

**Technical Report**

**TR-05-13**

**Summary of a GAMBIT Club  
Workshop on Gas Migration  
in Bentonite, Madrid  
29–30 October, 2003**

**A Report produced for the GAMBIT Club**

WR Rodwell, Serco Assurance

November 2005

**Svensk Kärnbränslehantering AB**

Swedish Nuclear Fuel  
and Waste Management Co  
Box 5864

SE-102 40 Stockholm Sweden

Tel 08-459 84 00

+46 8 459 84 00

Fax 08-661 57 19

+46 8 661 57 19



**Summary of a GAMBIT Club  
Workshop on Gas Migration  
in Bentonite, Madrid  
29–30 October, 2003**

**A Report produced for the GAMBIT Club**

WR Rodwell, Serco Assurance

November 2005

The full report including all Appendices is available as a pdf-file on the enclosed CD. The printed version contains only the main text and a list of the Appendices.

# **Abstract**

In order to review the status of understanding of gas migration in bentonite, and particularly the experimental data that provides the basis for such understanding as exists, the GAMBIT Club organised a workshop of invited participants that was held in Madrid during 29–30 October 2003. (The GAMBIT Club is a consortium of radioactive waste management agencies: SKB, ANDRA, Enresa, JNC, Nagra, and Posiva.) The motivation for the workshop was the difficulty found in developing models of gas migration in bentonite because of lack of detailed characterisation of its mechanism and controlling parameters.

This report provides a summary of the presentations made at the workshop and of the discussions that took place. Copies of the slides presented are provided in Appendix B.

May 2004

# Sammanfattning

The GAMBIT Club (SKB, ANDRA, Enresa, JNC och Posiva) arrangerade en workshop med inbjudna deltagare i Madrid 29–30 oktober 2003. Avsikten var att granska kunskapsläget kring förståelsen angående gastransport i bentonit och särskilt de experimentella data som ligger till grund för förståelsen. Motivet för workshopen var svårigheten att utveckla modeller för gastransport i bentonit på grund av avsaknaden av en detaljerad karaktärisering av dess mekanismer och styrande parametrar.

Den här rapporten ger en sammanfattning a presentationerna från workshopen och de diskussioner som fördes. Kopior av presentationerna finns som appendix B.

# Contents

<b>1</b>	<b>Introduction</b>	7
<b>2</b>	<b>Summary of presentations</b>	9
2.1	Overview of current status of experimental knowledge and understanding of gas migration in bentonite	9
2.2	Summary of GAMBIT club modelling of gas migration in compacted bentonite	12
2.3	A capillarity/advection model for gas break-through pressures	14
2.4	Recent experiments by JNC on gas migration in bentonite	19
2.4.1	Early gas migration experiments at JNC	19
2.4.2	Gas migration in an isotropically confined bentonite sample; recent experiments	20
2.4.3	Computer tomography imaging	20
2.4.4	Gas migration in sand-bentonite mixtures	21
2.4.5	Continuum modelling of gas migration	21
2.4.6	Conclusions	23
2.5	Gas flow in clays: experimental data leading to two-phase and preferential-path modelling ( <i>Eduardo Alonso</i> )	23
2.6	Gas movement in Mx80 bentonite under constant volume conditions	27
2.6.1	Background to test philosophy	28
2.6.2	Test geometry	28
2.6.3	Swelling and hydration behaviour	28
2.6.4	Baseline hydraulic properties	30
2.6.5	Gas migration behaviour	30
2.6.6	Process understanding (all tests)	33
2.6.7	Conclusions from the BGS CVRF and $K_0$ gas migration tests	34
2.7	Some practical observations on gas flow in clays and clay-rich rocks	35
2.7.1	Gas entry in unconfined clays at moisture contents between the liquid and plastic limits (particle-displacement mechanism)	35
2.7.2	Gas burps and mud volcanos	36
2.7.3	Gas migration in offshore geological environments	36
2.2.4	Inflammable gas emissions in the Hanford waste tanks	37
2.7.5	Study of gas migration in clay cores	38
2.7.6	Conclusions from the survey of gas migration data	39
2.8	Early large-scale experiments on gas break-through pressures in clay based materials	40
<b>3</b>	<b>Discussion</b>	43
	<b>References</b>	47

**Appendix B Presentations from workshop**

Overview of Current Status of Experimental Knowledge and Understanding of Gas migration in Bentonite (William Rodwell)

Summary of GAMBIT Club Modelling of Gas Migration in Compacted Bentonite (William Rodwell)

A Capillarity/advection Model for Gas Break-through Pressures (Marolo Alfaro, Jim Graham)

Recent Experiments by JNC on Gas Migration in Bentonite (Kenji Tanai, Mikihiro Yamamoto)

Gas Flow in Clays: Experimental Data Leading to Two-phase and Preferential-path Modelling (Eduardo Alonso)

Gas Movement in Mx80 Bentonite under Constant Volume Conditions (Jon Harrington, Steve Horseman)

Some Practical Observations on Gas Flow in Clays and Clay-rich Rocks (Steve Horseman, Jon Harrington)

Early Large-scale Experiments on Gas Break-through Pressures in Clay based Materials (Harald Hökmark)

# 1 Introduction

The GAMBIT Club is a consortium of radioactive waste management agencies consisting of SKB, ANDRA, Enresa, JNC, Nagra, and Posiva who have been funding the development, by Serco Assurance, of models of gas migration through saturated bentonite clay buffers used for the isolation of radioactive wastes in underground radioactive waste repositories. The discussions at GAMBIT Club meetings on model development have illustrated that there are substantial uncertainties in the understanding of the physical mechanism of gas migration in bentonite and about the implications of the range of different experimental results that have been obtained. These uncertainties hamper model development. GAMBIT Club members decided therefore to organise a workshop to consider the data currently available on gas migration in compacted bentonite and their interpretation in terms of mechanisms of gas migration through bentonite. The workshop was held at the offices of Enresa in Madrid on 29 and 30 October, 2003. This report is a summary of the workshop presentations, deliberations, and conclusions.

The main objectives of the workshop were:

- a) for experimental workers to present data on gas migration through bentonite to fellow experimentalists and model developers;
- b) for experimentalists and modellers to assess together the implication that the results of experiments and various theoretical considerations and modelling attempts have for the likely mechanism or mechanisms by which gas can migrate through bentonite buffers; and,
- c) to consider what, if any, new experimental or other work should be recommended to help to resolve current uncertainties in the mechanism of gas migration through compacted bentonite.

The focus of the workshop was on isothermal systems. Elevated temperatures and temperature gradients would occur in bentonite buffers around spent fuel and high level waste containers, before the waste had “cooled”, but elevated temperatures would tend to facilitate gas migration by promoting unsaturated conditions. The main issues arising in connection with the migration of gas would occur when saturated conditions had been established and were considered to be satisfactorily manifested in isothermal systems. These are already sufficiently complex for it to be desirable not to introduce additional complications into their evaluation by considering the effects of temperature variation. Furthermore, in the early stages, pore water will be undersaturated with  $H_2$ , thus gas dissolution and diffusion may prevent significant gas pressure buildup for some time.

The focus was also primarily on systems that have high initial water saturations, since it has been found that gas can pass relatively easily through bentonite when the water saturation is not high (say less than 90%). Ensuring that the initial water saturation is close to 100% can be difficult to achieve, but can be confirmed by weighing. (The standard Skempton-B geotechnical test for saturation would not be reliable for high density clays.)

The main performance assessment concerns arising from gas generation in wastes are the extent of any pressure rise that might occur as a consequence of the gas generation, and whether the gas can create preferential pathways for radionuclide transport.

The next section provides summaries of the presentations that were made at the workshop. The presentations themselves are being separately circulated to workshop participants, and the intention here is not to reproduce the details of those presentations, but to provide an overview of their main features and conclusions.

Section 3 provides an attempt to summarise the main views expressed and conclusions reached at the workshop.



## 2 Summary of presentations

The following technical presentations were made at the workshop, following a welcome address by Miguel Cuñado, and a statement by Patrik Sellin of the aims of the workshop as discussed in the Introduction:

- a) overview of the current status of experimental knowledge and understanding of gas migration in bentonite (William Rodwell);
- b) summary of GAMBIT Club modelling of gas migration in compacted bentonite (William Rodwell);
- c) a capillarity/advection model for gas break-through pressures (Marolo Alfaro, Jim Graham);
- d) recent experiments by JNC on gas migration in bentonite (Kenji Tanai, Mikihiko Yamamoto);
- e) gas flow in clays: experimental data leading to two phase and preferential path modelling (Eduardo Alonso);
- f) gas movement in Mx80 bentonite under constant volume conditions (Jon Harrington and Steve Horseman);
- g) some practical observations on gas flow in clays and clay-rich rocks (Steve Horseman and Jon Harrington);
- h) early large-scale experiments on gas break-through pressures in clay based materials (Harald Hökmark).

The first two presentations were primarily to provide context for the following talks on experiments on gas migration in bentonite, which formed the basis for the main purpose of the workshop, as described in the Introduction.

The overview of these presentations provided in the following subsections takes account of some of the discussion which took place in relation to the presentations. Where appropriate, some figures from the presentations have been included here for the purpose of illustrating the overview, but reference should be made to the presentations themselves for more extensive graphical illustrations.

### 2.1 Overview of current status of experimental knowledge and understanding of gas migration in bentonite

*(William Rodwell)*

This presentation attempted to provide an overview of the experimental data that exists on gas migration in bentonite, with the emphasis on saturated pure bentonite, but with an acknowledgement that data from related systems (e.g. other clays and sand-bentonite mixtures) may be relevant. Details of many of the experiments were provided in subsequent presentations. The presentation also noted possible interpretations of the data in terms of mechanisms that had been proposed, and discussed the relationship of these mechanisms with the experimental data and with modelling.

The conditions under which experiments on gas migration have been carried out vary significantly. Factors that differ between experiments include:

- the sample preparation method;
- the bentonite density;
- the confining conditions (e.g. constant volume or constant stress) and experimental geometry (linear or radial flow);
- the rate and manner of gas injection;
- the type of bentonite; and
- the range and type of measurements made.

An overview of the published experiments on gas migration in bentonite is provided in Table 2-1.

There is an obvious question of whether, and if so to what extent, the gas migration behaviour and mechanism is dependent on the experimental conditions.

The main features observed in the experiments on gas migration in bentonite may be summarised as follows:

- A threshold pressure for gas entry into the bentonite is observed in many experiments, the main exception being some Canadian experiments involving the long term application of a constant gas pressure (see Section 2.3). In some cases at least, this breakthrough pressure has been correlated with the swelling pressure.
- It appears that there is displacement of only small volumes of water from saturated bentonite by migrating gas, although the amount of water displaced has not often been determined.
- After breakthrough, gas flows at pressures below the threshold for initial flow, but flow ceases at pressures above the back pressure.
- Changes in porewater pressure and external stresses are observed in response to the applied gas pressure and the creation of gas pathways.
- There is evidence for macroscopic fracturing in radial flow experiments.

Turning to mechanisms of gas migration in compacted bentonite, three possible mechanisms of gas migration in have been proposed:

- Conventional two-phase porous medium behaviour. To model this type of flow mechanism, concepts of capillary pressure and relative permeability are invoked to relate the gas and water flows and pressures. Mechanisms in which water is displaced from capillary-like channels are considered to be the same type of mechanism.
- Microfissuring of the clay, in which new porosity is created to accommodate gas flow. This could involve compression of water and squeezing of water from clay particles (consolidation), as well as dilation of the whole sample. The clay sample is assumed to remain intact.
- Macroscopic fracturing of the clay. This is distinguished from microfissuring by the size of the fissures or fractures. For example, in the laboratory, the lengths of macroscopic fractures may be comparable to sample sizes.

**Table 2-1. Summary of experiments on gas migration in compacted bentonite.**

Authors	Bentonite	Dry density (Mg m <sup>-3</sup> )	Flow geometry	Gas flow controls	Confining conditions
/Pusch and Forsberg, 1983/†	Mx80	~ 1.35–1.65*	Linear	Constant pressure/pressure increments.	Constant volume oedometer.
/Pusch et al. 1985/	Mx80	~ 1.1–1.78*	Linear	Pressure increments.	Constant volume oedometer.
/Horseman and Harrington, 1997/	Mx80	1.5–1.7	Linear (axial) flow	Displacement of gas by water from an upstream reservoir.	Constant isotropic stress in flexible sleeve subject to external fluid pressure (8–22 MPa).
/Horseman and Harrington, 1997/	Mx80 paste	1.3–1.4	Point source and sink	Displacement of gas by water from reservoir.	Cylindrical pressure vessel with confining pressure (0.8–2.7 MPa) imposed on floating end cap.
/Tanai et al. 1997/	Kunigel VI, Fo-Co Clay	1.4–1.8	Linear	Pressure increments.	Constant volume cylinder.
/Gallé, 1998, 2000/	Fo-Co Clay	1.6–1.9	Linear	Pressure increments.	Constant volume oedometer cell.
/Graham et al. 2002; Hume, 1999/	Avonlea	0.6–1.4	Linear	Pressure increments/sustained pressure	Constant volume oedometer cell.
/Harrington and Horseman, 2003/	Mx80	1.577, 1.582	Approximately radial from central source	Displacement of gas by water from an upstream reservoir.	Constant volume cylindrical vessel.
/Harrington and Horseman, 2003/	Mx80	1.596	Linear	Displacement of gas by water from an upstream reservoir.	Cylindrical pressure vessel with confining pressure (10 MPa) applied to floating end caps.
/Tanai, unpublished 2002/	Mx80	1.63	Linear	Constant gas pumping rate.	Constant isotropic stress in flexible sleeve subject to external fluid pressure.

† Gas flow in these experiments may have occurred via diffusion of dissolved gas.

\* Estimated from saturated bulk density.

Despite evidence from tests on relatively lower density Canadian buffer, a consensus appears to be developing that gas migration in densely-compacted bentonite is not generally one of conventional two-phase flow. The reasons for this are:

- It is suggested that gas flow is localised (i.e. follows spatially isolated pathways) with very little displacement of water. This reasoning depends on the scale at which the mechanism is considered to apply.
- Conventional two-phase flow models do not generally address the possibility of the creation of new gas-occupied porosity.
- The high gas entry pressure is ascribed to capillary pressure in two-phase flow models. In terms of a capillary-bundle porous-medium model, this requires that the capillaries have a very small radius in order to reproduce the observed gas entry pressure, but then a very large number of these pathways are required in order to match the observed gas and water permeabilities.

On the other hand, if microfissuring/fracturing is not involved, it might be found possible to use a conventional two-phase modelling approach but with novel saturation functions to describe gas migration (e.g. with saturation functions/permeability that include a pressure dependence).

In a few experiments, there is clear evidence of macroscopic fracturing, but the arguments for microfissuring are more circumstantial. They include:

- the observation of the dilation of some samples;
- arguments that there are no connected gas accessible pores at least in highly compacted bentonite; and
- the fact that there is no gas entry until the stress in the clay is exceeded by the gas pressure in most experiments implies that gas pressure is needed to hold open fissures (but note flow continues at lower pressures once established).

It was noted that different mechanisms could occur under different circumstances. It was part of the purpose of the workshop to see whether the experimental data could be interpreted to provide a clearer picture of the likely mechanism of gas migration in bentonite.

## **2.2 Summary of GAMBIT club modelling of gas migration in compacted bentonite**

*(William Rodwell)*

This presentation was included to acquaint workshop participants who were not involved in the GAMBIT Club with the work on modelling gas migration in compacted bentonite that had been commissioned by the GAMBIT Club, and to bring GAMBIT Club members up-to-date with the current status of the latest work. Much of the work has appeared in reports and so is not described in detail.

The results of the modelling work were evaluated by comparisons with the results of experiments undertaken by BGS (funded by SKB). The features of these experiments which it was desired to reproduce were:

- there is a threshold pressure for gas entry that in some cases is correlated with swelling pressure;
- only small volumes of water are displaced;
- once established, flow continues at gas pressures below the threshold pressure for gas entry, but there is a “shut-in pressure” at which gas ceases to flow;
- changes in pore-water pressure are observed;
- experiments on radial flow of gas from small filters exhibit high threshold pressures and evidence for fracturing; and,
- gas pathways are resealed by resaturation.

The numerical model investigations carried out comprise mainly /Nash et al. 1998; Swift et al. 2002/:

- gas migration by fissure propagation;
- displacement of water from pre-existing capillary-like pathways;
- a continuum model of gas migration through newly-created gas-filled porosity;
- an attempt to represent the effect of the stress state of the clay on gas migration.

In the first model, gas invasion was assumed to occur by the formation of microfissures that could propagate when the gas pressure reached a critical value. Creation of gas pathways by fracture propagation was described in the model. Dilation of the gas pathways formed by fracture propagation was assumed to occur in response to changes in gas pressure, as such behaviour was implicated in the results of experiments on gas invasion of samples confined by a constant isotropic stress. The gas permeability was a function of the pathway dimensions. The behaviour of the clay itself was represented simply by its mechanical and fracture resistance properties; neither water movement nor the swelling properties of the clay were modelled.

The model based on the displacement of water from pre-existing capillary-like pathways was developed from the fracture propagation model by replacing the creation of gas pathways by fissuring by the displacements of water from capillaries.

The continuum model of gas migration through newly-created gas-filled porosity was developed with two main purposes:

- a) To provide a model that would be more readily upscalable to two- or three-dimensions and to field-scale problems than the fissure propagation model.
- b) To include some experimentally observed features of gas migration in bentonite that were not represented in the fissure propagation model. These were flow of water through the bentonite, coupling between the gas pressure and the water pressure as reported in some experiments /Horseman and Harrington, 1997; Harrington and Horseman, 2003/, resealing of the gas pathways after gas transport has finished and the clay is resaturated, and coupling of the water content and the stress state of the clay (swelling/suction behaviour). The last of these was modelled in a much simplified fashion.

The final investigation was an attempt to extend the continuum model to properly include the effect of the stress state of the clay on gas migration. The factors motivating this attempt were:

- a) The conceptual understanding of gas migration in clay (for example involving some dilation of the clay) has led to suggestions that a sensitivity to the stress state of the clay might be expected /e.g. Horseman and Harrington, 1997; Harrington and Horseman, 2003; Rodwell et al. 1999/.
- b) The international consensus expressed at the recent international workshop on gas generation and migration /NEA, 2001/ was that gas migration in bentonite would be sensitive to the stress state of the material.
- c) In upscaling a model of gas migration in bentonite to the scale of deposition holes it becomes important to consider the factors which might control the direction that is likely to be followed by gas migration pathways. The stress field is considered likely to be a factor having a strong influence on this direction as dilatation of the clay is expected to occur more easily normal to the lowest stress. Satisfactory treatment of the stress field may therefore become an important issue in upscaling, for reasons that make it less so in modelling laboratory experiments in which the gas flow direction is prescribed by the experimental geometry.
- d) A more thorough treatment of the mechanical behaviour of the bentonite may facilitate possible future extension of the model to gas migration in argillaceous host rocks in which there may be a pre-existing anisotropic stress field.

A particular difficulty with this attempt was that it requires the specification of the interactions between the stress field and the gas and water pressures and saturations but the nature of these couplings is not known (i.e. the constitutive behaviour of partially saturated bentonite subjected to applied gas and water pressures has not been fully understood).

In very general and abbreviated terms, the results of these modelling investigations are:

- The model of gas migration by fissure propagation can account semi-quantitatively for observed gas migration behaviour, but depends on some heuristic arguments, and only accounts for some features of bentonite behaviour on gas migration.
- Gas migration by water displacement requires a very large number of small capillaries (to reproduce the capillary entry pressures and permeabilities that are observed).
- The upscaleable continuum model gives agreement with experiment broadly comparable with other models and represents more of the observed experimental features.
- Extension of the continuum model to properly include stress effects has yet to be satisfactorily achieved, and suffers in particular from poor characterisation of the controls on gas pathway propagation, the couplings between physical parameters, and the mechanism involved in gas migration through bentonite.

### **2.3 A capillarity/advection model for gas break-through pressures**

*(Marolo Alfaro, Jim Graham)*

The topics of this presentation were the results of a large set of experiments on gas migration in Avonlea bentonite, illite, and bentonite-sand and illite-sand mixtures (both 50–50 mixtures), and the modelling of some of the results. Two distinct sets of tests were carried out.

In the first set of tests, pressures were incremented steadily at one end of a specimen over a period of time lasting from minutes to hours until an increase in pressure was observed at the other end of the specimen. The pressure at which this occurred was called the ‘gas breakthrough pressure’.

The second set of tests involved putting a pressure differential across a specimen and then waiting to see how long, or if, pressure would begin increasing at the downstream end of the specimen.

All testing was done in 50 mm diameter rigid wall cells. The dry density of the bentonite was in the range 0.6–1.45 Mg m<sup>-3</sup>.

The second set of tests was instigated because of difficulties experienced in the first set in obtaining gas breakthrough in the more saturated samples before the upstream gas pressure had exceeded the design limits for the apparatus, even when this was 50 MPa.

An important observation, which is potentially significant when comparing experimental results from different systems, is that for samples with the same dry density and degree of water saturation, the breakthrough pressure depends on the saturation of the sample when it is initially prepared, even if the saturation is increased to a common value by water injection. This is ascribed to the fact that the bi-modal micro- and macro-structure of compacted smectites depends on the water content at the time of hydration. Specimens with different degrees of initial saturation therefore have different microstructures.

Figure 2-1 confirms that there is no threshold pressure for gas migration at a water saturation less than 92–93% at the dry density of the samples shown. It is assumed that below this saturation, air-filled channels are already present before gas injection.

Figure 2-2 shows the dependence of the breakthrough pressure, in the incremental pressure tests, on a wider range of variables. Note the increase in breakthrough pressure with dry density.

A counter-intuitive result was obtained from examination of the distribution of water in a sample at the end of an experiment. It was found that the gas inlet end of the sample was wetter than the outlet end. This is illustrated in Figure 2-3 for results from incremental pressure tests on moderately compacted bentonite with a clay dry density of 1.10 Mg m<sup>-3</sup>.

An explanation of this was offered in terms of effective stress, with the effective stress being lower at the inlet than at the outlet end of the sample, which led to expansion of the sample at the inlet end (hence wetter) and compression at the outlet end (drier). This seemed to require water flow against the hydraulic gradient, which seemed to some workshop participants to need explaining.

It was also observed in a few tests using illite that the breakthrough time decreased with increasing pressure difference across the sample, so that the breakthrough pressure measured in these tests could be dependent on the test procedure (i.e. breakthrough might occur at lower pressures than first determined given sufficient time).

This motivated the second series of tests in which a constant upstream gas pressure was applied to samples for an extended period of time. These tests showed gas breakthrough at low applied gas pressures if sufficient time was allowed.

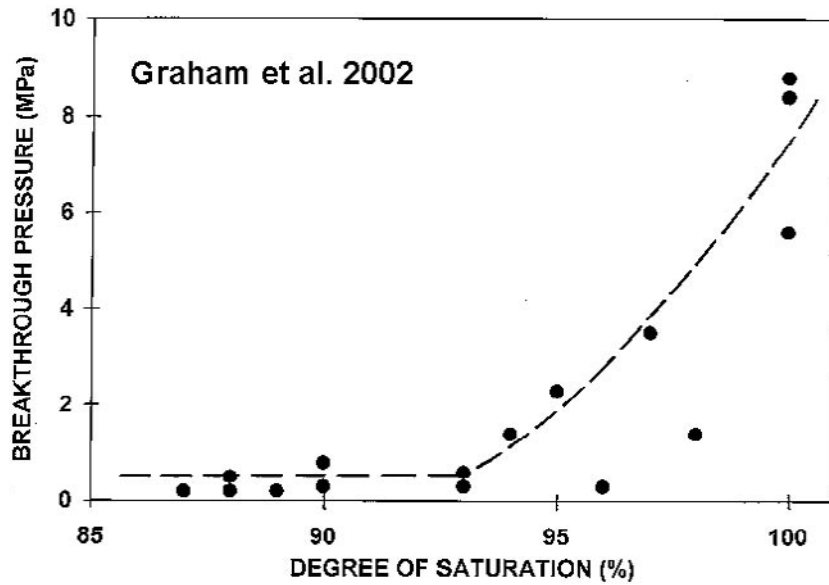


Figure 2-1. Breakthrough pressures from incremental pressure tests on bentonite as a function of degree of saturation.

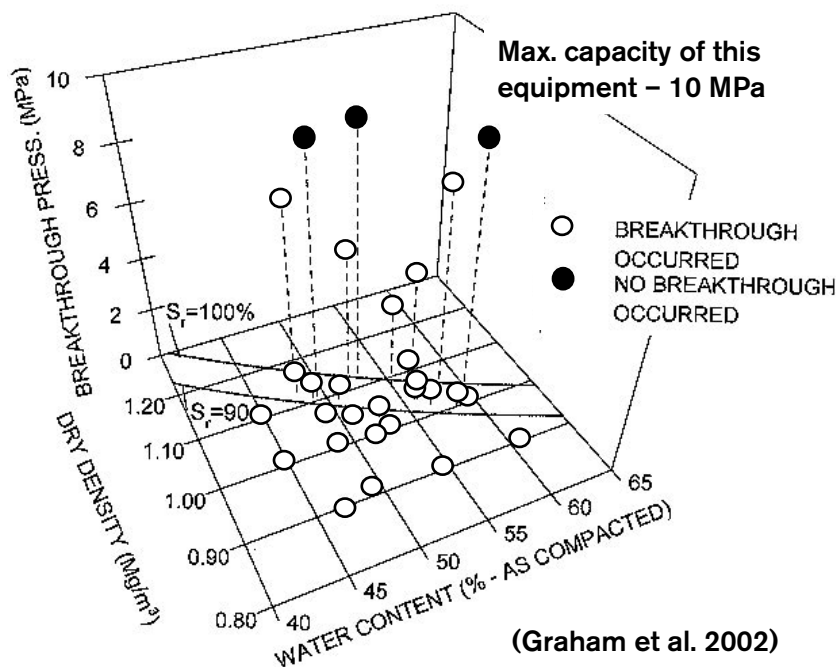
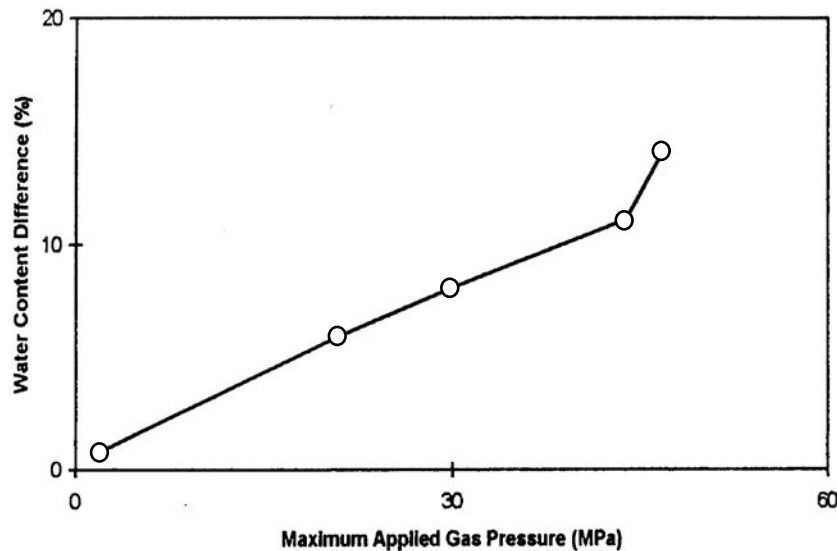


Figure 2-2. Breakthrough pressures from incremental pressure tests on unsaturated bentonite in terms of water content and dry density.





**Figure 2-3.** Differences in water content (inlet – outlet) related to gas pressure at end of test (dry density =  $1.10 \text{ Mg m}^{-3}$ ).

An explanation of this was offered in terms of gas displacement of water from capillary-like pathways present in the bentonite. The pore-size distribution measured for at least some bentonite samples using mercury intrusion shows bimodal characteristics (see Figure 2-4, in which the bimodal pore-size distribution for bentonite is contrasted with a unimodal distribution for illite).

Gas is presumed to displace water from the larger set of pores, leading to a simplified model for gas breakthrough:

- Below a certain degree of saturation, continuous gas channels are present and resistance to breakthrough is minimal.
- When the gas phase is not continuous, gas has to overcome capillarity to enter pores. Below a ‘gas entry value’ breakthrough will not occur.
- Gas pushes water advectively through larger pores until a continuous pore channel is formed.
- This permits gas breakthrough.

A model of water displacement by gas from uniform capillaries at a constant pressure difference across the sample leads to a gas breakthrough time that is inversely proportional to the pressure difference (note that, in these experiments, the inlet and outlet pressures are both measured in the gas phase, there being gas at both ends of the sample, so that any capillary pressure effects cancel). For bentonite with a low dry density ( $1.0 \text{ Mg m}^{-3}$ ), such a relationship was observed over a range of low pressure differences, but not over the whole range of pressure differences. For more compacted bentonites, this relationship was not quantitatively followed, as shown in Figure 2-5, but some reasonably systematic trends are seen:

- a) breakthrough times decrease with increasing pressure difference (hydraulic gradient),
- b) breakthrough times increase with increasing dry density (smaller pores, lower hydraulic conductivity).

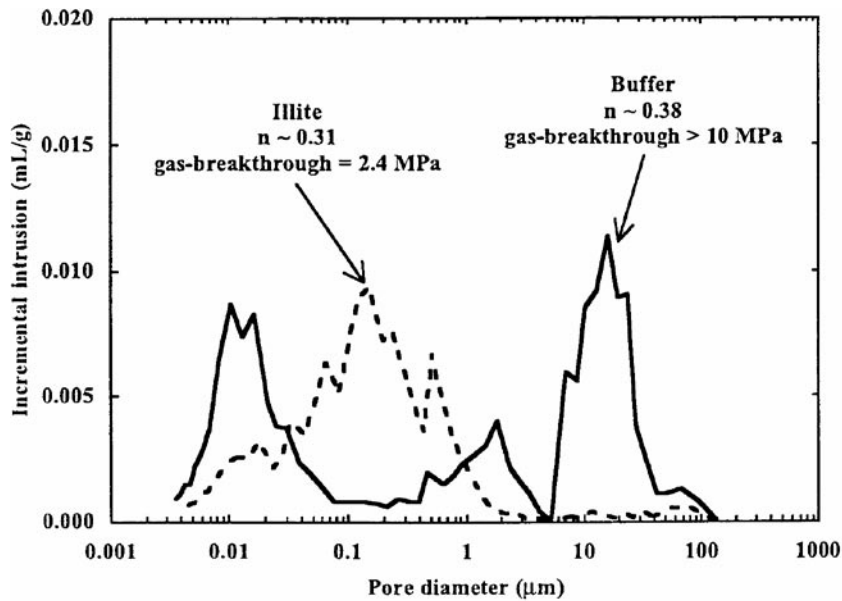


Figure 2-4. Pore size distributions: compacted illite and bentonite specimens /Gray et al. 1996/.

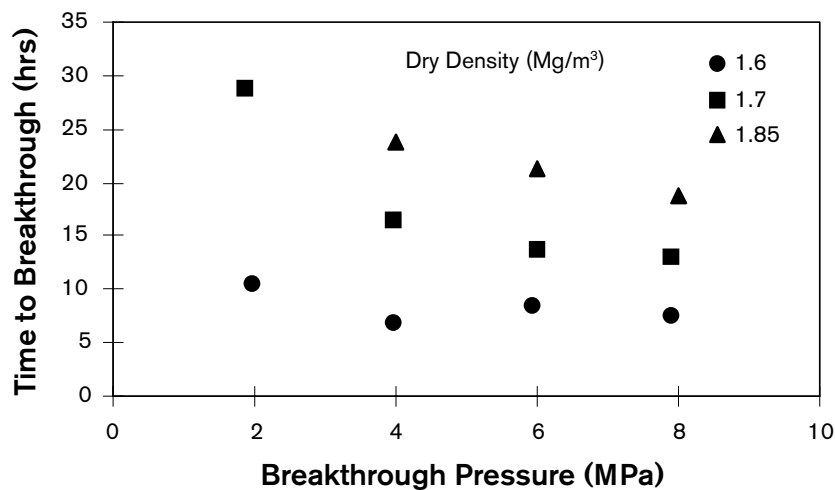


Figure 2-5. Time versus pressure difference relationship from bentonite – ‘constant pressure’ tests at 100% initial water saturation.

For specimens with lower, 95%, water saturations, trend (a) was not really apparent. Trend (b) was still followed reasonably consistently, and the breakthrough times were shorter than at the higher saturation.

The conclusions reached by these presenters are that:

- gas breakthrough occurs when the largest pore has fully drained;
- breakthrough times depend on pressure gradient;
- breakthrough times increase with effective clay dry density;
- resistance to breakthrough is low below a threshold degree of saturation;
- large diffuse double layers block small pores, create gel structures and inhibit water movement.

## 2.4 Recent experiments by JNC on gas migration in bentonite

*(Kenji Tanai, Mikihiro Yamamoto)*

This presentation covered the following topics:

- A summary of earlier gas migration experiments carried out by JNC and of the results obtained.
- A report on the current status of gas migration studies in JNC. This included an account of:
  - the latest experimental set up being used and the results obtained;
  - the use of CT tomography to try and see the effects of migrating gas;
  - simulation of a gas migration test on a sand-bentonite mixture using a modified version of the Tough-2 program.

The material presented is summarised under these headings in the following subsections.

### 2.4.1 Early gas migration experiments at JNC

The earlier gas migration study had been carried out in a conventional oedometer style test vessel (i.e. essentially constant volume). Bentonite and bentonite/sand mixtures were used as test materials, with samples placed in the test vessel and compacted uniaxially to predetermined dry densities. Water was supplied from the lower side of specimen by the water-head method or by using a water injection pump to saturate the samples. Hydrogen gas was injected from the lower side of the specimen, and the injection pressure increased stepwise. The outlet gas flow rate was monitored continuously, with the onset of flow being used to identify the breakthrough pressure, and subsequently to determine the effective permeability to gas.

The breakthrough pressure seems to correlate quite well with the experimentally determined swelling pressure. This is illustrated in Figure 2-6. On the other hand, the breakthrough pressure with a 10 cm thick sample is more than twice as large as that with 1 and 5 cm thick samples. It was postulated that there is a time lag between the gas pressure change in the clay and the expansion of cracks that serve as the gas pathways. In other words, the formation of the gas migration pathways occurs too late to follow the pressure rise, which resulted in the higher breakthrough pressure for the thicker sample. Breakthrough pressures measured on samples that had been resaturated following previous flow of gas through the sample showed values similar to those measured in the previous cycle, giving confidence in the resealing capacity of bentonite after gas migration.

The gas permeability for bentonite specimens was found to decrease with increasing effective clay density. A rather large variation in measured permeabilities with effective dry density was observed. The gas permeabilities obtained range from  $10^{-17}$  m<sup>2</sup> for mixtures with a 30% sand mass fraction at a dry density of 1.6 Mg m<sup>-3</sup> to  $10^{-20}$  to  $10^{-21}$  m<sup>2</sup> for pure bentonite at a dry density of 1.8 Mg m<sup>-3</sup>.

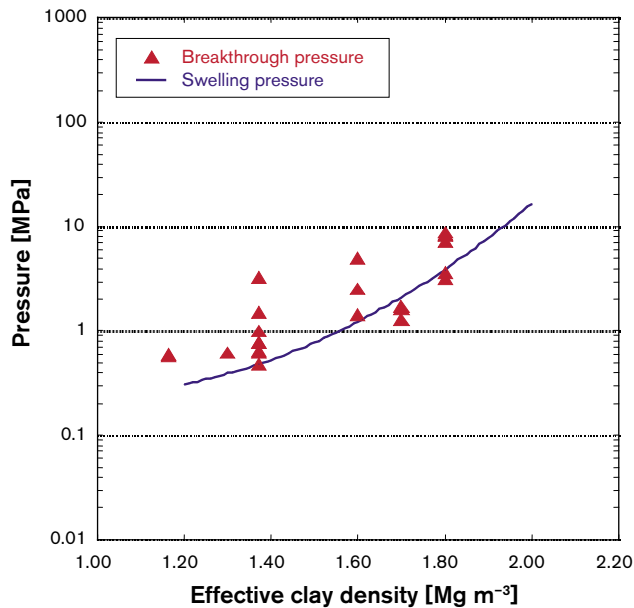


Figure 2-6. Comparison of breakthrough pressure and swelling pressures.

#### 2.4.2 Gas migration in an isotropically confined bentonite sample; recent experiments

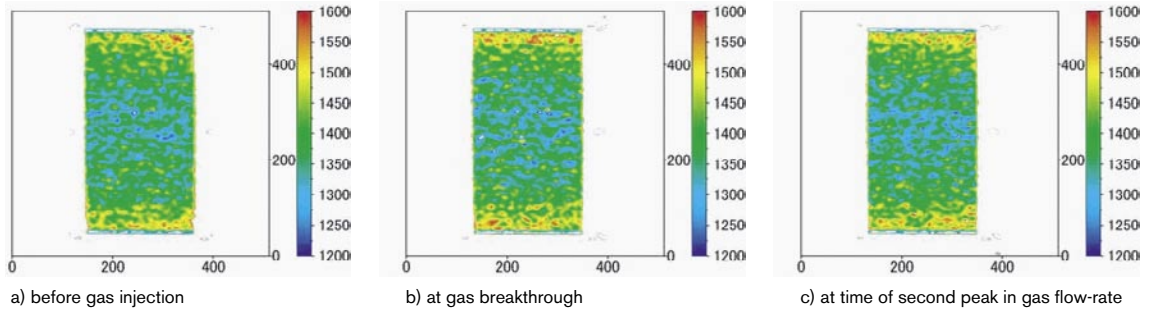
The more recent experiments made use of an alternative system for confining the clay samples. The clay was confined under isotropic stress in a pressure-controlled fluid path. It was initially resaturated by applying a fixed back-pressure of distilled water. An important objective of these experiments was to test whether X-ray computer tomography (CT) could be used to follow gas migration behaviour in bentonite. An attempt was made to use this technique to measure, non-destructively, the distribution of liquid or gas saturations in experimental samples.

Bentonite powder was compacted uniaxially to a dry density of  $1.6 \text{ Mg m}^{-3}$  in the test vessel and resaturated from the upstream face of the specimen by water injection. Starting from an upstream gas pressure of 600 kPa, gas (helium) was pumped into the gas volume upstream of the sample at  $0.05 \text{ mL m}^{-1}$ . The upstream gas pressure, gas flow rate and drainage volume of water were measured continuously.

The upstream gas pressure rose until substantial gas entry occurred at a gas pressure of 2.6 MPa, accompanied by an increase in the downstream gas flow rate (some much smaller flows occurred before this). This breakthrough pressure is larger than the swelling pressure of the bentonite, which was  $\sim 1 \text{ MPa}$ . The upstream pressure fell as gas escaped through the specimen, but a sudden large temporary increase in downstream gas flow was observed when the upstream pressure had dropped to 1.8 MPa. This second peak was considered probably indicative of the generation of a preferential pathway in the specimen; this might have been between the bentonite specimen and the test vessel.

#### 2.4.3 Computer tomography imaging

The CT scans were carried out prior to gas injection, at gas breakthrough, and at the time of the second peak in gas flow-rate. Some results are shown at these times in Figure 2-7 for the distribution of the “CT” value, which is a measure of X-ray attenuation of the X-rays (note that the axis of the core is horizontal in the figures). The CT parameter had previously been shown to be linearly proportional to the bulk density of the bentonite sample.



**Figure 2-7.** CT tomography results from gas migration experiments. The figures are for cross-sections parallel to the axis of the sample, with the axis in an horizontal orientation.

Prior to gas injection, the CT scan shows some increase in bulk density around the circumference of the sample relative to the core of the sample, presumably resulting from the method of the sample preparation. After gas breakthrough, there is some indication of an increase in this difference in CT values. Whether this is due to the presence of gas in the centre of the core cannot be ascertained, and the effect is neither clear cut nor pronounced. It is not possible to identify any discrete gas channels, but if they are present their widths are probably less than the resolution of the CT scanner.

#### 2.4.4 Gas migration in sand-bentonite mixtures

Example gas migration results were also shown for a 70/30 (by mass) mixture of Kunigel V1 bentonite (containing around 47% of smectite) and sand. It was possible to identify the displaced water volume in the sample as the volume of water expelled from the apparatus minus dead volumes in the apparatus, both upstream and downstream of the sand/bentonite mixture. From the experiment using low smectite content material, dehydration was estimated as 5% or more. Some graphs of results can be found in the copy of the presentation.

#### 2.4.5 Continuum modelling of gas migration

The final topic described in this presentation was of an attempt to use a modified conventional porous medium flow simulator (TOUGH2) to model the gas migration test in pure bentonite described above. The modifications to the program were in the specification of the gas permeability and relative permeability functions. It is assumed that the gas permeability is a function of pressure

$$k_{\infty}(p_c) = k_0 \left( \frac{-P_c - P_r}{P_e - P_r} \right) \exp \left( 4 \frac{-P_c - P_e}{G} \right)$$

and there is a time lag in the response of the permeability to pressure changes:

$$\frac{\partial k_{rg}}{\partial t} = -\lambda [k_{rg} - k_{\infty}(p_c)]$$

where

$p_c$  is the capillary pressure;

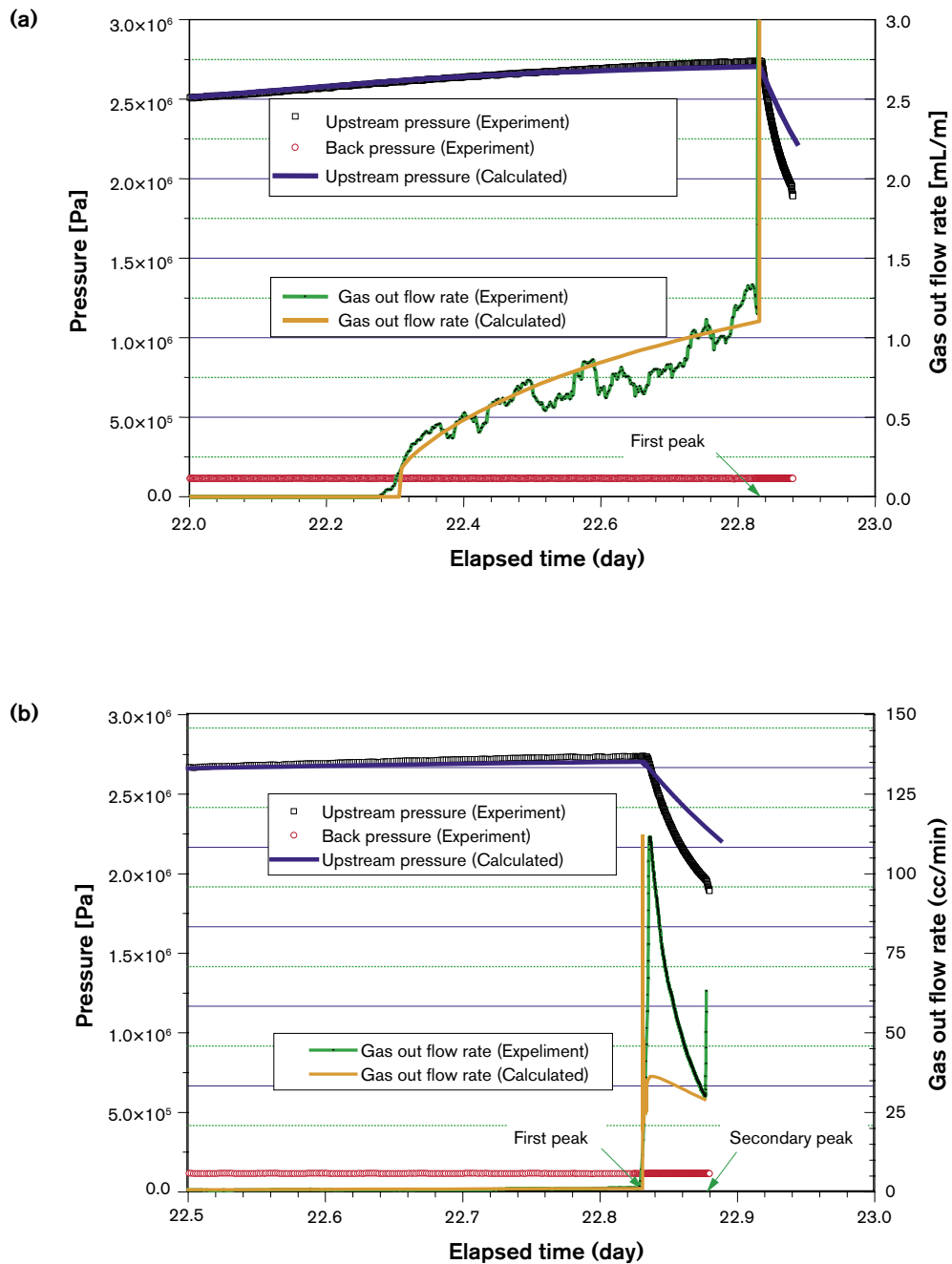
$p_e$  is the excess gas pressure (above the water back pressure);

$p_r$  is the excess pressure when the pathways reseal;

$k_{rg}$  is the gas relative permeability;  
 $k_{\Psi}$  is the steady state gas relative permeability;  
 $k_0, G, \lambda$  are constants.

Some results obtained with suitably chosen parameters for the first part of the experiment are shown in Figure 2-8.

The calculated results show encouraging agreement with the experimental observations of gas entry and breakthrough, up to a sudden large increase in gas out-flow, which corresponds to a gas permeability of  $10^{-17} \text{ m}^2$  and is considered likely to be associated with



**Figure 2-8.** Calculated versus experimental results for gas migration through saturated bentonite ((a) focuses on behaviour up to the peak in gas outflow; (b) on the behaviour after this peak).

the formation of a preferential pathway. The observed behaviour after this peak in gas outflow is less well reproduced by the calculation. It is not surprising that the computational model is less satisfactory in predicting the behaviour after this “burst flow”, as it does not, for example, contain features that can represent the formation of preferential pathways or a second peak that is seen in the gas outflow rate.

#### **2.4.6 Conclusions**

The overall conclusions of this presentation were:

- a) Early gas migration experiments at JNC showed some correlation between gas breakthrough pressure and swelling pressure, although the spread of experimental values was rather large. In later experiments in moderate density bentonite, the breakthrough pressure was substantially above the swelling pressure.
- b) Resaturation effectively sealed gas pathways.
- c) In later experiments, some instability was apparent in gas pathways after breakthrough.
- d) The use of X-ray tomography to map density variations in bentonite samples, before and after gas migration, has been successfully demonstrated, but the technique did not provide identification of the characteristics of the pathways followed by the gas, possibly because the pathways were smaller than the resolution of the technique.
- e) The use of a conventional porous medium flow simulator that had been modified to include a pressure dependent gas permeability was, with appropriately chosen parameters, successful in simulating the first part of a gas migration experiment, including gas entry and breakthrough, up to the point of a sudden large increase in gas flow rate. After this, agreement was less satisfactory, as the model did not include any mechanisms that would be able to simulate instabilities after the large increase in gas flow rate, which may have involved the generation of fracture-like gas pathways.

### **2.5 Gas flow in clays: experimental data leading to two-phase and preferential-path modelling**

*(Eduardo Alonso)*

The main thrust of this presentation was the development of a model of gas migration in bentonite starting from the premise that heterogeneities in the bentonite mean that there are predetermined pathways in the clay that will be preferentially followed by the gas.

Evidence used to suggest that this starting was reasonable included:

- f) Bentonite dismantled after it had been saturated in the Febex experiment showed continuing evidence of the presence of joints between the blocks from which the bentonite buffer was assembled in situ.
- g) Measurements of pore-size distributions in bentonite show bimodal character (e.g. in Febex bentonite with a density of 1.6–1.8 Mg m<sup>-3</sup>, the peaks in the bimodal distribution were at pore radii of 10 nm and 10–100 μm).
- h) Electron microscope images show the presence of macro-pores between clay particles containing only internal micropores.
- i) Hysteresis in the variation in volumetric strain with total suction may be attributed to the effect of macropores in the bentonite.

The generally accepted picture was recognised that there were a number of potential mechanisms by which gas could migrate through saturated clay buffers, and any number of which could potentially occur together. At low enough gas generation rates, diffusion of dissolved gas could transport all the gas produced, but at higher rates gas flow could occur by:

- j) flow through the matrix of the clay, displacing water (conventional two-phase flow);
- k) flow through fissures and discontinuities, which could be either existing discontinuities, or discontinuities generated by crack propagation.

It was argued that gas-carrying channels might dilate in response to the gas pressure if the gas migration rate is in equilibrium with the gas generation rate, but crack propagation might occur if the tensile strength of the clay at the tip of the dilating channel were exceeded due to a fast pressure build up.

The idea that gas migration would tend to follow localised pre-existing features, which may, for example, be interfaces, shear zones, or schistosity/sedimentation planes, provided the motivation for a model of gas migration in clays. These planar features would behave different properties from other parts of the porous medium.

This concept was explored in a simple illustrative example in which the fracture zone properties were represented through the dependence of the permeability and capillary pressure on porosity: above a critical porosity, perhaps representing the point at which the fracture becomes active, the increase in permeability with porosity was greater than below that porosity. Correspondingly, the capillary pressure decreased more rapidly with porosity above the critical porosity than below it. The stress/strain (with porosity depending on strain) behaviour of the illustrative model was governed by a deformable soil model including a contribution from matric suction. Using a model to simulate gas migration with an initial porosity that was above the critical porosity in the fracture zone, but below it elsewhere, resulted in focusing of the gas flow along the fracture zone. There was an increase in porosity in this zone, representing fracture opening, and a decrease elsewhere.

Based on this example, a more general model was described. The basic features of this model are:

- the definition of pre-existing fracture zones containing the fracture planes to be activated;
- normal deformations to the reference plane result in fracture opening: in an element of the fracture zone, all the strain normal to the fracture plane is assumed to be associated with opening of the fracture passing through the element;
- the mechanical model for the fracture zone and other rock is based on an elastoplastic model, which includes the effect of changes in suction on drying and swelling and a tensile strength that depends on suction;
- the permeability of the fracture is described by a laminar flow model (cubic dependence on aperture), which gives an anisotropic total permeability for the fracture zone.

The presentation of this work included some mathematical details of the generalised model (see attached slide presentation).

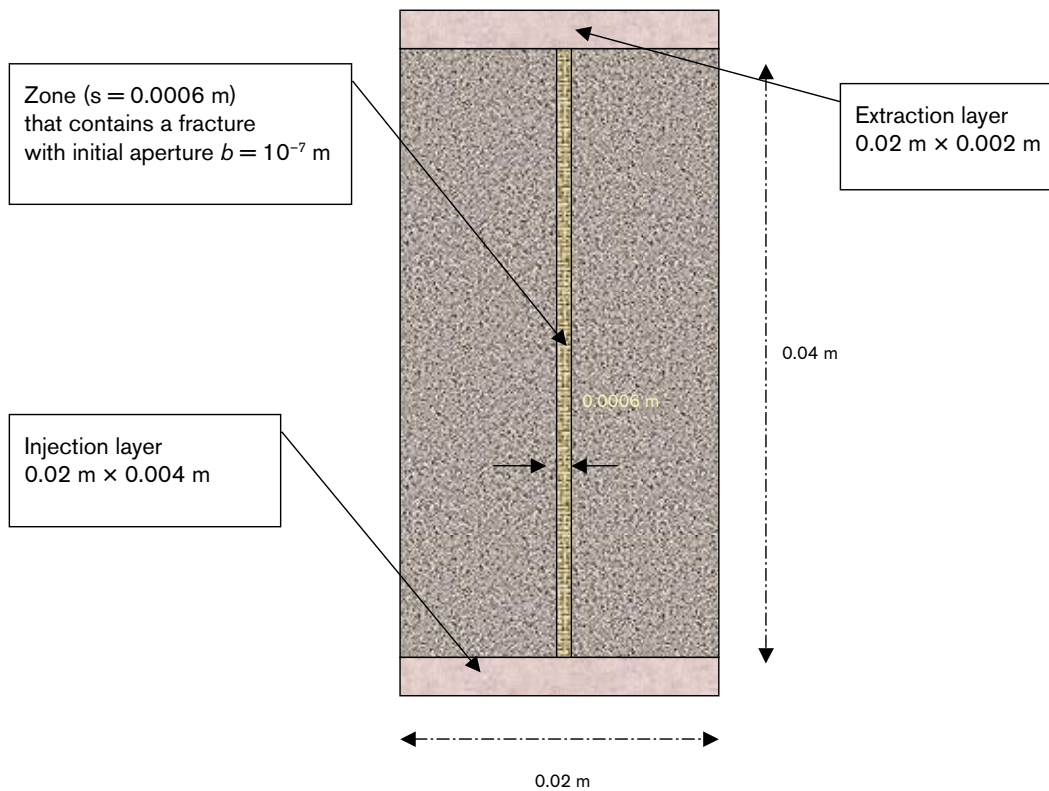


The generalised model was applied to the simulation of a permeability test sequence carried out on a 30 mm diameter mini Opalinus Clay core by Rummel and Weber for the Mont Terri Project. The test program consisted of:

- sample drying at 105°C;
- pressure pulse testing with argon under triaxial load;
- fracture initiation by axial deformation;
- pressure pulse testing with argon to determine the permeability of the fractured sample;
- water flooding carried out as a combination of constant pressure and constant rate injection to heal the sample;
- further pressure pulse testing with argon at increasing pressures up to the confining pressure.

Figure 2-9 shows the model dimensions.

It is assumed in the model that initially the fracture exists but is closed. Deviatoric stresses open the existing fracture.



**Figure 2-9.** Schematic of model used to model the Rummel and Weber tests on an Opalinus Clay core.

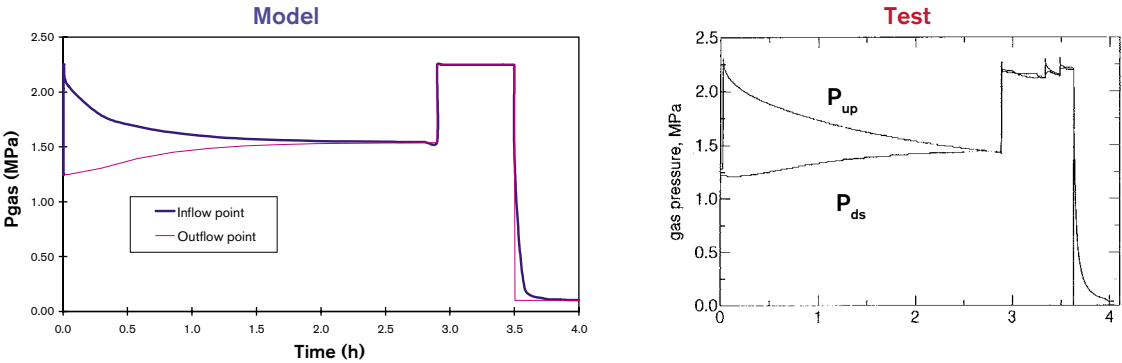
Figure 2-10 compares the results of the gas injection tests on the dried sample with the model results. Results from time 0 to 3 hours correspond to the initial gas injection pulse test. At 3 hours the fracturing process is initiated, and the second argon pulse test is carried out at 3.5 hours. The rapid equilibration of the gas pressures in the second test compared with the first indicates the much increased permeability resulting from the fracturing ( $1.2 \cdot 10^{-16} \text{ m}^2$  compared with  $5.2 \cdot 10^{-19} \text{ m}^2$ ). The model results evidently reproduce behaviour similar to the experiments, although with a more rapid equilibration of the gas pressures than seen in the experimental results.

Figure 2-11 shows the progress of the saturation of the sample. This consisted of a sequence of constant-pressure water injection followed by three sequences of constant flow-rate water injection. It is not known why there is a substantial difference in pressure fall-off at the end of the test between the experimental and modelled results.

Finally, Figure 2-12 shows the modelled and experimental pressure histories for gas injection pulse tests carried out on the sample after saturation, for successively increased injection pressures. The agreement between modelled and experimental results can be seen to be reasonable; the largest differences between the two are in the behaviour after the injection of the final pulse. The model appears to have reproduced the fall in permeability to about  $4 \cdot 10^{-20} \text{ m}^2$  resulting from saturation of the sample.

By way of summary of this modelling approach, the following points were made:

- l) Porous-medium based transport phenomena and flow through discrete features such as fractures may occur simultaneously in gas migration through barriers and host rock.
- m) A procedure to simulate gas flow through pre-existing but not necessarily currently active discontinuities has been described, and can be readily integrated into general coupled HM two-phase continuum formulations.
- n) Coupling between gas flow along discontinuities and a mechanical response allows some singular features observed in experiments to be reproduced (delayed breakthrough, output gas flow peaks).
- o) A complex set of laboratory triaxial tests involving flow in damaged and subsequently healed samples of Opalinus clay has been modelled satisfactorily.



**Figure 2-10.** Experimental and model results for the gas permeability tests before and after fracturing on the dried core.

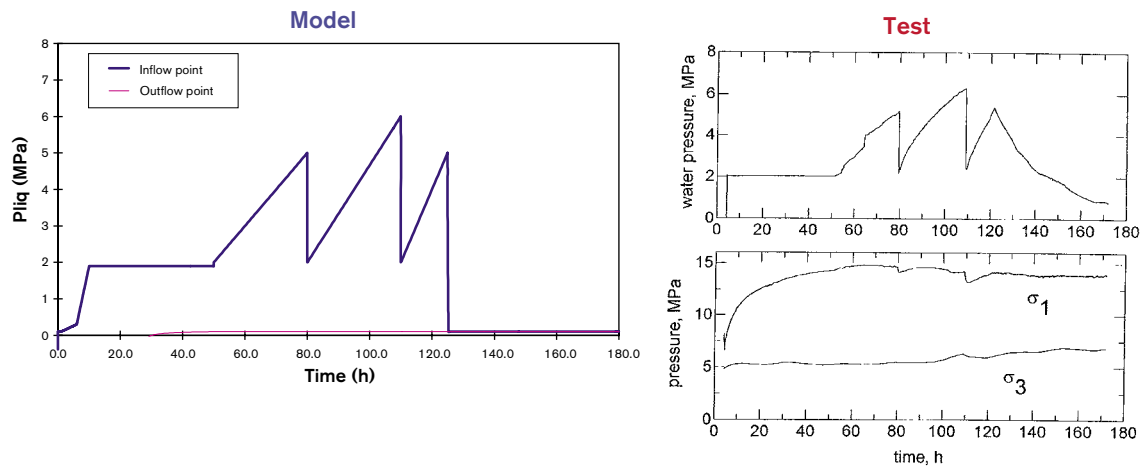


Figure 2-11. Modelled and experimental pressure variations during the saturation of the sample.

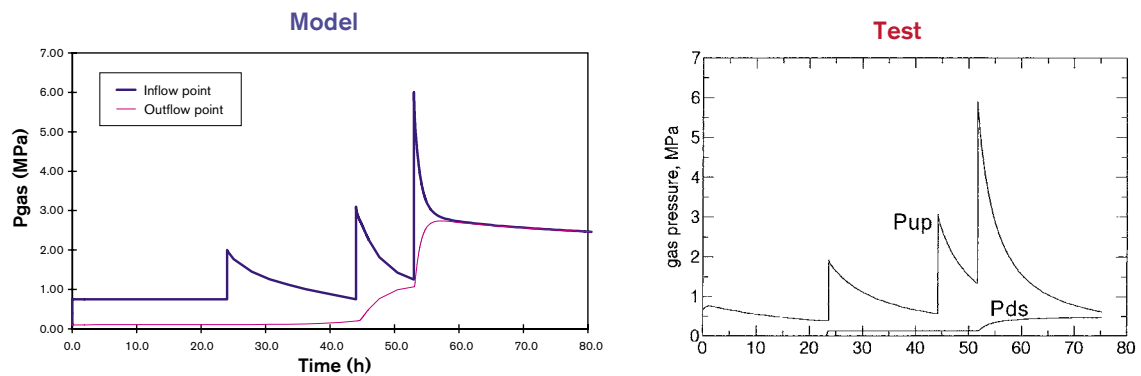


Figure 2-12. Modelled and experimental results for the gas pulse tests after saturation of the sample.

## 2.6 Gas movement in Mx80 bentonite under constant volume conditions

(Jon Harrington, Steve Horseman)

This presentation was of the results of the more recent of a series of tests of careful experiments on gas migration through compacted and saturated bentonite carried at the British Geological Survey (BGS) over a number of years. The tests discussed were carried out in two geometrical configurations:

- p) a constant volume cylindrical cell in which gas was injected in a central filter and exited the cell at collection points (sinks) on the radial boundary (the CVRF – constant volume radial flow – geometry);
- q) a cell with a fixed radius as for the CVRF cell but with the sample constrained in the axial direction by a constant applied stress ( $K_0$  geometry).

A summary of the presentation is provided here. More details can be found in the presentation itself and in the published report of the experiments /Harrington and Horseman, 2003/.

### 2.6.1 Background to test philosophy

An important motivation for this work was to explore the effect of boundary conditions on the characteristics of gas migration through saturated bentonite.

The test philosophy was motivated by a number of observations from previous work:

- r) The gas breakthrough pressure is strongly dependent on the degree of water saturation. At low saturations (between 70% and 90%) the buffer contains a network of inter-connected cracks resulting in little or no gas threshold; as the clay approaches full saturation, gas breakthrough pressure increases rapidly.
- s) With experiments on saturated isotropically-consolidated specimens, gas breakthrough occurs at a pressure marginally greater than the sum of the swelling pressure and the porewater pressure.
- t) After gas testing, it has been argued that saturations remain close to 100% suggesting that gas may pass through a relatively small number of discrete pathways /Harrington and Horseman, 2003/
- u) Experiments by BGS on gas injection into unconfined clay pastes /Donohew et al. 2000/ suggest that a saturated clay dilates during gas entry, with changes in gas content accommodated by an increase in the total volume of the clay. Although this is consistent with gas flow through a network of pressure-induced pathways, it cannot be reconciled with the more usual soil mechanics concept of desaturation by direct displacement of porewater.

If dilatancy is a pre-condition for gas entry, a question arises about whether gas transport mechanisms are sensitive to the boundary conditions constraining the sample.

### 2.6.2 Test geometry

Two experiments were carried in the CVRF apparatus. These were designated Mx80-8 and Mx80-10. The bentonite sample had a diameter of 60 mm and length of 120 mm.

One experiment, designated Mx80-9, was carried out in the  $K_0$  geometry. The diameter and length of the sample were equal at 51 mm.

Diagrams of both apparatus are shown in the slides from the presentation. They were fitted with gas sinks in arrays around the circumference of the sample jackets, water pressure sensors, and boundary stress measuring sensors.

The values quoted for the sample properties were in the ranges: water mass fraction, 26.7–27.1; dry density, 1.568–1.582 Mg m<sup>-2</sup>; and water saturation, 97.6–98.6%.

### 2.6.3 Swelling and hydration behaviour

For one of the experimental systems (Mx80-10), studies were made of the swelling and hydration behaviour of the sample. The build up of stress was monitored as a function of time as hydration took place at a constant applied water pressure (1MPa). Equilibrium was established at a total average stress of 6.4 MPa, with a variation in stress measurements at equilibrium of from 6.0 to 6.6 MPa. This measured total stress is rather less than would have been predicted from previously reported empirical relationships relating swelling pressure and void ratio /Horseman and Harrington, 1997/ and references therein.

The total stress is generally taken to be, by the definition of swelling pressure, the sum of the swelling pressure and the applied external water pressure. To test that the swelling pressure is not a function of the water back pressure, that is, it only a function of the clay density, the effect on the total stress of increasing and then decreasing the external applied water pressure in a series of steps was investigated. The system was allowed to reach equilibrium after each change in water pressure, and the equilibrium results are plotted in Figure 2-13. The graph shows hysteresis in the response of the stress to changing water pressure.

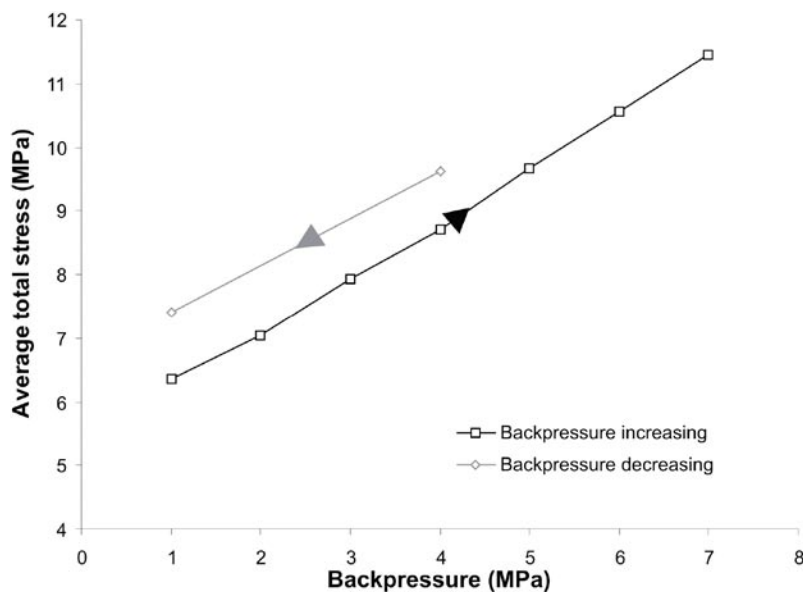
The plots for increasing and decreasing water pressure were fitted by lines of the form

$$\sigma = \Pi + \alpha p_w$$

where

- $\sigma$  is the total stress in the sample;
- $\Pi$  is the swelling pressure;
- $\alpha$  is a fitting parameter; and
- $p_w$  is the external water pressure.

A value of  $\alpha = 1$  would indicate that an increase in water pressure produces the same increase in total stress. This is not precisely observed, with  $\alpha = 0.86$  ( $\Pi = 5.4$  MPa) with the water pressure increasing, and  $\alpha = 0.74$  ( $\Pi = 6.7$  MPa) with it decreasing.



**Figure 2-13.** Average total stress plotted against externally-applied water pressure.

## 2.6.4 Baseline hydraulic properties

The permeability and specific storage were determined from hydraulic tests for samples Mx80-8 and Mx80-9. Because of the geometry of the source and sink system used in the hydraulic tests in the CVRF geometry, finite element flow modelling had to be used to interpret the results of the hydraulic tests.

The results showed that the average permeability from the CVRF test is  $1.4 \times 10^{-21}$ – $1.7 \times 10^{-21}$  m<sup>2</sup>, with a specific storage in the range  $1$ – $9 \times 10^{-6}$  m<sup>-1</sup>. This small value of specific storage is indicative of a fully-saturated constant volume system. For the K<sub>0</sub> geometry the permeability was  $9.5 \times 10^{-21}$  m<sup>2</sup>, and the specific storage  $3.8 \times 10^{-4}$  m<sup>-1</sup>.

## 2.6.5 Gas migration behaviour

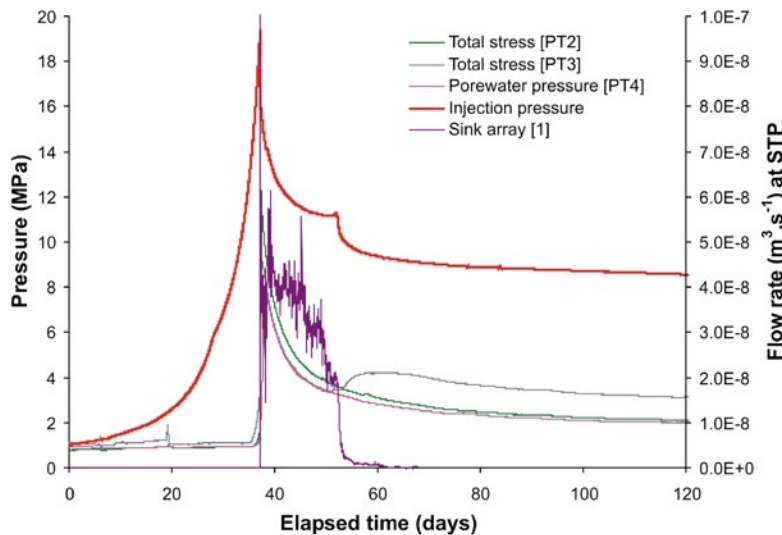
A comprehensive set of results was provided and discussed in detail in the slide presentation, to which reference should be made (with the published report /Harrington and Horseman, 2003/) for these details. It is only intended to attempt a summary here, without going into some of the considerable complexity in the results.

Following the approach developed at BGS, gas injection was carried out by pressurising a volume of gas in an upstream storage vessel by pumping water at a controlled rate into that vessel. The gas pressure rises until at some point it enters the sample. The evolution of the upstream pressure provides information about the flow of gas into the sample. The flow of fluids from the outlet ports against an applied water backpressure is monitored. An experimental history would typically include the effect of making step changes in the rate of pumping of water into the upstream vessel.

### ***Mx80-8 gas migration test results***

The main features found in the gas injection tests with the CVRF geometry and sample Mx80-8 were:

- As the upstream gas pressure rose, a very small amount of fluid was produced from the sinks at a gas pressure of 13.8 MPa (accompanied by a rise in axial and radial stress). At 18.7 MPa, the gas pressure dropped slightly (axial stress increased) but then increased again. This was interpreted as the opening of a gas pathway that failed to intersect any of the 12 sinks around the circumference of the sample.
- A peak gas pressure of 19.4 MPa was reached (Figure 2-14); this was much larger than reached in previous experiments on isotropically constrained samples with a similar density of bentonite. At this point there was flow of large quantities of gas to one set of sink arrays (99.9%), indicating channelled gas flow. After breakthrough, the upstream gas pressure fell to a steady-state value of 11.2 MPa. When the injection pump was turned off, the upstream value fell towards a “shut-in pressure” of around 8 MPa at which flow from the sample ceased.
- A small flux of fluid was noted to the two other sink arrays during gas injection (6.8 ml in total). Given the high gas and porewater pressures and the uniform distribution of flow between these two areas it was considered likely this fluid was exclusively water (predominantly from end filters plus a small amount from pressure-induced consolidation).



**Figure 2-14.** *Mx80-8 first gas breakthrough and shut-in.*

- When the original pumping rate was re-established after the first shut-in, no conspicuous peak in the upstream gas pressure was produced. Flow from the sample evolved to a steady-state pressure of 11.5 MPa, but temporal variations in outgoing flux between the three sink areas was observed. This was taken to demonstrate the existence of multiple, unstable gas pathways of varying aperture. The shut-in pressure to which the upstream gas pressure converged when pumping was stopped was again around 8 MPa. The steady-state and upstream pressures were similar to those found for the first cycle of gas injection.

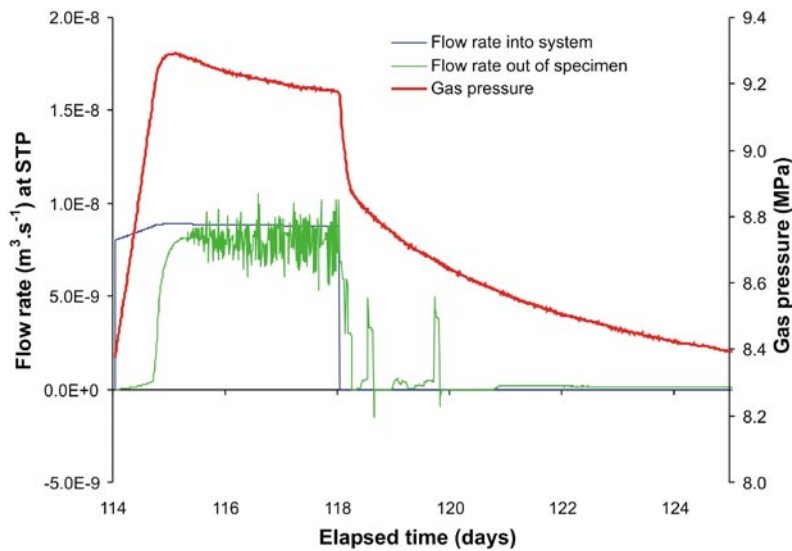
### ***Mx80-9 gas migration test results***

The tests in the  $K_0$  geometry with sample Mx80-9 were carried out with a stress of 10 MPa applied to the floating end caps, and a water backpressure of 1 MPa applied to the sinks on the circumference of the sample.

In this test, the water injection pump was turned off when the pressure had reached 8.8 MPa (before gas breakthrough) and the upstream pressure kept at this value for ~ 80 days. This was to test whether the breakthrough pressure was time dependent and whether gas flow would occur at lower pressures if sufficient time were allowed, as reported for the experiments with Avonlea bentonite described above. While the pressure was increasing, a small flow from the sample was observed. The rate of this flow increased to a peak, but then declined when the pumping was stopped. It was interpreted as slug flow of liquid displaced from the sample, for example from tubing and the porous plugs at the end of the sample.

When gas injection was resumed, the following features were observed:

- There was a major gas breakthrough at a peak pressure fractionally below 10 MPa, followed by a rapid decline in pressure, which included an “undershoot” in pressure before pressure and flow stabilised. This was argued to be consistent with the presence of unstable gas pathways. The shut-in pressure was around 8.2 MPa.



**Figure 2-15.** *Mx80-9 second gas injection history.*

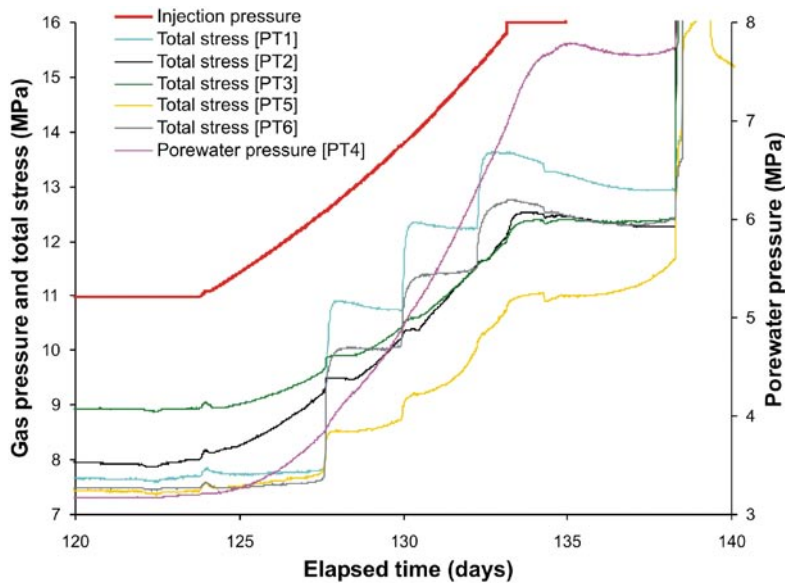
- When pumping was restarted after shut-in (Figure 2-15), the flow rate out of the specimen began at around 8.5 MPa. Gas pressure increased to a peak value of 9.3 MPa before decaying slightly to a steady state pressure of 9.2 MPa. No conspicuous peak in flow was seen. A break seen in the slope of the pressure decline curve after pumping was terminated was considered indicative of pathway closure.

### **Mx80-10 gas migration test results**

The results of the CVRF Mx80-10 gas migration tests, the most recently completed, were described in some detail. The results are quite complex, and include substantial information from pore water pressure and boundary stress measurements; the technique for the measurement of the boundary stresses had been refined prior to this experiment. The main features of the results described in the presentation were:

- During the initial period while the upstream pressure was increased, the pump was twice turned off and the upstream pressure kept constant: for 33 days at a pressure of 6 MPa and for 54 days at a pressure of 11 MPa. Shortly after the pump was stopped for the second time, breakthrough of gas to the sink arrays was observed, with the outgoing flux unevenly distributed amongst the filters. This breakthrough was accompanied by a sharp increase in total stress, which suggests that dilation of the fabric occurs during gas flow.
- After pumping was restarted and the pressure rise continued, the stress sensors showed step-like responses, which were again interpreted as being correlated with propagation events. There were no corresponding increases in discharge to the sink arrays, so it was inferred that none of the pathways actually intersected sink filters.
- At an upstream pressure of 16 MPa, the injection pump was again switched to constant pressure, and shortly afterwards (27 hours) gas flow to two of the sinks increased spontaneously. A need to reprime the system resulted in some water injection which “resealed” pathways, so that when pumping was restarted, gas breakthrough did not restart until a peak pressure of 22.1 MPa had been reached, when major flows of gas to two of the sinks occurred.





**Figure 2-16.** Evidence of gas pathway formation from stress responses.

- A sharp drop in pressure after the peak is suggestive of a breakdown in tensile strength and the development of conductive gas pathways. Mass balance considerations confirm the flow was predominantly gas. The drop in gas pressure was accompanied by an increase in all stress and porewater pressure sensors, which was taken to be a consequence of fracture propagation. At breakthrough, the peak gas pressure is around 2.7 MPa above the maximum total stress, this difference being attributable to the tensile strength of the sample. After breakthrough the gas pressure tends to a steady-state value of ~ 10 MPa, close to the average total stress.
- After the pump is turned off, the upstream gas pressure tends towards a zero flow value estimated to be 7 MPa.
- A hydraulic test was performed at this point, and the results showed that, after resaturation, gas migration had no long-term effect on permeability to water
- Reinstating the original pumping rate after the hydraulic tests produced no obvious signs of early gas flow. A first small outflow was observed at 9.4 MPa, and the peak gas pressure was 12.8 MPa; which is substantially lower than for the first injection cycle (22.1 MPa), indicating that although the resaturation had restored the hydraulic properties, some “memory” of the previous gas migration was retained in the sample.
- After this second peak, changes in the boundary stresses and in the pressure are taken as further indications of pathway propagation events, and of the existence of a tensile strength in the bentonite.

### 2.6.6 Process understanding (all tests)

The following is a summary of the explanations offered for the various features seen in the test results:

**Peak behaviour:** This was interpreted from linear fracture elasticity as the pressure needed to create a radial fracture around the injection filter, taking into account the elevation of the porewater pressure caused by the gas injection.

**Post-peak behaviour:** Post-peak, the fracture will lie beyond the region of stress concentration around the filter and the clay will have lost its tensile strength so that to a first approximation the gas pressure will be equal to the total stress.

**Capillary-pressure behaviour:** Since the capillary pressure is the difference between the gas pressure and the porewater pressure, and since the post-peak gas pressure is argued above to be equal to the total stress, it follows that the capillary pressure is equal to the total stress minus the porewater pressure; that is, the capillary pressure is equal to the local effective stress.

**Shut-in behaviour:** Since gas pathways should become blocked by water (assuming water availability) when the gas pressure falls below the sum of the capillary pressure and the external water pressure, then this provides a lower bound to the shut-in pressure. (the local water pressure may be higher than the external water pressure). Measured shut-in pressures are consistent with this.

**Transport mechanism:** It has been argued that gas should displace water from bentonite by a conventional displacement mechanism. No measurable desaturation of the bentonite samples was found, and prolonged application (5–13 months) of gas pressures greater than 8 MPa do not produce any passage of gas through the sample.

**Self-sealing:** It was argued that evidence for spontaneous closure of pathways and re-establishment of the tensile strength of the samples indicated a capacity for “self-sealing”. Restoration of the original permeability on rehydration also supported this assertion.

## 2.6.7 Conclusions from the BGS CVRF and $K_0$ gas migration tests

The main conclusions drawn from the results of the experiments described were:

- Gas entry and breakthrough under constant volume boundary conditions causes a substantial increase in the total stress acting on the clay and in the internal porewater pressure.
- It was argued that the fact that gas entry, breakthrough, peak and steady-state gas pressures vary with test boundary conditions (e.g. constant volume versus constant stress), suggests that the process of gas entry is accompanied by dilation of the bentonite fabric. Prior to breakthrough, gas pressure under constant volume conditions can significantly exceed the sum of the swelling pressure and externally-applied porewater pressure (recall that the swelling pressure depends on the degree of compaction of the bentonite, as, for example, defined by its dry density).
- The sharp pressure drop after the peak is indicative of a breakdown in the tensile strength of the bentonite. This is associated with increases in total boundary stress. Increases in total stress can be interpreted as a due to fracture propagation events.
- Experimental evidence is consistent with the development of a relatively small number of crack-like pathways, which are highly unstable (for example, the distribution of flow between sinks is non-uniform and often changes abruptly and spontaneously during the course of an experiment).
- No convincing evidence was found of porewater displacement, desaturation or conventional two-phase flow, although a case can be made for internal consolidation of the clay (i.e. some water may be squeezed from fully water-saturated regions of the clay as a result of compaction of the clay by the application of gas pressures exceeding the total local stress).

- There is no evidence from these tests that the development of pressure-induced gas pathways compromises the sealing capacity of the bentonite barrier. Gas pathways appear to be ephemeral features of the buffer which tend to close up when gas pressure falls.

## **2.7 Some practical observations on gas flow in clays and clay-rich rocks**

*(Steve Horseman, Jon Harrington)*

This presentation provided a review of data on gas migration in clays from a variety of sources. The authors aim is to draw conclusions about the mechanisms of gas migration in clays and their relationship to the properties of the clay. There is an implicit assumption that the behaviour of bentonite with respect to gas migration can be fitted into a general framework of understanding that applies across a broad spectrum of clays and even other porous materials.

The data considered was from the following sources:

- v) gas entry in unconfined clays at different moisture contents;
- w) gas burps and mud volcanos;
- x) gas migration in offshore geological environments;
- y) seabed pockmarks;
- z) inflammable gas emissions in the Hanford waste tanks;
- aa) study of gas migration in clay cores.

A brief summary of the review presented of the data from each of these summaries follows, and more details can be found in the presentation slides:

### **2.7.1 Gas entry in unconfined clays at moisture contents between the liquid and plastic limits (particle-displacement mechanism)**

Experiments had been carried out at BGS by injecting gas from a needle into the body of water saturated clay pastes in an open vessel. Both the clay type and the water content were varied. The upstream gas pressure was increased continuously until air entry into the clay took place. The pressure at air entry was measured and the nature of the migration pathways formed by the gas was noted.

A relationship was found between the breakthrough pressure and the gravimetric water content of the clay, with a trend in that behaviour being associated with the plasticity of the clay. In addition, some systematic variations in the nature of gas pathways formed were noted. At one extreme, the gas pathway was formed by fracturing the clay, sometimes with sound emission; at the other extreme, gas transport occurred as bubbles. The mechanisms were categorised as:

- BB – buoyancy driven bubble transport;
- TFR – rapid, audible fracture propagation at high gas entry pressures;
- TFG – gentle (slow) fracture propagation at low gas pressures.

The variation of these mechanisms with water content and gas entry pressure are shown in Figure 2-17. The main feature to which attention is drawn for the present purposes is that for clays at low water contents and high gas entry pressures, gas entry occurs by fracturing the clay; for softer clays, deformation of the clay can accommodate the gas without fracturing.

**2.7.2 Gas burps and mud volcanos**

Photographs were presented of natural gas escape through muds, as for example found in hydrothermal regions (see presentation). It was observed that in muds close to their liquid limit, the gas formed bubbles that burst and collapsed back into the sea of mud, but that in stiffer muds a “volcano” like structure built up and provided a pathway that was reused by the gas for a time, with more mud being driven up the core of the volcano and deposited over its slopes to build up the volcano.

**2.7.3 Gas migration in offshore geological environments**

Two forms of evidence of gas migration in offshore geological environments were discussed:

- gas chimneys above gas reservoirs;
- gas seeps and “burps” in soft seabed sediments.

Seismic images from around the world were shown of gas migrating through formations overlying gas reservoirs. A number of features of the flow of the gas were pointed out:

- evidence of slow seepage and rapid venting of gas;
- a distribution of the gas that suggested localisation of flows along fractures or faults;
- evidence for sediment deformation associated with the pathways followed by the gas.

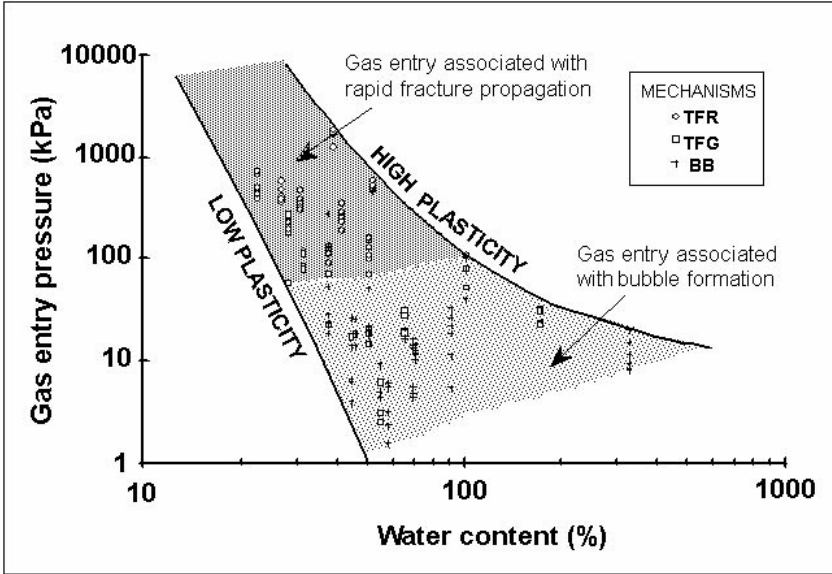


Figure 2-17. Zonation of particle-displacing gas entry mechanisms on injection into clay pastes.

The last feature in particular raised the question of whether gas migration might be associated with fracturing and dilation of sediments.

Gas releases through soft seabed sediments were evidenced by the widespread occurrence of seabed pockmarks. It was noted that these may exhibit the following characteristics:

- are ubiquitous on the shallow continental shelf;
- are mostly caused by rapid passage of gas through soft sediment;
- may produce very large measured methane fluxes;
- are a few metres to many hundreds of metres in diameter;
- cause fine-grained sediments to be ruptured, deformed, and ejected into the sea;
- may form linear “strings” over deep-seated faults.

Examples of pockmark occurrences from around the world were provided to illustrate the above points. The pockmarks clearly provide evidence of sediment deformation. They are also suggestive of the occurrence of episodic flow. Possible sources of the gas released during pockmark formation could be the migration of gas from deeper accumulations via gas chimneys, as discussed in the previous subsection, or the decomposition of sub-seabed gas hydrates.

Note was made of published efforts to simulate the processes of gas migration through soft-sediments, both using theoretical particle interaction models and laboratory analogues. Gas bubbles formed in gelatine were found to develop a discoidal shape, suggestive of a fracture propagation like mechanism of bubble growth.

#### **2.2.4 Inflammable gas emissions in the Hanford waste tanks**

Hydrogen gas is formed in some of the waste tanks at the Hanford site in the USA. Studies of this inflammable gas release have been undertaken /Stewart et al. 1996; Gauglitz et al. 1996/.

In waste tanks containing settled sludges, intermittent discharge of gas is observed. This is most conspicuous in tanks containing clay-like wastes. It was noted that although the sludges are “wet” sludges, interesting trends in behaviour are observed.

Laboratory experiments using bentonite /water mixes have been used to simulate the gas release mechanisms seen in the waste tanks.

Two types of bubble development were reported:

- pore-filling gas bubbles; and
- particle displacing gas bubbles.

The pore-filling gas bubbles were confined to the pre-existing pore volume and developed by the displacement of interstitial fluid. They were found in deep layers of waste or in waste that had large pores and a high yield strength. They existed as pore-filling networks, and were referred to as litho-dendritic bubbles.

The particle displacing bubbles occurred most often in waste layers that were under little stress or had low yield strength and small pore sizes. Two categories of particle-displacing bubbles were differentiated: hydrostatic bubbles that had not merged into networks, and hydro-dendritic bubbles that had formed networks. A simple dimensionless number determined which type of particle displacing bubble was formed, as follows.

If  $\frac{\tau_s D}{\gamma} \gg 1$ , hydro-dendritic bubbles formed; if  $\frac{\tau_s D}{\gamma} \ll 1$ , hydrostatic bubbles formed,

where

$\tau_s$  is the shear strength;

$D$  is the bubble diameter;

$\gamma$  is the surface tension.

That is, hydro-dendritic bubbles are formed if the capillary pressure is much greater than the tensile stress.

The maximum extent of gas retention in the sludges differed between the litho-dendritic bubbles and the particle-displacing bubbles. The volume of retained gas was limited in the case of pore-filling bubbles by the porosity. The limit on gas retention in particle displacing bubbles was higher because additional porosity could be created by particle displacement.

The retention of particle-displacing bubbles was summarised /Gauglitz et al. 1996/ in the diagram shown in Figure 2-18, which was developed from consideration of buoyancy effects and Bingham-type plasticity behaviour.

The experiments carried out by /Gauglitz et al. 1996/ demonstrated gas percolation through a network of hydro-dendritic bubbles in the stronger clays. Gas release occurs when a hydrodendritic bubble propagates to the surface and provides a pathway for gas percolation. Bubbles in one region of the clay column become dendritic as they expand, then contract as they reach the percolation threshold and discharge part of their gas into a higher region which in turn expands and eventually discharges. The gas column grows by this process until it becomes quasi-stationary and releases gas nearly continuously but at varying rates. A hydro-dendritic percolation release could leave some marks of its occurrence on the waste surface. Entrained slurry brought to the surface repeatedly through the same vent could produce mud cones.

When both particle displacing and hydrostatic bubbles were considered, the map of gas retention/migration behaviour shown in Figure 2-19 was obtained.

### **2.7.5 Study of gas migration in clay cores**

The final example of visualisation of gas migration in clays was from tests of gas migration in saturated bentonite and Opalinus Clay cores. Samples that had been subject to tests involving gas migration through the samples were removed from the test cells, immersed in glycerol, and warmed. The expansion of the gas remaining in the samples resulted in the emergence of streams of gas bubbles from the surface of the samples, indicating movement of gas within the samples.

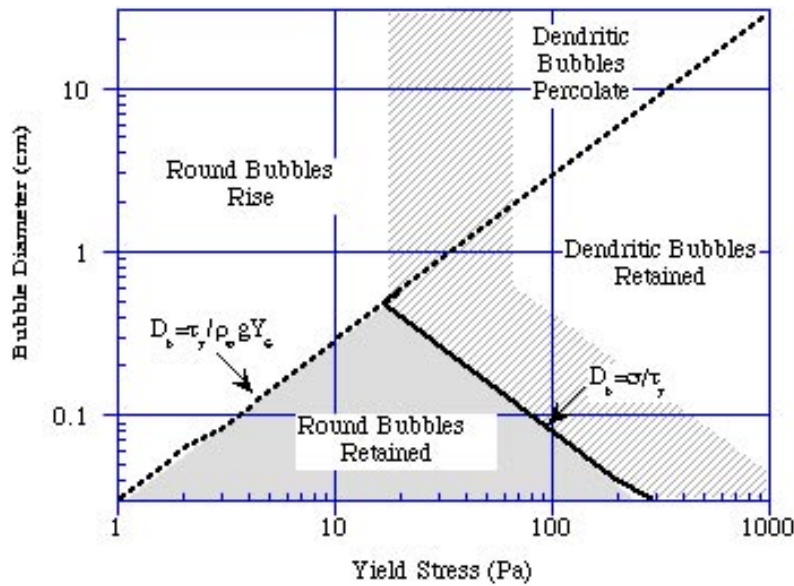


Figure 2-18. Retention of particle displacing bubbles /Gauglitz et al. 1996/.

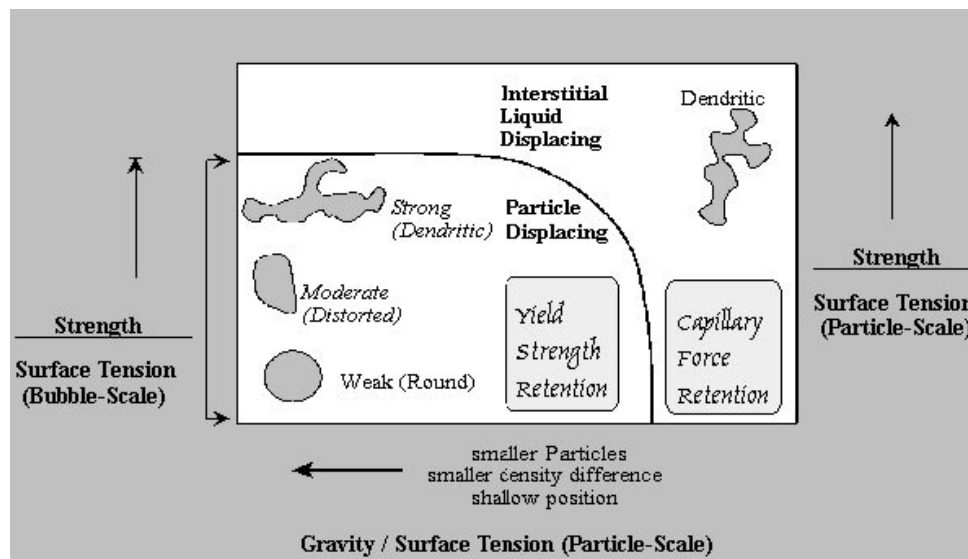


Figure 2-19. Gas migration/retention behaviour map for Hanford waste sludges /Gauglitz et al. 1996/.

### 2.7.6 Conclusions from the survey of gas migration data

The observations detailed above have been drawn together to suggest that a pattern of gas migration behaviour exists across a range of clay media. In “softer”, low-strength clays, gas migration is seen to occur by creation of new porosity to accommodate the gas by simply displacing the clay particles. In stiff, higher strength clays, gas migration occurs by a fracture-like mechanism, with crack-like pathways propagating through the medium to accommodate gas flow. It is argued that nowhere in the spectrum of gas migration behaviour in clay materials considered in this presentation is migration by a conventional two-phase flow mechanism, involving direct displacement of water by gas from the porosity of the clay, seen. Water can be displaced from the clay by a consolidation mechanism in

which water is squeezed from the water-filled porosity as a consequence of increased stress on the clay resulting from the application of gas pressure. (In conventional two-phase porous-medium flow, the pore structure is generally regarded as substantially unchanged, beyond relatively small storage or consolidation effects, by the invasion of the saturated medium by gas, or any other fluid flow process. During steady-state two-phase flow of gas and water, the two phases would generally be considered to flow predominantly in separate channels, although of course if the saturations are changing, the fluid whose saturation is increasing will displace the other fluid from some pores. In contrast, the mechanisms described in this presentation all involve the creation of gas pathways by the development of new porosity through modification of the structure of the clay.)

## **2.8 Early large-scale experiments on gas break-through pressures in clay based materials**

*(Harald Hökmark)*

This presentation was of early experiments on gas breakthrough pressures in bentonite under conditions expected to be encountered for SFR buffer bentonite /Pusch and Hökmark, 1987/. In contrast to the small-scale experiments described in other presentations, these experiments were carried out on a large scale: the bentonite sample was 78 cm in diameter and 30 cm deep (megapermeameter).

The objectives of the experiments were to:

- determine the critical gas pressure by repeated pressurization of a large sample;
- test the hypothesis that gas phase penetration through water-saturated bentonite takes place when the gas pressure is the sum of the “true”critical gas pressure (zero water back pressure) and the water pressure /Pusch et al. 1985/.

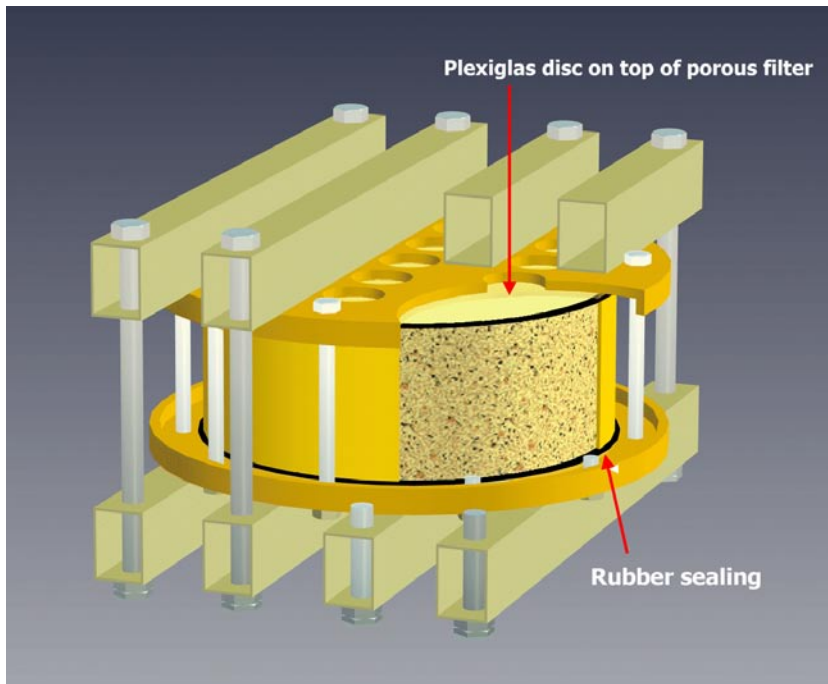
The bentonite used was a low density GEKO/QI, with a water-saturated density of  $1,680 \text{ kg m}^{-3}$ . It was intended for use as wall fill to isolate the concrete silo in the SFR storage. The swelling pressure was less than 500 kPa. Water of an artificial composition to mimic the natural ground water at the Forsmark site was used. The gas injected was nitrogen.

The experimental technique was to

- bb) apply a water back pressure to top of the permeameter and an equally large gas pressure at the bottom;
- cc) while keeping the water back pressure constant, increase the gas pressure at the bottom in steps, with sufficient time between steps to allow for transients to disappear, and record gas inflow and gas/water outflow;
- dd) after gas break-through, reset the equipment, allow for “rest”, and repeat with the same or a new water back pressure.

A schematic of the apparatus is shown in Figure 2-20.





**Figure 2-20.** Schematic of megapermeameter.

The results obtained from the experiments are summarised in Figure 2-21. The values in the yellow boxes indicate the water back pressure that was applied in each experiment. The gas pressures were increased by the steps shown in each experiment until breakthrough occurred, except in experiment 10, in which some leakage occurred without breakthrough being achieved. This leakage prevented the back pressure being varied over a sufficiently wide range to verify or falsify the critical pressure hypothesis. The times (days) in red show the intervals between experiments. It can be seen that gas phase breakthrough occurred at gas over-pressures in the range 165 kPa–240 kPa.

Other observations from the work were:

- ee) The amount of water successively displaced during pressure build-up was, at most, a few parts per thousand of the water contained in the sample.
- ff) Point (a) implies that only a small fraction of the pore space; that is, the largest continuous pores, were involved in the gas transport.
- gg) Capillary analogy estimates suggest that the smallest diameter of the largest continuous pores was 1–2  $\mu\text{m}$ .
- hh) The first test gave a larger amount of water displaced before breakthrough than the following tests (at least twice as much).

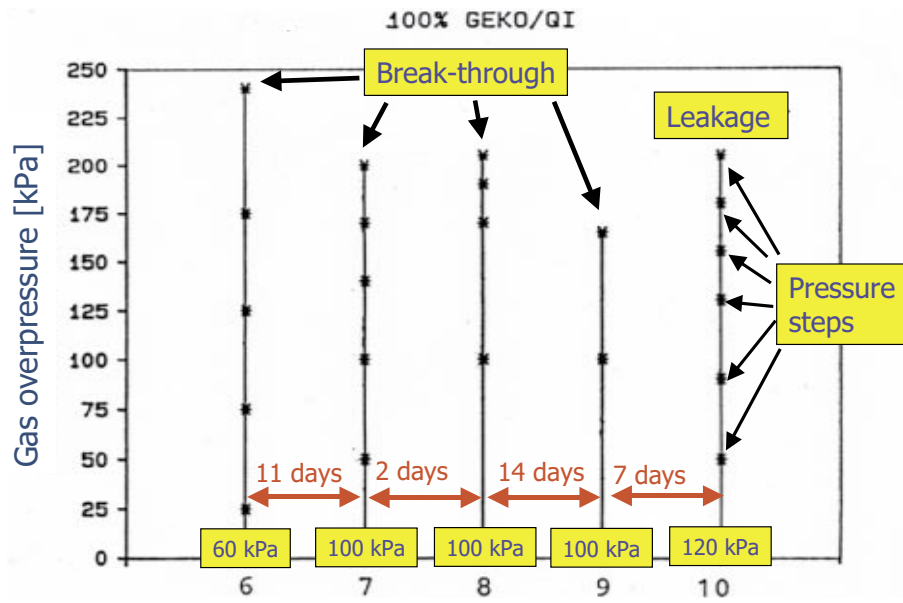


Figure 2-21. Summary of results from the megapermeameter experiments.

### 3 Discussion

A number of possible basic mechanisms have been proposed for gas invasion of water-saturated compacted bentonite. The main distinction is between behaviour of the bentonite as a conventional porous medium with direct displacement of the porewater by gas, and mechanisms which require significant deformation of the clay to create the gas pathways, with little direct displacement of water. In the former, the conventional porous medium model, the gas flow is governed by conventional concepts of capillary pressure and relative permeability. In the latter, the formation of fractures or fissures is considered the likely mechanism by which gas pathways are created.

It is possible that there is a spectrum of behaviour involving combinations of the above mechanisms simultaneously.

Examination of the experimental data has not produced a unique explanation of the experimental results in terms of these mechanisms, and in relation to this the following observations can be made:

- ii) In a few experiments, the “radial” flow experiments at constant volume /Harrington and Horseman, 2003/, there is compelling evidence that fracturing or fissuring is involved in the establishment of gas pathways.
- jj) In these “radial” flow experiments, explanations can be found of the high gas entry pressures (e.g. much higher than the swelling pressure) in terms of the development of the radial stresses around the source leading to tensile failure of the clay. However, it is not clear how such arguments relate to the threshold pressures (where they exist) required for gas entry into the end face of bentonite samples in a linear flow geometry (the stress applied to the end face of a linear sample by the application of gas pressure does not induce tensile stresses in the sample, in contrast to the application of stresses in the same way to the surface of an internal void within the sample). This raises the question of whether different modes of failure might be involved in the different geometries.
- kk) The high gas entry pressure in some constant volume experiments may be suggestive that the threshold pressure is sensitive to the boundary conditions, although theoretical studies /Swift et al. 2001/ suggest that the amount of deformation of the clay required for the formation of gas pathways may be too small for gas flow to be strongly influenced by boundary conditions. This may particularly be the case for field-scale system, in which the gas at the entry point to the clay may not “see” the more distant boundary condition.
- ll) Where stresses and porewater pressures have been measured, couplings between gas flow events and these parameters have been observed, but the physics which controls these couplings has not been satisfactorily established. Progress with the modelling of gas invasion of bentonite would benefit from a sound constitutive model of these aspects of bentonite behaviour, including fracture formation.

- mm) In the cases in which a threshold pressure for gas entry into the clay is observed experimentally, which is most cases, once gas flow is established it is found that the flow will continue until the gas pressure is reduced substantially below the threshold pressure. Precisely why the gas flow continues at pressures considerably below the entry pressure and what controls the upstream pressure at which gas flow finally stops has not been fully established. For example, does it arise from mechanical closure of pathways or from capillary pressure effects. It has been suggested in this workshop that capillary effects are involved and that the spontaneous closure of pathways is associated with reestablishment of the tensile strength of the clay.
- nn) Some experiments have shown intermittency and instability in the flow of gas from the downstream end of the sample; this suggests that closing and reopening of pathways occurs. What controls this is not clear, although the discussion of the above bullet point may also relate to this issue.
- oo) There is a difficulty in modelling regarding the way the downstream boundary condition should be defined. For models in which the gas permeability is dependent on gas pressure it is found that, for the gas pressure change with distance, most of the pressure drop occurs close to the downstream boundary. There is no data to determine whether this is a modelling artefact or a real feature of the systems.
- pp) Modelling suggests that if gas flow occurs by capillary displacement, then this must involve a large number of very small capillaries in order to reproduce the gas entry pressures and provide the observed gas permeability after breakthrough. A fissure propagation mechanism for creating gas pathways is thought likely to involve a very much smaller number of pathways. This implies a distinct difference in the nature of the gas pathways that are formed by these two mechanisms, although experimental data on the dimensions and numbers of gas pathways that might discriminate between the two seems difficult to obtain.

These uncertainties constitute considerable difficulties in the development of models of gas migration in bentonite, because of the ambiguity that results in the constitutive relationships needed for such models. The development of a picture of gas migration across a spectrum of clay-rich materials with little evidence of conventional porous-medium type flow was considered by several workshop participants to give weight to the suggestion that gas migration in saturated compacted bentonite necessarily involves some deformation, probably fissuring, of the clay. However, this view was not universally accepted at the workshop. In particular, the work with low density Avonlea bentonite was evidence to others of porous-medium type flow, with time to failure dependent on pressure difference and flow length.

Despite remaining uncertainties, it should be noted that the experimental data that have been collected does give a substantial degree of confidence that saturated compacted bentonite will function satisfactorily as a buffer material:

- qq) It has been shown that gas can pass through saturated bentonite buffers (although whether the rather high entry pressures that have been observed in recent “radial” flow experiments would actually be observed or be acceptable in full-scale systems is a matter for further consideration).
- rr) Very little water is expelled from the buffer by migrating gas.
- ss) When resaturated, the buffer seems to reseal, with restoration of the hydraulic and transport properties that it possessed prior to the passage of gas.

These features are seen to be key conditions for the performance of a buffer as far as gas migration is concerned. Note that if the buffer water saturation is not close to unity, gas migration through the buffer is expected to occur easily.

In attempts to illuminate some of the issues that were raised by the presentations, a few observations were made in the concluding discussions of the workshop:

- tt) There was discussion of the differences observed between experiments on Avonlea bentonite, for which gas breakthrough occurred at excess gas pressures that exceeded a rather low threshold value (gas entry values), given sufficient time, and results obtained by workers using other materials, for which a larger threshold pressure for gas breakthrough was required, even if substantial gas pressures (below this threshold) were applied for a considerable time. The explanation for these differences remained obscure. It could result from differences in the way samples were prepared. For example, the clay microstructure depends on the water content on initial compaction. Some samples were prepared from pelletised bentonites, others were not.
- uu) There was a question mark about how reliable mercury intrusion porosimetry was in determining the pore size distribution of compacted bentonites, since it could not really be carried out without perturbing the bentonite.
- vv) It needs to be remembered that the conditions measured at the boundary of a sample, would be different from those in the body of the sample. For example, internal stresses would differ from those on the boundary. Modelling was a route into exploring the relationship between the conditions in the sample and those on the boundaries (as had been attempted in the GAMBIT programme /Swift et al. 2001; Hoch et al. 2004/).

Finally the workshop considered whether the material discussed pointed to the need for experimental work additional to that already being carried out. It was recognised that the development of experiments that would allow gas pathways created in compacted bentonite to be counted and characterised would be helpful in establishing the mechanism(s) of gas migration in bentonite. However, no clearly practicable technique was identified by which the presence of gas in bentonite could be imaged with sufficient resolution to allow gas pathways in the bentonite to be characterised.

Although there remained uncertainty in the mechanisms of gas migration in bentonite, it was believed that the research into the subject being carried out in a number of laboratories was satisfactorily addressing the key issues with relevance to the effect of gas generation on the safety performance of bentonite buffers in radioactive waste repositories. They were also leading to advancement in the understanding of gas migration in clays. No fundamental redirection of or addition to these programmes was therefore recommended.

## References

- Donohew A T, Horseman S T, Harrington J F, 2000.** Gas Entry into Unconfined Clay Pastes between the Liquid and Plastic Limits. Chapter 18, in *Environmental Mineralogy – Microbial Interactions, Anthropogenic Influences, Contaminated Land, and Waste Management* (eds J.D. Cotter-Howells, L.S. Campbell, E. Valsami-Jones, and M Batchelder), Mineralogical Society, London, Special Publication No. 9, pp 369–394.
- Gallé C, 1998.** Migration des Gaz et Pression de Rupture dans une Argile Compactée Destinée à la Barrière Ouvragée d'un Stockage Profond, *Bull. Soc. Géol.*, 169 (5), 675–680.
- Gallé C, 2000.** Gas Breakthrough Pressure in Compacted Fo-Ca Clay and Interfacial Gas Overpressure in Waste Disposal Context, *Applied Clay Science*, 17, 85–97.
- Graham J, Gray M, Halayko K G, Hume H, Kirkham T, Oscarson D, 2002.** Gas Breakthrough Pressures in Compacted Illite and Bentonite, *Engineering Geology*, 64, 273–286.
- Gauglitz P A, Rassat S D, Brecht P R, Konynenbelt J H, Tingey S M, Mendoza D P, 1996.** Mechanisms of Gas Bubble Retention and Release: Results for Hanford Waste Tanks 241-S-102 and 241-SY-103 and Single-Shell Tank Simulants, Report PNNL-11298, Pacific Northwest National Laboratory, Richland, Washington.
- Harrington J F, Horseman S T, 2003.** Gas Migration in KBS-3 Buffer Bentonite: Sensitivity of Test Parameters to Experimental Boundary Conditions, SKB TR-03-02, Svensk Kärnbränslehantering AB.
- Hoch A R, Cliffe K A, Swift B T, Rodwell W R, 2004.** Modelling Gas Migration in Compacted Bentonite: GAMBIT Club Phase 3 Final Report, Serco Assurance Report SA/ENV-0481.
- Horseman S T, Harrington J F, 1997.** Study of Gas Migration in Mx80 Buffer Bentonite, BGS Internal Report WE/97/7 to SKB.
- Hume H B, 1999.** Gas Breakthrough in Compacted Avonlea Bentonite, MSc Thesis, University of Manitoba, Canada.
- Nash P J, Swift B T, Goodfield M, Rodwell W R, 1998.** Modelling Gas Migration in Compacted Bentonite, Posiva Report 98-08.
- NEA, 2001.** Proceedings of an NEA/EC Workshop on Gas Generation and Migration in Radioactive Waste Disposal: Safety-relevant Issues, 26–28 June 2001, Reims, France, (OECD Paris).
- Pusch R, Forsberg T, 1983.** Gas Migration through Bentonite Clay, SKBF/KBS Technical Report TR-83-71.
- Pusch R, Hökmark H, 1987.** Megapermeameter Study of Gas Transport through SFR Storage Buffers, SKB Report AR SFR 87-06 (In Swedish).
- Pusch R, Ranhagen L, Nilsson K, 1985.** Gas Migration through Mx-80 Bentonite, Nagra Technical Report 85-36.

**Rodwell W R, Harris A W, Horseman S T, Lalieux P, Müller W, Ortiz Amaya L, Pruess K, 1999.** Gas Migration and Two-Phase Flow through Engineered and Geological Barriers for a Deep Repository for Radioactive Waste. A Joint EC/NEA Status Report published by the EC, European Commission Report EUR 19122 EN.

**Stewart C W, Meyer P A, Brewster M E, Recknagle K P, Gauglitz P A, Reid H C, Mahoney L A, 1996.** Gas Retention and Release Behaviour in Hanford Single-Shell Waste Tanks, Report PNNL-11391, UC-230, Pacific Northwest National Laboratory, Richland, Washington.

**Swift B T, Hoch A R, Rodwell W R, 2001.** Modelling Gas Migration in Compacted Bentonite: GAMBIT Club Phase 2 Final Report, Posiva Report 2001-02.

**Tanai K, Kanno T, Gallé C, 1997.** Experimental Study of Gas Permeabilities and Breakthrough Pressures in Clays, Proceedings of the Scientific Basis of Nuclear Waste Management Conference Number XX, held in Boston, USA, December, 1996, Material Research Society.

# Appendix A

## List of participants

<b>Name</b>	<b>Company</b>	<b>Country</b>
Mr. Lawrence Johnson	Nagra	Switzerland
Mr. Salo Jukka-Pekka	Posiva Oy	Finland
Mr. Heikki Juhani Raiko	VTT Processes	Finland
Mr. Patrik Sellin	SKB	Sweden
Mr. Harald Hökmark	Clay Technology	Sweden
Mr. Marolo C Alfaro	University of Manitoba	Canada
Mr. William R Rodwell	Serco Assurance	UK
Mr. Steve T Horseman	British Geological Survey	UK
Mr. Jon F Harrington	British Geological Survey	UK
Mr. Jean Talandier	ANDRA	France
Mr. Miguel Cuñado	Enresa	Spain
Mr. Kenji Tanai	JNC	Japan
Mr. Mikihiro Yamamoto	Toyo Engineering Co.	Japan
Mr. Jim Graham	University of Manitoba	Canada
Mr. E Alonso	UPC-ETSICCP	Spain
Mrs. A Cortés	E.E.A.A. (Enresa)	Spain





serco

Serco Assurance

**Status of Experimental  
Knowledge and  
Understanding of Gas  
Migration in Bentonite**

**William Rodwell**

# Status of Experimental Knowledge and Understanding of Gas Migration in Bentonite

- Aim is to provide context for workshop
- Background: development of models of gas migration in bentonite buffers is currently impeded by lack of understanding of detailed physics and mechanisms of gas migration in bentonite
- Provide overview of the range of reported experimental work on gas migration in bentonite
- Briefly review current interpretations in terms of possible mechanisms
- Preliminary identification of areas of uncertainty and needs for future work

# Overview of Experimental Data on Gas Migration in Bentonite

- **Emphasis here is on experiments on saturated “pure” bentonite**
  - some data on sand-bentonite mixtures may be relevant (and also other clays)
- **Experimental conditions vary significantly, e.g.**
  - sample preparation method
  - bentonite density
  - confining conditions and geometry
  - rate and manner of gas injection
  - type of bentonite
  - range and type of measurements
- **How dependent is gas migration mechanism on the experimental conditions?**

# Experiments on Gas Migration through Compacted Bentonite

Authors	Bentonite	Dry Density (Mg m <sup>-3</sup> )	Flow geometry	Gas Flow Controls	Confining Conditions
Pusch and Forsberg [1983] <sup>1</sup>	Mx80	~1.35 - 1.65*	Linear	Applied gas pressure (1-10 MPa)	Constant volume oedometer
Pusch et al. [1985]	Mx80	~1.1 - 1.78*	Linear	Pressure increments	Constant volume oedometer
Horseman and Harrington [1997]	Mx80	1.5 - 1.7	Linear (axial) flow	Displacement of gas by water from an upstream reservoir.	Constant isotropic stress in flexible sleeve subject to external fluid pressure (8 - 22 MPa)
Horseman and Harrington [1997]	Mx80 paste	1.3 - 1.4	Point source and sink	Displacement of gas by water from reservoir.	Cylindrical pressure vessel with confining pressure (0.8 - 2.7 MPa) imposed on floating end cap
Tanai et al. [1997]	Kunigel VI, Fo-Co Clay	1.4 - 1.8	Linear	Pressure increments	Constant volume cylinder
Gallé [1998]	Fo-Co Clay	1.6 - 1.9	Linear	Pressure increments	Constant volume oedometer cell
Graham et al. [1998]; Hume [1999]	Avonlea	0.6 - 1.4	Linear	Pressure increments	Constant volume oedometer cell
Harrington and Horseman [2003]	Mx80	1.577 / 1.582	Approximately radial from central source	Displacement of gas by water from an upstream reservoir.	Constant volume cylindrical vessel.
Harrington and Horseman [2003]	Mx80	1.568	Linear	Displacement of gas by water from an upstream reservoir.	Cylindrical pressure vessel with confining pressure (10 MPa) applied to floating end caps.
Tanai [unpublished 2002]	Mx80	1.63	Linear	Constant gas pumping rate	Constant isotropic stress in flexible sleeve subject to external fluid pressure (? MPa)

\*From saturated density; <sup>1</sup>Gas flow may have been by aqueous phase diffusion

# Swedish work

- **Threshold pressure**
- **Threshold pressure correlated with swelling pressure, but range of breakthrough gas pressures quite large**
- **Entry pressure also explained as capillary entry pressure for pre-existing pathways**
- **Microstructural analysis of clays carried out**
- **Microstructural model developed involving clay fabric, gel properties and pore sizes**
  - Gas entry related to sizes of gel-filled pores
  - What is nature of connectivity?

# Japanese and French work

- **Threshold pressure for gas invasion observed**
- **Correlation with swelling pressure**
- **In CEA work, distinction drawn between gas entry and rupture pressure - close together for saturated bentonite**
- **Work at range of initial water saturations**
- **Work at constant volume and constant stress**

# Canadian Work

- **Experiments carried out on bentonite and illite and on clay-sand mixtures, and at range of initial saturations**
  - Concentrate on bentonite at near 100% water saturation
  - At lower water saturations, gas migration can occur easily through pre-existing gas-filled pathways
- **Very large gas entry pressures when fast build-up of pressure**
- **Gas flow at low excess pressures with sustained application of pressure**
- **Do not believe relationship with swelling pressure**
- **Suggest capillary displacement model of gas invasion of clay**

# UK (BGS) Work

- **Experiments under a variety of conditions:**
  - Isotropic stress; K0 geometry; constant volume “radial” flow
- **Designs allow post-breakthrough behaviour to be studied**
- **Breakthrough pressure observed in all systems even after extended application of large gas pressures**
  - Correlates with swelling pressure under isotropic conditions
  - Large breakthrough pressures above swelling pressure for constant volume systems
- **Evidence for macroscopic fracturing in constant volume systems**
- **Measurement of stresses and pore fluid pressures**
  - Relationship seen between pore water and gas pressures
- **Outflow shows instabilities (e.g. pulsating and changing location)**



# Summary of Features of Data on Gas Migration in Bentonite

- **Threshold pressure for gas entry observed in many experiments (exception: long term Canadian experiments)**
  - **Related to swelling pressure?**
- **Displacement of only small volumes of water?**
- **After breakthrough, gas flows at pressures below the threshold, but flow ceases at pressures above back pressure**
- **Changes in porewater pressure in response to applied gas pressure**
- **Evidence for macroscopic fracturing in radial flow experiments**

# Possible mechanisms of gas migration

- **Conventional two-phase porous medium behaviour**
  - invoke concepts of capillary pressure and relative permeability
  - capillary displacement models
  
- **Microfissuring of the clay**
  - new porosity created to accommodate gas flow (compression / water displacement)
  - clay sample remains intact
  
- **Macroscopic fracturing of the clay**
  - in laboratory, fracture lengths are comparable to sample sizes
  - discrete fracture episodes or slow fracture propagation?

# Conventional two-phase / capillary pathway flow models

- Generally not thought applicable to gas migration in bentonite. Why?
- Suggested that gas flow is localised (i.e. follows spatially isolated pathways) with very little displacement of water (importance depends on possibility of defining suitable representative volume)
- Does not address possibility of the creation of new gas occupied porosity
- High gas entry pressure is ascribed to capillary pressure - requires very large number of very small pathways to match entry pressure and gas permeability
- If microfissuring / fracturing is not involved, is it possible to use a conventional two-phase modelling approach but with novel saturation functions to describe gas migration (e.g. with saturation functions / permeability that include a pressure dependence)?
  - May not provide insights into mechanisms (need process models)

# Fracture propagation / microfissuring

- **Clear evidence of macroscopic fracturing in some experiments**
- **Arguments for microfissuring are more circumstantial**
  - Dilation of samples?
  - No accessible pores in highly compacted bentonite
  - No gas entry until stress in clay is exceeded in most experiments - implies gas pressure needs to hold open fissures (but note flow continues at lower pressures once established)
- **Very little displacement of water (NB water could be displaced by consolidation of clay as well as by displacement of gas from pores)**

# What are the Implications of Experimental Data for Process Understanding?

- **Relative importance of gas migration mechanisms?**
  - two-phase flow / water displacement
  - microfissures that dilate
  - macroscopic fracturing
  
- **Factors controlling gas breakthrough pressure?**
  - swelling pressure
  - local stress field
  - capillary pressure / viscous resistance
  - clay adhesion
  
- **Evolution of gas permeability**
  - pressure dependent?
  - creep effects?
  
- **Importance of clay fabric?**

# Experimental Questions

- **Are experiments possible that determine distribution and properties of gas-filled pathways?**
- **How confident are we that microstructural analysis of distressed clay samples after water flow or gas migration experiments provides an accurate picture of the characteristics of the clay under experimental, high stress, conditions?**
- **Introduction of thermal / resaturation effects adds new factors which will eventually require better understanding**



serco

Serco Assurance

**Modelling Gas Migration  
through Compacted  
Bentonite: Work of the  
GAMBIT Club**

**William Rodwell  
Andrew Hoch  
Ben Swift et al**

Madrid October 2003

# The GAMBIT Club

- **Consortium of Radioactive Waste Management Agencies formed initially to support development of models of gas migration through water-saturated compacted bentonite**
  - SKB
  - Andra
  - Enresa
  - JNC
  - Nagra
  - Posiva
  
- **Work funded by these organisations and carried out by Serco Assurance**



# Presentation

- **Summary of experimental results on gas migration through buffer bentonite**
- **Describe a number of models of gas migration examined in GAMBIT Club**
- **Comparison with experimental results obtained by BGS**
- **Conclusions**

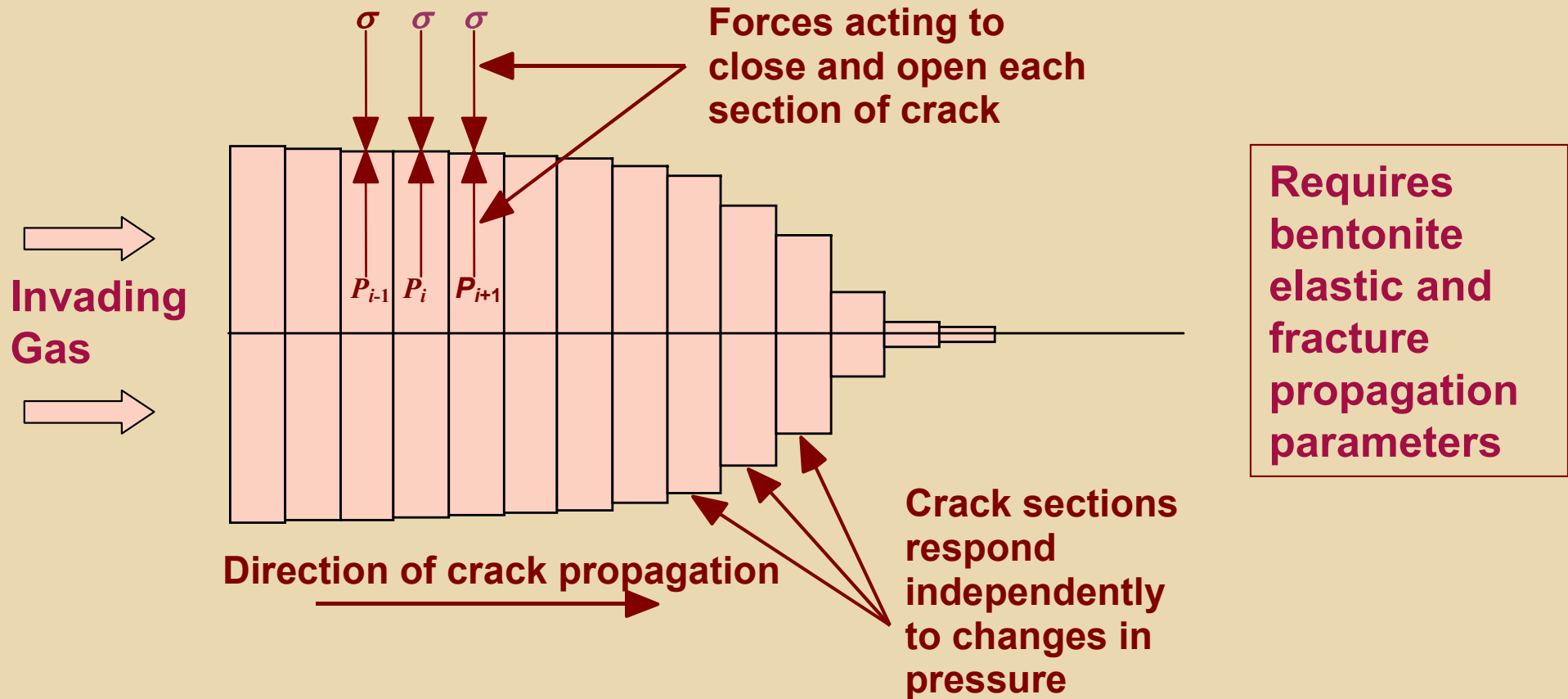
# Summary of Experimental Observations

- **Threshold pressure for gas entry**
  - Sometimes correlated with swelling pressure
- **Displacement of only small volumes of water**
- **Once established, flow continues at gas pressure below threshold pressure; “shut-in pressure” at which gas ceases to flow**
- **Changes in pore-water pressure observed**
- **Experiments on radial flow of gas from small filters exhibit high threshold pressures and macroscopic fracturing**
- **Gas pathways resealed by resaturation?**
- **Gas migration may be sensitive to stress state of clay?**

# Numerical Models Investigated

- **Gas migration by fissure propagation**
- **Displacement of water from pre-existing capillary-like pathways**
- **Continuum model of gas migration through newly-created gas-filled porosity**
- **Inclusion of the effect of the stress state of the clay on gas migration**

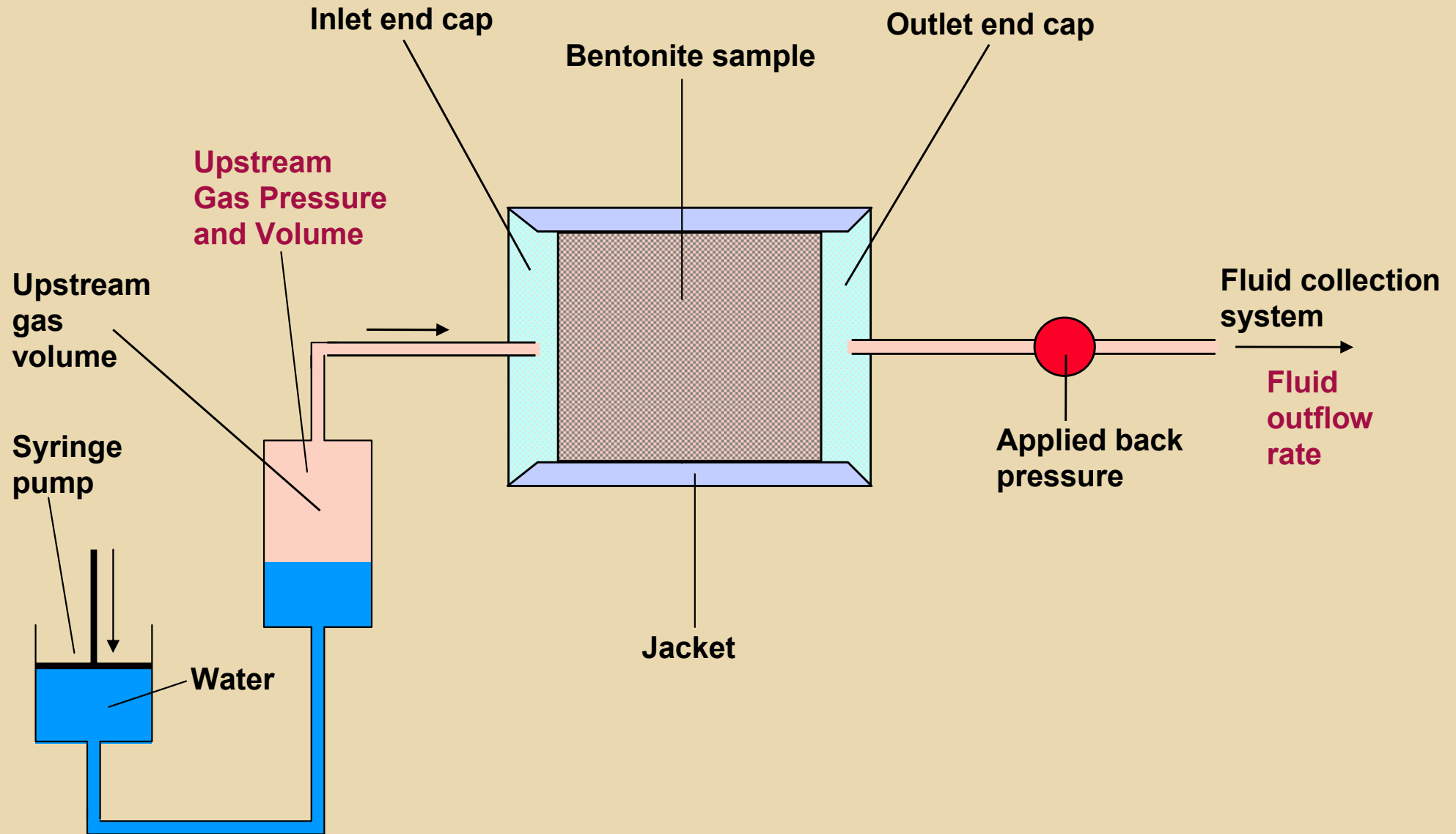
# Gas Migration by Fracture Propagation - first model tried



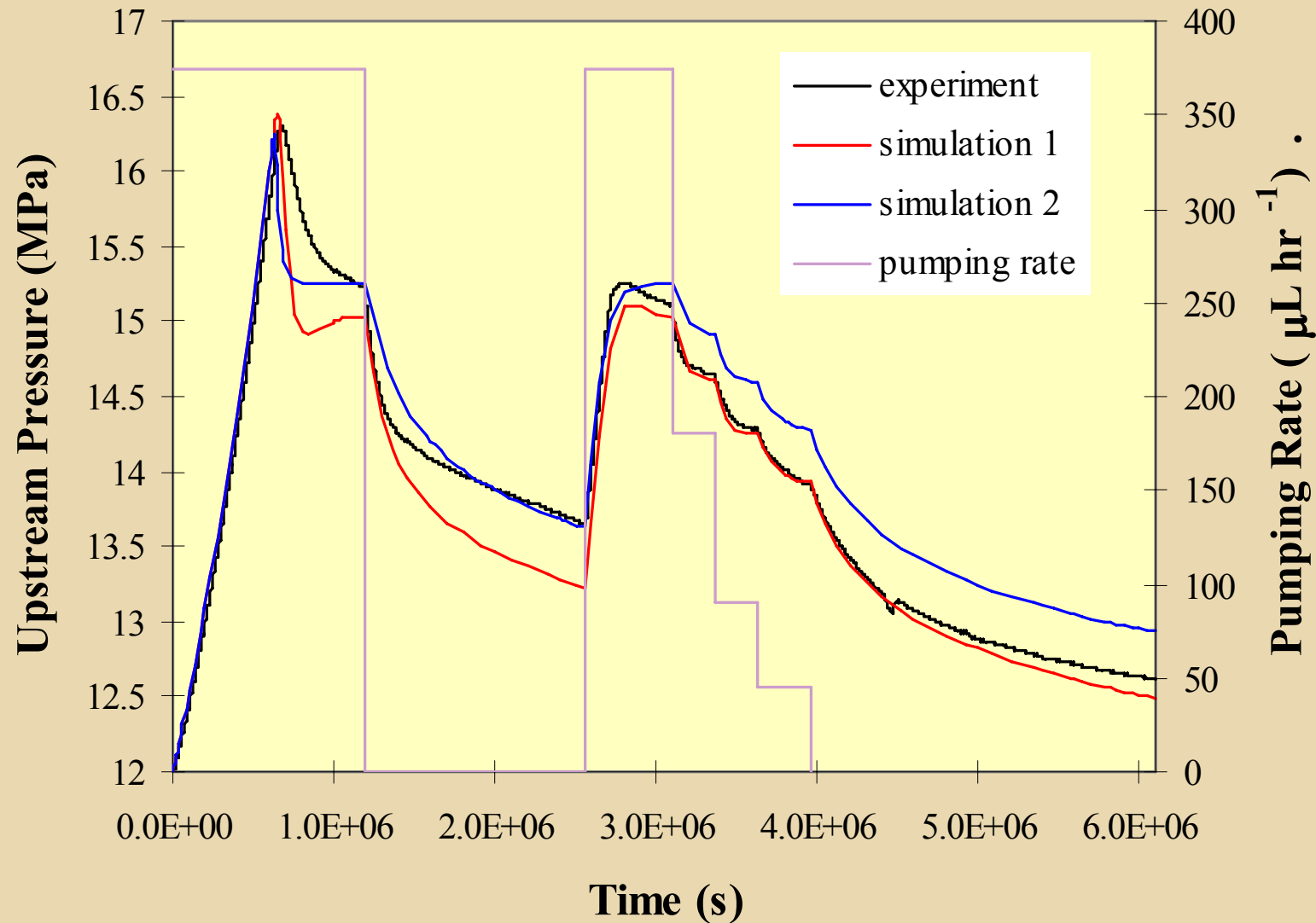
# Features of Original Model of Gas Invasion by Fracture Propagation

- **Model propagation of individual (or groups of identical) gas pathways**
- **Threshold pressure depends on critical stress intensity (i.e. classic model of fracture propagation)**
- **Dilation of pathways with gas pressure**
- **Time dependence in dilation behaviour (basis of hysteresis in permeability)**

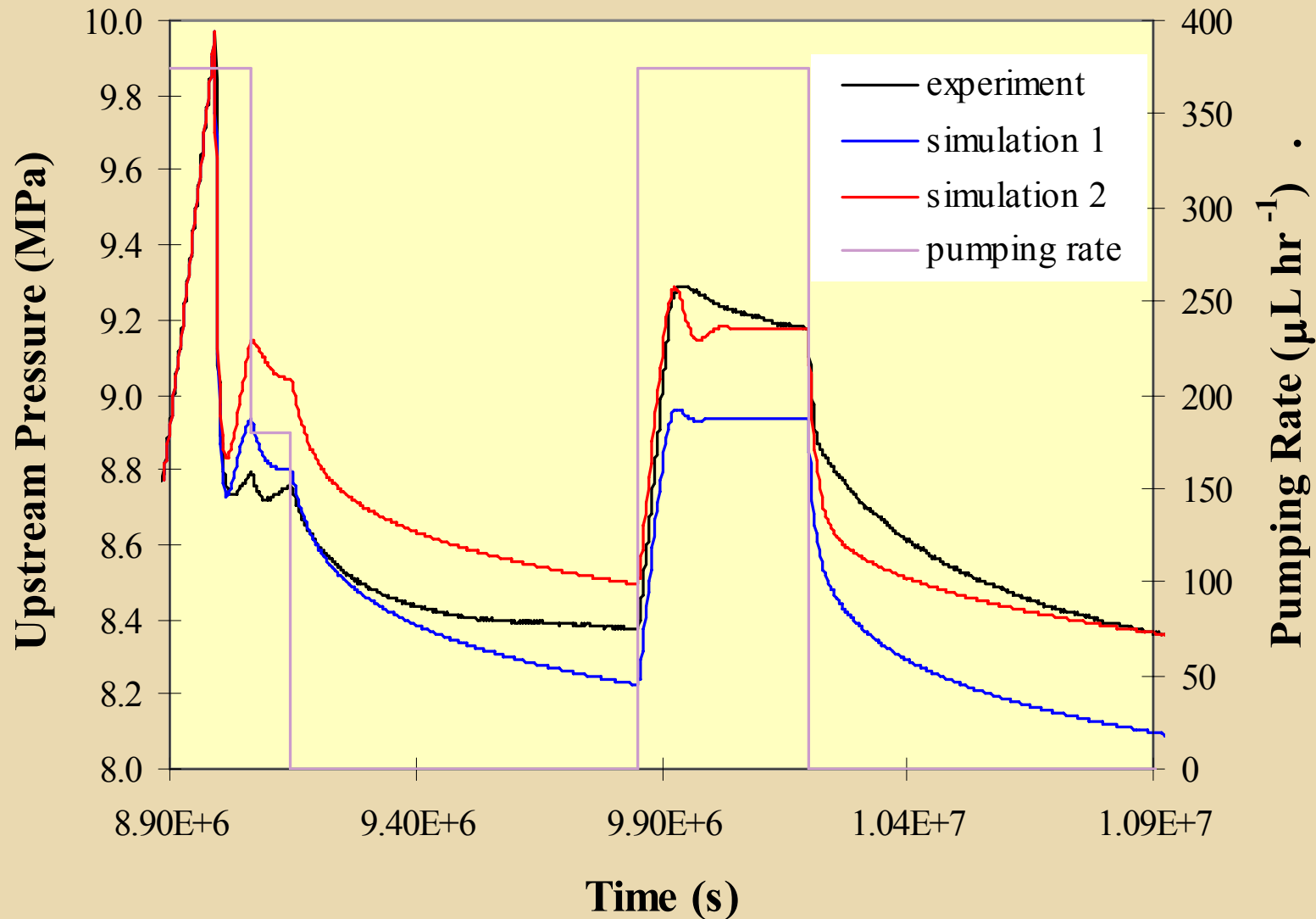
# Schematic of Experimental Set up Used by Horseman and Harrington



# Fit of Fracture Propagation Model Results to BGS Experiments - Isotropically Constrained Linear Flow



# Fit of Fracture Propagation Model Results to BGS Experiments - Constant Radial Strain & Axial Stress





# Results for Fracture Propagation Model

- Requires heuristic model adjustments to keep pathways open after breakthrough (explained as clay creep)
- Introduce time lag in response to pressure changes to provide hysteresis in gas permeability
- Gives good agreement to sections of experimental histories for isotropically constrained samples, but not able to match whole of history
  - Significance depends on experimental reproducibility
- Qualitative agreement for  $K_0$  geometry

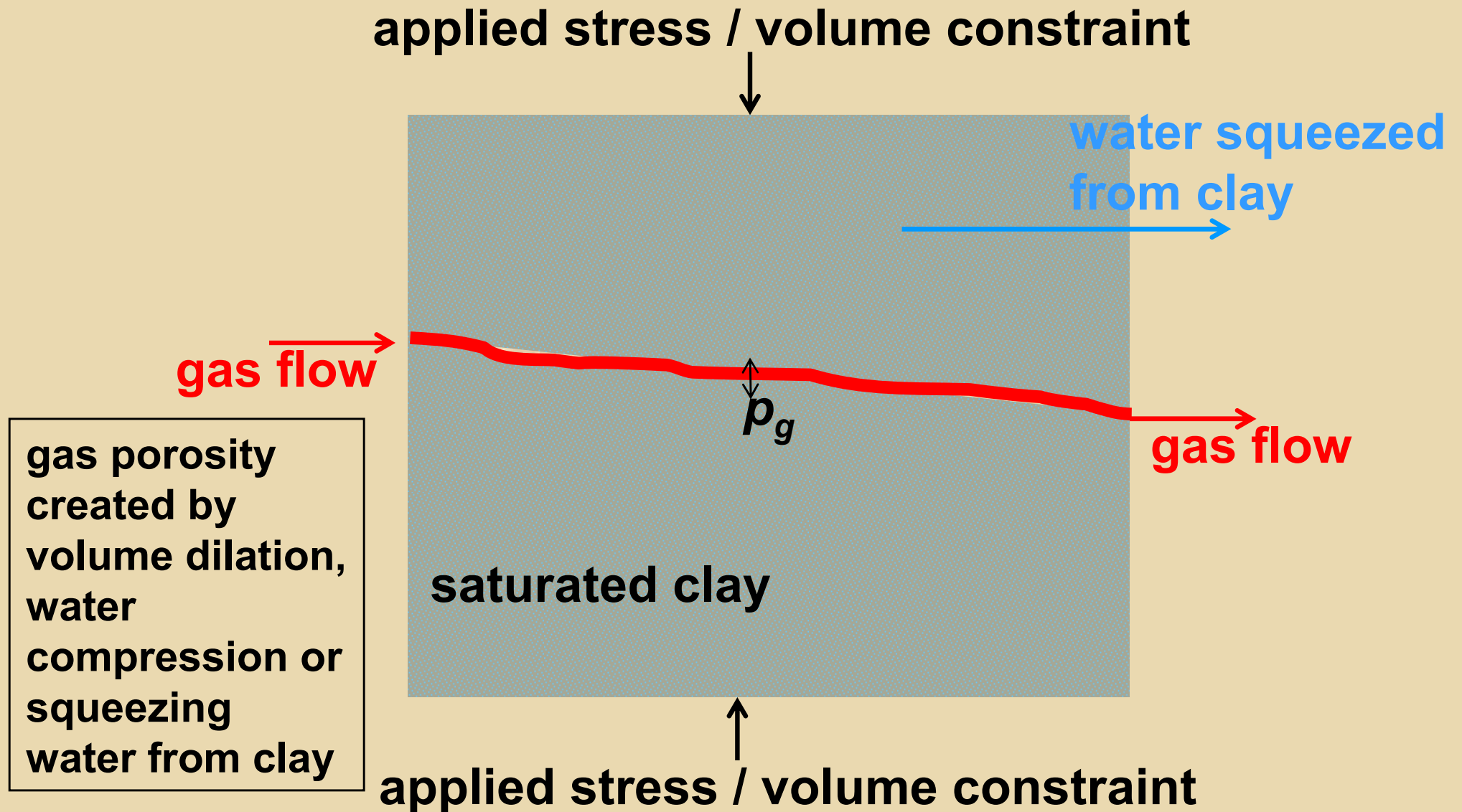
# Fissure Propagation Models / Limitations

- **The fissure propagation model treats clay simply as an elastic medium with fracture toughness properties so does not feature:**
  - Flow of water through the clay
  - Coupling between gas and porewater pressures as seen in some experiments
  - Resealing of gas pathways after gas transport is over
  - Coupling of the water content and stress state of the clay (swelling / suction behaviour)
- **Pathway propagation models present upscaling difficulties both in size and dimensionality**
- **Alternative “continuum” model developed**

# Rationale for Developing the Alternative “Continuum” Model

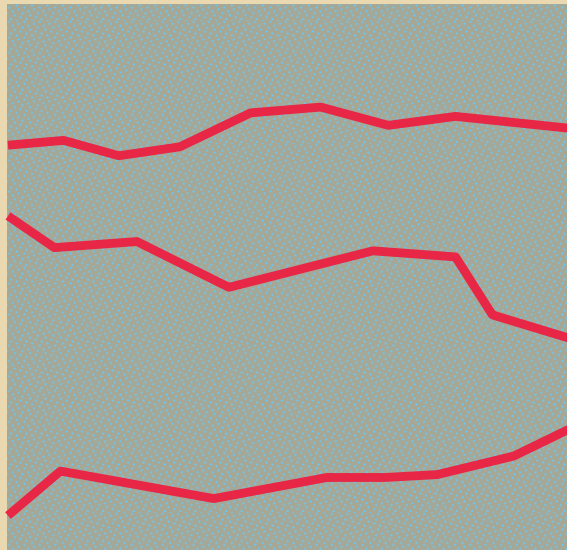
- **At field-scale, not necessary to account for details of pathway propagation (occurs too quickly compared with timescales of interest)**
- **Need to represent in appropriate detail the features missing from the pathway propagation models**
- **Should be readily upscaleable to develop a tool applicable at the scale of canisters/deposition holes**
- **Bears an understandable relationship to the physics of clay behaviour and gas migration (including the maintenance of pathways after breakthrough)**

# Conceptual Basis of Continuum Model / 1



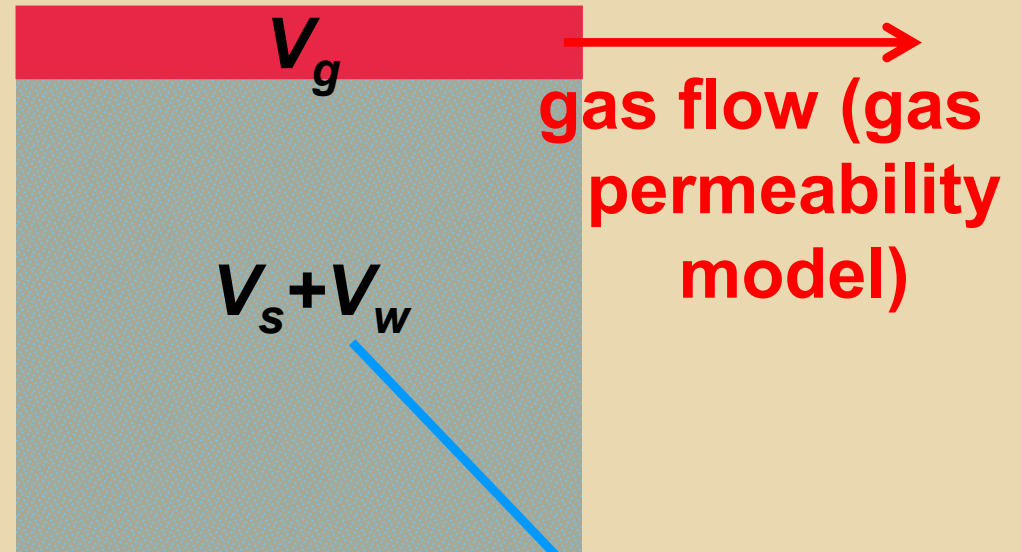
# Conceptual Basis of Continuum Model / 2

## Actual Fissures



Idealisation →

## Idealised Concept

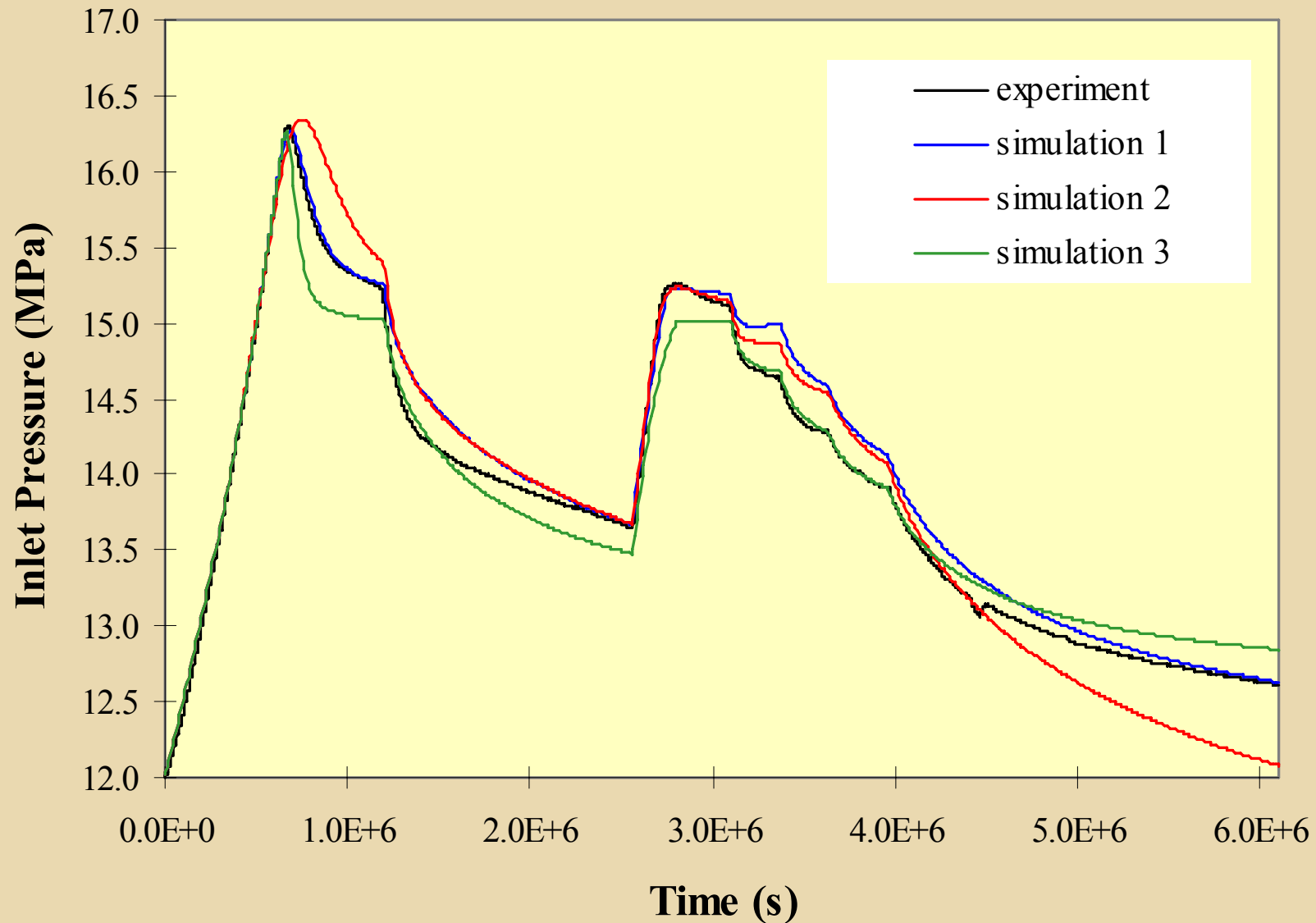


water squeezed from clay (swelling behaviour)

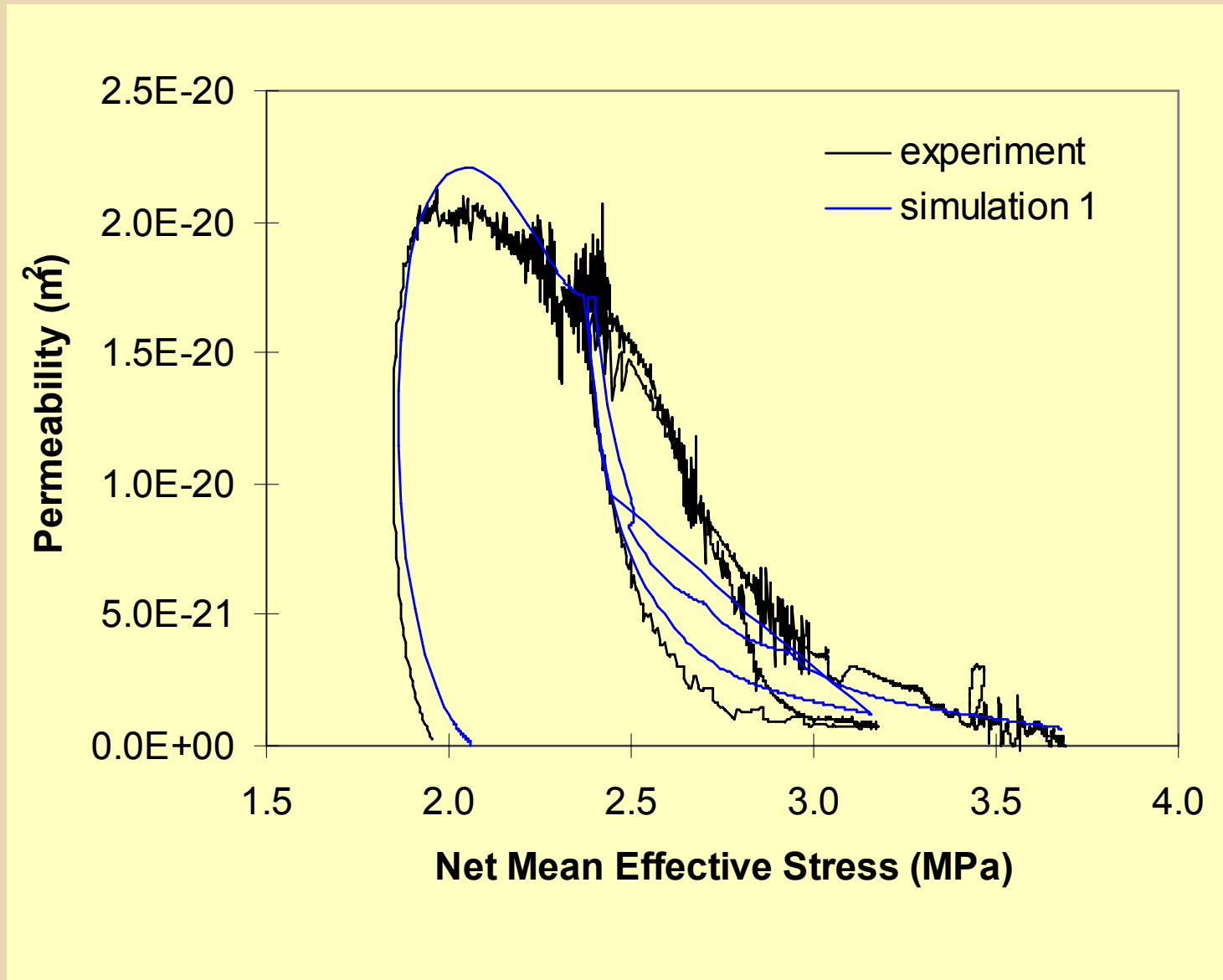
# Parameters for Continuum Gas Migration Model

- **Water permeability**
- **Gas permeability as a function of gas-filled porosity**
  - parameters for function, e.g. critical gas saturation
  - alternative models
- **Swelling pressure as a function of void ratio**
- **Water compressibility**
- **(Simple dependence of sample volume on stress)**

# Fit of Continuum Model Results to BGS Experiments - Isotropically Constrained Linear Flow

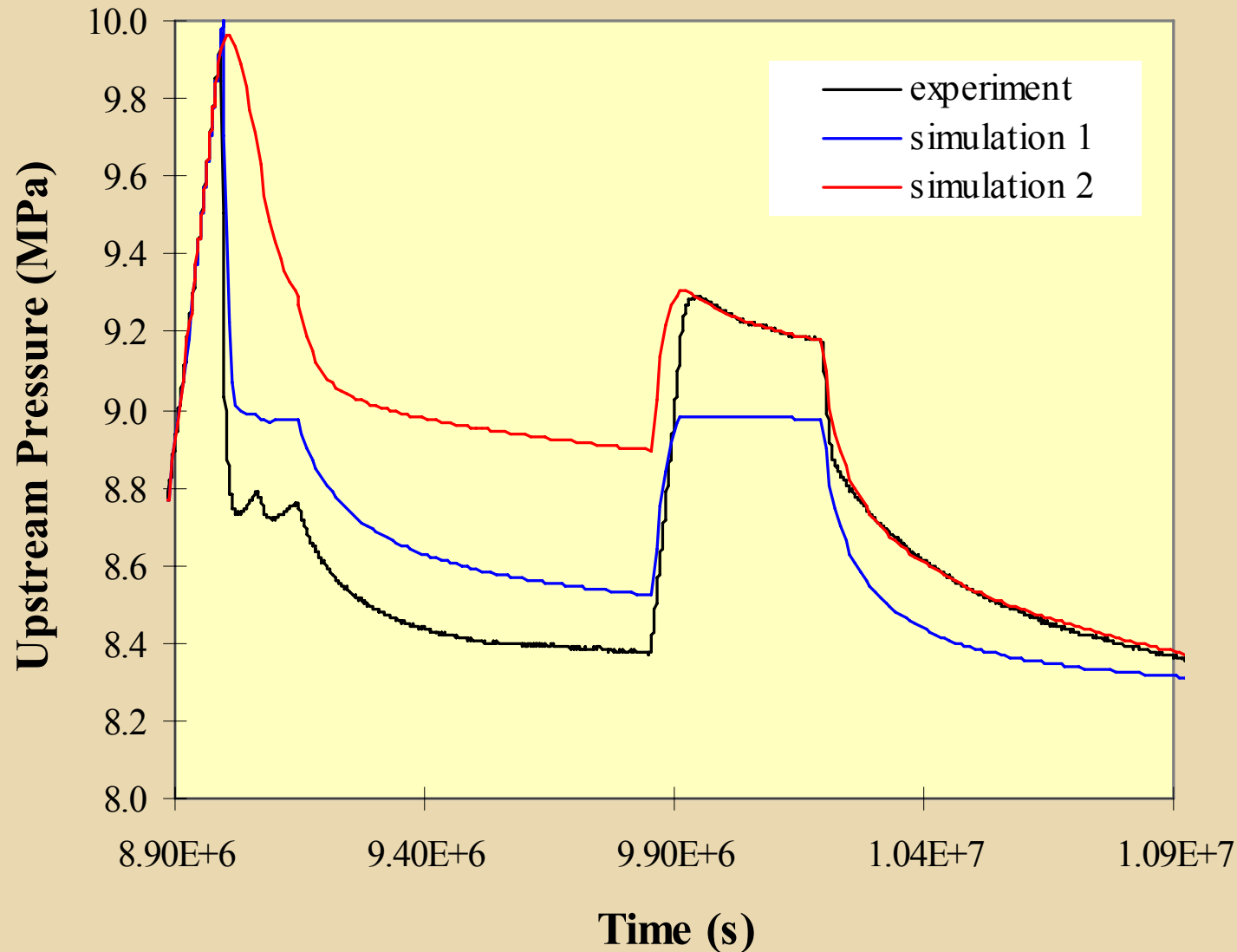


# Gas permeability from Continuum Model - Isotropically Constrained Linear Flow





# Fit of Continuum Model Results to BGS Experiments - Isotropically Constrained Linear Flow



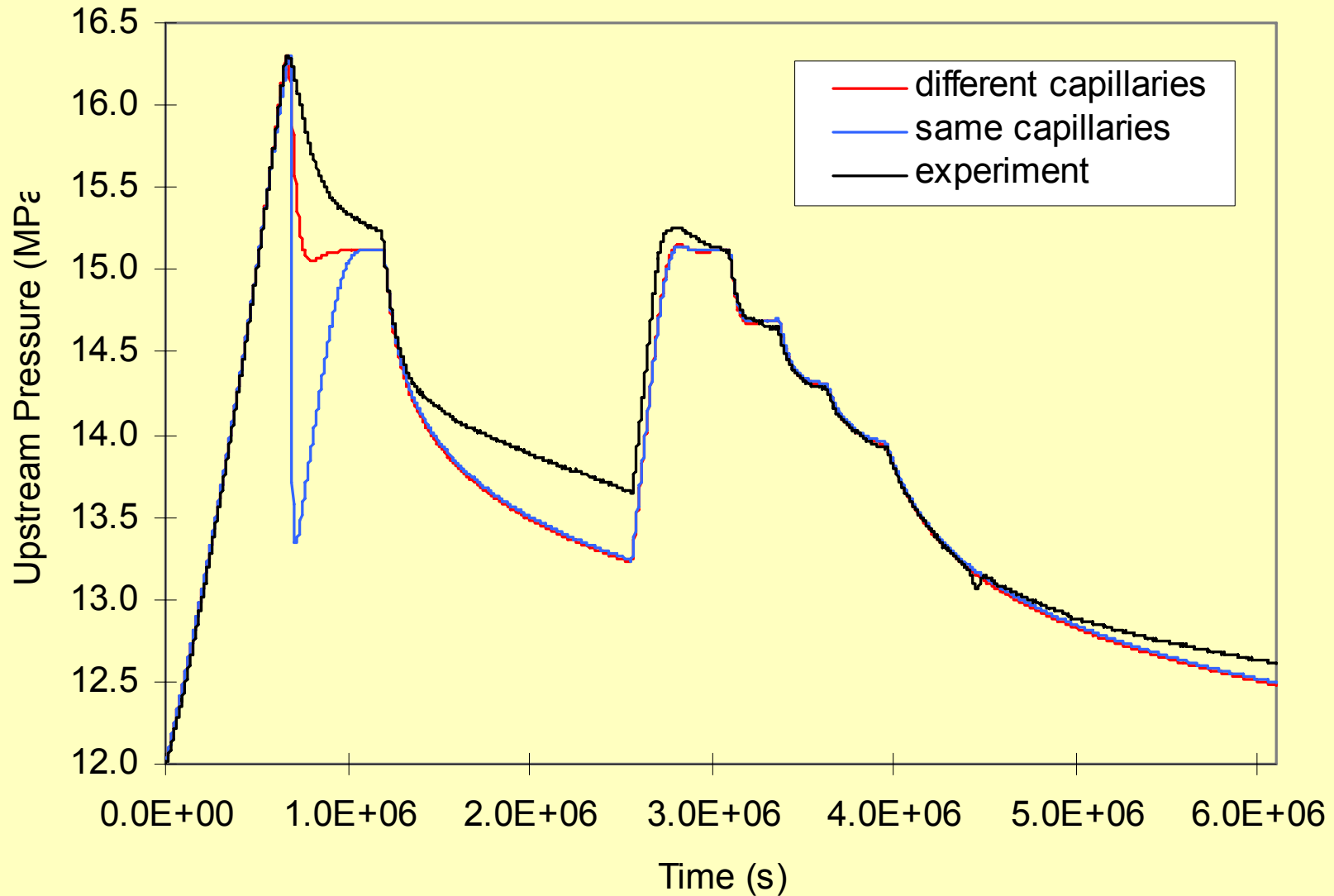
# Results of Continuum Model Development

- **Gives comparable agreement to fracture propagation model for experiments with isotropically constrained sample**
- **Less good agreement for experiment in  $K_0$  geometry**
  - Large difference between first and second cycles presents greater challenge
  - Due to limited representation of time-lag effects
  - Attempts to represent a dual porosity aspect of the clay fabric did not improve fits
- **Pathways naturally stay open after gas invasion until resaturation causes resealing**
- **Small magnitude of gas porosity created suggests insensitivity to stress boundary conditions?**

# Capillary displacement model

- **Modification of fracture propagation model in which pathways formed by displacement of water from pre-existing capillaries**

# Results from capillary displacement model / 1



# Results from capillary displacement model / 2

- Require different capillary radius before and after breakthrough to give good agreement with experiment
- Small capillary radius ( $\sim 10^{-8}\text{m}$ ) required to give large capillary pressure ( $\sim 14\text{MPa}$ )
- Larger continuous gas pathway radius ( $\sim 10^{-6}\text{m}$ ) required to support flow after breakthrough
- Increase in number of pathways allows decrease in continuous pathway radius
- $10^{10} - 10^{11}$  pathways required before continuous gas pathway radius comparable with capillary radius
- Very different concept to the localised pathway model
- Similar limitations to fracture propagation model

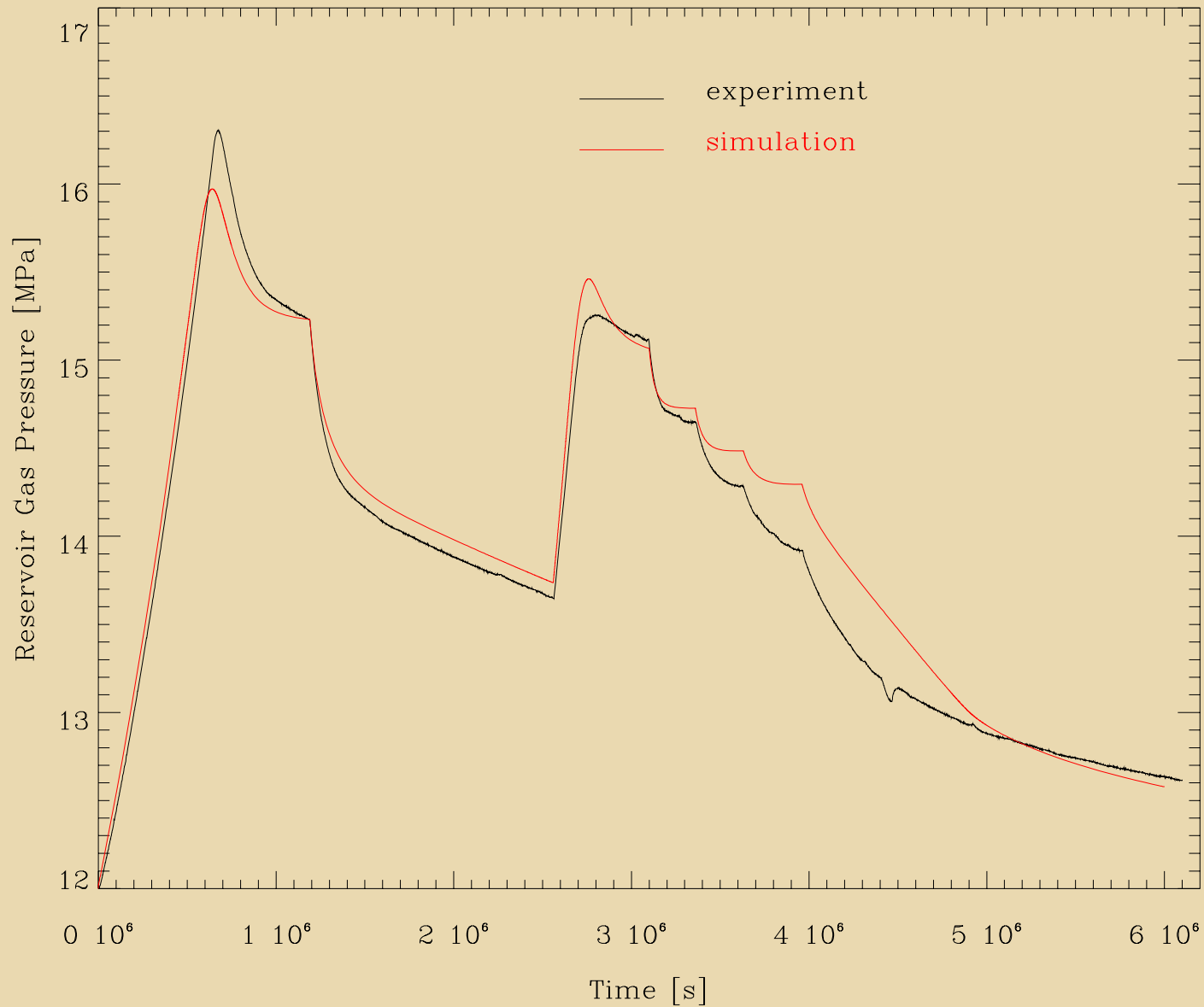
# Inclusion of Effect of Full Stress State of Clay on Gas Migration

- **Have been attempting to extend models to properly include the effect of the stress state of the clay on gas migration**
  - **Anticipate effect on direction of migration?**
- **Need to include interactions between stress field and gas and water pressures; nature of coupling not satisfactorily characterised experimentally**
- **Investigation into numerical method needed to find suitable method to allow gas front to propagate**
- **Use ENTWIFE to automatically generate finite element computer code from a model specification**
  - **Allows different models to be easily explored**
- **Results similar to earlier examples obtained for linear flow experiments**
- **Difficulties experienced with instabilities in two-dimensional flow in defining and controlling gas “pathway” propagation**

# Issues addressed in new model

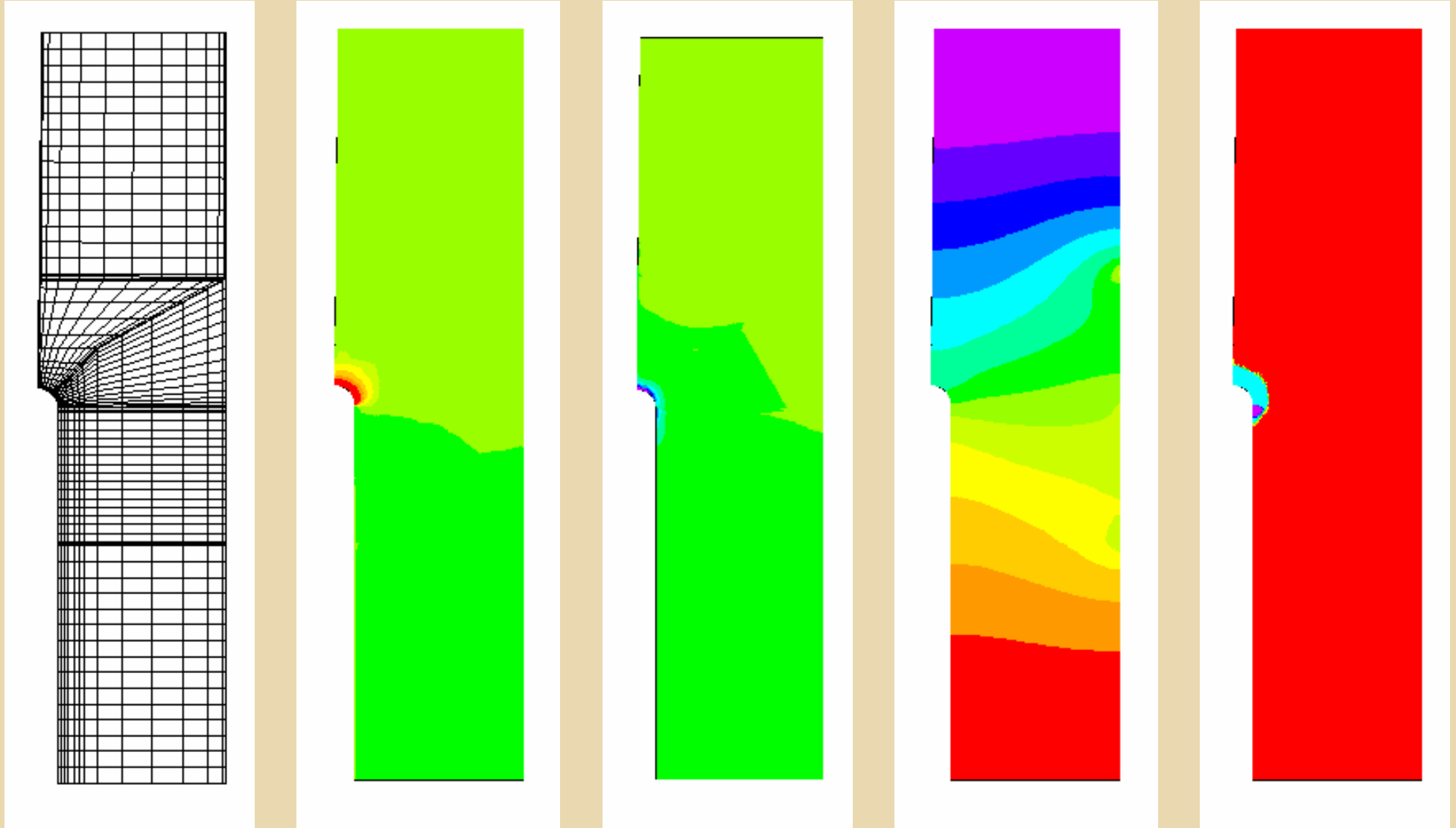
- **Gas entry condition**
  - Gas enters when pressure exceeds minimum principal effective stress
  
- **Gas permeability**
  - Currently treated as an isotropic function of saturation
  - Direction depends on gas entry condition, not permeability
  
- **Relationship between gas and water pressure**
  - Generalised Hooke's law contains a term in the matric suction (pore water pressure is subsumed into treatment in terms of effective stress)
  - Gas saturation dependence on matric suction includes "failure" term and "dilation" term

# Results from Attempts to Couple Gas Migration to Stress in Model - Linear Model





# Current status of work on radial flow experiment - modelling up to gas breakthrough



# Conclusions

- **Model of gas migration by fissure propagation can account semi-quantitatively for observed gas migration behaviour, but depends on some heuristic arguments**
- **Gas migration by water displacement requires very large number of small capillaries**
- **Upscaleable continuum gives agreement with experiment broadly comparable with other models and represents more of the observed experimental features**
- **Extension of continuum model to properly include stress effects suffers from poor characterisation of couplings and controls on gas pathway propagation**
- **Experimental data needed on mechanism of gas migration in bentonite**

# A CAPILLARITY/ADVECTION MODEL FOR GAS BREAK-THROUGH PRESSURES



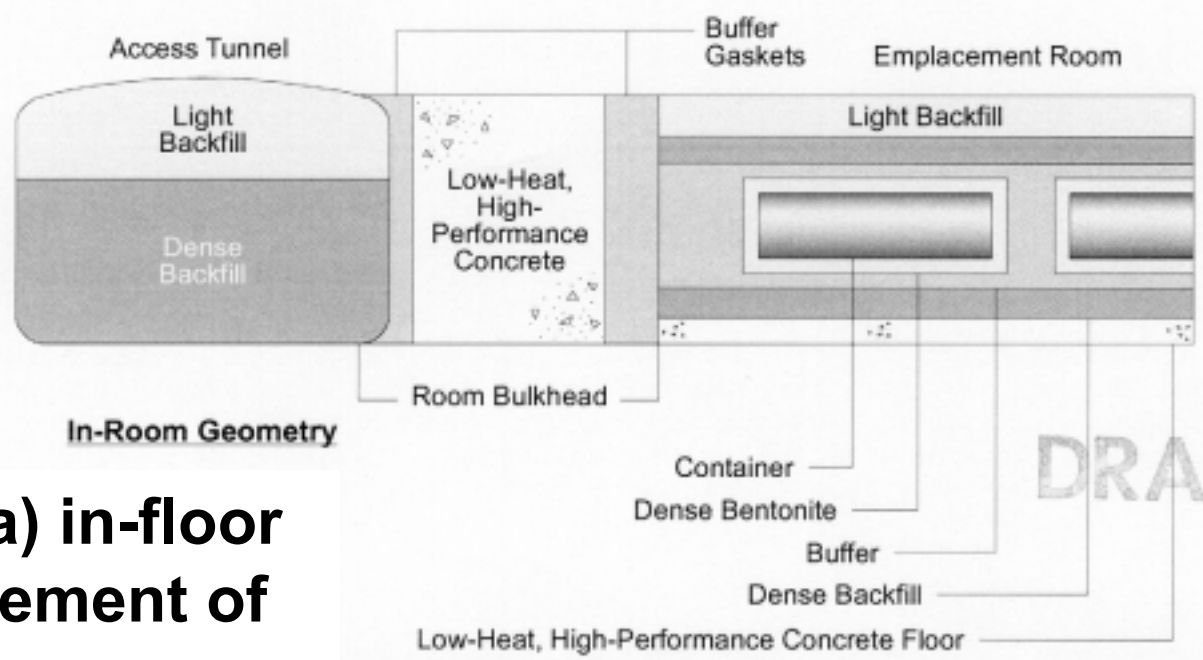
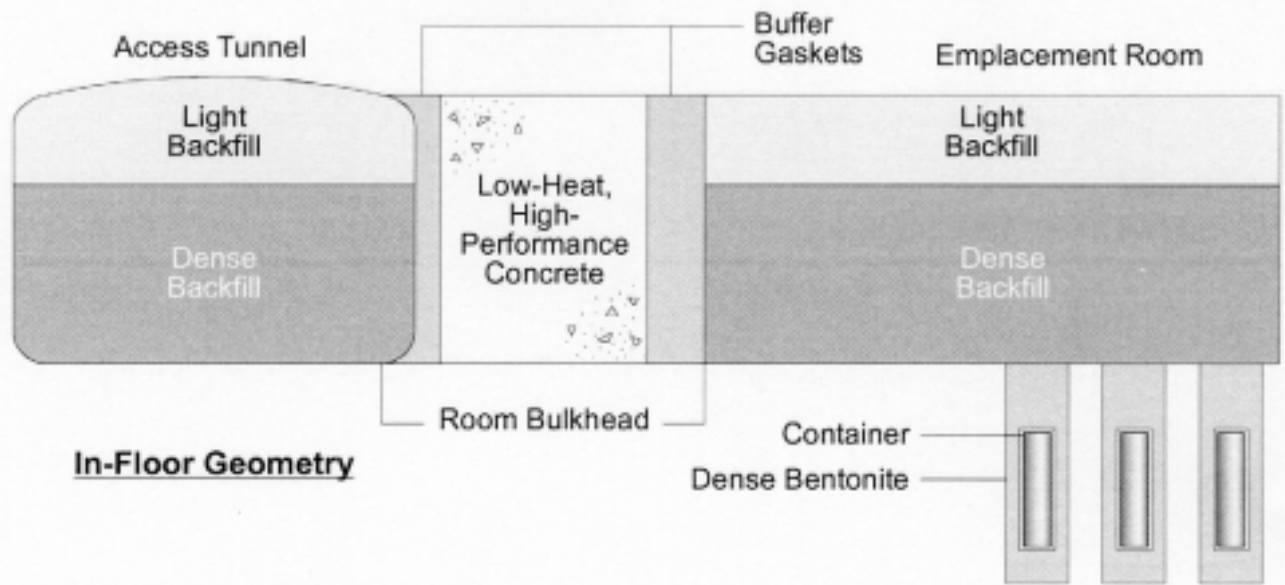
**JIM GRAHAM**

- Professor Emeritus, Univ. Manitoba
- Secretary General, Canadian Geotechnical Society
- Keller Visiting Professor, Queen's University, Belfast

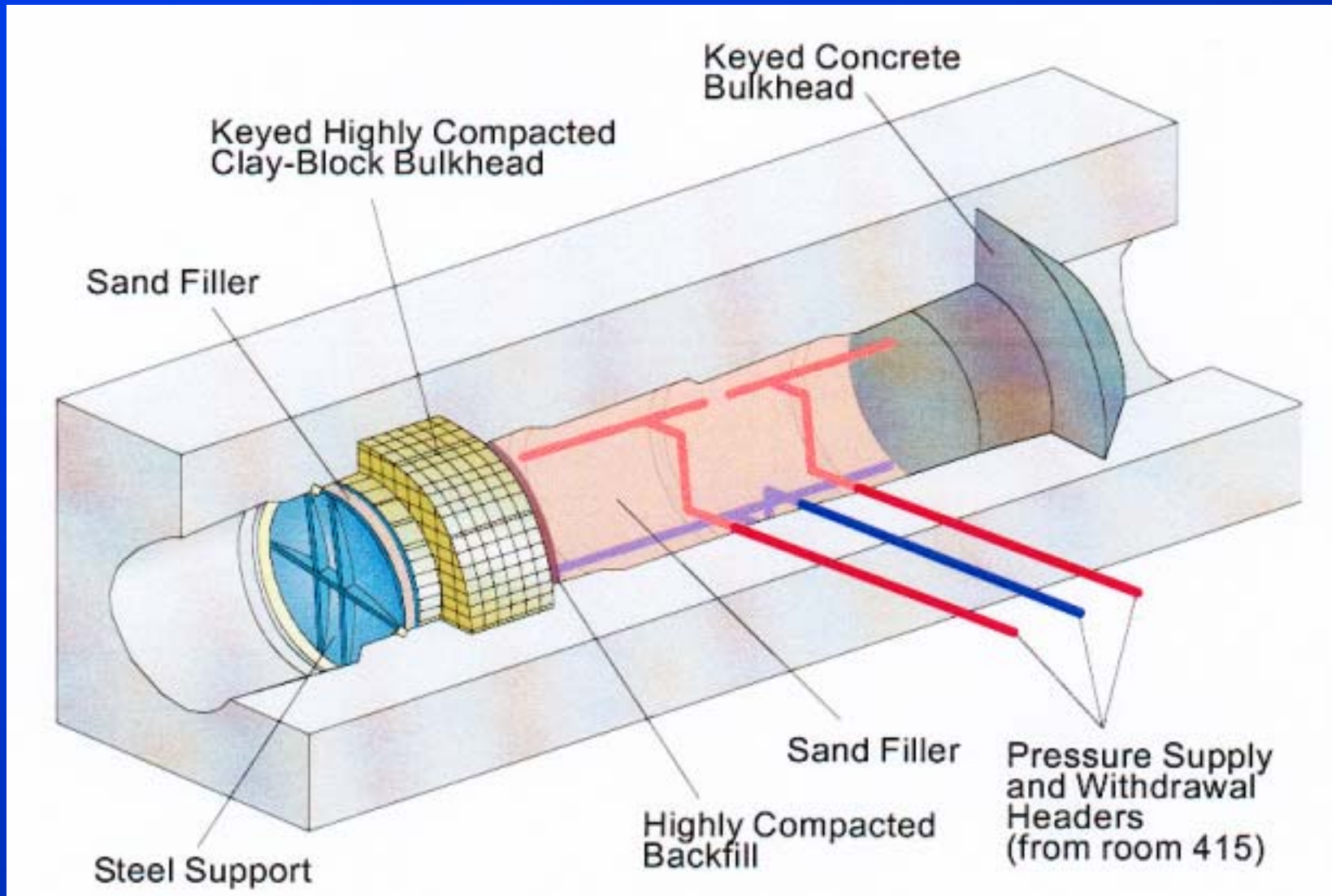


**MAROLO ALFARO**

- Assistant Professor, University of Manitoba



**Canadian concept for a) in-floor and b) in-room emplacement of waste-fuel containers Read/Chandler**



## The Tunnel Sealing Experiment (TSX) Underground Research Laboratory, AECL, Pinawa MB

Read/Chandler

## ***Issues of gas generation, gas pressure buildup, and gas breakthrough***

- ***generated by biological degradation of organic materials, anaerobic corrosion of metals in the repository, or by radiolysis (methane, hydrogen)***
- ***increased pressure on container***
- ***damage to fabric of clay-based barriers***
- ***burst-out and vector for radionuclides***

## ***Two distinct test procedures:***

- 1. pressures at inlet to specimens incremented at fixed rates until 'breakthrough'***
  - 'INCREMENTAL PRESSURE TESTS'***
- 2. constant pressure difference applied across specimens to examine relationship between 'time to breakthrough' and pressure gradient***
  - 'CONSTANT PRESSURE TESTS'***

***Both sets of tests done in rigid-wall cells***

## ***Materials:***

- illite and sand-illite mixtures***
- bentonite and sand-bentonite mixtures***

### ***Range of Parameters in Test Program***

---

Soil type	$\gamma_{\text{dry}}$ Mg/m <sup>3</sup>	w.c. %	S <sub>r</sub> %
Illitic clay	1.85 – 2.10	10 – 16	67 – 100
Bentonitic clay	0.6 – 1.45	30.0 – 63.5	60 – 100
Sand-illite	1.97 – 2.30	5.4 – 13.0	45 – 100
Sand- bentonite	1.67	11.4 – 20.4	50 - 89

---



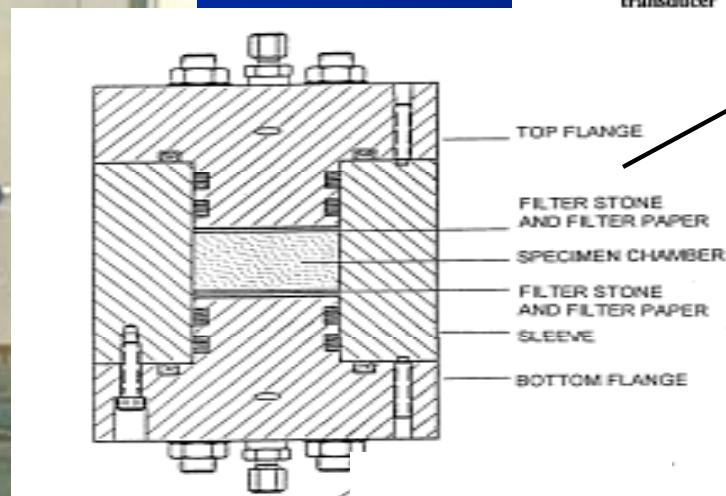
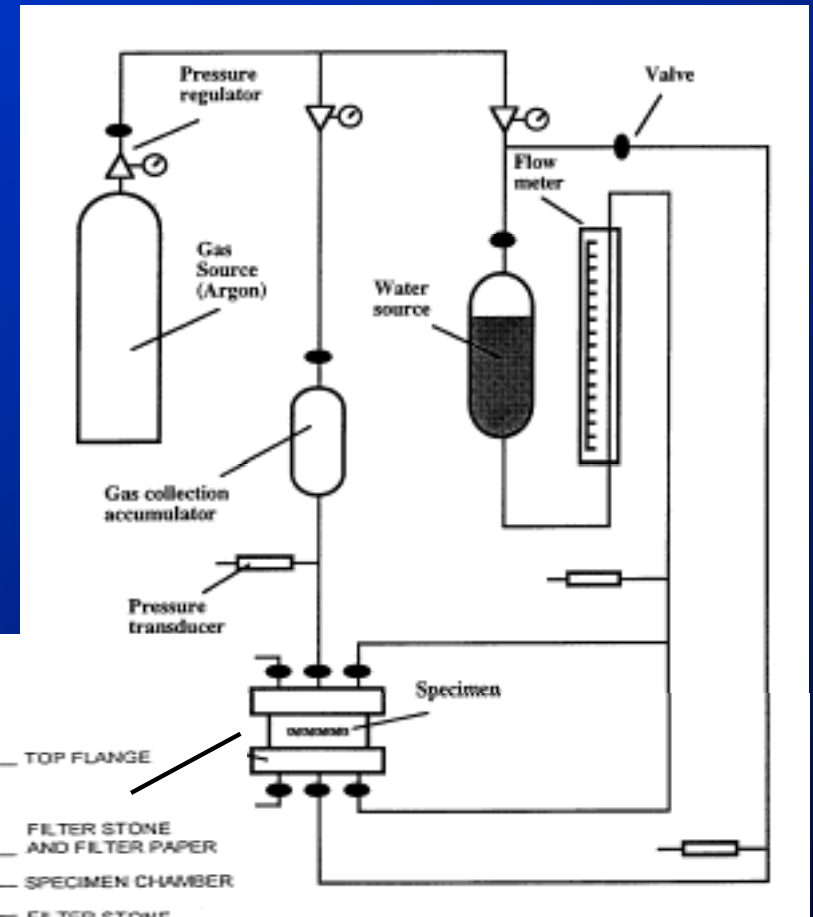
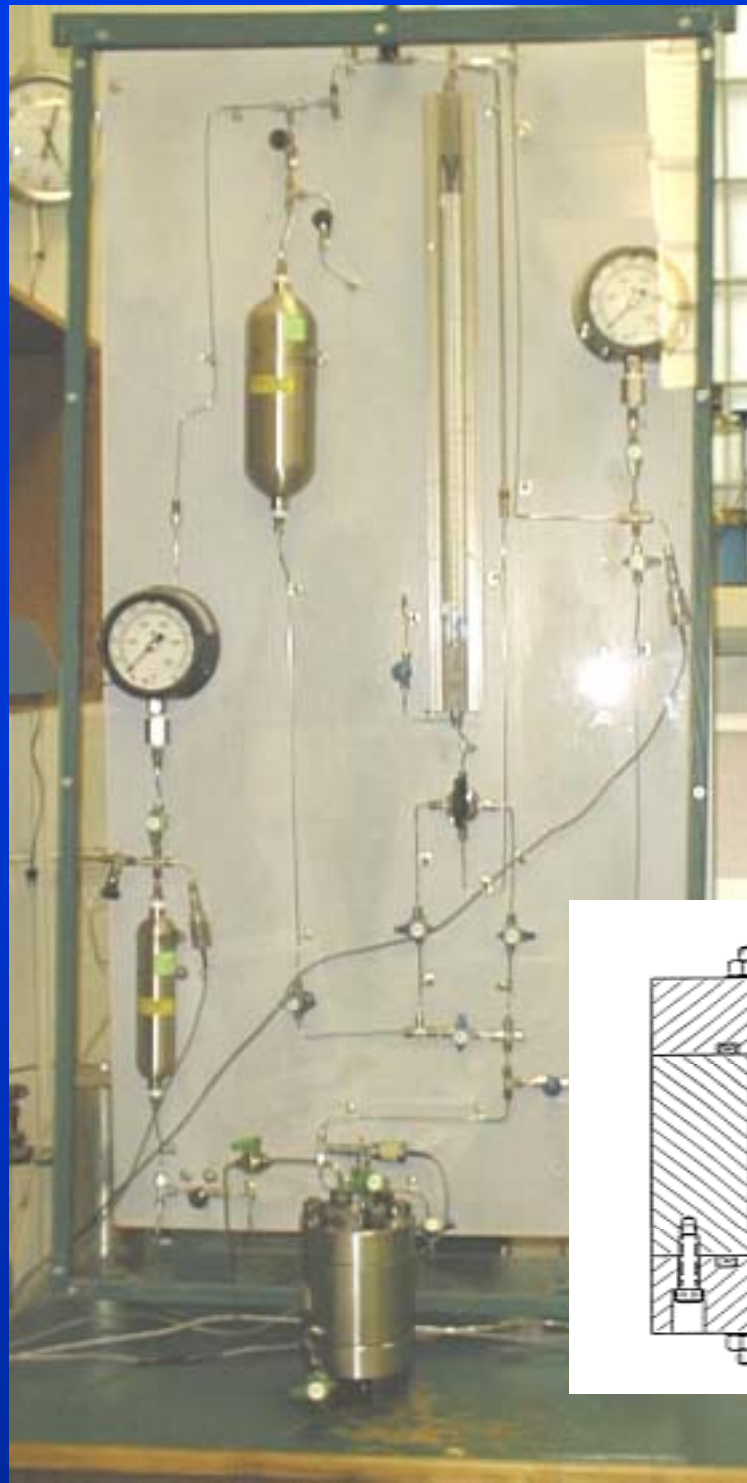
## *Comparison of the properties of illite and bentonite used in the tests*

---

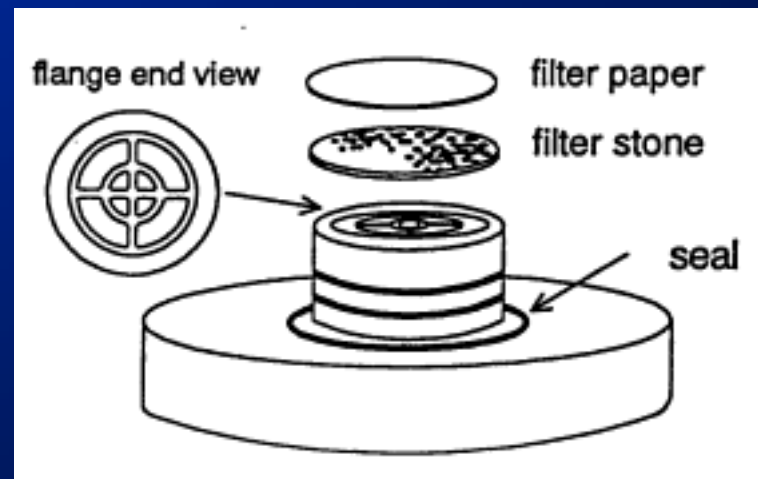
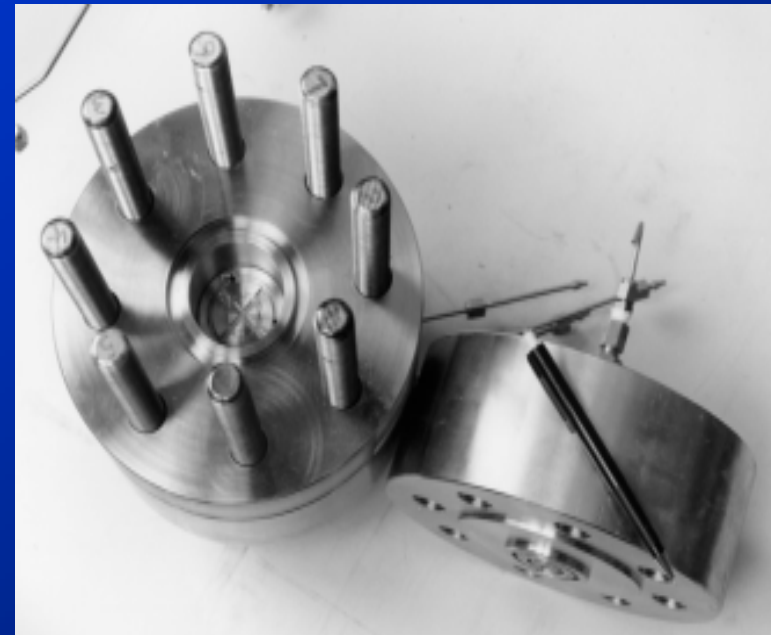
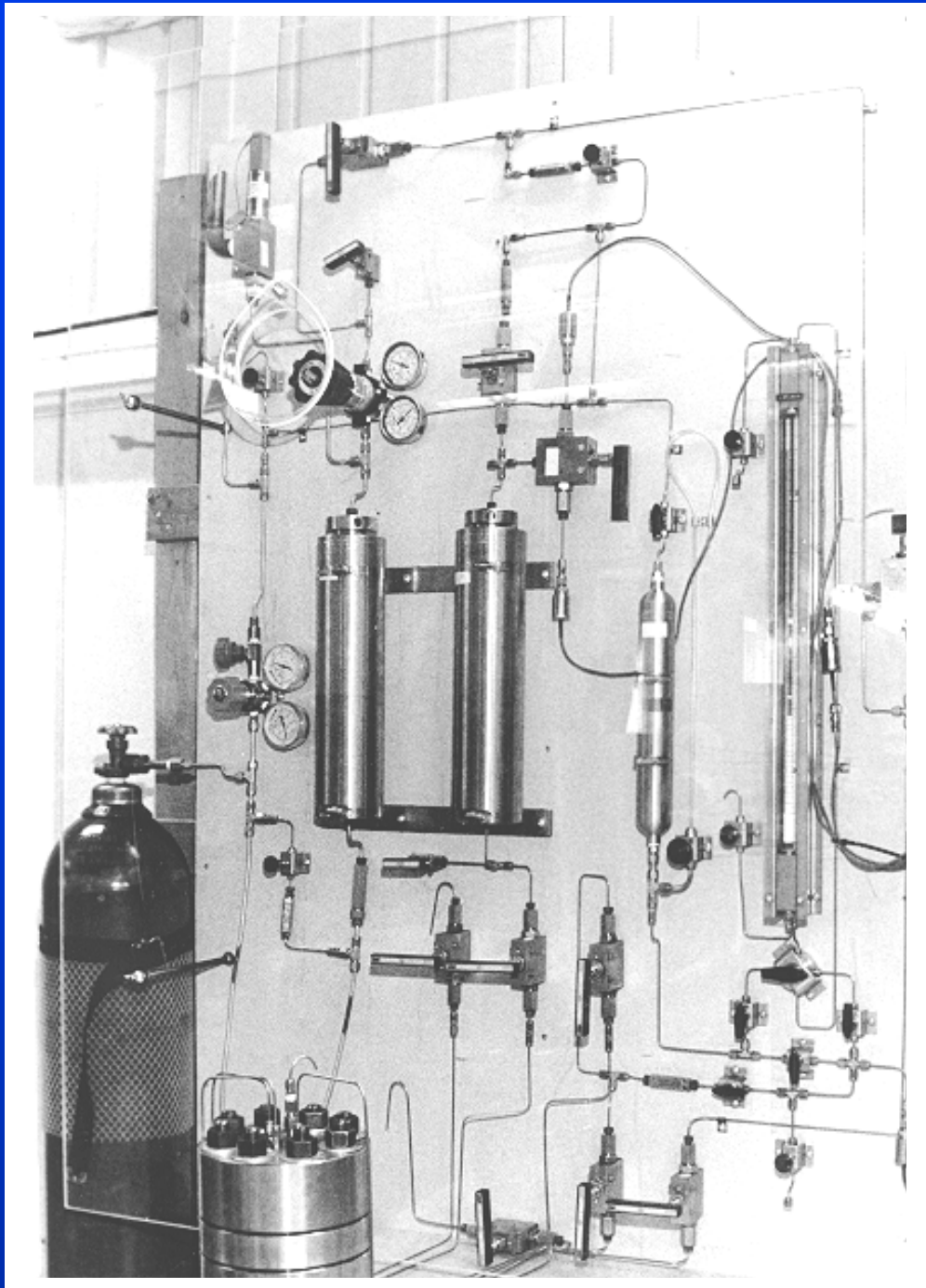
Property	Illite	Bentonite
Primary clay mineral	hydrous mica	montmorillonite
Plasticity index $I_p$	11	208
Liquid limit $w_L$	31	257
Plastic limit $w_p$	20	49
Unified Soil Classification	CL	CH
Specific weight	2.76	2.75
Spec. surface area $m^2/g$	43-81	519-631
Free swell volume ml/g	<1	>9
optimum w.c % from Modified Proctor Test	12	10*

---

# Gas breakthrough testing – 10 MPa equipment



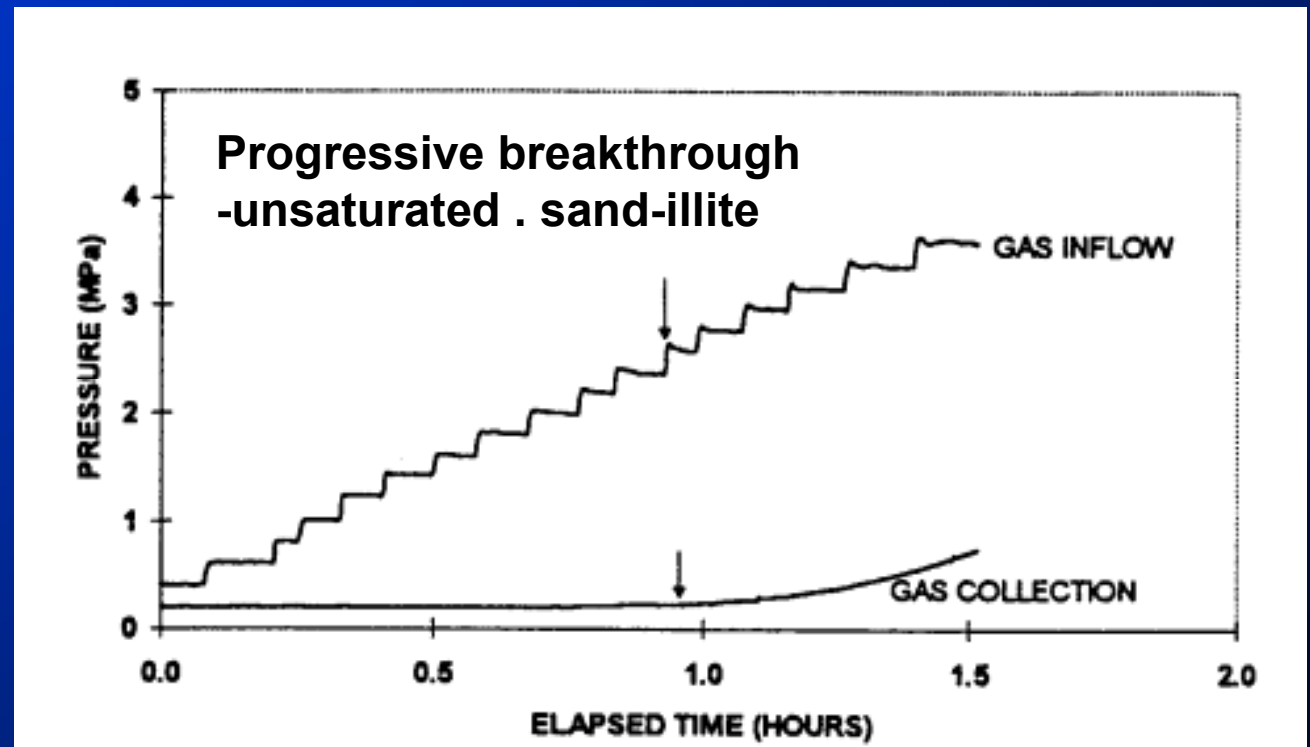
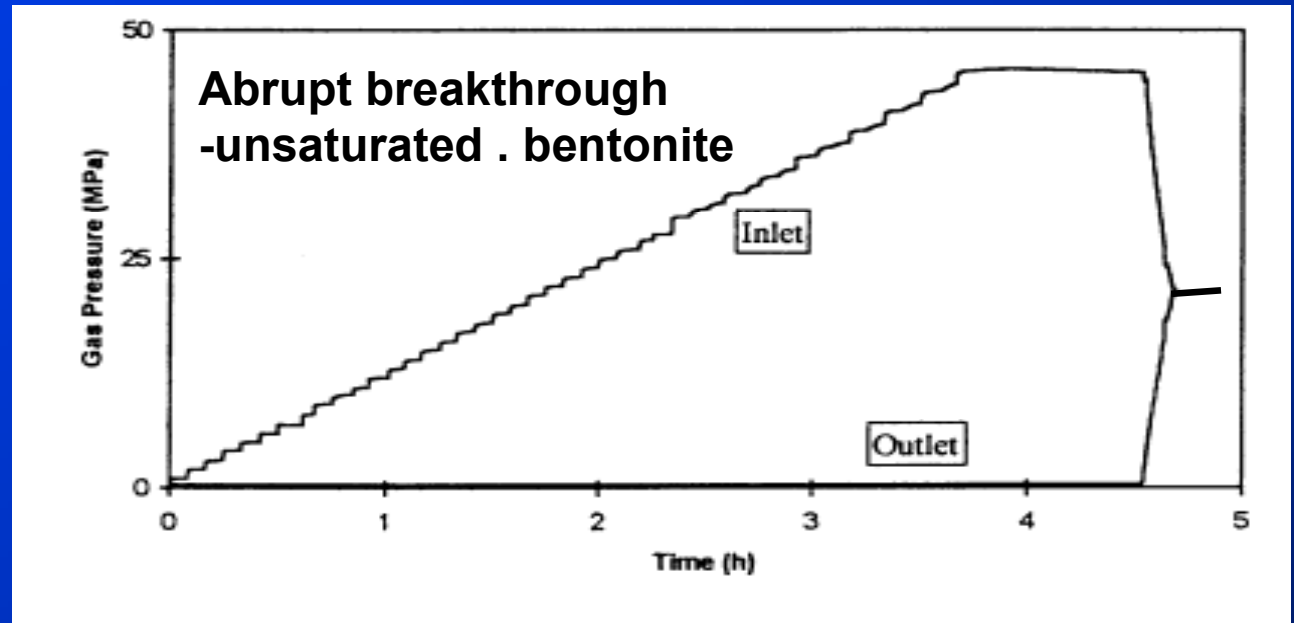
# Gas breakthrough testing – 50 MPa equipment



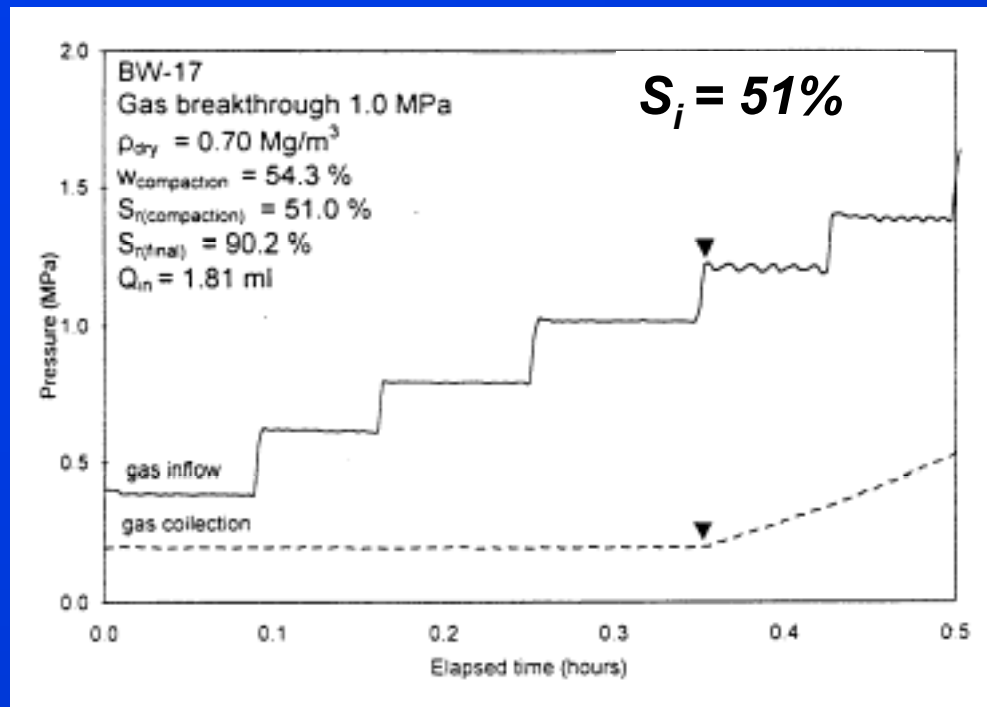
***'Incremental pressure tests: standardized pressure increments used to determine 'breakthrough pressure related to:***

- ***Initial dry density (specifically dry density of the clay phase)***
- ***material – illite, sand-illite, bentonite, sand-bentonite***
- ***some specimens tested at 'as-compacted' degrees of saturation***
- ***others given uptake of water at a controlled water back-pressure to produce high initial saturations.***

**Incremental loading tests (0.2 MPa/5 min)**

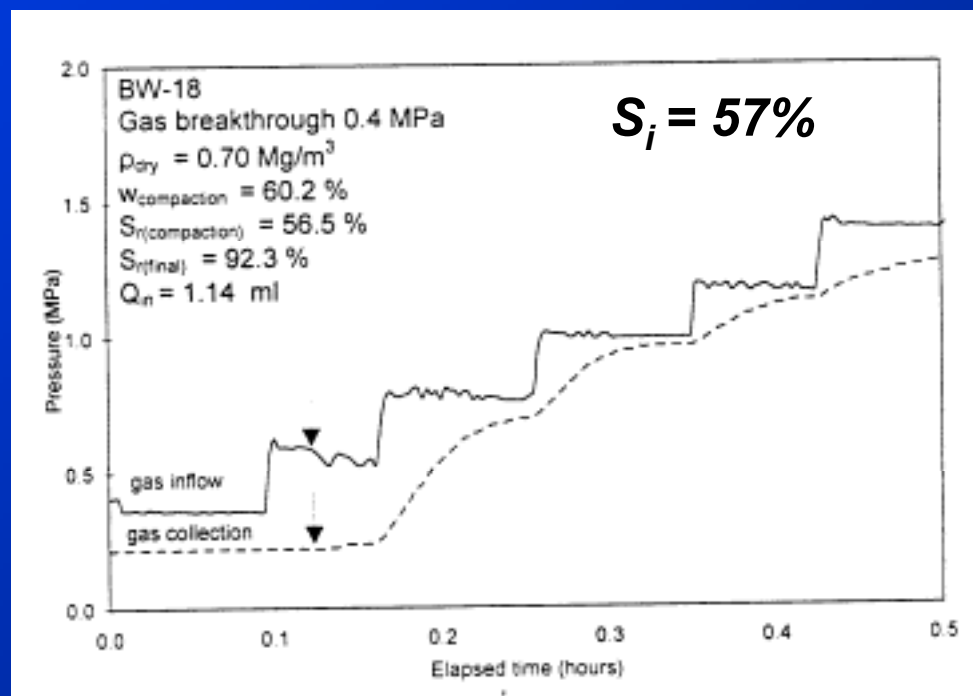


Kirkham 1995



*Same initial dry density but different water contents produce different initial saturations and pore size distribution – followed by back pressuring to  $S_f > 90\%$*

*- bentonite, with back pressuring – 1.0 MPa*



*‘Breakthrough’ at 0.4 MPa followed by time-dependent equalization of inflow and collection pressures.*

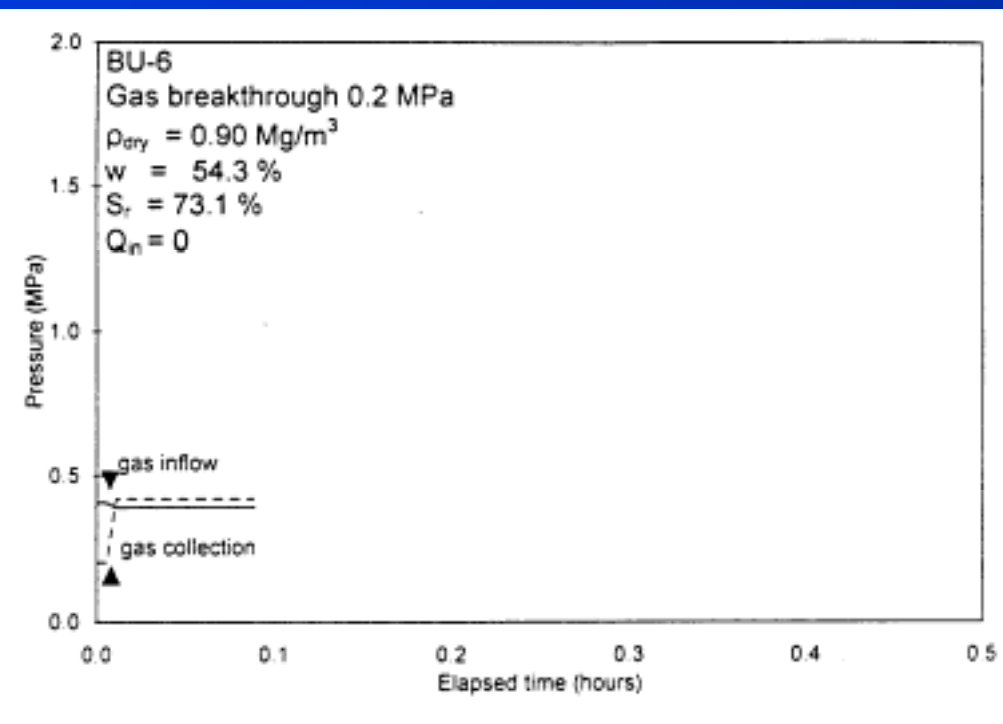
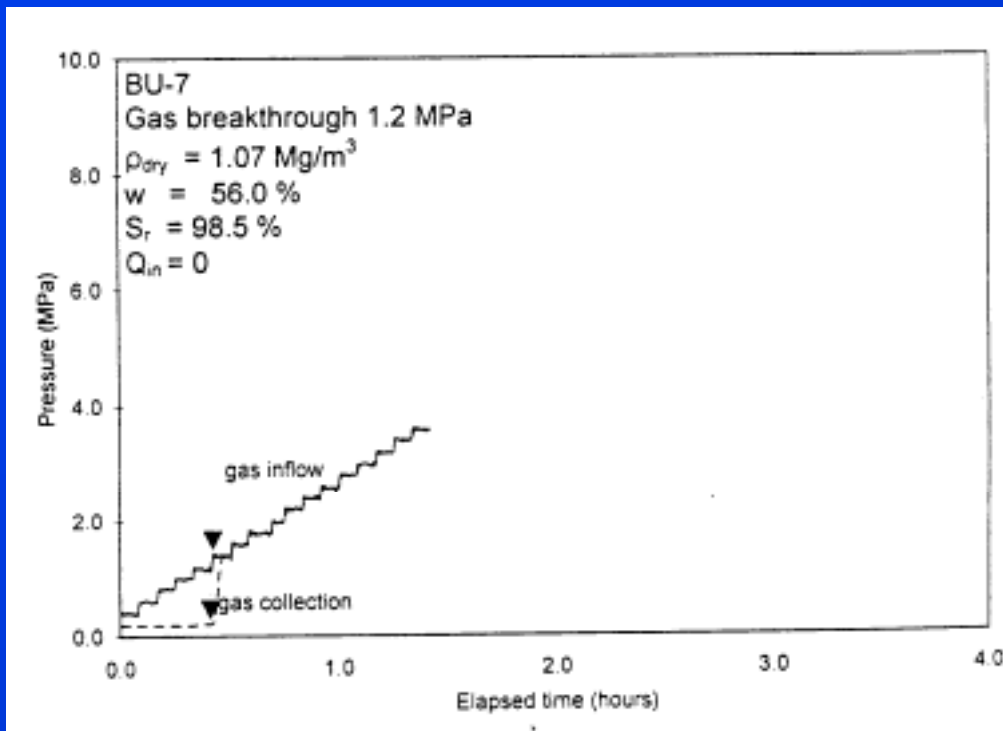
Halayko 1998

**Same water contents, but different dry densities and initial saturations**

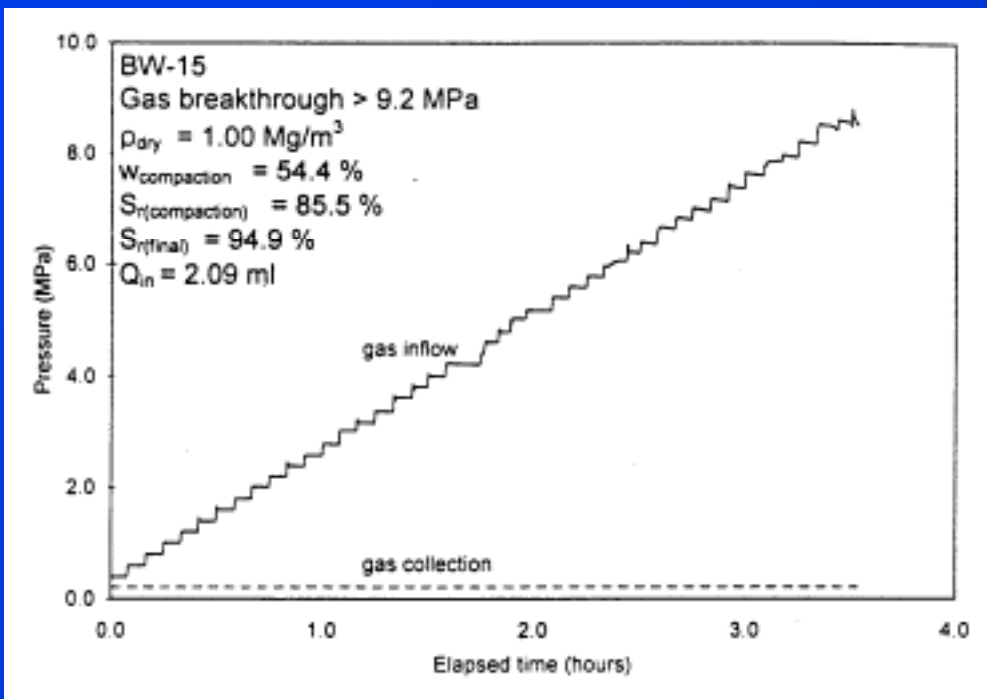
**– unsaturated bentonite without backpressure**

$$\gamma_i = 1.07 \text{ Mg/m}^3 \quad p_g = 1.2 \text{ MPa}$$

$$\bullet \gamma_i = 0.90 \text{ Mg/m}^3 \quad p_g = 0.2 \text{ MPa}$$

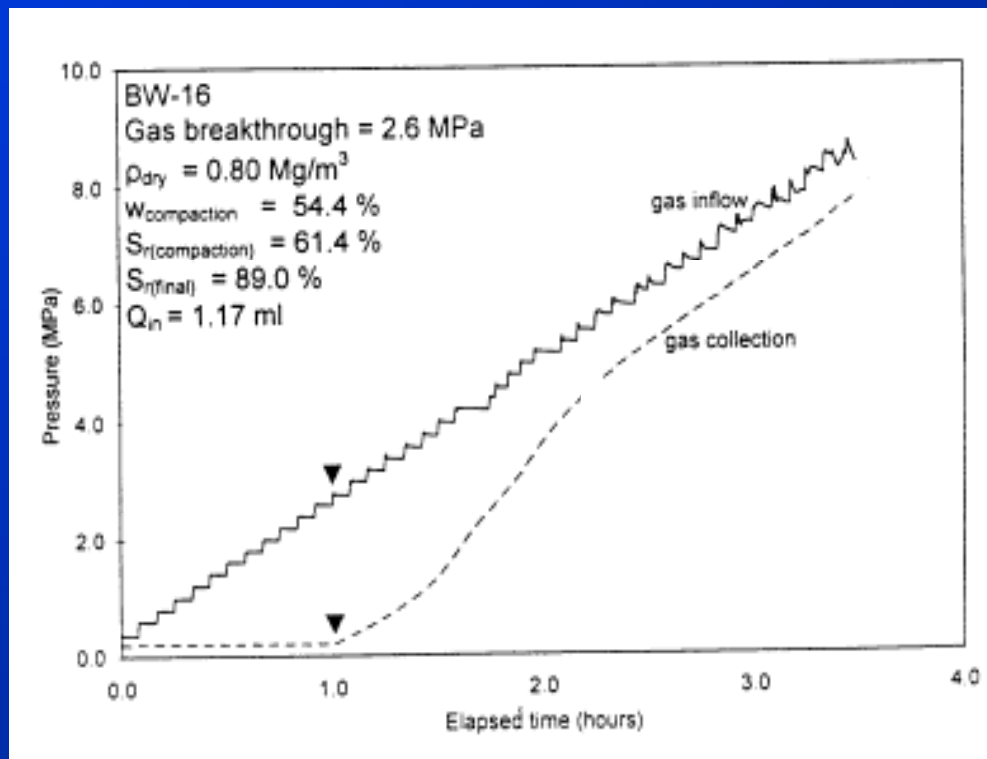


Halayko 1998



**Same initial water contents  
but different dry densities  
and initial saturations  
- bentonite, with  
backpressuring**

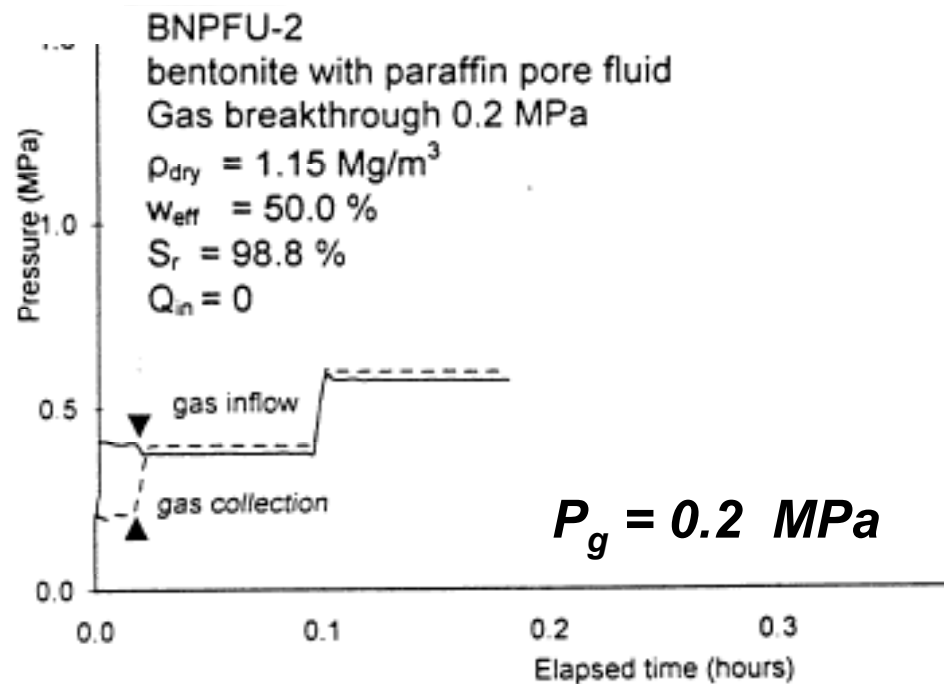
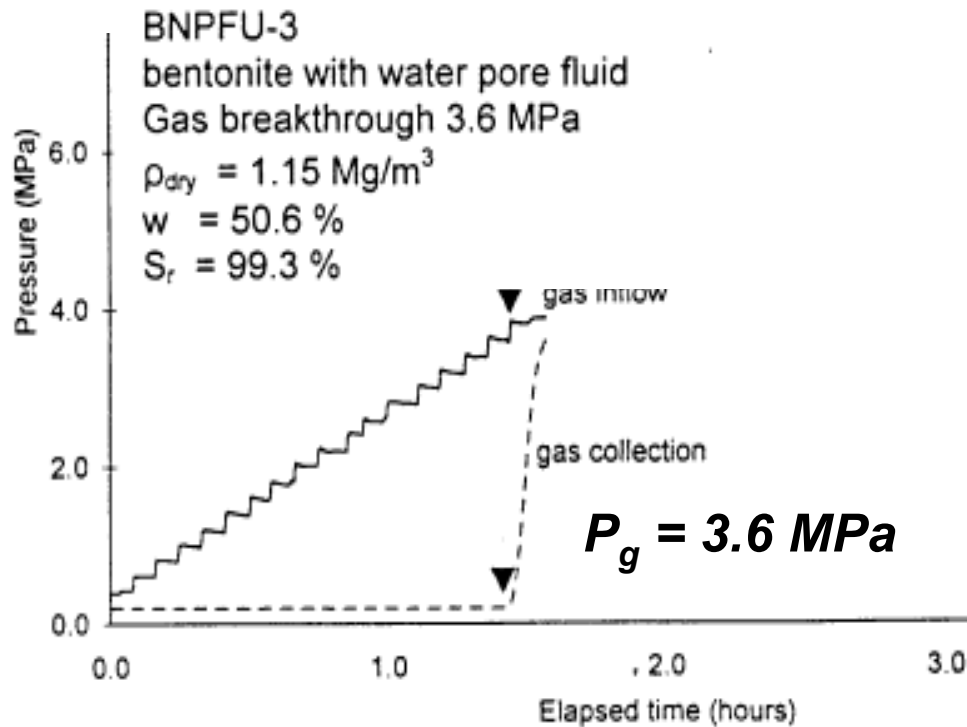
- $S_i = 86\%$ ,  $S_f = 95\%$   
 $p_g > 9.2 \text{ MPa}$



- $S_i = 61\%$ ,  $S_f = 89\%$   
 $p_g = 2.6 \text{ MPa}$

Halayko 1998



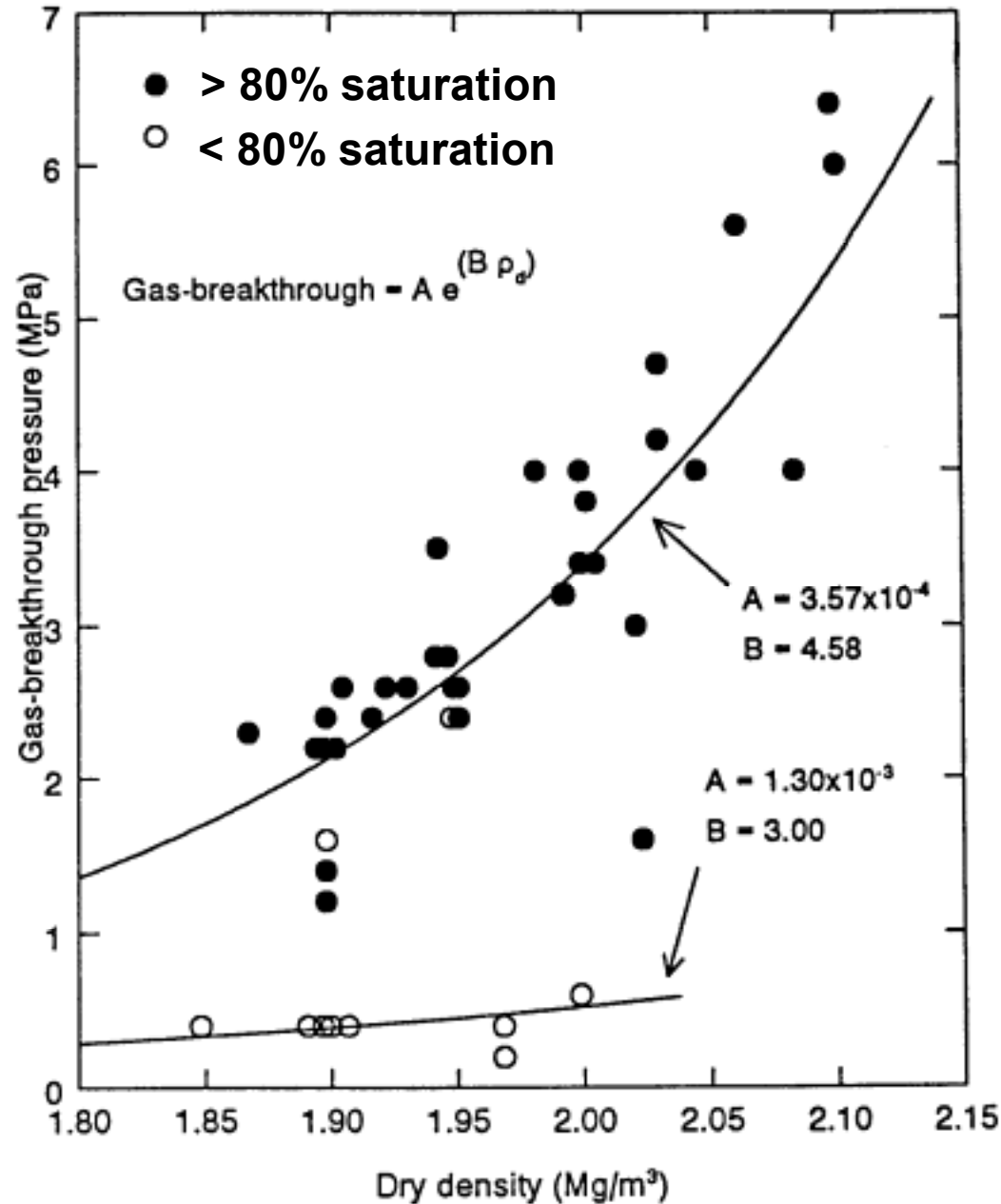


***Influence of pore-fluid chemistry:  
same initial dry density,  
fluid content, saturation.***

***- Pore fluid, water***

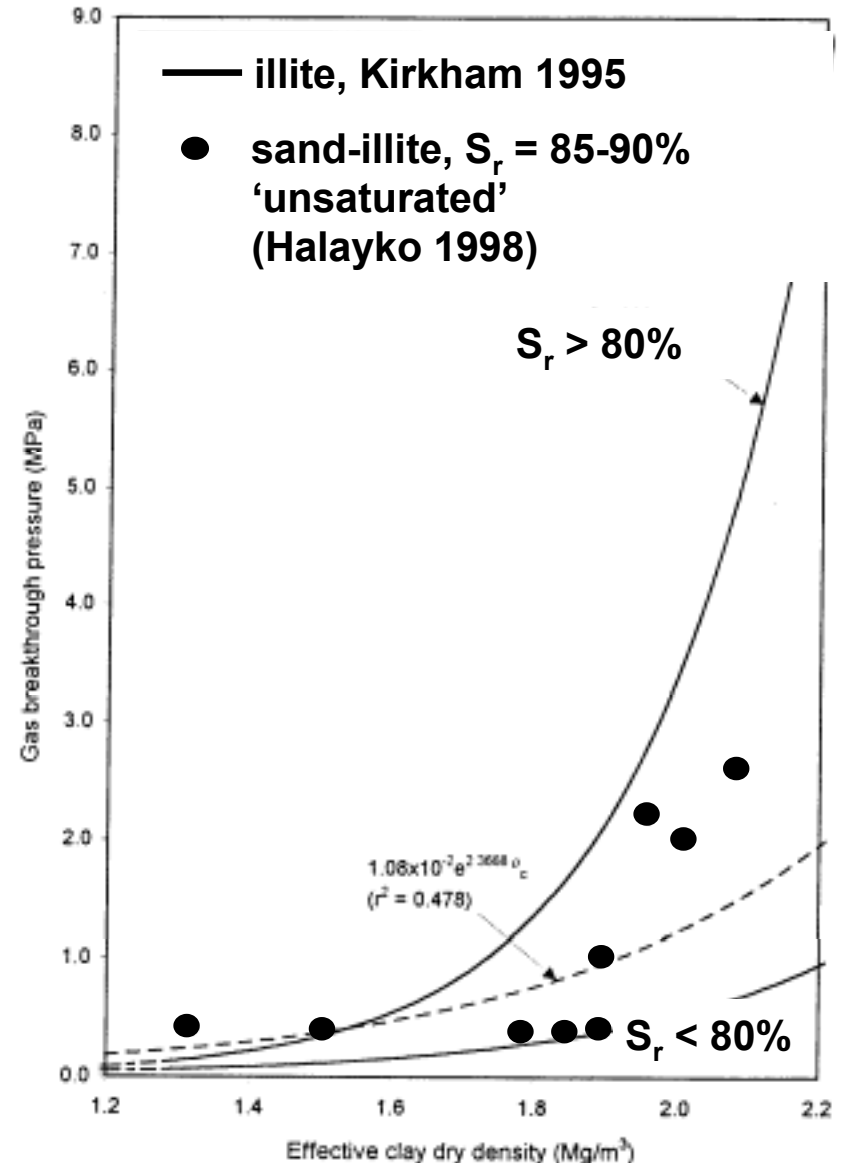
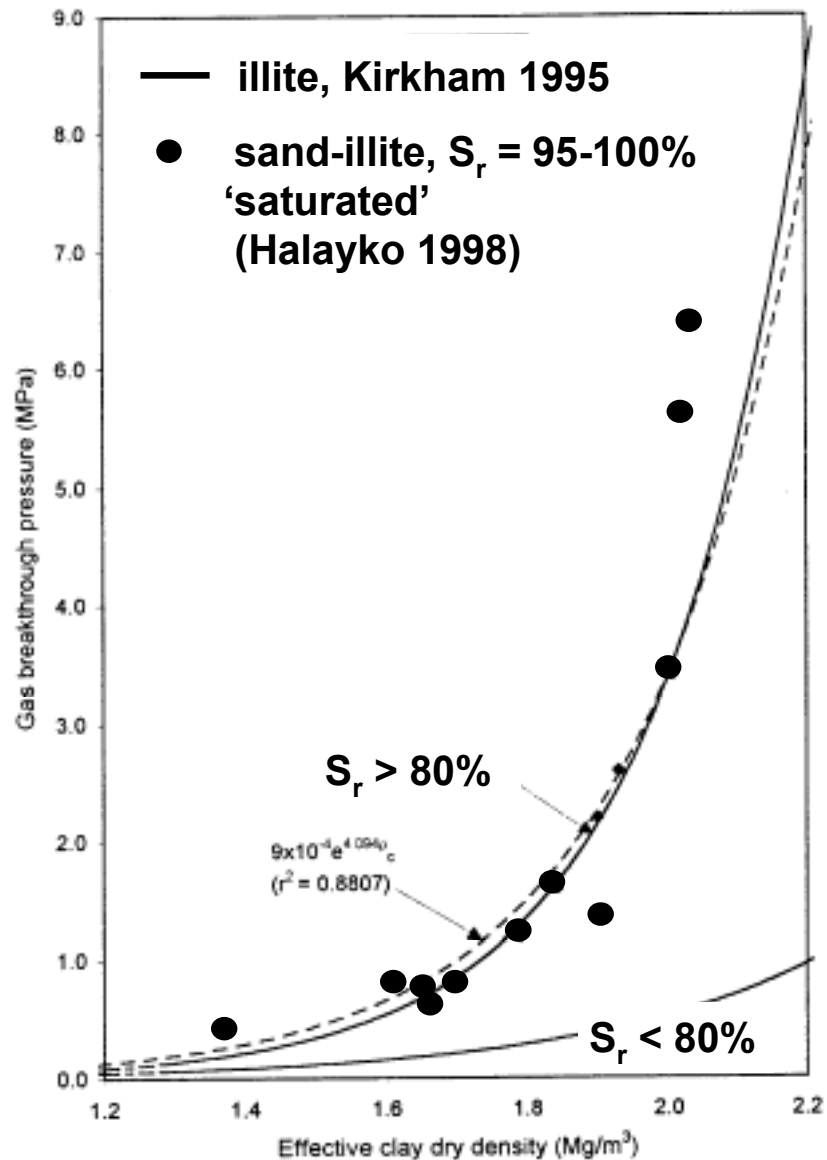
***- Pore fluid, paraffin***

Halayko 1998

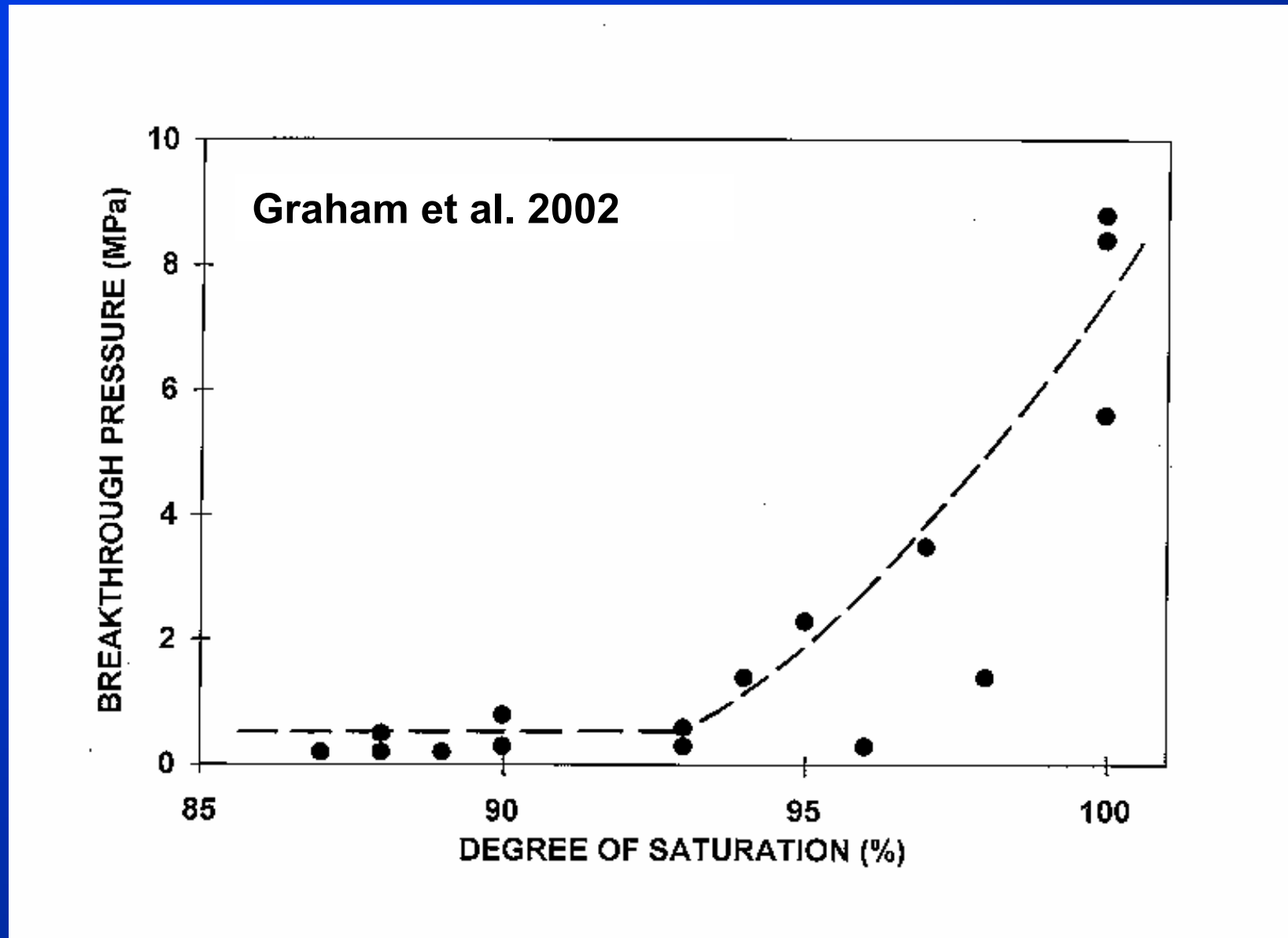


*Gas breakthrough pressure – dry density relationship in illite for saturations above and below 80% saturation (Gray et al. 1996)*

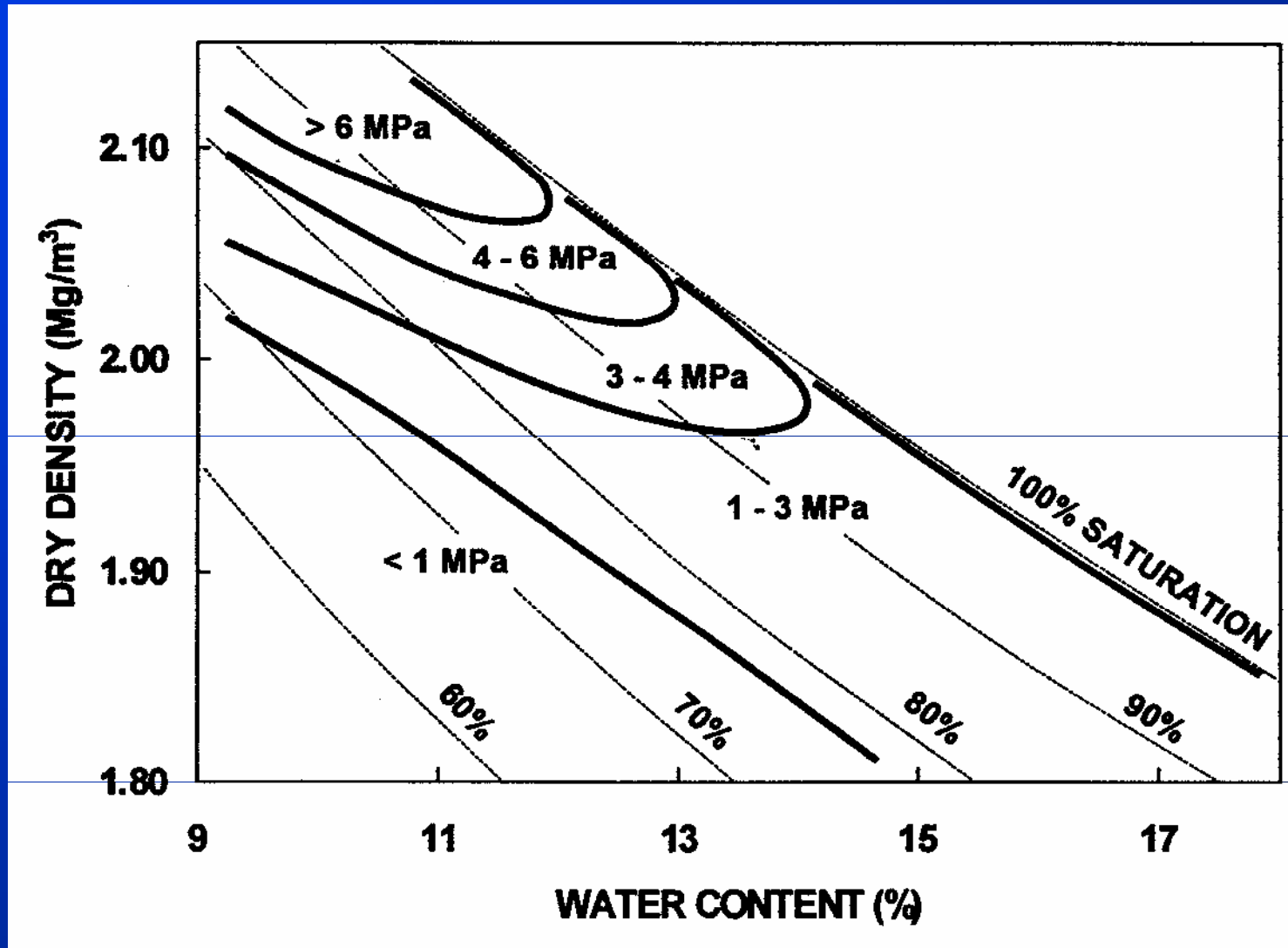
# Illite and sand-illite results consistent when plotted as breakthrough pressure vs. effective clay dry density



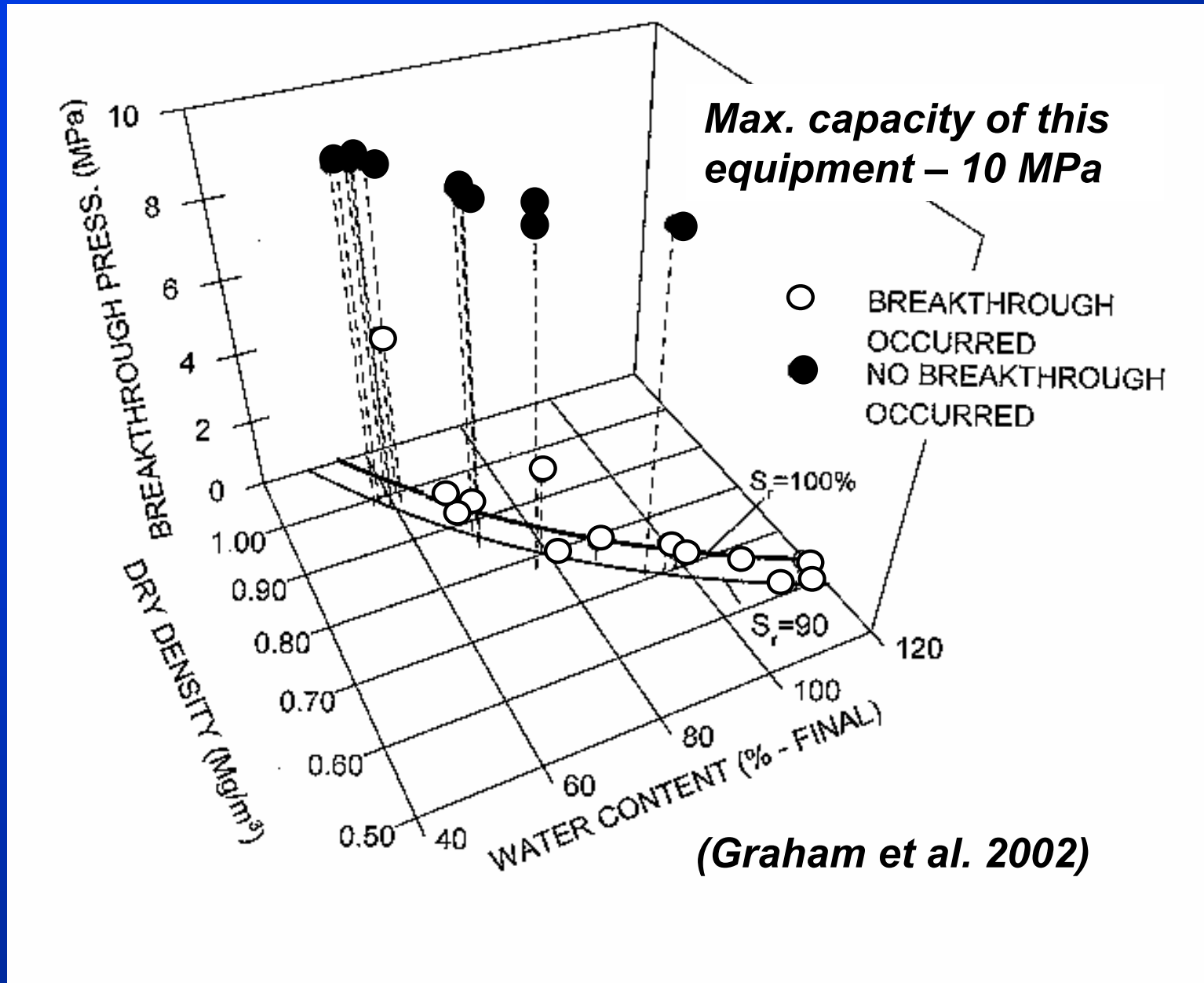
# *Breakthrough pressures from incremental pressure tests on bentonite as a function of degree of saturation*



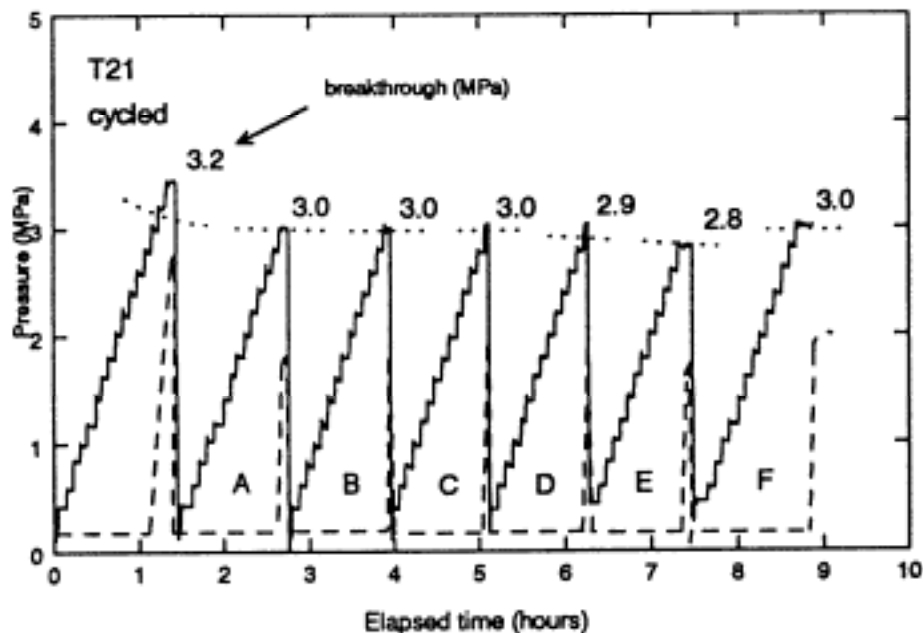
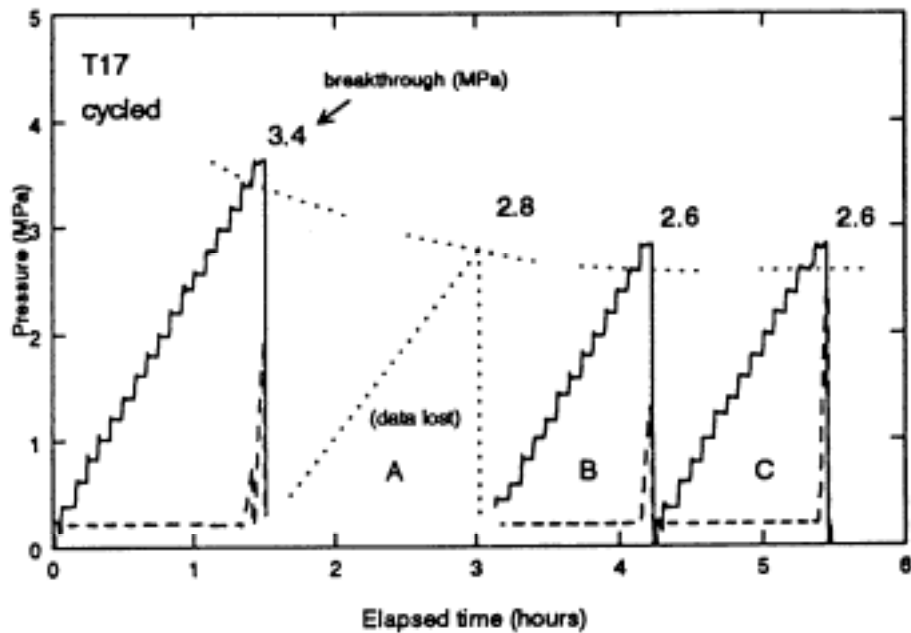
**Breakthrough pressures from incremental pressure tests on illite in terms of water content, dry density and degree of saturation. (Graham et al. 2002)**



# Breakthrough pressures from incremental pressure tests on illite in terms of water content and dry density







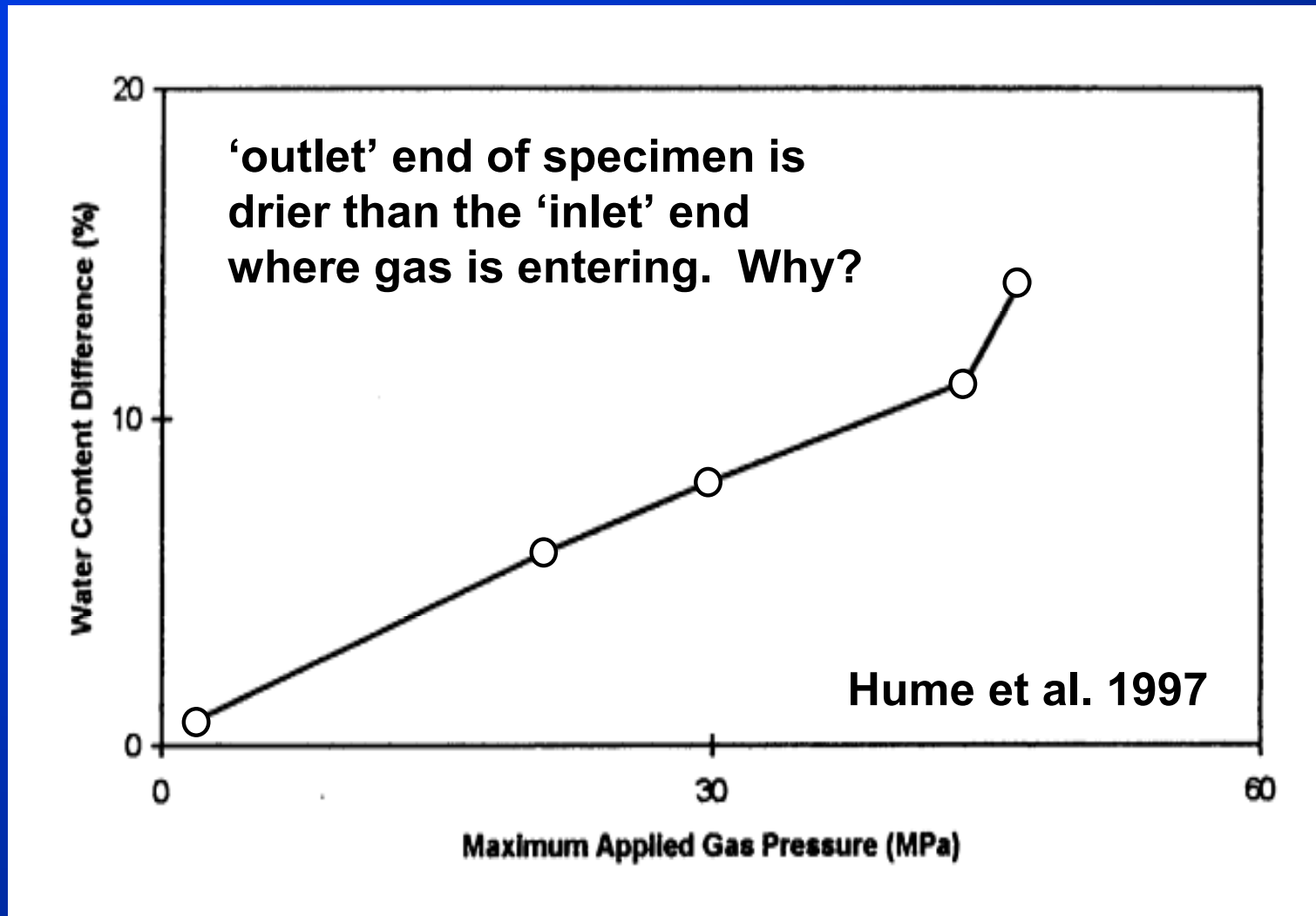
*Once breakthrough has occurred, what is the resistance to subsequent increasing pressures?*

- *pressure increase until breakthrough in compacted illite,*
- *pressure release,*
- *repeated pressure cycling*
- *self sealing.*

**Kirkham 1995**



**Differences in water content (inlet – outlet) related to gas pressure at end of test (bentonite  $\gamma_c = 1.10 \text{ Mg/m}^3$ )**



***What happens if a constant gas pressure difference is applied across the specimen?***

***Breakthrough times from 'constant pressure' tests on 'saturated' illite:***

Number	$S_r$ %	$p_b$ (MPa)	time $t_b$ (hours)
1	97.2	0.8	>336
2	96.9	1.8	22.7
3	96.9	2.8	0.3
4	97.2	2.8	0.2

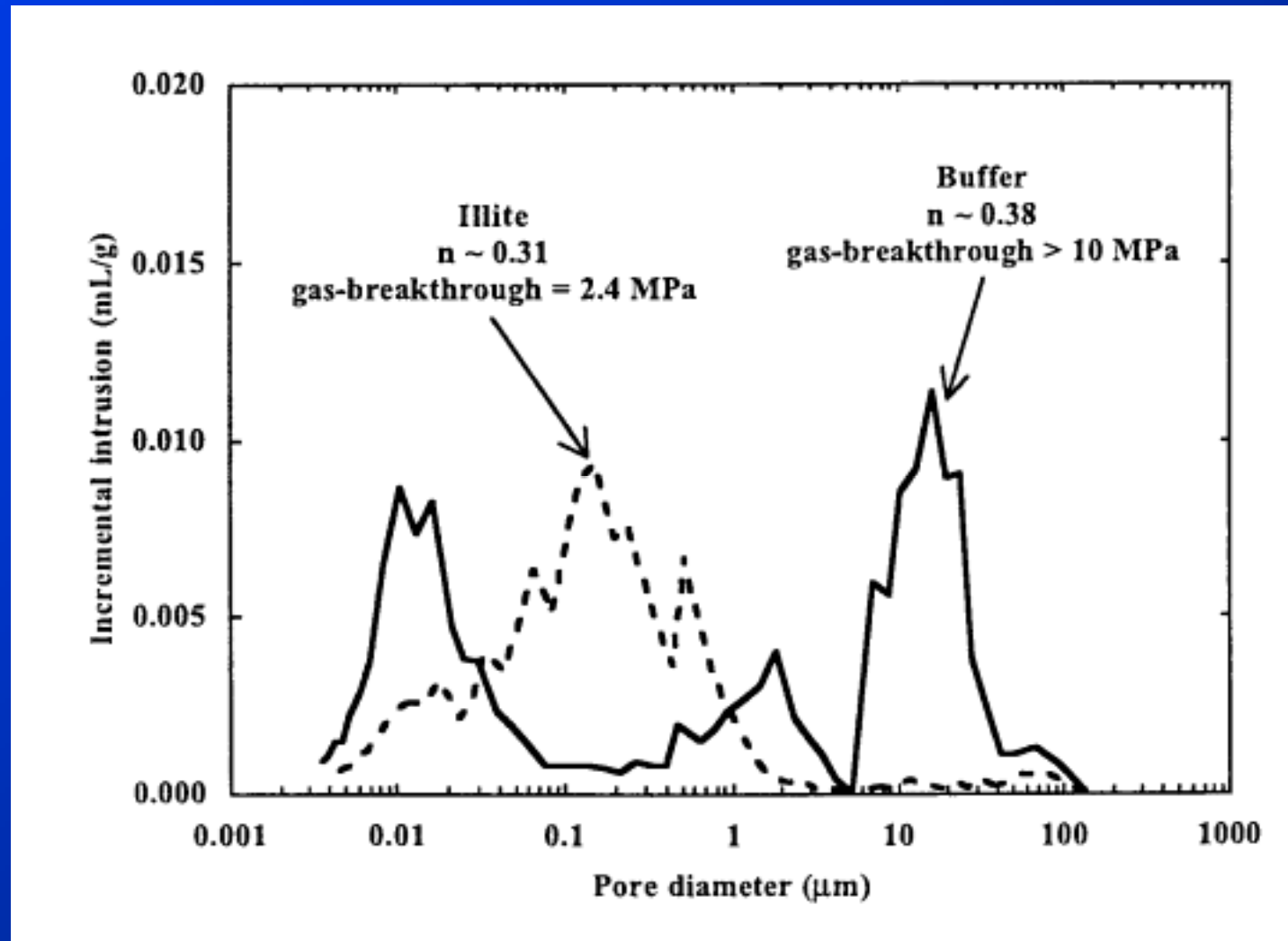
***Breakthrough times decrease with increasing pressure difference (hydraulic gradient).***

*The tests appear to produce results that depend on the test procedures – clearly not a fundamental study of the processes involved.*

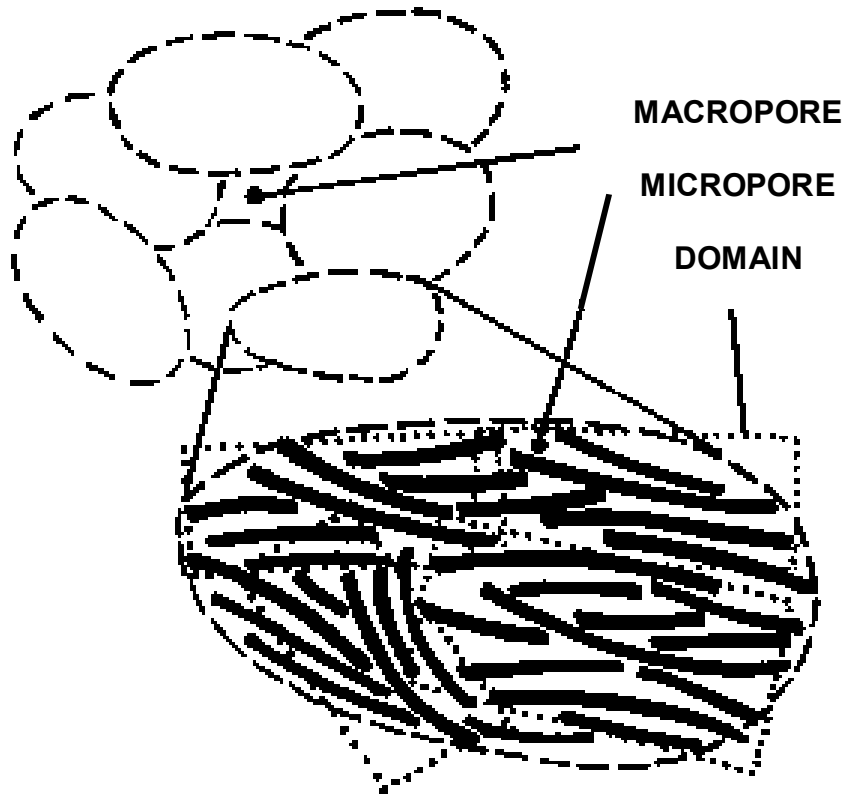
*The rest of this presentation deals with:*

- *pore size distributions*
- *effective stresses in the specimens*
- *capillarity and advection*
- *results from ‘CONSTANT PRESSURE’ tests*

# *Pore size distributions - Compacted illite and bentonite specimens*

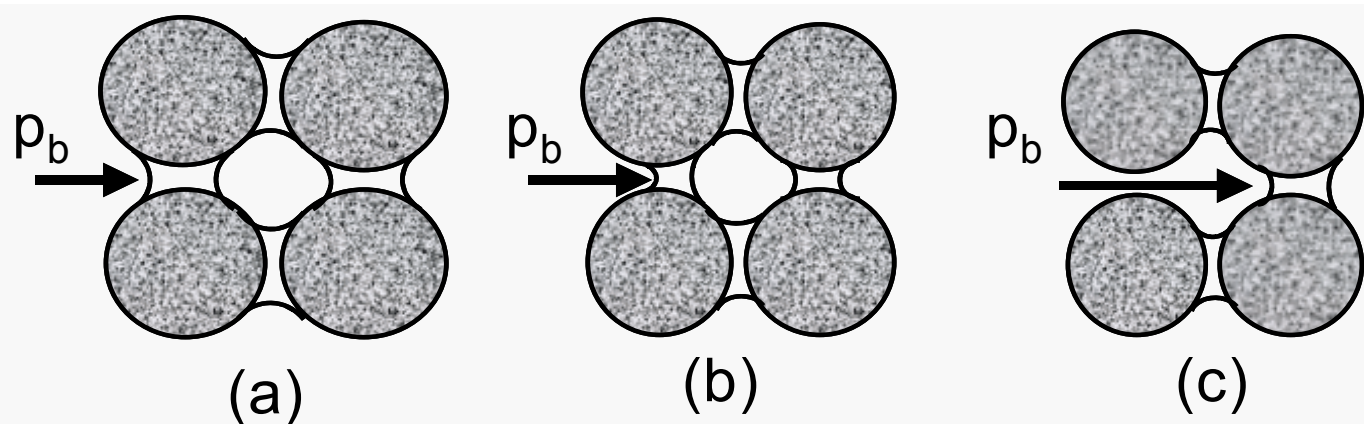


Gray, Kirkham, Wan, Gray 1996

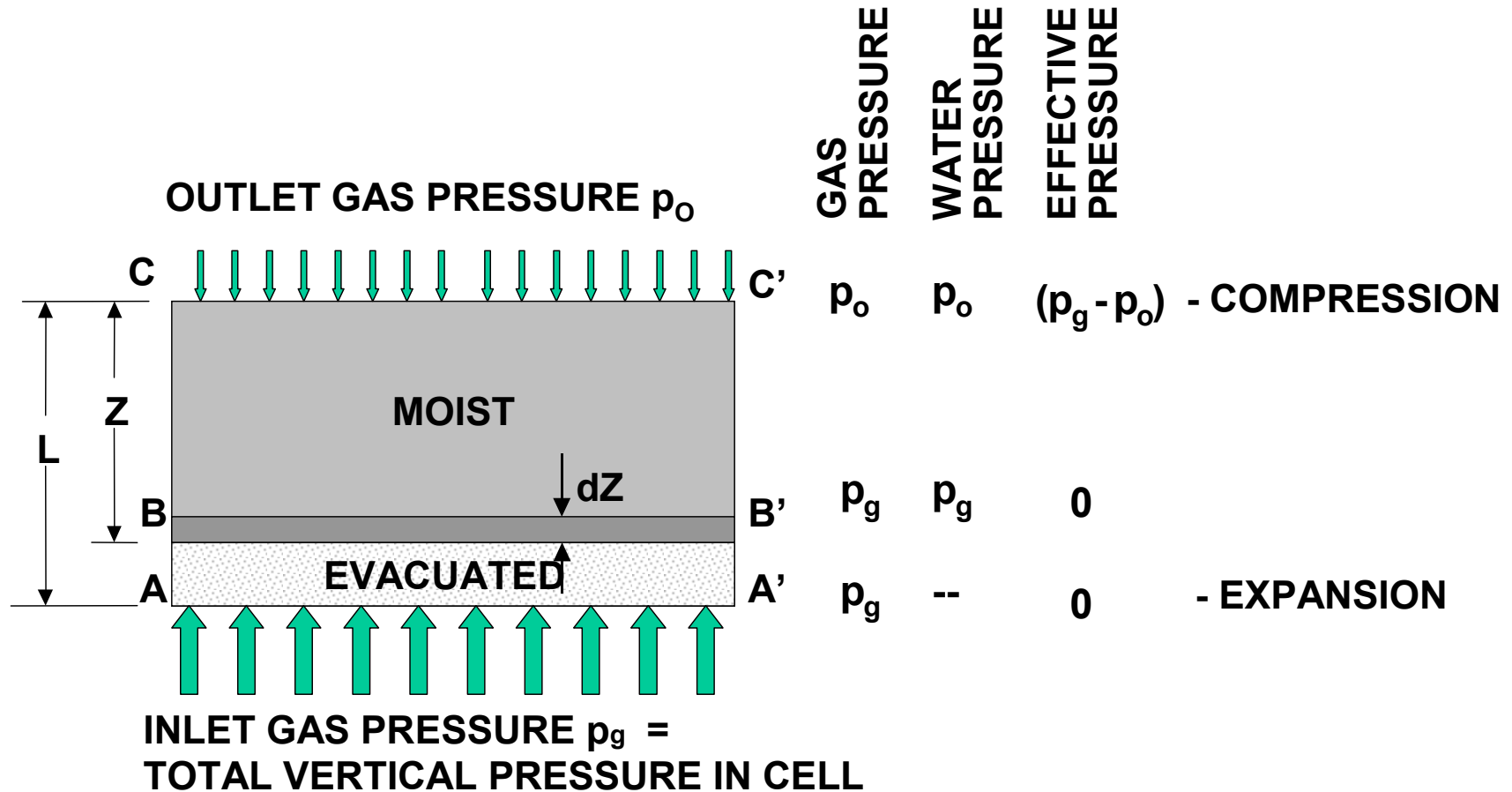


**(1) Pedal structures, bi-modal PSDs, macropores and micropores**

**(2) 'Gas entry' pressure, capillarity-advective flow (Bannister, Graham, Gray 2000).**



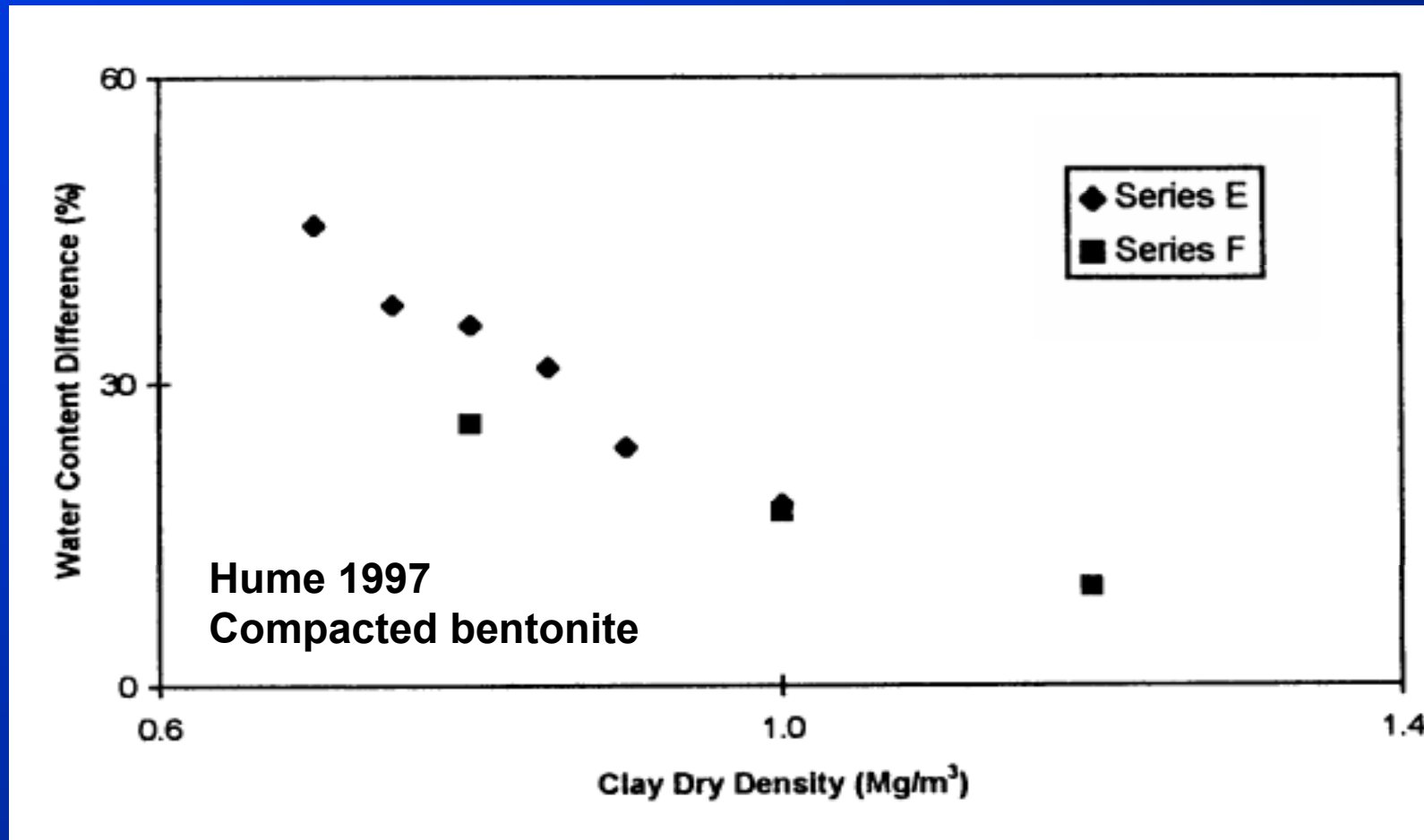
# Gas, water and effective pressures in a partly evacuated specimen



***Another example of the gas inlet end of the specimens being wetter than the outlet end.***

***- at inlet, low effective stress = swelling***

***- at outlet, higher effective stress = compression***


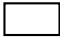




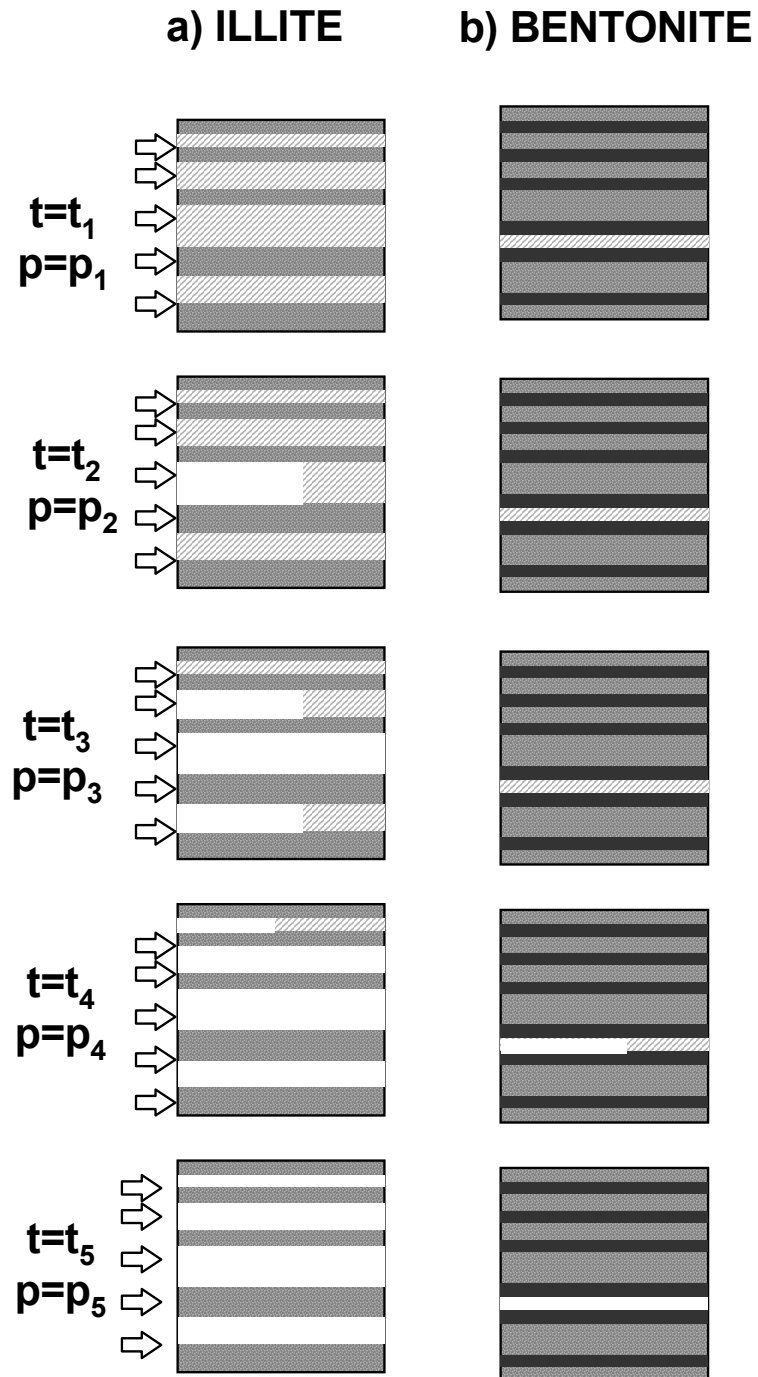
## *Simplified model for gas breakthrough*

- **Below a certain degree of saturation, continuous gas channels are present and resistance to breakthrough is minimal.**
- **When the gas phase is not continuous, gas has to overcome capillarity to enter pores. Below a 'Gas Entry Value' breakthrough will not occur.**
- **Gas pushes water advectively through larger pores until a continuous pore channel is formed.**
- **This permits gas breakthrough.**

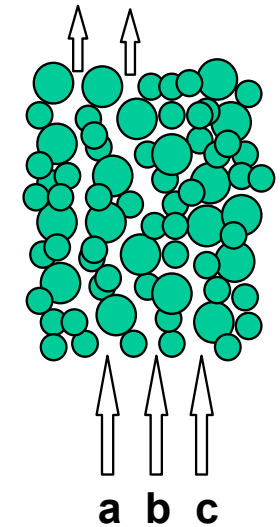


**Simplified representation of pore structures:**  
**a) illite,**  
**b) bentonite,**  
**c) open and occluded channels**

 soil matrix  
 gas  
 water  
 bound water



**c) OPEN AND OCCLUDED CHANNELS**



## **CAPILLARITY :**

***Gas must be able to get into the (larger) pore spaces***

***Gas Entry Value  $GEV = 2T_s/r$***

***Where  $T_s$  = surface tension,  $r$  = radius. But which radius in material with variable pore size distribution?***

## **ADVECTION:**

***As gas extrudes water, the hydraulic gradient increases and the progression of the gas-water interface accelerates***

$$t_b = \frac{L^2 \gamma_w n}{2kp}$$

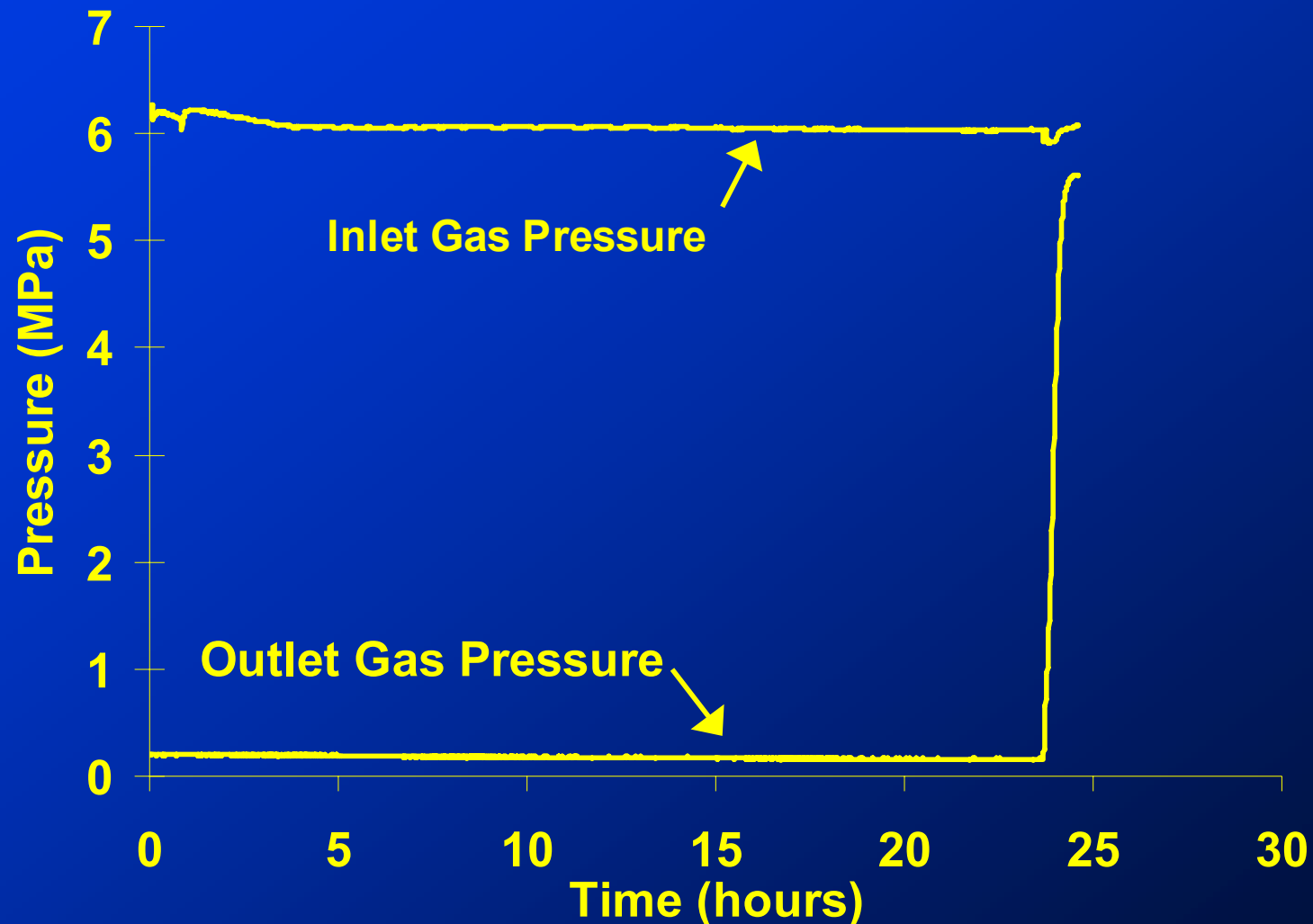
***$t_b$  = time to breakthrough***  
 ***$n$  = porosity***  
 ***$k$  = hydraulic conductivity***  
 ***$p = p_g - p_w$  = pressure difference***

## ***'Constant pressure' tests to determine***

- ***the relationship between pressure and 'time to breakthrough'***
  - constant pressure tests under higher gradients for different dry densities and degrees of saturation
- ***degree of saturation at which the gas phase becomes continuous***
  - constant pressure tests under low pressure gradients.

## Constant pressure tests:

- typical results from a Constant Pressure Test
- sand-bentonite, (Bannister et al. 2000)

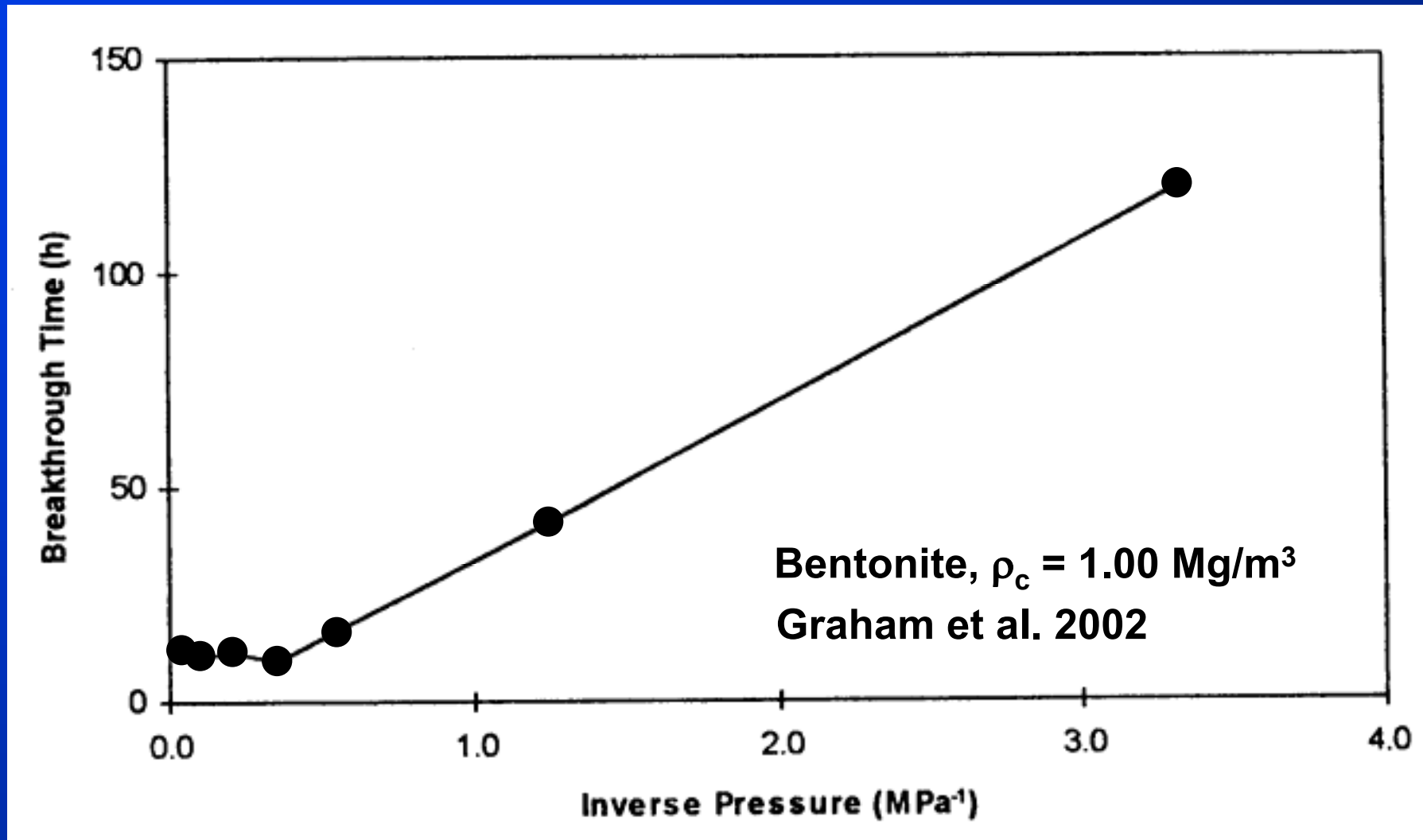


## *Range of parameters in Constant Pressure Test Program*

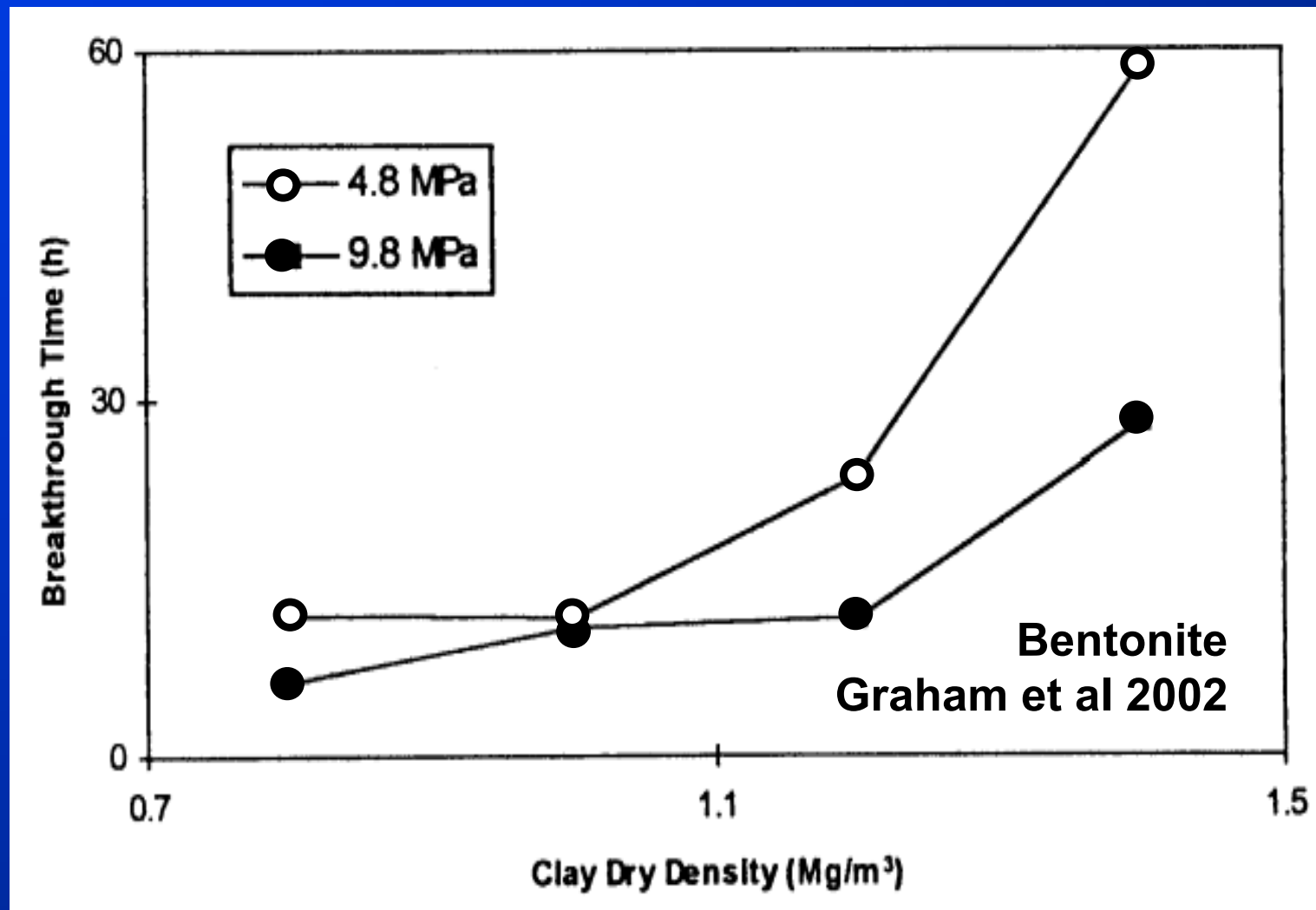
Degree of Saturation %	Dry density Mg/m <sup>3</sup>		
	1.6	1.7	1.85
80	n/a	n/a	2, 4, 6, 8*
85	n/a	n/a	2, 4, 6, 8
90	n/a	n/a	2, 4, 6, 8
95	2, 4, 6, 8	2, 4, 6, 8	2, 4, 6, 8
100	2, 4, 6, 8	2, 4, 6, 8	2, 4, 6, 8

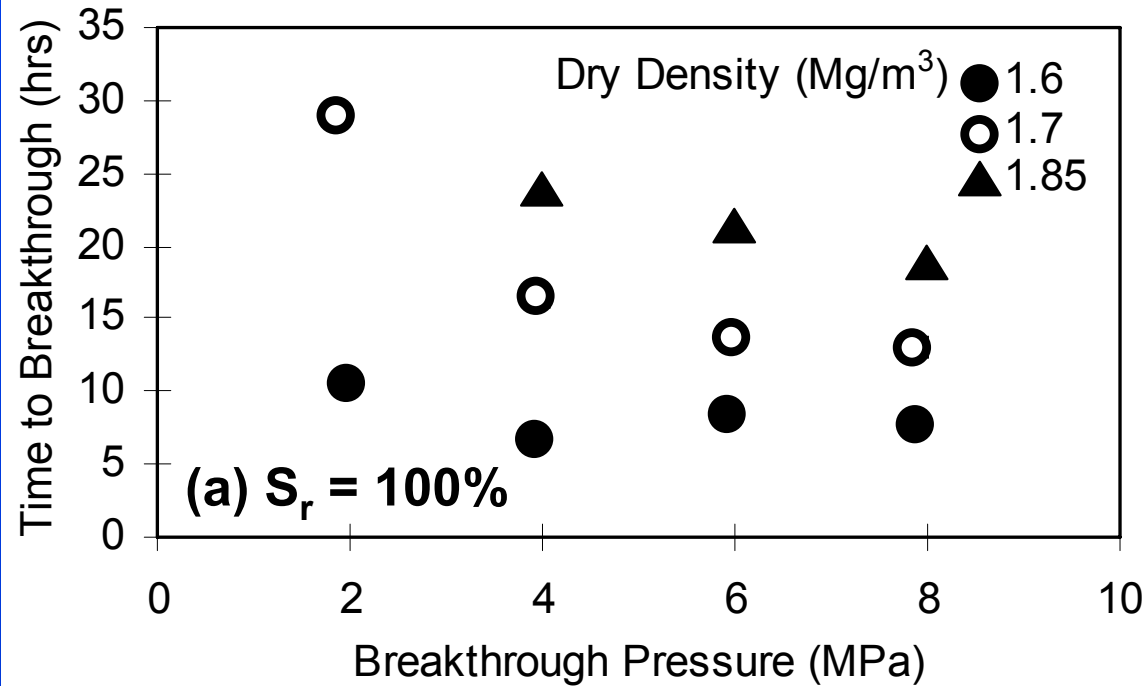
***\* The numbers in the cells denote the applied pressure differences in MPa***

- Relationship between breakthrough time and (pressure)<sup>-1</sup>**
- bentonite,  $\gamma_c = 1/00 \text{ Mg/m}^3$
  - high pressure difference = small (pressure)<sup>-1</sup> = short time



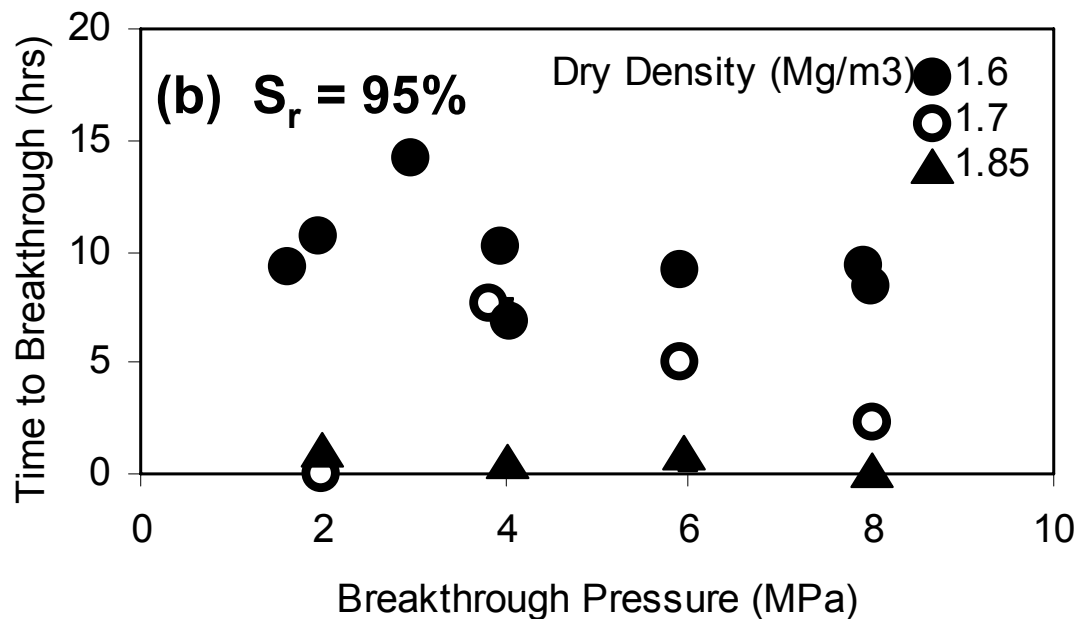
- Breakthrough times for 'constant pressure' tests at various effective clay dry densities – 2 pressure differences**
- higher clay densities = longer breakthrough times
  - higher pressure differences = shorter breakthrough times





***Time – Pressure  
Difference  
relationship***

***Bentonite - ‘constant  
pressure’ tests***

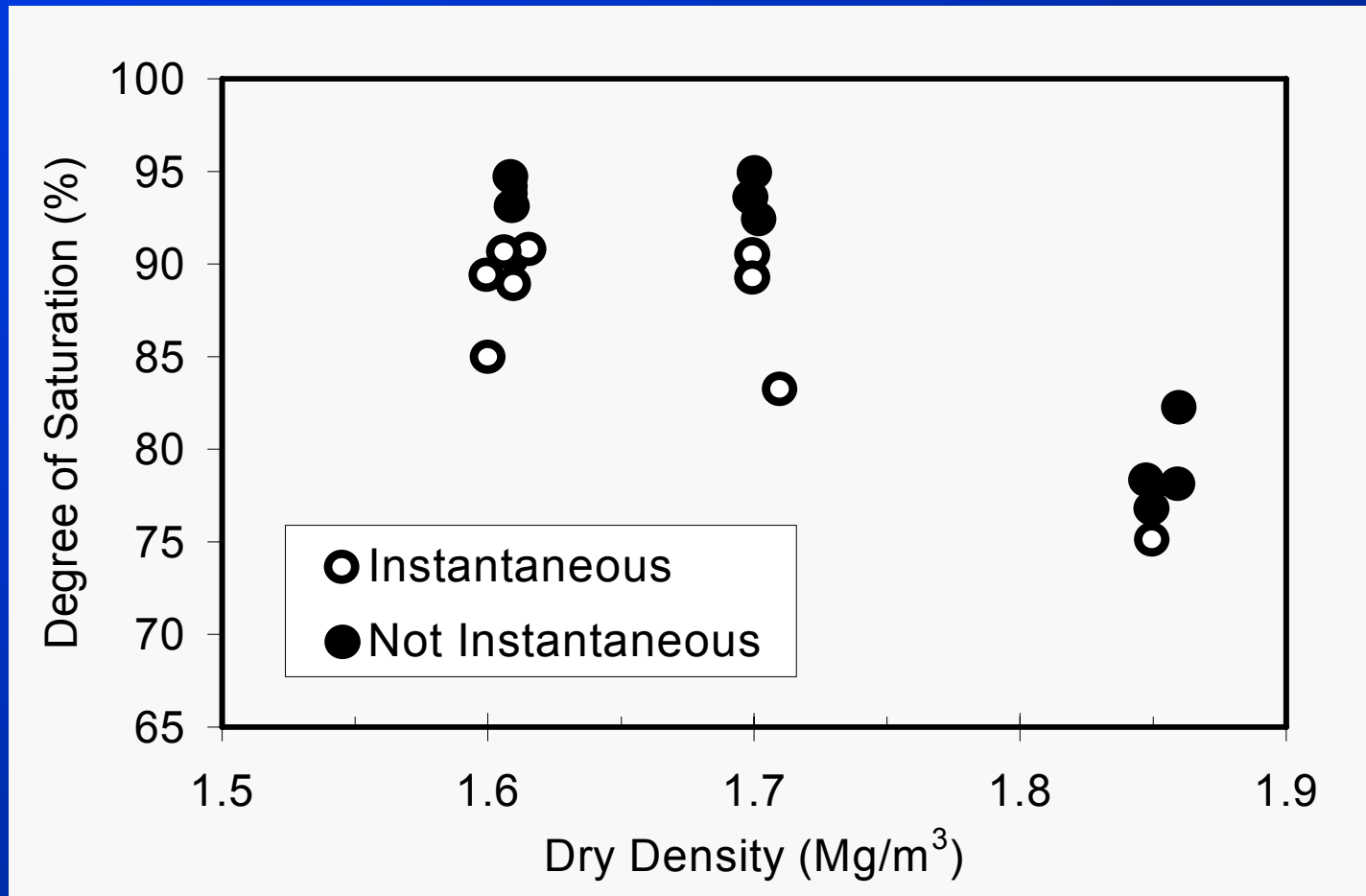


***Time to breakthrough  
is approximately  
inversely proportional  
to pressure difference***

**Bannister et al. 2000**

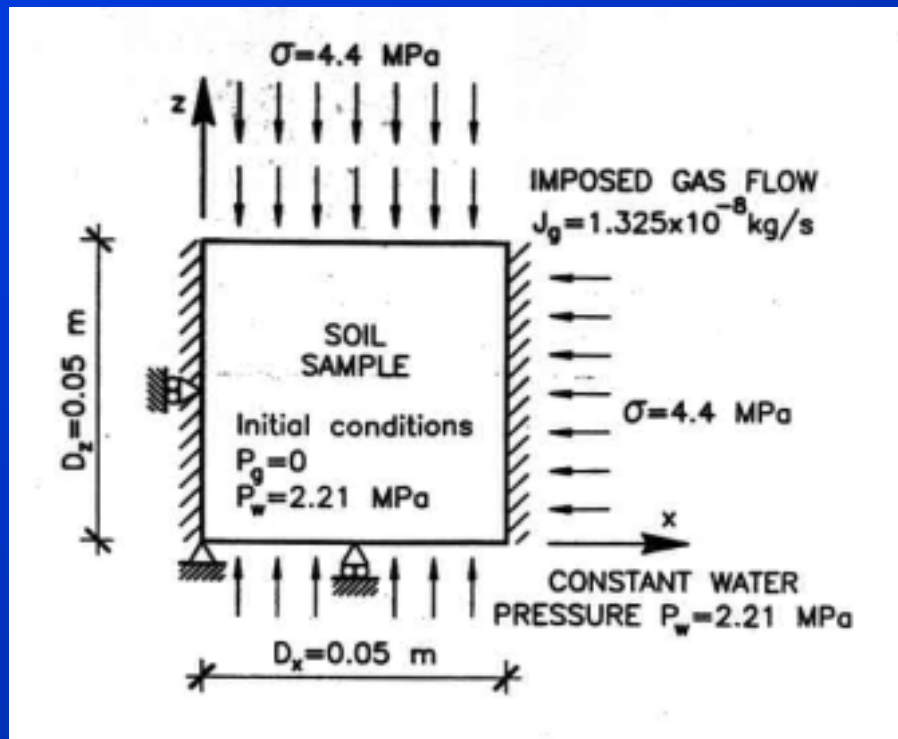


**Summary of breakthrough results from constant-pressure tests at different degrees of saturation  
- sand-bentonite,  $p_g = 0.2$  MPa**

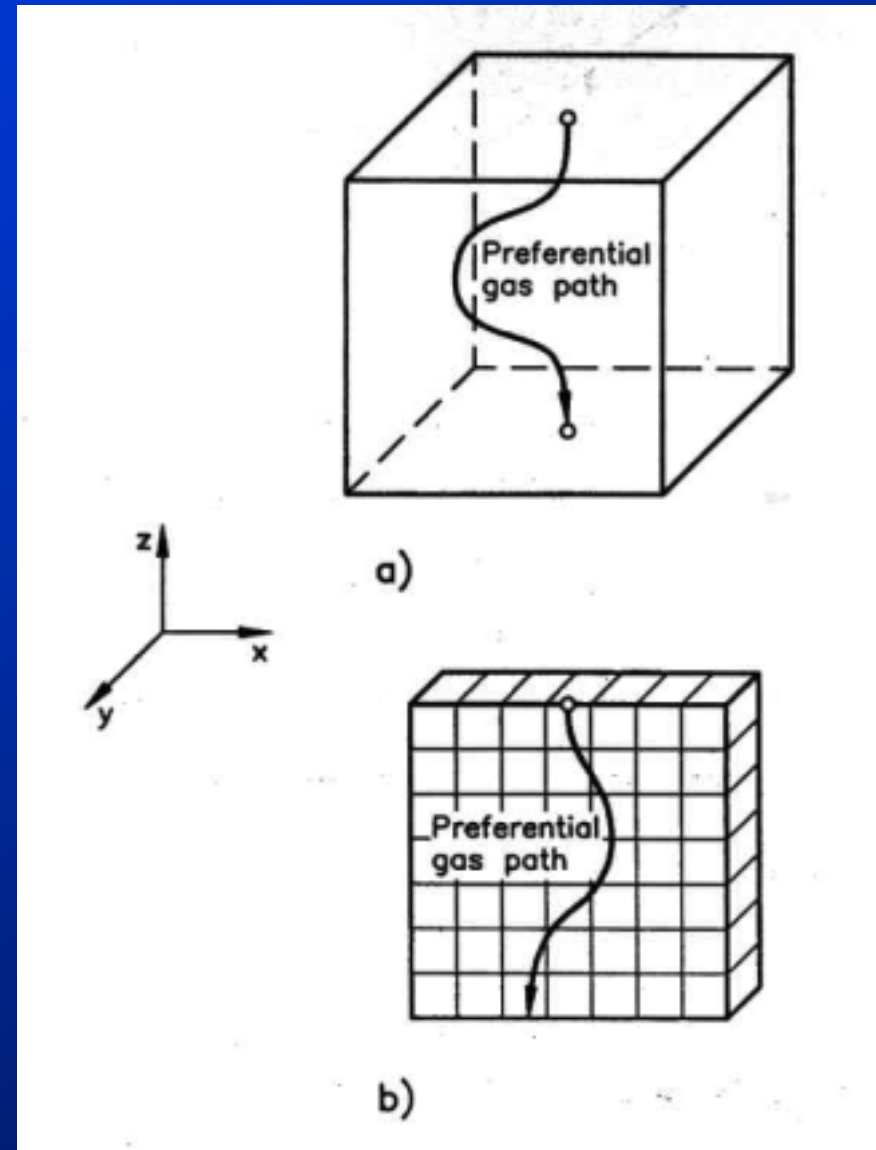


***(Bannister , Graham and Gray al. 2000)***

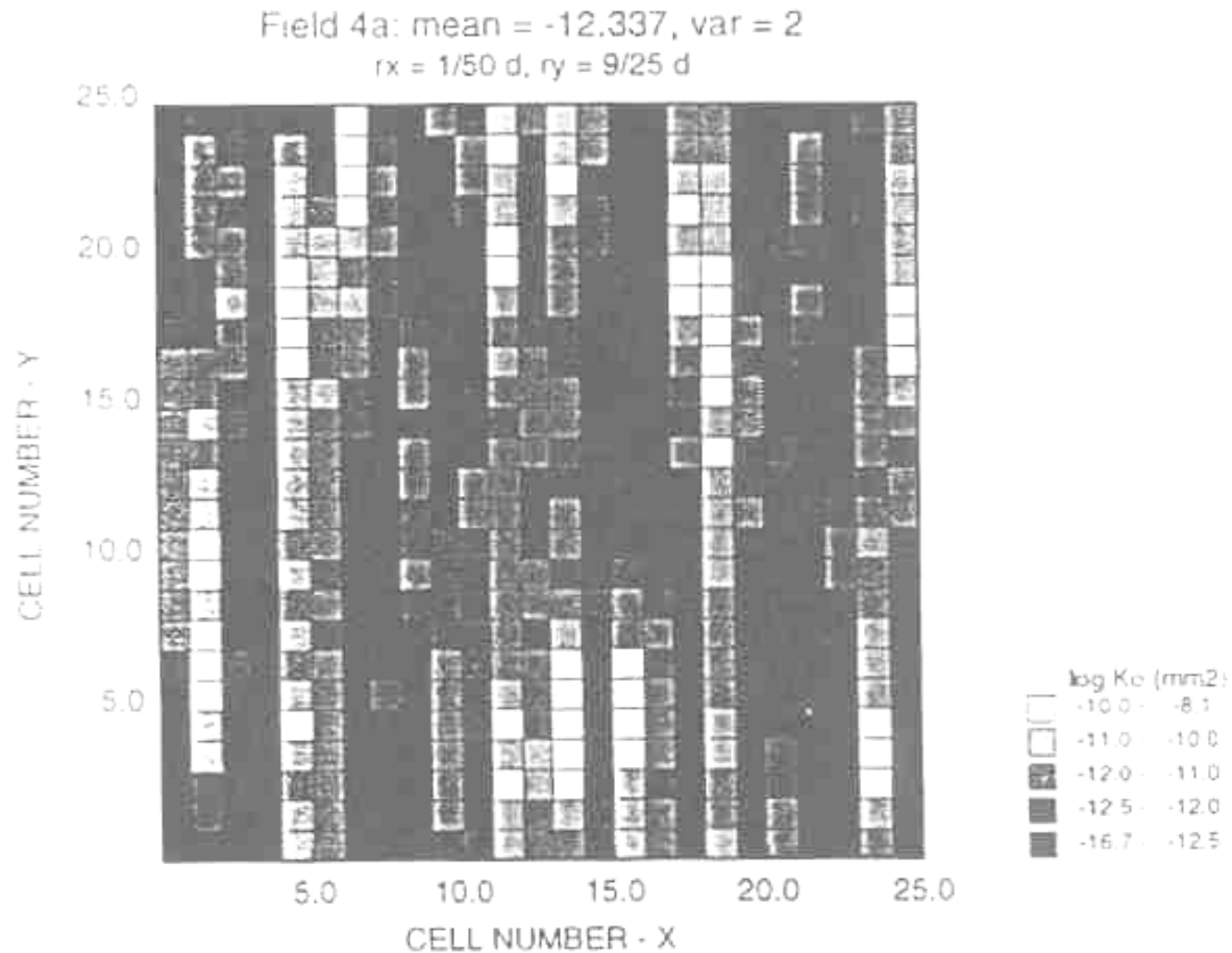
**Simulation of soil heterogeneity and preferential paths for gas migration (Delahaye and Alonso, 1998).**



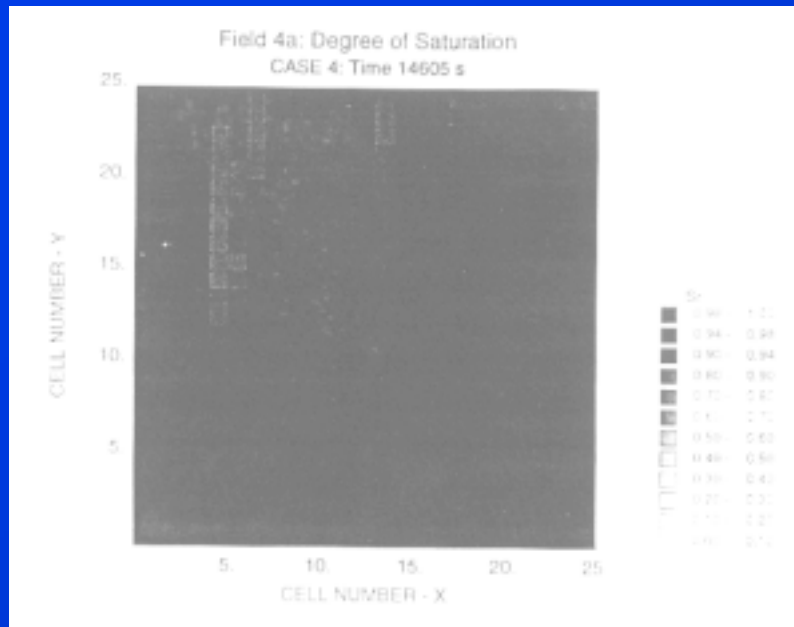
**Problem definition**



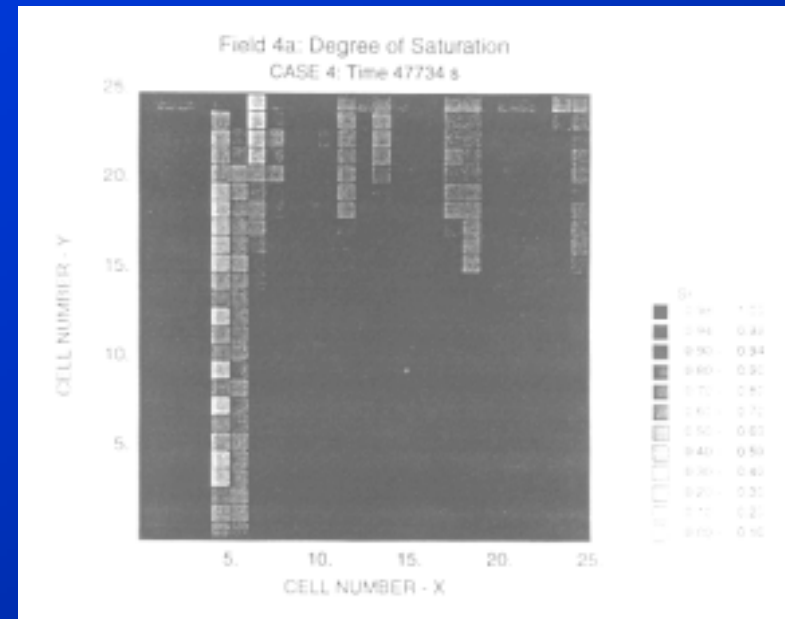
**Preferential path in a heterogeneous sample**



***Random intrinsic permeability fields  
(Delahaye and Alonso, 1998).***

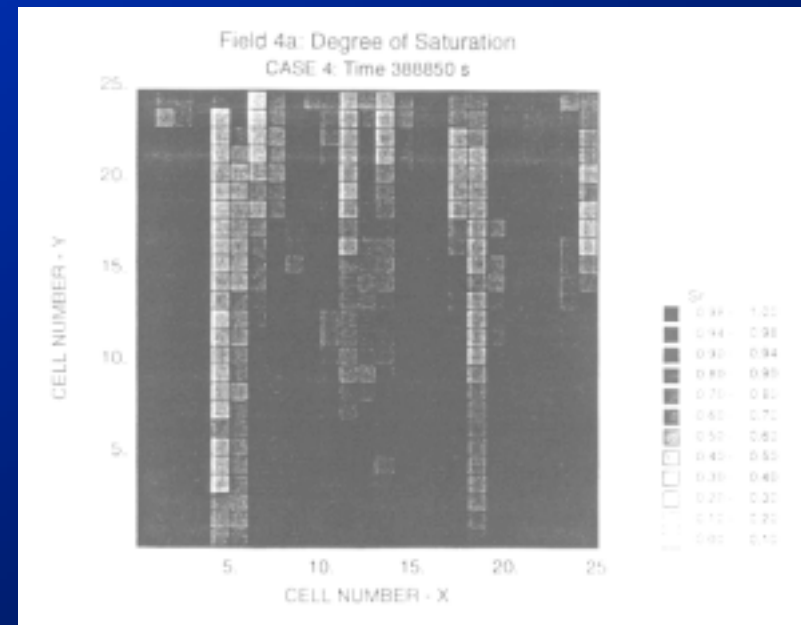


**(a) Time = 4 hours**



**(b) Time = 13 hours**

**Preferential path formations (Delahaye and Alonso, 1998).**



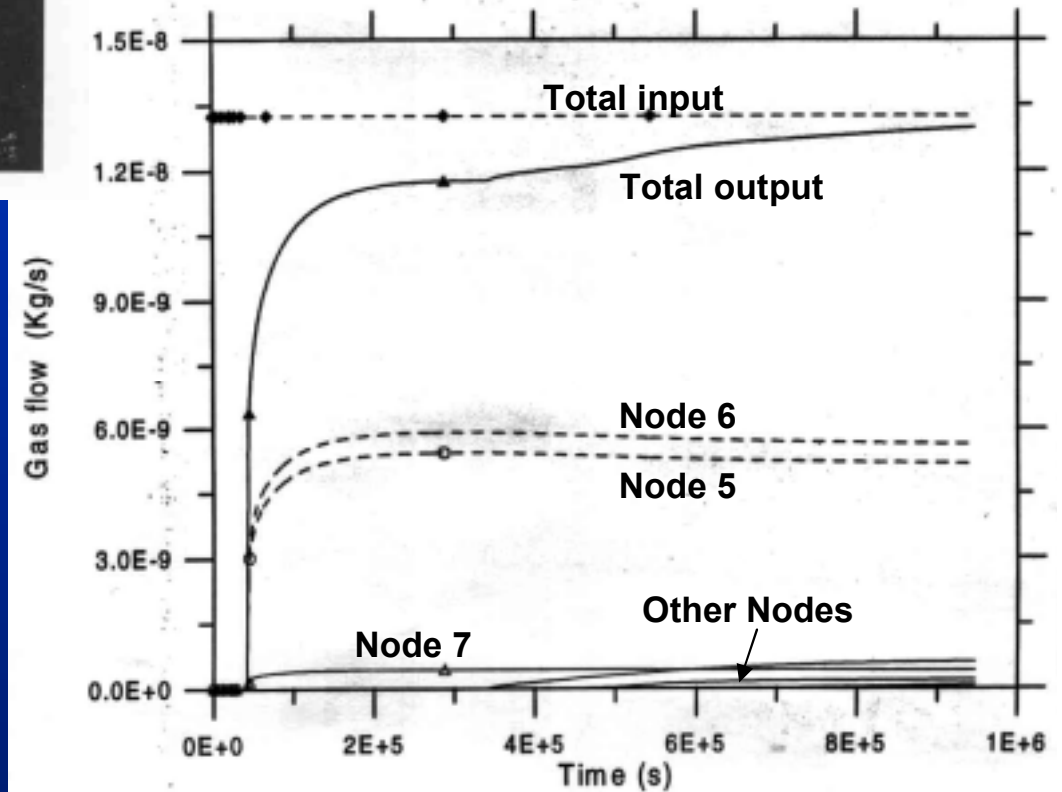
**(c) Time = 108 hours**



**Computed gas flow output  
(Delahaye and Alonso,  
1998).**



**Gas velocity contours  
(Delahaye and  
Alonso, 1998).**



## **Conclusions:**

- *Breakthrough occurs when the largest pore has fully drained*
- *Breakthrough times depend on pressure gradient.*
- *Breakthrough pressures increase with effective clay dry density*
- *Resistance to breakthrough is low below a threshold degree of saturation*
- *Large DDLs block small pores, create gel structures and inhibit water movement*



**Marolo  
Alfaro**



**James  
Blatz**



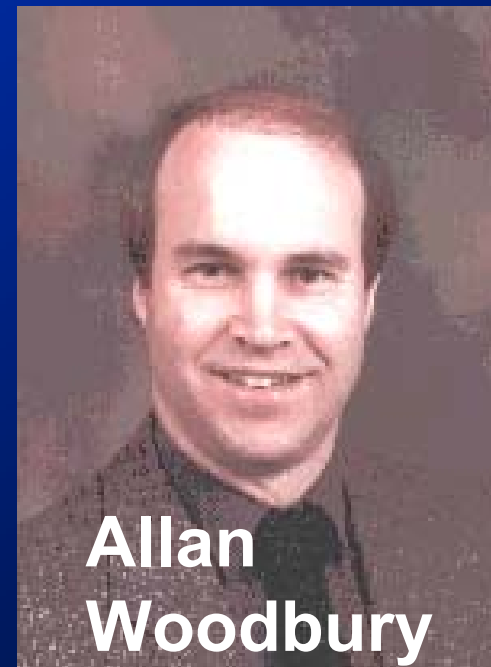
**Jim  
Graham**



**Brian  
Stimpson**



**Jamie  
van Gulck**



**Allan  
Woodbury**



**The University of Manitoba, Geotechnical Group**

## *Possible future studies?*

- *Refinement of 'capillarity advection model'*
  - *Identification of 'representative' pore size*
  - *Incorporation of swelling at inlet and  $k = k(\gamma)$*
- *Measure GEV and high 'threshold' pressures*
- *Longer duration tests, and confirmation of 'threshold' pressure below which no breakthrough will occur.*
- *Tests for migration by diffusion*
- *CAT imaging for 'fingering'*
- *Measure tensile strength and model mode of failure for 'fracture' mechanisms*



# **Acknowledgements**

- 1) Atomic Energy of Canada Limited**
- 2) Natural Sciences and Engineering Research Council of Canada**
- 3) CANDU Owners Group (COG)**
- 4) Ontario Power Generation**
- 5) UM Graduate Students**  
**(Alan Wan, Tim Kirkham, Krista Halayko, Harold Hume, Kent Bannister)**
- 6) Keller Ground Engineering who support the Visiting Chair in Geotechnics at the Queen's University, Belfast**

***Questions?***

# Current Status of Gas Migration Study on Compacted Bentonite in Japan

Kenji TANAII (JNC)

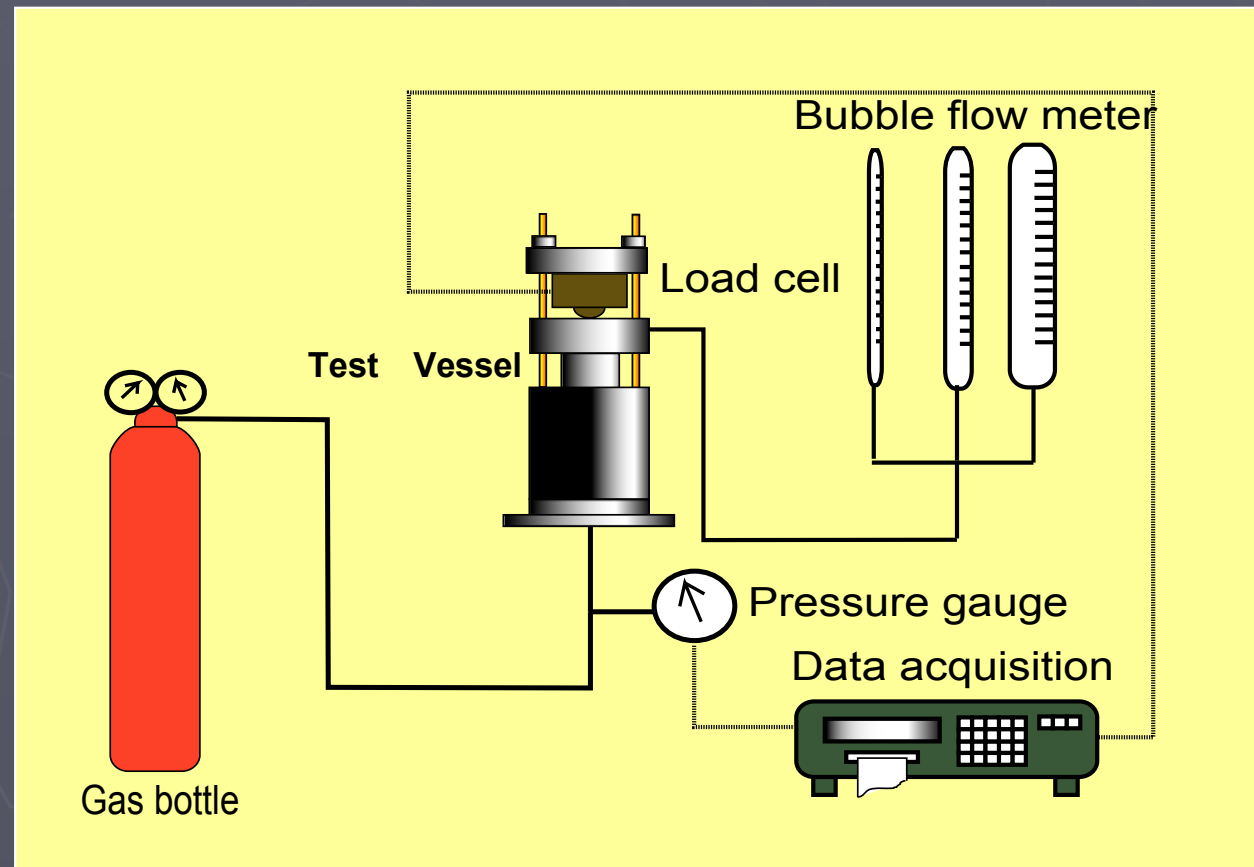
Mikihiko YAMAMOTO (TEC)

# Outline

- **Previous studies in JNC**
  - **Experimental outline**
  - **Experimental results**
- **Current status of gas migration study in JNC**
  - **Gas migration test**
  - **Simulation of the gas migration test by modified Tough-2 code**
- **Conclusions**

## Previous studies in JNC (experimental outline)

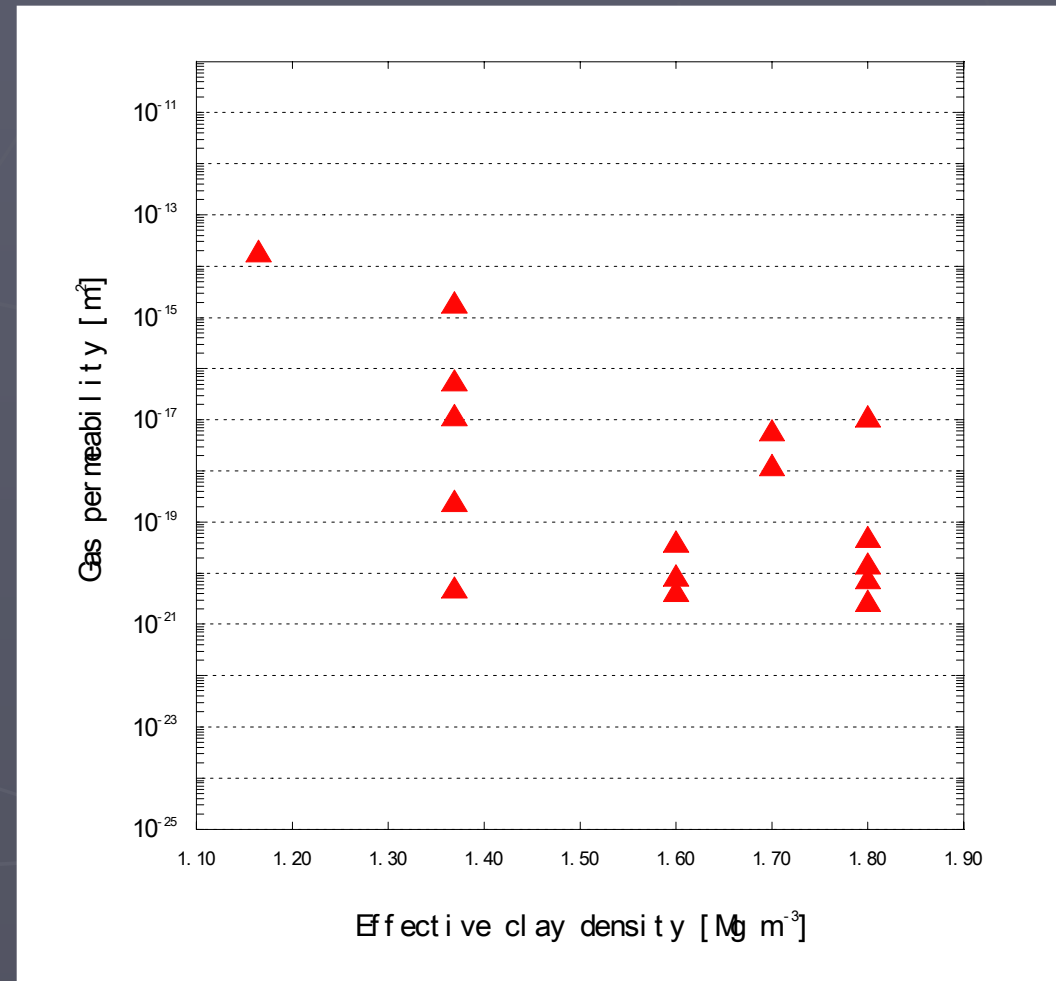
In this study, bentonite and bentonite/sand mixtures material are used as test materials. Buffer samples are placed in the test vessel and compacted uniaxially to predetermined dry densities. Water is supplied from the lower side of specimen by water-head method or water injection pump. Hydrogen gas is injected from the lower side of the specimen and injection pressure is increased stepwise up to a pressure at which breakthrough occurs. In these experiments, the breakthrough pressure and gas flow rate are measured continuously. All tests are conducted at room temperature conditions.



Test apparatus

# Results of previous study (1) (gas permeability)

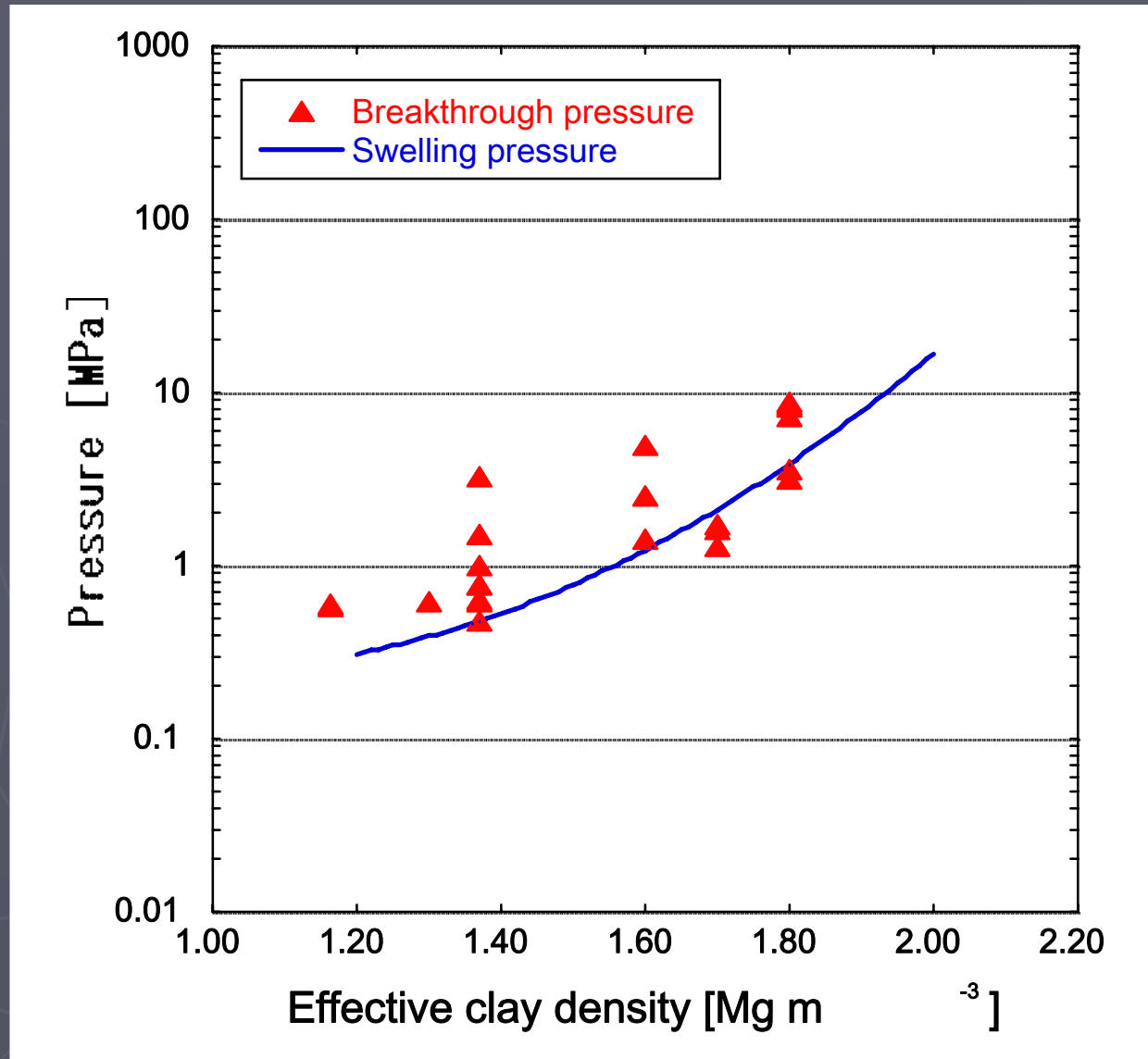
This Figure shows the relationship between effective clay density and gas permeability. This Figure shows that as expected, the gas permeability for bentonite specimen tends to decrease for increasing effective clay density. In any case, gas flow rate gradually shifts to dynamic flow from leisurely flow (a very small amount flow) through the bentonite specimen. And, data dispersion is probably indicative of influence of heterogeneity of the sample and/or experimental conditions such as increase method of gas pressure etc,. The gas permeabilities obtained are  $10^{-17} \text{ m}^2$  for the 30 wt% sand mixtures at a dry density of  $1.6 \text{ Mg m}^{-3}$  and  $10^{-20}$  to  $10^{-21} \text{ m}^2$  for the bentonite at a dry density of  $1.8 \text{ Mg m}^{-3}$ .



Relationship between effective clay density and gas permeability

# Results of previous study (2) (breakthrough pressure & swelling pressure)

The breakthrough pressure seems to be almost the same as the swelling pressure from experimental results. On the other hand, the breakthrough pressure with 10 cm thick sample is more than twice as large as the pressure with the 1 and 5 cm thick samples. It may be that there is a time lag between the gas pressure change in the clay and the expansion of cracks that serve as the gas pathways as the sample thickness increases. In other words, the formation of the gas migration pathways occurs too late to follow the pressure rise, which resulted in the high breakthrough pressure.



## Results of previous study (3) (Recovery of gas pathways )

Test No.	Breakthrough pressure	
	First step	Second step
1	8.88 MPa	8.14 MPa
2	0.60 MPa	0.59 MPa
3	0.62 MPa	0.65 MPa
4	3.59 MPa	3.15 MPa
5	1.64 MPa	1.70 MPa

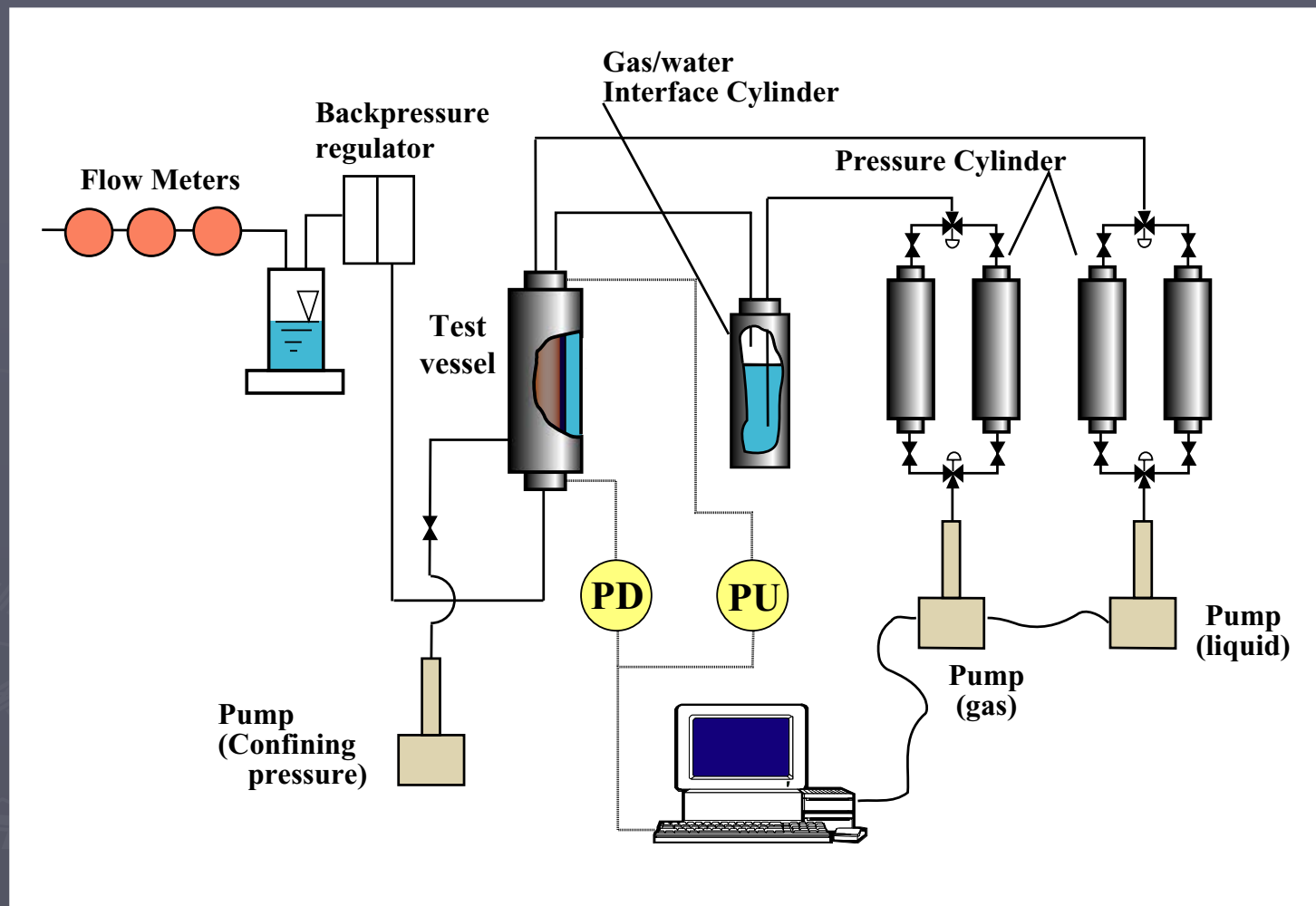
It is assumed that gas first accumulates at the overpack-buffer interface, followed by gas migration through the buffer occurring repeatedly during the operational life time of an actual repository. It is important to evaluate if the gas migration pathway, once formed, can recover by the self-sealing ability of bentonite. The reproducibility of the gas breakthrough pressure is measured to estimate the recovery of gas pathways. Results of tests are shown in this table. As to reproducibility of the breakthrough pressure, it is observed that first and second breakthrough pressure are almost the same for the specimens. This suggests that gas pathways created during the first gas injection period are closed due to bentonite swelling during the resaturation period.



## Current status of gas migration study

- **New gas migration test using X-ray CT technique performed to more clarify the gas migration behaviour in bentonite. In this study, distribution of liquid or gas saturation was measured to demonstrate that X-ray CT was a reliable new technique for the non-destructive measurement of the gas migration behaviour in bentonite.**
- **And, an analysis by the modified TOUGH2 code using gas migration test result performed to evaluate of applicability of this model.**

# Gas migration test apparatus



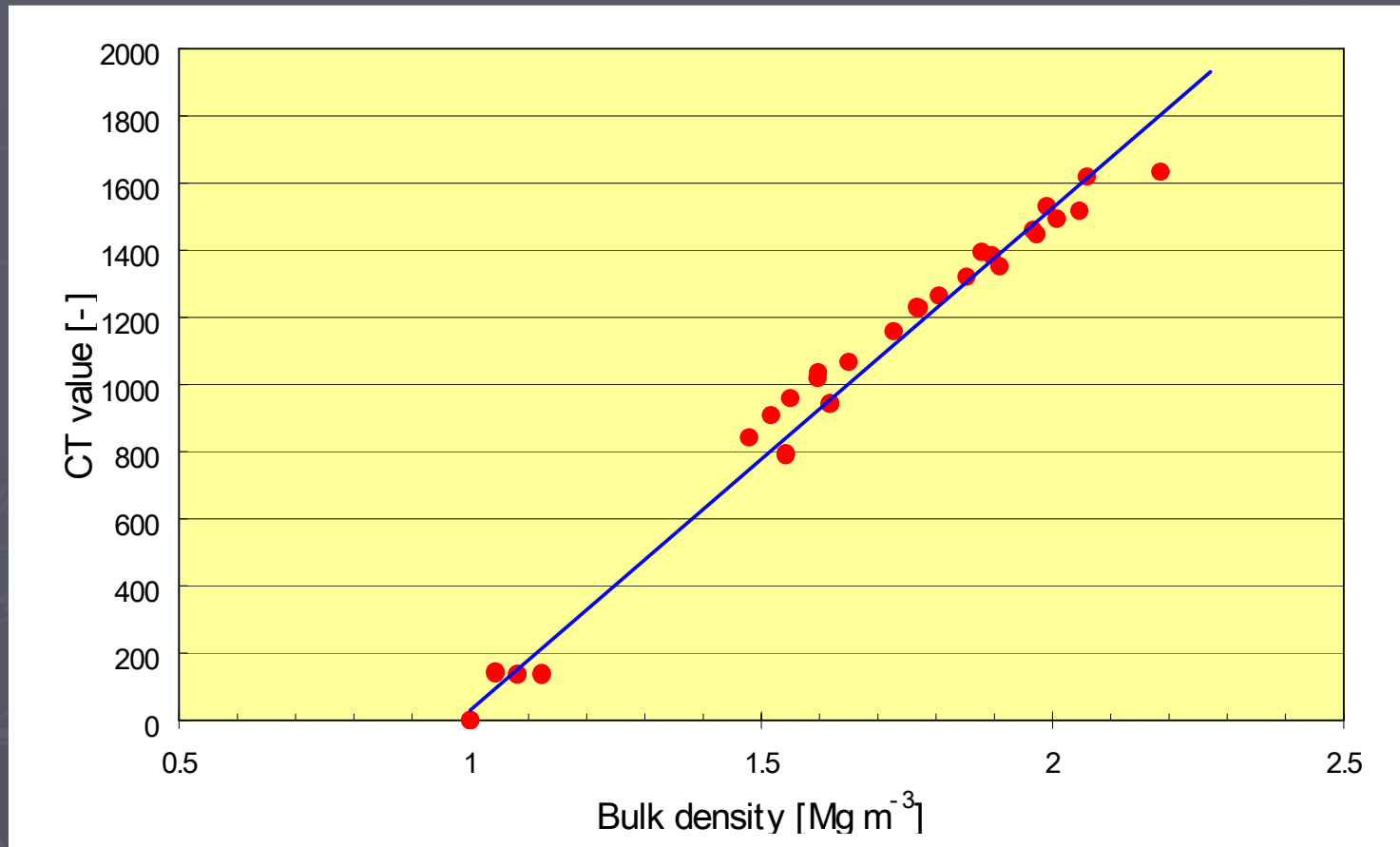
The set up of the gas migration test apparatus is shown schematically in Figure-4. This apparatus comprises four main components: (a) a specimen assembly, (b) fluid injection system together with its associated pressure control pump, (c) a backpressure system, and (d) a microcomputer-based data acquisition system. The clay is equilibrated by backpressuring with distilled water at a fixed pressure. A 3.8 cm diameter cylindrical clay specimen is placed between sintered stainless steel porous filters.

## X-ray CT scanner

An X-ray CT scanner, Asteion VI was used in this test. It is the third-generation medical scanner (Photograph-1). A target in an X-ray tube is attacked by electrons accelerated at 135 kV with a 200 mA current. An X-ray fan-beam from the tube penetrates a sample on a bed made of carbon. The intensity of the X-ray beam after the sample penetration is measured by 896 detectors. The expose time of X-ray is 1.0 sec (time for the 360° rotation of the X-ray tube). The time for the image reconstruction by Fourier transformation is 3.0 sec.



# Relationship between bulk density and CT value of Kunigel V1 bentonite

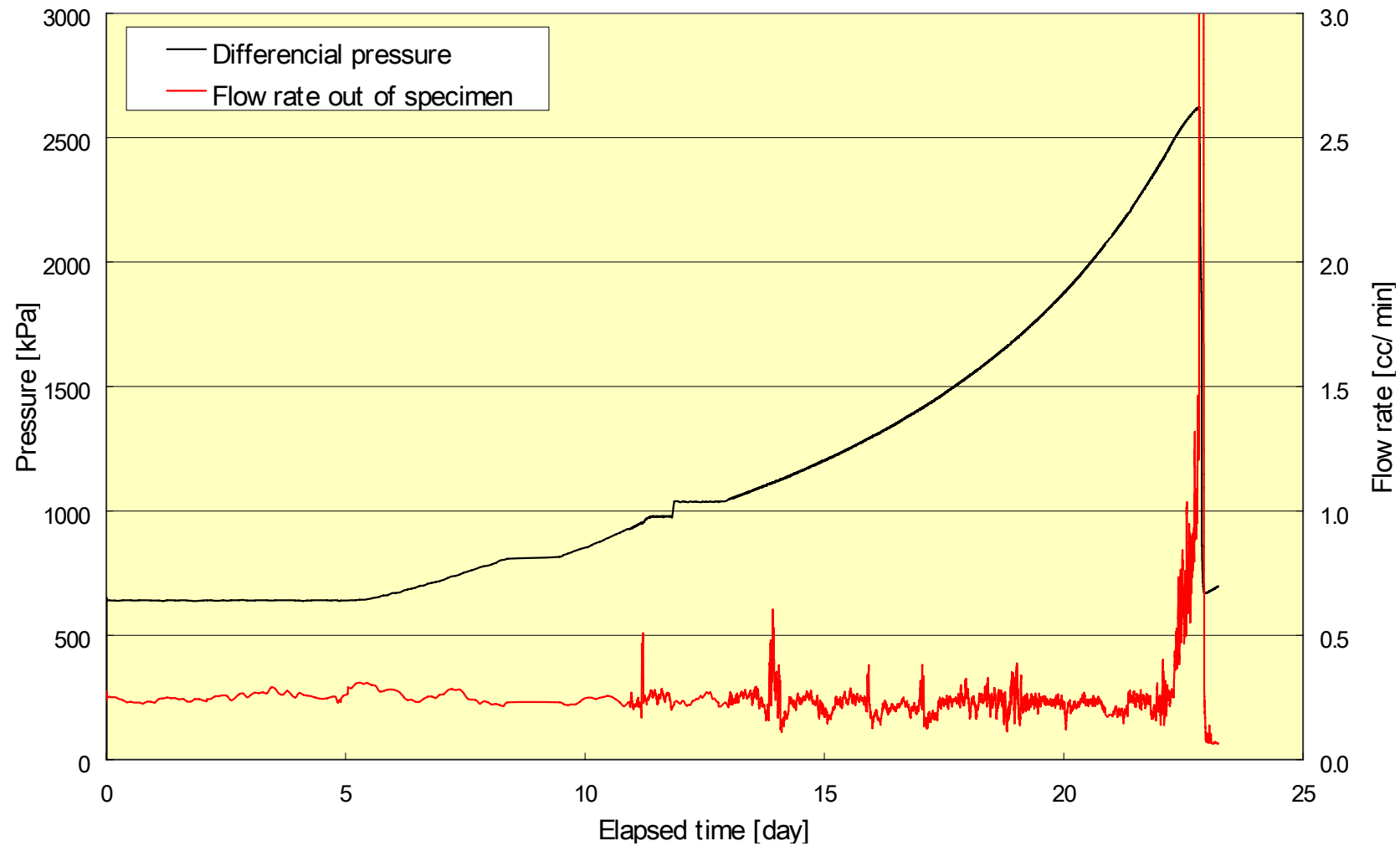


The degree of X-ray attenuation increases linearly with the bulk density of sample. This Figure shows relationship between bulk density and CT value of Kunigel V1 bentonite.

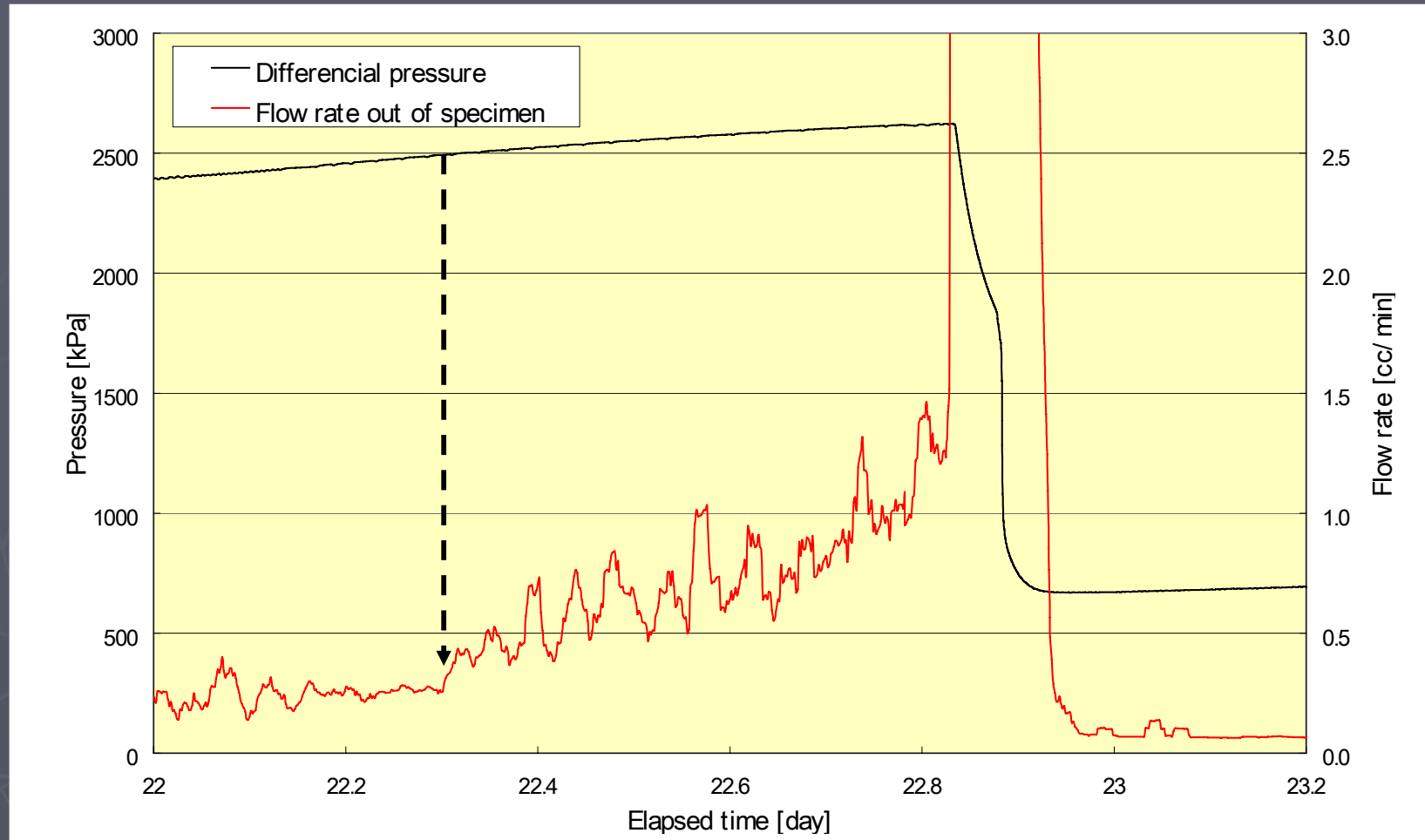
## Test procedures

- 1) Bentonite powder is placed in the test vessel and compacted uniaxially to dry density of  $1.6 \text{ Mg m}^{-3}$ .
- 2) Water was supplied from the upstream of the specimen by water injection pump. After saturated of the specimen, helium was admitted into the upper part of the gas-water interface cylinder and the tubing and porous disc were gas-flushed.
- 3) The initial gas pressure in the injection system was set using a regulator (600 kPa). The injection pump was set to constant flow rate mode and pumping rate of  $0.05 \text{ cc min}^{-1}$  was used in this test.
- 4) In this experiment, the breakthrough pressure, gas flow rate and drainage volume of water are measured continuously.

# Results of gas migration test (1)

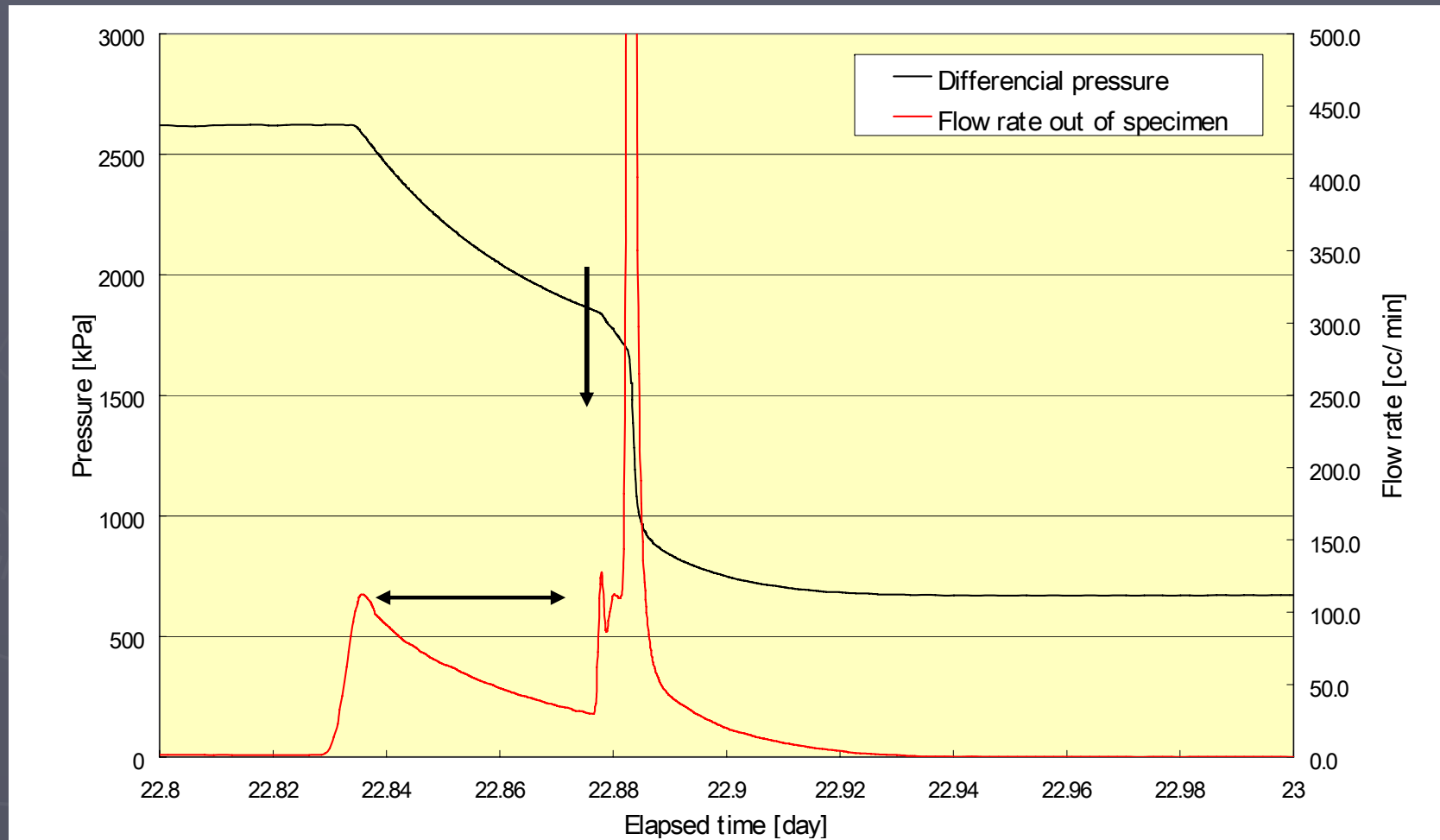


# Results of gas migration test (2)



This Figure shows differential gas pressure and gas flow rate history after a period of 22 days. A very small amount of flow was observed at a gas pressure of 2.5 MPa. Gas pressure continued to rise until major gas entry occurred at a gas pressure of 2.6 MPa, accompanied by an increase of gas flow rate. Breakthrough pressure is larger than the swelling pressure of the bentonite.

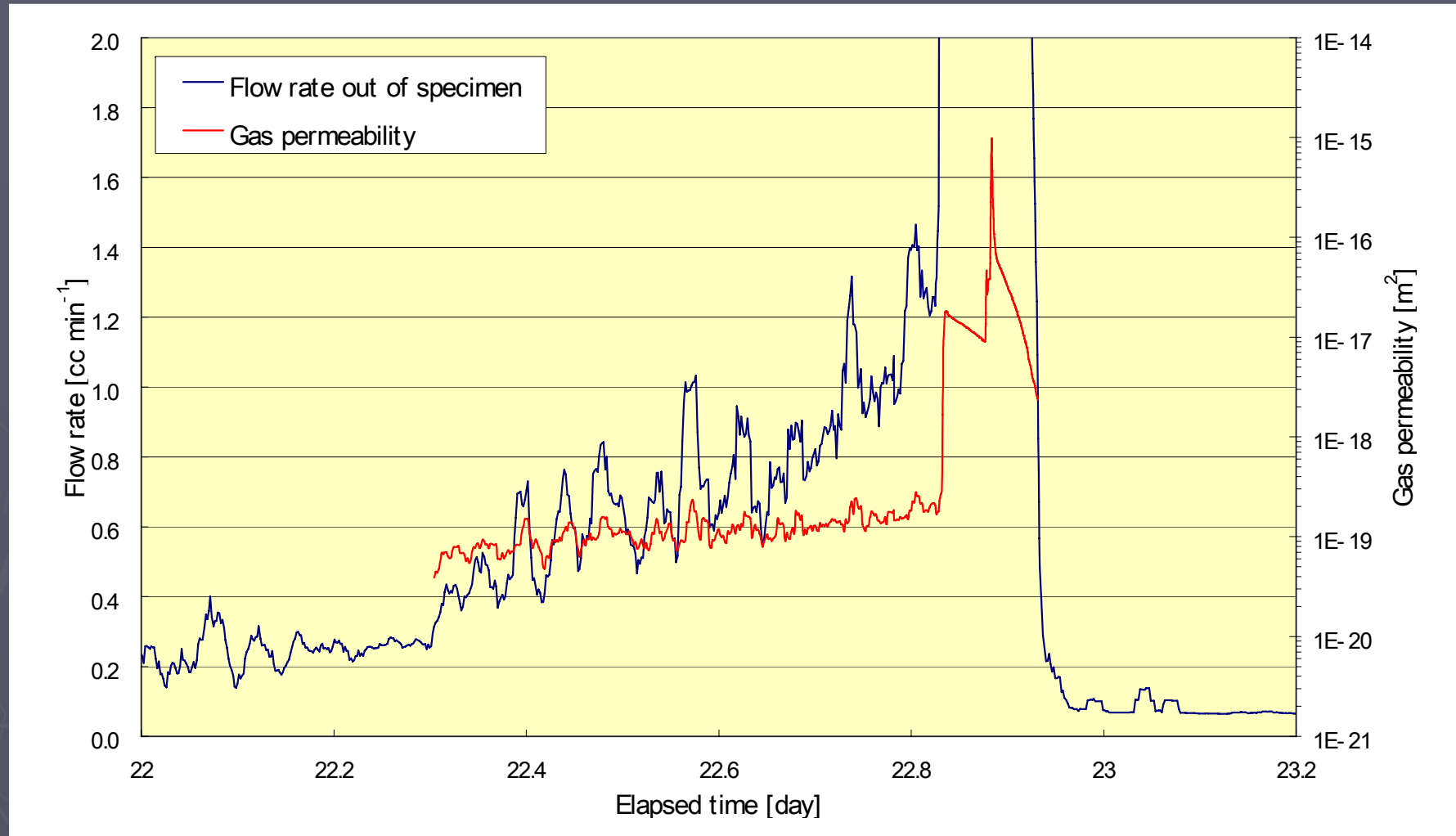
# Results of gas migration test (3)



Differential gas pressure and gas flow rate after breakthrough was spontaneously decreased to 22.87 days. And, the secondary peak of gas flow rate occurs at pressure of approximately 1.8 MPa. Maximum gas flow rate at this point was approximately  $1,667 \text{ cc min}^{-1}$ . After the secondary peak, steady-state gas flow was observed at a pressure of approximately 0.67 MPa. The secondary peak is probably indicative of generation of prominent pathway in the specimen and/or at interface between the bentonite specimen and test vessel.

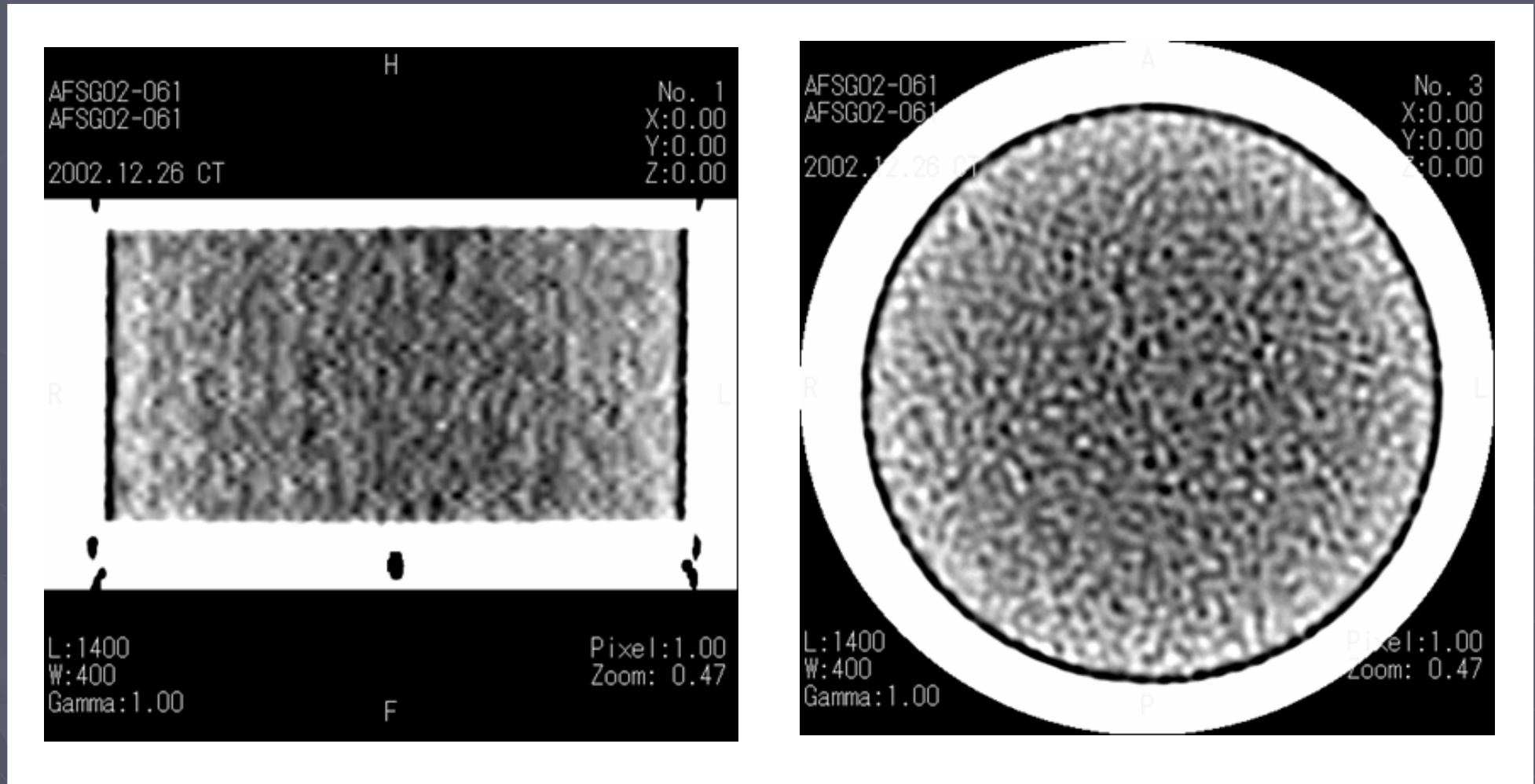


# Results of gas migration test (4)



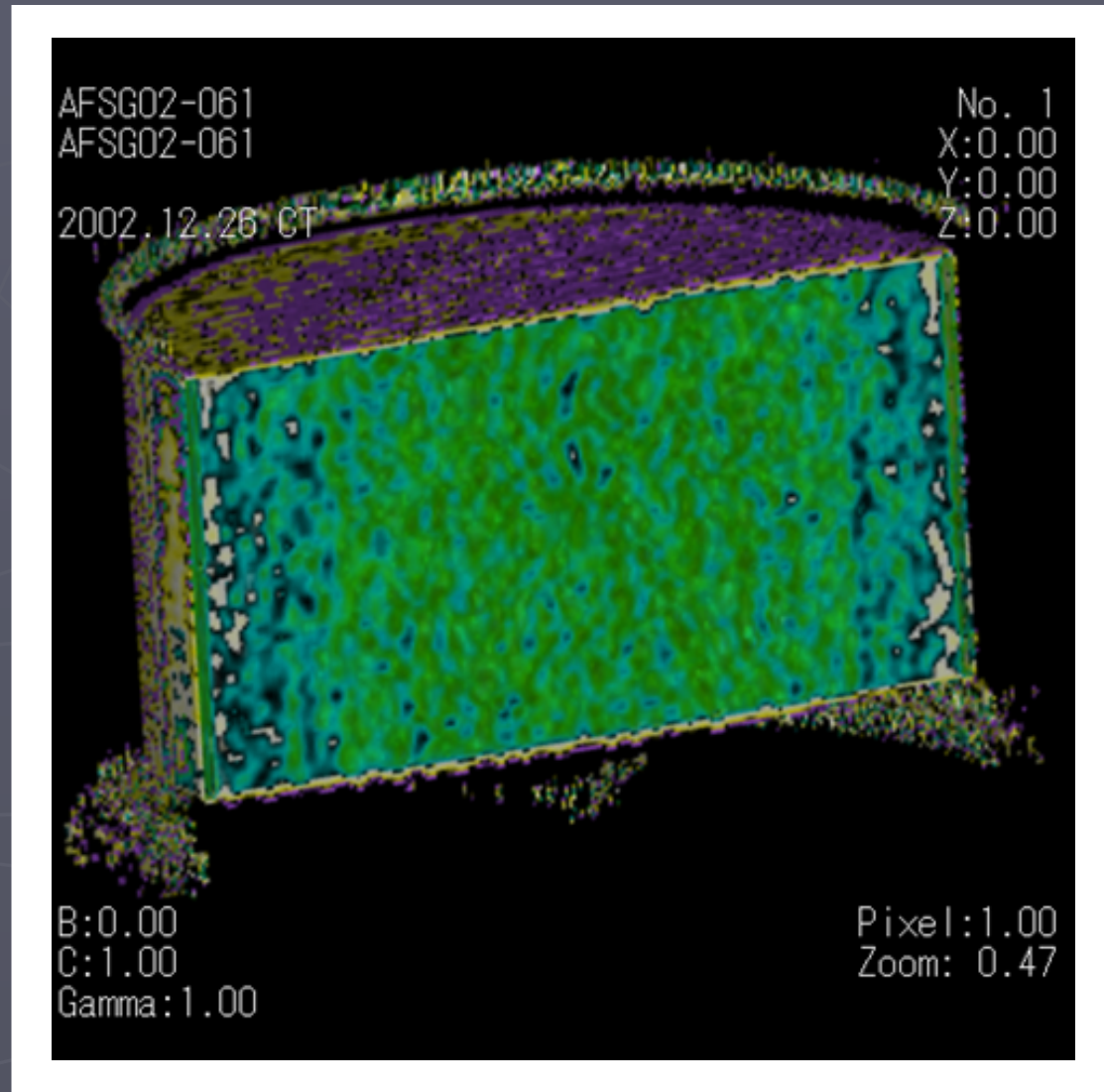
The gas permeabilities obtained are  $3.8$  to  $6.0 \times 10^{-20} \text{ m}^2$  at pressure of  $2.5 \text{ MPa}$  and  $9.9 \times 10^{-16} \text{ m}^2$  at pressure of approximately  $1.8 \text{ MPa}$ . The secondary peak is probably indicative of generation of prominent pathway at interface between the bentonite specimen and test vessel.

# Two-dimensional X-ray CT images

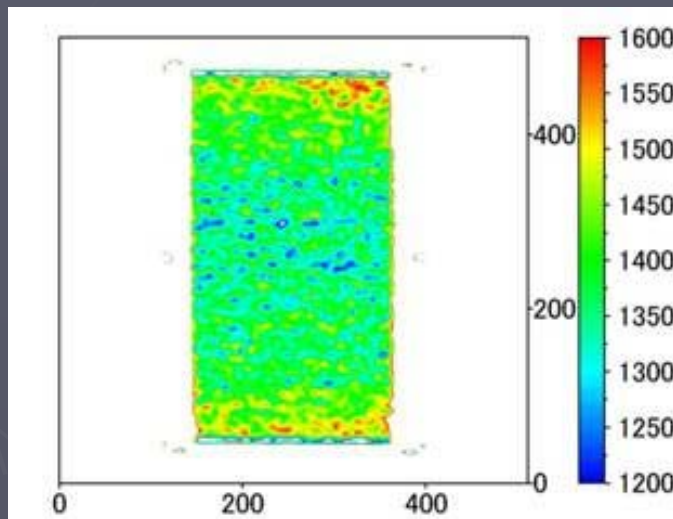


The CT images are drawn with black color for low CT value and white color for high CT value and the total number of levels on the gray level distribution is 256.

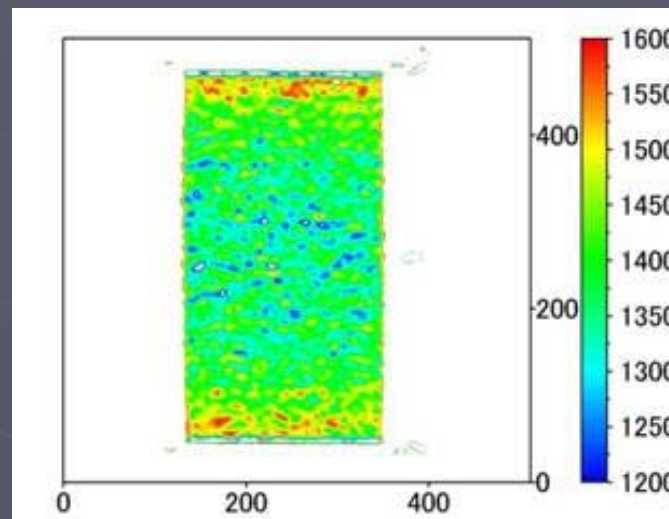
# 3-D images of specimen (at breakthrough occur)



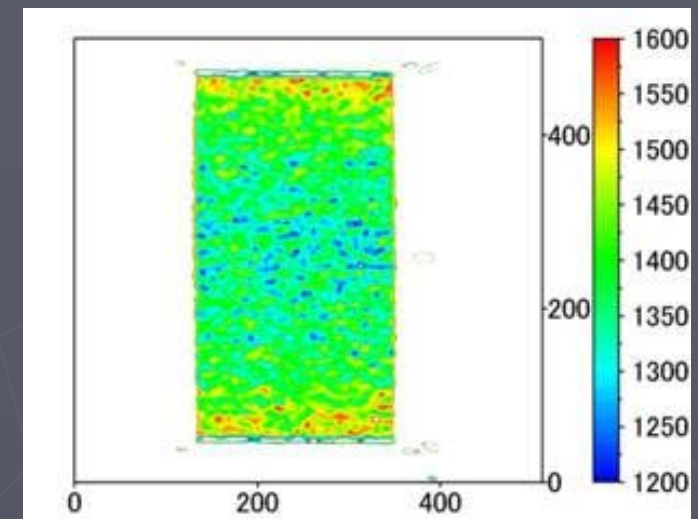
# Images of CT value distribution



a) before gas injection



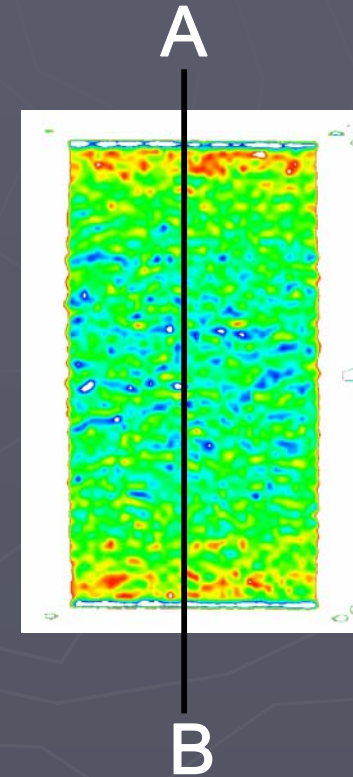
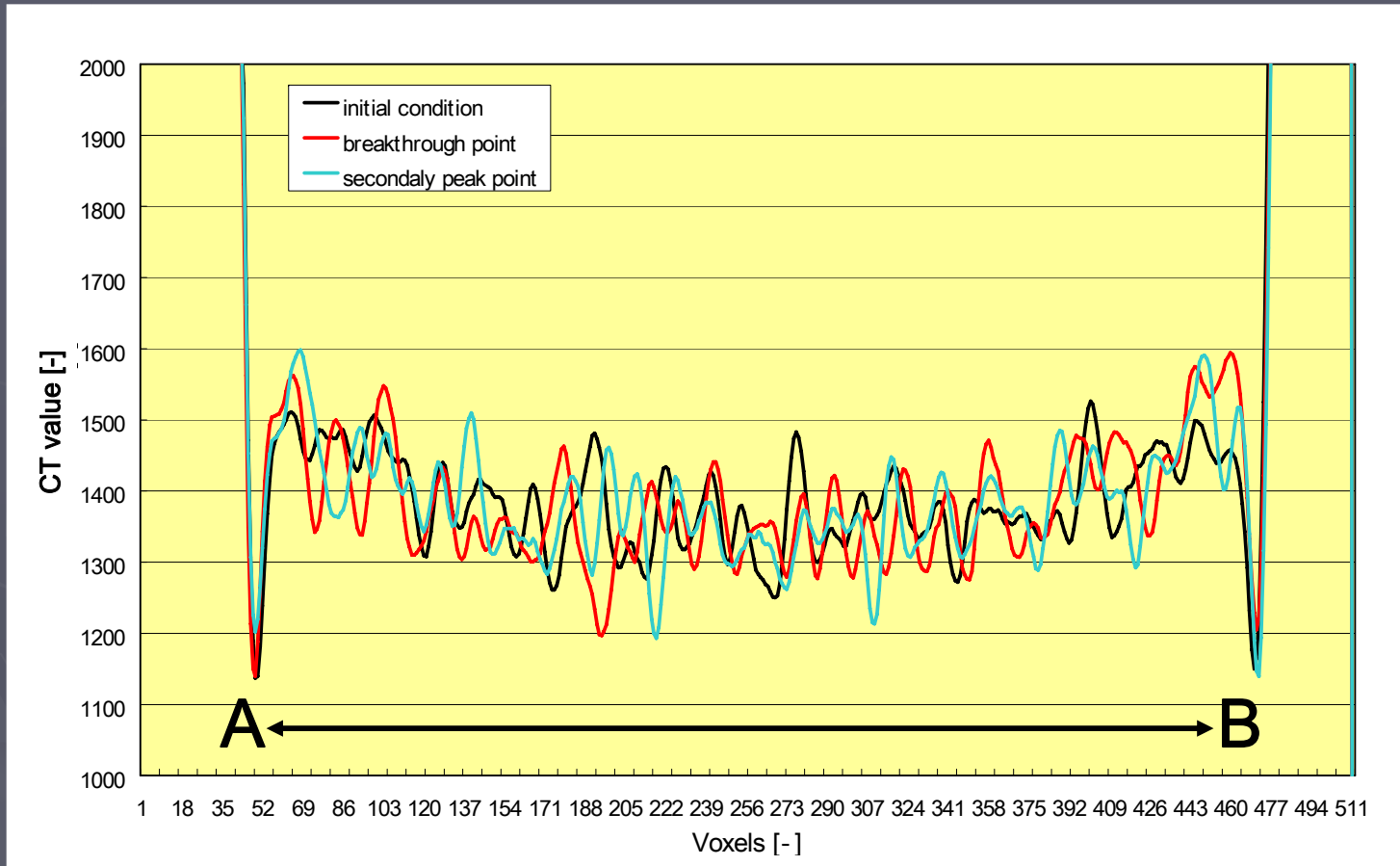
b) breakthrough point



c) secondary peak point

The distribution of liquid saturation was measured to demonstrate that X-ray CT was reliable new technique for the non-destructive measurement of gas migration through bentonite specimen. This figure shows 2-D images of the CT value distribution. Contrast differences in the CT images represent bulk density differences in the bentonite specimen.

# Line profile of CT value of the bentonite specimen



This Figure shows line profile of CT value at center position of 2-D images. The alteration of liquid saturation in this test specimen is not observed from this test case. But, these experimental result are probably indicative of migration along preferential pathway rather than uniform flow in the matrix of bentonite specimen.

## Conclusions (1)

The knowledge obtained from previous studies are as follows,

- i) The gas permeabilities are  $10^{-17}$  m<sup>2</sup> for the 30wt% sand mixtures at a dry density of 1.6 Mg m<sup>-3</sup> and  $10^{-20}$  to  $10^{-21}$  m<sup>2</sup> for the bentonite (100%) at a dry density of 1.8 Mg m<sup>-3</sup>,
- ii) The breakthrough pressure seems to be almost the same as the swelling pressure at constant volume condition,
- iii) Gas pathways created during the first gas injection period are closed due to bentonite swelling during the resaturation period.

## Conclusions (2)

In this test, it is obtained two peak of gas flow rate. In particular, maximum flow rate at secondary peak is obtained approximately  $1,667 \text{ cc min}^{-1}$ . This peak is probably indicative of generation of prominent pathway at interface between bentonite specimen and test vessel. Breakthrough pressure (2.5 MPa) is larger than the swelling pressure of the bentonite. It may be that there is a time lag between the gas pressure change in the clay and expansion of cracks due to large pumping rate. The gas migration pathways are unstable due to stress condition in bentonite specimen and/or heterogeneity of the specimen.

## Conclusions (3)

The distribution of liquid saturation was measured to demonstrate that X-ray CT was reliable new technique for the non-destructive measurement of gas migration through bentonite specimen. The degree of X-ray attenuation depends on the bulk density of the bentonite specimen. However, alteration of water content in the sample is calculated by CT value of the sample. The alteration of liquid saturation in this test specimen is not observed from this test case. But, these experimental results are probably indicative of migration along preferential pathway rather than uniform flow in the matrix of bentonite specimen.

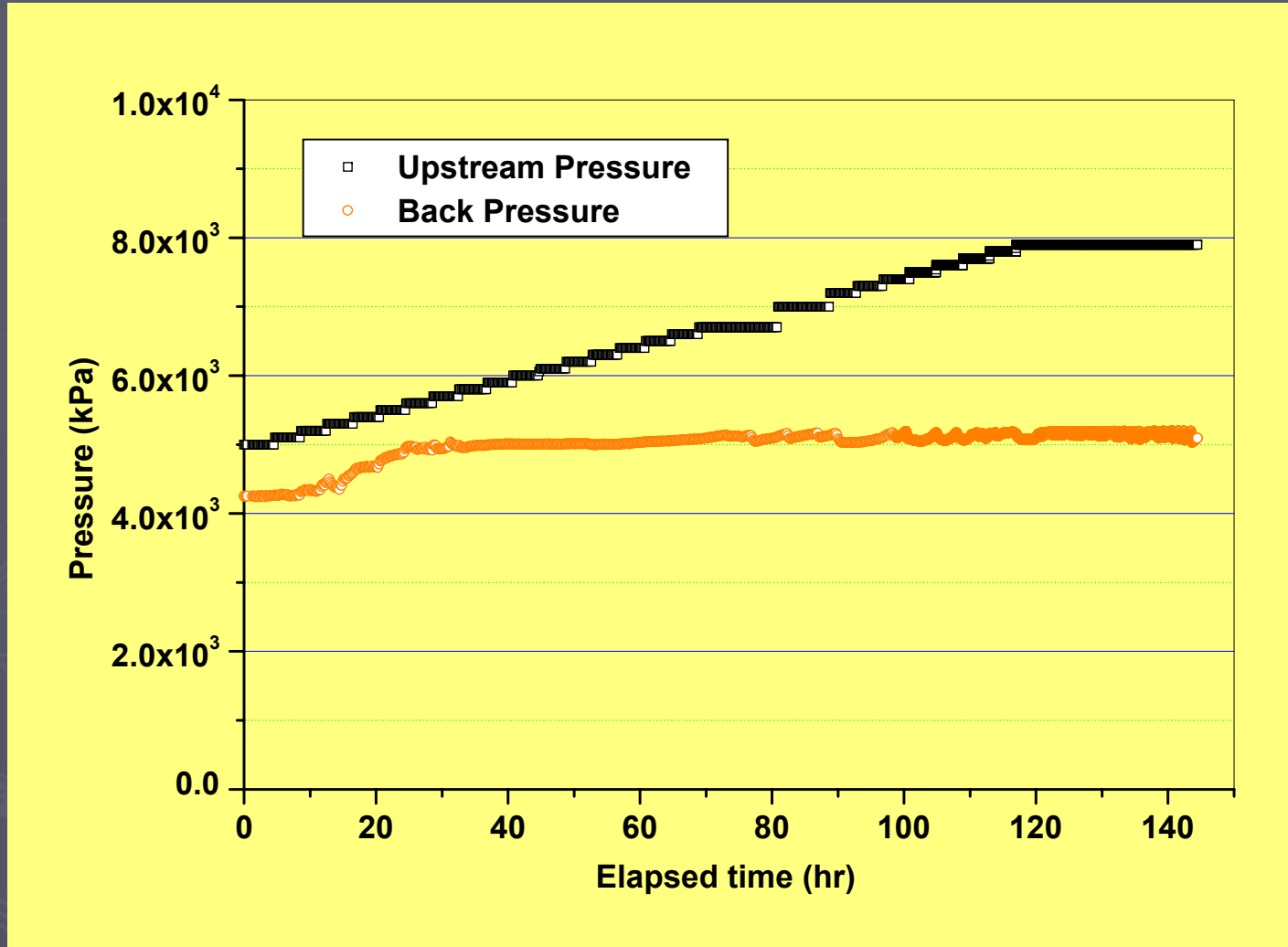


## Test procedures - bentonite/sand mixture

- 1) Bentonite/sand mixture (70/30 wt%) is placed in the test vessel (57.2mm  $\phi$  30mm H) and compacted to dry density of 1.6 Mg m<sup>-3</sup>.
- 2) The specimen was saturated by water injected from both up- and down-stream of the specimen at 5 MPa. After that, humidified nitrogen gas was admitted into test vessel.
- 3) The initial gas injection pressure was set at 5 MPa. The gas injection pressure increased step by step basis at 100 kPa/4 hr.
- 4) After the gas out flow was observed, the gas injection pressure was controlled at constant value.
- 5) Breakthrough pressure, gas flow rate and volume of expelled water were measured.

# Results of gas migration test (5)

(bentonite/sand 70/30  $\rho_d=1.6 \text{ E}+3 \text{ kg m}^{-3}$ )



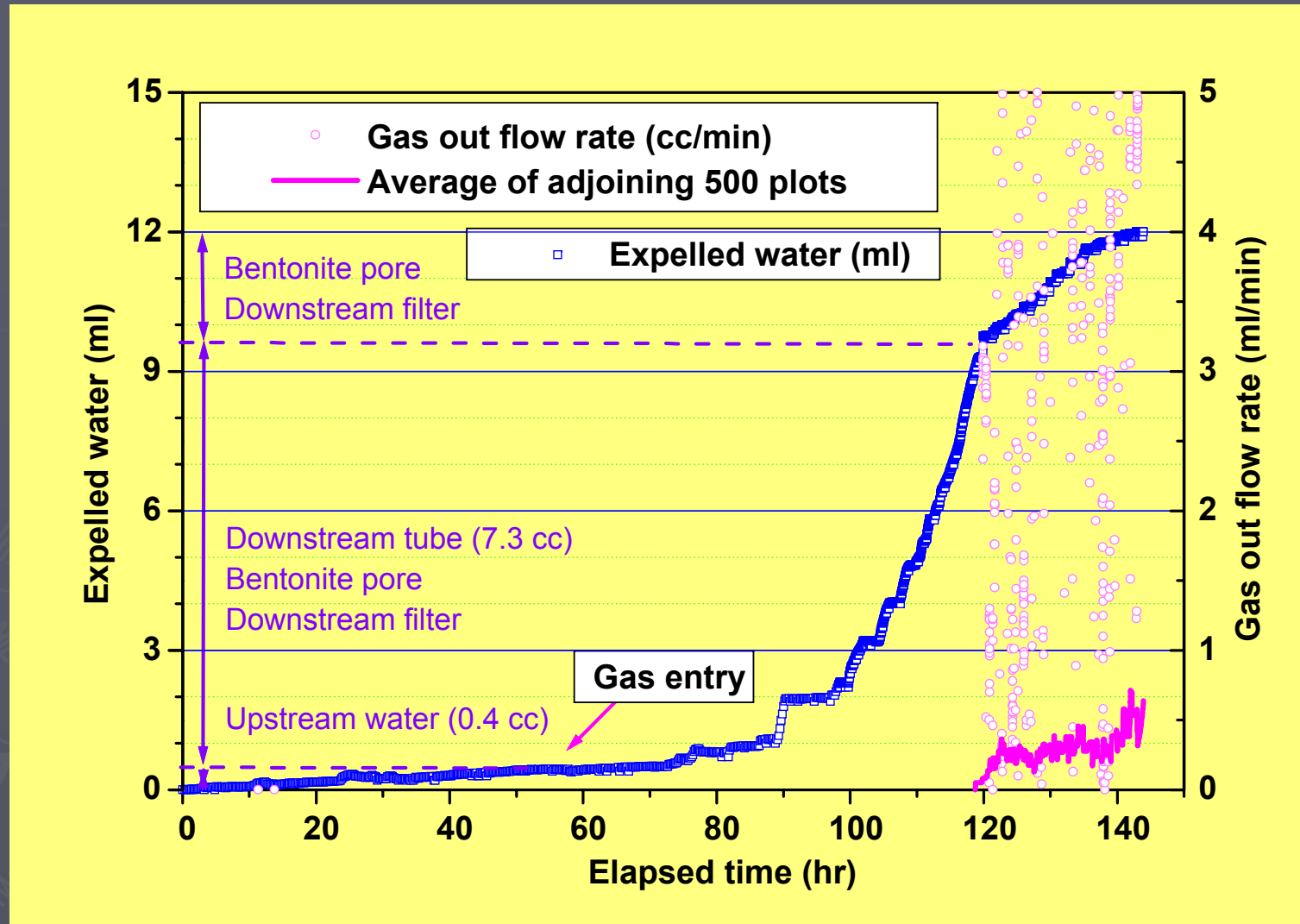
The test conditions are constant volume cell, non confining pressure applied and backpressure of 5MPa.

The initial gas injection pressure was 5 MPa and increased step by step basis at 100 kPa/4 hr.

Water permeability is  $7.9 \text{ E}-20 \text{ (m}^2\text{)}$ . Porosity is 0.43. Upstream pressure at breakthrough was

# Results of gas migration test (6)

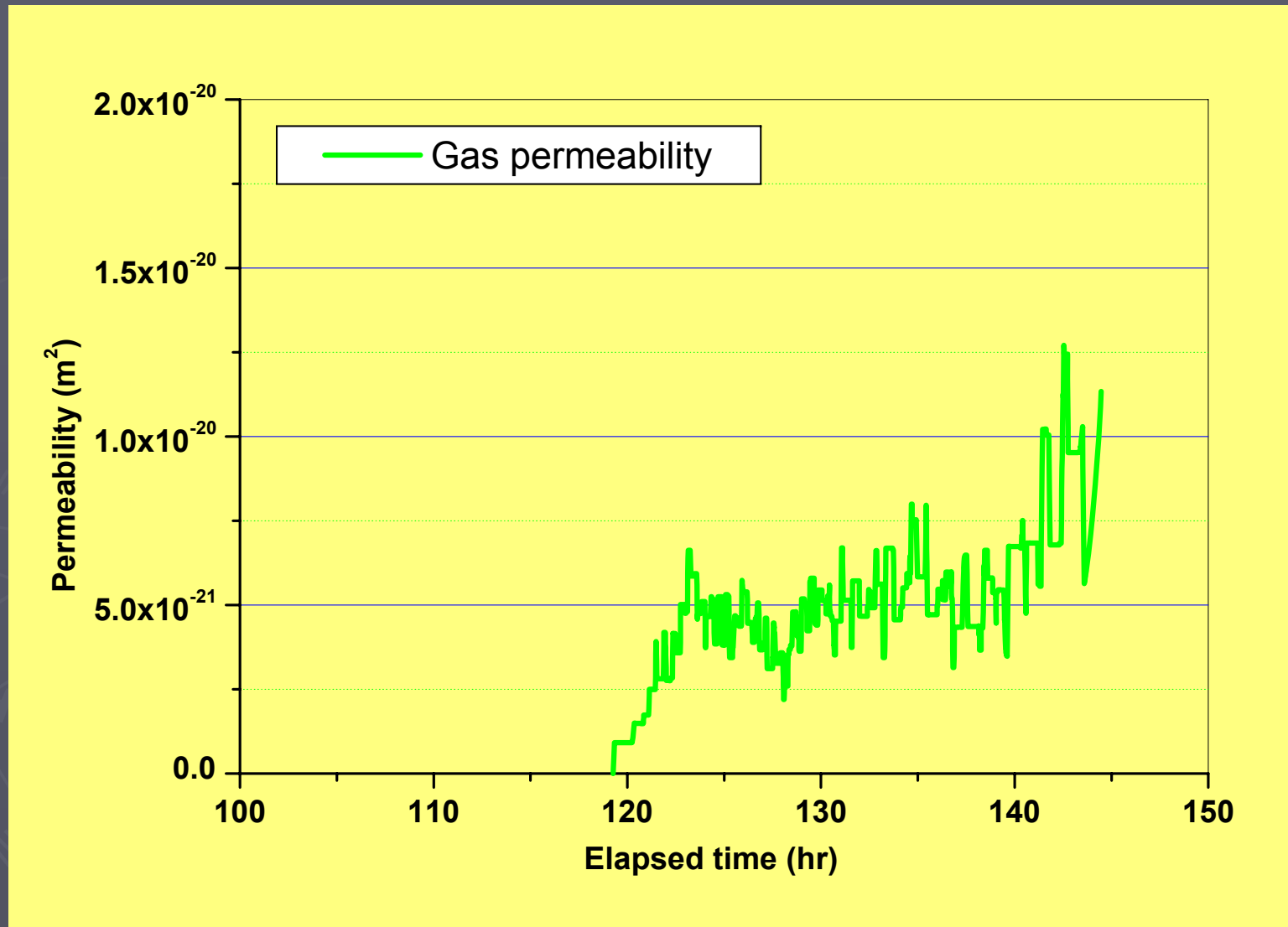
(bentonite/sand 70/30  $\rho_d = 1.6 \text{ E}+3 \text{ kg m}^{-3}$ )



The excess pressure at which gas enters exists between 1.2 MPa and 1.7 MPa. From 10 to 20 % of pore water in the bentonite/sand sample is estimated to be expelled.

# Results of gas migration test (7)

(bentonite/sand 70/30  $\rho_d=1.6 \text{ E}+3 \text{ kg m}^{-3}$ )



# Simulation of the gas migration test by modified TOUGH2 code (Mathematical formulation 1)

- De-coupling the water and gas flows
- gas permeability function that matches the experiments

$$k_{rg}(t = t_e) = k_0$$

$$k_{rw} = \text{Select from any functions}$$

$k_{rg}$  : Relative permeability of gas  
 $k_{rw}$  : Relative permeability of water  
 $t_e$  : Gas entry time (s)  
 $k_0$  :  $k_{rg}$ , at gas entry

- Kozeny-Carman relationship for gas flow model

$$S_g = \frac{C k_{rg} k \left( \frac{-P_c}{\sigma} \right)^2}{\phi \tau}$$

$k$  : Absolute permeability (m<sup>2</sup>)  
 $S_g$  : Saturation of gas  
 $P_c$  : Capillary pressure (Pa)  
 $\sigma$  : Surface tension (Pa m)  
 $\phi$  : Porosity  
 $\tau$  : Tortuosity  
 $C$  : Shape factor

## Mathematical formulation 2

- A threshold gas entry pressure and a shut-in gas pressure
- An gas permeability in response to a gas pressure

$$k_{\infty}(p_c) = k_0 \left( \frac{-P_c - P_r}{P_e - P_r} \right) \exp \left( 4 \frac{-P_c - P_e}{G} \right)$$

$k_{\infty}$  : Maximum  $k_{rg}$  value at  $P_c$  (m<sup>2</sup>)  
 $P_r$  : Shut-in pressure (Pa)  
 $P_e$  : Gas entry pressure (Pa)  
 $G$  : Elastic material constant (Pa)

- A 'time-lag' between gas pressure and the dilation of the pathways

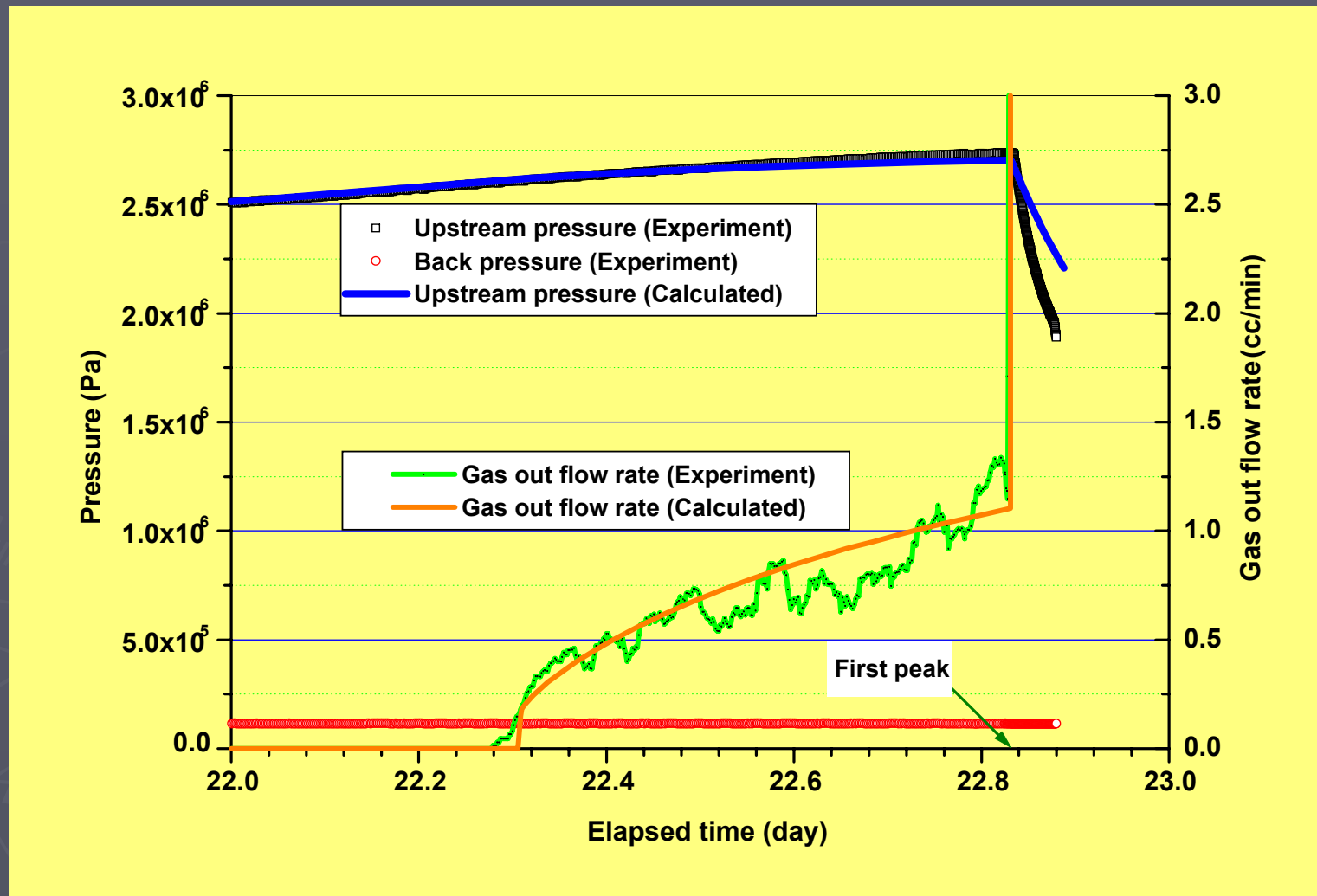
$$\frac{\partial k_{rg}}{\partial t} = -\lambda [k_{rg} - k_{\infty}(p_c)]$$

$\lambda$  : Time-dependence constant (s<sup>-1</sup>)

# Parameter values : pure bentonite

Parameter	Chose value		Remarks
<b>Initial condition</b>			
$P_g$	7.54 E+5	Pa	Experimental result
$P_w$	1.12 E+5	Pa	Experimental result
<b>Pre-Breakthrough : First region</b>			
$k$	5.0 E-20	m <sup>2</sup>	Experimental result
$k_0$	1.0 E +1		Based on experimental result
$P_e$	2.48E+6	Pa	Experimental result
$P_r$	8.01E+5	Pa	Experimental result
$G$	3.1 E +6	Pa	Fitting parameter
$\lambda$	3.0 E -5		Fitting parameter
$C$	5.0 E -4		Fitting parameter
<b>At First Peak : Second region</b>			
$k$	5.0 E-20	m <sup>2</sup>	Experimental result
$k_0$	3.75 E+5		Based on experimental result
$P_e$	2.48E+6	Pa	Experimental result
$P_r$	8.01E+5	Pa	Experimental result
$G$	3.1 E +6	Pa	Fitting parameter
$\lambda$	5.0 E -2		Fitting parameter
$C$	5.0 E -4		Fitting parameter

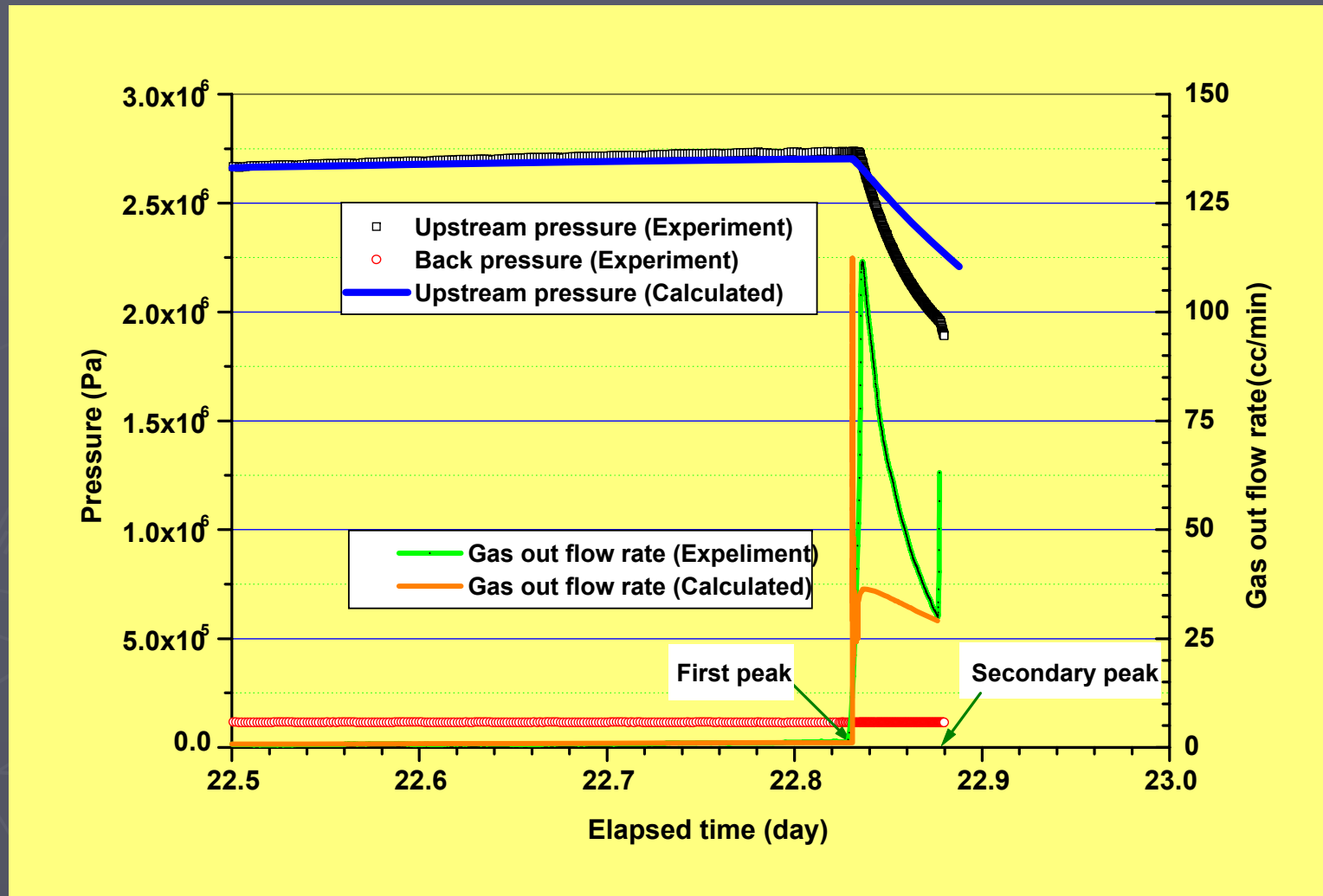
# Simulation results of pure bentonite (1)



Within the first region, the level of agreement for the gas breakthrough time, history of the gas out flow rate which is relatively low and increasing moderately and history of the upstream pressure is satisfying.



# Simulation results of pure bentonite (2)



In the second region, the calculation gives a good agreement with the first peak value of gas out flow rate, but the predicted behaviour of gas out flow reduction is significantly rapid compared with observed value.

## Conclusions (4)

The modified TOUGH2 simulator which has a gas flow model based on Kozeny-Carman relationship was applied.

The results of the simulation were in reasonably agreement with obtained experimental data around gas breakthrough phenomenon.

But, it has some difficulties to simulate “burst flow” which has extremely large and instantaneous increase of gas out flow.

Despite these difficulties the continuum 2 phase model approach coupled with mechanical nature is one of the potential methods of describing gas migration in clay material.

**“Workshop on Gas Migration in Bentonite: Experimental  
Data and Interpretation”**

**Madrid, October 29-30, 2003**

**GAMBIT**

**GAS FLOW IN CLAYS. EXPERIMENTAL DATA  
LEADING TO TWO PHASE AND PREFERENTIAL  
PATH MODELLING**

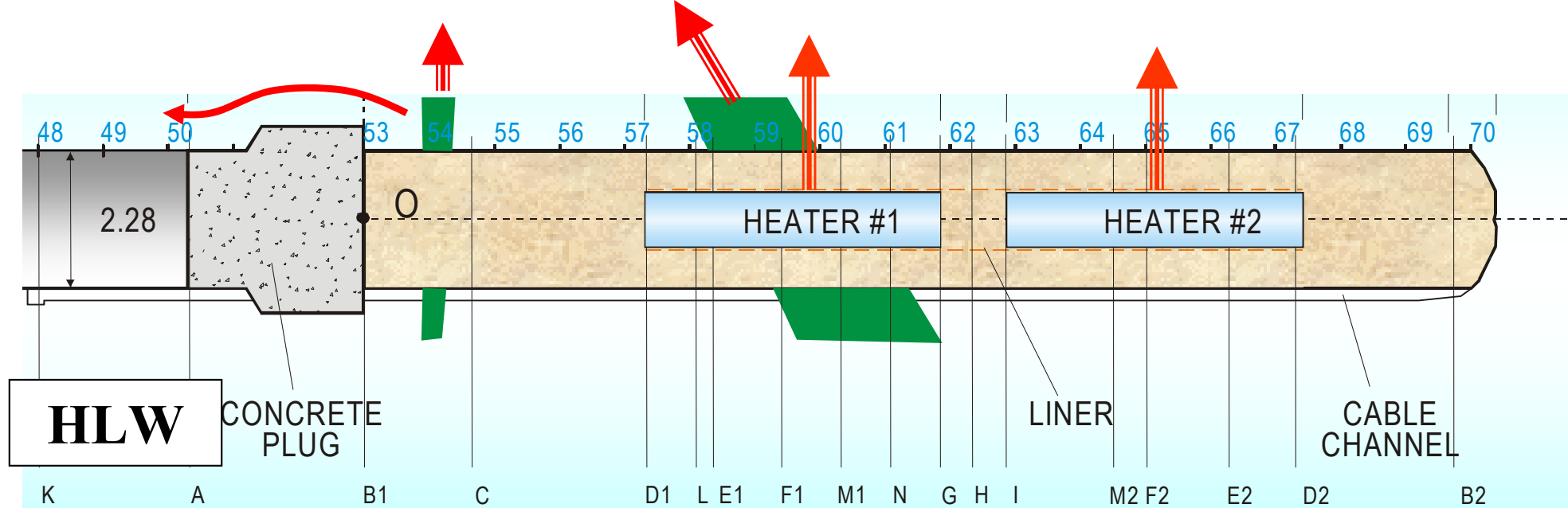
E. E. Alonso and S. Olivella



Department of Geotechnical Engineering and Geosciences

UPC, Barcelona

Enresa, Madrid. Wednesday, Oct. 29, 2003



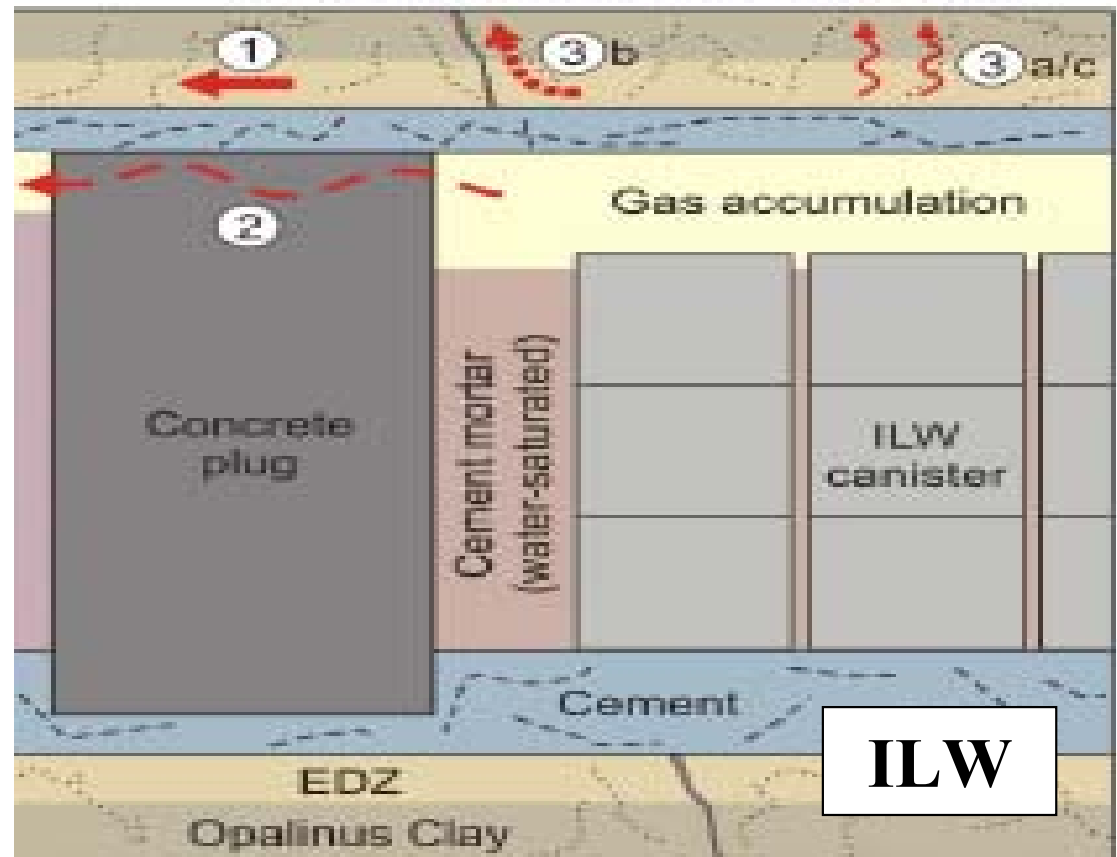
**ILW emplacement tunnel**

## GAS FLOW IN THE NEAR FIELD

Normalised gas generation rates:

**HLW:** 0.04 - 0.4 m<sup>3</sup> Gas/ m<sup>3</sup> waste /a / m disp. Tunnel  
**ILW:** 0.16 - 0.19

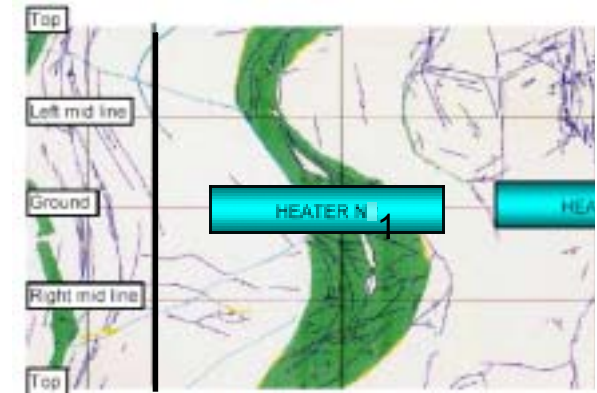
*(Marschall, 2002)*



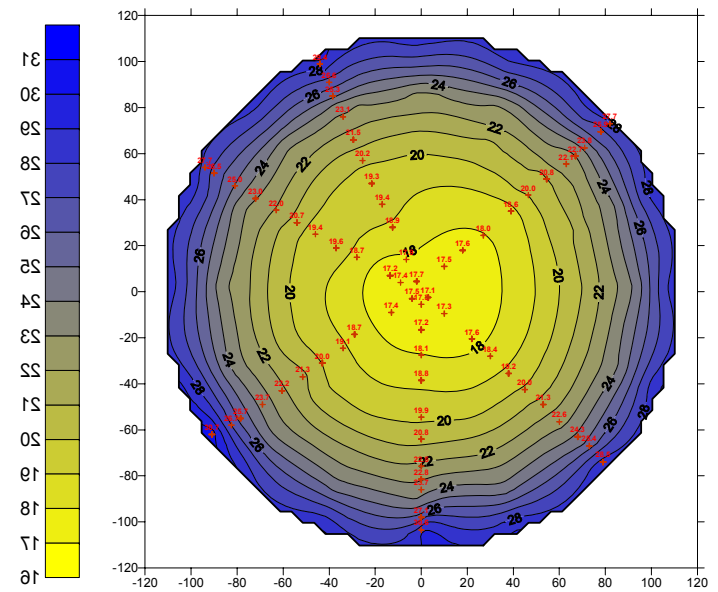


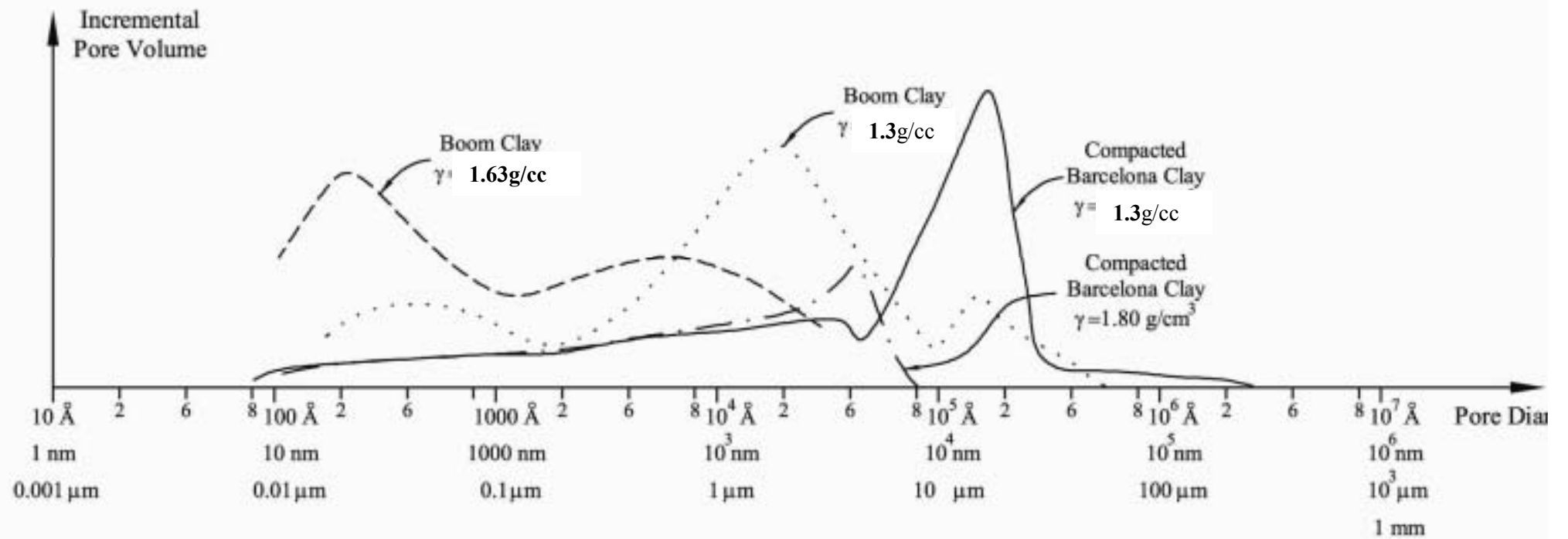
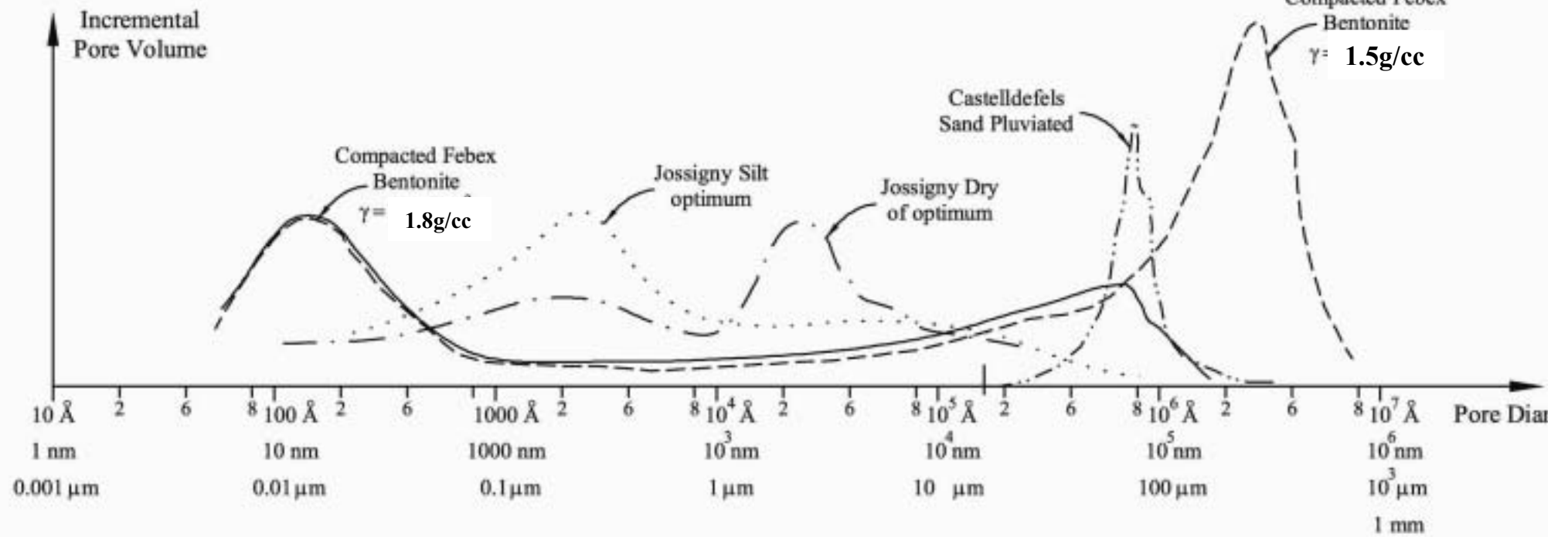
# Dismantling of FEBEX test

**Section 15**  
**x=327 cm**

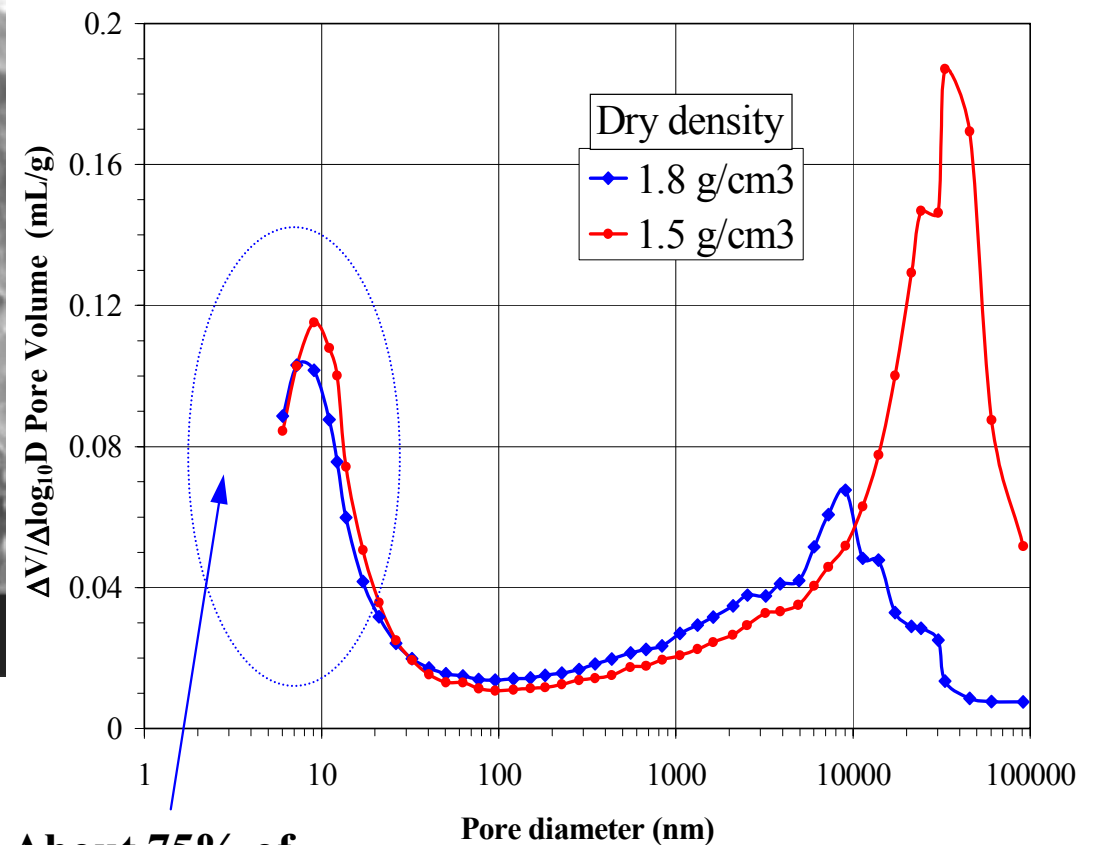
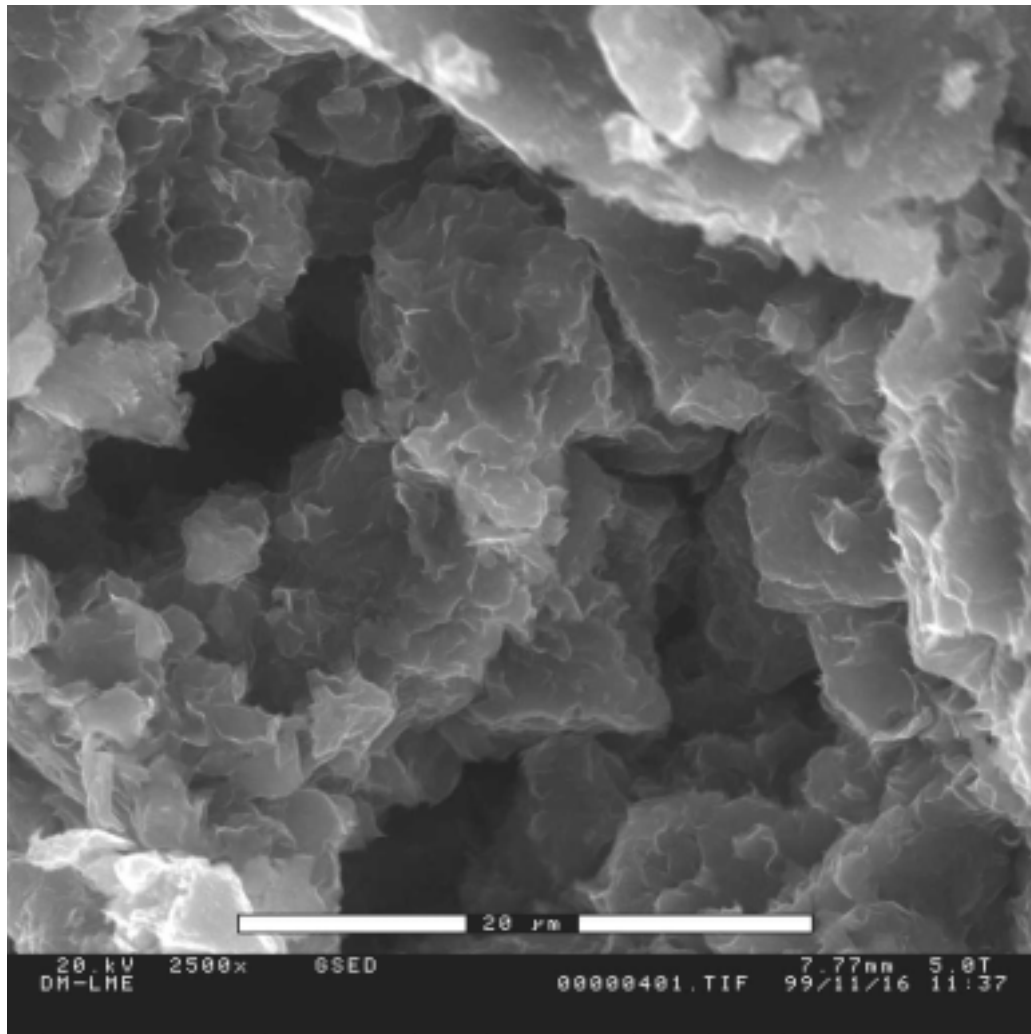


**Mean water content**  
**24.01 (%)**





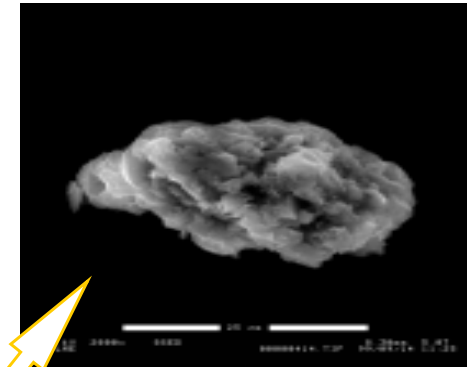
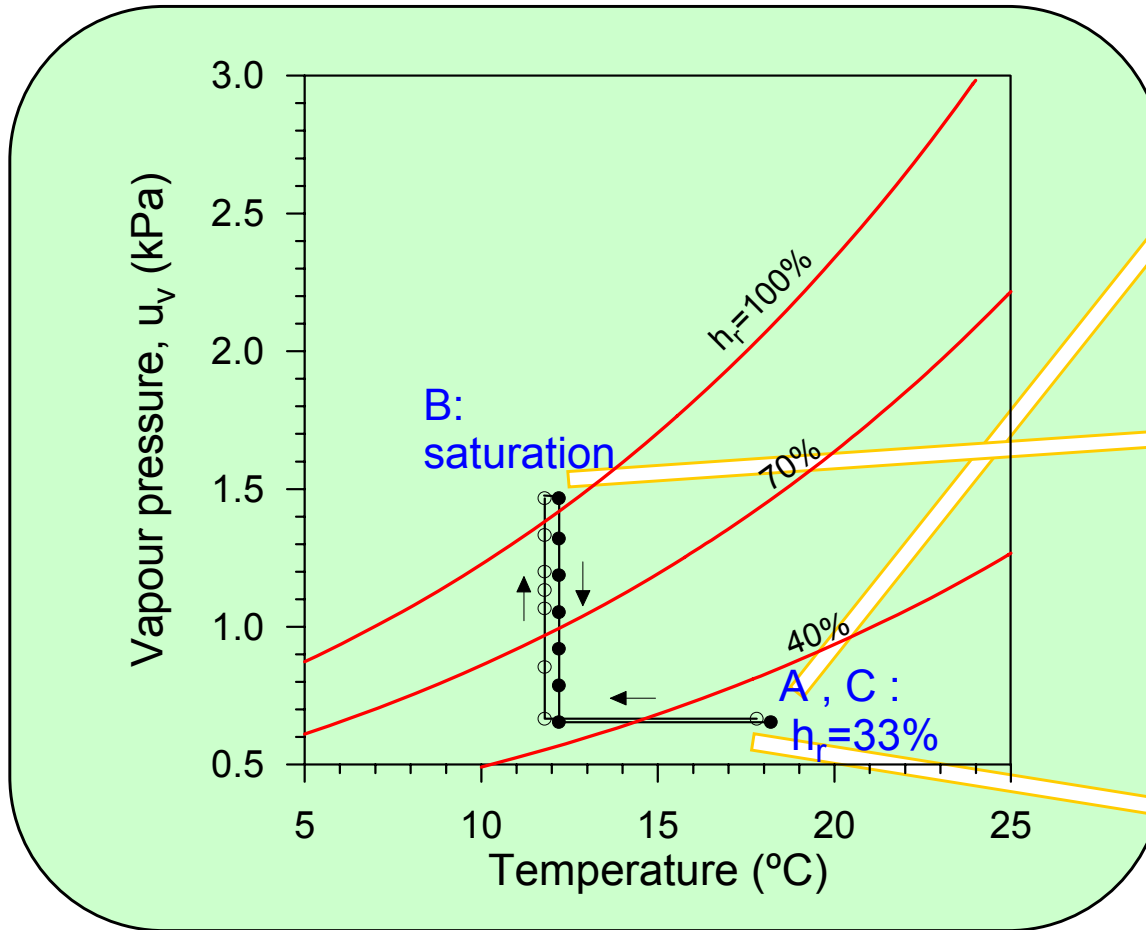
# Microstructure of FEBEX bentonite



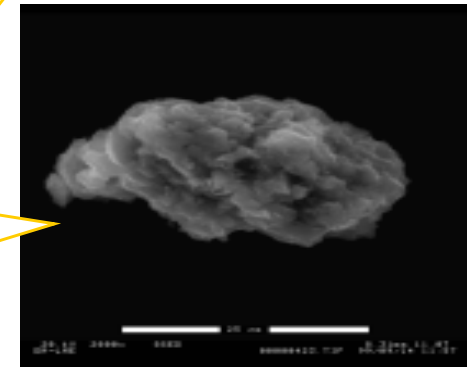
About 75% of  
total pore volume

# Interaction micro-macro

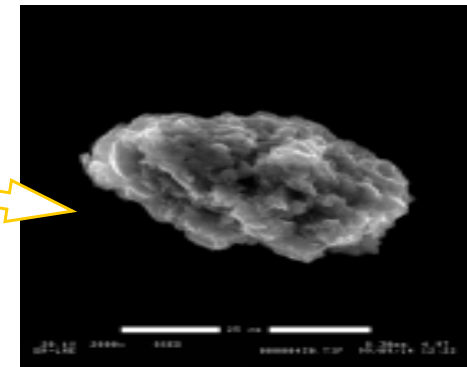
## ESEM observations



A

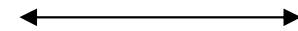


B



C

Wetting-drying cycle

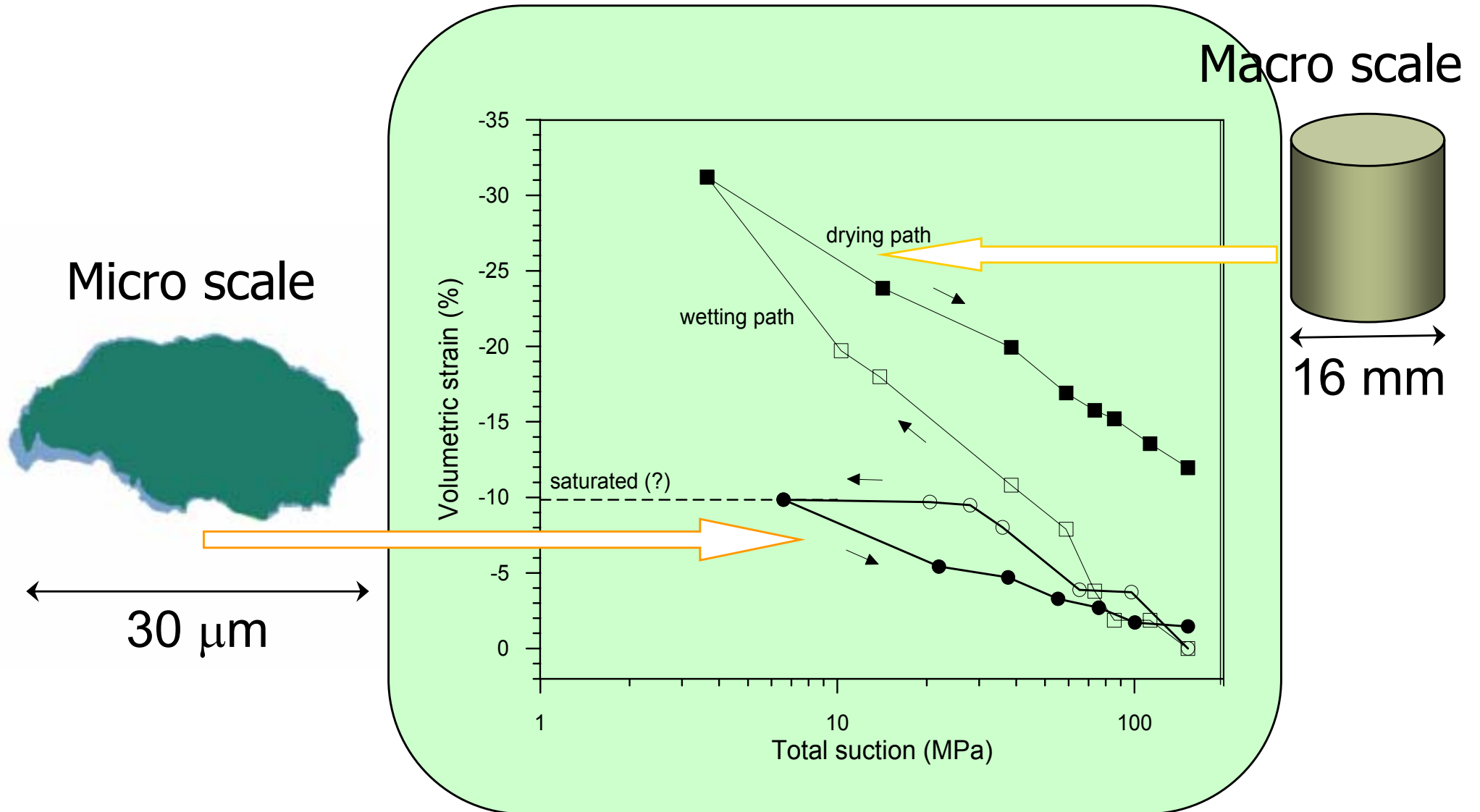


30  $\mu\text{m}$



# Interaction micro-macro

## ESEM observations / Swelling measurements



## MECHANISMS OF GAS TRANSPORT:

- Gas dissolved in water migrates through diffusion/convection. (Significant if low gas generation rates)
- Gas flow through the matrix of clay, partially displacing water (TWO PHASE FLOW). **Role of clay heterogeneity?**
- Gas flow through fissures and discontinuities
  - Existing discontinuities
  - Crack generation

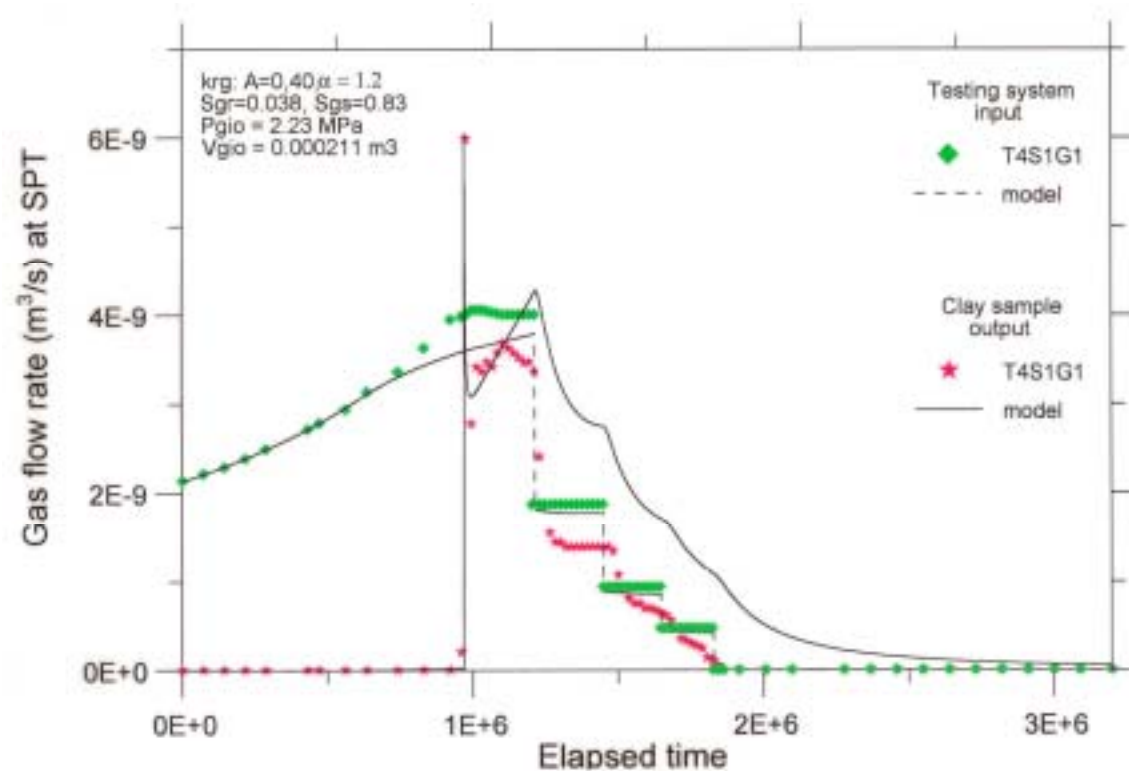
All the mechanisms may be present to a certain degree in a given case

# TWO PHASE FLOW. MAIN ISSUES

- Relative permeability
- Water retention

$$k_{rg} = A S_{eg}^{\alpha}$$

$$S_{eg} = (S_g - S_{gr}) / (S_{gs} - S_{gr})$$



(BGS T4S1G1 TEST, Horsemann, 1998)

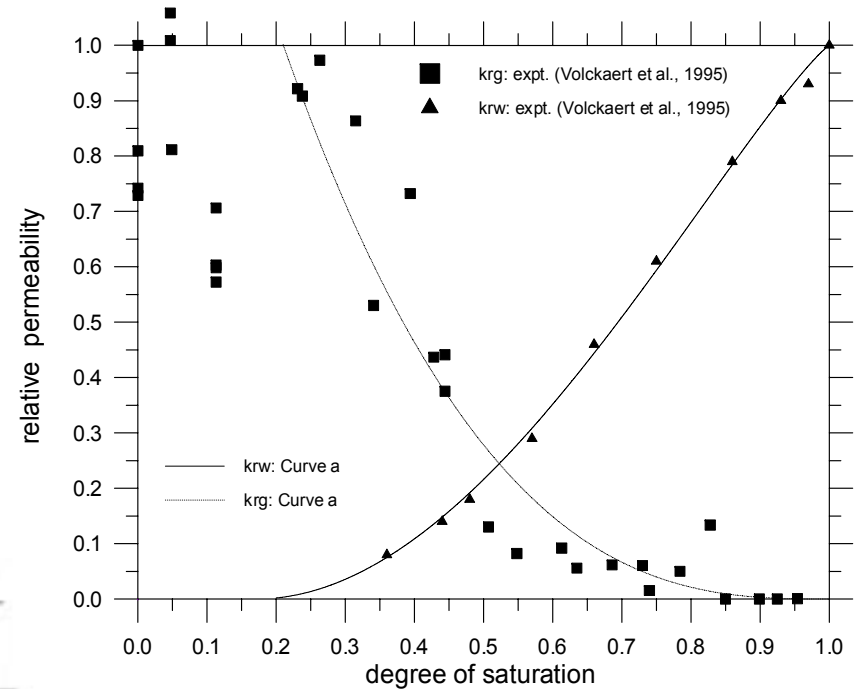
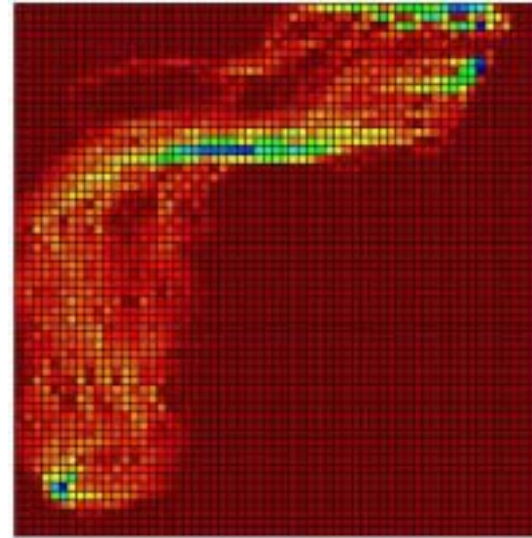


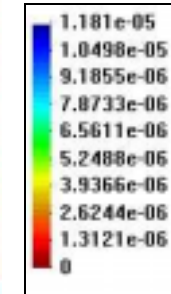
Fig. 2.2: Relative permeability data of Boom clay specimens and relationships adopted for the homogeneous and heterogeneous cases

EFFECT OF  
HETEROGENEITY.  
SIMULATION OF  
DIPOLE TESTS IN A  
PLANAR FRACTURE

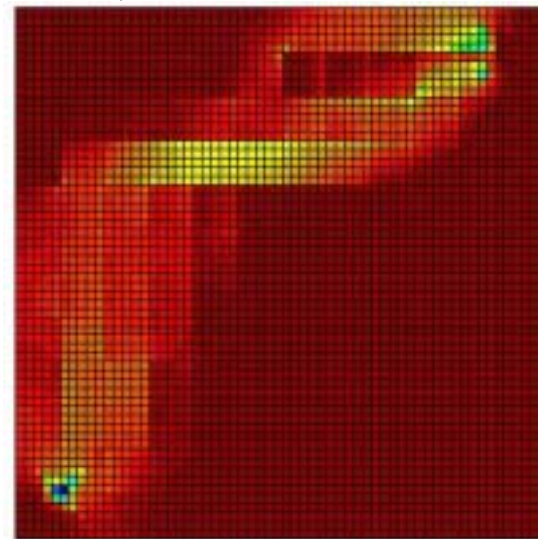
a) 60X60 ORIGINAL



“Point”  
properties

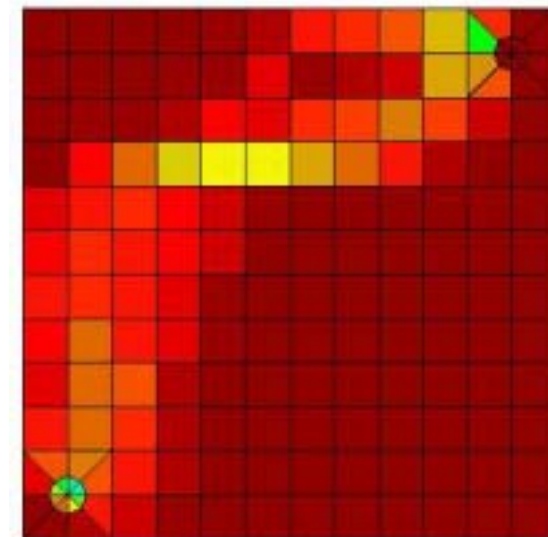


b) 60X60 UPSCALED



Averaged  
properties  
(upscale)

c) 12X12 UPSCALED

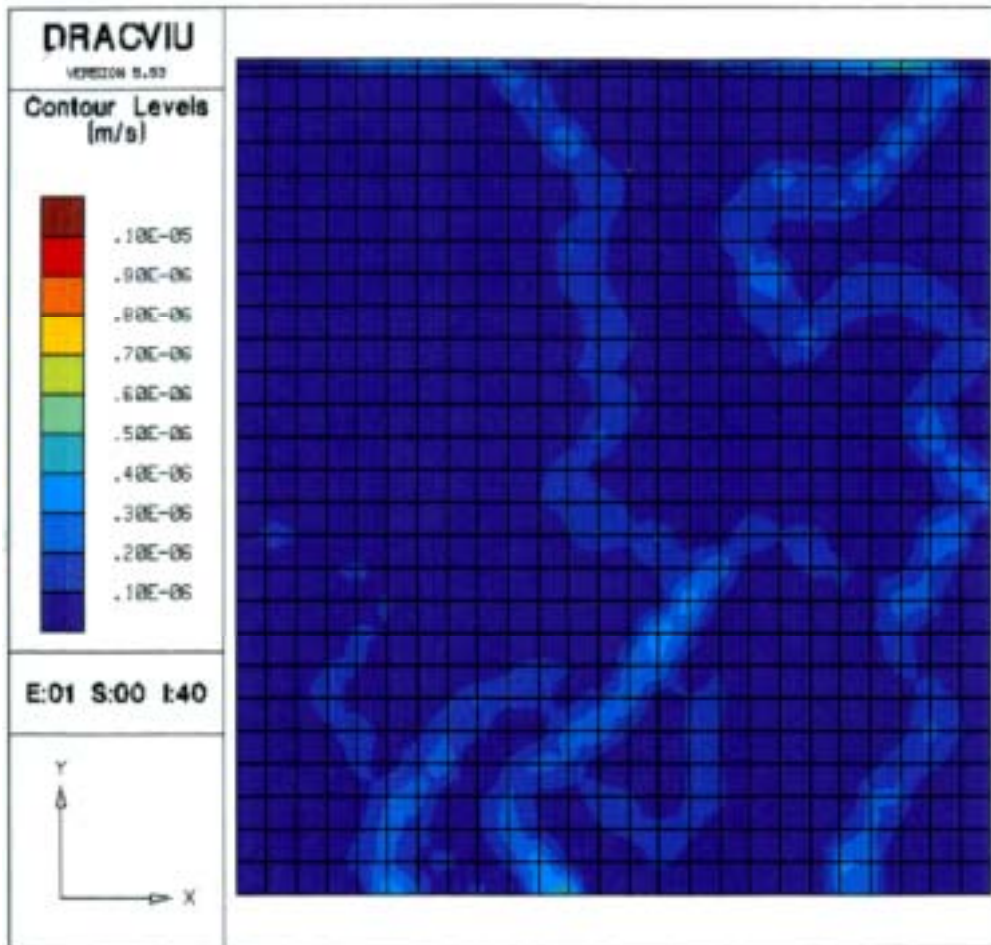


**Fig.7:** Gas fluxes obtained when performing the dipole test in the different fine and coarse grids at one particular time (6.7min).

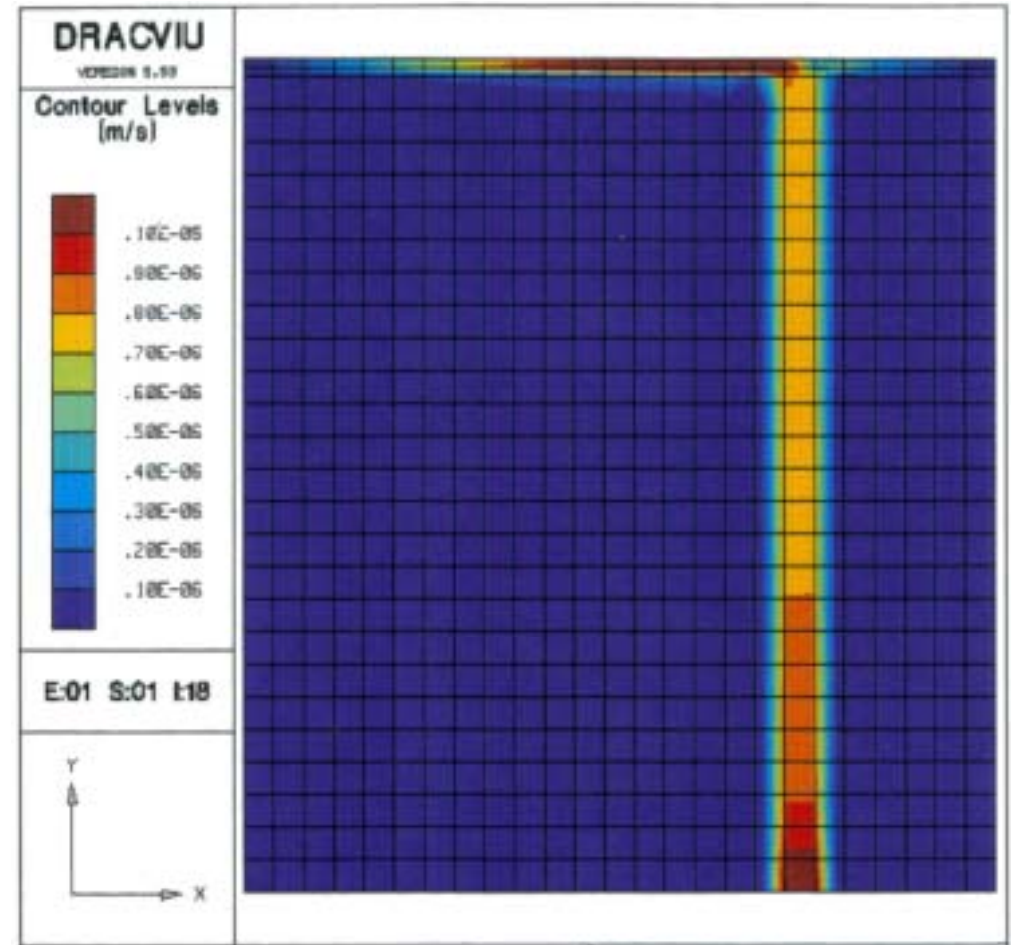
(H. Ramajo, S. Olivella, J. Carrera, X. Sánchez-Vila, 2002.

“Simulation of gas dipole tests in fractures at the intermediate scale using a new upscaling method” )

# PREFERENTIAL PATHS (GAS VELOCITY CONTOURS AT STEADY STATE) FOR ISOTROPIC AND ANISOTROPIC RANDOM FIELDS



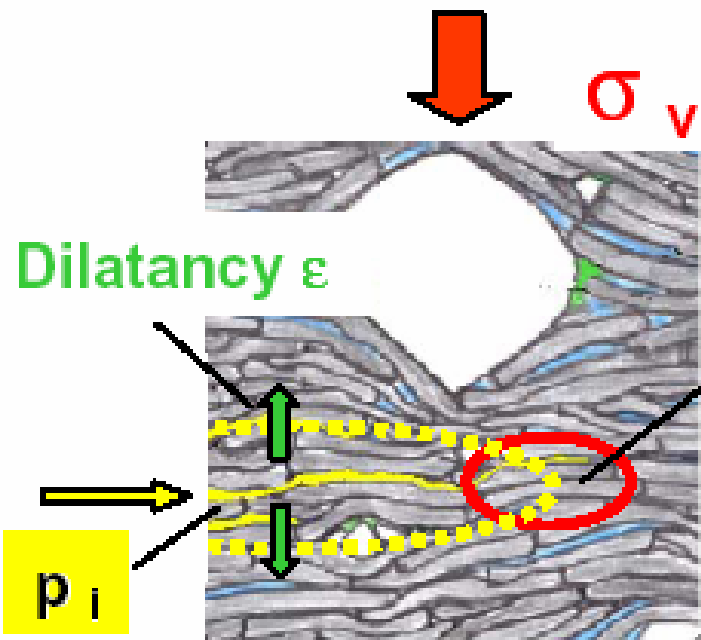
Random field 4: Isotropic



Random field 4b: H.anisotropic

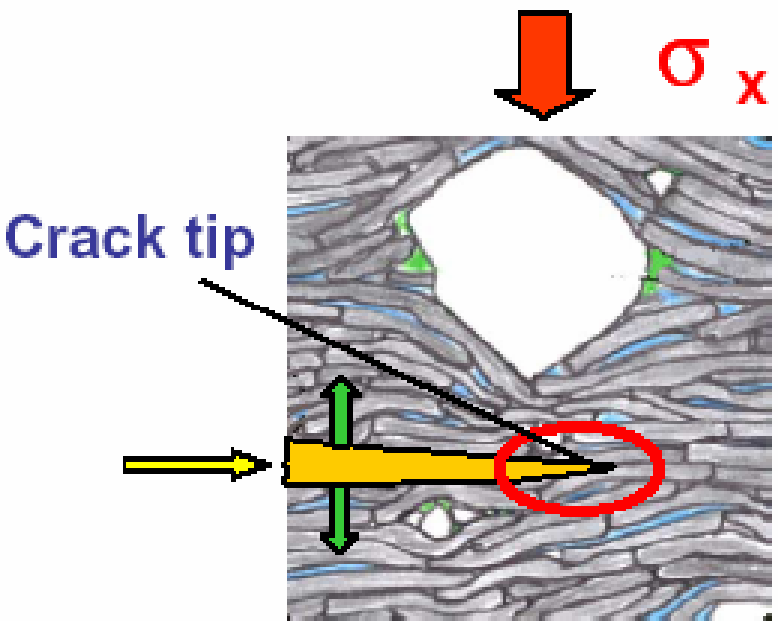
(CH Delahaye and E.E. Alonso, 2002. "Soil heterogeneity and preferential paths for gas migration".)

**MECHANISMS OF  
PATH FORMATION  
IN CLAY RICH  
BANDED ROCKS**



**Quasi-stationary  
damage zone  
propagation**  
(gas generation in  
equilibrium with  
dilatancy rate)

**Microscopic pathway dilation**



**Tensile strength  
exceeded due to  
fast pressure build-  
up**

**Macroscopic gas frac**

*(Marschall, 2002)*

# BALANCE EQUATIONS FOR THM ANALYSIS IN POROUS MEDIA

## SOLID PHASE

$$\frac{D_s \phi}{Dt} = \frac{1}{\theta_s} \left[ (1 - \phi) \frac{D_s \theta_s}{Dt} \right] + (1 - \phi) \nabla \cdot \frac{d\mathbf{u}}{dt}$$

## MASS BALANCE OF WATER

$$\phi \frac{D_s (\theta_l^w S_l + \theta_g^w S_g)}{Dt} + (\theta_l^w S_l + \theta_g^w S_g) \frac{D_s \phi}{Dt} + ((\theta_l^w S_l + \theta_g^w S_g) \phi) \nabla \cdot \frac{d\mathbf{u}}{dt} + \nabla \cdot (\mathbf{j}_l^w + \mathbf{j}_g^w) = f^w$$

## MASS BALANCE OF AIR

$$\phi \frac{D_s (\theta_l^a S_l + \theta_g^a S_g)}{Dt} + (\theta_l^a S_l + \theta_g^a S_g) \frac{D_s \phi}{Dt} + ((\theta_l^a S_l + \theta_g^a S_g) \phi) \nabla \cdot \frac{d\mathbf{u}}{dt} + \nabla \cdot (\mathbf{j}_l^a + \mathbf{j}_g^a) = f^a$$

## MOMENTUM BALANCE FOR THE MEDIUM

$$\textcircled{\text{R}} \quad -\boldsymbol{\tau} , \quad \mathbf{b} > \mathbf{0}$$

## INTERNAL ENERGY BALANCE FOR THE MEDIUM

$$\frac{\partial}{\partial t} (E_s \rho_s (1 - \phi) + E_l \rho_l S_l \phi + E_g \rho_g S_g \phi) + \nabla \cdot (\mathbf{i}_c + \mathbf{j}_{Es} + \mathbf{j}_{El} + \mathbf{j}_{Eg}) = f^Q$$

# A MODEL FOR GAS FLOW IN OPENING DISCONTINUITIES EMBEDDED IN A POROUS MEDIUM

1. The effect of local concentration of porosity along a given plane

- 1.1. Example

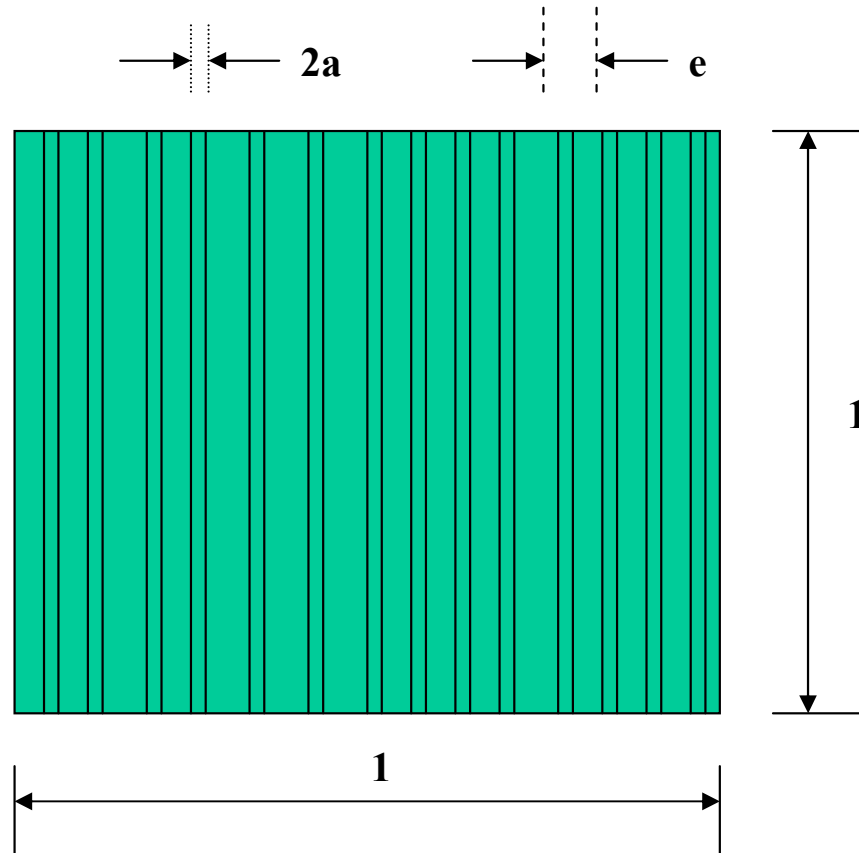
2. Generalization of the model

3. Modelling Rummel and Weber gas flow tests on Opalinus clay



# 1. The effect of local concentration of porosity along a given plane

## Flow along a set of channels. Viscous “Poiseuille” flow



$$\text{FLOW RATE : } q = 2aN.A.\frac{\gamma}{\mu}.(2a)^2.l \quad (1)$$

$$\text{Number of channels: } N = \frac{1}{e} = \frac{1}{D_{10}}$$

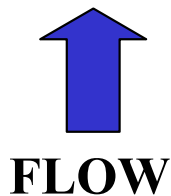
$$\text{Porosity : } n = \frac{2a}{e} = 2aN$$

**INTRINSIC PERMEABILITY, from (1):**

$$k = A \frac{n^3}{N^2} \quad \longrightarrow \quad dk = 3A \frac{n^2}{N^2} dn$$

$$k = An^3D_{10}^2 \quad \longrightarrow \quad dk = 3An^2D_{10}^2 .dn$$

N “channels”



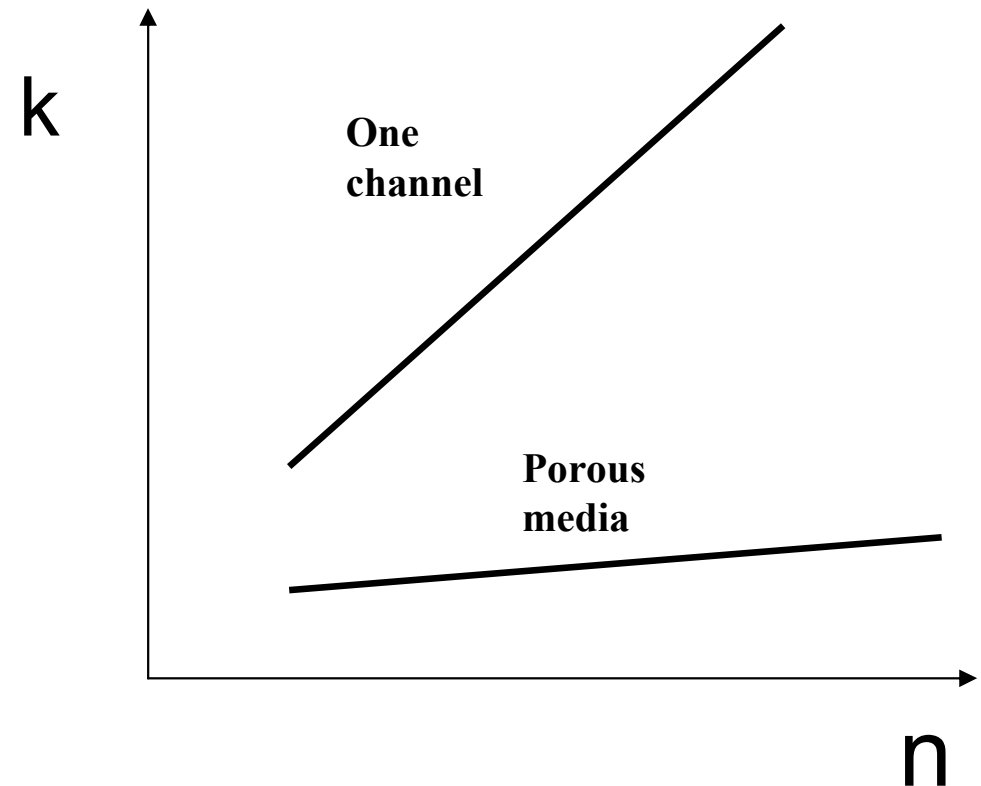
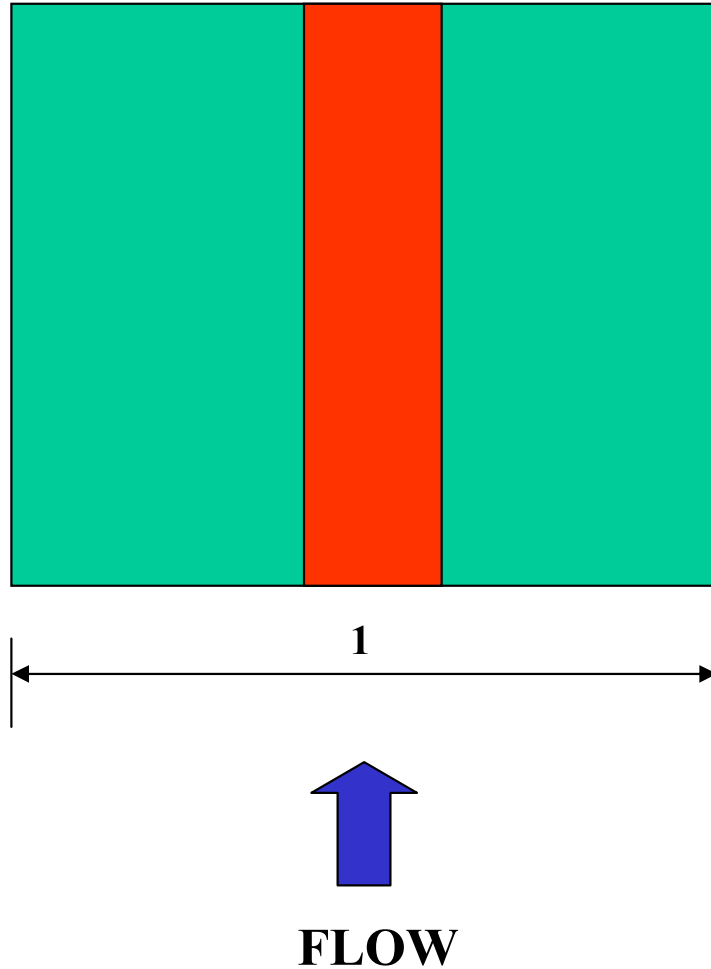
# 1. The effect of local concentration of porosity along a given plane

## Flow along a single channel. Viscous “Poiseuille” flow

Porosity is maintained :  $n$

Now,  $N=1$

$$k = An^3 \longrightarrow dk = 3An^2 \cdot dn$$



# 1. The effect of local concentration of porosity along a given plane

A finite number of channels ( $N_f$ ) become active beyond a threshold critical porosity,  $n_c$

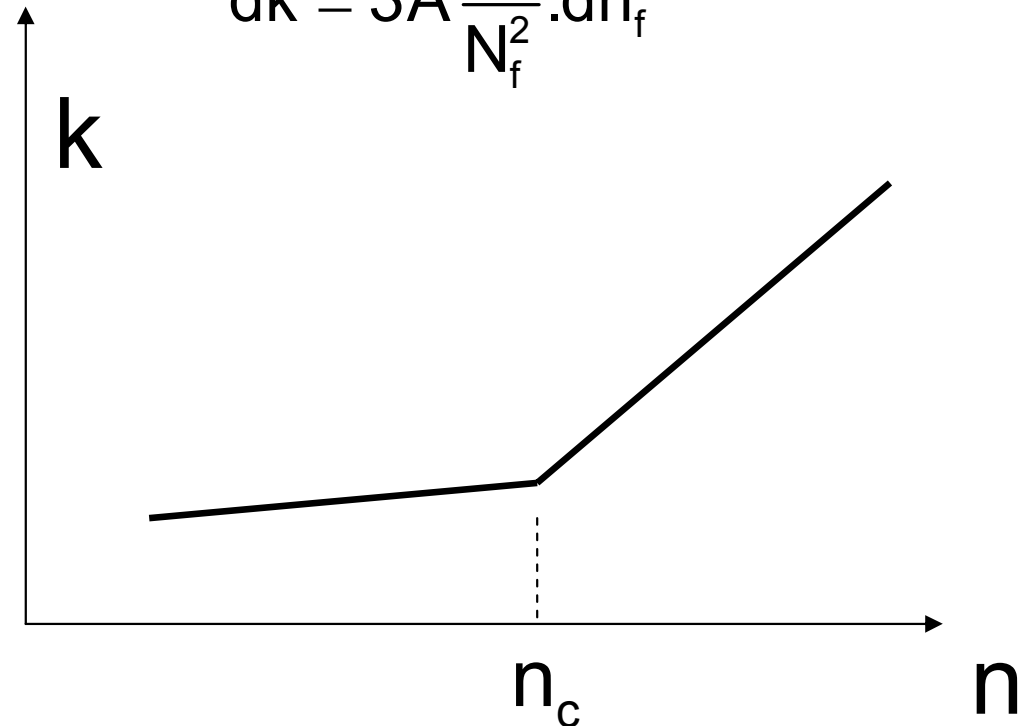
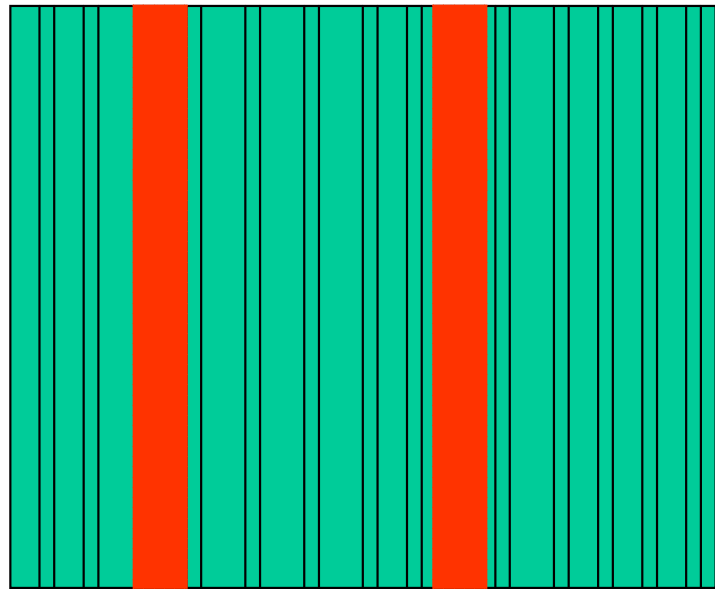
$n < n_c$  : Porous medium

$n > n_c$  : Porous medium + Open channels

$$n = n_c + n_f$$

$$k = An_c^3 D_{10}^2 + A \frac{n_f^3}{N_f^2} = k_{n_c} + A \frac{n_f^3}{N_f^2}$$

$$dk = 3A \frac{n_f^2}{N_f^2} \cdot dn_f$$



# 1. The effect of local concentration of porosity along a given plane

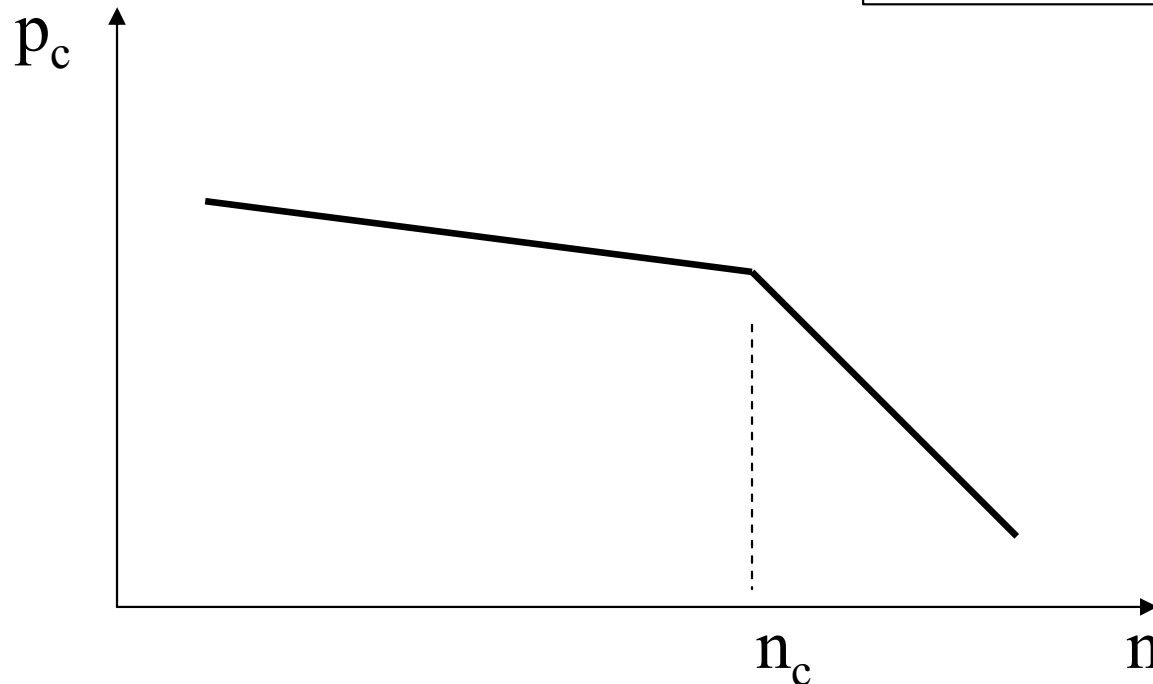
---

## Effect on air entry value

Laplace →  $p_c = \frac{2\sigma}{d}$

Flow in tubes →  $k = Cd^3$

$$p_c = \frac{2\sigma}{\sqrt[3]{k/C}}$$



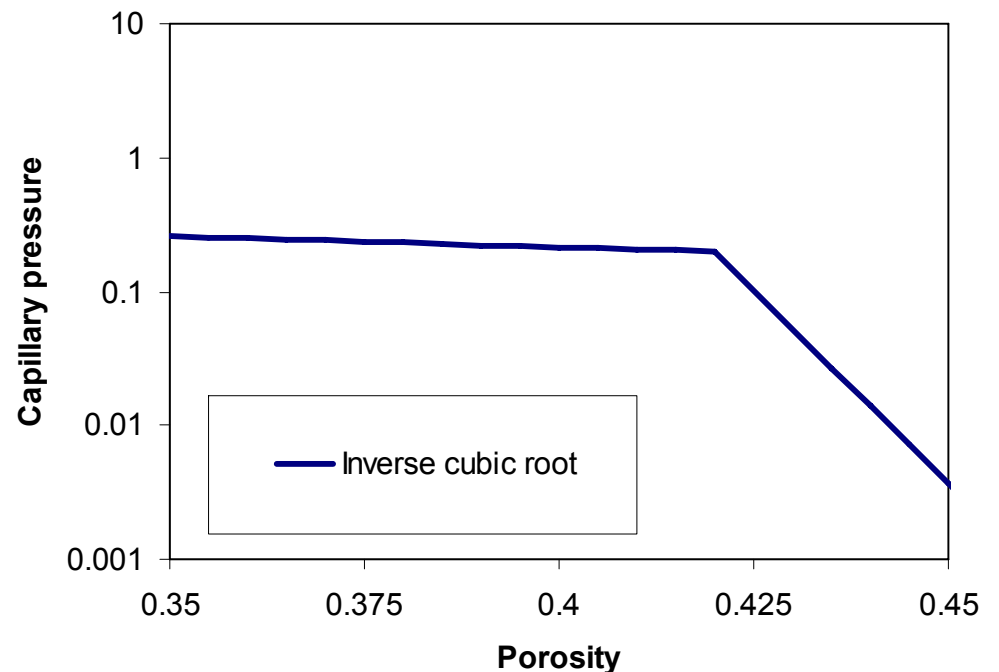
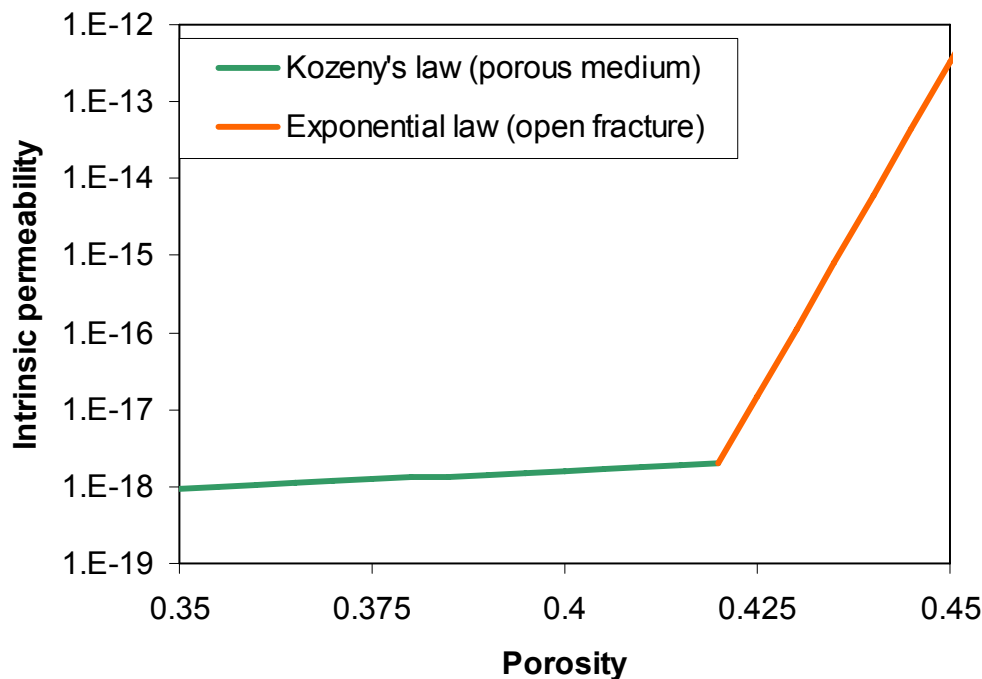
# 1. The effect of local concentration of porosity along a given plane. Example

Consider the following permeability and capillary pressure relationships:

● Permeability function for  
A material that can change  
the structure from porous to  
fractured medium:

● Capillary pressure  
for van Genuchten law  
calculated as:

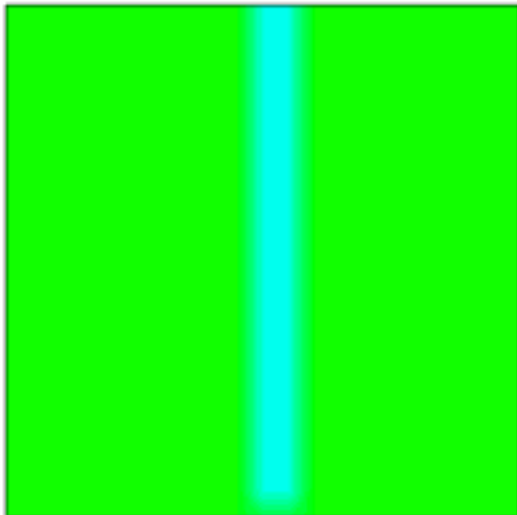
$$P = P_o \left( \frac{k_o}{k} \right)^{1/3}$$



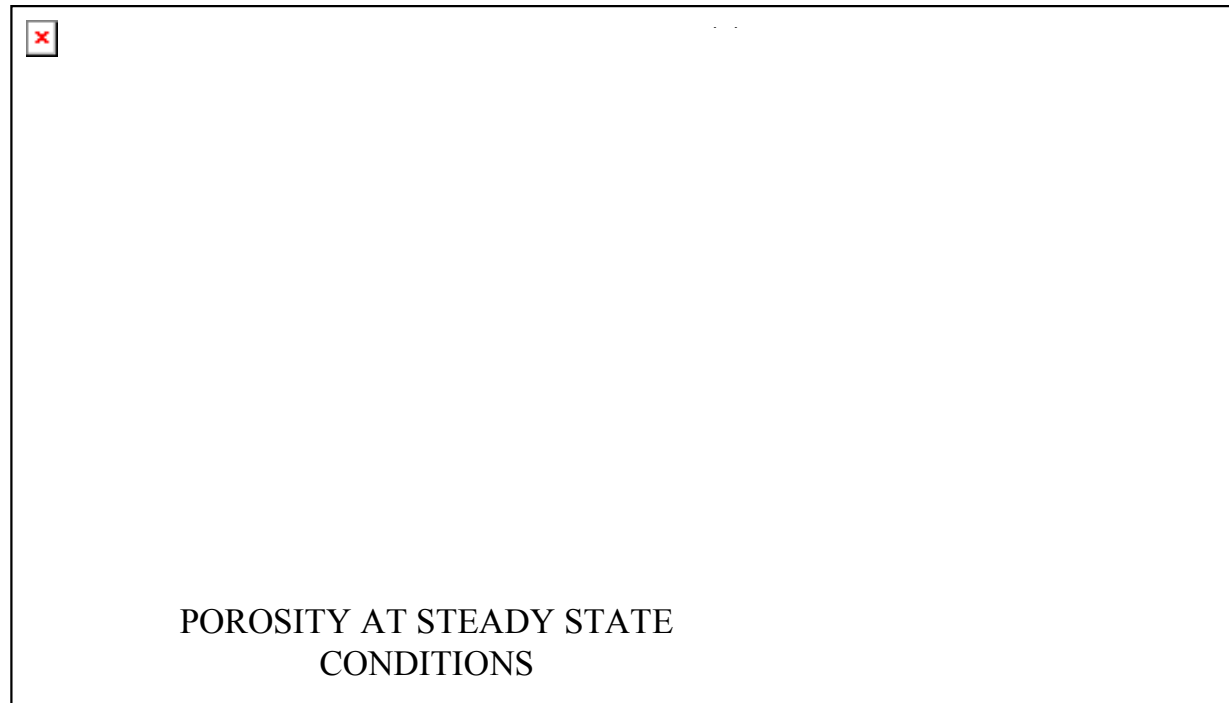
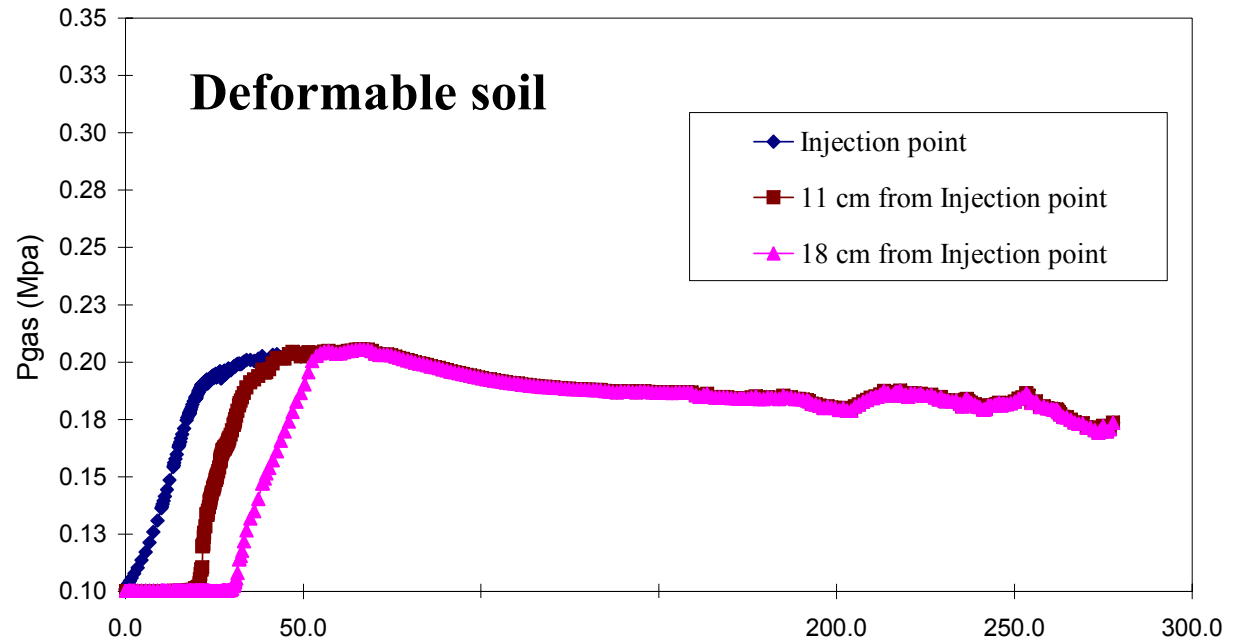
# 1. The effect of local concentration of porosity along a given plane. Example

SAMPLE (20 x 20 cm)  
WITH POROSITY  
EQUAL TO 0.40 AND  
INCLUDING A NON-  
HOMOGENEOUS ZONE  
(width = 1 cm ) WITH  
POROSITY EQUAL TO  
0.425.

**Constant gas inflow rate**



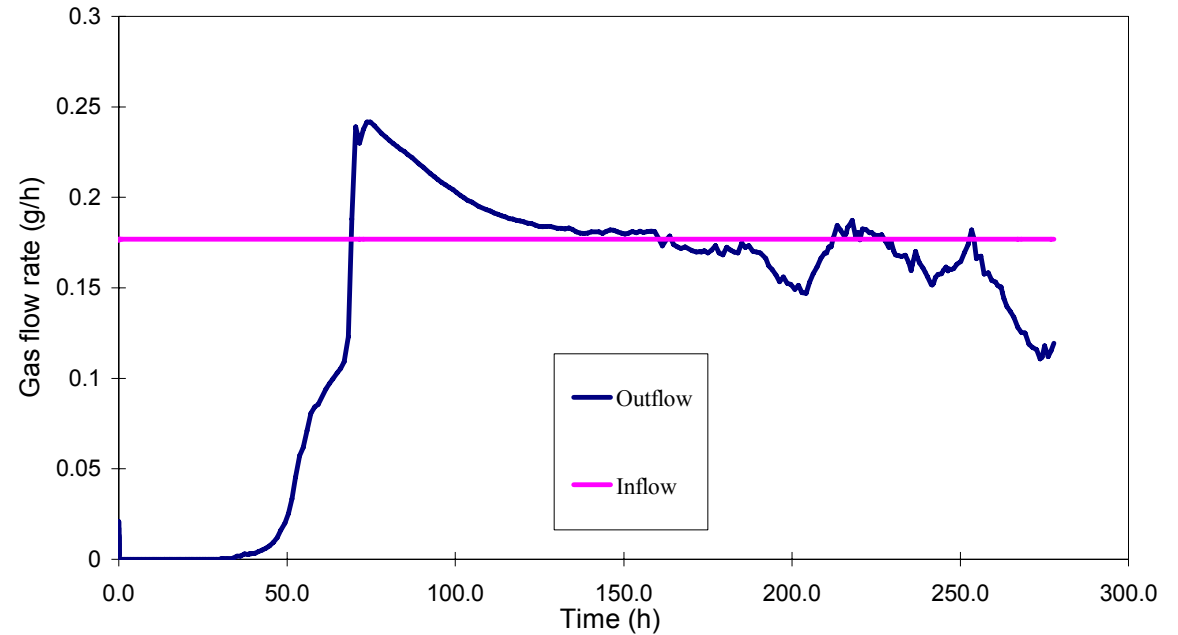
One dimensional analysis. Time evolution of  $P_{gas}$ .



# 1. The effect of local concentration of porosity along a given plane. Example

Time evolution of Gas Outflow

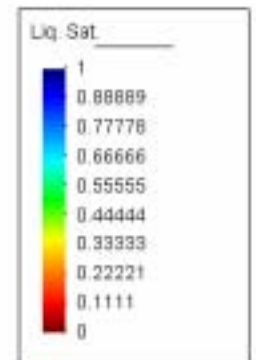
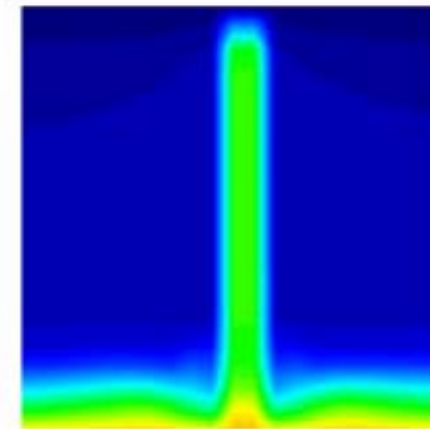
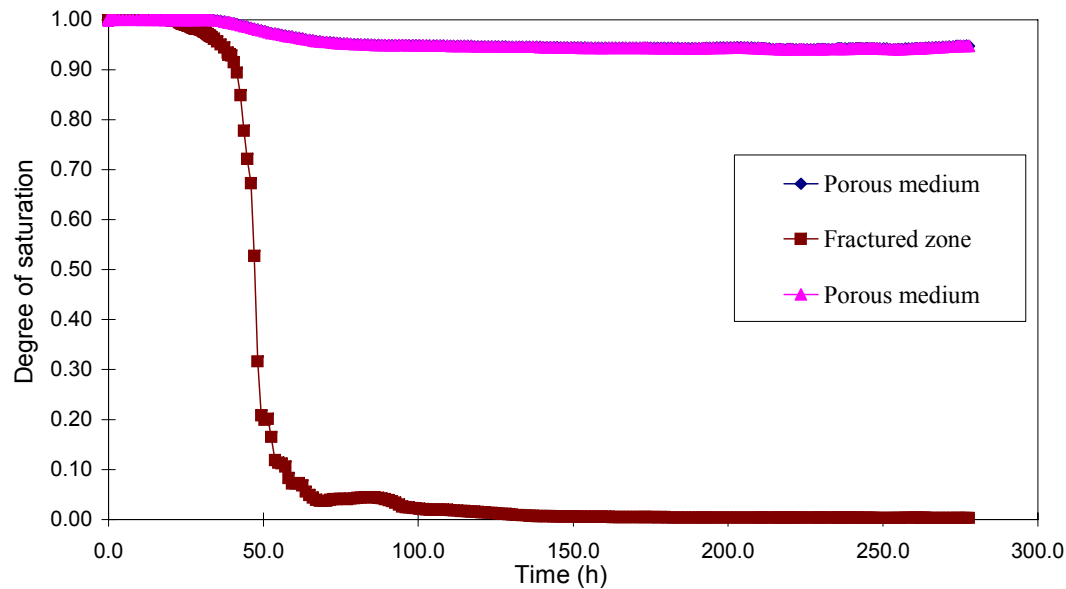
Evolution of gas flow rate



Evolution of degree of saturation

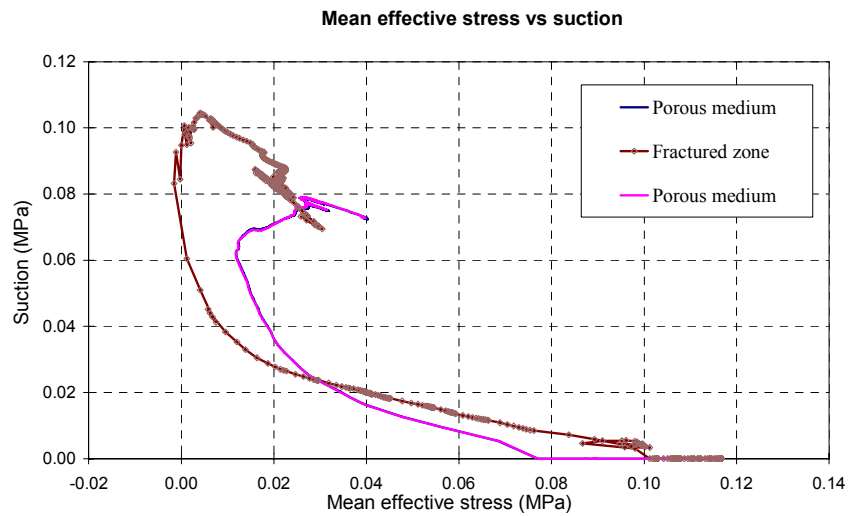


Degree of saturation

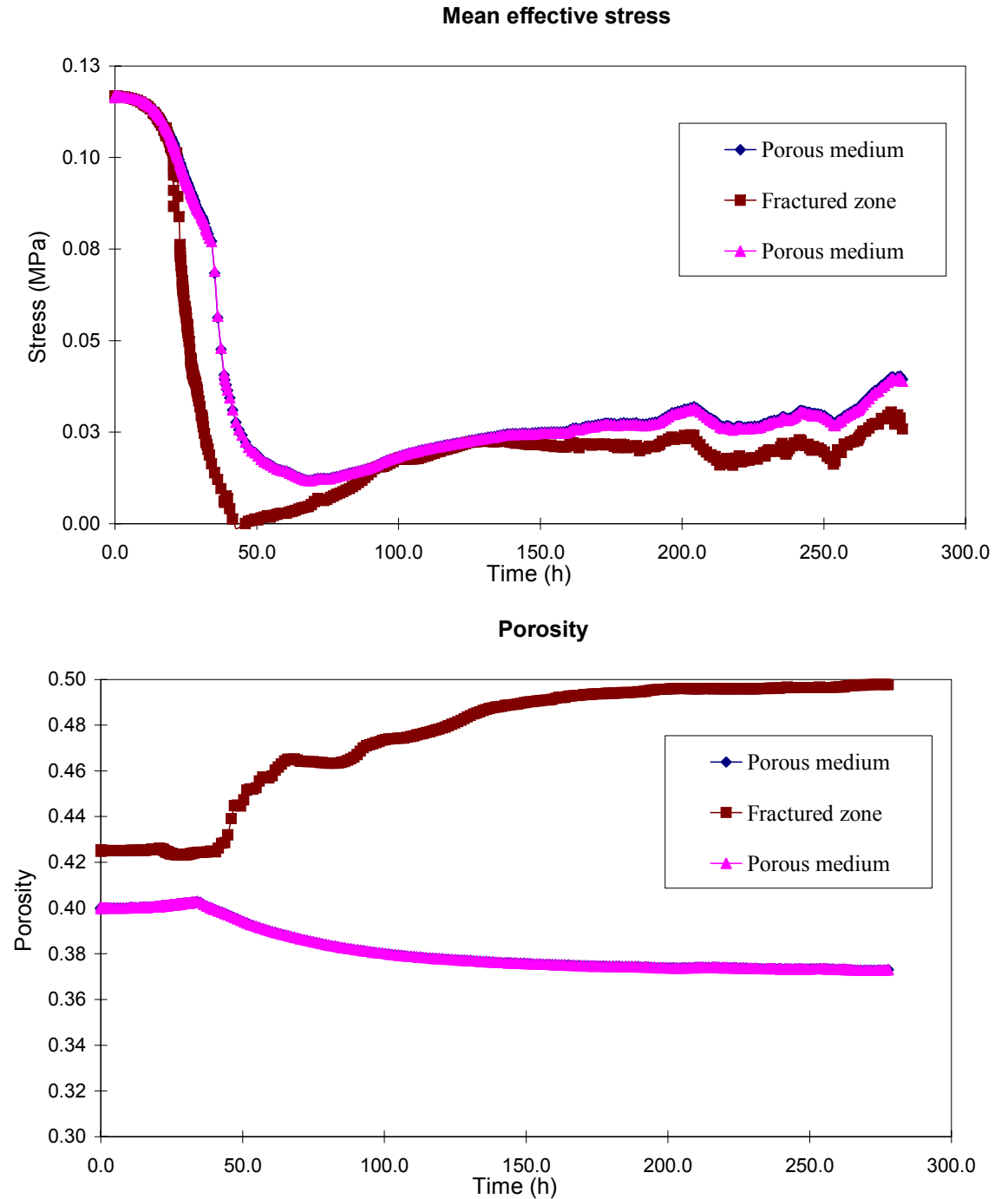


# 1. The effect of local concentration of porosity along a given plane. Example

Evolution of net mean stresses



Evolution of porosity





## 2. Generalization. Model description

---

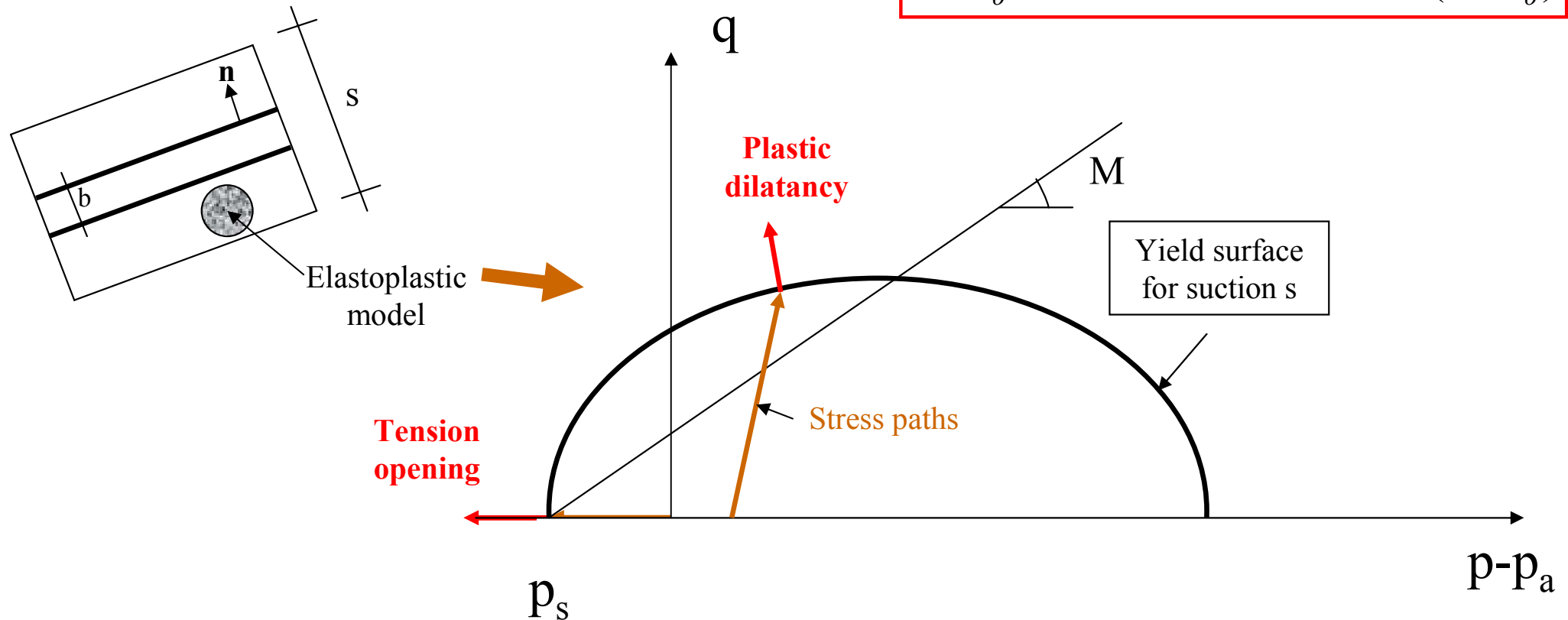
### Main ideas

- Gas flow takes place along a given surface/plane
- The plane is included in a “damaged” zone
  - Interfaces
  - Shear zones
  - Schistosity/Sedimentation planes
- Normal deformations to the reference plane result in fracture opening. Flow properties are modified accordingly (strong **anisotropy** of flow properties is induced)
- An appropriate elastoplastic (continuum) constitutive law defines the damaged zone

## 2. Generalization. Model description

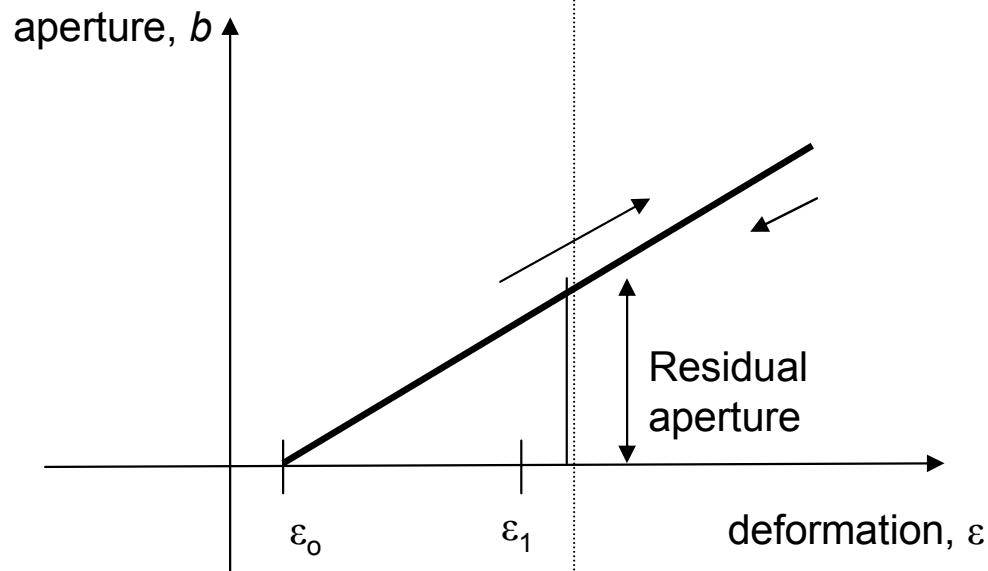
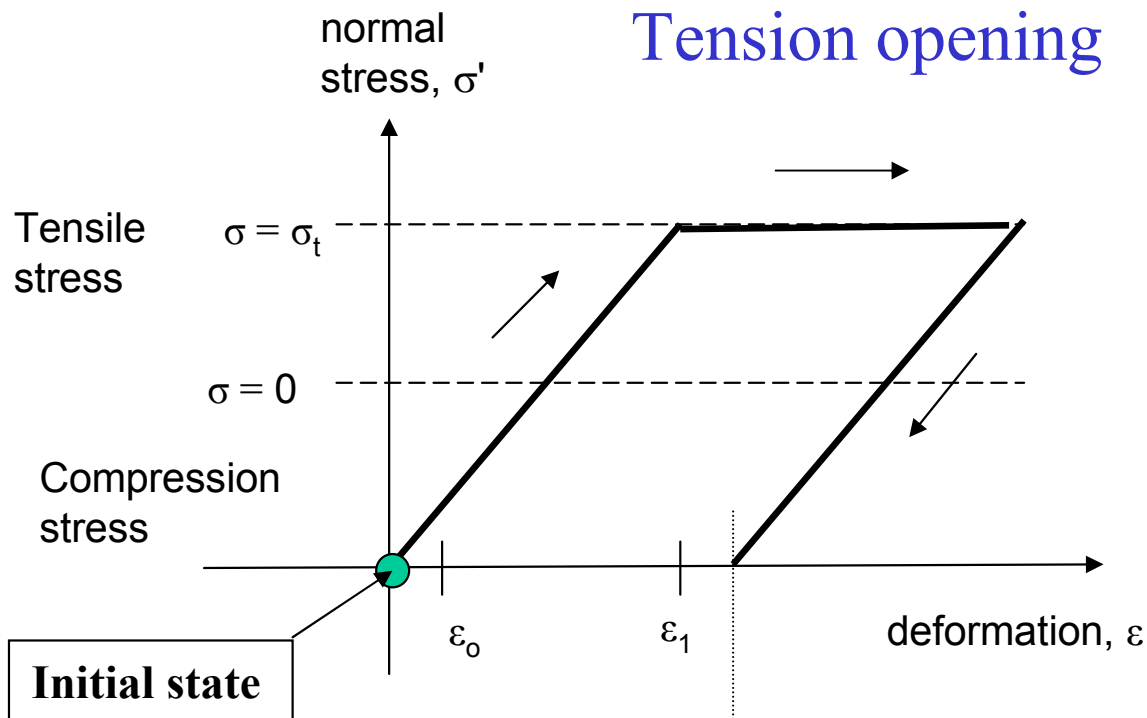
Accumulation of normal deformations in a given plane within a fractured zone.

$$b = b_o + \Delta b \quad \text{and} \quad \Delta b = s\Delta\epsilon = s(\epsilon - \epsilon_o)$$



- Model for damaged zone based on elastoplastic BBM
- Suction changes (drying-wetting) induces shrinkage/swelling
- Tensile strength depends on current suction

## 2. Generalization. Model description



$\epsilon_0$ : threshold deformation to start fracture opening

$\epsilon_1$ : deformation corresponding to tensile strength

$\sigma_t$ : tensile strength of the fracture

Cases:

Existing fracture

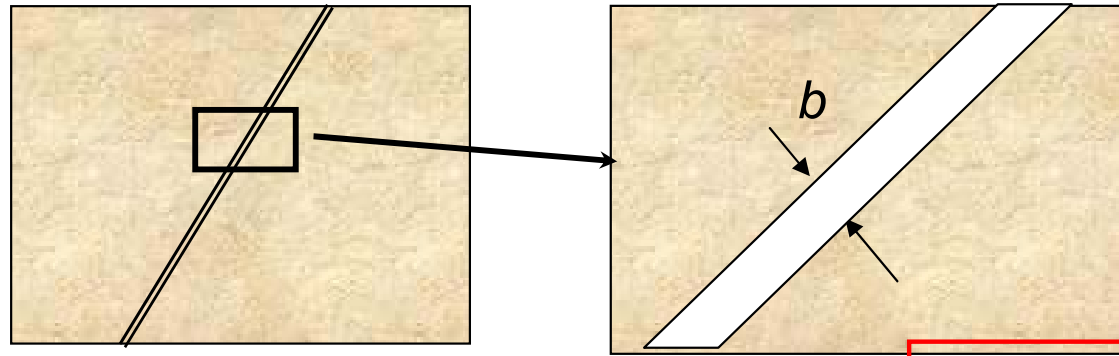
$$\sigma_t = 0, \epsilon_0 \approx 0$$

Non existing fracture:

$$\sigma_t \neq 0 \text{ and } \epsilon_0 = \epsilon_1 \neq 0$$

## 2. Generalization. Model description

### Hydraulic characterization of fracture element



$$k_{fracture} = \frac{b^2}{12}$$

- Intrinsic permeability (laminar flow):

- Equivalent permeability of fracture:

$$k_{equivalent} = k_{fracture} \frac{b}{s} = \frac{b^3}{12s}$$

- Equivalent permeability of element:

$$k_{element} = k_{fracture} \frac{b}{s} + k_{porous} \frac{s-b}{s} \cong \frac{b^3}{12s} + k_{porous}$$

## 2. Generalization. Model description

---

### Hydraulic characterization of fracture element

- Capillary air entry pressure:

$$P = P_o \frac{\sqrt[3]{k_{fracture\_o}}}{\sqrt[3]{k_{fracture}}}$$

- Updated permeability:

$$k_{new} = k_{old} \frac{b_{new}^3}{b_{old}^3}$$

- Adopted initial permeability :

$$k_{element} = \frac{b^3}{12s} = \frac{(10^{-7})^3}{12 \times 0.001} \cong 10^{-19} \text{ m}^2$$

Typical of a low porosity rock such as Opalinus clay

## 2. Generalization. Model description

### Elastoplastic model for the rock and fractured zones

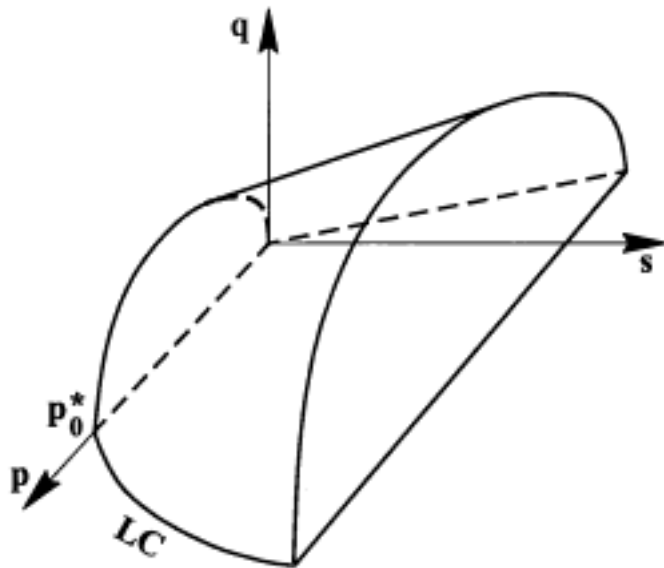
#### Yield function

$$F > F(p', J, \rho, \phi_v^p, s^*)$$

$$p' > \frac{1}{3} (\tau'_x, \tau'_y, \tau'_z)^*$$

$$J > \frac{1}{2} \text{trace}(ss) \quad s > \tau' \cdot p' \mathbf{I}$$

$$\rho > \frac{1}{3} (\sin^{-1}) 1.5\sqrt{3} \det s / J^3 \quad (\text{Lode's angle})$$



$$F > \frac{3J^2}{g_y^2} \cdot L_y^2 p', P_s^*) P_o \cdot p'^* > 0$$

$$L_y > \frac{M}{g_y} \rho > \frac{\theta}{6}^*$$

$$P_o = P^c \left( \frac{P_o^*}{P^c} \right)^{\frac{\lambda(o)-kio}{\lambda(s)-kio}}$$

$$\lambda(s) = \lambda(o) [(1-r) \exp(-\beta s) + r]$$

$$P_s = k s + P_{so}$$

## 2. Generalization. Model description

---

### Elastoplastic model for the rock and fractured zones

#### Hardening

$$dP_o^* = \frac{1+e}{\lambda(0) - k_{io}} P_o^* d\varepsilon_v^p$$

#### Plastic potential (non associated)

$$G = \frac{3J^2}{g_p^2} - \alpha L_p^2 (p' + P_s)(P_o - p')$$

$$L_p > \frac{M}{g_p \rho > \cdot \theta/6^*}$$

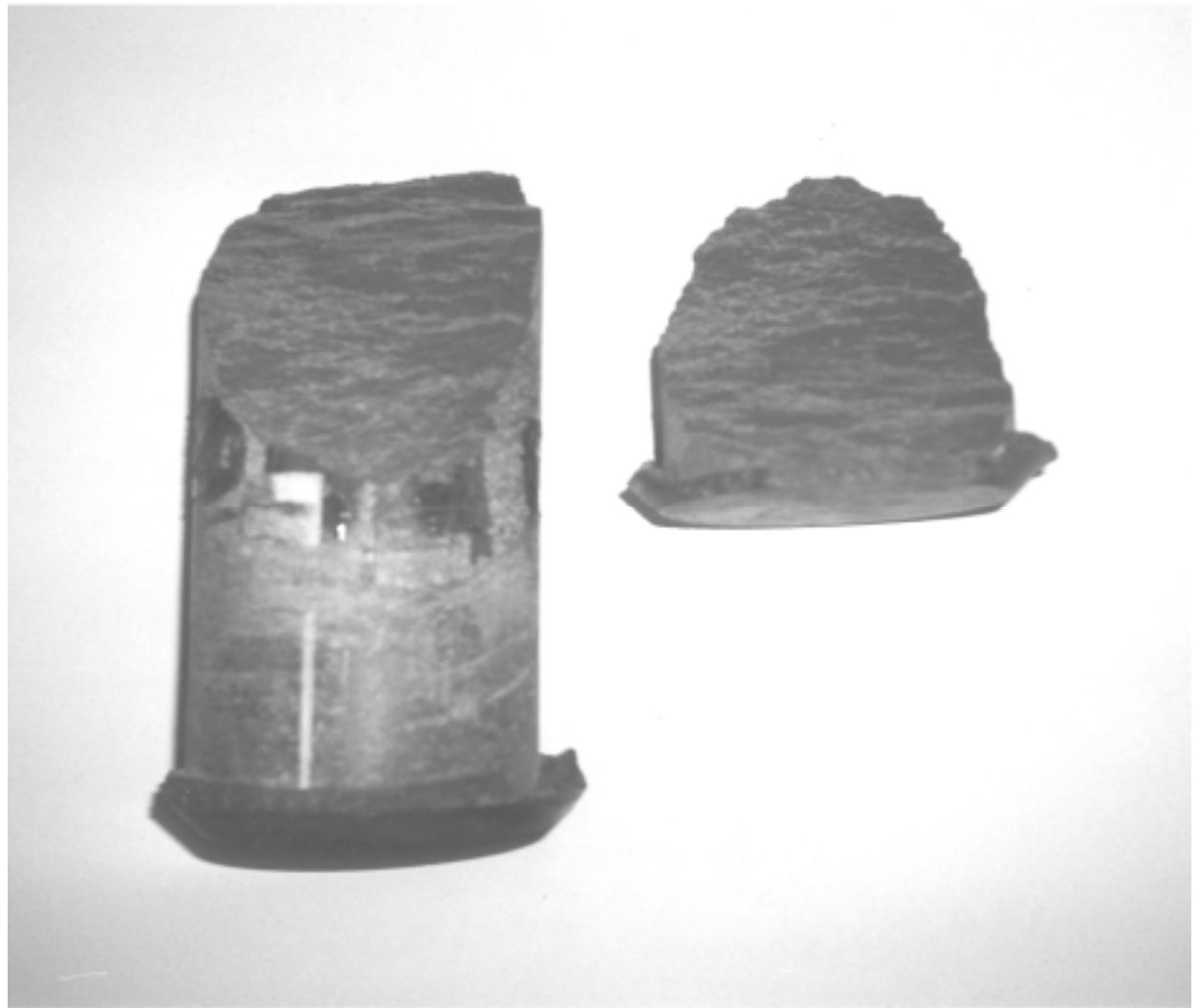
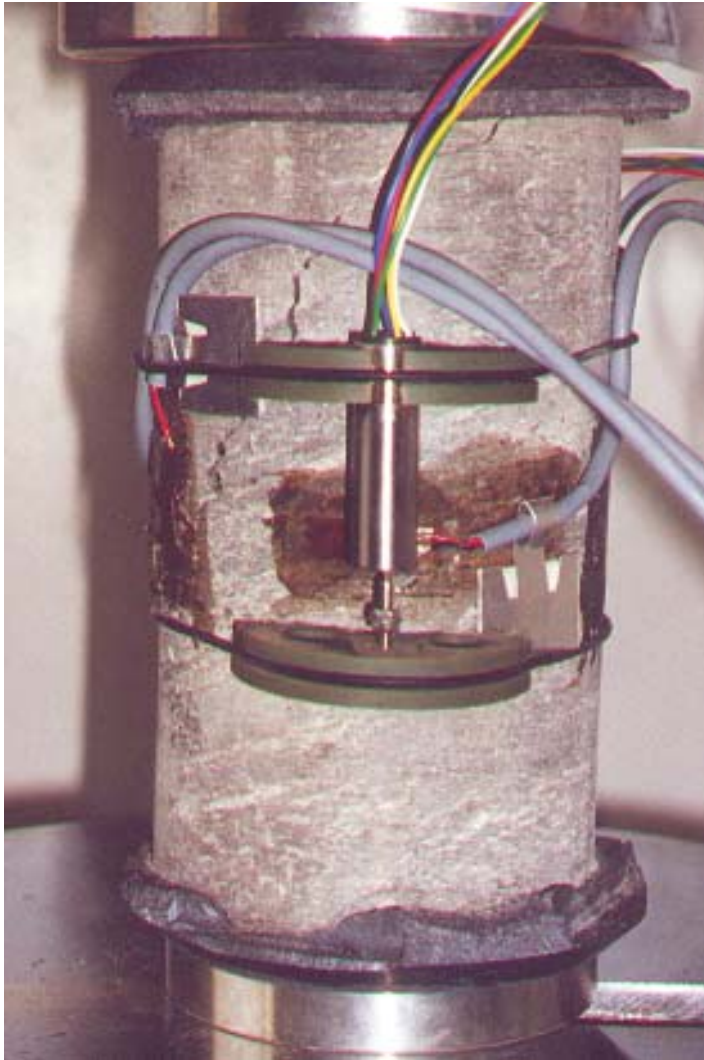
#### Elastic strains

$$d\varepsilon_v^e = \frac{1}{K} dp' + \underbrace{\frac{k_s}{1+e} \frac{ds}{s+0.1}}_{\text{Model for swelling and shrinkage deformations}}$$

Model for swelling and shrinkage deformations

# MONTERRI “OPALINUS” CLAYSTONE, Switzerland

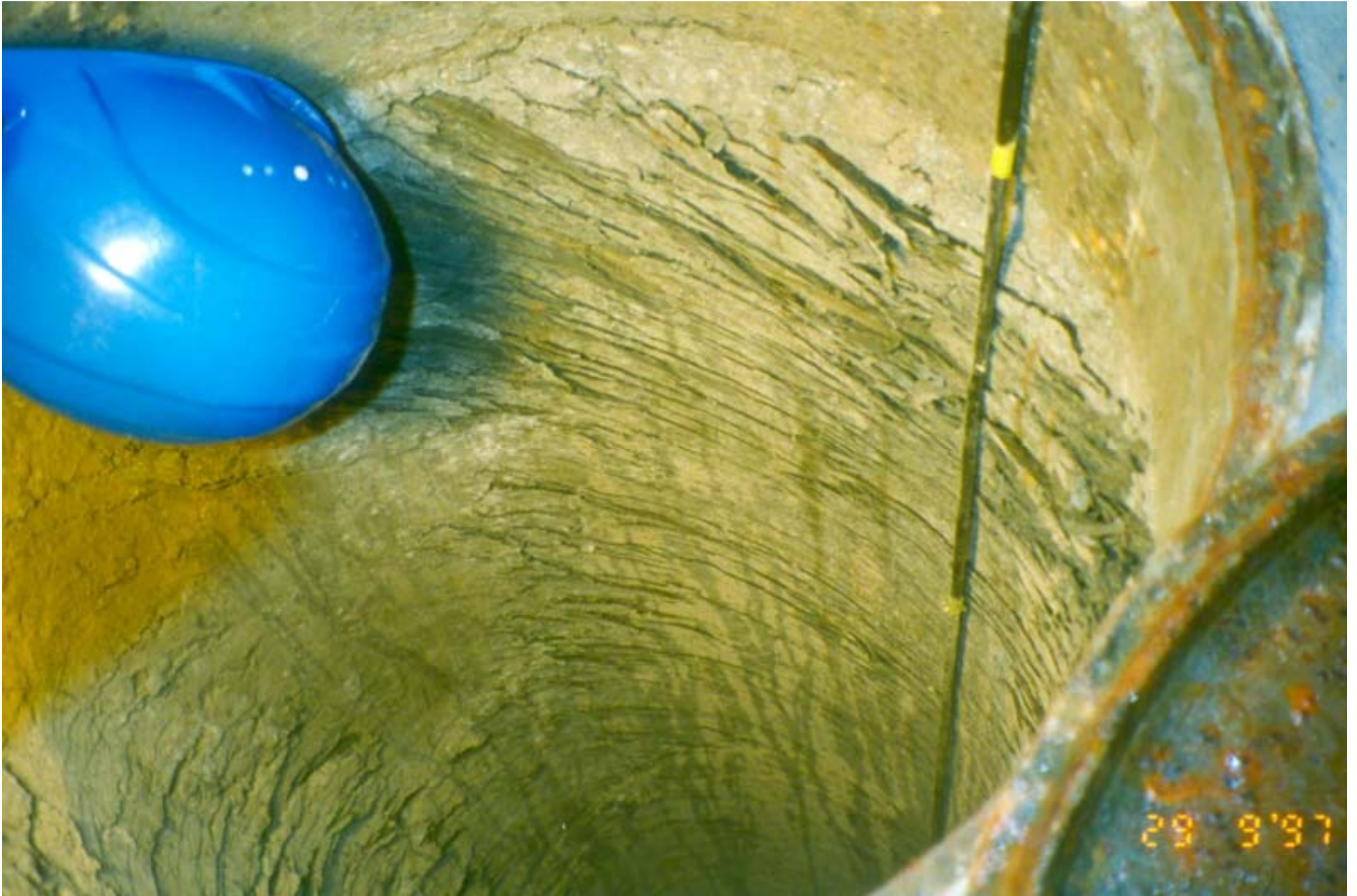
---





# MONTERRI "OPALINUS" CLAYSTONE, Switzerland

---



## Mineralogy (M. Hohner & P. Bossart)

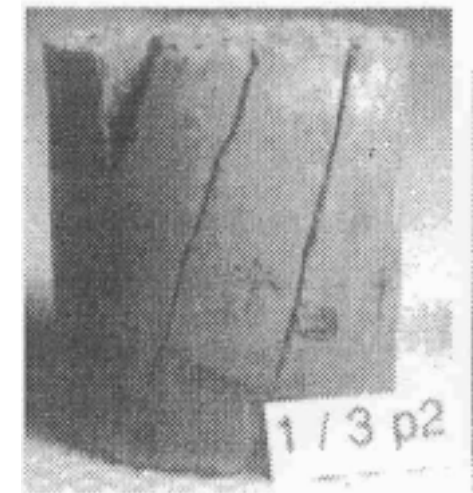
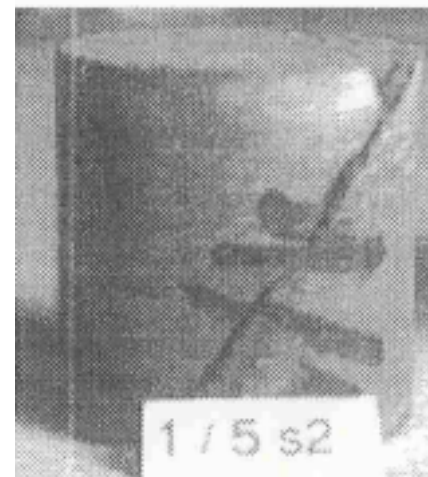
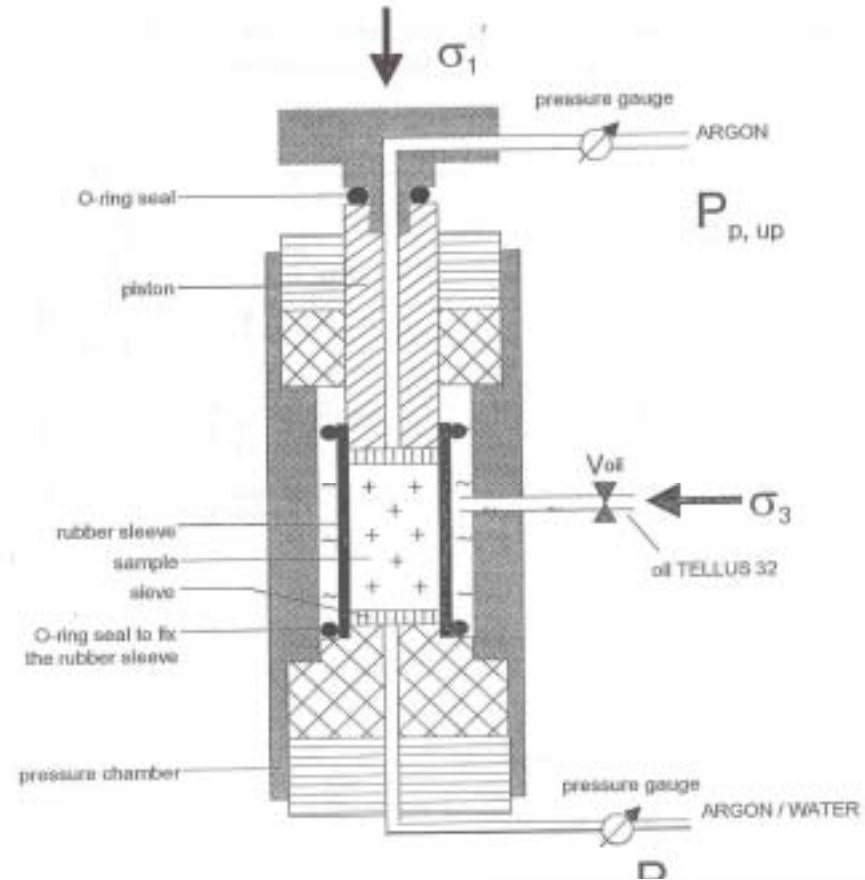
Illite [%]	16.6 – 27.0
Chlorite [%]	9.2 – 13.2
Kaolinite [%]	16.6 – 25.7
Illite/smectite ML [%]	7.6 – 15.9
Quartz	9 – 14
Feldspars	0 – 2
Carbonates	
-Calcite	4 – 25
-Siderite	1 – 7
-Ankerite	< 1
Pyrite	0.3 – 1.7
Organic carbon	0.3 – 1.3

### 3. Modelling Rummel and Weber tests

- Triaxial+gas and water injection tests on intact and broken samples

#### TEST PROTOCOL

- Initial gas pulse test on intact samples
- Rock sample broken when a deviatoric stress state was applied.
- Gas tests show the change in permeability induced by fracture formation
- Water flooding carried out to heal the sample.
- Further gas pulse tests to check permeability



### 3. Modelling Rummel and Weber tests

---

Tests were interpreted in terms of permeability changes associated with different states of the rock

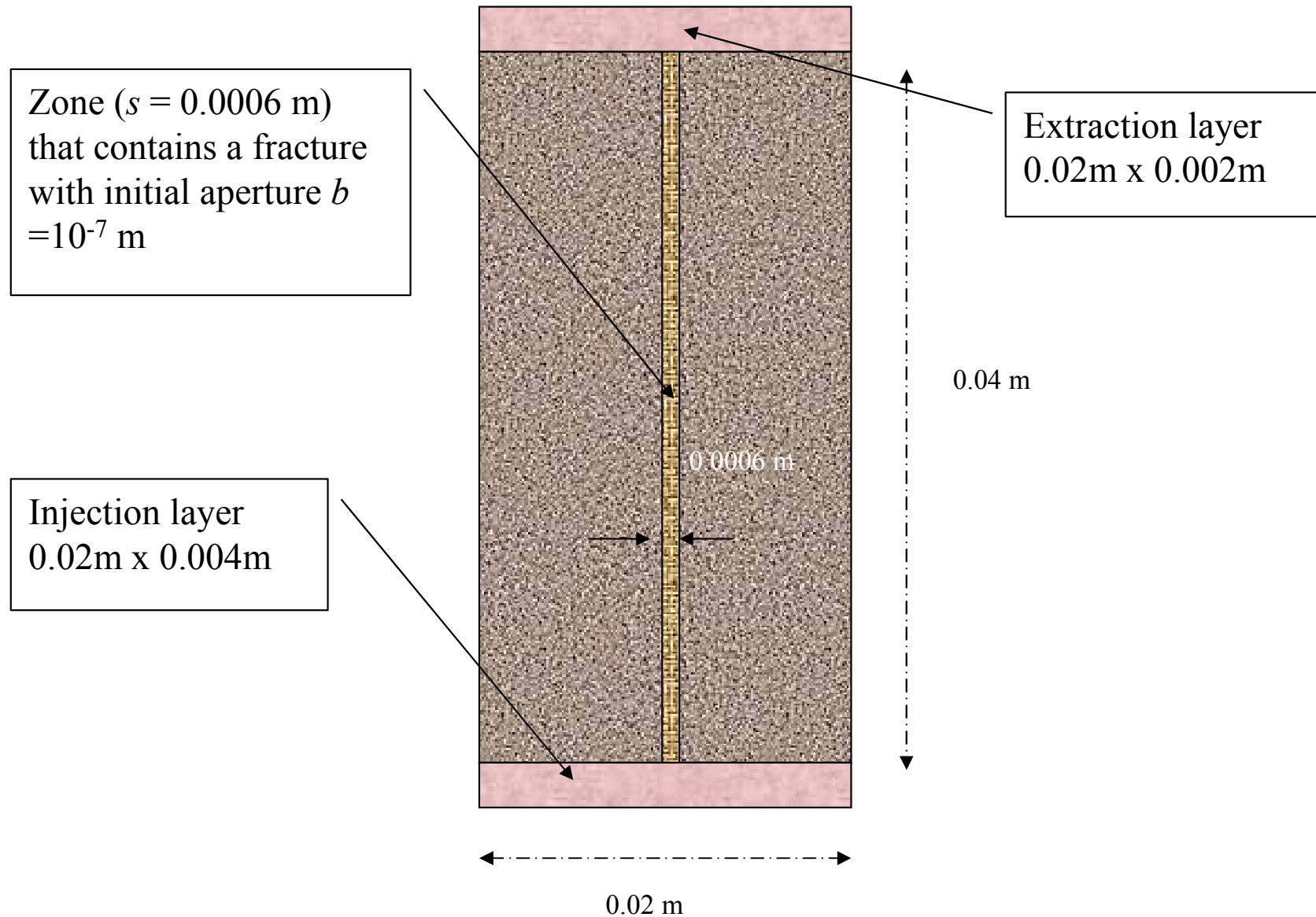
#### Measured permeabilities where:

- Intact:  $5.2 \times 10^{-19} \text{ m}^2$
- Broken sample:  $1.2 \times 10^{-16} \text{ m}^2$
- Begin. water injection:  $1.0 \times 10^{-18} \text{ m}^2$
- End water injection:  $4.0 \times 10^{-20} \text{ m}^2$

But these tests have much more information...

### 3. Modelling Rummel and Weber tests

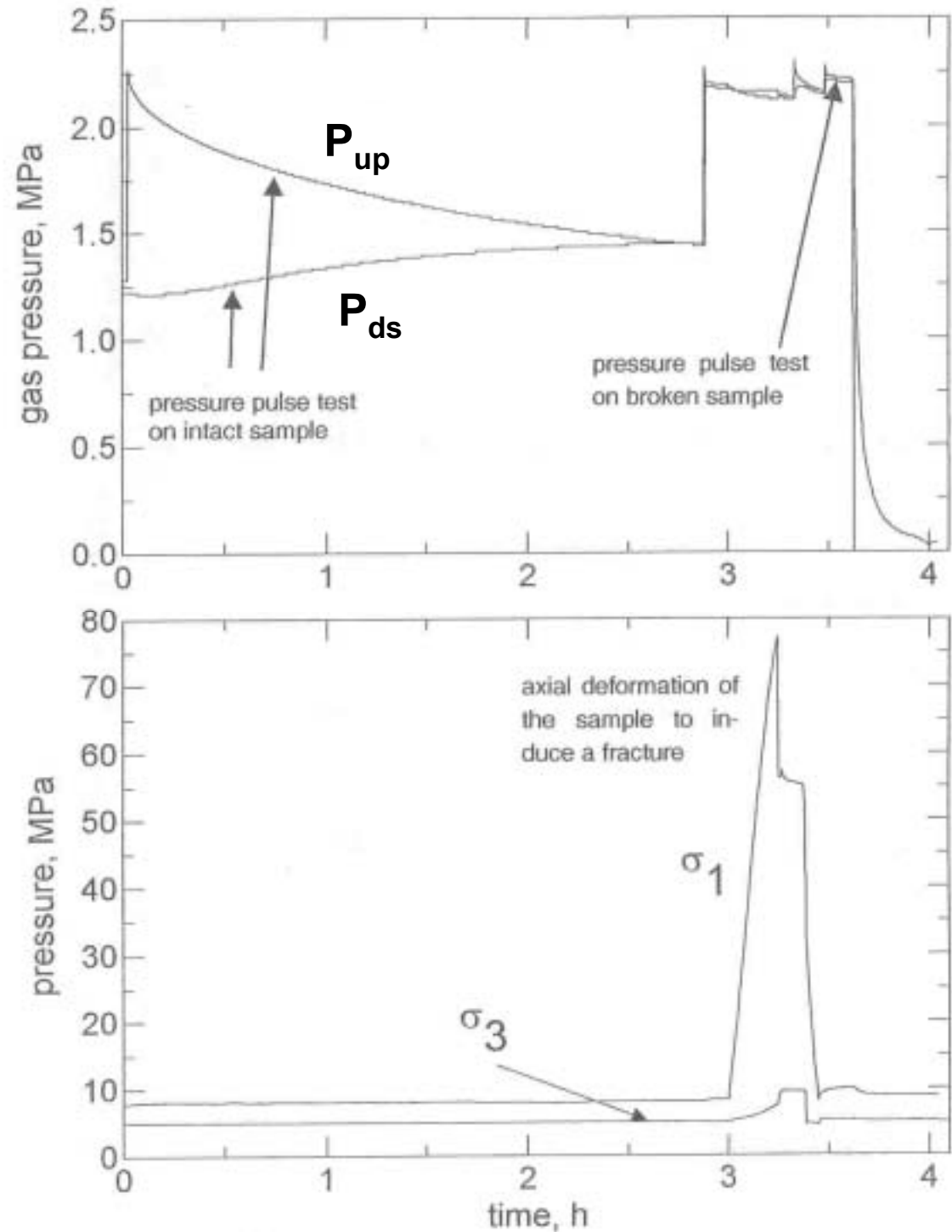
#### Simulation through a 2-D elastoplastic model



### 3. Modelling Rummel and Weber tests

---

- 1st stage: Gas pulse tests before and after sample fracture (4 hours)



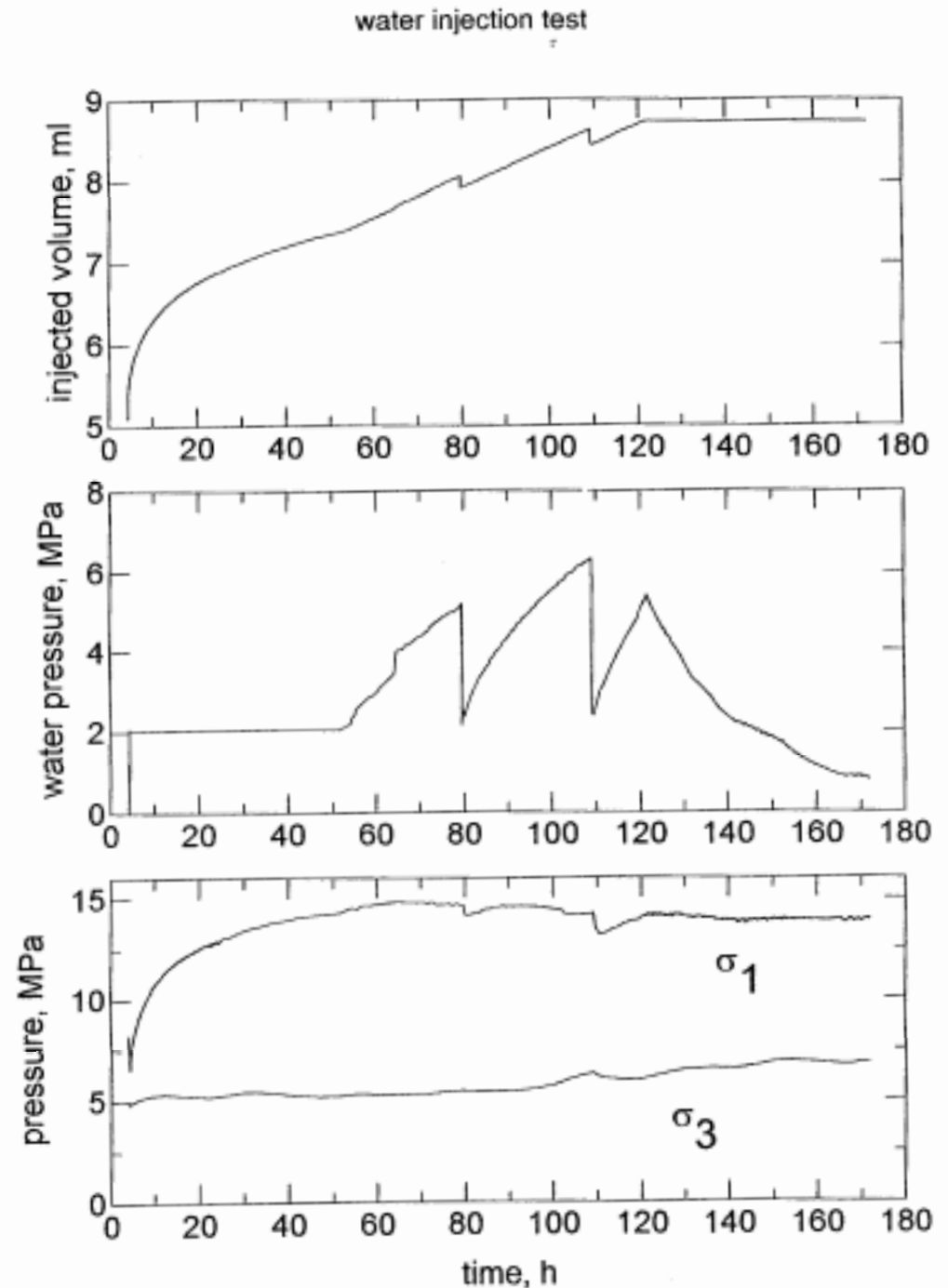
(Sample 1/5s2A. Argon gas)

### 3. Modelling Rummel and Weber tests

---

- 2nd stage: Water flooding to induce crack healing (180 hours)

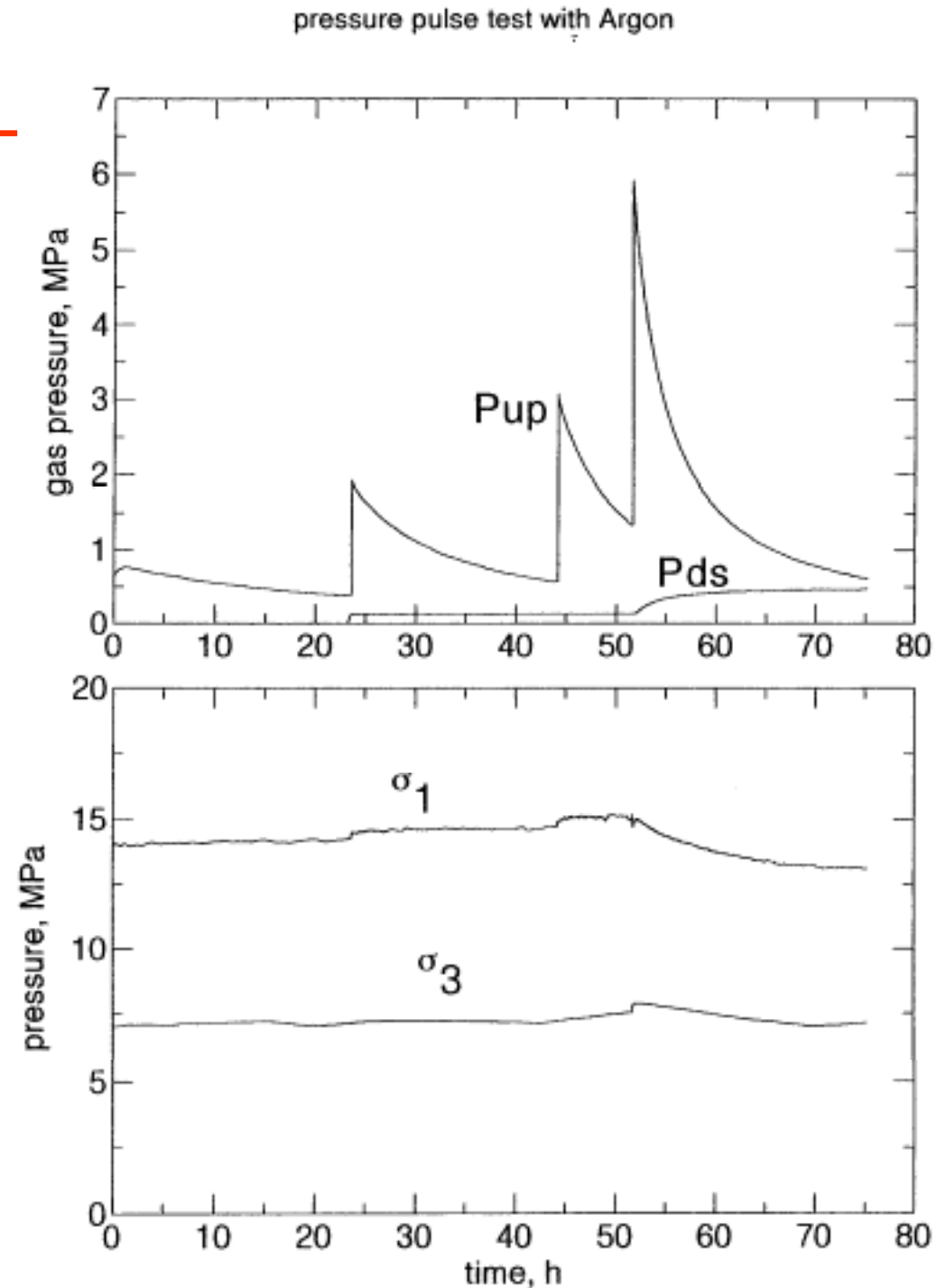
Sample : 1 / 5 s2



### 3. Modelling Rummel and Weber tests

---

- 3rd stage: Gas pulse tests to check healing effects (80 hours)





### 3. Modelling Rummel and Weber tests

---

#### Some simulation parameters

- Rock matrix permeability:  $k=3 \times 10^{-9} \text{ m}^2$
- $V_{inflow}/V_{\text{pores-sample}} = (0.002 * 0.02) / (0.02 * 0.04 * 0.11) = 0.45$
- $k_{so} = 0.001$  and  $0.003$
- Elastic modulus: 20000 MPa and 10000 MPa
- Fracture-element size: 0.0006 m
- Fracture strain threshold:  $10^{-5}$
- Fracture tension stress: 0 MPa
- Note: it is assumed that the fracture exists but it is closed.  
Deviatoric stresses open the existing fracture

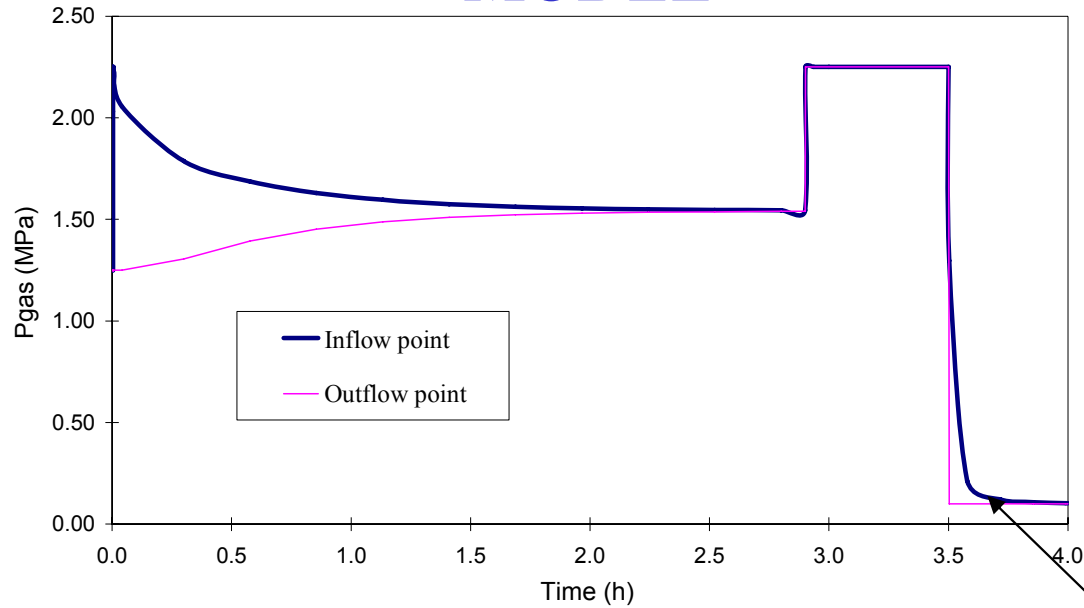
Table 4.1: Material parameters considered for simulation of tests

Parameter	Value	Reference / Remarks
Porosity	0.11	Measured density of the samples is $2.45 \text{ g/cm}^3$ , which implies $n = (2.75-2.45)/(2.75-1.0)=$
Intrinsic permeability of rock matrix	$3 \times 10^{-19} \text{ m}^2$	Corresponds to the permeability of the rock matrix. Permeability of the fracture according to model described in Chapter 2.  Rummel and Weber (2000) measured $5.2 \times 10^{-19} \text{ m}^2$ for the sample that is modelled here.
Retention curve, $P_o$ in VG model	0.3 MPa	Same as in the scoping calculations
Retention curve $\lambda$ in VG model	0.50	Same as in the scoping calculations
Relative permeability $n$ (a power function is used: $k_{rl}=S_l^n$ )	3	Same as in the scoping calculations
Elastic Modulus $K$	10000 MPa	$E = 3K(1 - 2\nu) \approx 15000 \text{ MPa}$
Poisson Modulus $\nu$	0.26	The values of $E$ and $\nu$ correspond well with values measured by Rummel and Weber (2000)
Critical state $M$	1	Corresponds to a friction angle of $25^\circ$ ( $M=6 \sin \phi' / (3 - \sin \phi')$ )
Tensile Strength rock matrix ( $p_s$ , see section 2).	10 MPa	Same as in the scoping calculations.
Tensile Strength for the fractured zone	0.0 MPa	The fracture is assumed to exist.
Threshold strain	0.00001	

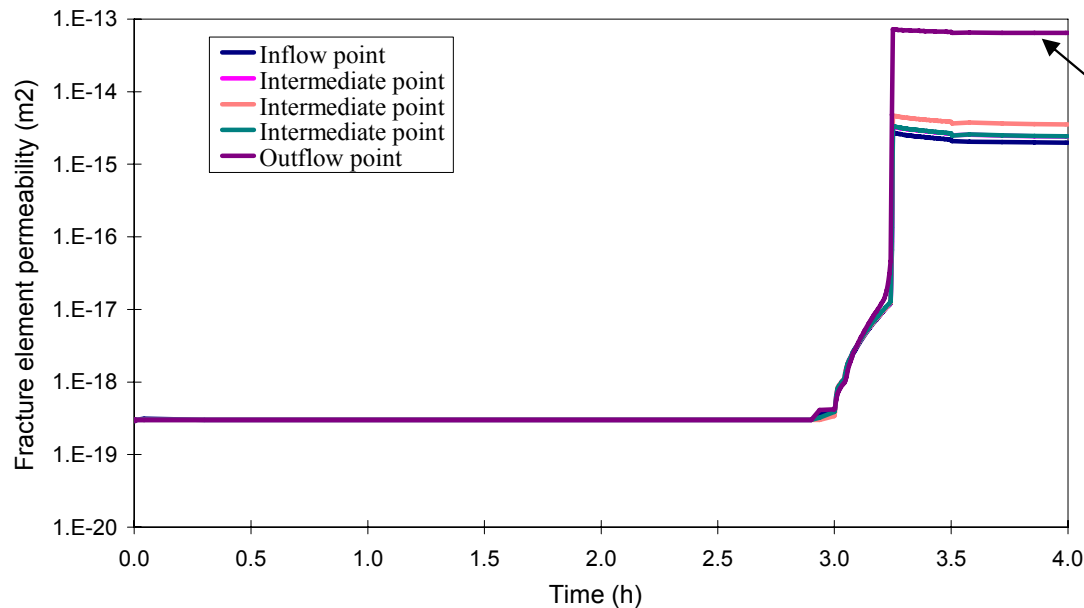
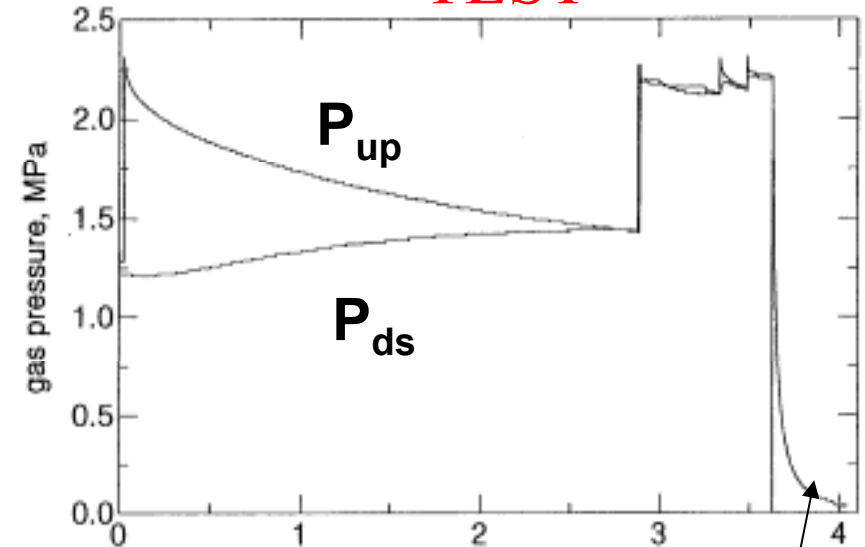
# 3. Modelling Rummel and Weber tests

## 1st stage: Gas pulse tests and sample fracture

MODEL



TEST

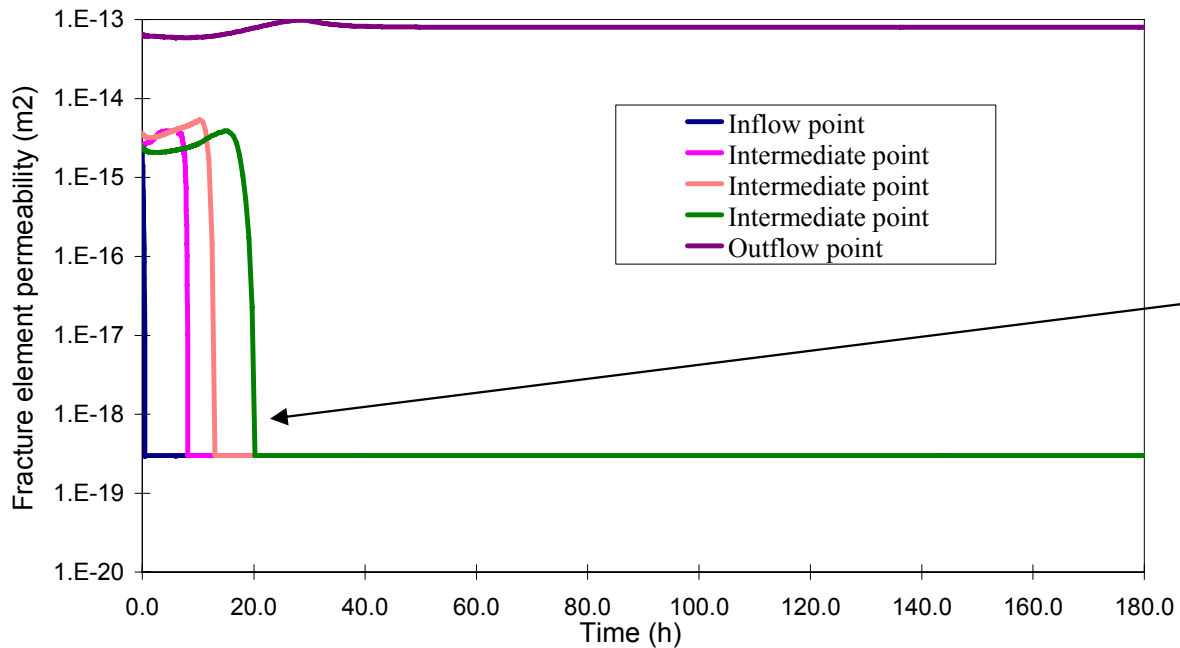
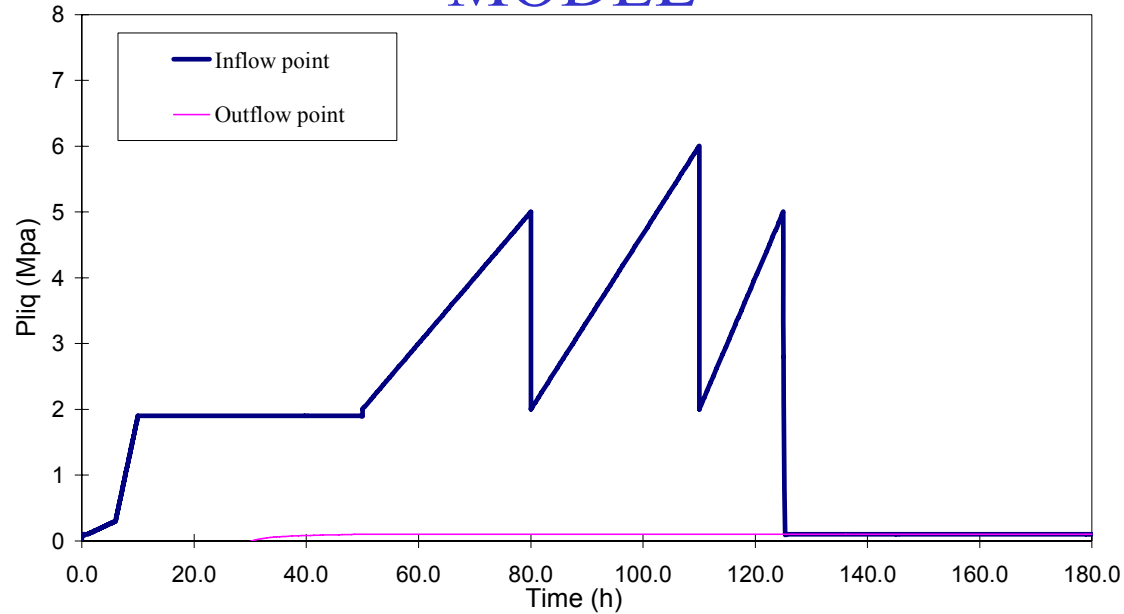


Fast gas pressure dissipation due to high permeability

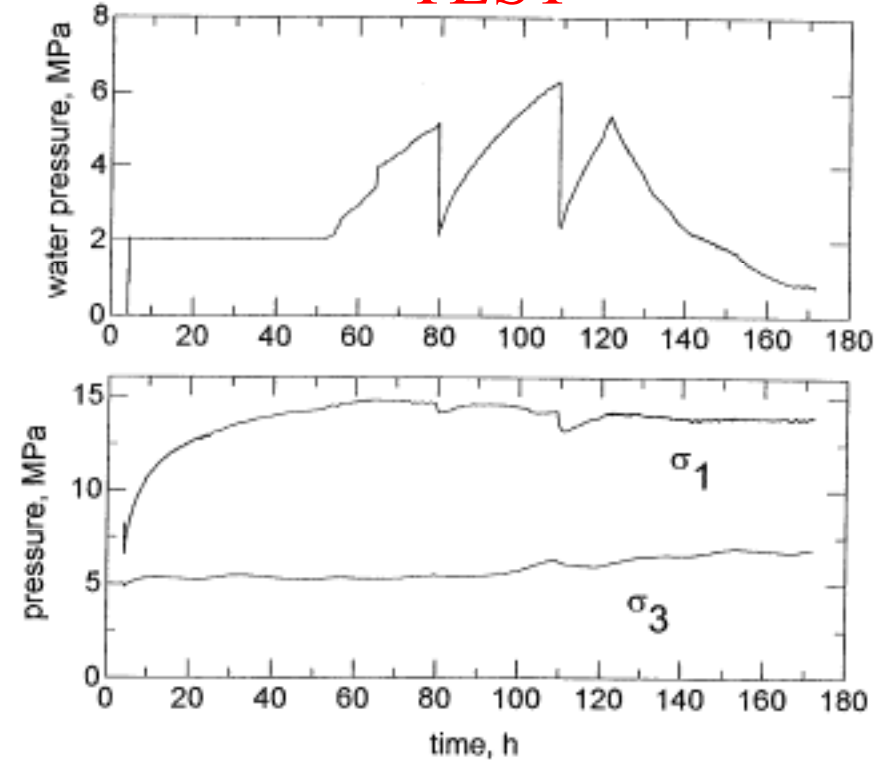
# 3. Modelling Rummel and Weber tests

## 2nd stage: Water flooding

### MODEL



### TEST

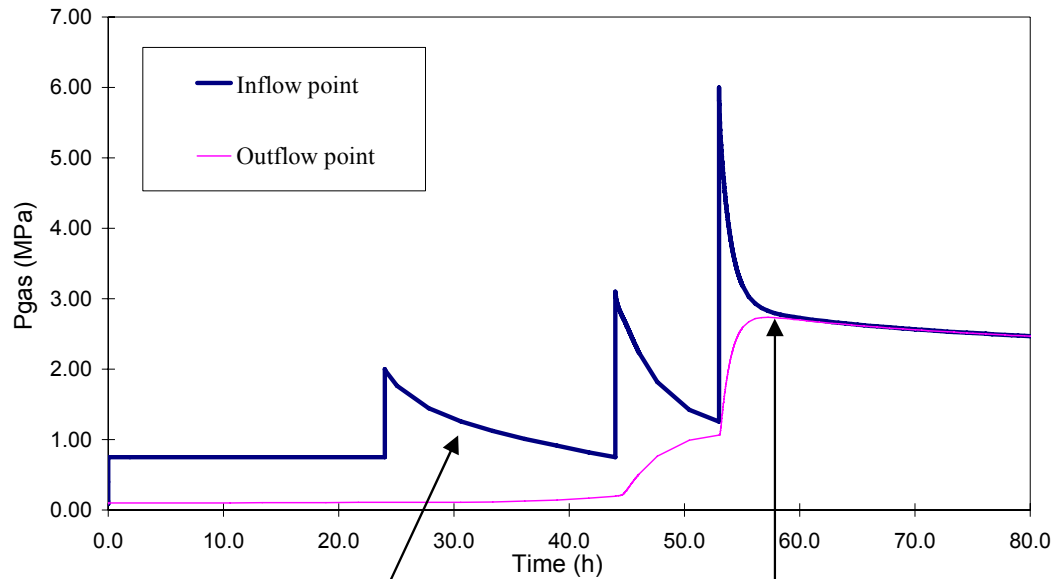


**During wetting,  
permeability  
decreases due to  
fracture closure and  
swelling**

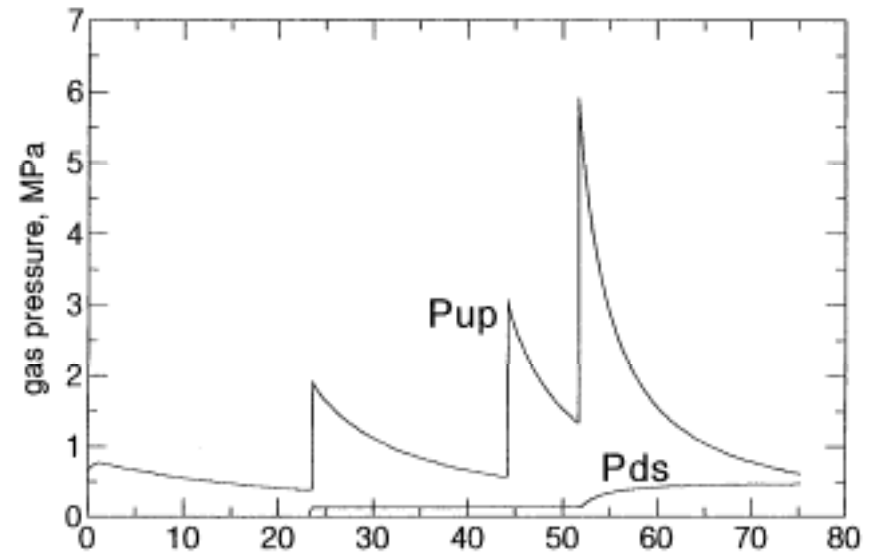
# 3. Modelling Rummel and Weber tests

## 3rd stage: Gas pulse tests

### MODEL



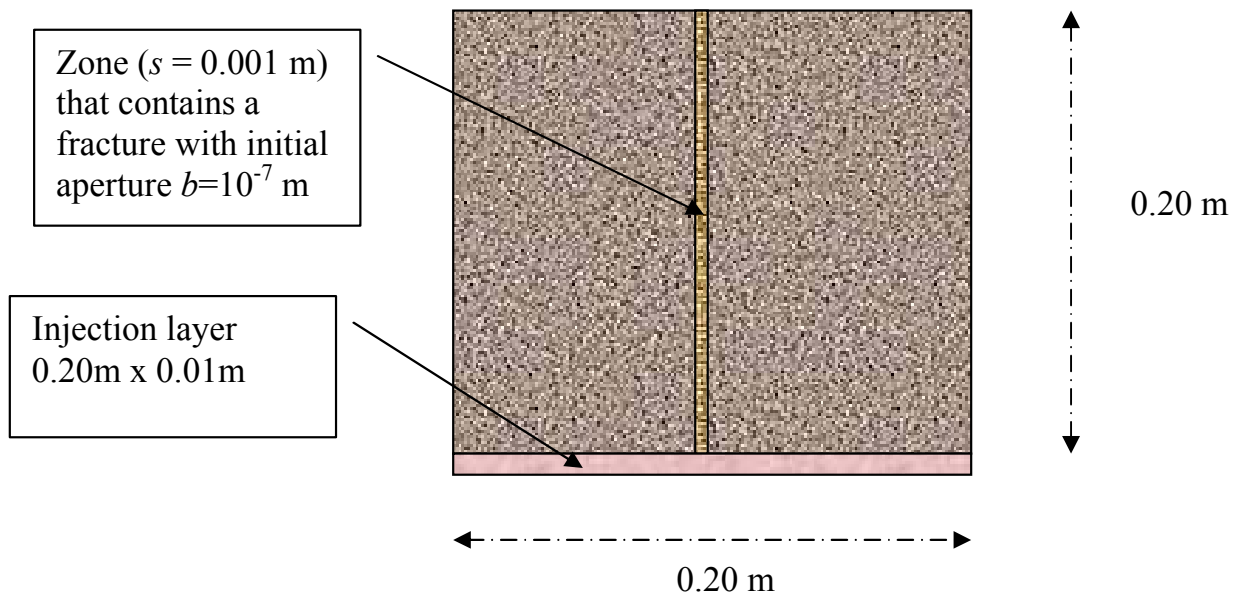
### TEST

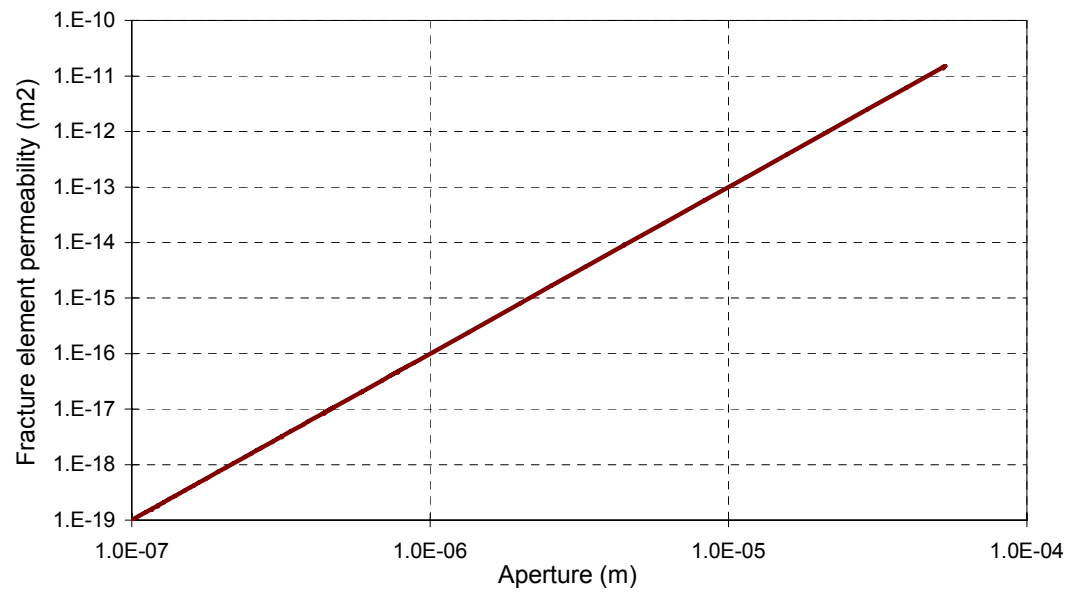
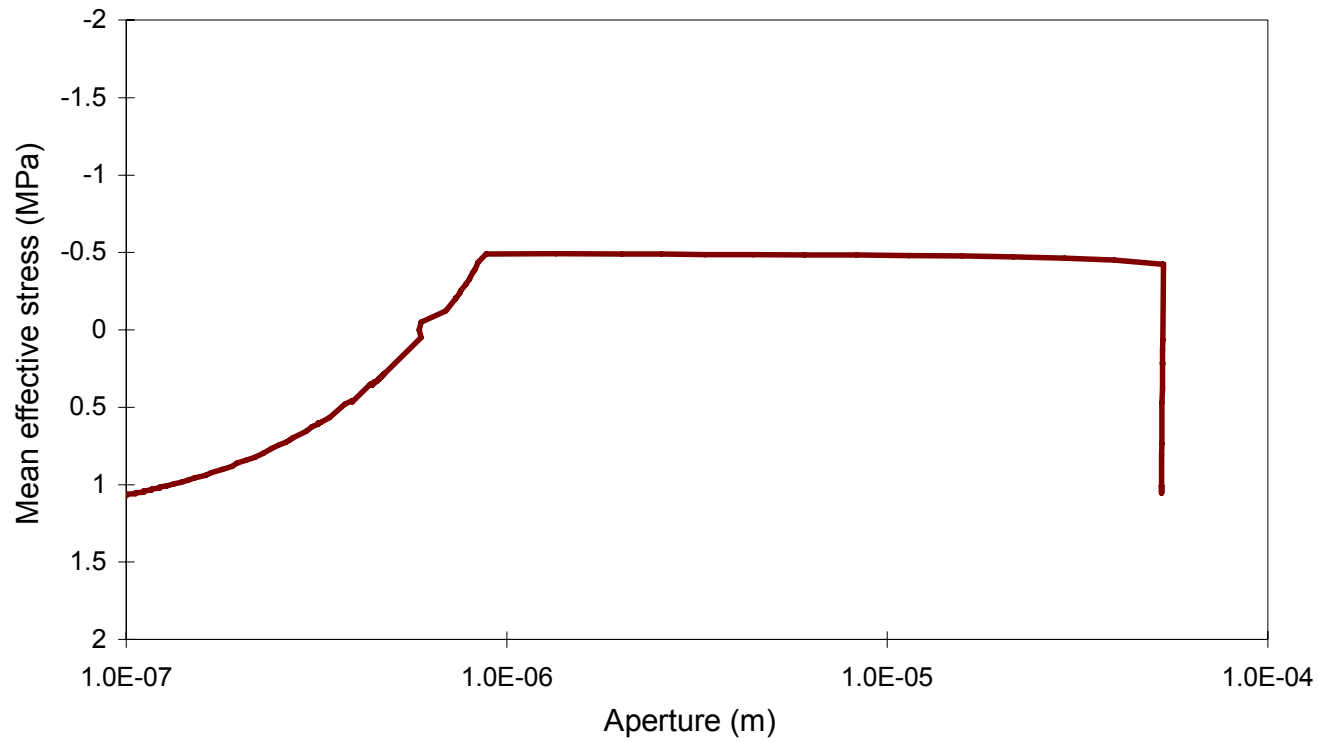


**Gas pressure dissipation due to low permeability. Healing effect leads to permeability similar to intact rock permeability. Progressive desaturation is observed**

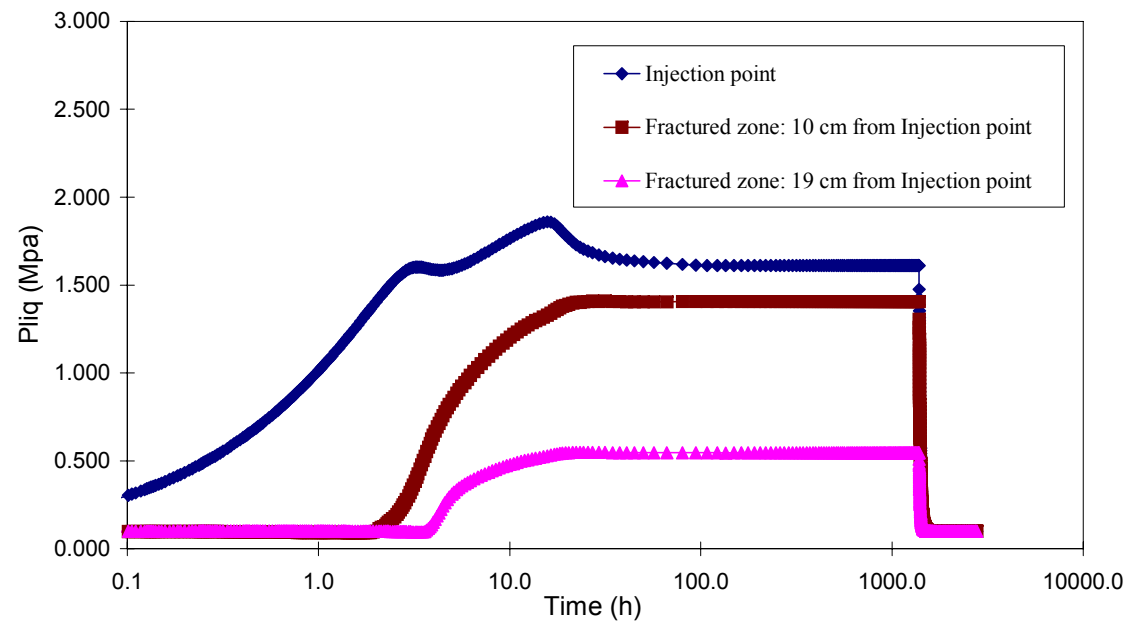
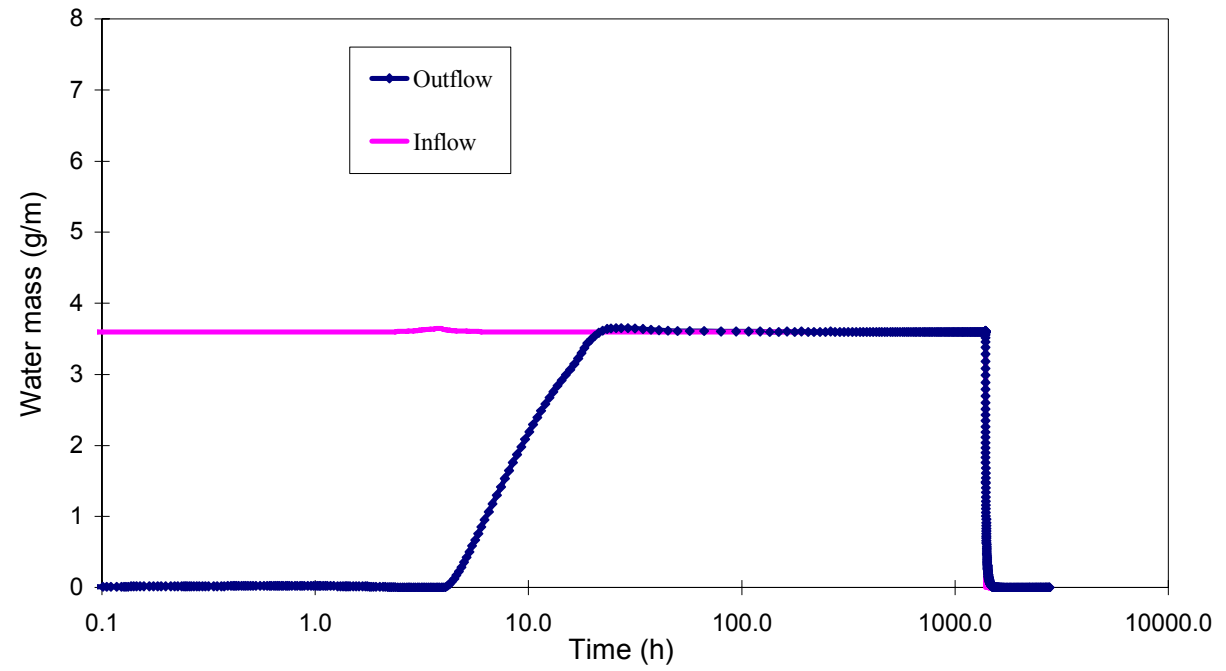
## CONCLUDING REMARKS

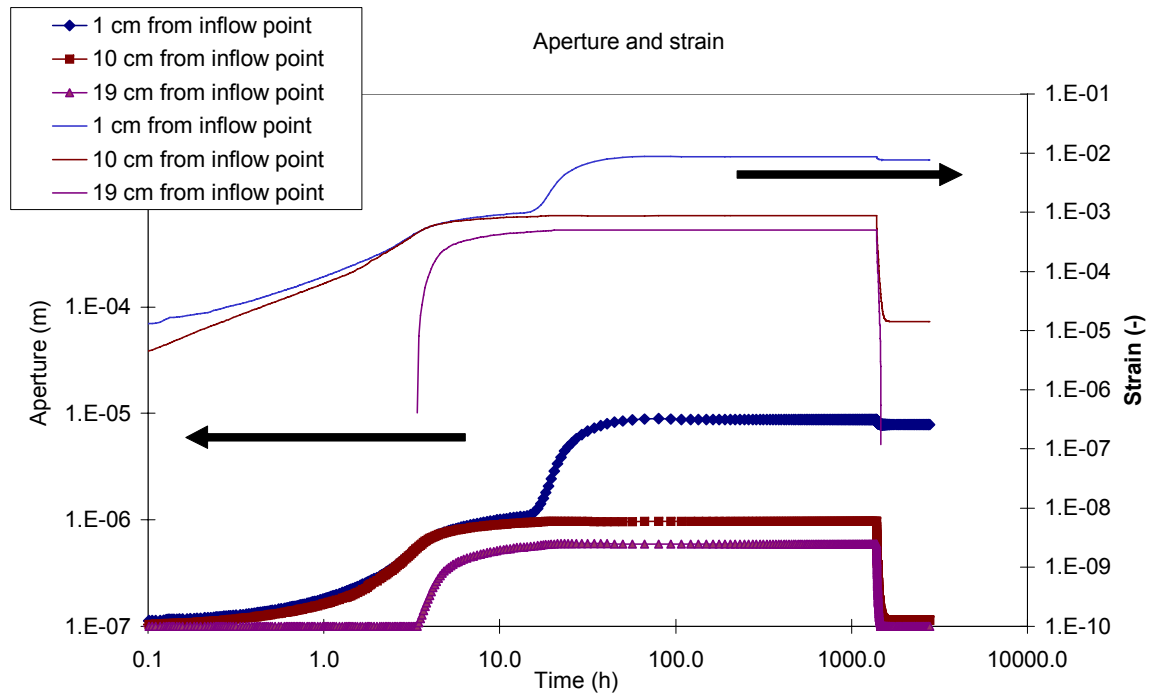
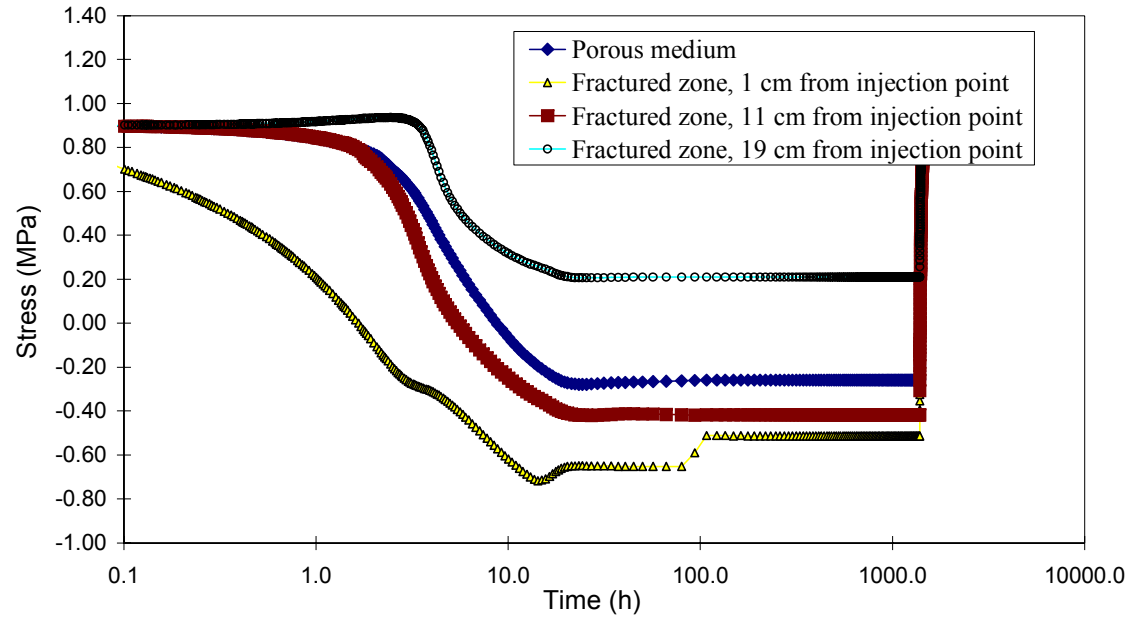
- Porous-based transport phenomena and singular path flow may be present in gas migration through barriers and host rock
- A procedure to simulate gas flow through discontinuities has been described
- It is integrated in general coupled HM two-phase continuum formulations
- Gas flow-mechanical coupling along discontinuities explains some singular features observed in experiments (delayed breakthrough, output gas flow peaks)
- A complex set of laboratory triaxial tests involving flow in damaged and subsequently healed samples of Opalinus clay has satisfactorily been modelled
- The model presented may be implemented, at a limited effort, in current computer codes for THM analysis

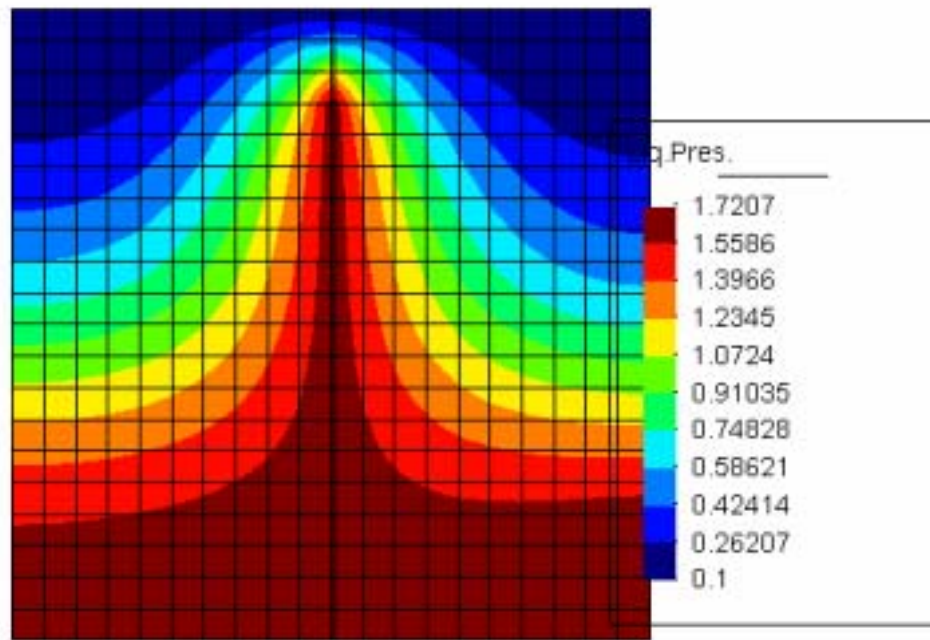
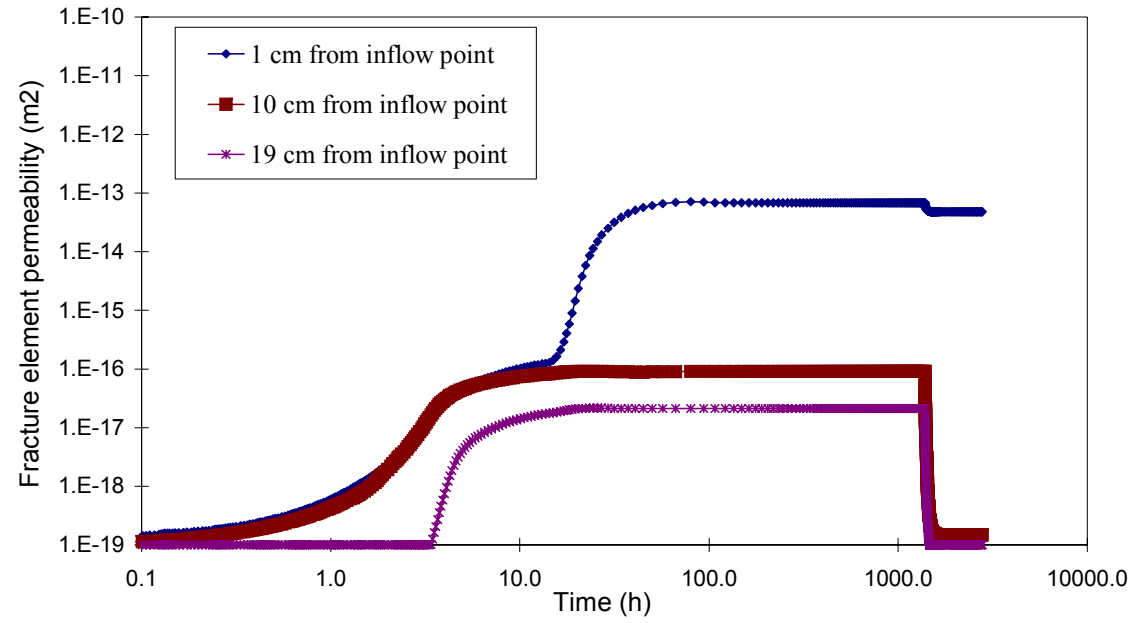


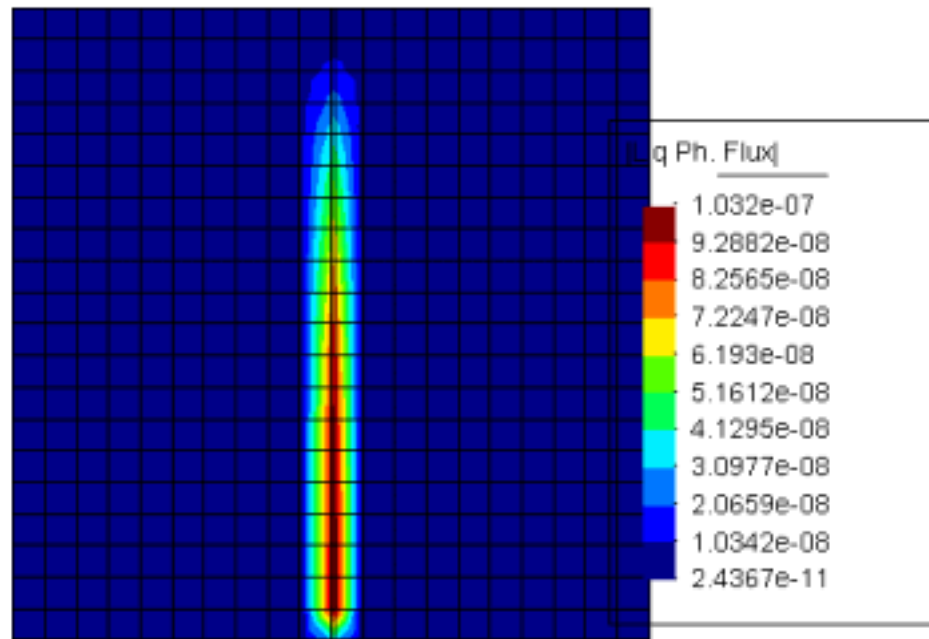


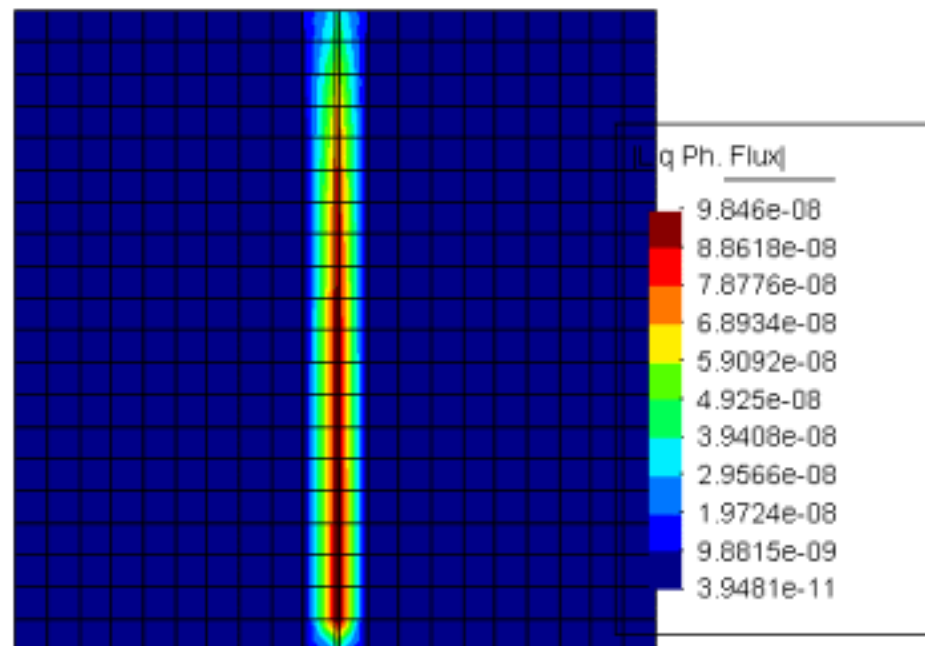
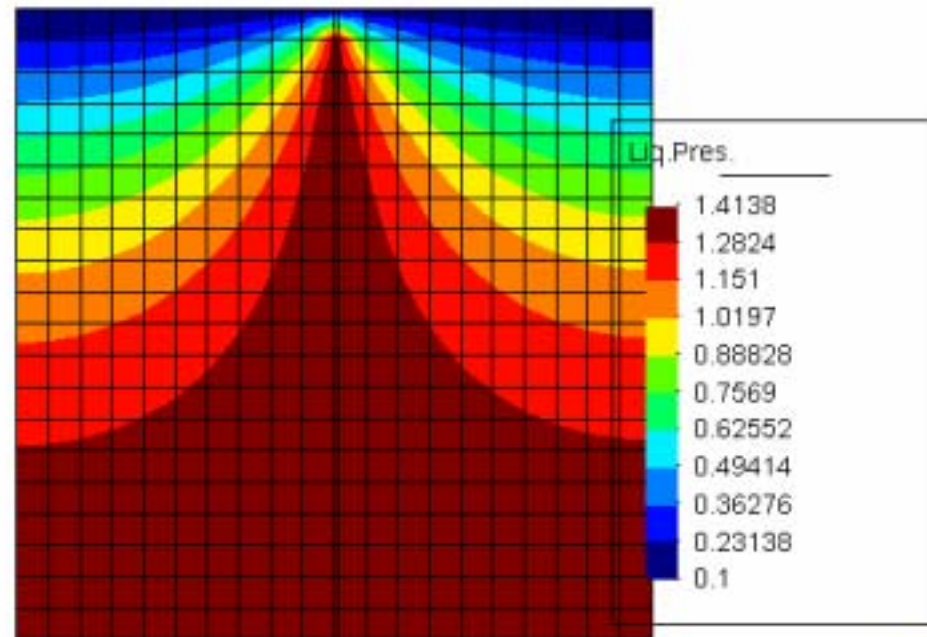


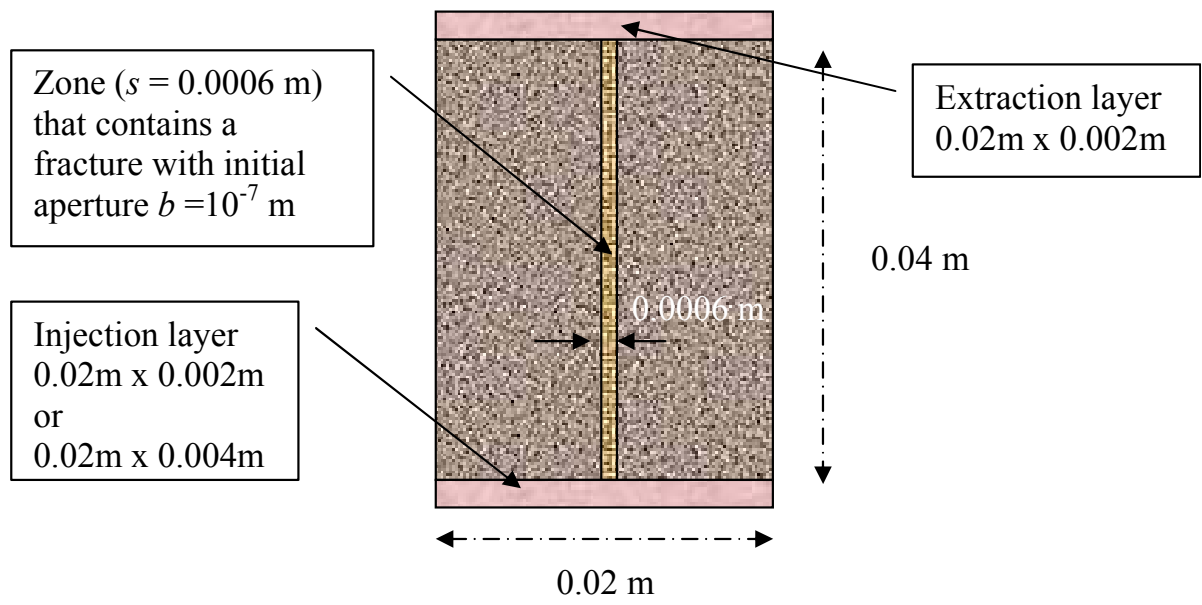




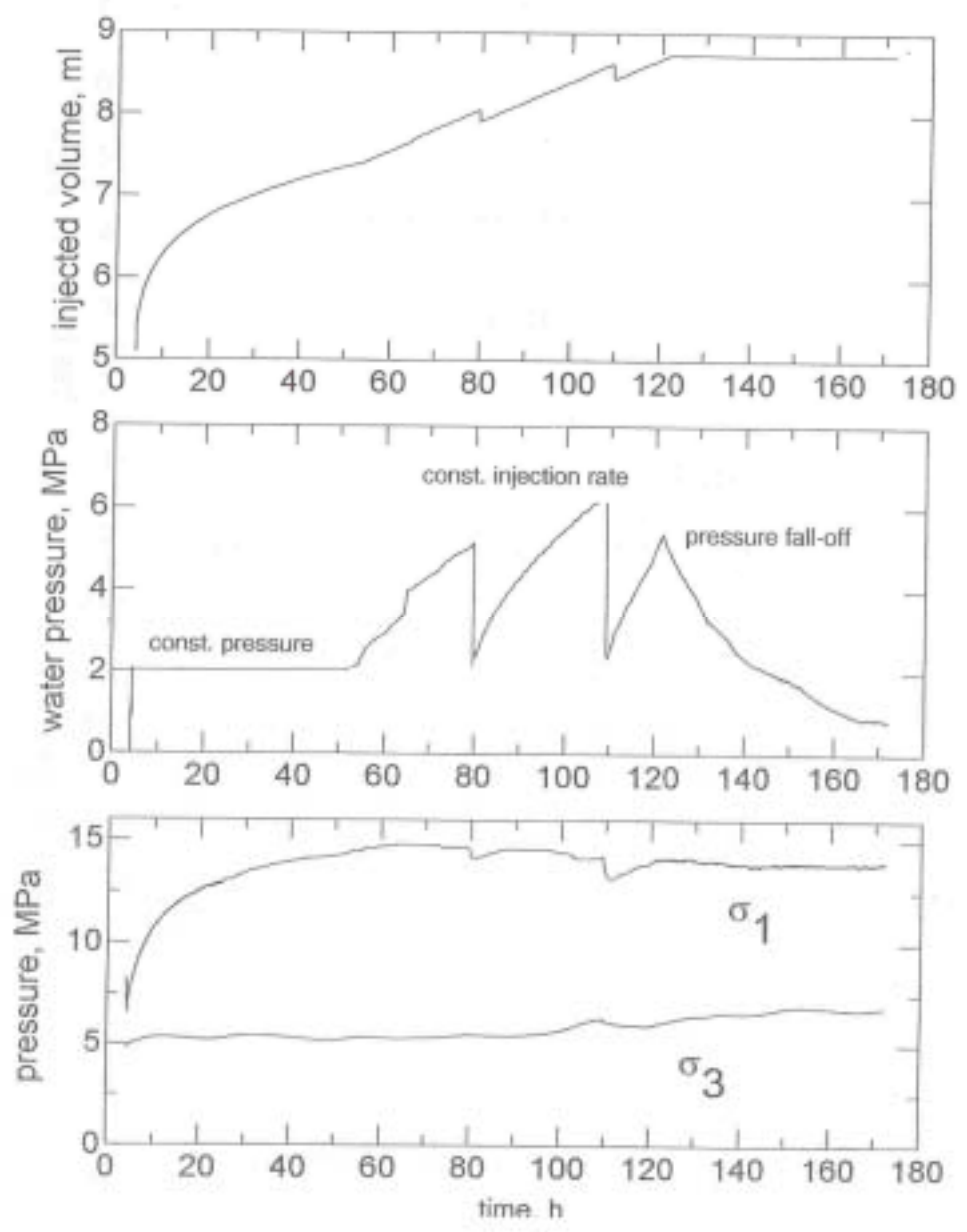




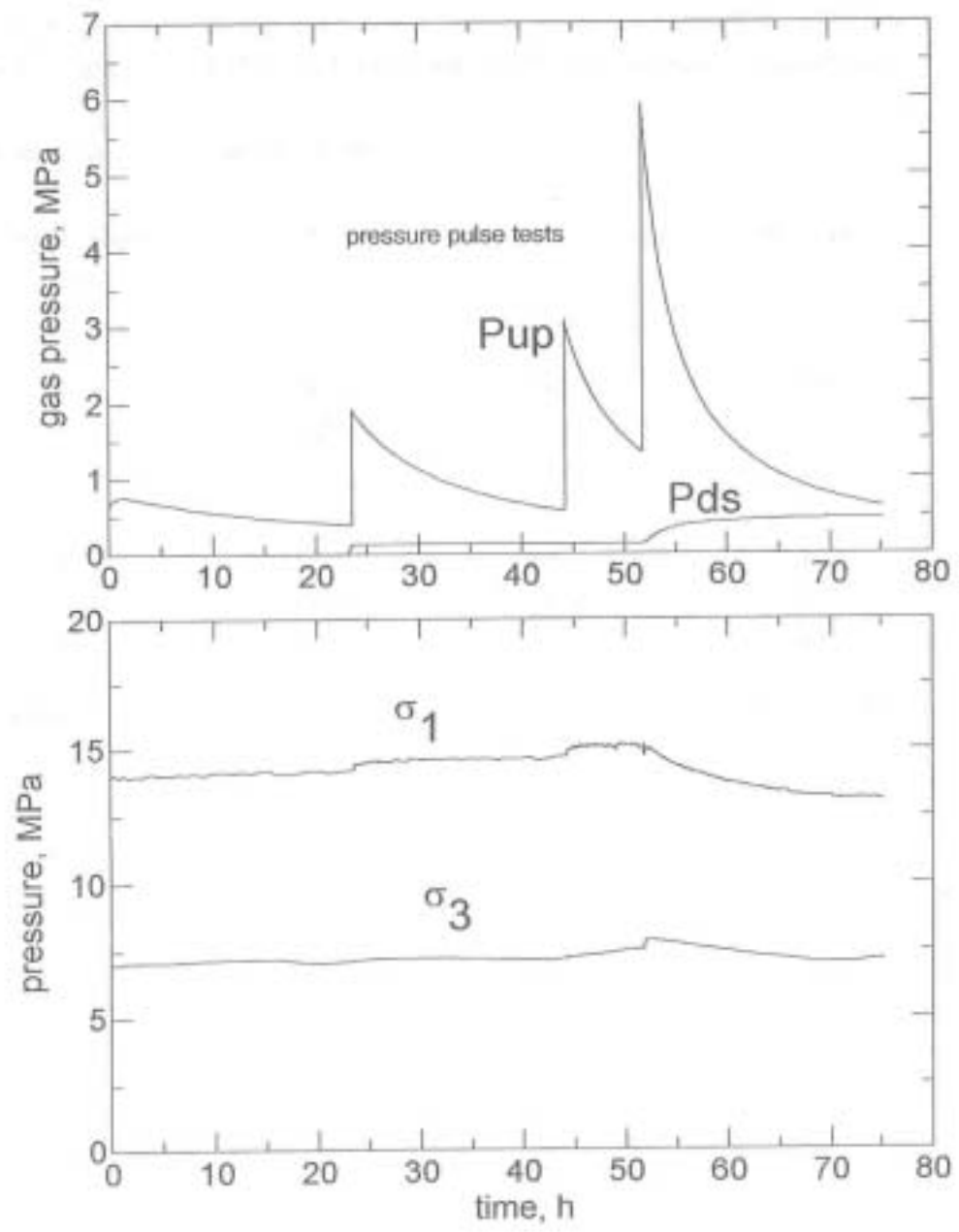


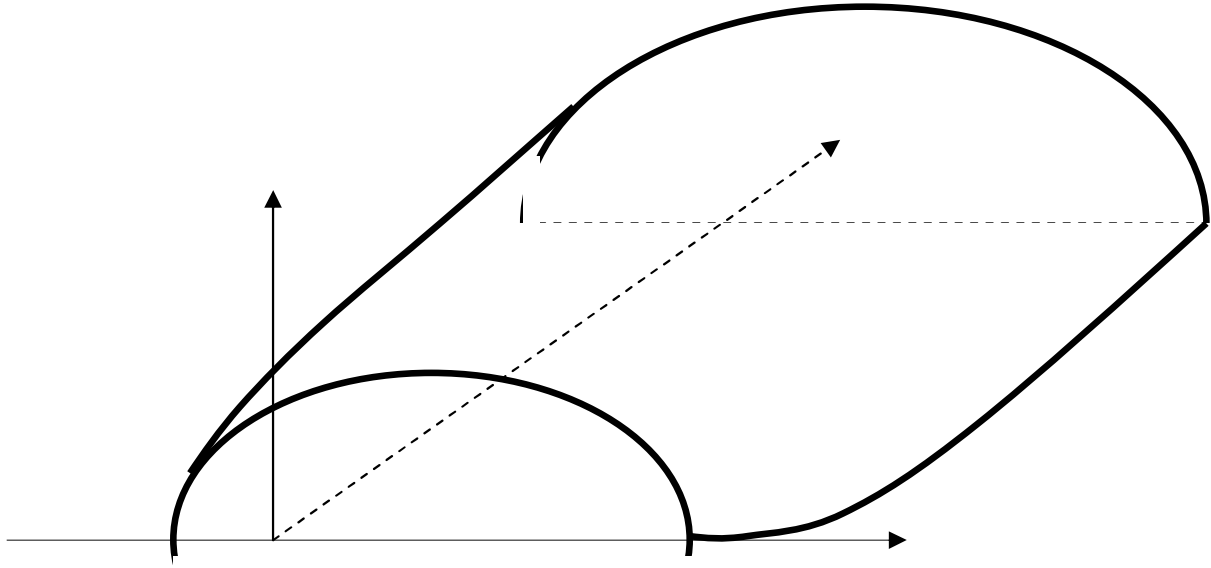


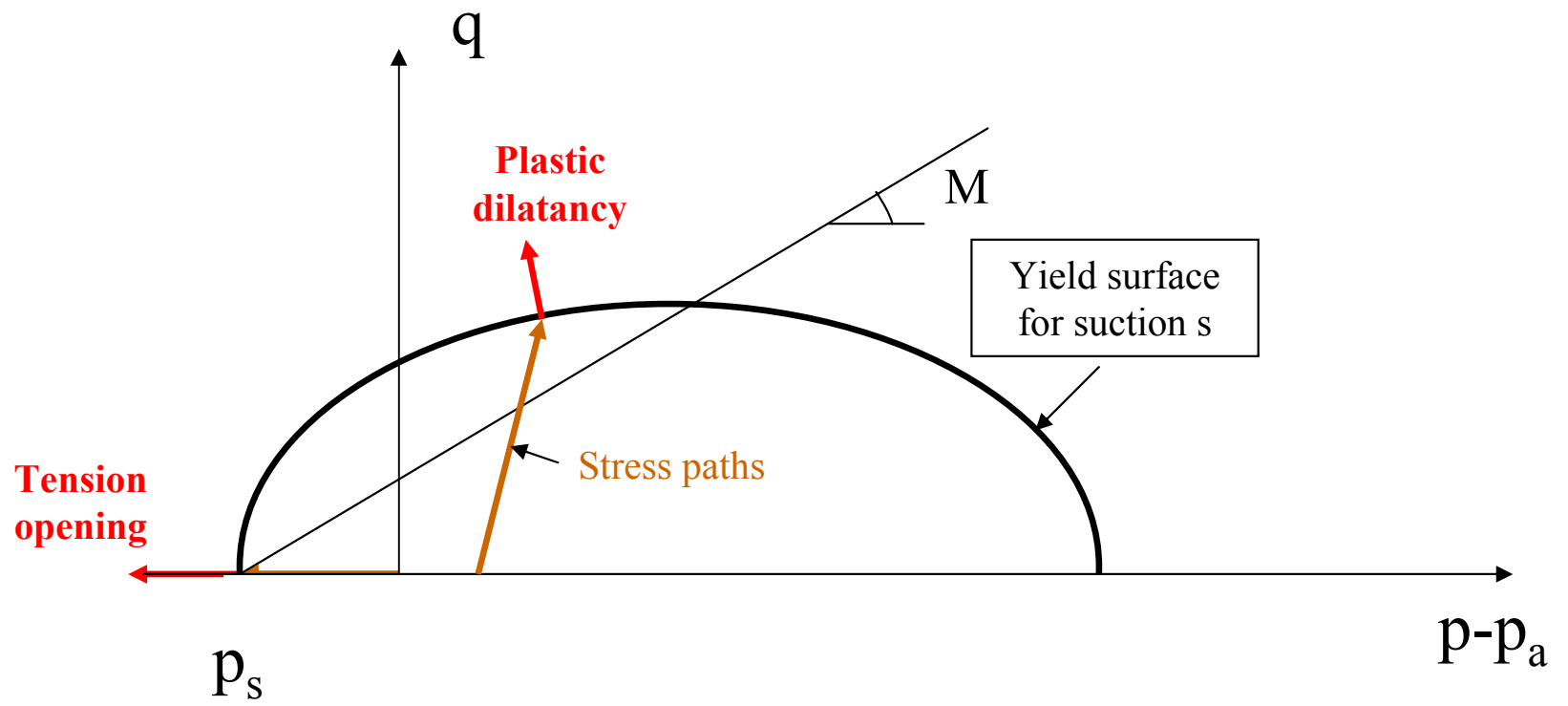
Parameter	Value	Reference / Remarks
Porosity	0.11	Measured density of the samples is 2.45 g/cm <sup>3</sup> , which implies $n = (2.75-2.45)/(2.75-1.0) =$
Intrinsic permeability of rock matrix	$3 \times 10^{-19} \text{ m}^2$	Corresponds to the permeability of the rock matrix. Permeability of the fracture according to model described in Chapter 2.  Rummel and Weber (2000) measured $5.2 \times 10^{-19} \text{ m}^2$ for the sample that is modelled here.
Retention curve, $P_o$ in VG model	0.3 MPa	Same as in the scoping calculations
Retention curve $\lambda$ in VG model	0.50	Same as in the scoping calculations
Relative permeability $n$ (a power function is used: $k_{rl} = S_l^n$ )	3	Same as in the scoping calculations
Elastic Modulus $K$	10000 MPa	$E = 3K(1 - 2\nu) \approx 15000 \text{ MPa}$
Poisson Modulus $\nu$	0.26	The values of $E$ and $\nu$ correspond well with values measured by Rummel and Weber (2000)
Critical state $M$	1	Corresponds to a friction angle of 25° ( $M = 6 \sin \phi' / (3 - \sin \phi')$ )
Tensile Strength rock matrix ( $p_s$ , see section 2).	10 MPa	Same as in the scoping calculations.
Tensile Strength for the fractured zone	0.0 MPa	The fracture is assumed to exist.
Threshold strain	0.00001	



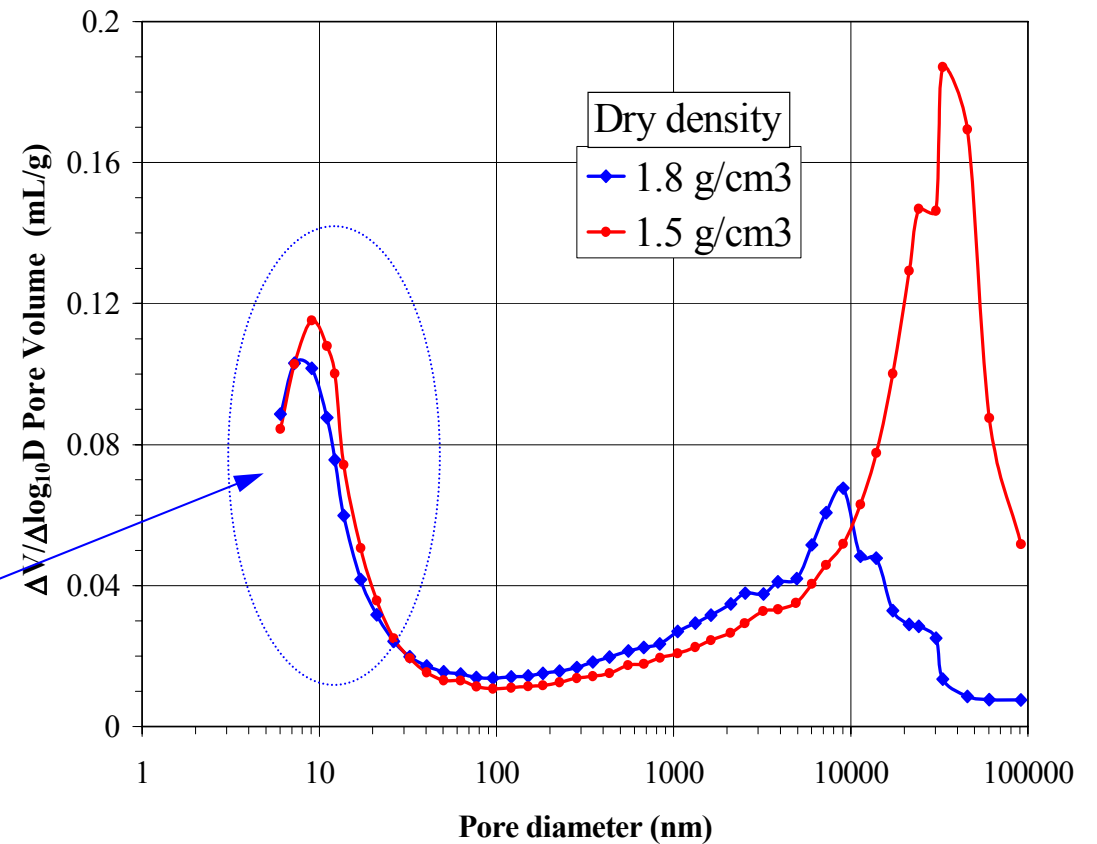
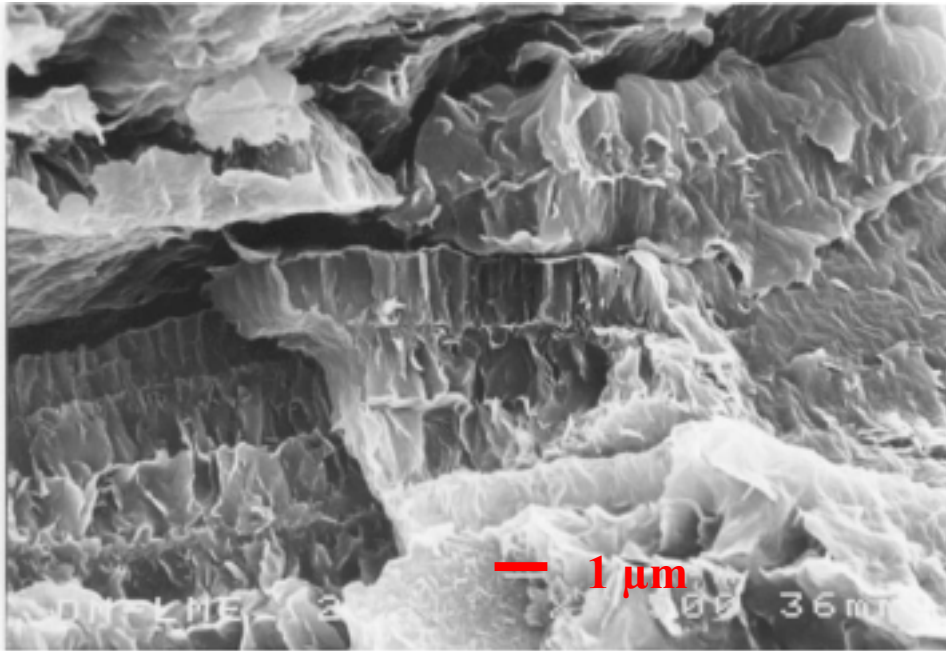








# FEBEX bentonite structure

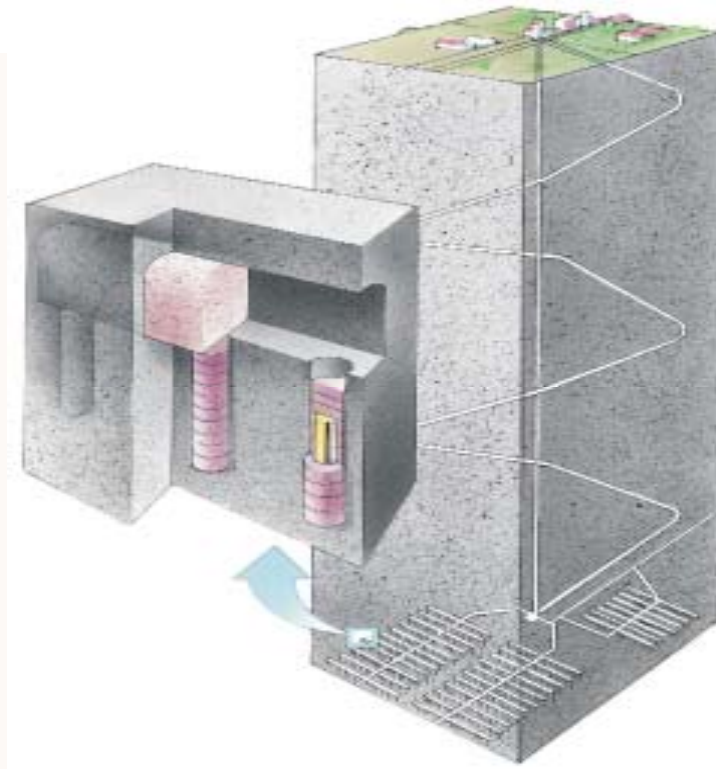


About 75% of total pore volume



# Gas flow in buffer bentonite under $K_0$ and constant volume conditions

J.F. Harrington and S.T. Horseman



Kingsley Dunham Centre  
Keyworth  
Nottingham NG12 5GG  
Tel 0115 936 3100

© NERC All rights reserved



# Contents of presentation

- Background to test philosophy
- Constant volume radial flow (CVRF) test geometry ([Mx80-8](#), [-10](#))
- Radially constrained ( $K_0$ ) test geometry ([Mx80-9](#))
- Basic material properties ([all tests](#))
- Swelling and hydration behaviour ([Mx80-10](#))
- Baseline hydraulic properties ([Mx80-8](#) and [Mx80-9](#))
- Gas migration behaviour ([all tests](#))
- Process understanding ([all tests](#))
- Conclusions

**Mx80-8 =  $K_0$ ; Mx80-9 & -10 = CVRF**



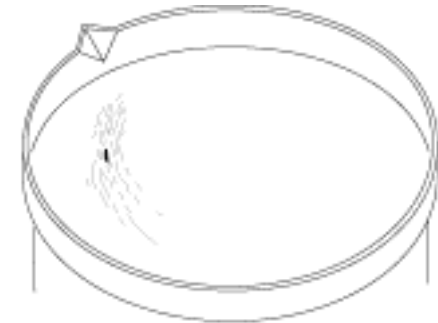
## Background (1)

- **Gas breakthrough pressure**
  1. Strongly dependent on the degree of water saturation
  2. At low saturations ( $S_w > 70 < 90\%$ ) the buffer contains a network of interconnected cracks resulting in little or no gas threshold
  3. As the clay approaches full saturation, gas breakthrough pressure increases rapidly
  4. Experiments on saturated isotropically-consolidated specimens show gas breakthrough occurs at a pressure marginally greater than the sum of the swelling pressure and the porewater pressure
- **After gas testing saturations remain close to 100% (Pusch and Forsberg, 1983) suggesting that gas may pass through a relatively small number of discrete pathways**



## Background (2)

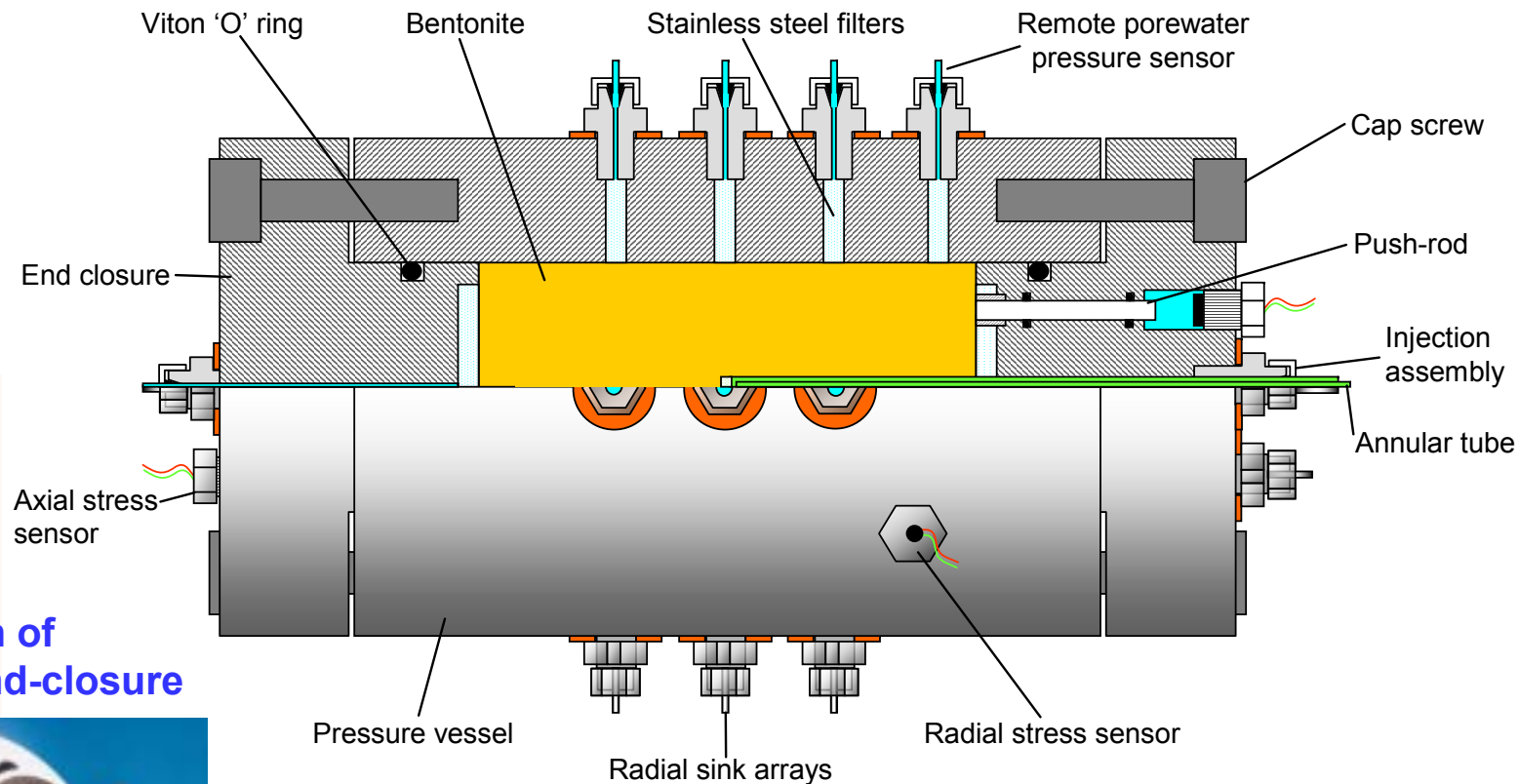
- Experiments by Donohew (2000) suggest that a saturated clay dilates during gas entry and changes in gas content are accommodated by an increase in the total volume of the clay
- Although this is consistent with gas flow through a network of pressure-induced pathways, it cannot be reconciled with the more usual soil mechanics concept of desaturation by direct displacement of porewater
- If dilatancy occurs during gas entry, are the gas transport mechanisms sensitive to the nature of the boundary conditions of the experiment?



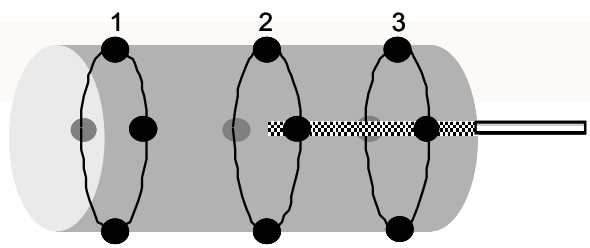




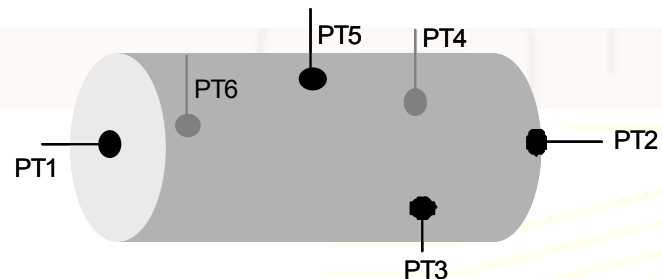
# Cut-away diagram of CVRF apparatus



Photograph of injection end-closure



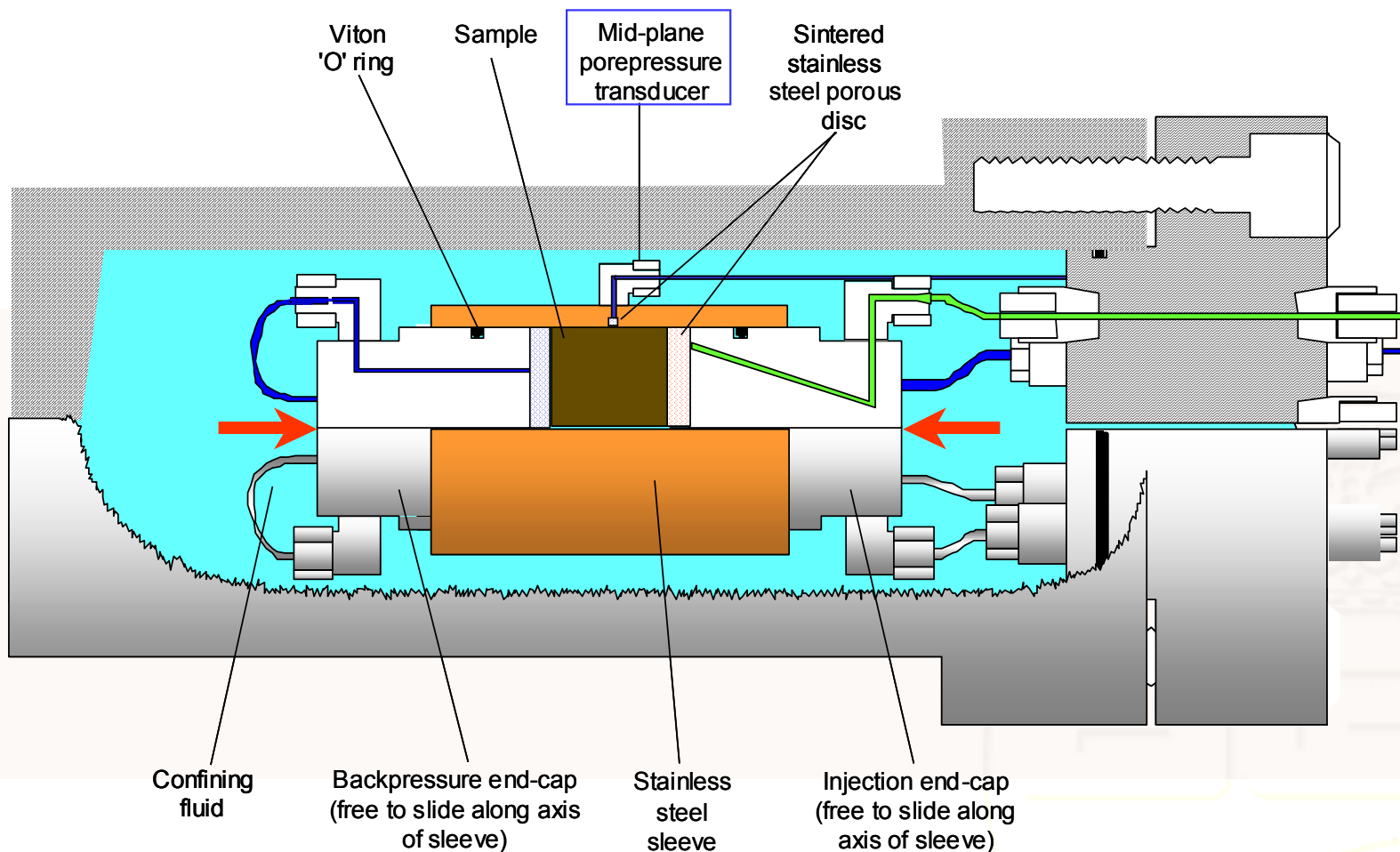
Sink configuration



Stress sensor locations



# Cut-away diagram of $K_0$ apparatus





## Specimen details

Specimen number	Test type	Orientation to compression axis	Diameter (mm)	Length (mm)	Pre-test volume (ml)
Mx80-8	CVRF	Perpendicular	60	120	337.6
Mx80-9	K0	Perpendicular	51	51	103.6
Mx80-10	CVRF	Perpendicular	60	120	337.6

Specimen number	Block number	Water content (wt-%)	Bulk density (Mg.m <sup>-3</sup> )	Dry density (Mg.m <sup>-3</sup> )	Void ratio	Initial saturation (%)
Mx80-8	BGS4	26.7	1.997	1.577	0.756	97.6
Mx80-9	BGS4	27.1	1.993	1.568	0.767	98.0
Mx80-10	BGS99	26.7	2.005	1.582	0.751	98.6



British  
Geological Survey

NATURAL ENVIRONMENT RESEARCH COUNCIL



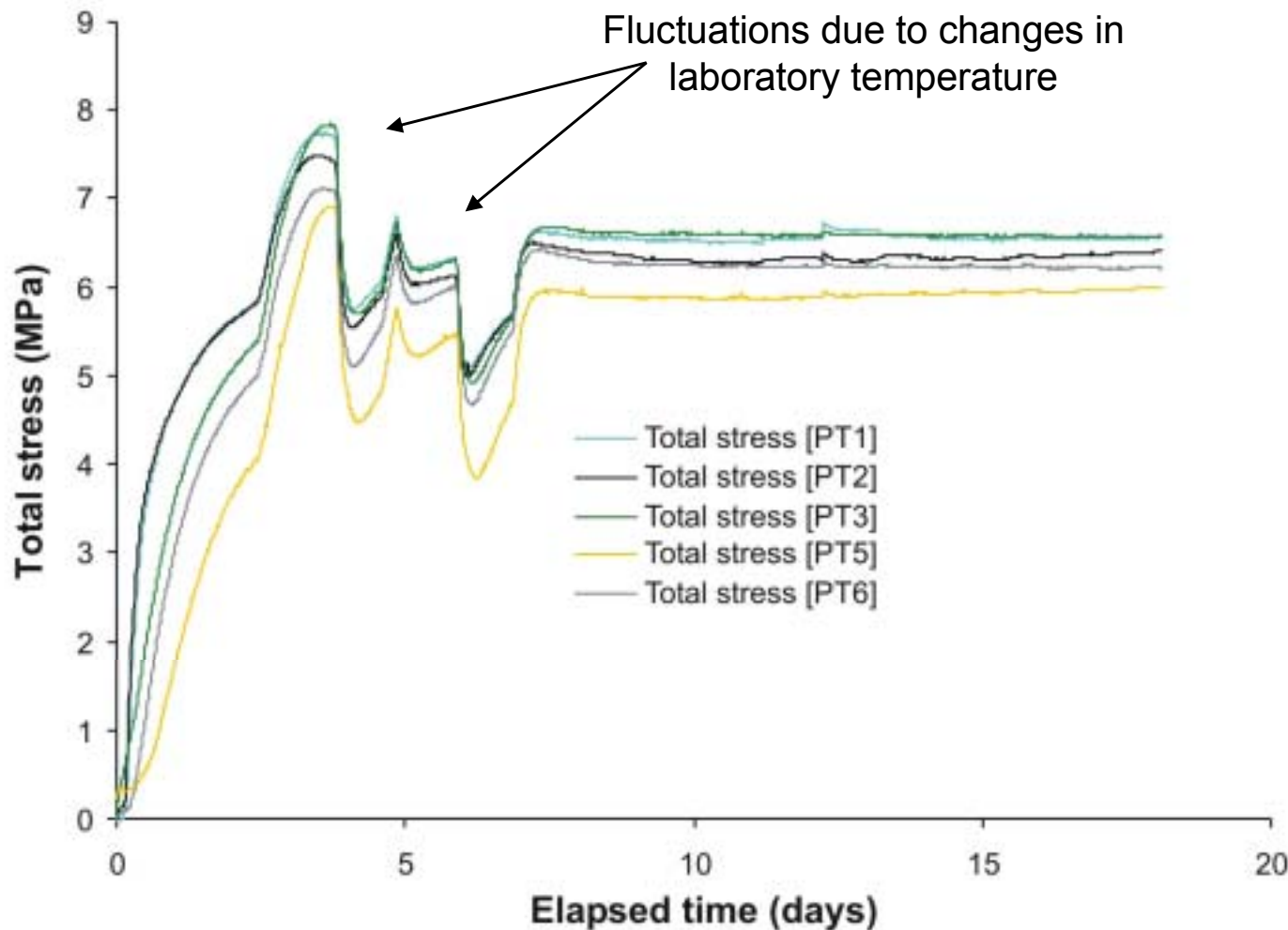
[www.bgs.ac.uk](http://www.bgs.ac.uk)

# Swelling and hydration behaviour (Mx80-10)





# Mx80-10 initial hydration stage



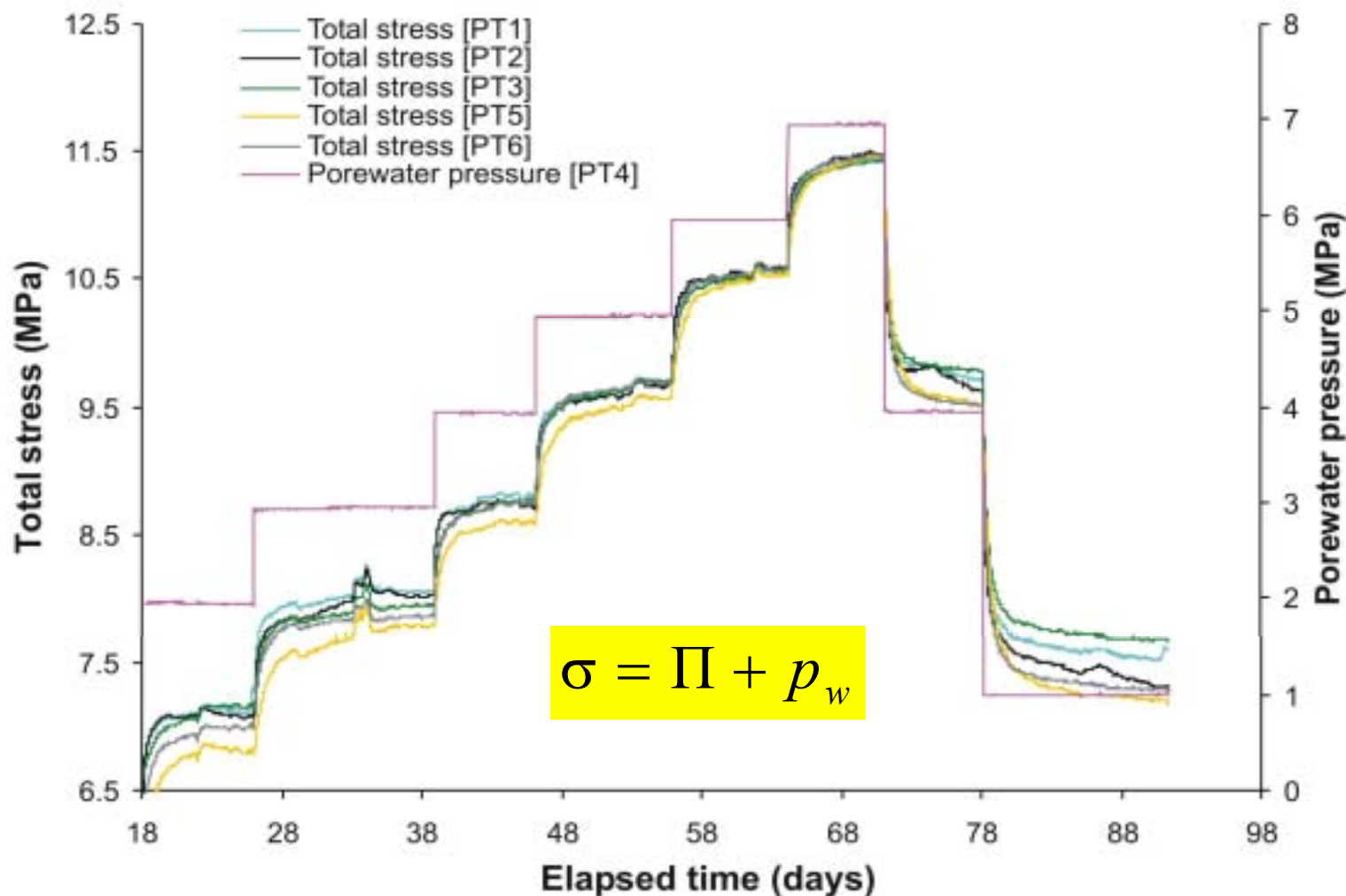
Total stress varies from **6.6 MPa** close to the end-closures, to **6.0 MPa** at the mid-point of the specimen

Average total stress = **6.4 MPa**

$$\sigma = \Pi + p_w$$

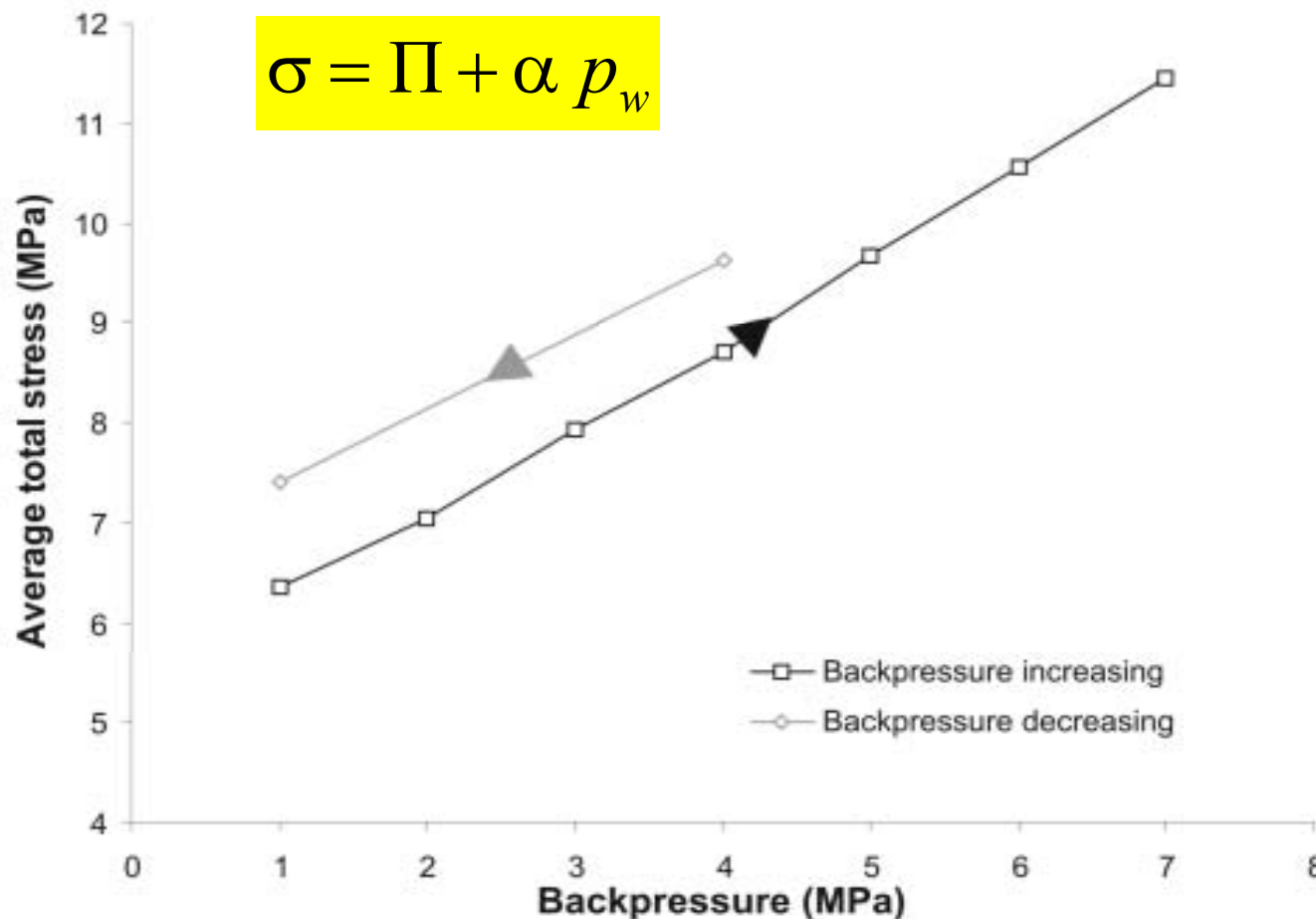


# Mx80-10 validity of stress equation





# Average total stress plotted against externally-applied water pressure



Hysteretic response

Backpressure increasing:

$\alpha = 0.86$

$\Pi = 5.4 \text{ MPa}$

Backpressure decreasing:

$\alpha = 0.74$

$\Pi = 6.7 \text{ MPa}$



British  
Geological Survey

NATURAL ENVIRONMENT RESEARCH COUNCIL



[www.bgs.ac.uk](http://www.bgs.ac.uk)

# Baseline hydraulic properties (Mx80-8 and Mx80-9)





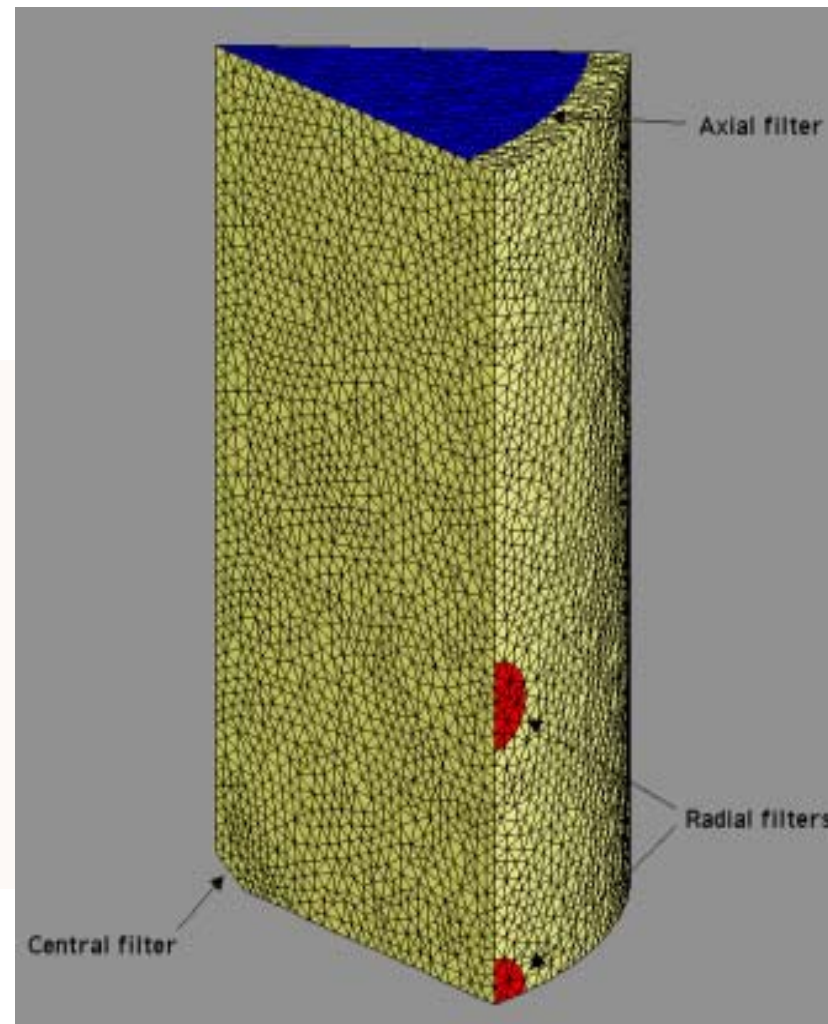


## Base-line hydraulic properties: CVRF geometry

To interpret the hydraulic data, inverse modelling was undertaken using the FESTIG 3-D finite element groundwater flow code.

A 3-D finite element mesh of one sixteenth of the CVRF specimen was developed.

This comprised 33,916 tetrahedral elements connecting 9,294 nodes.

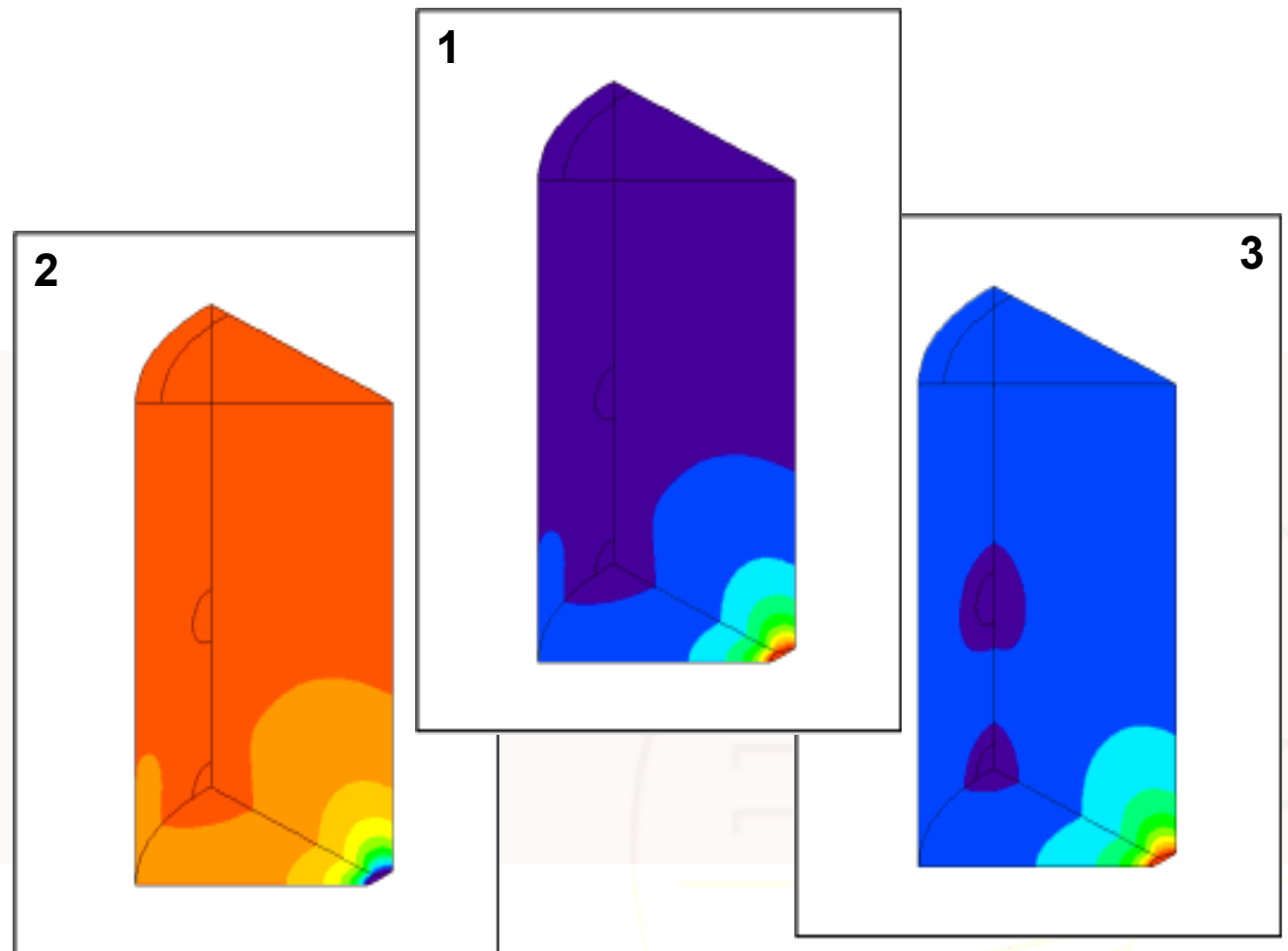




# BLHP – CVRF boundary conditions

## Measurement details:

- (1) high pressure (10 MPa) applied to the central filter and low pressure (1 MPa) applied to the axial and radial filters
- (2) low pressure applied to the central filter and high pressure applied to the axial and radial filters and
- (3) high pressure applied to the central filter and low pressure applied to the radial filters (with no flow from the axial filter).

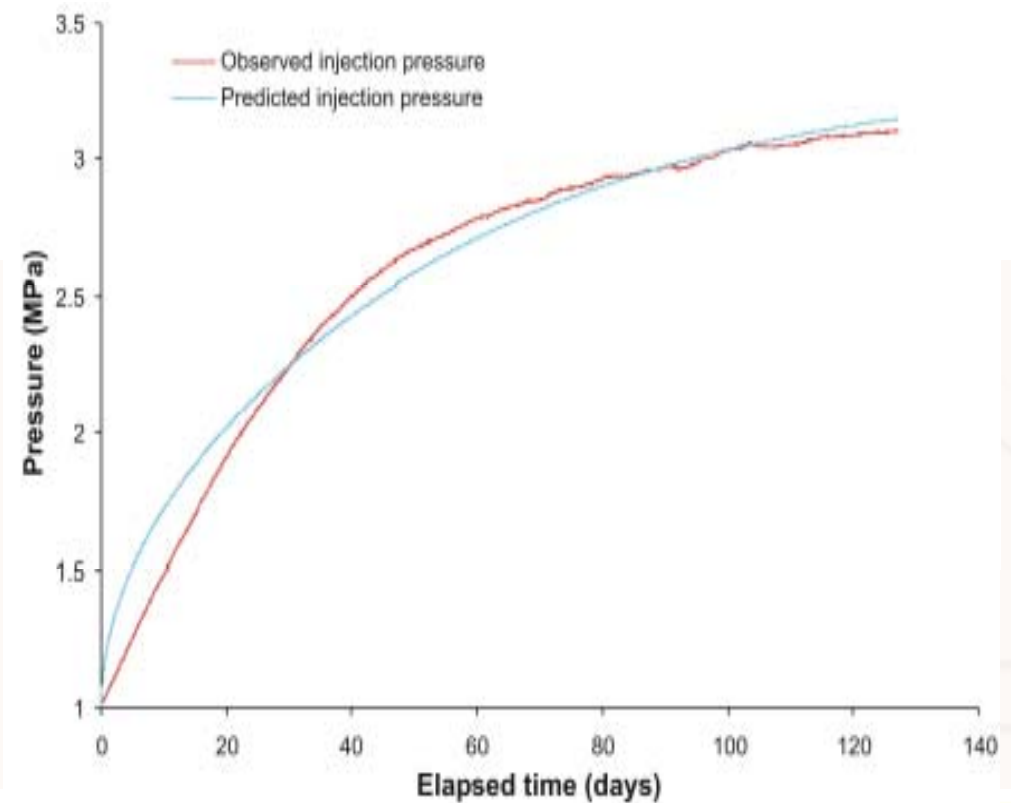
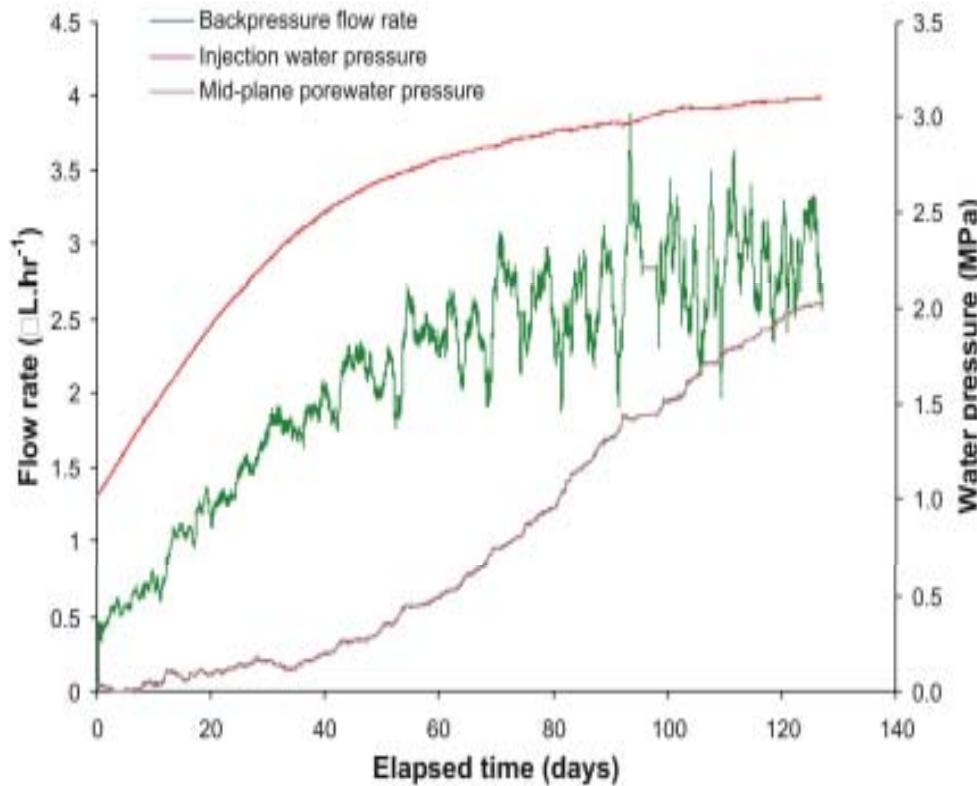


Pressure contours at 1.0 MPa intervals



# BLHP – $K_0$ boundary conditions

- Total stress = 10 MPa, porewater pressure = 1 MPa



Linear pressure distribution at steady-state

Non-linear least squares fitting routine



## Permeability data for Mx-80 bentonite with a dry density of $1.6 \text{ Mg.m}^{-3}$

Test number	Test geometry	Test configuration	Applied pressure gradient (MPa)	Steady-state flow rate ( $\mu\text{l.hr}^{-1}$ )	Hydraulic permeability ( $\text{m}^2 \times 10^{21}$ )
Mx80-8	CVRF	(A)	9.0	1.34	1.4
		(B)	9.0	2.23	2.3
		(C)	9.0	0.35	0.4
Mx80-9	$K_0$	-	2.1	2.90	9.5

- Average hydraulic permeability from CVRF test is  $1.4 \times 10^{-21} \text{ m}^2$ . Analysis of the transient flow data gives an average permeability of  $1.7 \times 10^{-21} \text{ m}^2$  and a specific storage in the range  $1 \text{ to } 9 \times 10^{-6} \text{ m}^{-1}$
- Storage value exceptionally small as one might anticipate for a fully-saturated constant volume system
- $K_0$  hydraulic permeability  $9.5 \times 10^{-21} \text{ m}^2$  ( $S_s = 3.8 \times 10^{-4} \text{ m}^{-1}$ )



British  
Geological Survey

NATURAL ENVIRONMENT RESEARCH COUNCIL



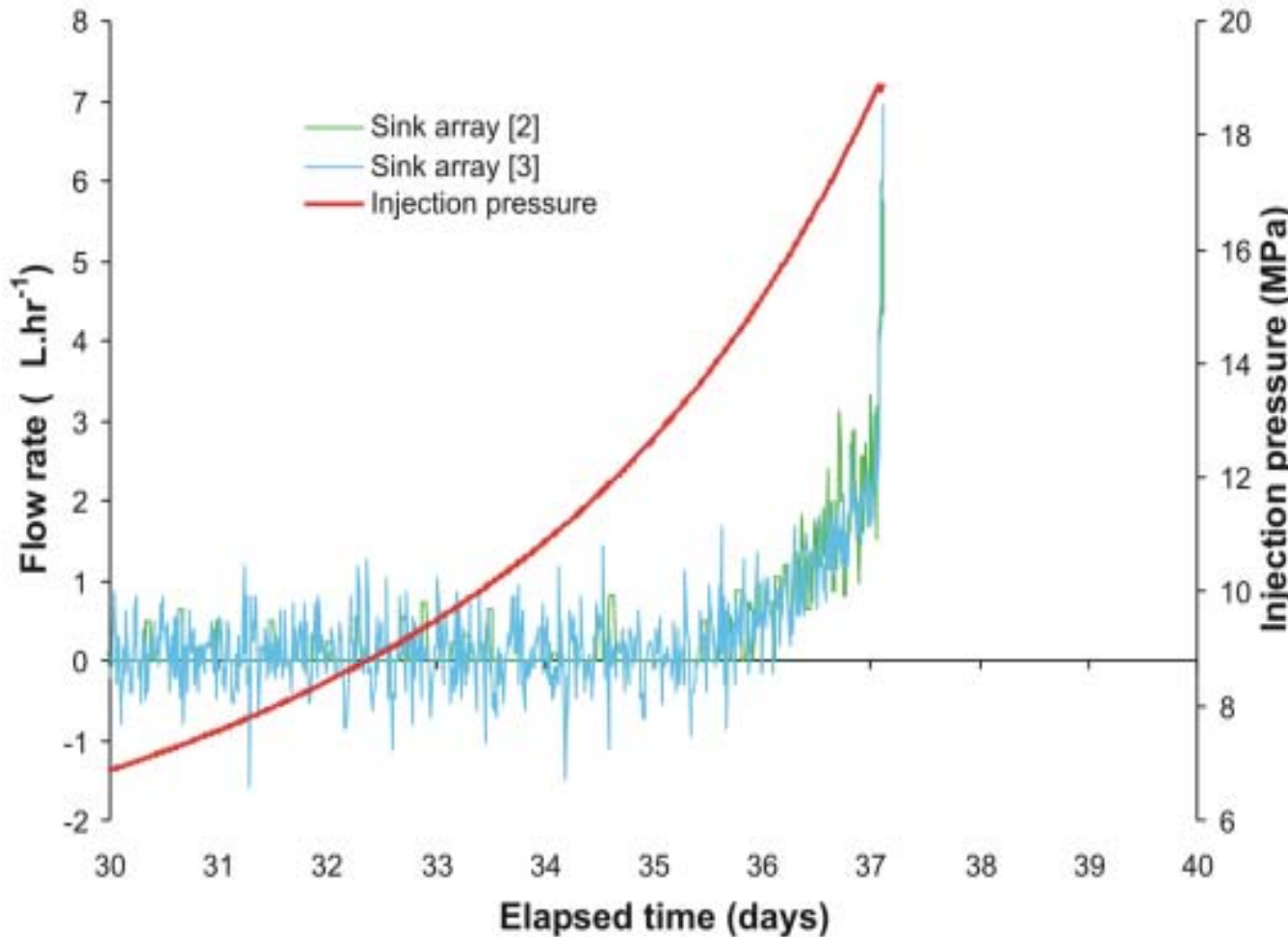
[www.bgs.ac.uk](http://www.bgs.ac.uk)

# Gas migration behaviour (all tests)





# Mx80-8 initial fluid flow

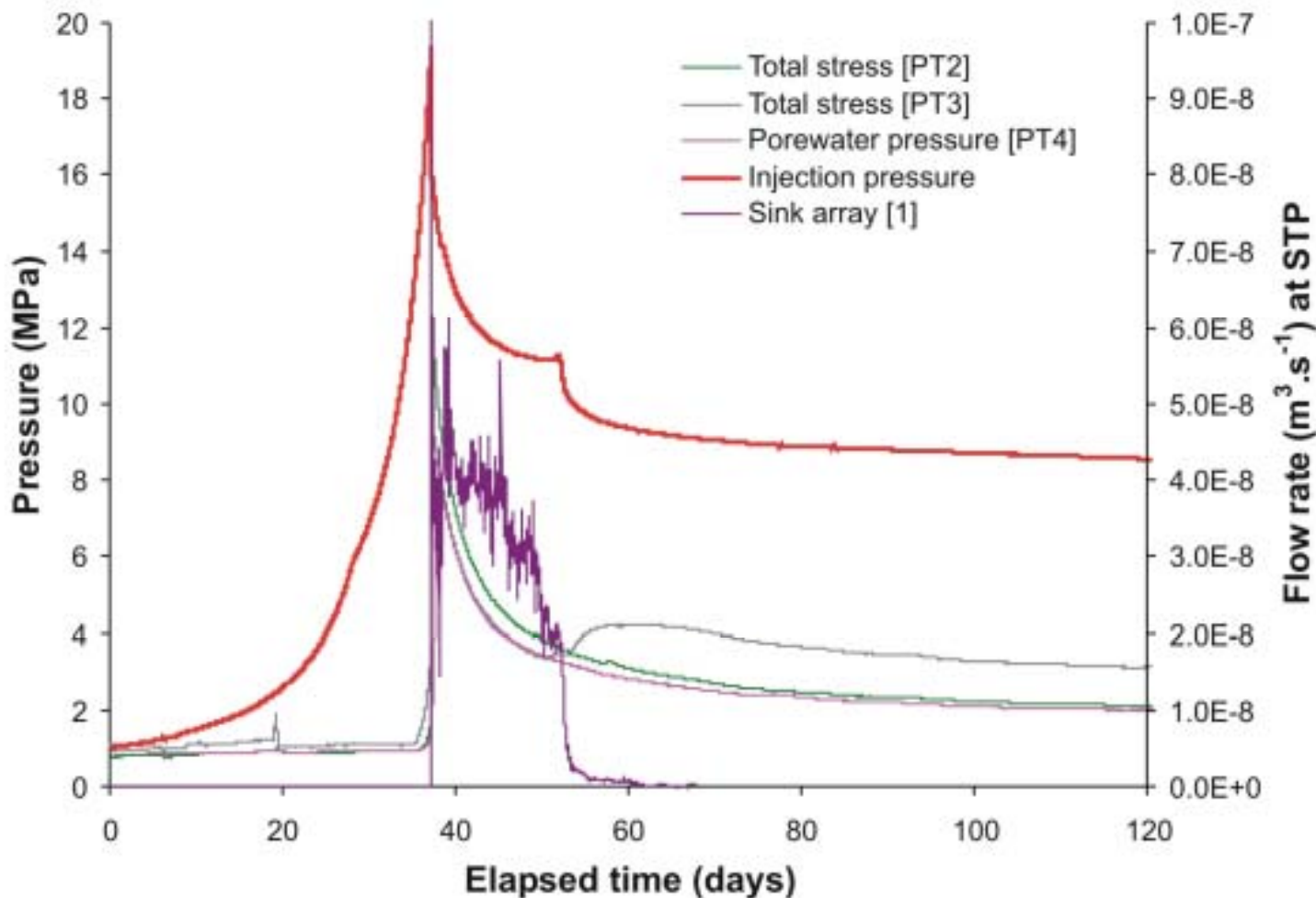


A very small amount of fluid was observed at a gas pressure of **13.8 MPa** (accompanied by a rise in axial and radial stress)

At **18.7 MPa** gas pressure dropped slightly (axial stress increased), gas pressure then increased again – pathway failed to intersect sink



# Mx80-8 first gas breakthrough and shut-in



Peak gas pressure  
**19.4 MPa**

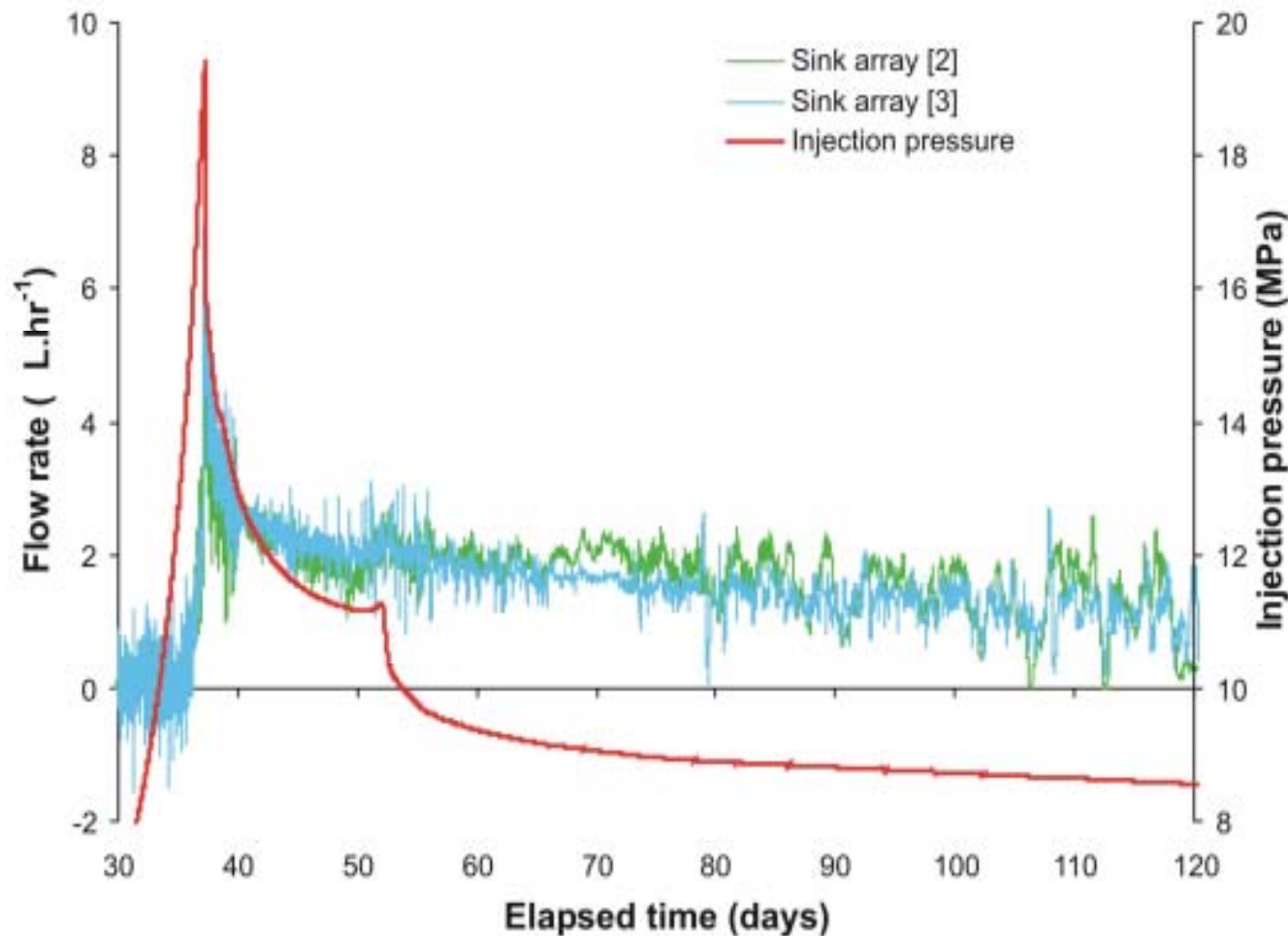
Large quantities of gas flow to sink array [1] (**99.9%**) i.e. non-uniform gas flow

High steady-state pressure of **11.2 MPa**  
( $p_g > \Pi + p_{we}$ )

Shut-in pressure around **8 MPa**



# Mx80-8 background flow from sink arrays



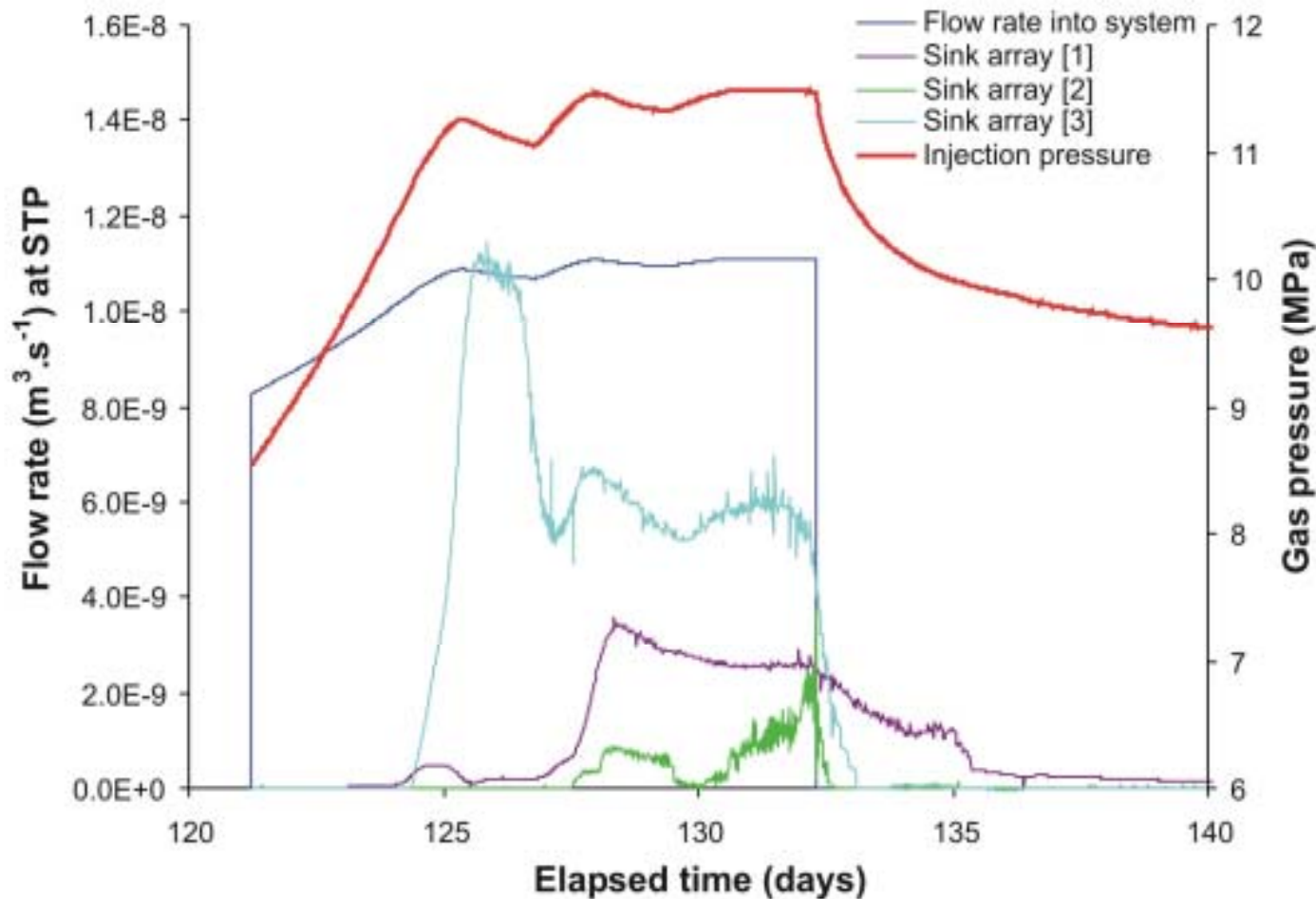
A small flux of fluid was noted to arrays [2] and [3] during gas injection (6.8ml in total)

Given the high gas and porewater pressures and the uniform distribution of flow, it seems likely this fluid is exclusively water (predominantly from end filters plus a small amount from pressure induced consolidation)





# Mx80-8 second gas injection history



No conspicuous peak

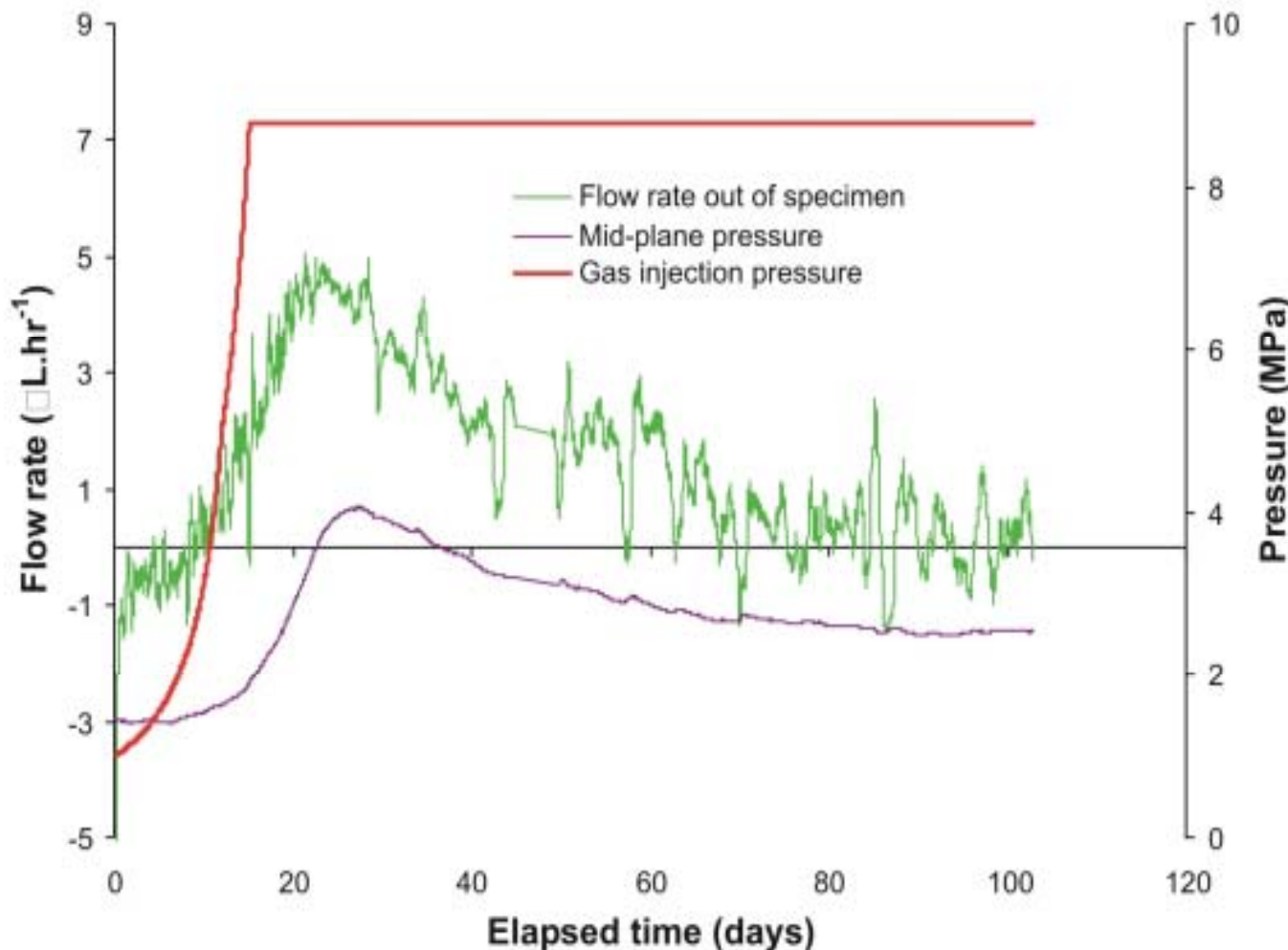
Flow evolves to a steady-state pressure of **11.5 MPa**

Temporal variations in outgoing flux demonstrate the existence of multiple, unstable gas pathways of varying aperture

Shut-in pressure around **8 MPa**



# Mx80-9 first 100 days of gas test



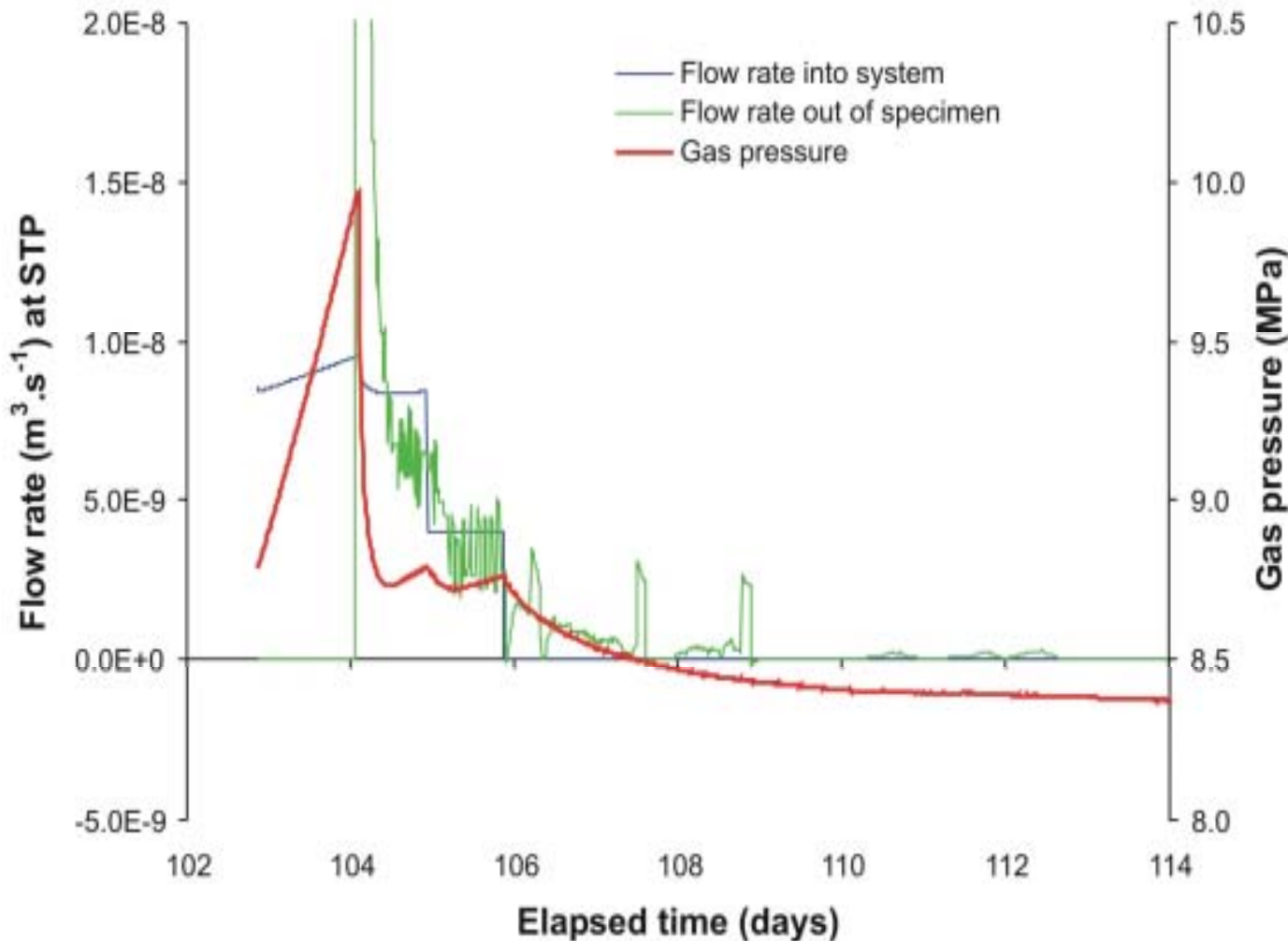
Confining and porewater pressures **10 MPa** and **1 MPa** respectively

At a gas pressure of **8.8 MPa**, the injection pump was switched to constant pressure mode

Flow rate increased to a peak then decline – interpreted as slug flow



# Mx80-9 main gas breakthrough event



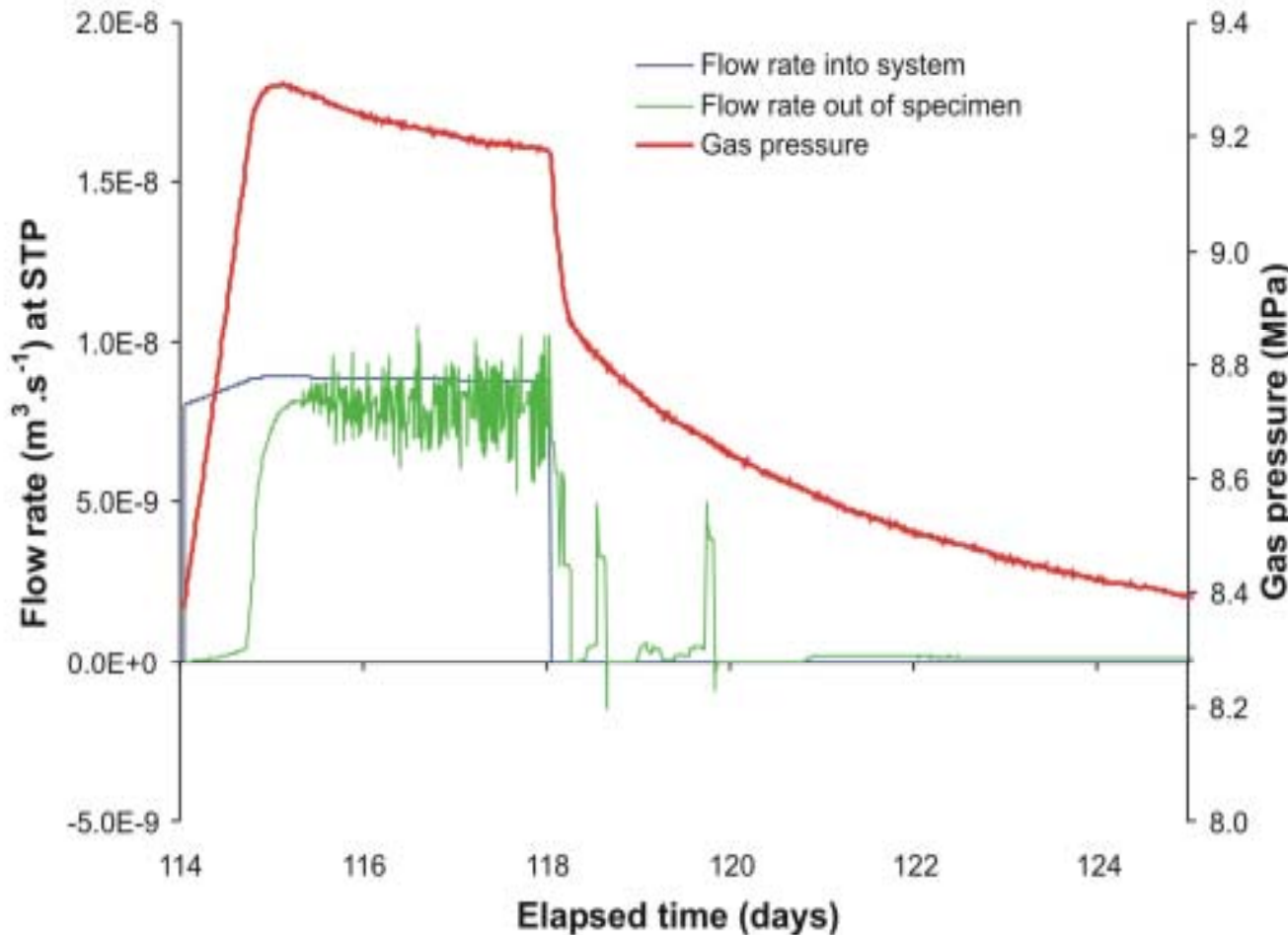
Major gas breakthrough at a peak pressure fractionally below **10 MPa**

Followed by a rapid decline in pressure – evidence of an “undershoot” in pressure – consistent with unstable gas pathways

Shut-in pressure around **8.2 MPa**



# Mx80-9 second gas injection history



Flow rate out of the specimen began at around **8.5 MPa**

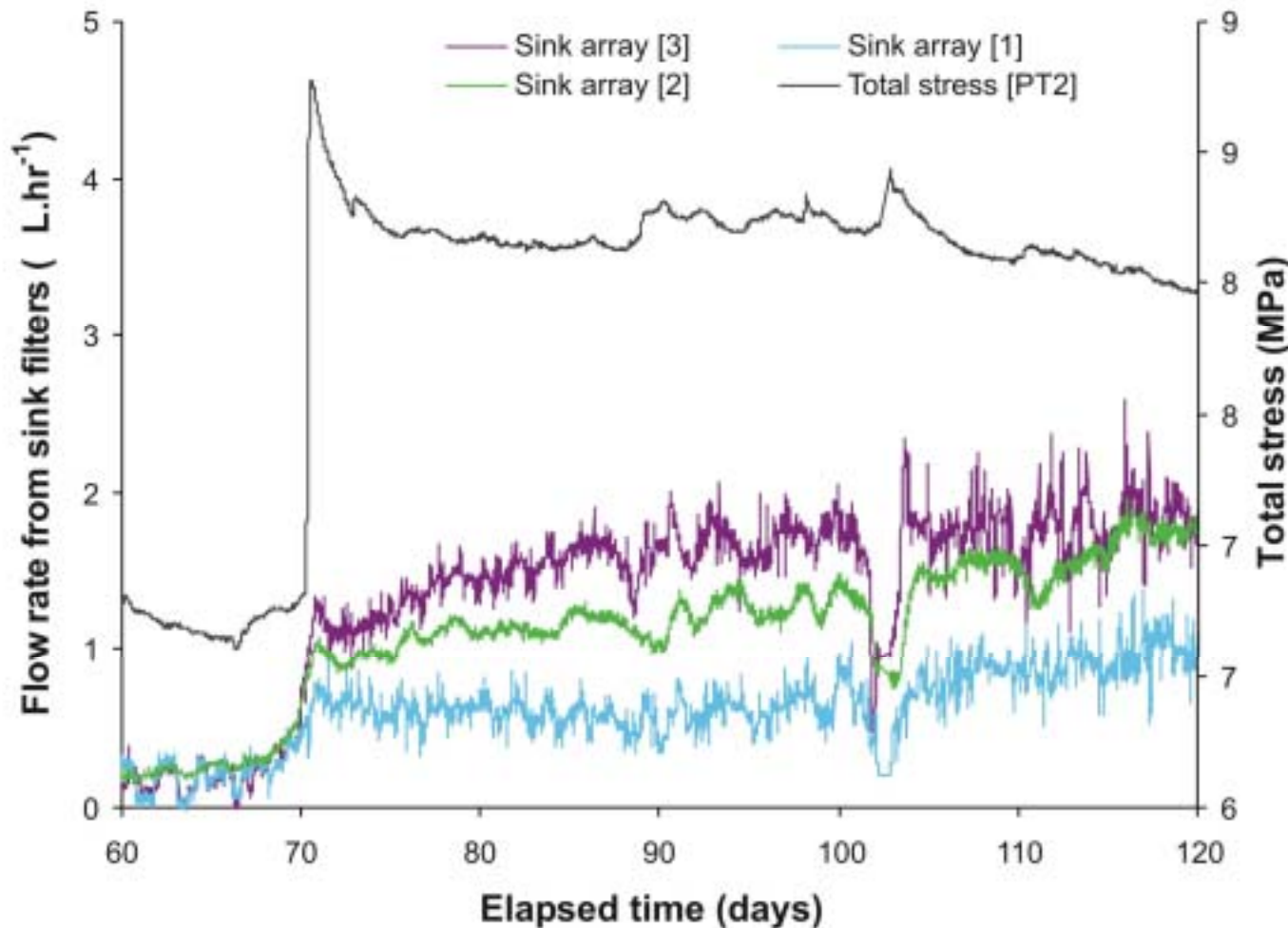
Gas pressure increased to a peak value of **9.3 MPa** before decaying slightly to a steady state pressure of **9.2 MPa**

No conspicuous peak in flow

Break in shut-in slope indicative of pathway closure



# Mx80-10 Change in total stress at gas breakthrough



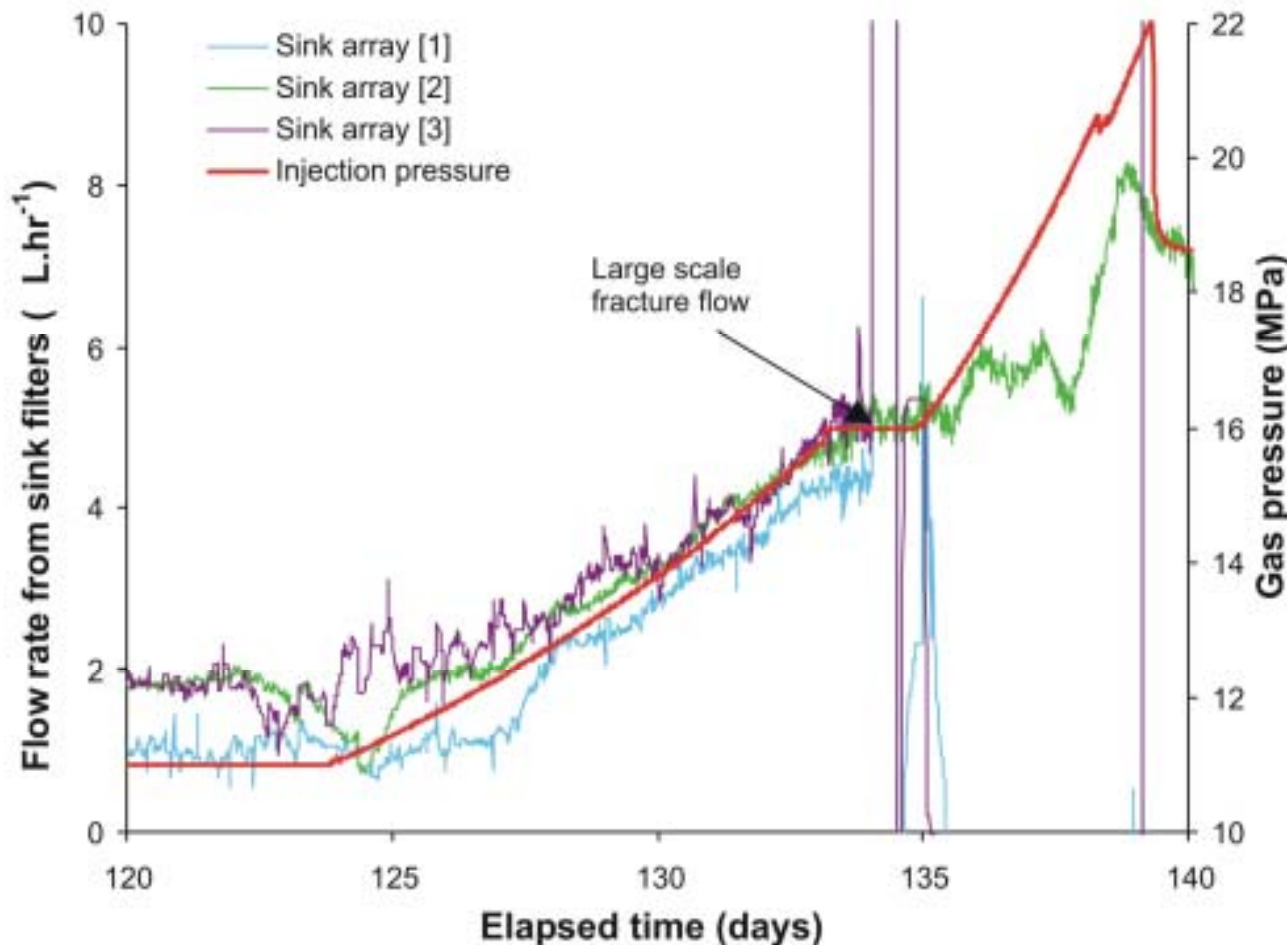
Gas breakthrough accompanied by a sharp increase in total stress

Suggests dilation of the fabric occurs during gas flow

Outgoing flux is unevenly distributed amongst filters



# Mx80-10 distribution of flow with increasing gas pressure



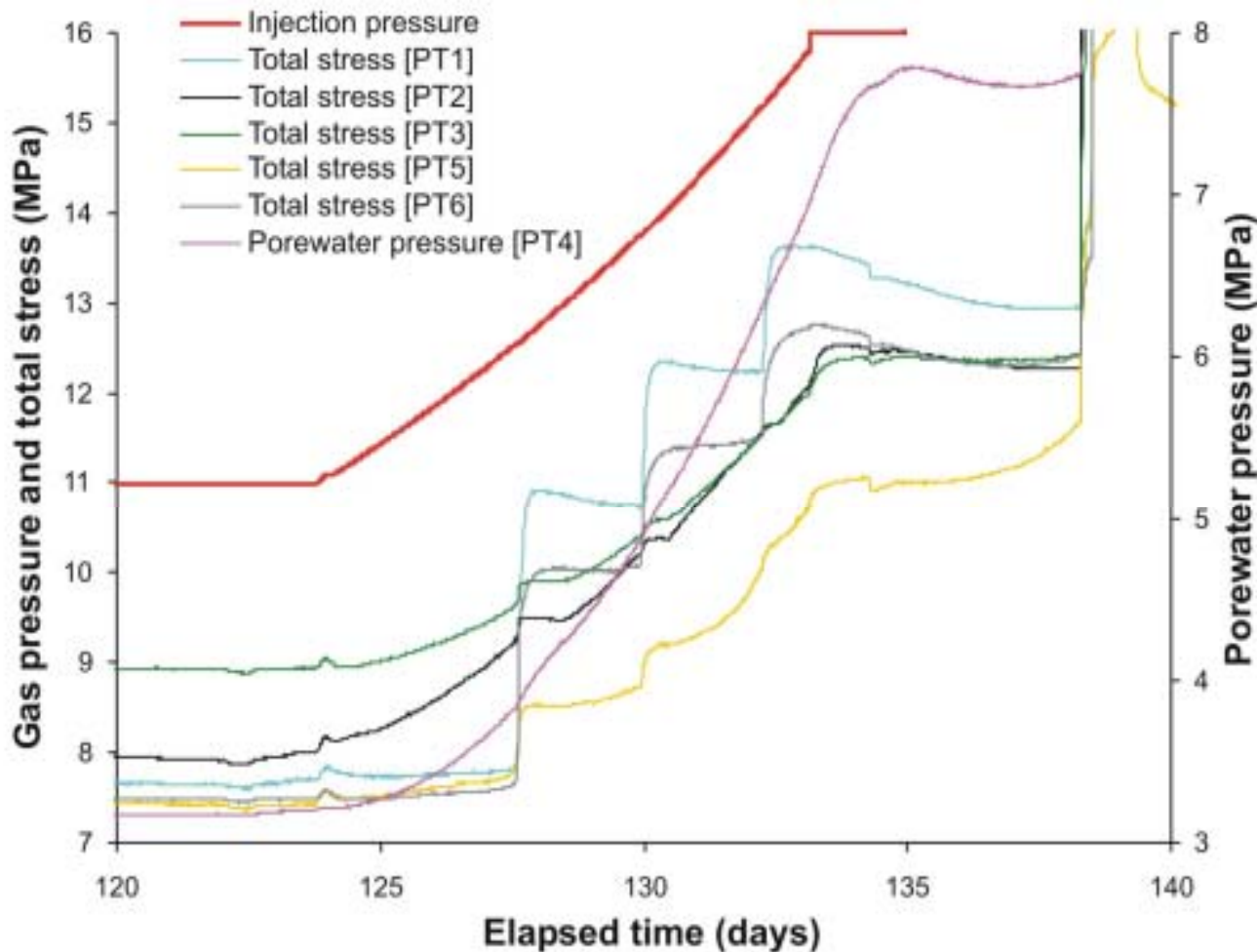
Discharge rate to [3] increased immediately while [1] and [2] lagged behind 2-3 days

At 16 MPa pump switched to constant pressure. After 27 hours gas flow to [1] and [3] increased spontaneously

Water injected which “resealed” pathways (peak pressure 22.1 MPa)



# Mx80-10 evidence for pathway development



Stress sensors show step-like responses which correlate with propagation events

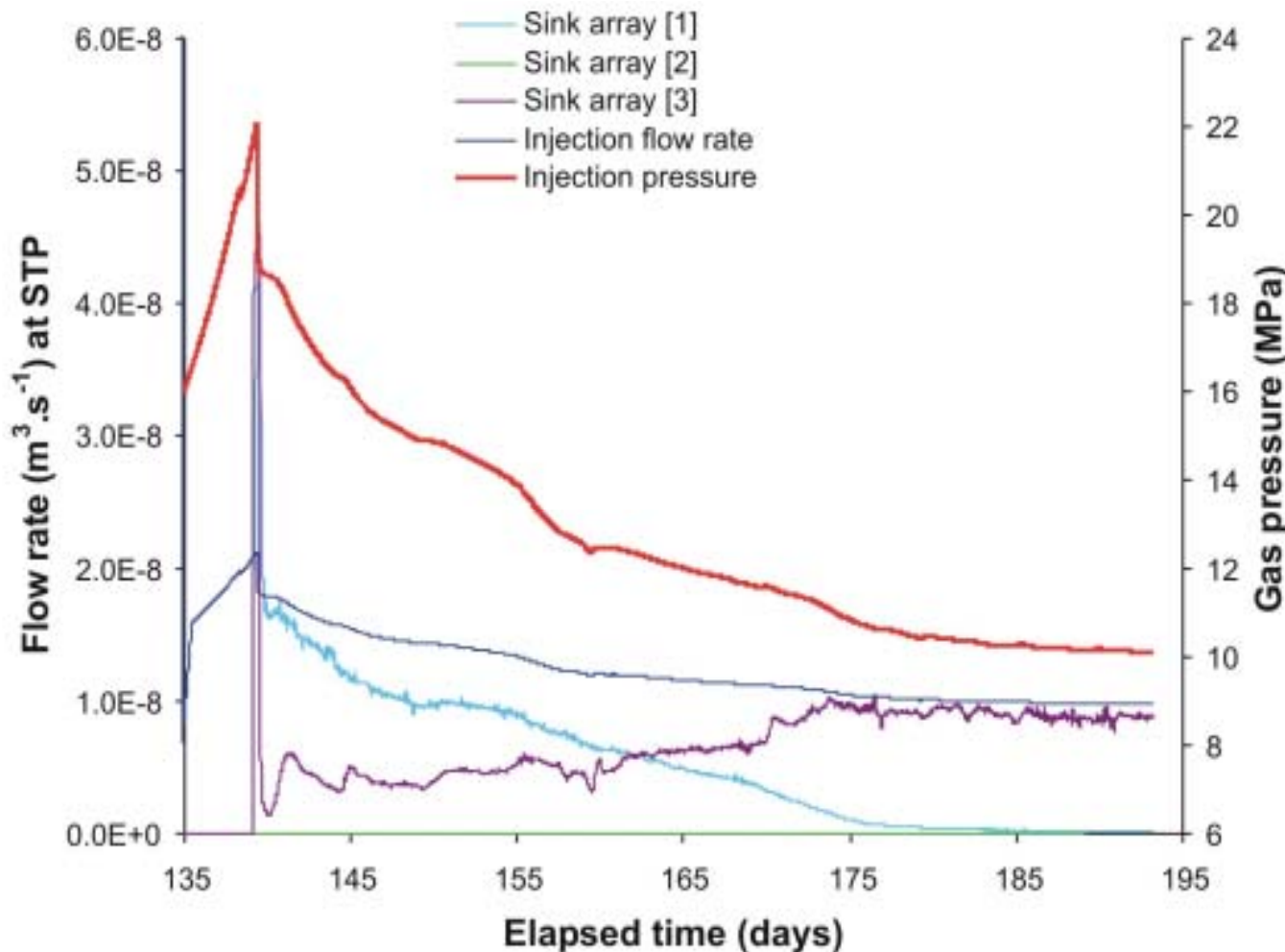
There were no corresponding increases in discharge to the sink arrays

Therefore it can be inferred that none of the pathways actually intersected sink filters

Gas pressure > total stress (pre-peak behaviour)



# Mx80-10 breakthrough and steady-state gas flow



Major flow occurs to arrays [1] and [3]

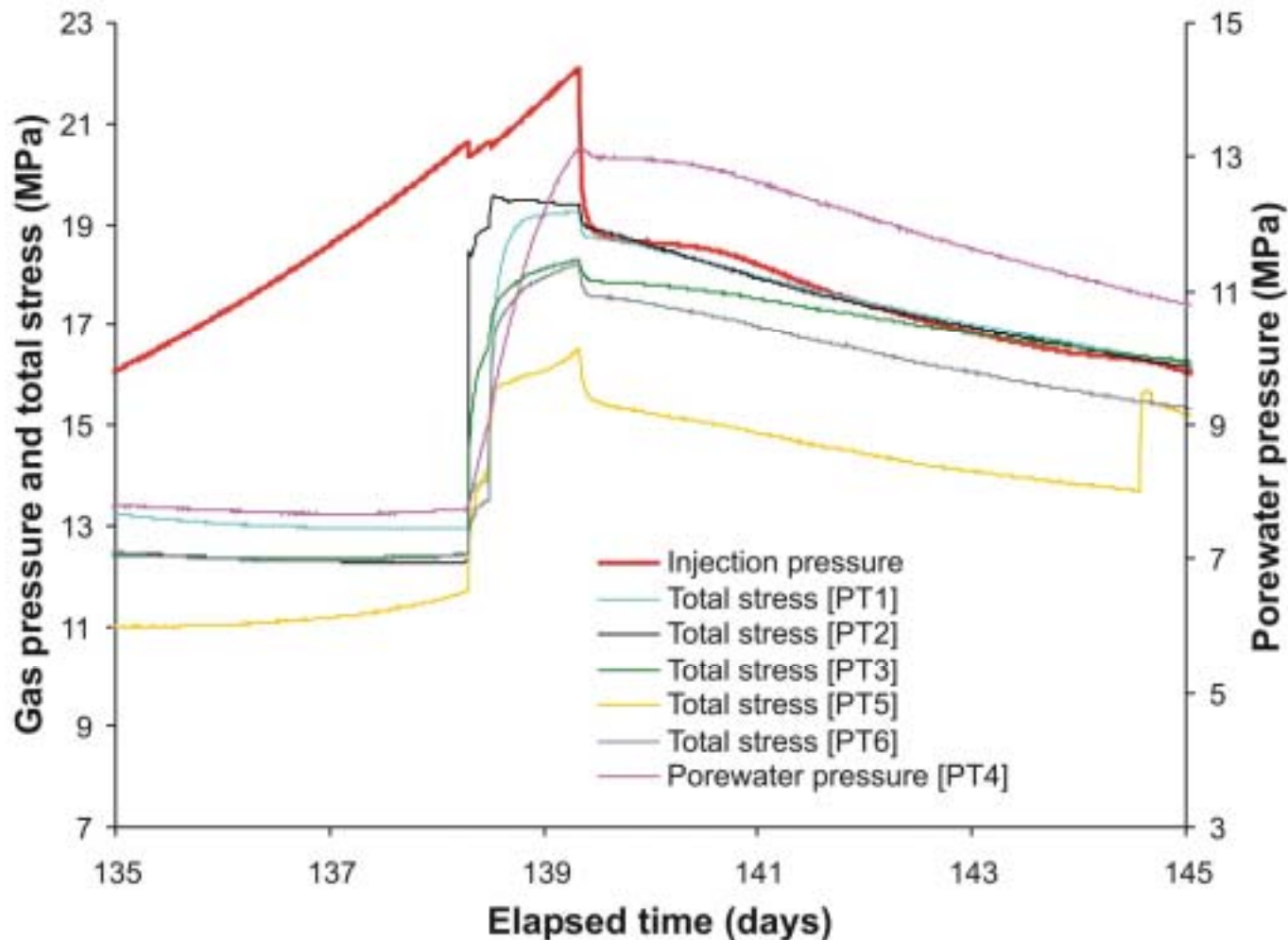
Sharp drop in pressure after the peak is suggestive of a breakdown in tensile strength and the development of conductive gas pathways

Mass balance considerations confirm the flow is predominantly gas





# Mx80-10 stress distribution at peak pressure



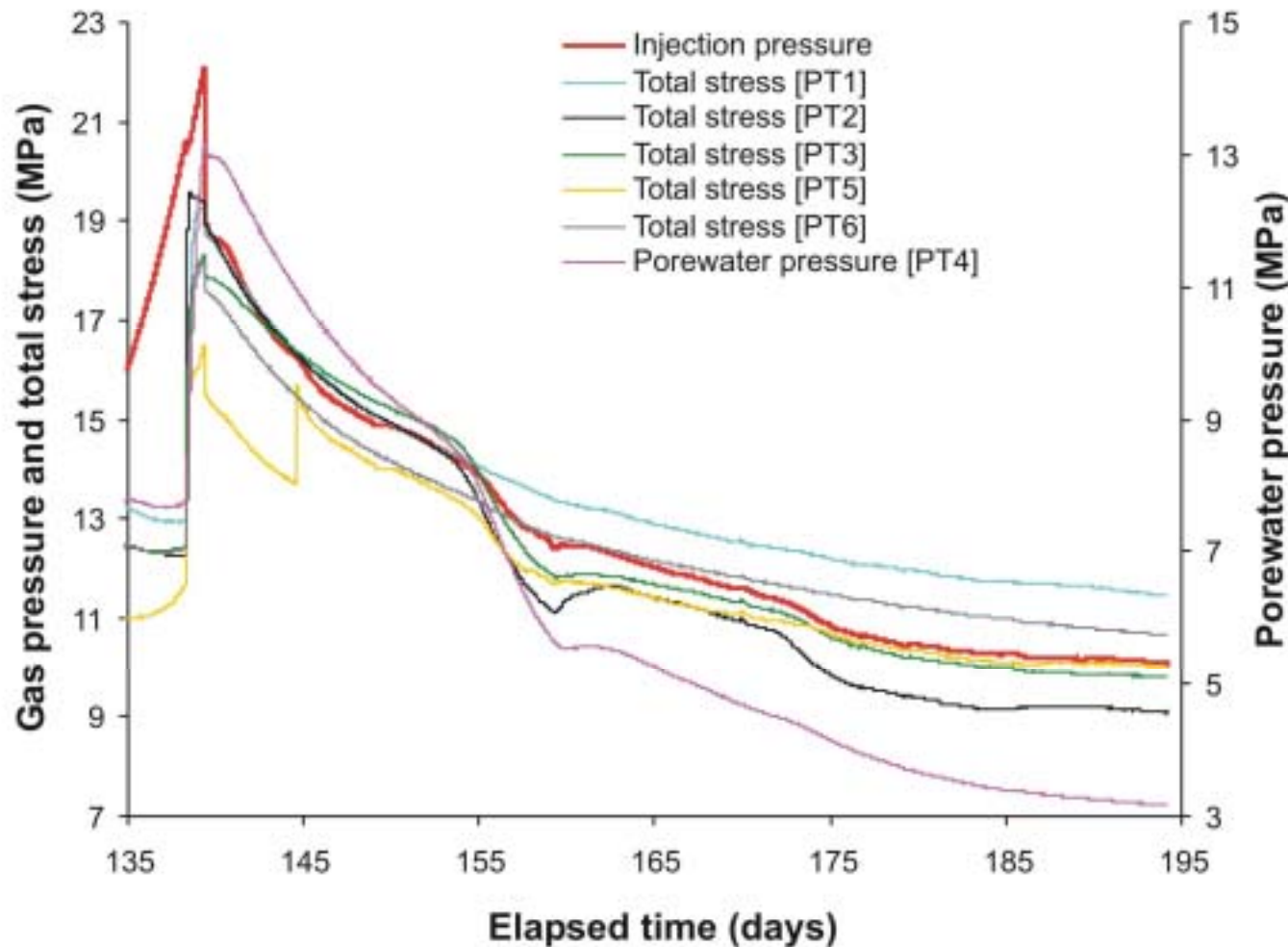
Drop in gas pressure accompanied by an increase in all stress and porewater pressure sensors - a consequence of fracture propagation

Initial fractures have a radial orientation

At breakthrough peak gas pressure is around **2.7 MPa** above maximum total stress i.e. tensile strength



# Mx80-10 post peak stress and porewater pressure behaviour



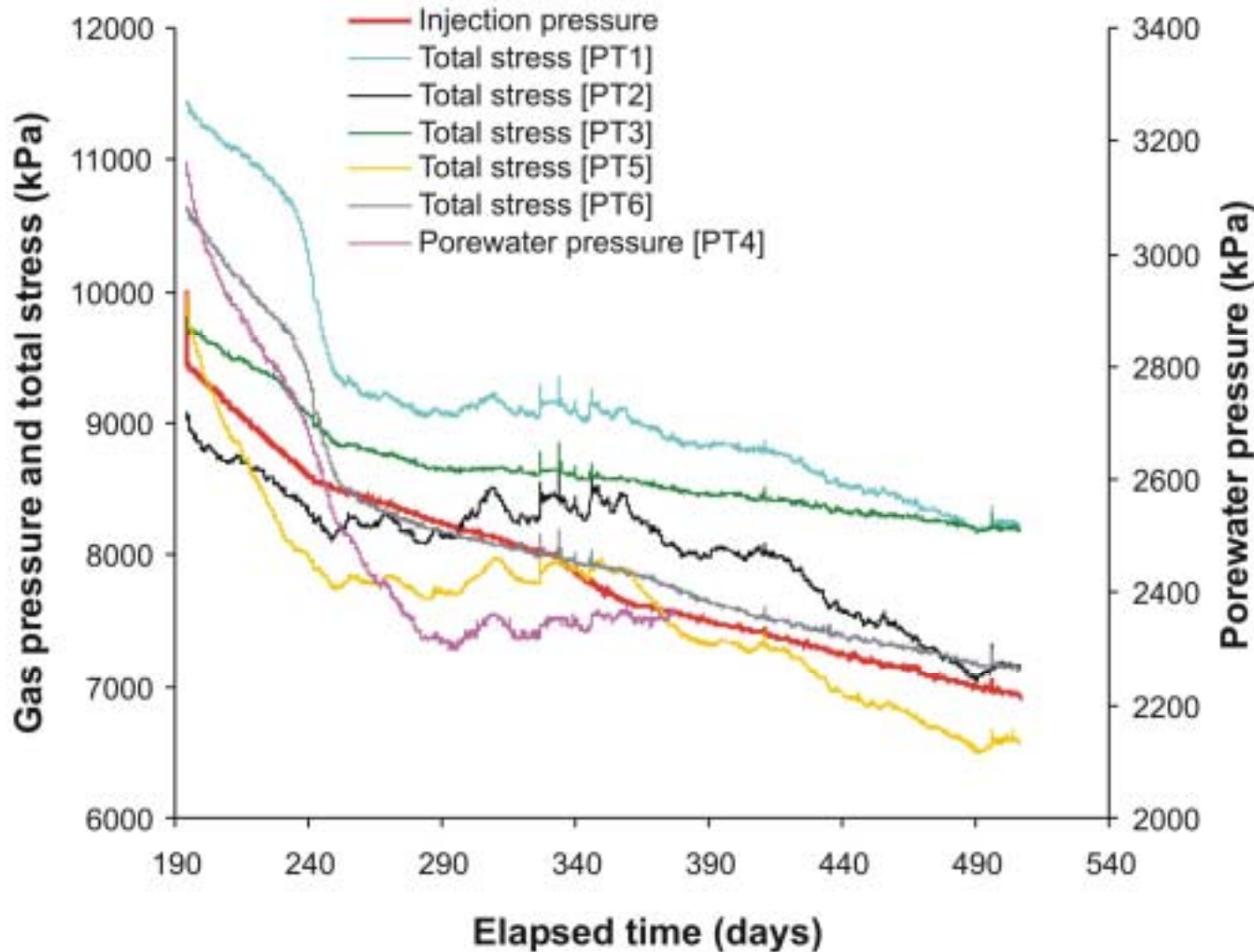
Gas pressure transient shows signs of changes in pathway aperture

Post peak gas pressure is close to the average total stress (contrast to pre-peak)

Gas pressure slowly declines to a steady-state value of around **10.1 MPa**



# Mx80-10 shut-in response



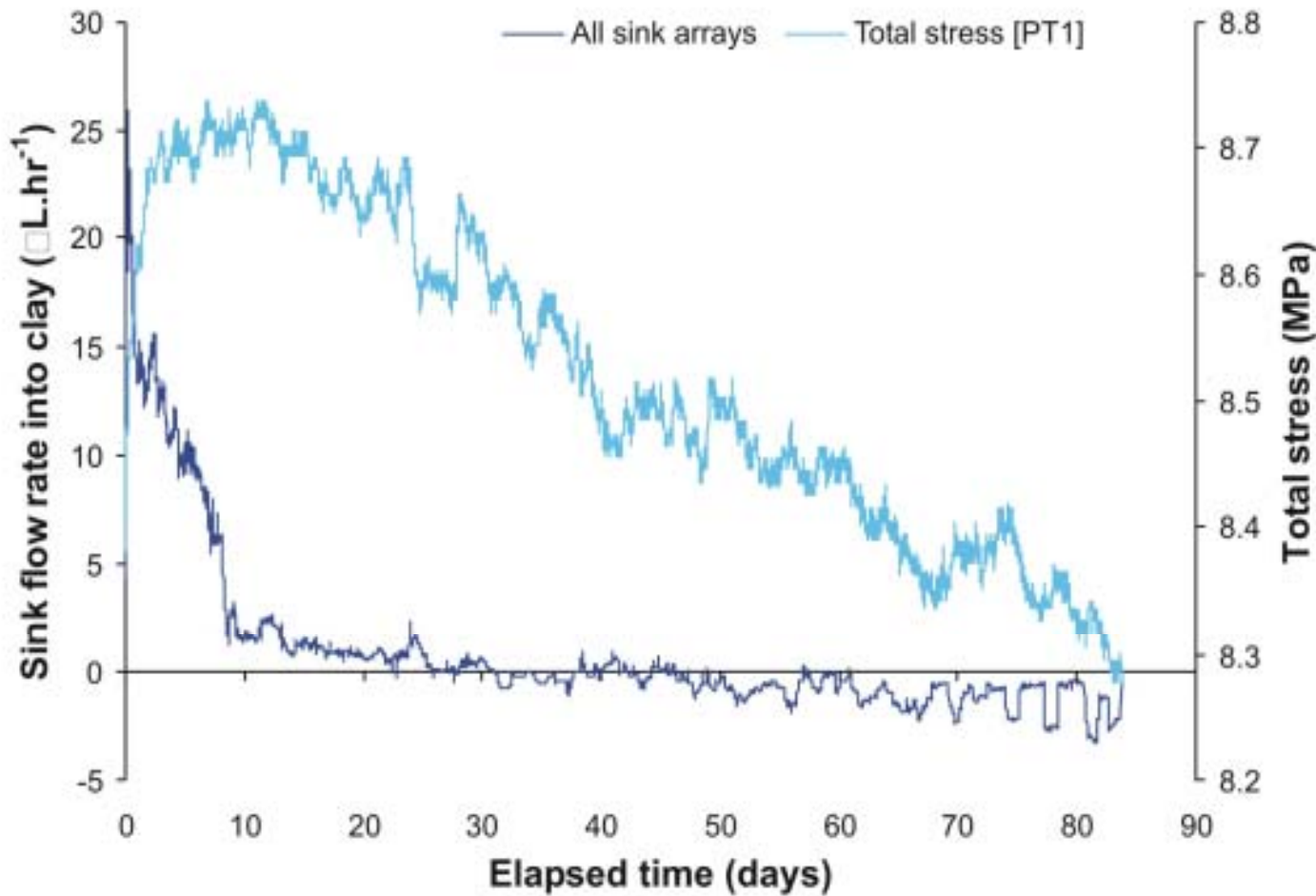
Changes in slope are indicative of a change in pathway aperture

During much of the shut-in transient gas pressure exceeds porewater pressure by around **5.8 MPa**

Zero flow asymptote estimated to **7 MPa**



# Mx80-10 post gas hydraulic testing



A hydraulic test was performed identical to that of Mx80-8

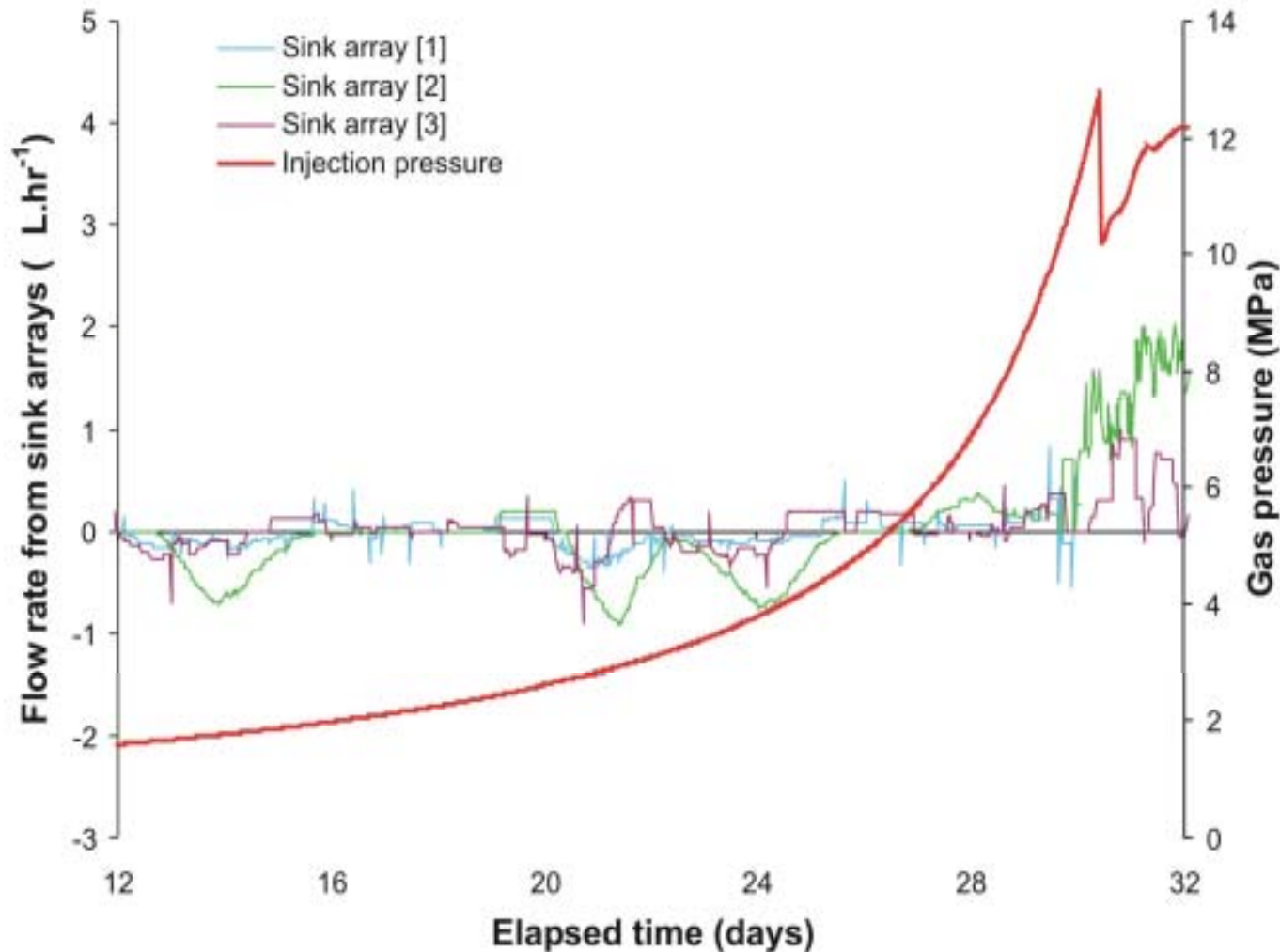
Breaks in flow rate at 1 and 9 days are indicative of reduction in permeability

Average flow  $1.4 \mu\text{L.hr}^{-1}$

Same as Mx80-8, indicating gas pathways had no long-term effect on permeability to water



# Mx80-10 second gas injection history



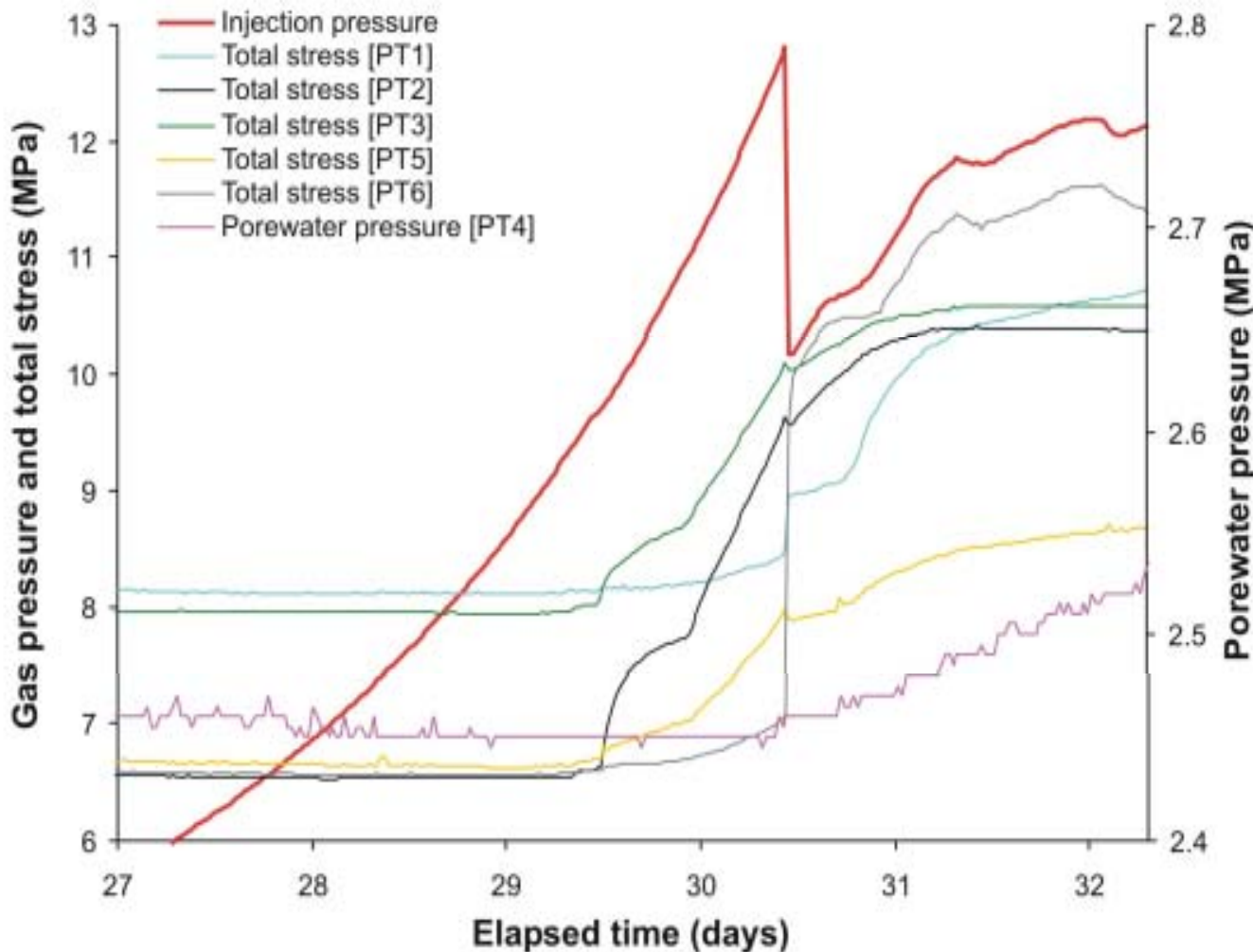
No obvious signs of early gas flow

At **9.4 MPa** a small outflow was detected

Peak gas pressure was **12.8 MPa** which is substantially lower than before (**22.1 MPa**)



# Mx80-10 second gas injection history



Outflow of fluid at 9.4 MPa coincides with a small increase in total stress

Another fracture propagation event marked by a sharp rise in [PT2] and [PT3] sensors coincided with a small change in gas pressurisation curve

Post peak gas pressure drop indicates the clay regained part of its tensile strength (“self-sealing”)



British  
Geological Survey

NATURAL ENVIRONMENT RESEARCH COUNCIL



[www.bgs.ac.uk](http://www.bgs.ac.uk)

# Process understanding (all tests)





## Peak behaviour

- Using linear elastic stress analysis the gas fracturing pressure of clay around the filter is given by:

$$p_g \text{ (peak)} = T + 2\sigma_{eff} + p_w$$

where  $T$  is the tensile strength of the clay,  $\sigma_{eff}$  is the isotropic effective stress (outside the region of the stress concentration) and  $p_w$  is the porewater pressure (just before fracturing)

- For saturated bentonite the isotropic effective stress must be equal to the swelling pressure
- Substituting values for test Mx80-10 ( $T = 2.7 \text{ MPa}$ ;  $\sigma_{eff} = 5.5 \text{ MPa}$  and  $p_w = 7.7 \text{ MPa}$ ) gives a gas fracturing pressure of  $21.4 \text{ MPa}$  (close to the observed peak gas pressure value of  $22.1 \text{ MPa}$ )



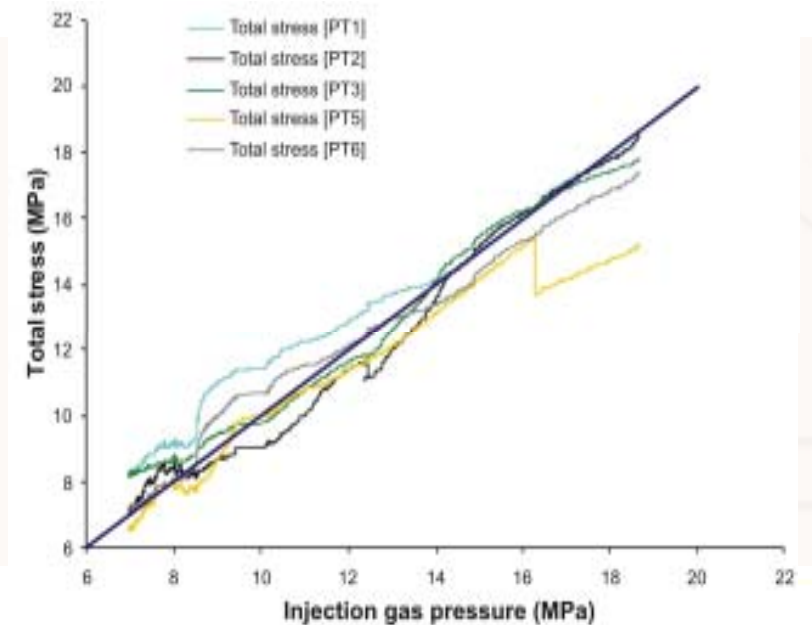


## Post-peak behaviour

- Post-peak the fracture will lie beyond the region of stress concentration region around the filter and the clay will have lost its tensile strength ( $p_g = \sigma$ )

$$p_g \text{ (post - peak)} = \sigma = \sigma_{eff} + p_w$$

- At an elapsed time of 145 days  $p_w = 10.8 \text{ MPa}$  ( $\sigma_{eff} = 5.5 \text{ MPa}$ ) which gives a post peak gas pressure of  $16.3 \text{ MPa}$  (close to the observed value of  $16.1 \text{ MPa}$ )
- The average total stress at this time  $15.8 \text{ MPa}$
- The shape of the post-peak transient is governed by a couple between gas and porewater pressure





## Steady state behaviour

- At steady-state the gas permeability of the fracture network must remain more or less constant with time
- Under constant volume conditions mechanical equilibrium of forces demands that total stress be moderately homogenous (any variation governed by the shear strength). Total stress sensors indicate a variability of around 3 MPa
- Since conductive fractures are propped by gas then the gas pressure gradient must also be close to 3 MPa (the same can be said for internal porewater pressure)
- The existence of a porewater pressure gradient at steady-state supports the hypothesis of “pressure induced consolidation” which in turn may question the “uniqueness” of permeability values



# Capillary pressure behaviour

- Capillary pressure is defined as:

$$p_c = p_g - p_w$$

- Taking an average value over 170 days of the shut-in Mx80-10 gives a capillary pressure of **5.8 MPa** (close to measured swelling pressure)
- Rewriting post-peak equation we obtain:

$$\sigma_{eff} = p_g \text{ (post - peak)} - p_w$$

which shows that capillary pressure and effective stress are equal over the entire post-peak history

- Leads to the conclusion that effective stress is equal to swelling pressure



## Shut-in behaviour

- Theoretically under constant volume conditions, gas pressure cannot fall below the sum of the capillary pressure and externally applied water pressure

$$p_g \text{ (shut - in)} = p_c + p_{we}$$

- Taking capillary pressure as **5.8 MPa** (Mx80-10) and  $p_{we}$  as **1.0 MPa** gives a lower bound value of **6.8 MPa**
- Independent measurements from CVRF testing gives shut-in pressures of **7 – 8 MPa**



# Evidence for porewater displacement

- It has been suggested that the rate of gas pressurisation in laboratory experiments is usually so large that gas fracturing becomes the dominant mechanism and advection in original pores therefore remains undetected

Test specimen	Initial saturation (%)	Initial volume of gas voids (cm <sup>3</sup> )	Net inflow of water (cm <sup>3</sup> )	Final saturation (%)	Time period at over 8 MPa (days)	Total gas flow at STP (litres)
Mx80-8	97.6	3.49	3.73	100.2	195	55.5
Mx80-9	98.3	0.89	1.54	101.4	139	4.5
Mx80-10	98.9	1.59	3.51	101.3	390	60.4

- Specimens were exposed to gas pressures **>8 MPa** for periods of time ranging from **5 –13 months**
- It is possible to pass up to **60L** (STP) of helium through the specimens without causing any measurable desaturation



## Evidence for self-sealing behaviour

- Strong evidence that gas flows through a network of pressure-induced pathways
- Very little if any displacement of water occurs during gas movement
- In CVRF tests, spontaneous changes in slope of the pressure transients and temporal variations in the amount of gas discharged to sinks collectively demonstrates the unstable nature of the pathways
- Evidence from Mx80-10 that the clay regained part of its tensile strength during the rehydration stage
- Spontaneous closure of pathways and re-establishment of strength in tension can each be interpreted as a capacity for “self-sealing”



## CVRF conclusions (1)

- Gas entry and breakthrough under constant volume boundary conditions causes a substantial increase in the total stress acting on the clay and the internal porewater pressure
- Since gas entry, breakthrough, peak and steady-state gas pressures are sensitive to test boundary conditions, it indicates the process of gas entry is accompanied by dilation of the bentonite fabric
- The sharp pressure drop after the peak is indicative of a breakdown in the tensile strength of the bentonite
- Breakthrough and peak pressures may also be affected by the number, location and geometry of the sink filters and the rate of gas pressurisation



## CVRF conclusions (2)

- Gas pressure under constant volume conditions can significantly exceed the sum of the swelling pressure and externally-applied porewater pressure
- Abrupt drops in gas pressure, accompanied by increases in total stress, can be interpreted as fracture propagation events
- Gas is always non-uniformly distributed between the sink arrays. Furthermore, the distribution of flow between sinks often changes abruptly and spontaneously during the course of an experiment
- Experimental evidence is consistent with the development of a relatively small number of crack-like pathways which are highly unstable





## Conclusions (3)

- Since gas entry, breakthrough, peak and steady-state pressure are all sensitive to test boundary conditions, it confirms advective gas flow is accompanied by dilation of the bentonite fabric
- After intense scrutiny of the data we are unable to find any convincing evidence of porewater displacement, desaturation or conventional two-phase flow – though a case can be made for internal consolidation
- There is no evidence from these tests that the development of pressure-induced gas pathways compromises the sealing capacity of the bentonite barrier. Gas pathways appear to be ephemeral features of the buffer which tend to close up when gas pressure falls



British  
Geological Survey

NATURAL ENVIRONMENT RESEARCH COUNCIL



[www.bgs.ac.uk](http://www.bgs.ac.uk)

# Some practical observations on gas flow in clays and clay-rich rocks

S.T. Horseman and J.F. Harrington

**GAMBIT 4 Workshop, Madrid 2003**

Kingsley Dunham Centre  
Keyworth  
Nottingham NG12 5GG  
Tel 0115 936 3100

© NERC All rights reserved



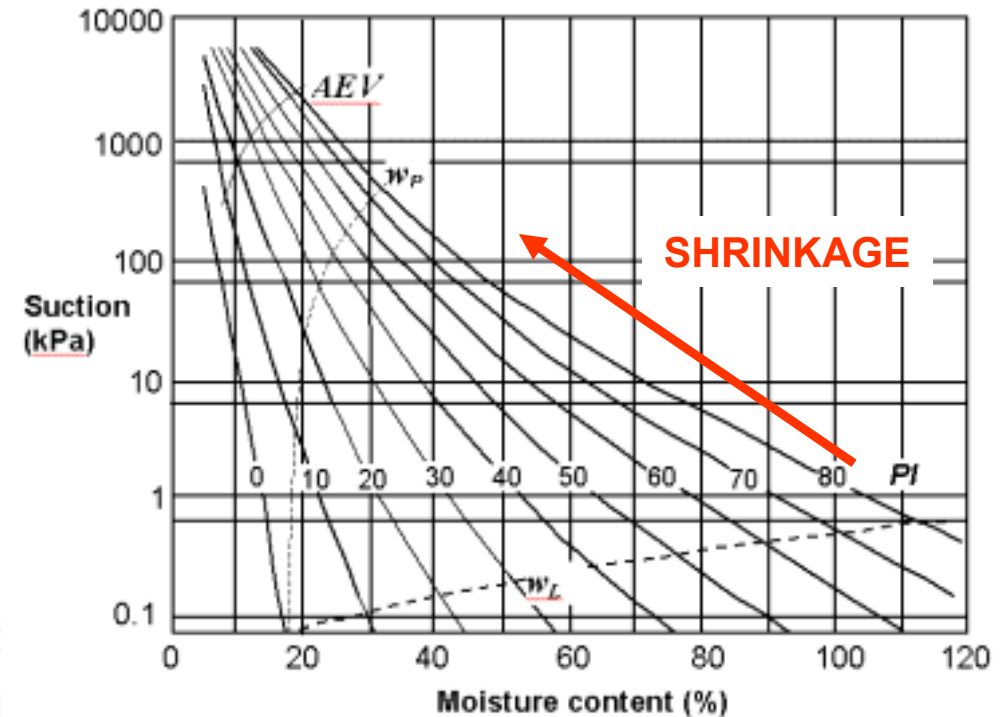
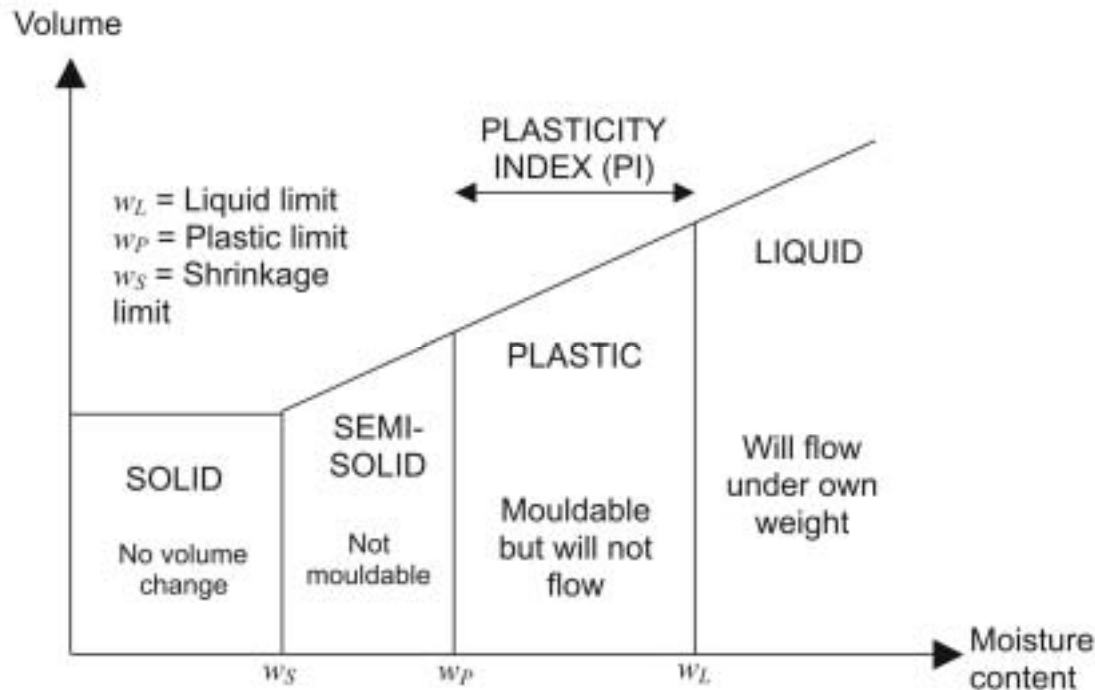


# Contents of presentation

- **Study of gas entry in unconfined clays at moisture contents between the Liquid and Plastic Limits (particle-displacement mechanism)**
- **Gas burps and mud volcanos**
- **Gas migration in offshore geological environments**
- **Seabed pockmarks**
- **Study of inflammable gas emissions in the Hanford Waste Tanks**
- **Study of gas migration in clay cores**
- **Concluding remarks**



## Study of gas entry in unconfined clays at moisture contents between the Liquid and Plastic Limits



INCREASING SHEAR STRENGTH

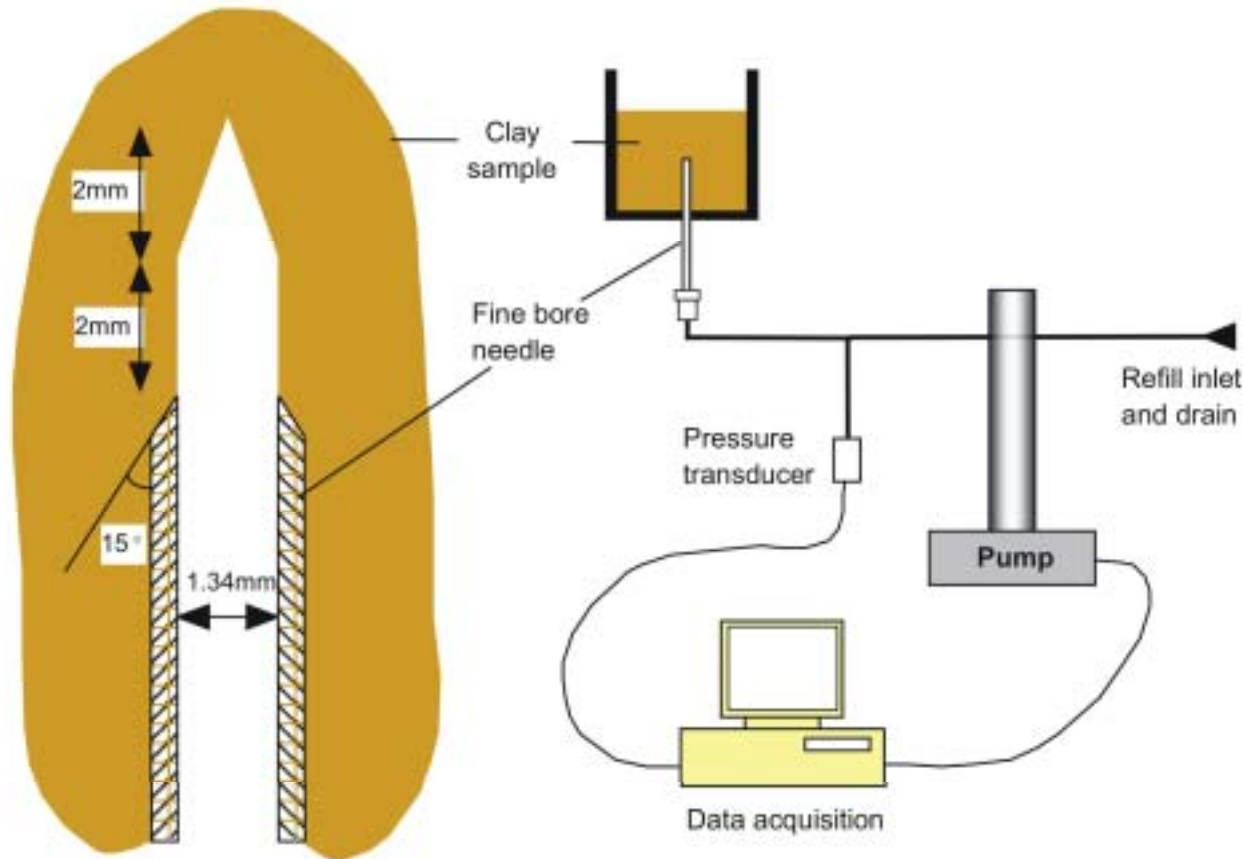


## Details of the clay samples

	Liquid limit (%)	Plastic limit (%)	Plasticity index (%)	Specific surface (m <sup>2</sup> .g <sup>-1</sup> )
<b>Kaolinite</b>	<b>60</b>	<b>35</b>	<b>25</b>	<b>29</b>
<b>London Clay</b>	<b>56</b>	<b>24</b>	<b>32</b>	<b>138</b>
<b>Ball Clay (Illite)</b>	<b>72</b>	<b>33</b>	<b>39</b>	<b>101</b>
<b>Blauton</b>	<b>72</b>	<b>29</b>	<b>43</b>	<b>176</b>
<b>Gault Clay</b>	<b>91</b>	<b>45</b>	<b>46</b>	<b>260</b>
<b>Bentonite</b>	<b>332</b>	<b>38</b>	<b>294</b>	<b>ca 750</b>



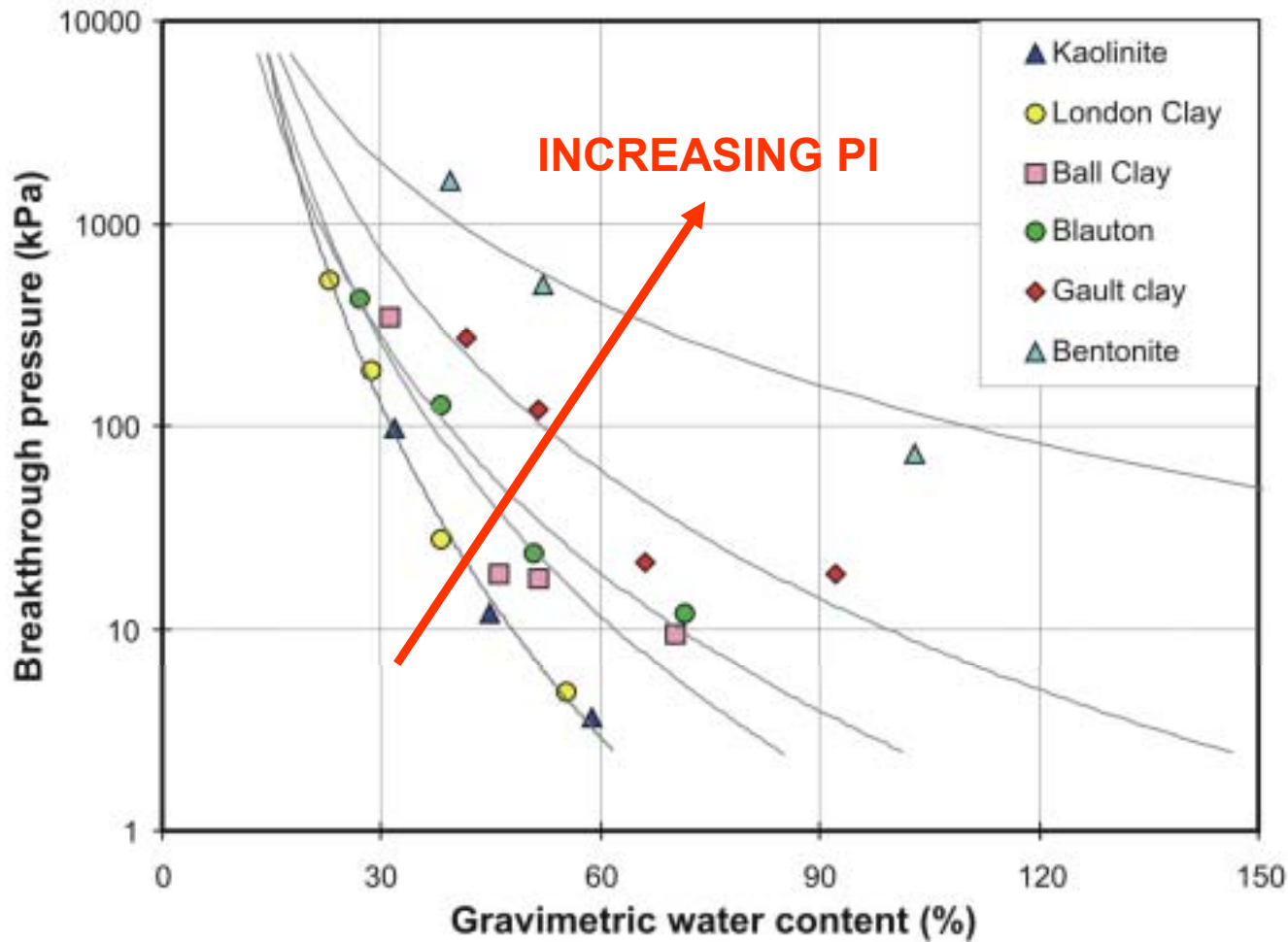
## Experimental method



1. Dried and ball milled to fine powder
2. Mixed with de-aired distilled water to preset moisture contents
3. Place in test container, avoiding air entrainment
4. Tested at constant air flow rate
5. Peak pressure determined
6. Samples sketched



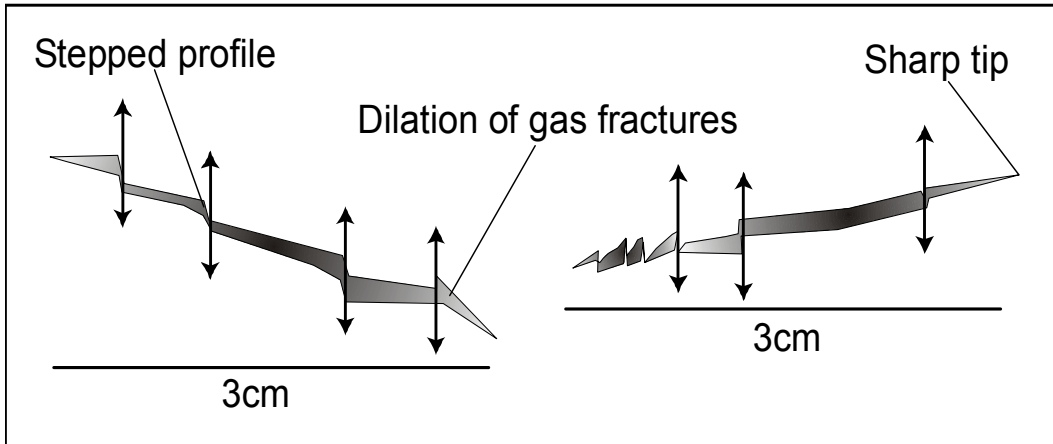
## Breakthrough pressure against water content



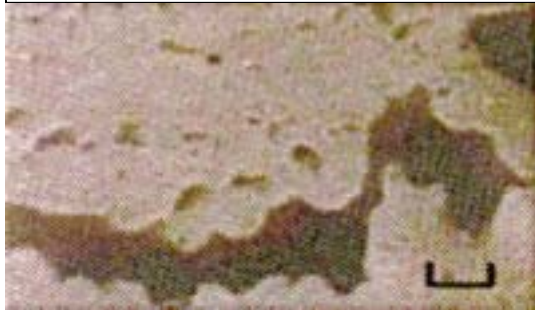
Each point is the average of 4 to 6 tests



# Typical features of samples after testing



Breakthrough pressure less than 100 kPa



Gas fracs

Breakthrough pressure more than 100 kPa



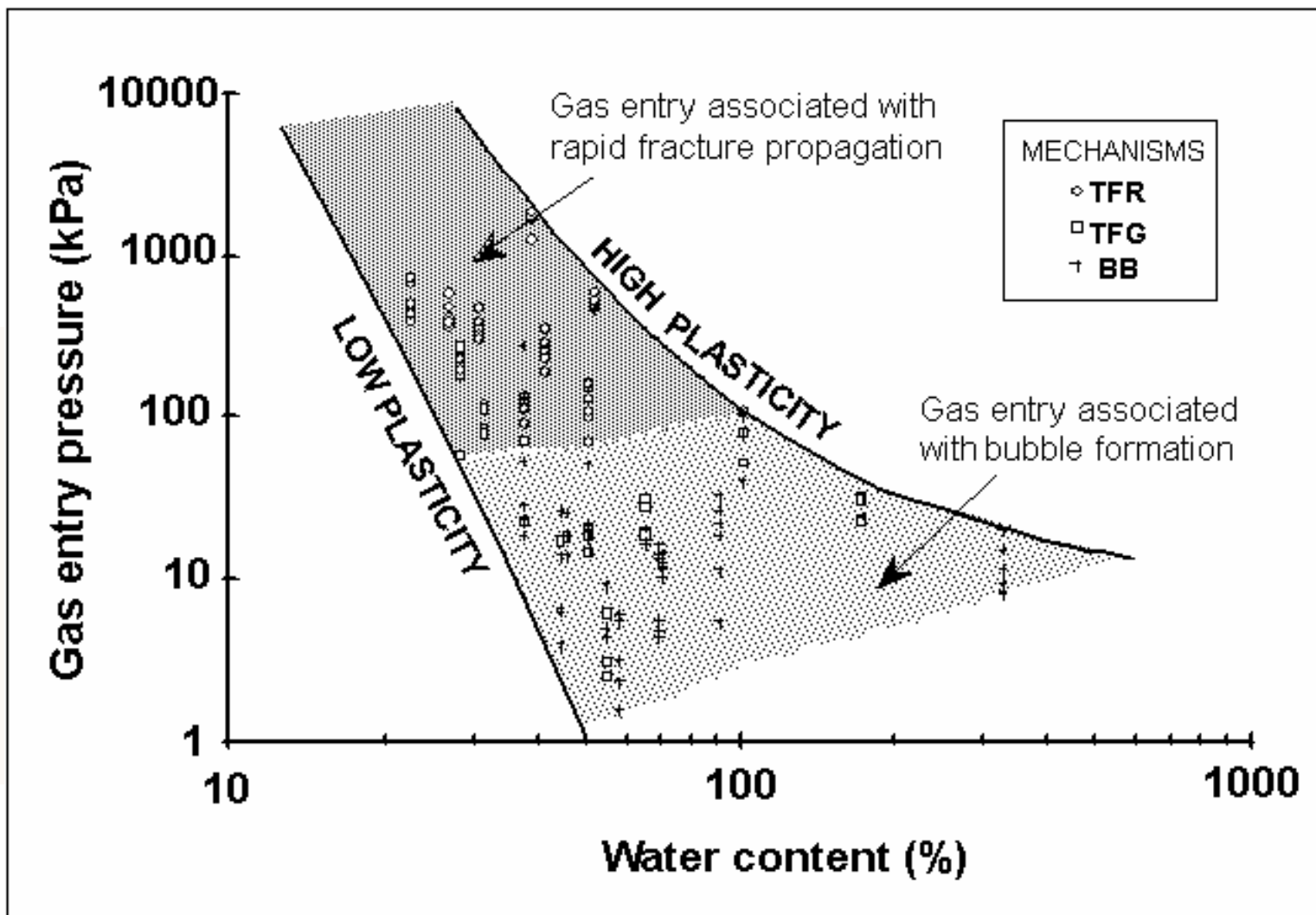
Pockmarks and gas burps







# Zonation of particle-displacing gas entry mechanisms





## Gas burps and mud volcanos



Moisture content close to Liquid Limit



Moisture content between the Liquid and Plastic Limits (USGS Photo)



## More gas bubbles in wet mud



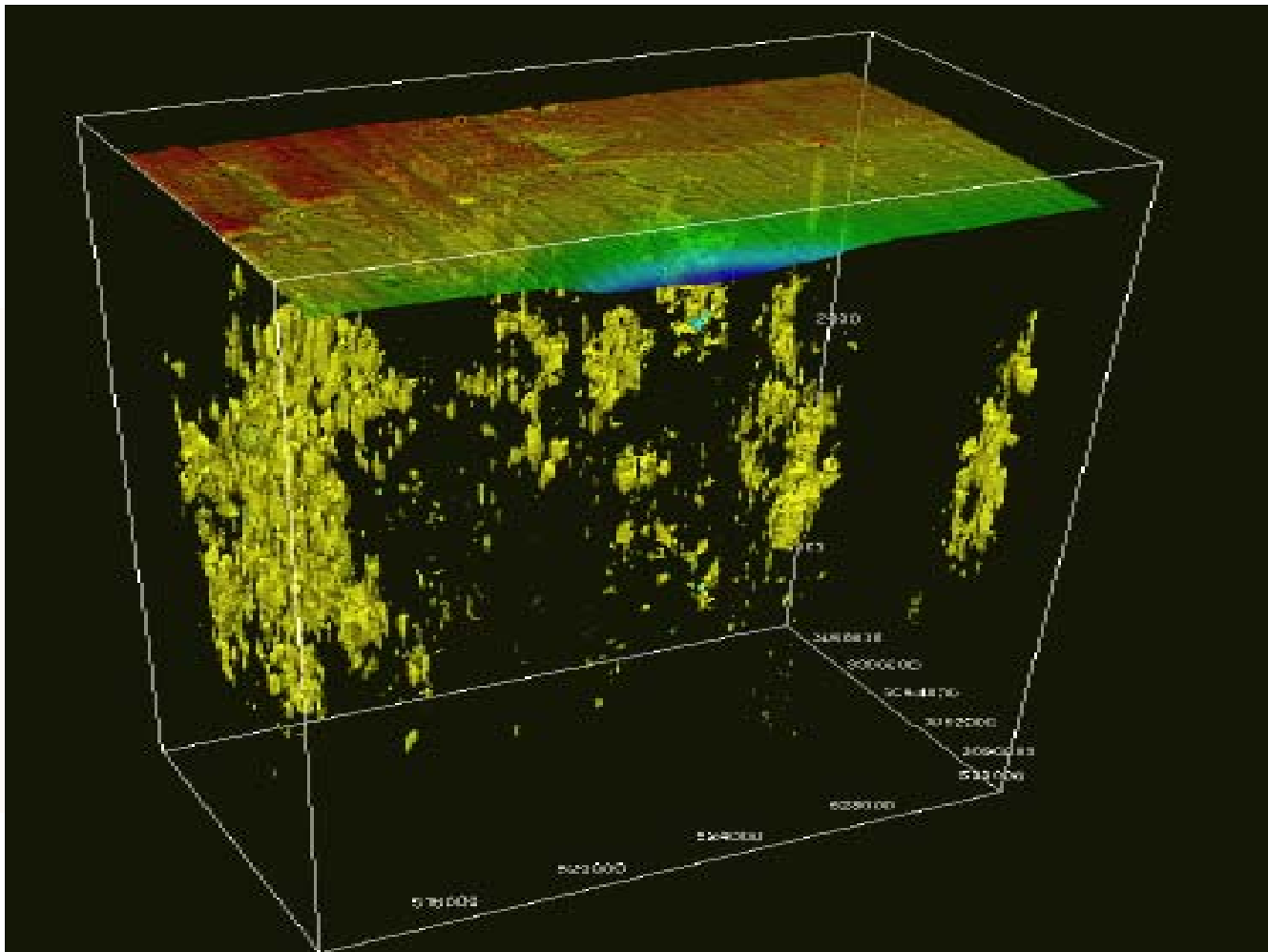


## Gas migration in offshore geological environments

- Gas chimneys above gas reservoirs
  - Sediment deformation
  - Link with fracturing and dilatancy?
  - Role of faults?
- Gas seeps and burps in soft seabed sediments
  - Pockmarks indicative of sediment deformation
  - Episodic flow?
  - Link with gas chimneys?
  - Gas hydrates?



## 3-D seismic visualisation of gas chimneys cutting through mixed sedimentary lithologies. Slow seepage and rapid venting of gas.



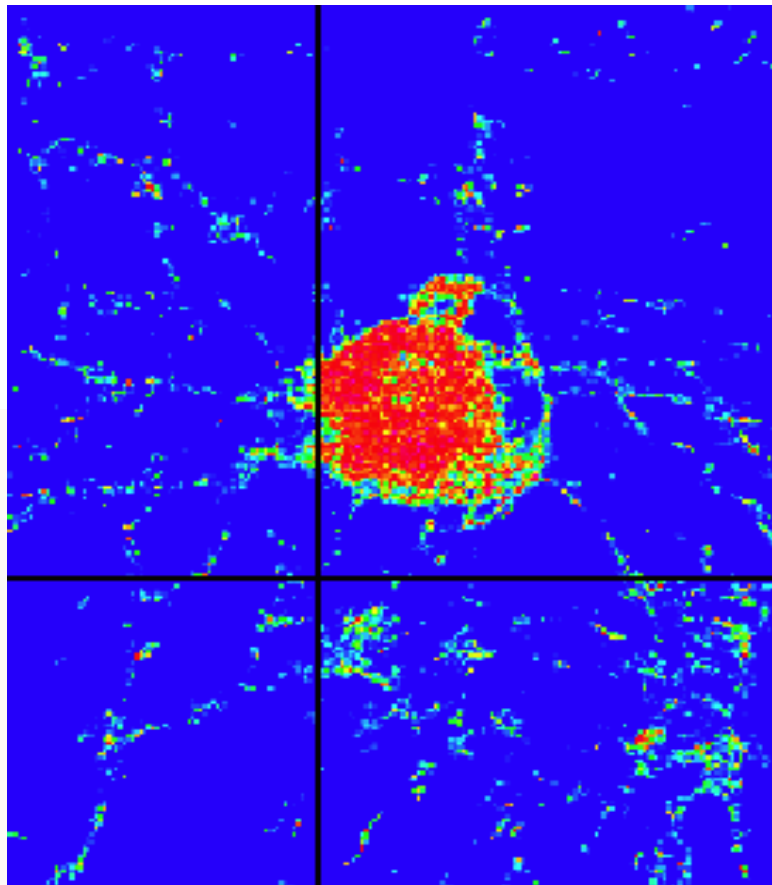
Survey techniques included: (a) high resolution seismics, side-scan sonar, 3-D seismics and direct observation of the seabed.

Identified rapid venting and slow seepage mechanisms

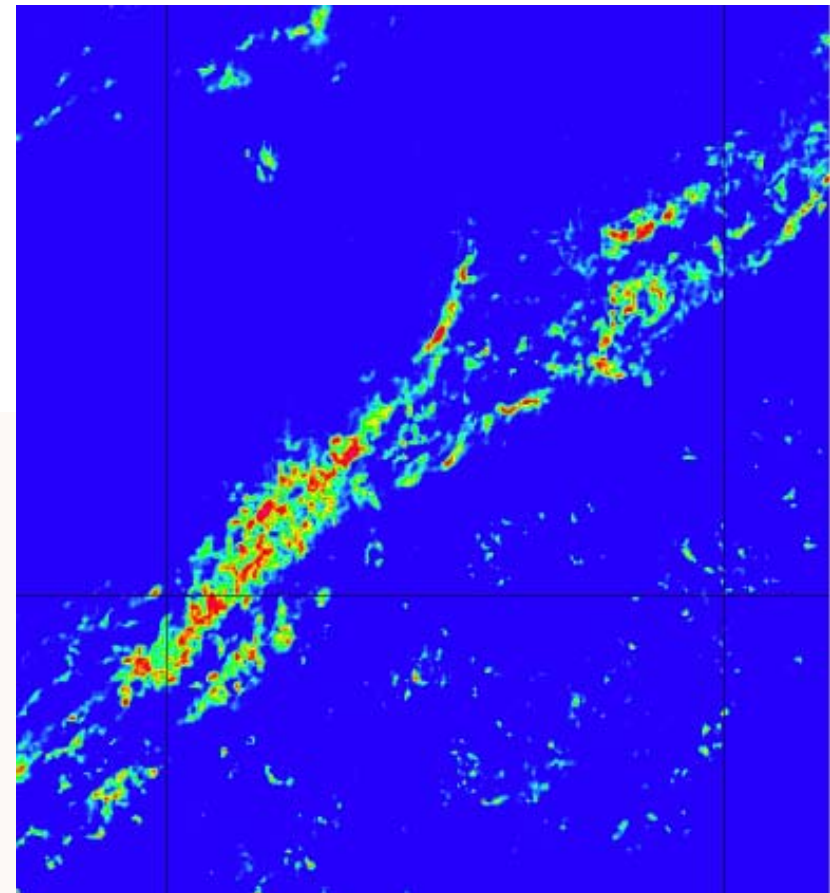
**Roberts (2001)**



## 3-D seismic visualisation of gas chimneys: horizontal slice



Equal time slice through 3-D seismic visualisation showing a cigar-shaped gas chimney with radial pattern linked to fracturing.



Equal time slice through 3-D seismic visualisation showing probable relationship between this gas chimney and faulting (off West Africa)



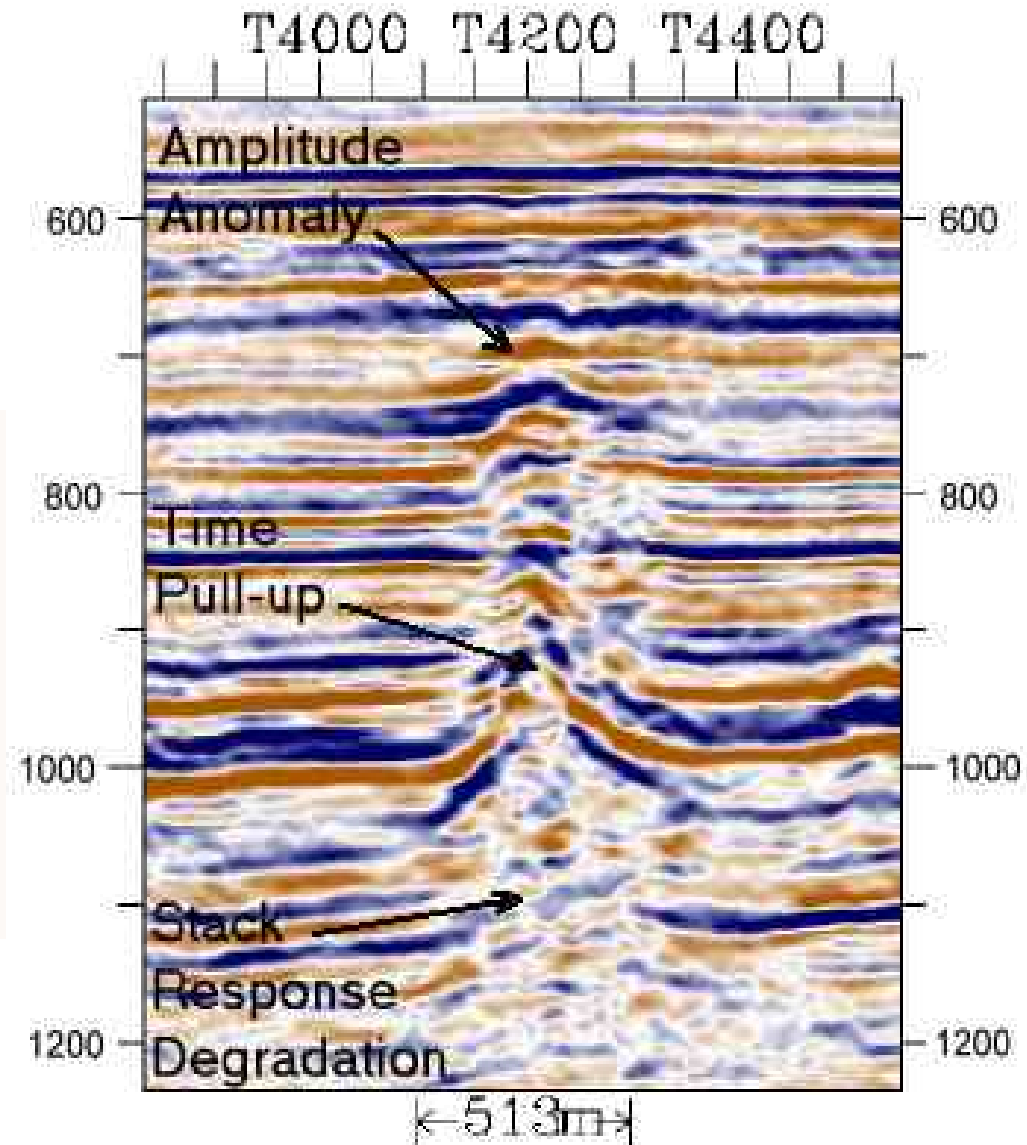
## Typical seismic signature of a gas chimney

Tahbilk gas discovery in the southern Vulcan Sub-basin, Bonaparte Basin, Australia.

What is the gas migration mechanism?

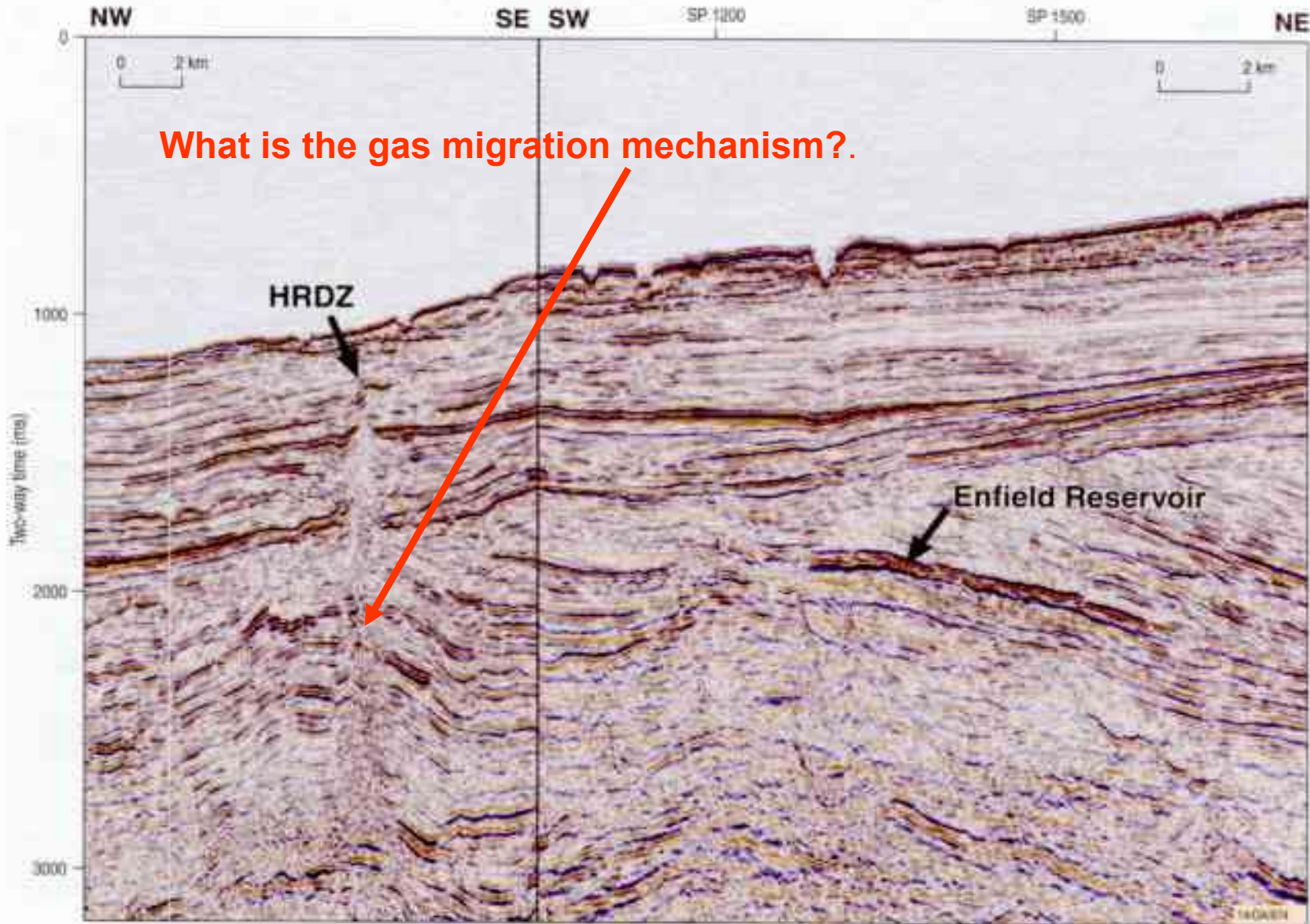
Note: 1000 milliseconds two-way travel time is around 1000 m depth for these rocks.

Cowley and O'Brien (2003)





## Gas chimney: Carnarvon Basin, Australia



HRDZ

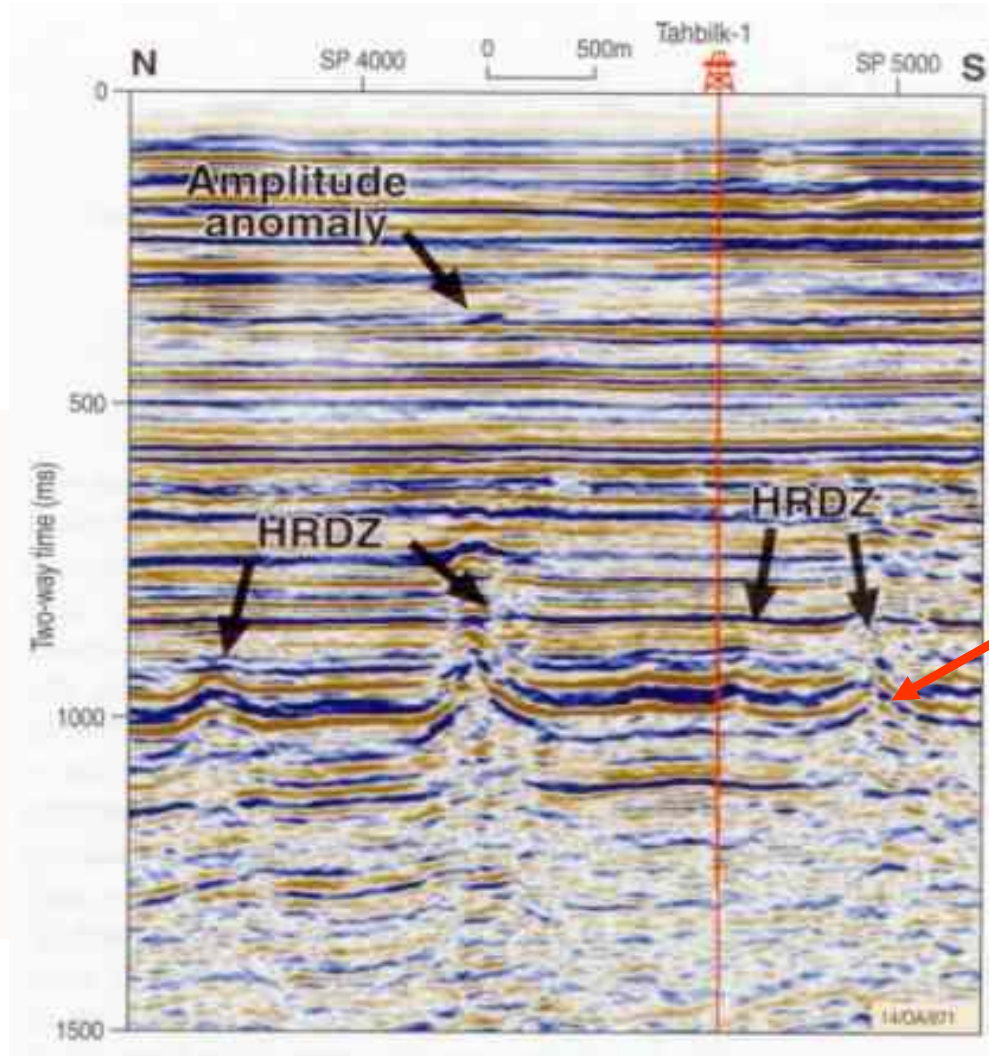
Hydrocarbon-related diagenesis zone

Schlumberger  
Geco-Prakla  
(2003)





## Gas chimneys: Tahbilk gas accumulation, Australia

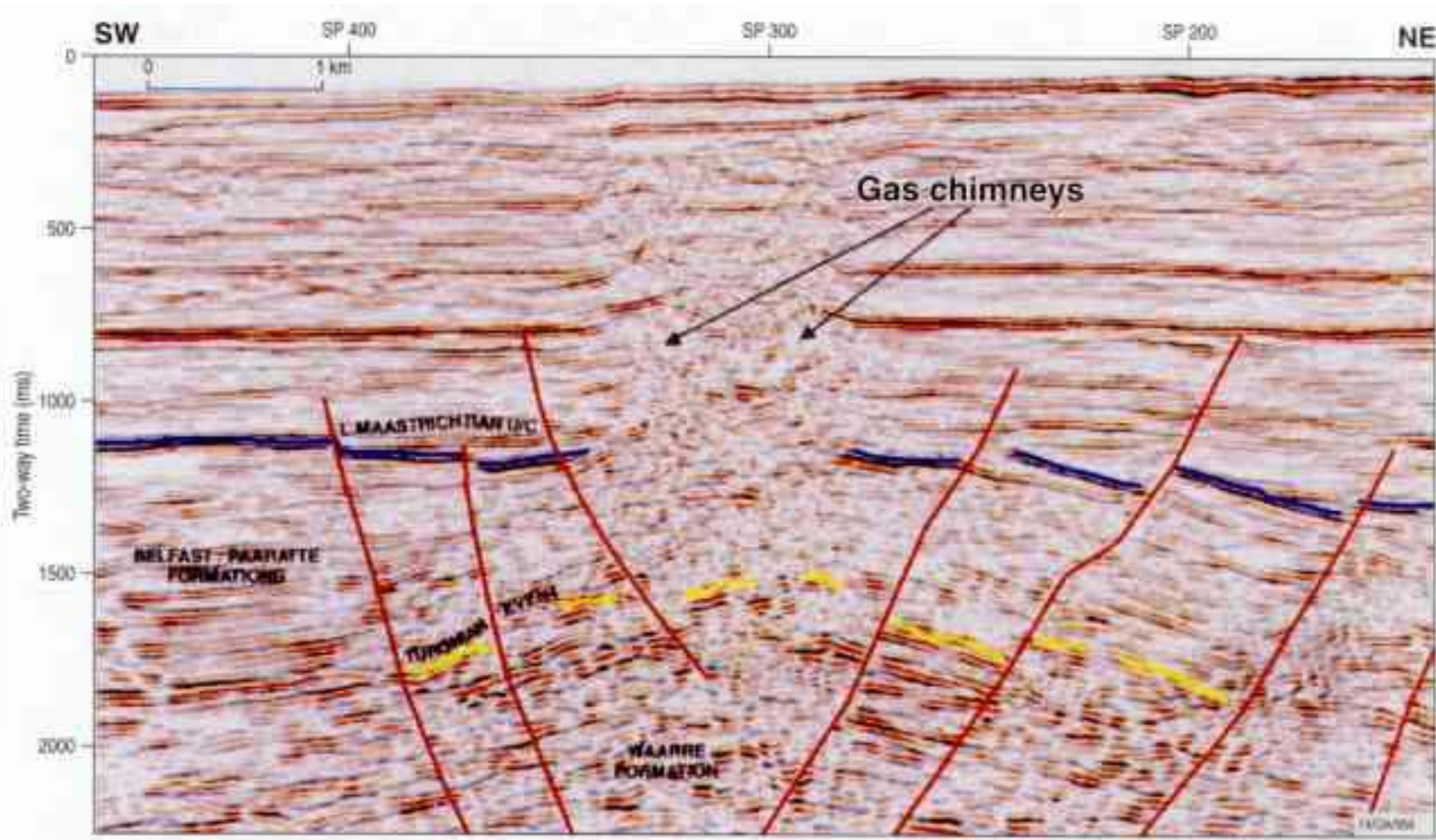


What is the gas migration mechanism?

Cowley and O'Brien (2003)



## Gas chimney: Otway Basin, south-eastern Australia





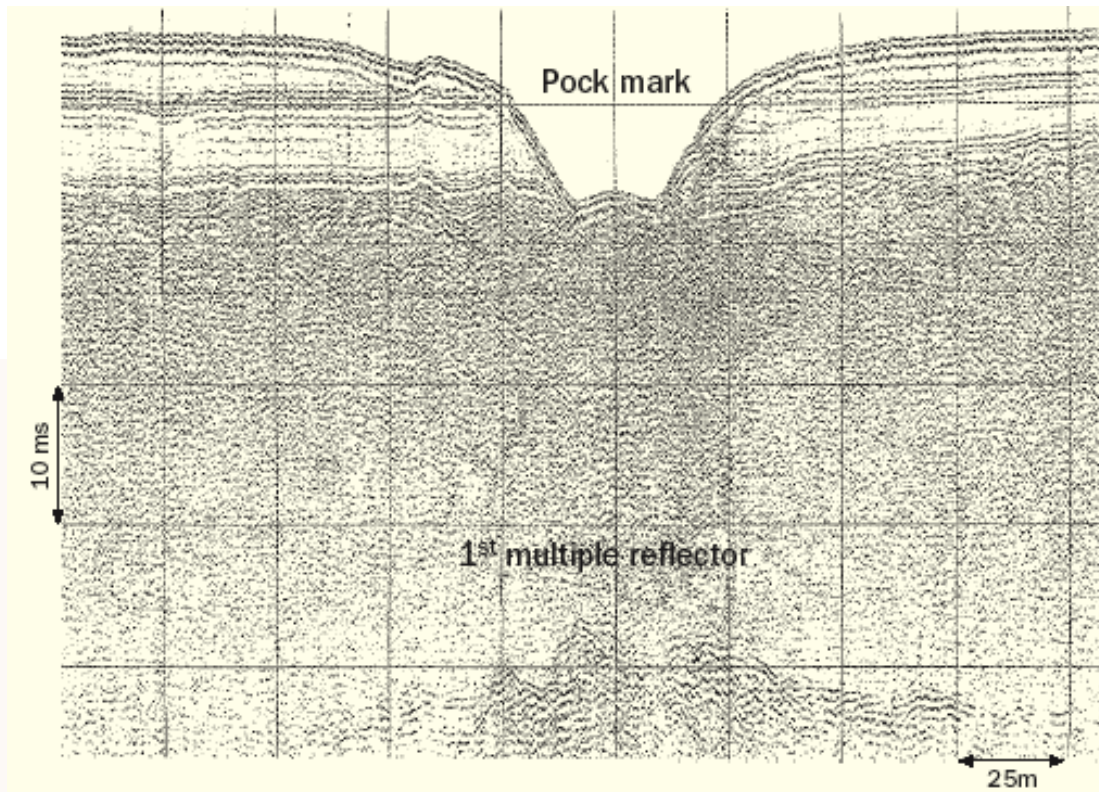
## Seabed pockmarks

- Ubiquitous on the shallow continental shelf
- Mostly caused by rapid passage of gas through soft sediment.
- Very large methane fluxes measured.
- Few metres to many hundreds of metres in diameter.
- Fine-grained sediment ruptured, deformed and ejected into sea.
- May form linear “strings” over deep-seated faults.

**What do they tell us about gas flow in deformable sediments?**

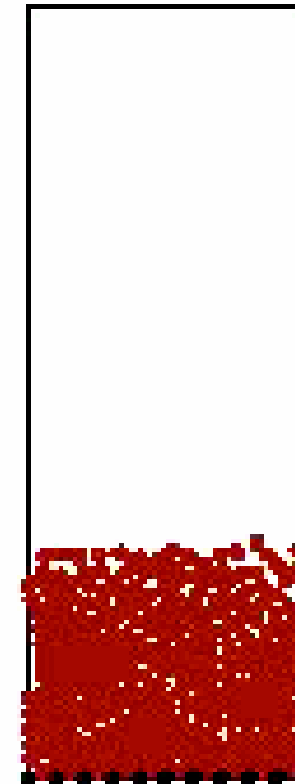


## Pockmarks in shallow, fine-grained seabed sediments



Boomer survey of a pockmark in seabed sediments in the northern North Sea.

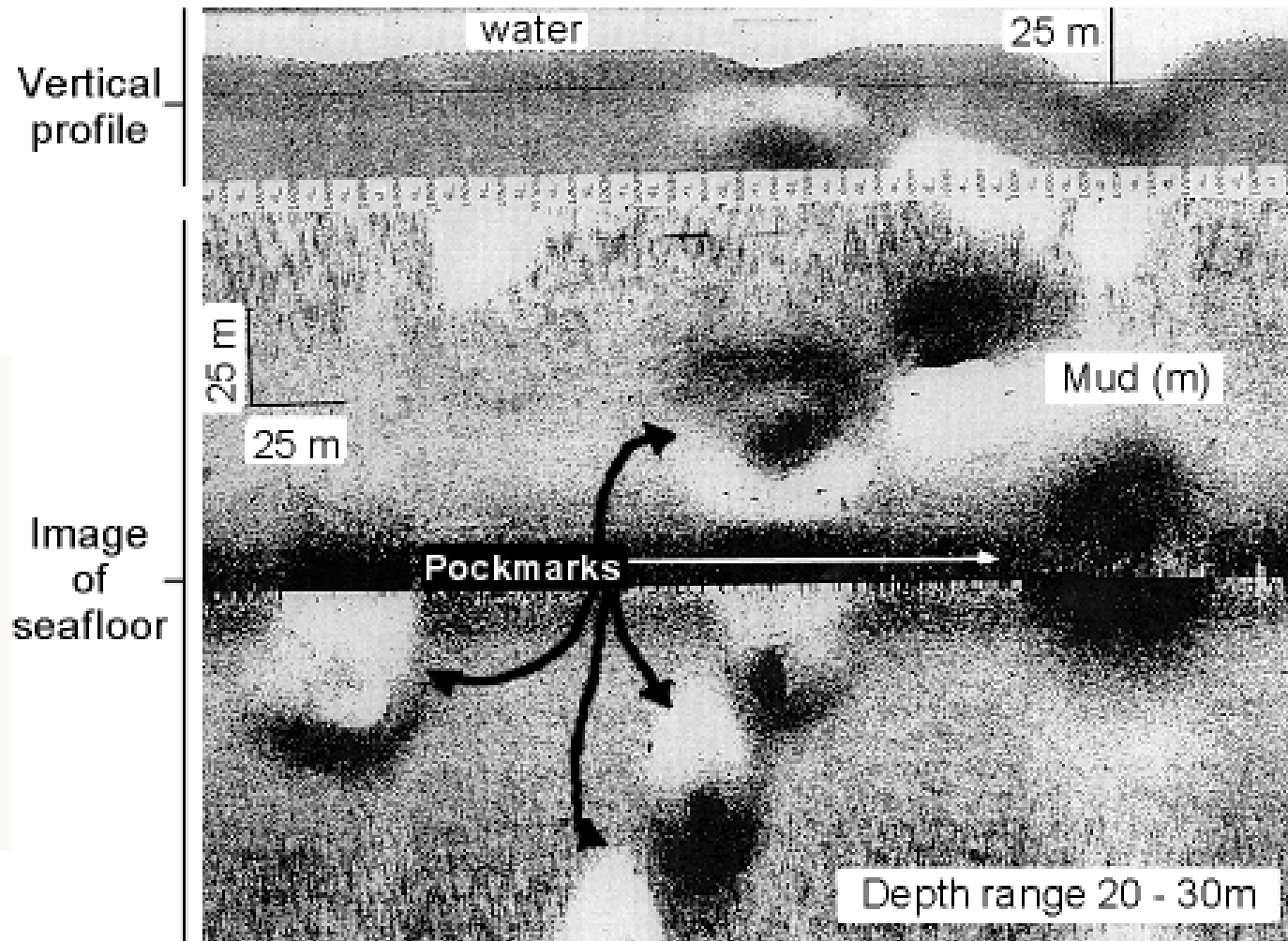
(TNO, 2000)



Kyoto University, 2003

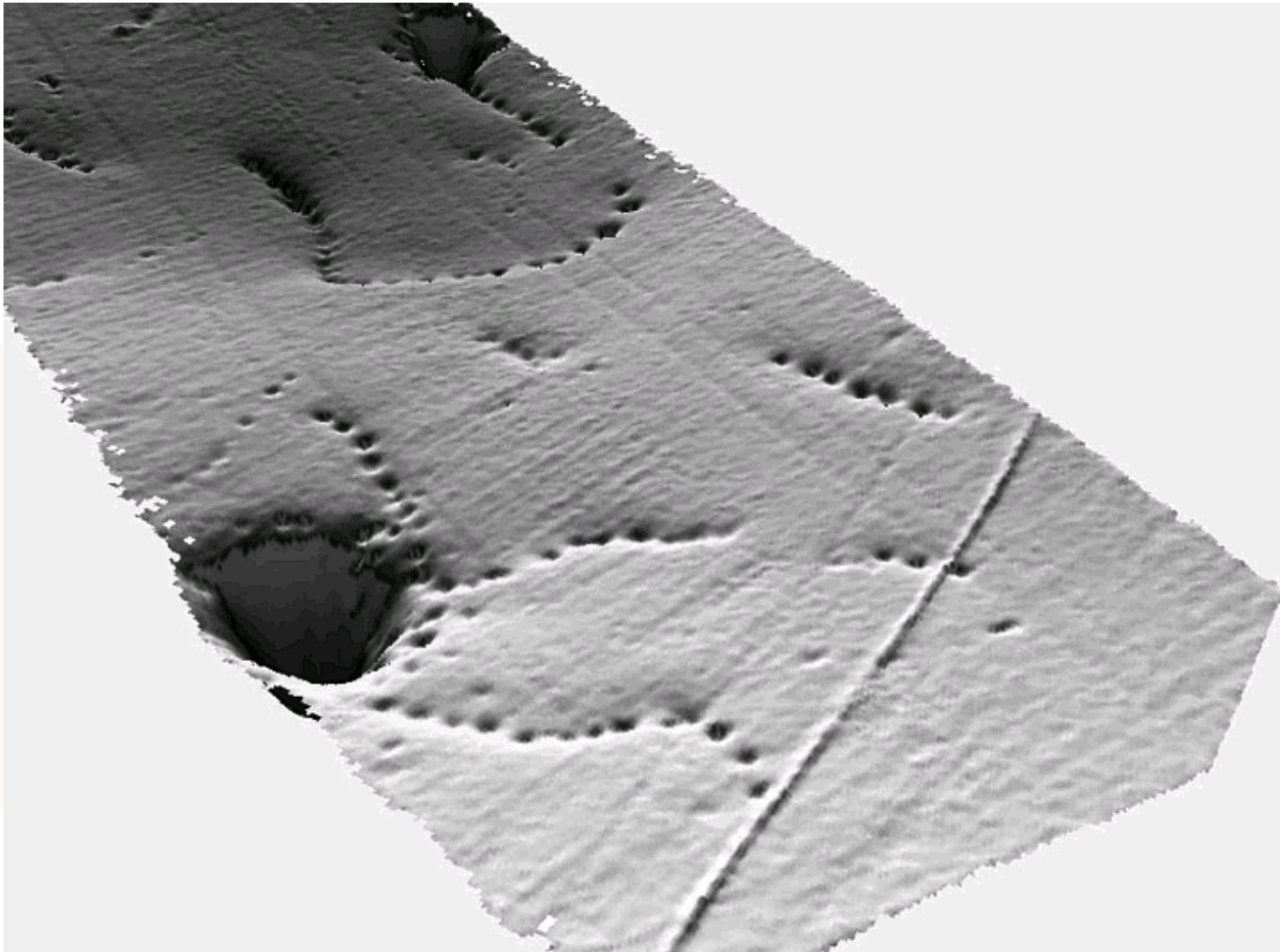


## Pockmarks in muddy seabed sediments - profile and plan



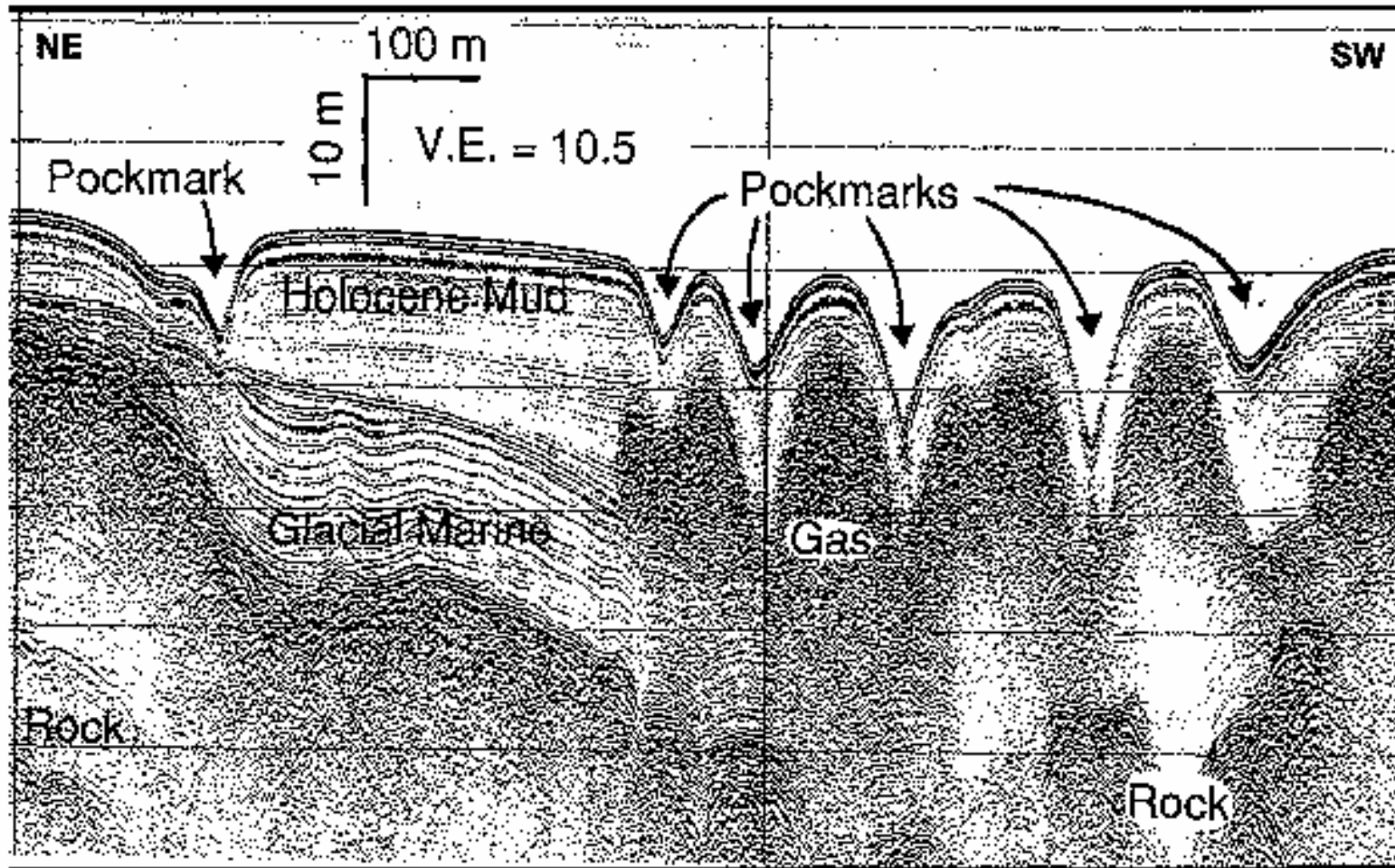


## Pockmarks adjacent to the route of a seabed gas pipeline





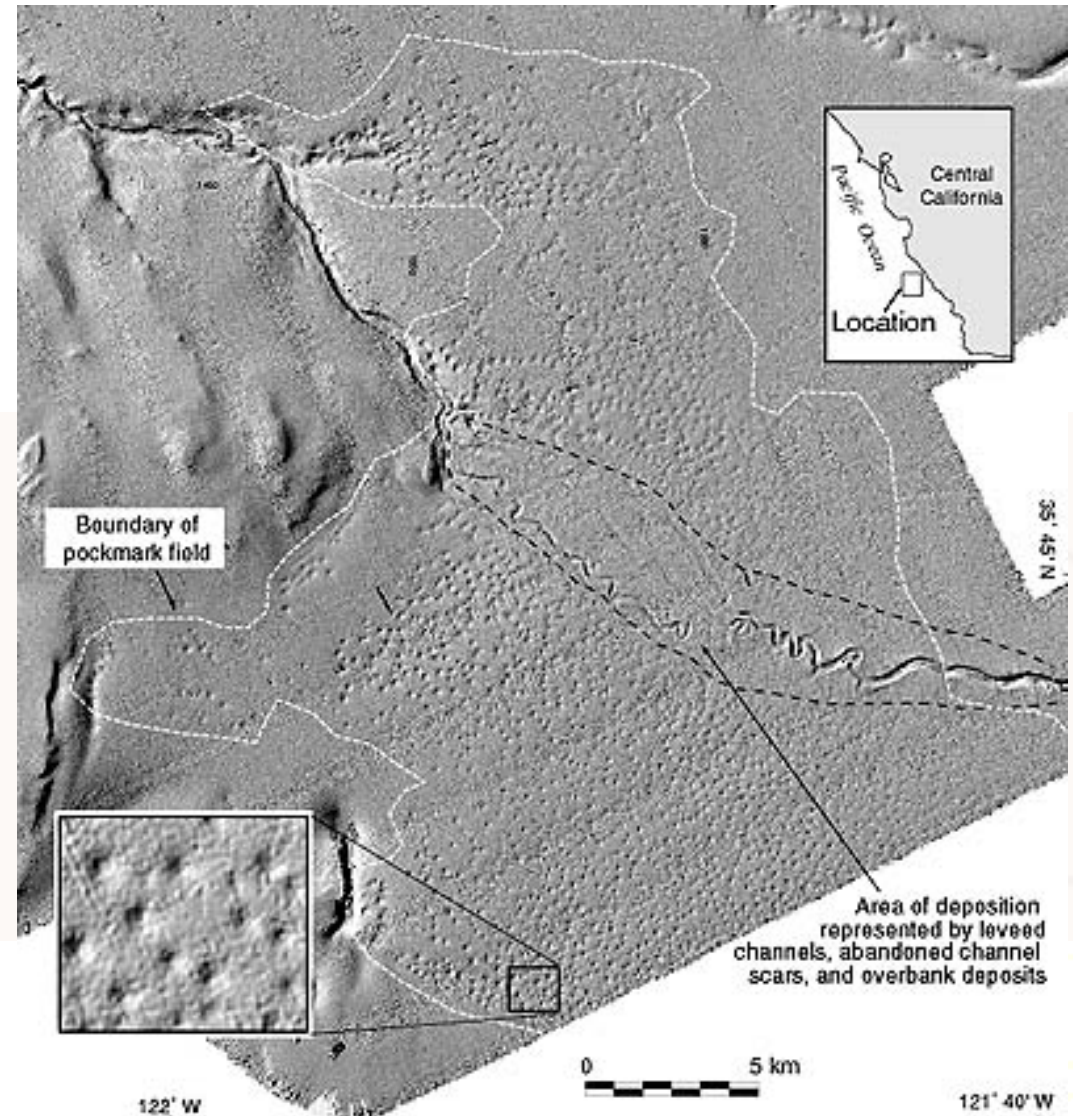
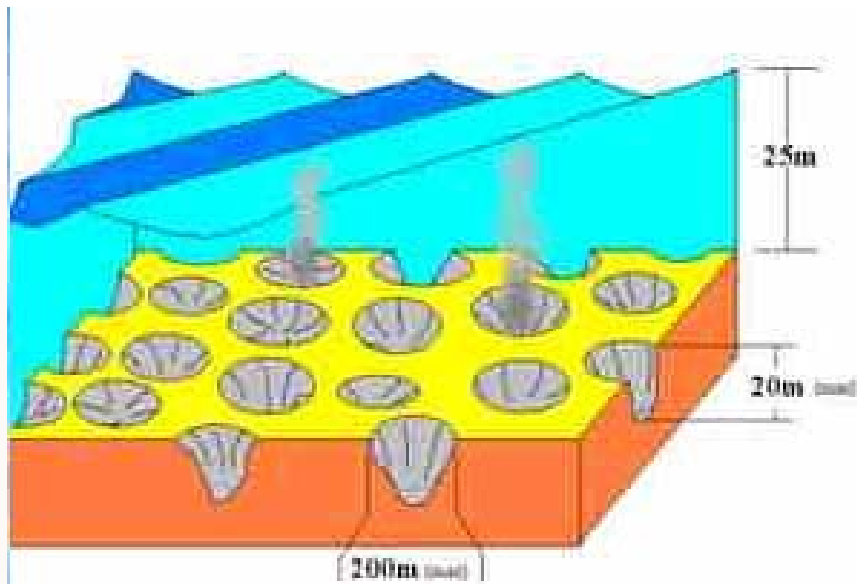
## Seismic reflection profile of pockmarks (Belfast Bay, Maine)



Kelley (1994)



## Pockmark field off the coast of California

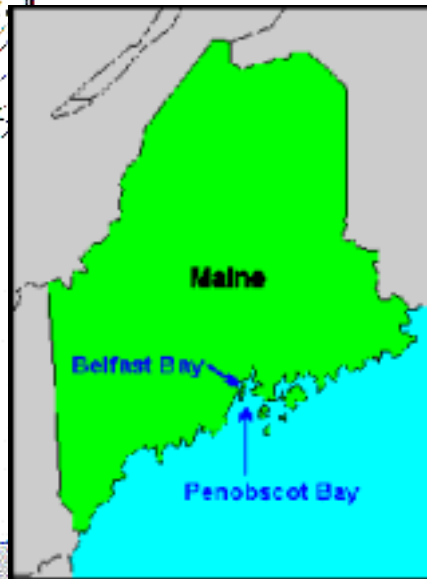
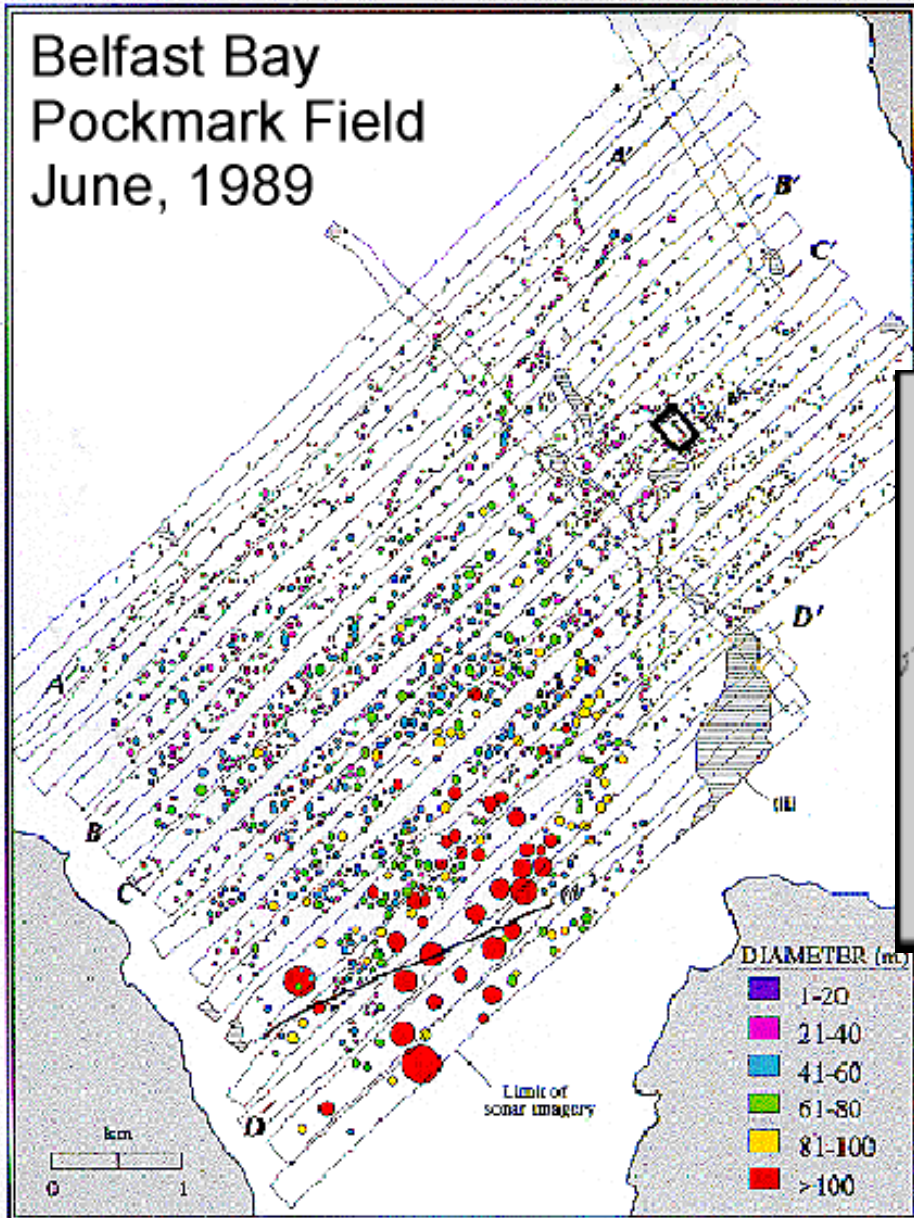






## Extensive pockmark field off the coast of Maine

Belfast Bay  
Pockmark Field  
June, 1989

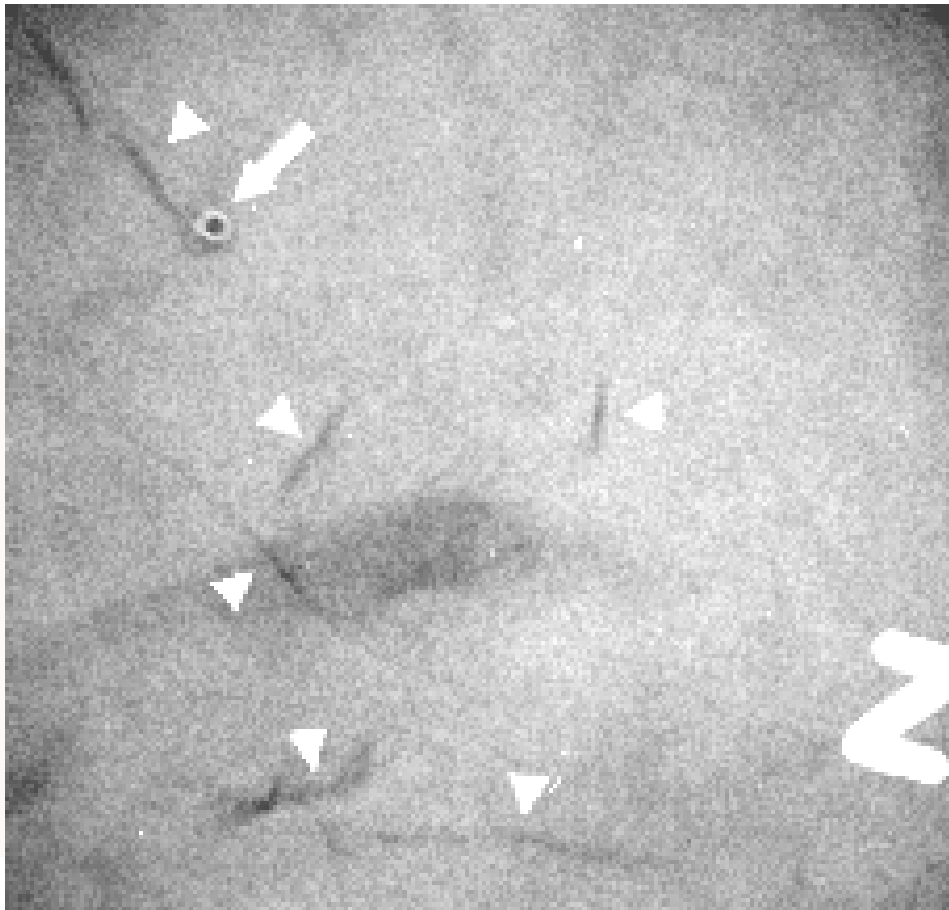


Maine Geological Survey





## Mechanical response of sediment to bubble growth: LEFM Approach, Dept. Oceanography, Dalhousie University, Nova Scotia



X-ray image of discoidal gas bubbles in a simulated marine sediment



Ellipsoidal (discoidal) bubble in gelatine

When does a bubble become a fracture?



## Study of inflammable gas emissions in the Hanford Waste Tanks

- Intermittent discharge of gas from tanks containing settled waste sludges.
- Most conspicuous in tanks containing clay-like waste.
- Bentonite/water used to simulate behaviour in laboratory.
- These are “wet” sludges, but the trends are very interesting.

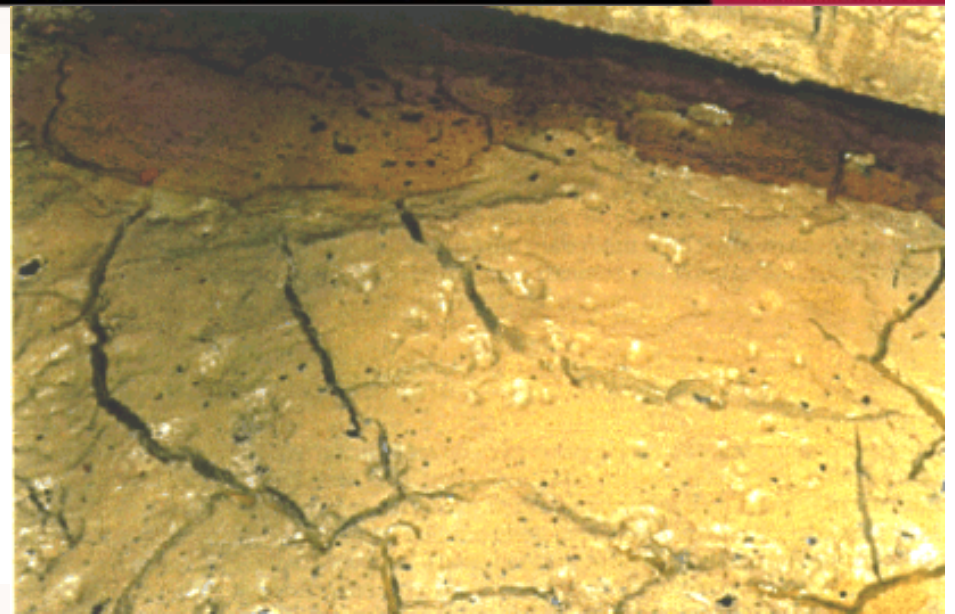
### References:

Stewart, P.A. et al. (1996). Gas retention and release behavior in Hanford single-shell waste tanks. Rept. No. PNNL-11391, UC-2030 , Pacific Northwest National Laboratory, Richland, Washington.

Gauglitz P.A et al. (1996). Mechanisms of Gas Bubble Retention and Release: Results for Hanford Waste Tanks 241-S-102 and 241-SY-103 and Single-Shell Tank Simulants.. Rept. No. PNNL-11298, Pacific Northwest National Laboratory, Richland, Washington.



Large gas vent of fumarole (arrow) in Tank SY-101



Pockmarks formed by gas upwelling in Tank T-104

Another gas vent  
in Tank SY-101



## Hanford Waste Tanks



## General observations on the Hanford sludges

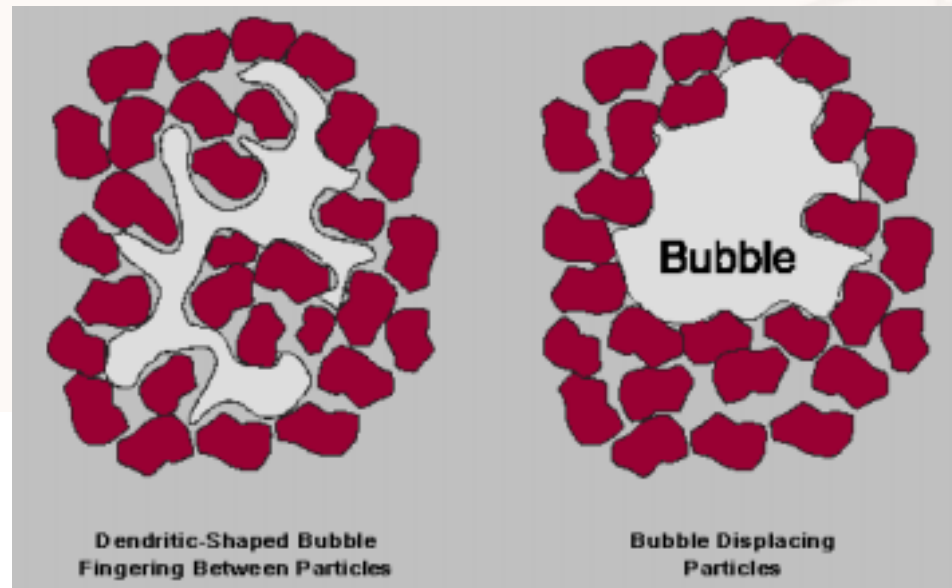
1. Particle-displacing bubbles occur most often in waste layers that are under little stress or have low yield strength and small pore size.
2. The particle-displacing bubbles were called **hydrostatic** if they had not merged into networks, **hydro-dendritic** if they had.
3. Bubbles that are confined to the pore volume often appeared in deep layers of waste or in waste that has large pores and high yield strength. These bubbles, which displace only the interstitial liquid, existed as pore-filling networks and were referred to as **litho-dendritic** bubbles.
4. The maximum gas retention due to pore-filling bubbles is limited by the porosity; the upper limit on gas retention by particle-displacing bubbles is higher, because porosity is not relevant for this bubble type.



## Proposed mechanisms of gas retention in Hanford sludges

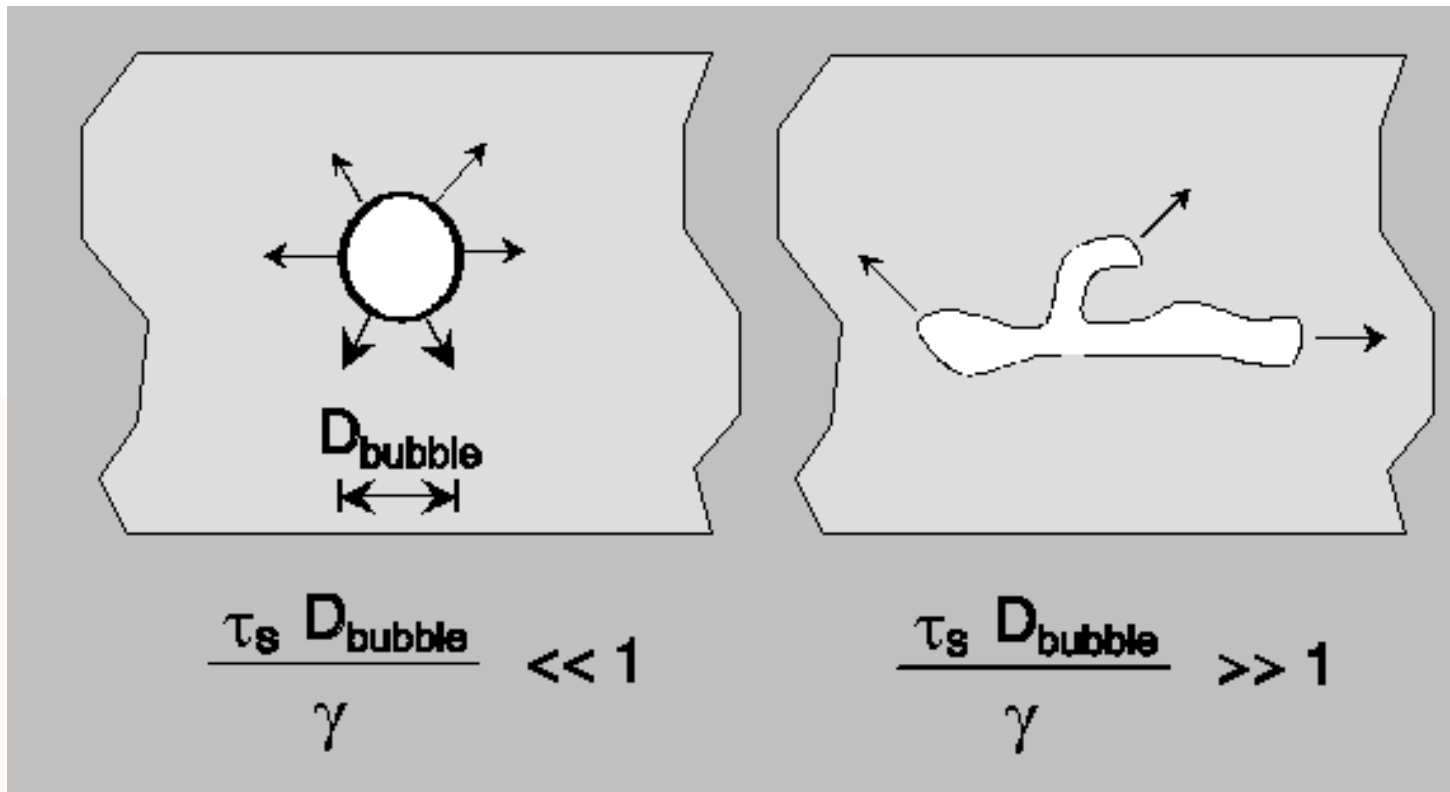
1. Pore-filling gas bubbles (coarse-grained sludges and/or deep)
2. Particle displacing gas bubbles (fine-grained sludges and/or shallow)
  - a) Spherical in sludges with low shear strength
  - b) Dendritic in sludges with higher shear strength

Particle displacing  
mechanism





## The particle-displacing mechanism



For example, the largest spherical bubbles observed in a clay with a yield strength of 67 Pa had a diameter less than about 2 mm.

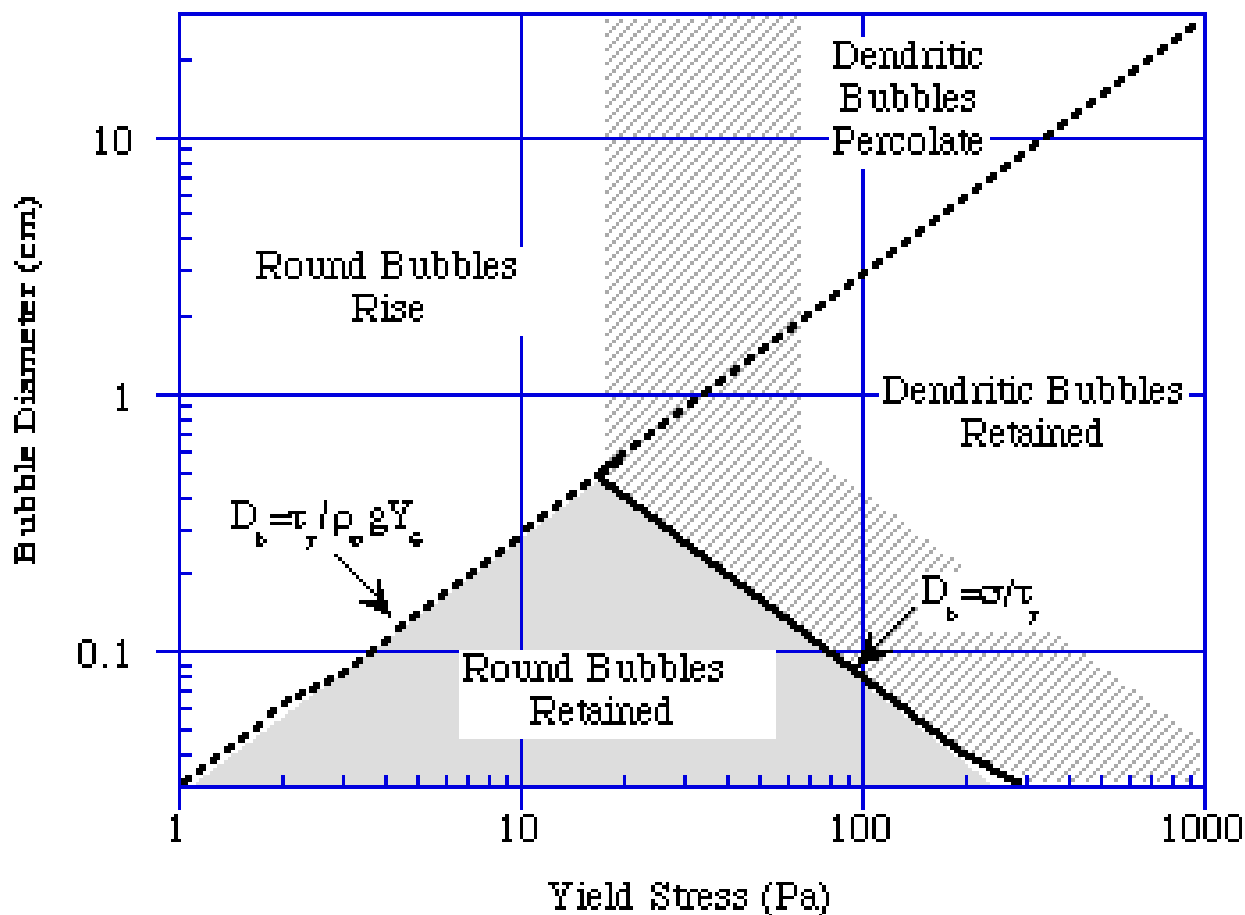
$\tau_s$  = shear strength,  $D_{bubble}$  = diameter of bubble,  $\gamma$  = surface tension coefficient

Spherical bubble forms can be separated from dendritic forms by a dimensionless ratio.

(Gauglitz P.A. et al., 1996).



## Retention of particle-displacing bubbles in the sludge



Considers buoyancy but ignore “pressure drive”

Bingham-type plasticity assumed.

(Gauglitz P.A. et al., 1996)



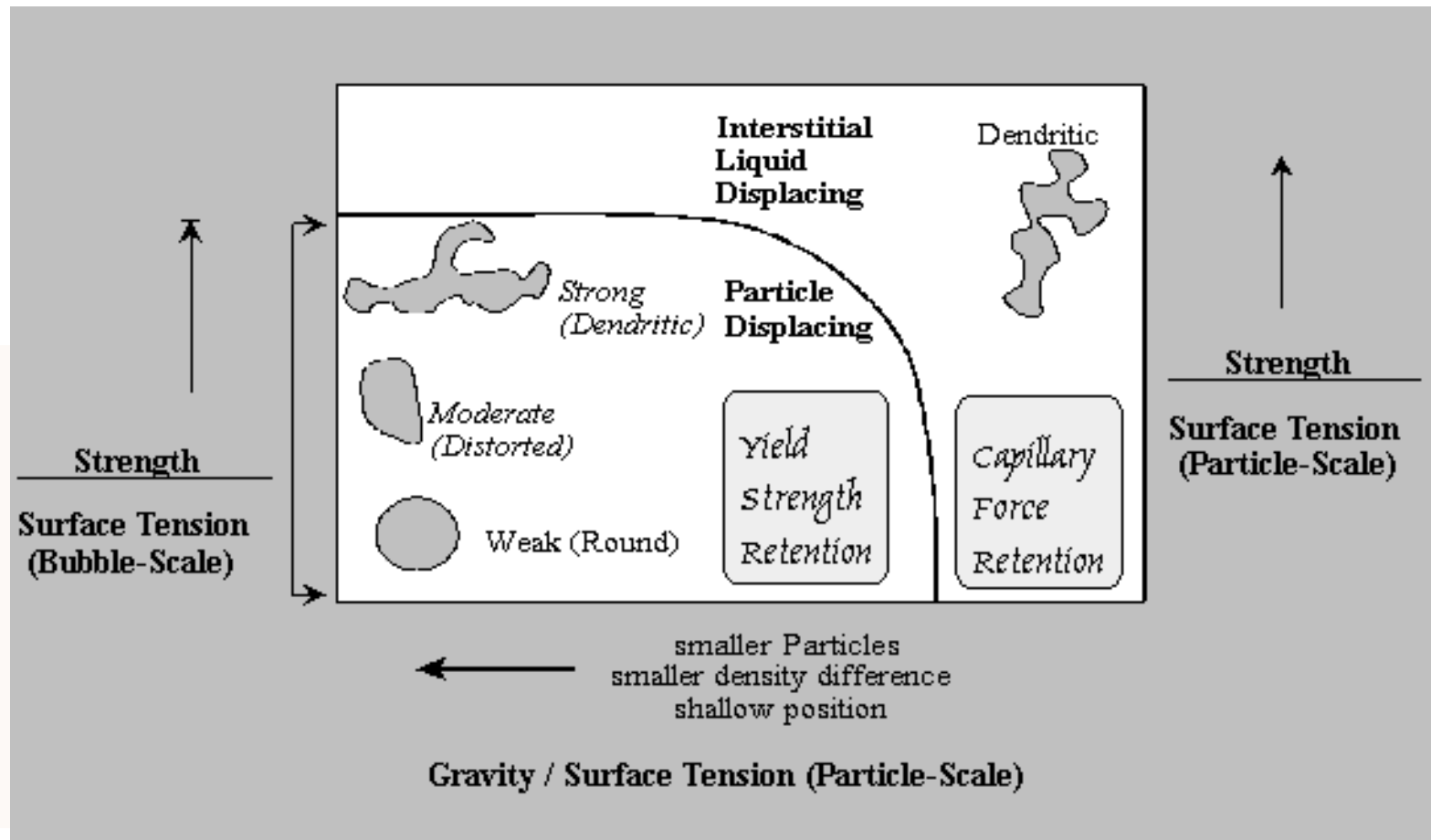


## Dynamics of hydro-dendritic bubble percolation

- Gas release occurs when a hydro-dendritic bubble propagates through to the waste surface and gas percolates through it.
- Gauglitz et al. (1996) performed experiments which clearly demonstrated gas percolation through a network of hydro-dendritic bubbles in the stronger clays.
- Bubbles in one region of the clay column become dendritic as they expand, then contract as they reach the percolation threshold and discharge part of their gas into a higher region which in turn expands and eventually discharges.
- The column grows by this process until it becomes quasi-stationary and releases gas nearly continuously but at varying rates.
- A hydro-dendritic percolation release could leave some marks of its occurrence on the waste surface. Entrained slurry brought to the surface repeatedly through the same vent could produce mud cones, such as those visible in Tank SY-101.



## Gas retention mechanism map for Hanford sludges



(Gauglitz P.A. et al., 1996)



# Gas retention mechanism map (Gauglitz P.A. et al., 1996).

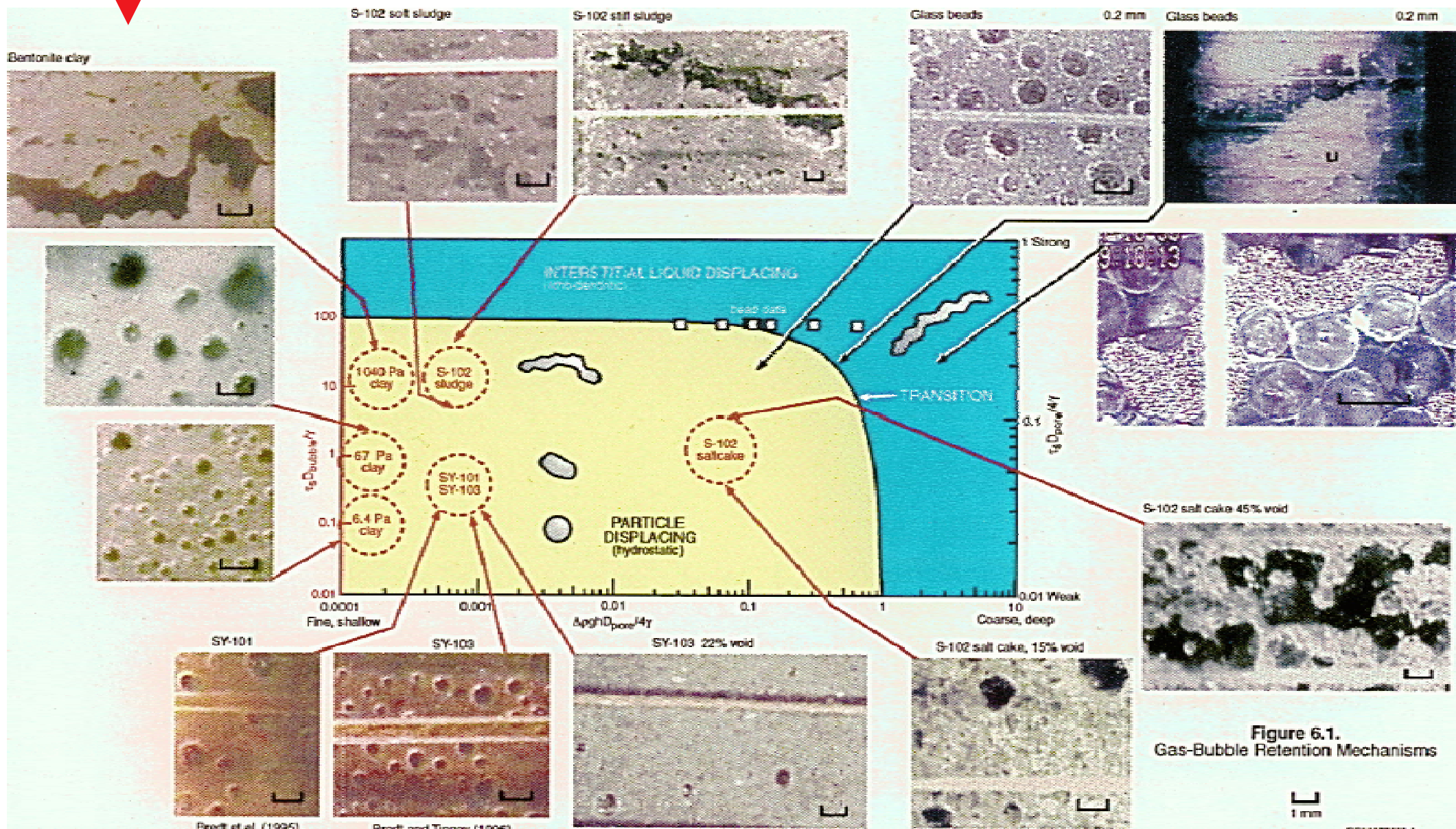


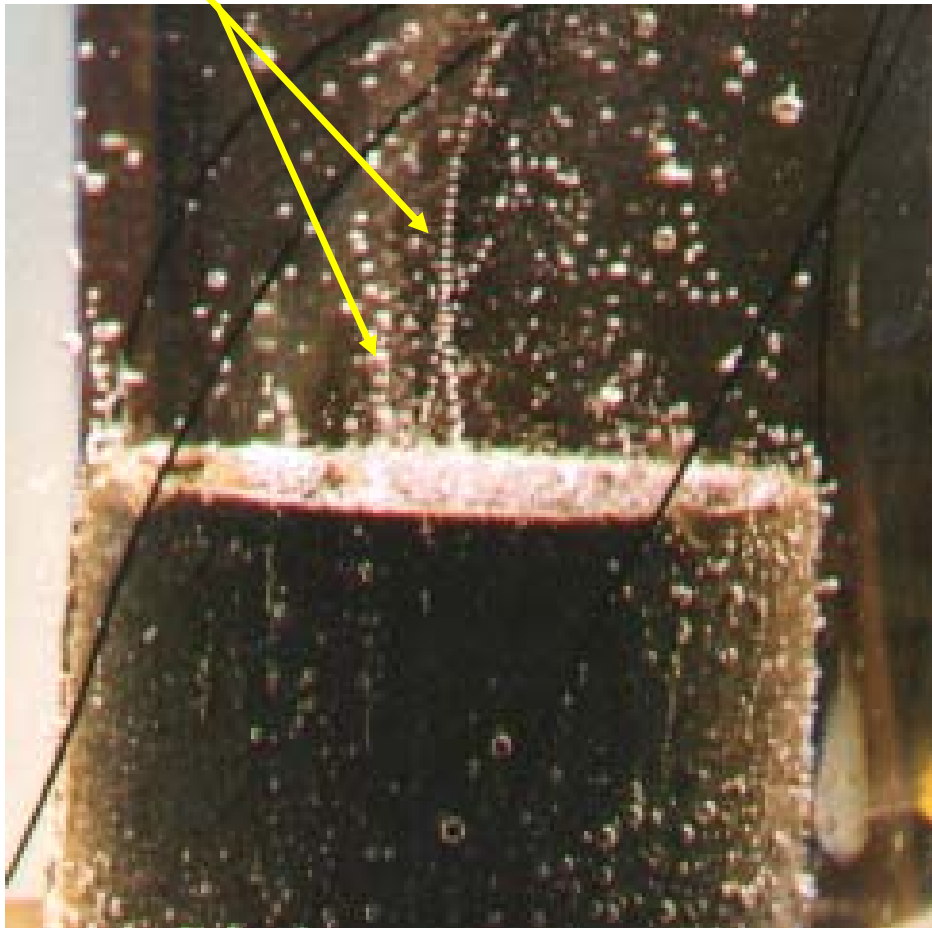
Figure 6.1. Gas-Bubble Retention Mechanisms

1 mm

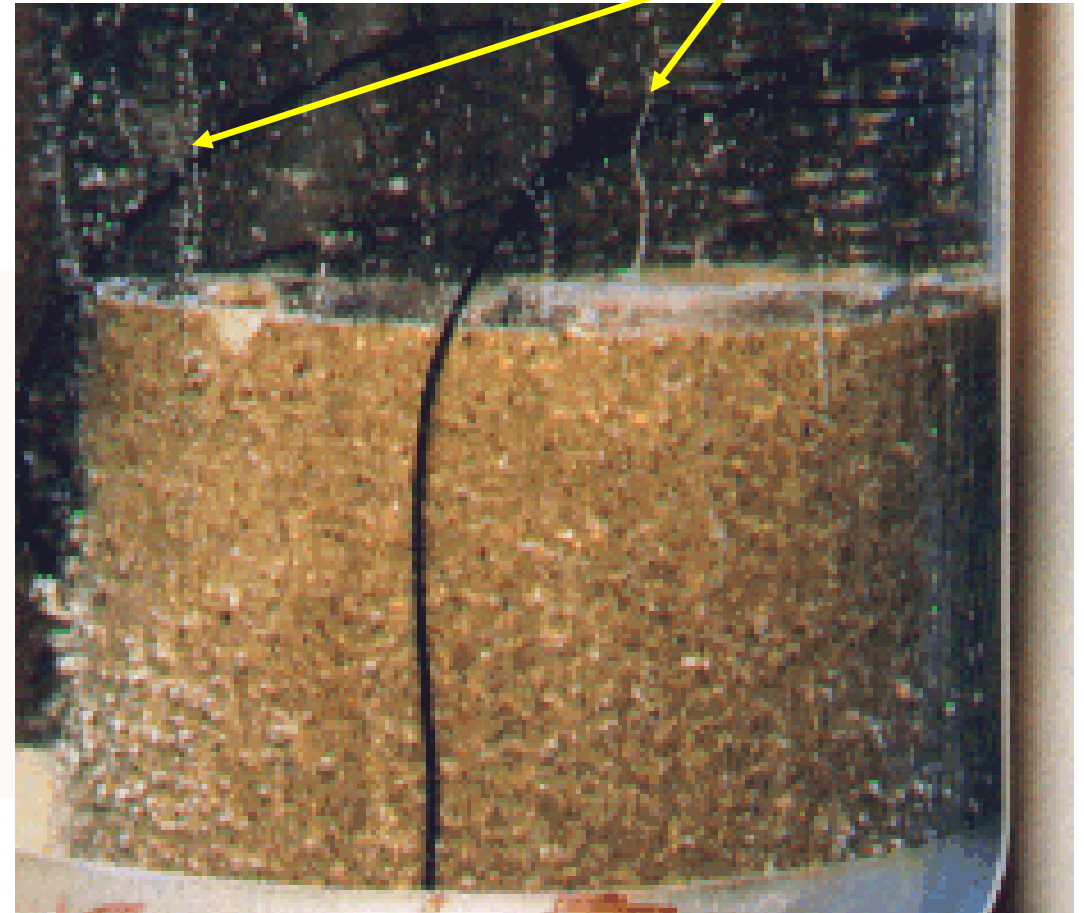


## Bentonite specimens after gas testing (immersion and warming in glycerol)

Bubble streams



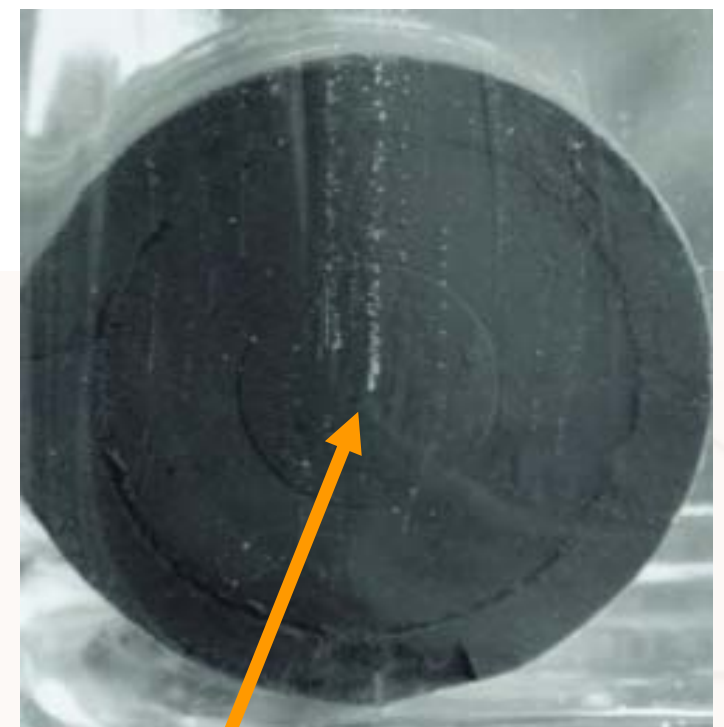
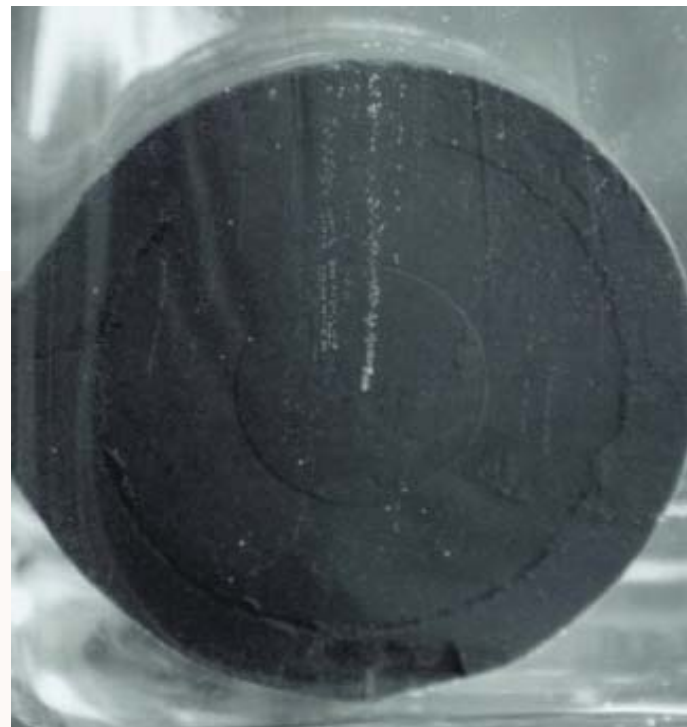
Bubble streams





## Opalinus Clay specimens after gas testing (immersion and warming in liquid paraffin)

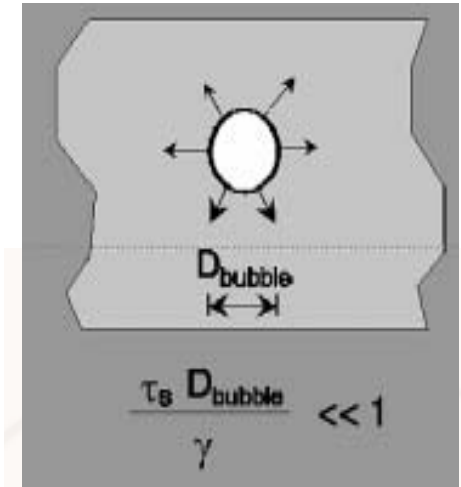
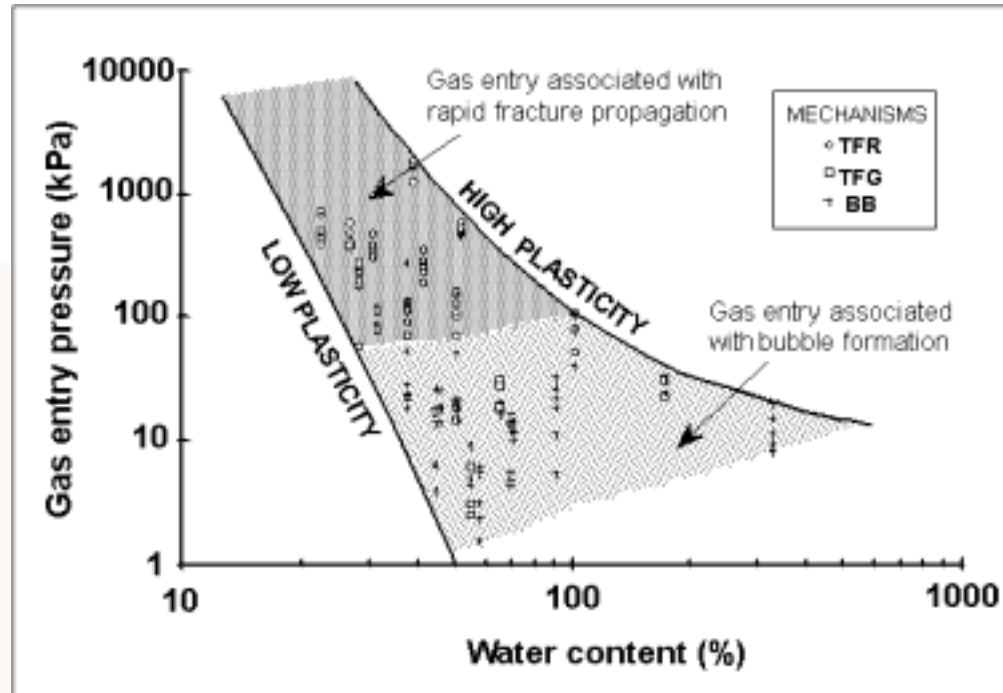
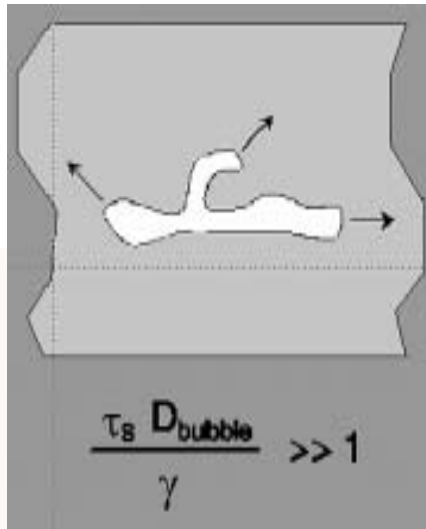
**Filter arrangement**



**Gas trapped in the rock during testing can be seen emerging from the rock, predominantly in the region of the injection filter.**



# Concluding comments



# Early large scale experiments on gas breakthrough pressures in clay-based materials

Harald Hökmark, Clay Technology AB, Lund Sweden

Based on SKB work performed in 1986, reported in:

Pusch R., Hökmark H., 1987. Megapermeameter study of gas transport through SFR storage buffers.

# Objectives of the Megapermometer test

- To determine the critical gas pressure by repeated pressurization of a large sample
- To test the hypothesis that gas phase penetration through water-saturated bentonite takes place when the gas pressure is the sum of the critical gas pressure and the water pressure

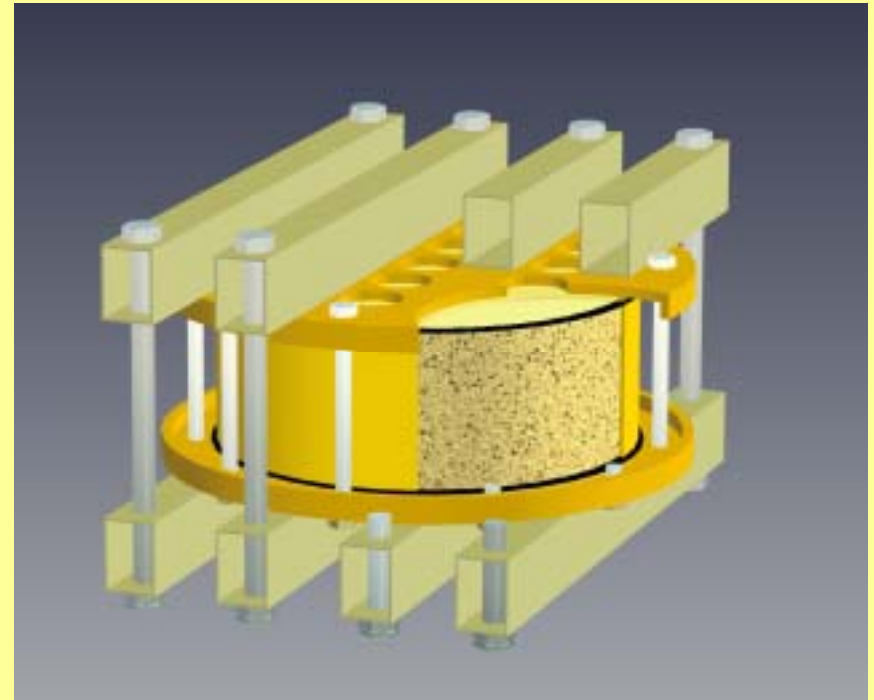




# Experimental principle

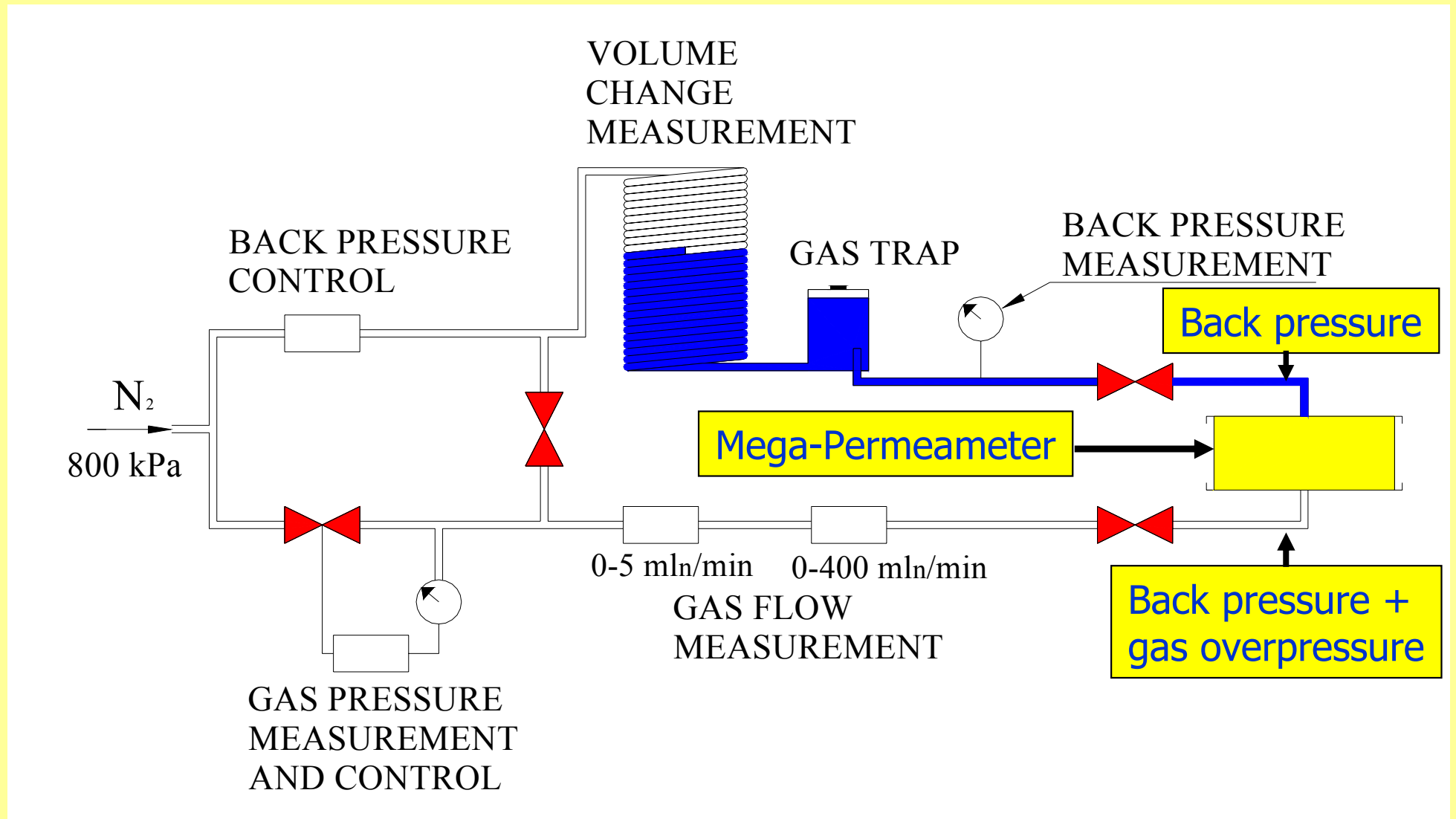
- Apply back pressure to top (water) and to bottom (gas)
- While keeping the water back pressure constant, increase gas pressure at the bottom in steps, with sufficient time between steps to allow for transients to disappear, and record gas inflow and gas/water outflow.
- After gas break-through: reset, allow for "rest" and repeat with same or new back-pressure

Back pressure

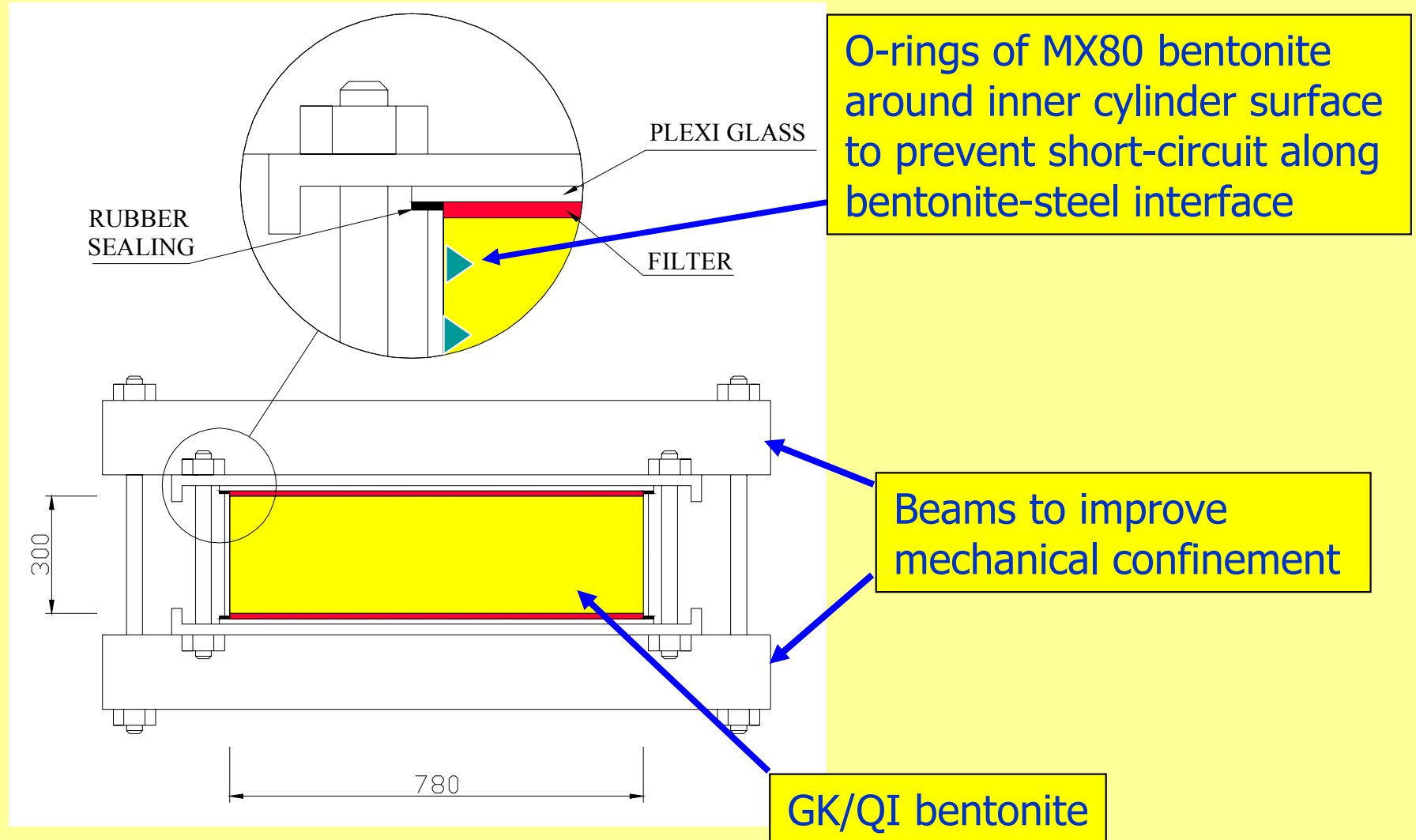


Back pressure +  
gas overpressure

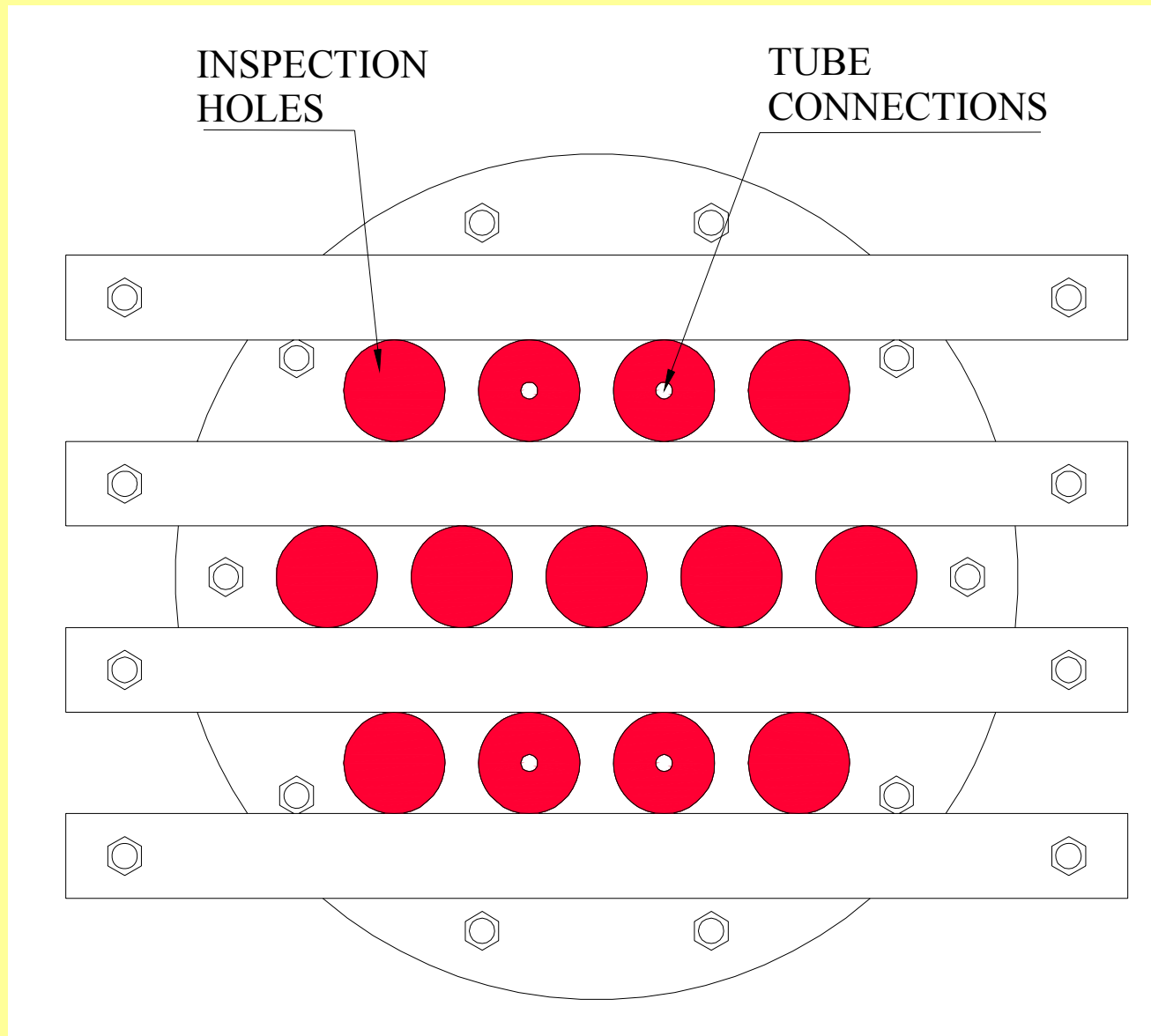
# Experiment layout



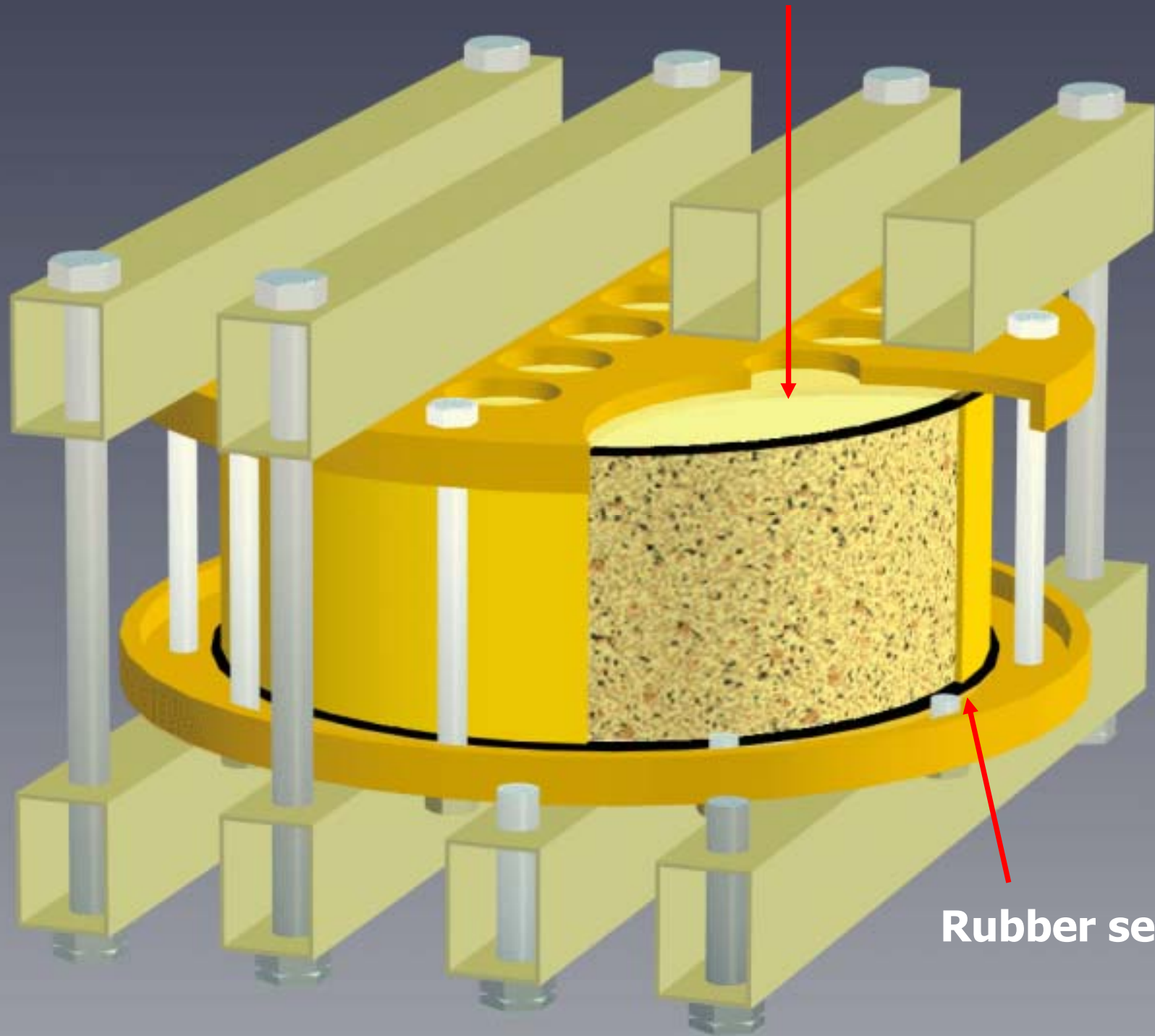
# Mega-Permeameter, vertical cross section



# Mega-Permeameter, top view

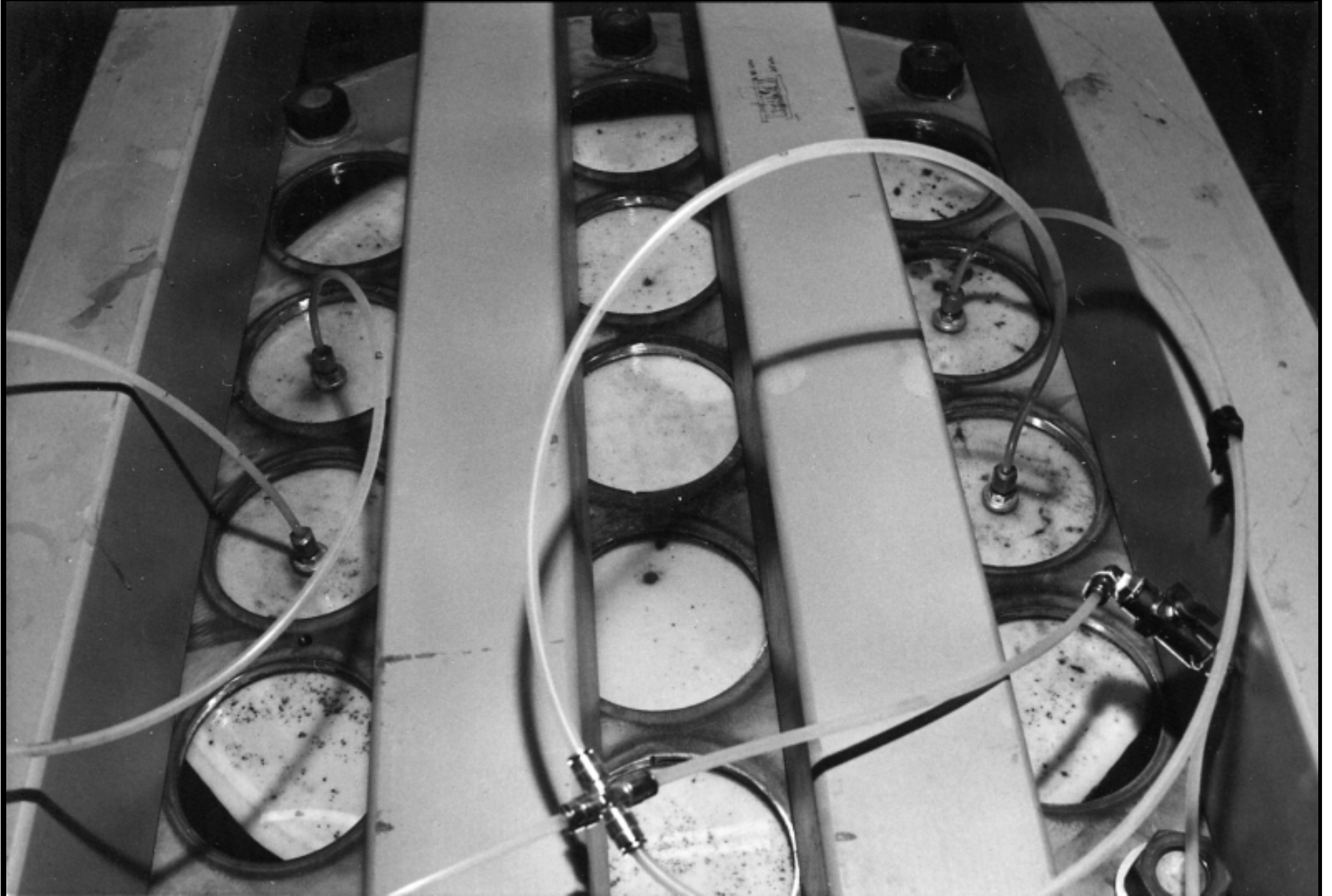


**Plexiglas disc on top of porous filter**

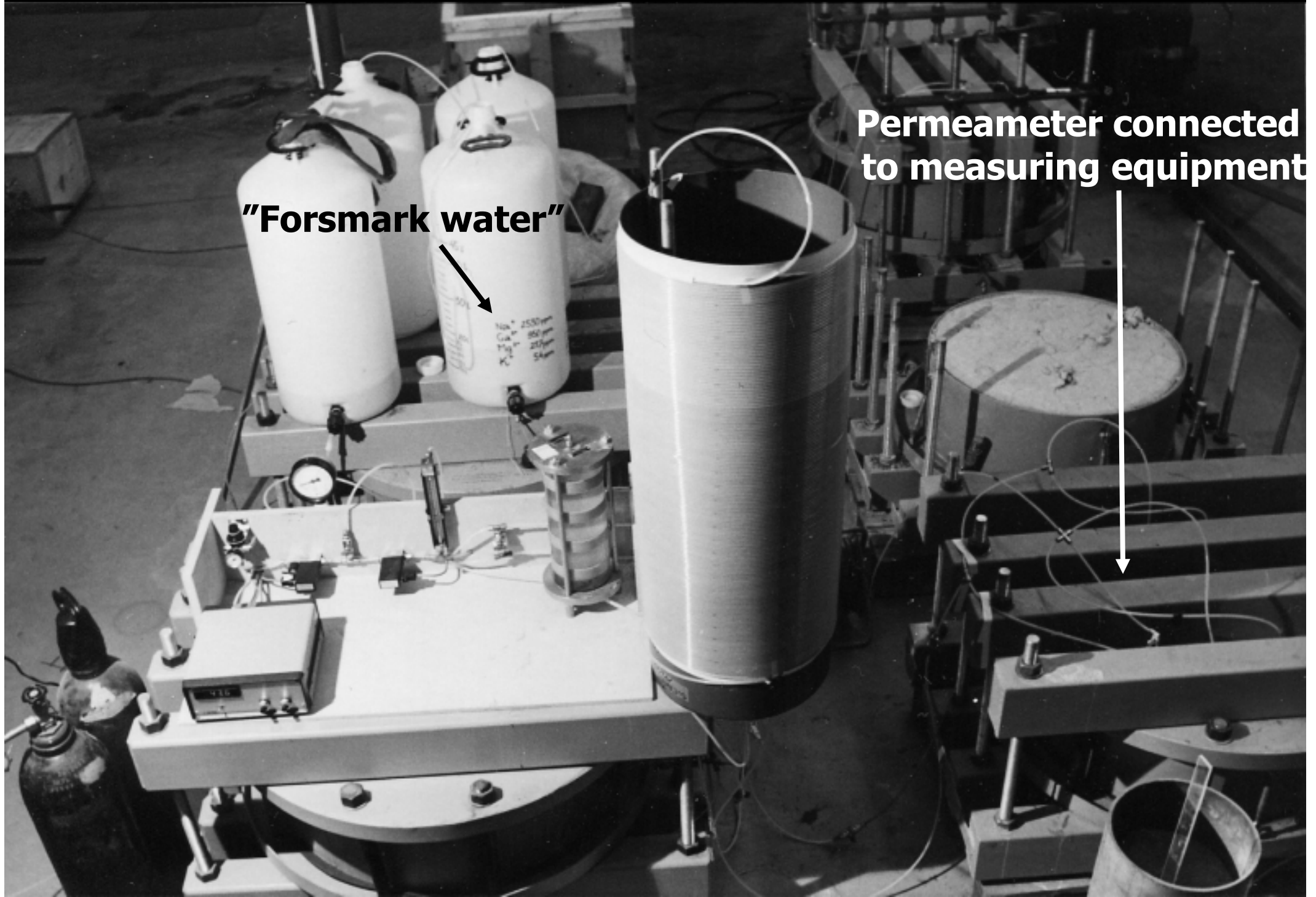


**Rubber selaing**

# Inspection holes and connection tubes



# Experiment set-up, overview



**"Forsmark water"**

**Permeameter connected  
to measuring equipment**



# Experiment set-up, measuring equipment

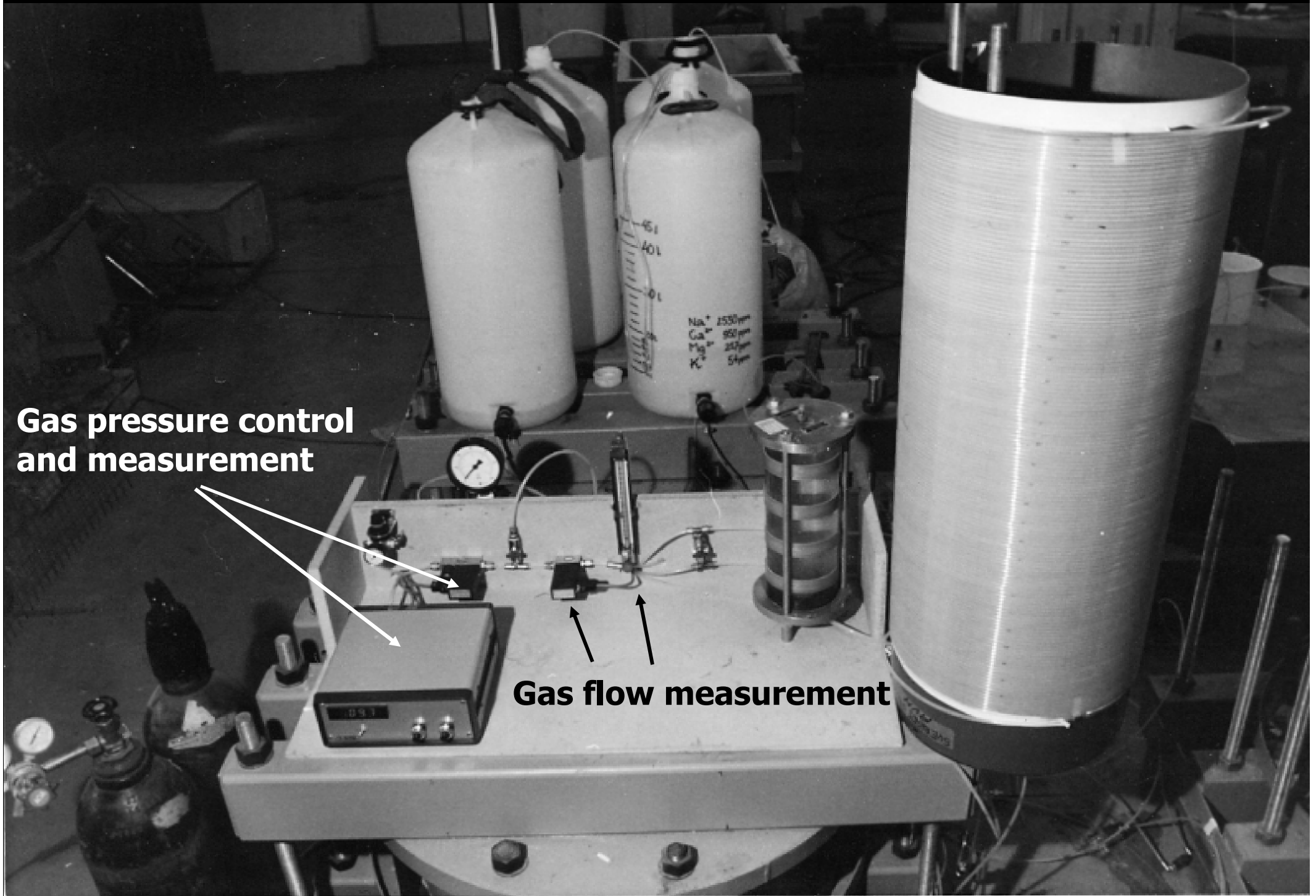
Back pressure control  
and measurement



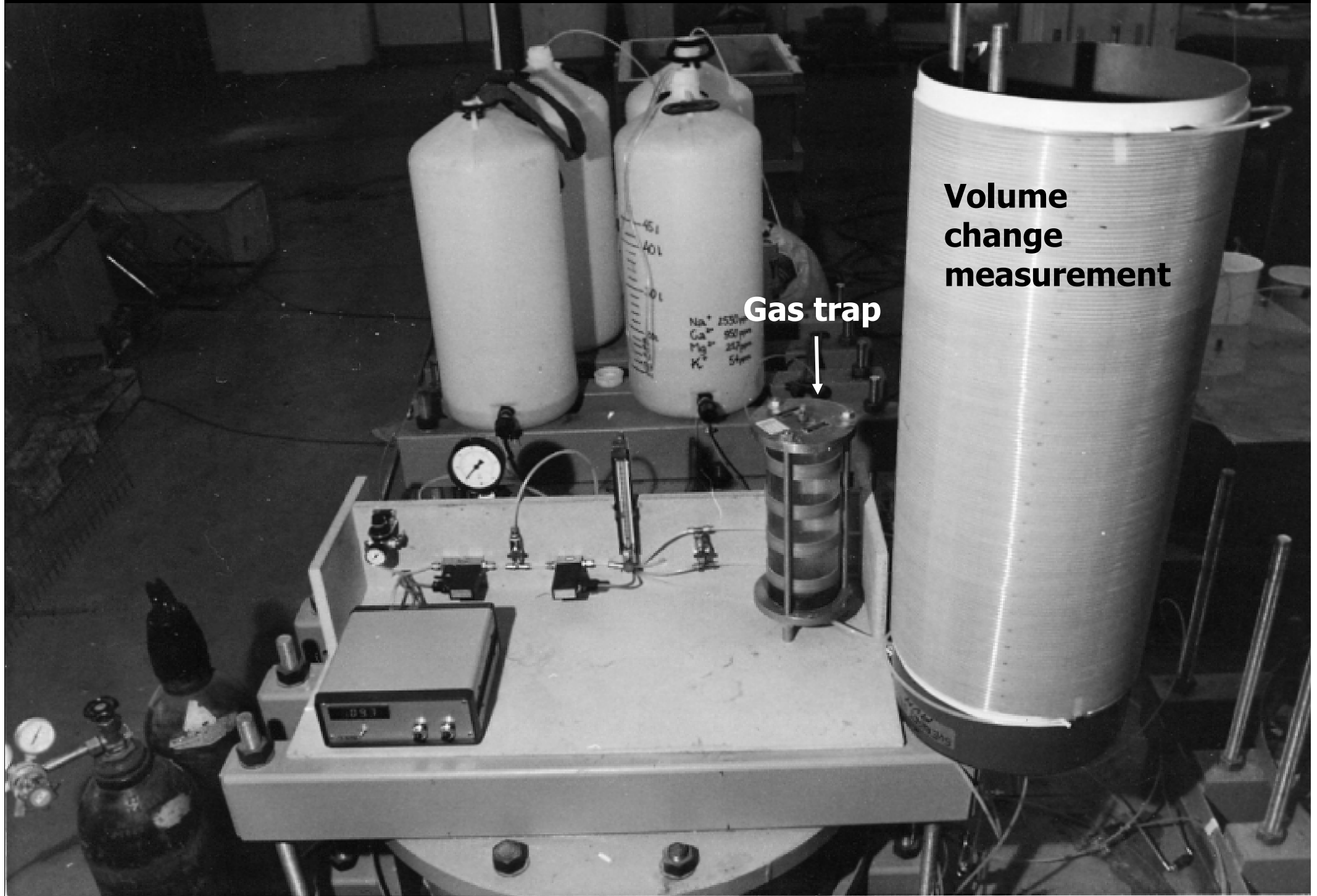
# Experiment set-up, measuring equipment

Gas pressure control and measurement

Gas flow measurement



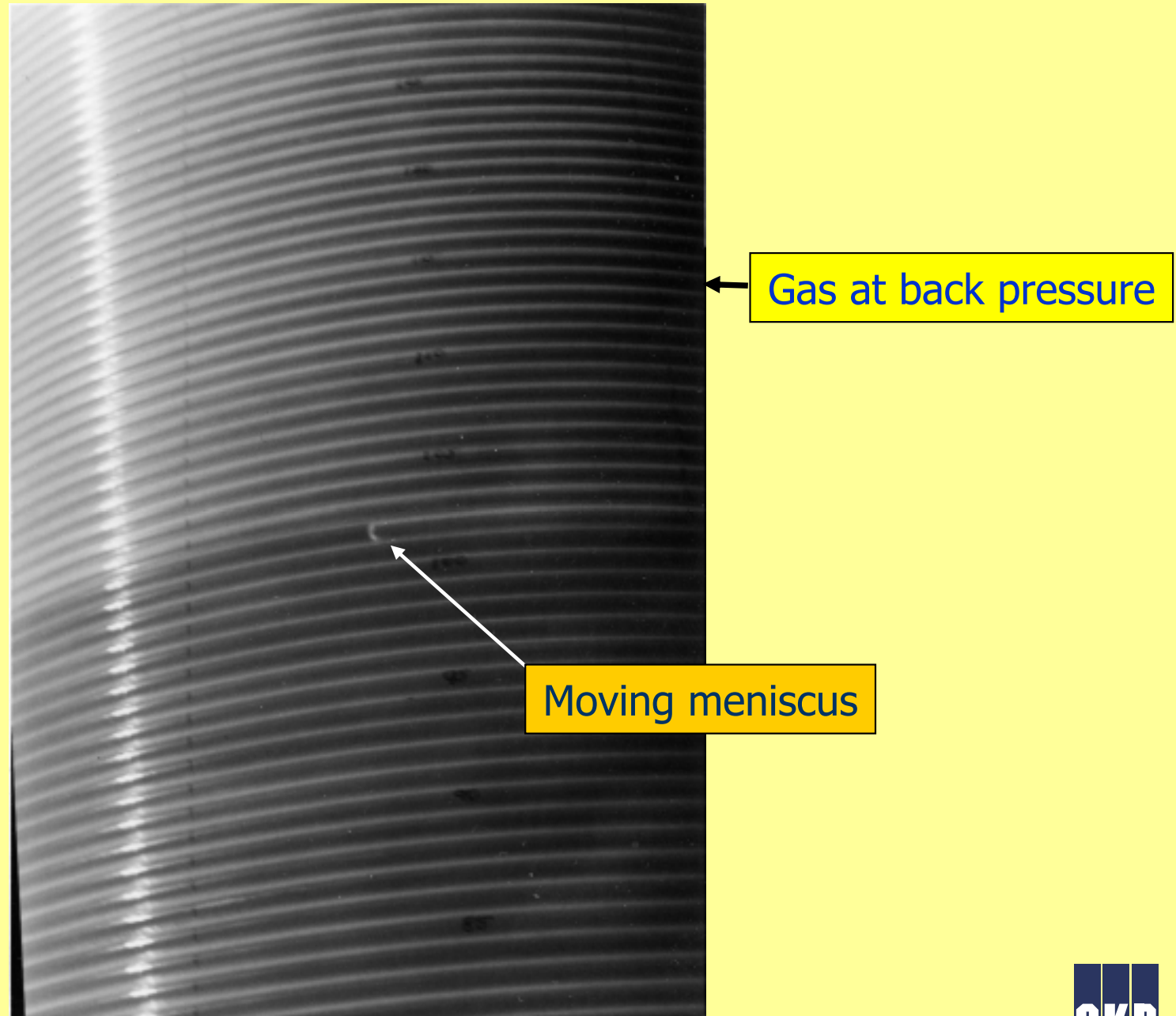
# Experiment set-up, measuring equipment



**Volume  
change  
measurement**

**Gas trap**

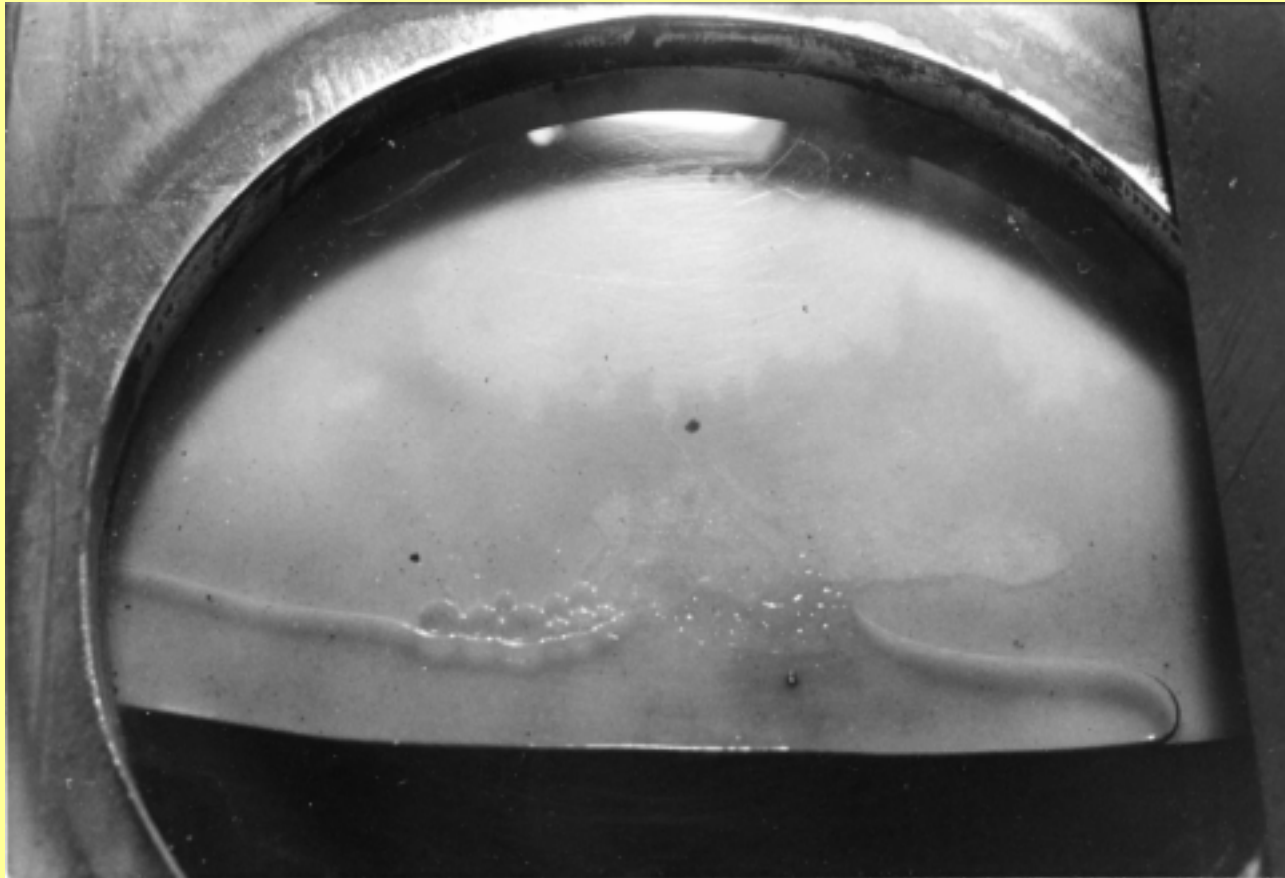
# Volume measurement of expelled water/gas



# Gas break-through



# Gas break-through



# Test 6 (Back pressure 60 kPa)

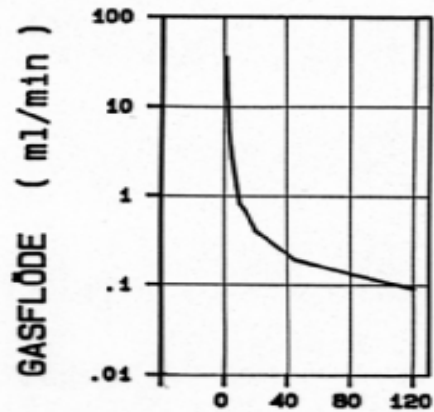
Pressure step 1: 25 kPa

Pressure step 2: 75 kPa

Pressure step 3: 125 kPa

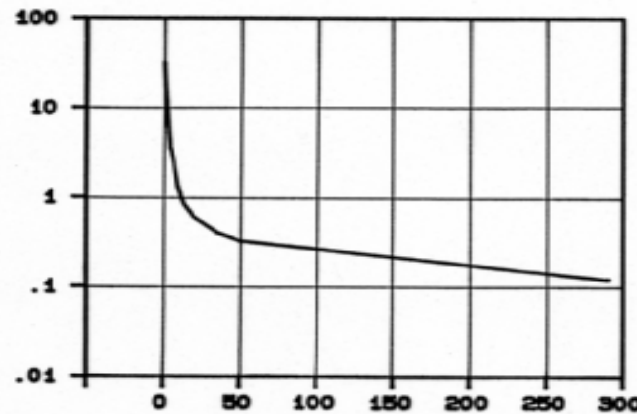
Upper: gas flow into sample;  
Lower: water flow out of sample

120 min: ~ 0.1 ml/min



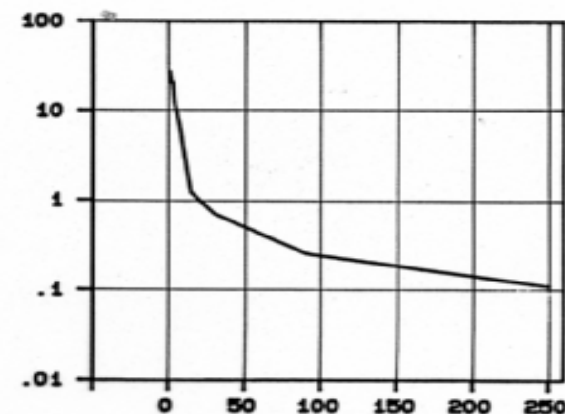
25 kPa

300 min: ~ 0.1 ml/min



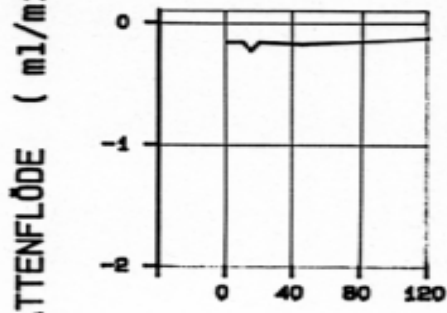
75 kPa

250 min: ~ 0.1 ml/min

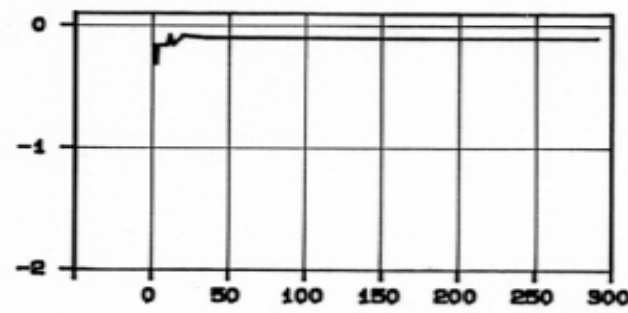


125 kPa

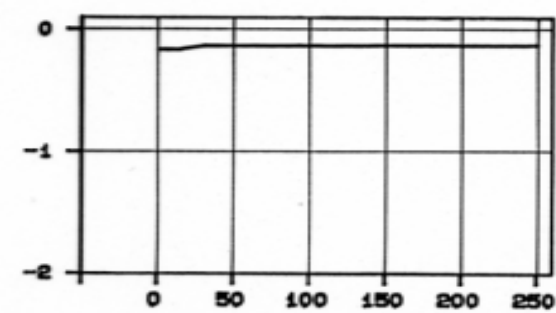
120 min: ~ 0.1 ml/min



300 min: ~ 0.1 ml/min



250 min: ~ 0.1 ml/min



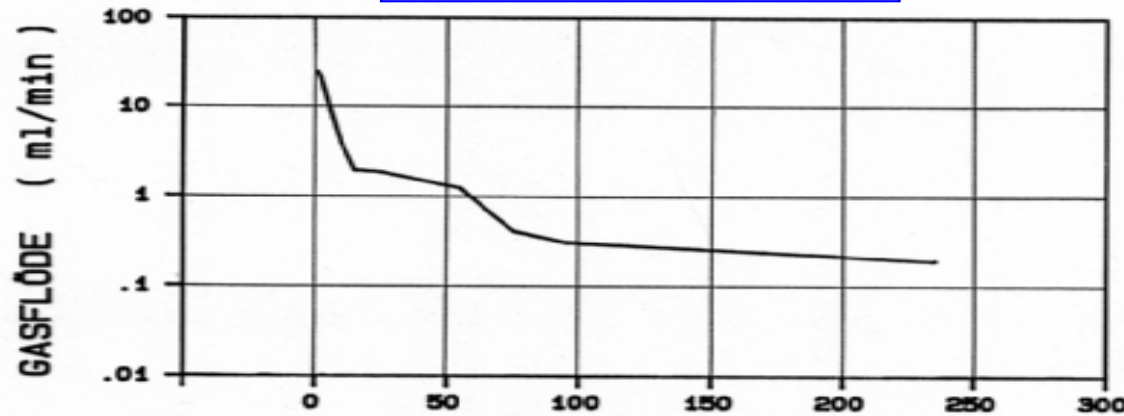
# Test 6 (Back pressure 60 kPa)

Pressure step 4: 175 kPa

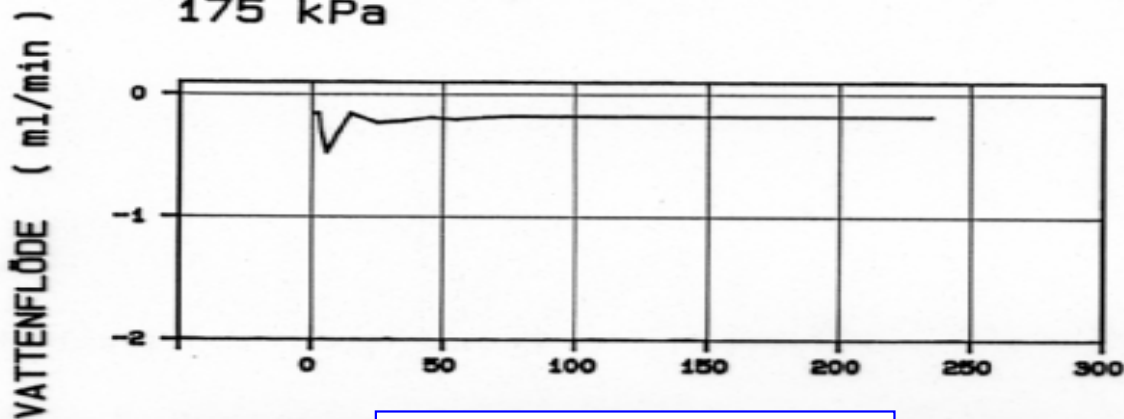
Pressure step 5: 240 kPa

Upper: gas flow into sample;  
Lower: water flow out of sample

300 min: ~ 0.2 ml/min

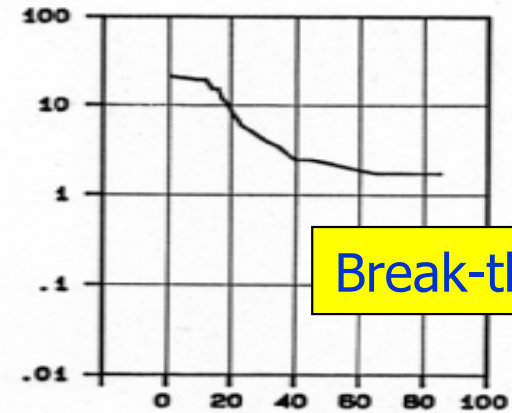


175 kPa

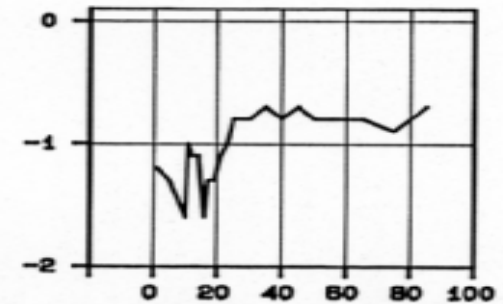


300 min: ~ 0.2 ml/min

100 min: ~ 1 ml/min



240 kPa



100 min: <0.1 ml/min

Break-through



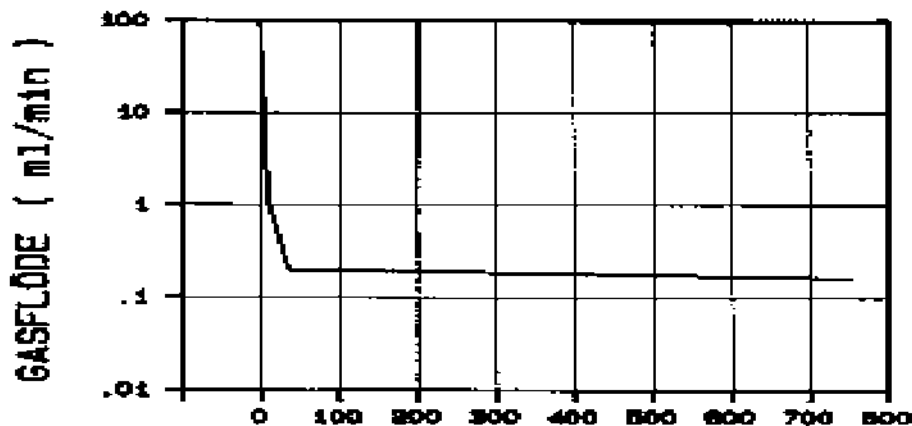
# Test 7 (Back pressure 100 kPa)

Pressure step 1: 50 kPa

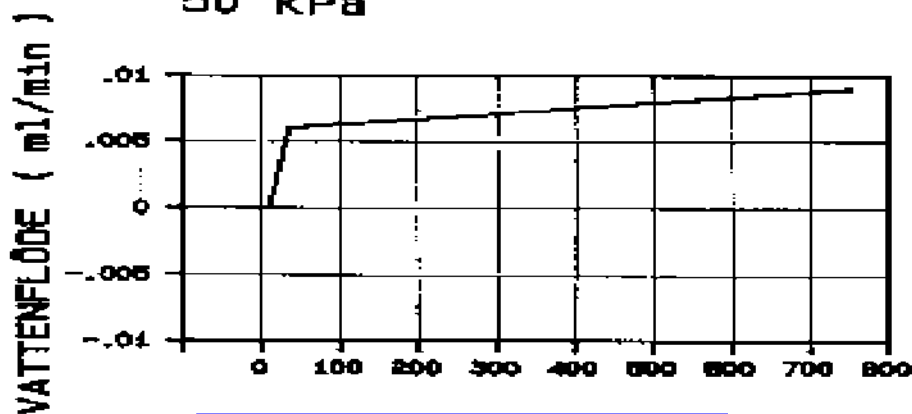
Pressure step 2: 100 kPa

Upper: gas flow into sample;  
Lower: water flow out of sample

800 min: ~ 0.2 ml/min

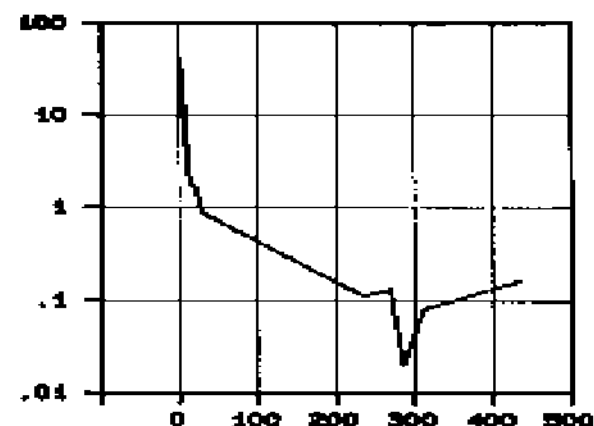


50 kPa

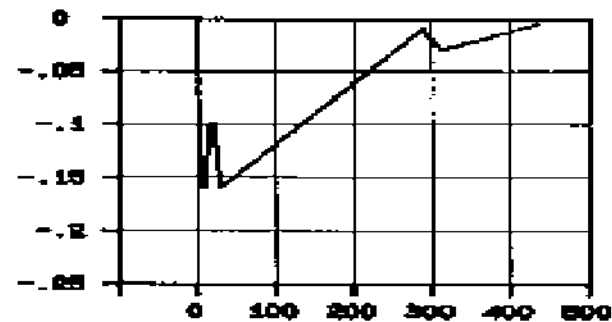


800 min: <0.01 ml/min

500 min: ~ 0.1 ml/min



100 kPa



500 min <<0.01 ml/min

# Test 7 (Back pressure 100 kPa)

Pressure step 3: 140 kPa

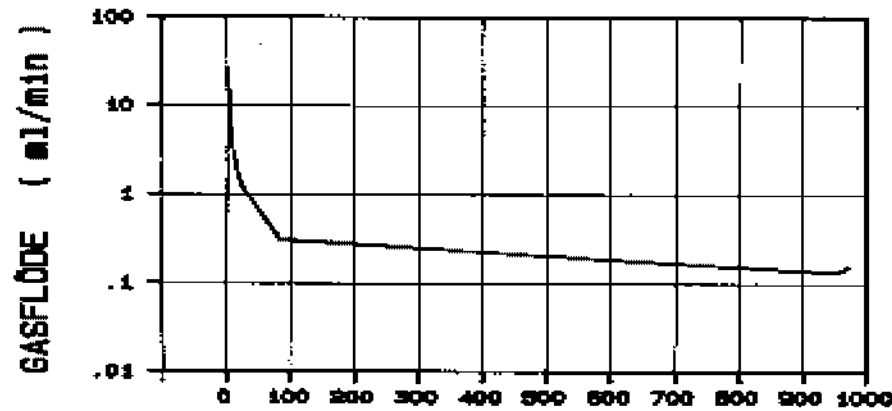
Pressure step 4: 170 kPa

Pressure step 5: 200 kPa

Upper: gas flow into sample;

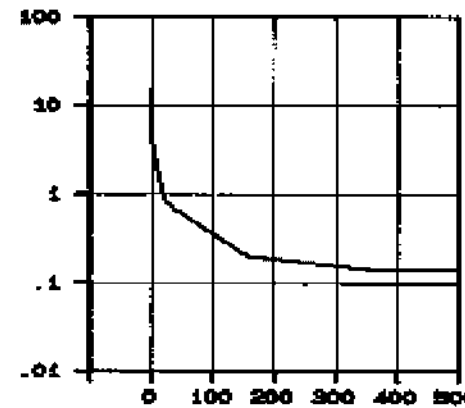
Lower: water flow out of sample

1000 min: ~ 0.1 ml/min



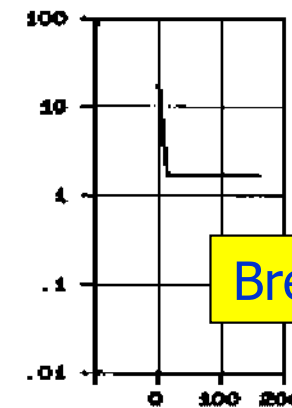
140 kPa

600 min: ~ 0.1 ml/min



170 kPa

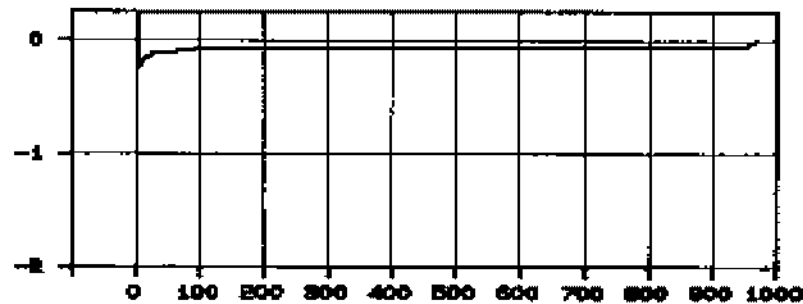
200 min: > 1 ml/min



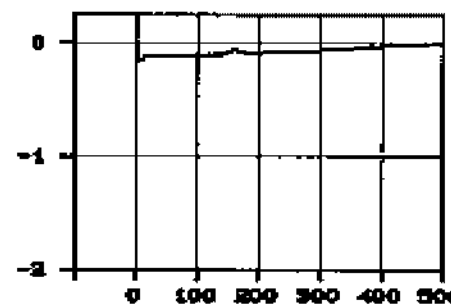
200 kPa

Break-through

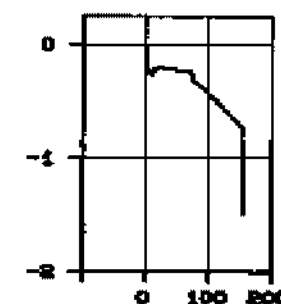
VATTENFLÖDE ( ml/min )



1000 min: <0. 1 ml/min



600 min <0. 1 ml/min



200 min: >1 ml/min

# Test 8 (Back pressure 100 kPa)

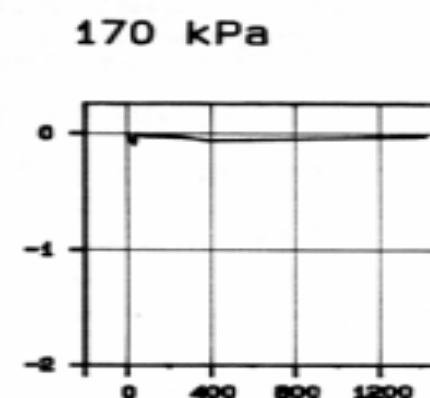
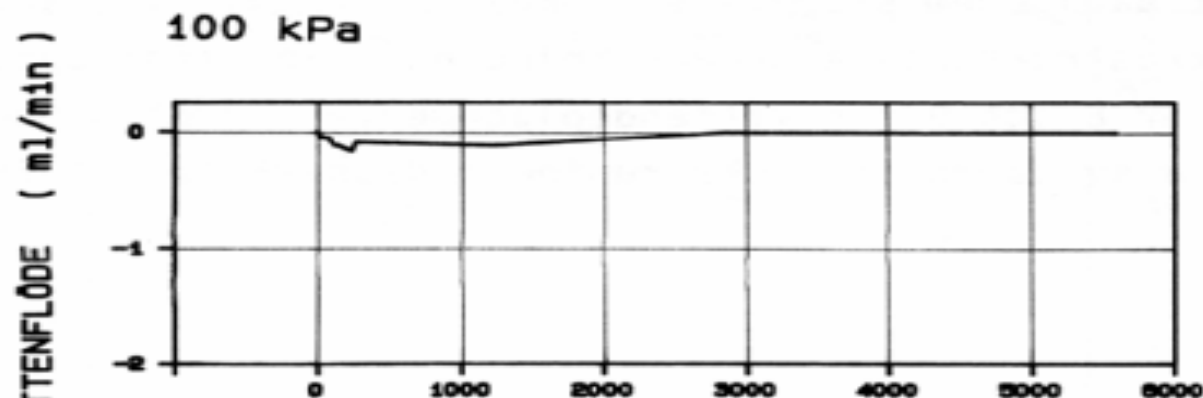
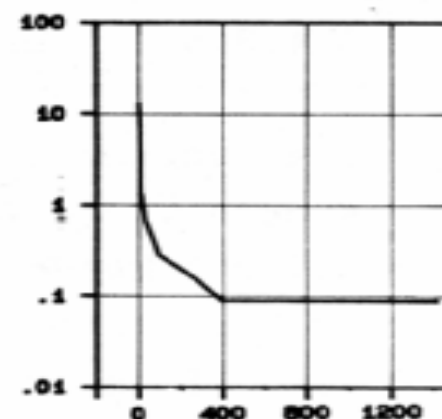
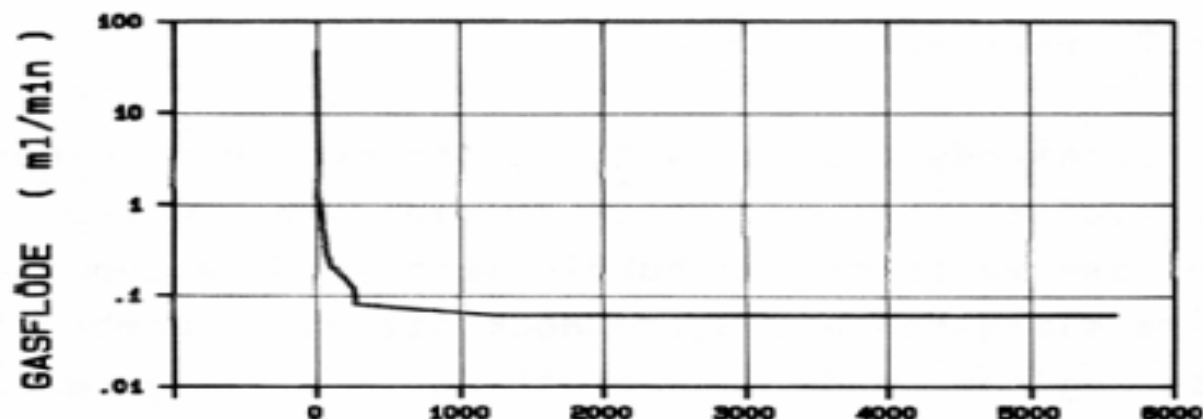
Pressure step 1: 100 kPa

Pressure step 2: 170 kPa

Upper: gas flow into sample;  
Lower: water flow out of sample

6000 min < 0.1 ml/min

1200 min: ~1 ml/min



6000 min: <0.1 ml/min

1200 min < 1 ml/min

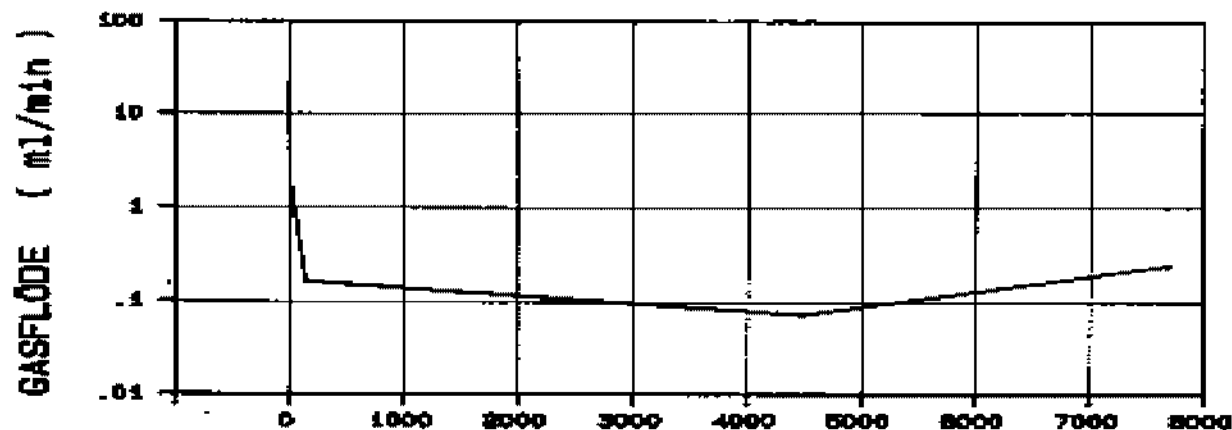
# Test 8 (Back pressure 100 kPa)

Pressure step 3: 190 kPa

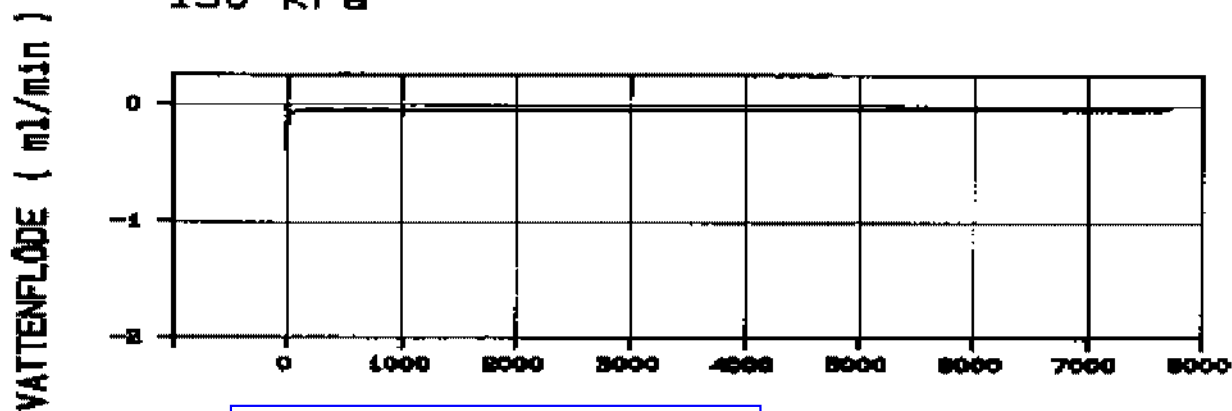
Pressure step 4: 205 kPa

Upper: gas flow into sample;  
Lower: water flow out of sample

8000 min ~ 0.2 ml/min

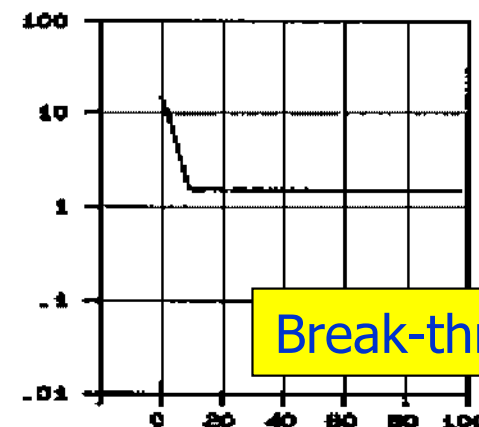


190 kPa



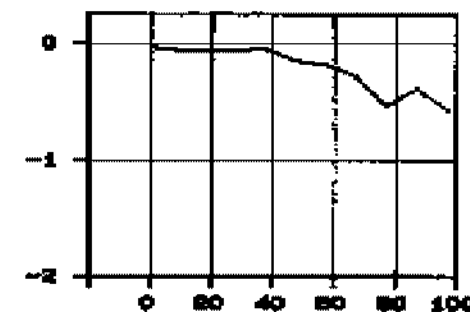
8000 min: <0.1 ml/min

100 min: >1 ml/min



Break-through

205 kPa



100 min ~ 1 ml/min

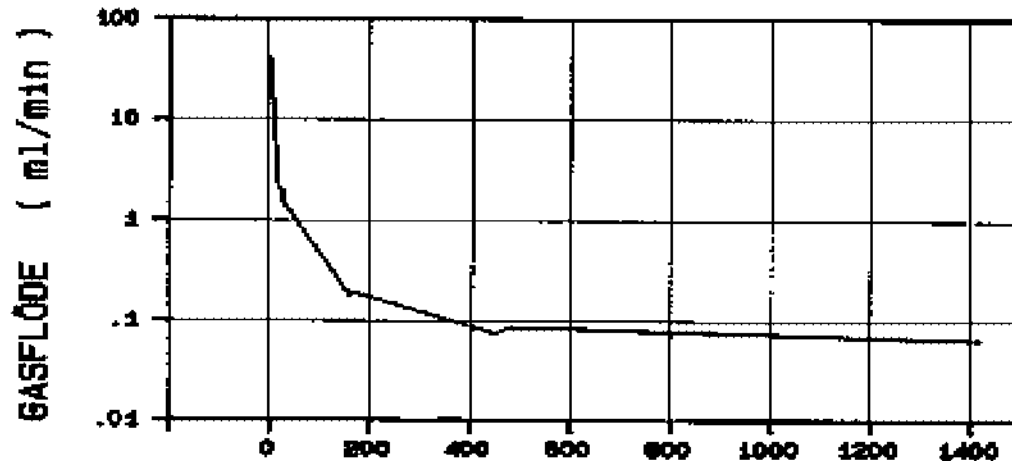
# Test 9

Pressure step 1: 100 kPa

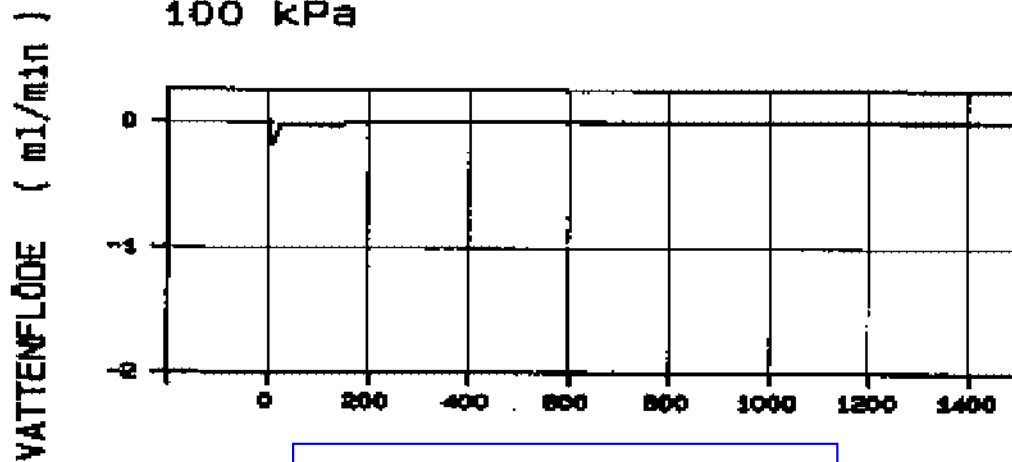
Pressure step 2: 165 kPa

Upper: gas flow into sample;  
Lower: water flow out of sample

1400 min: <0.1 ml/min

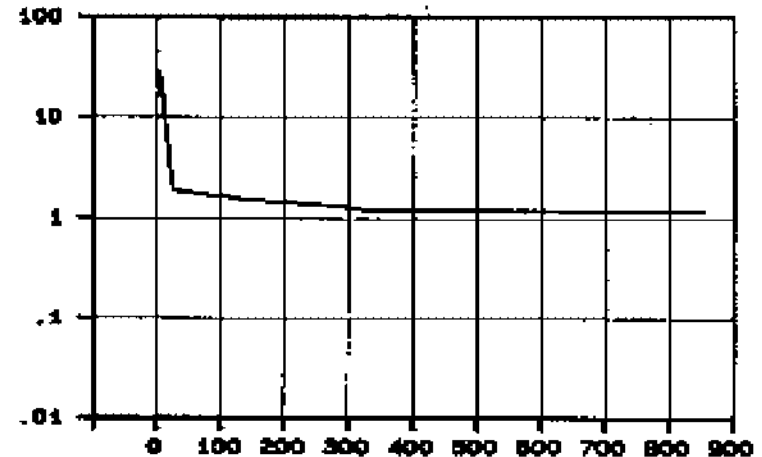


100 kPa

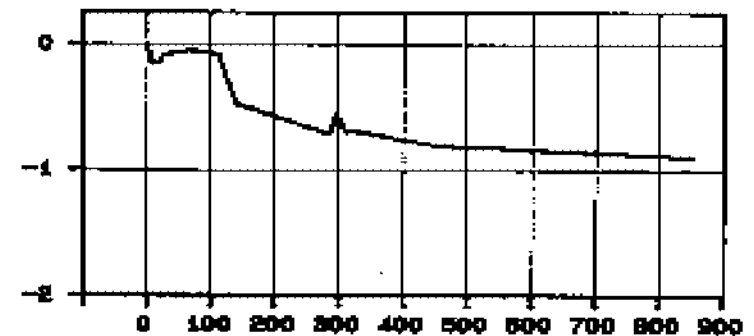


1400 min: <0.1 ml/min

800 min: 1 ml/min



165 kPa



800 min: 1 ml/min

# Test 10 (Backpressure 120 kPa)

Pressure step 1: 50 kPa

Pressure step 2: 90 kPa

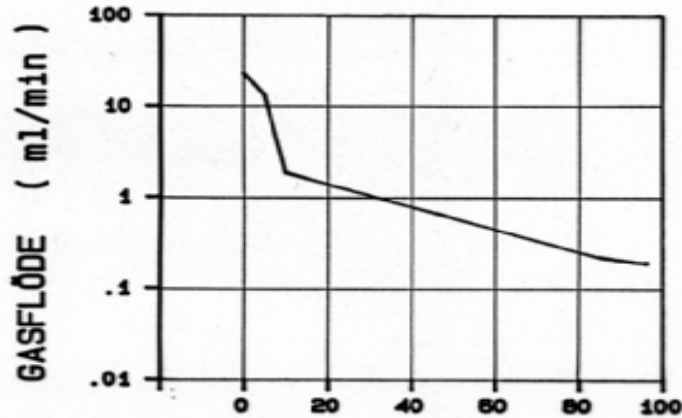
Pressure step 3: 130 kPa

Upper: gas flow into sample;  
Lower: water flow out of sample

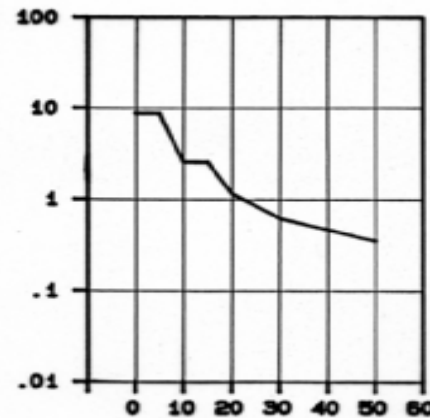
100 min: ~ 0.2 ml/min

60 min: ~ 0.2 ml/min

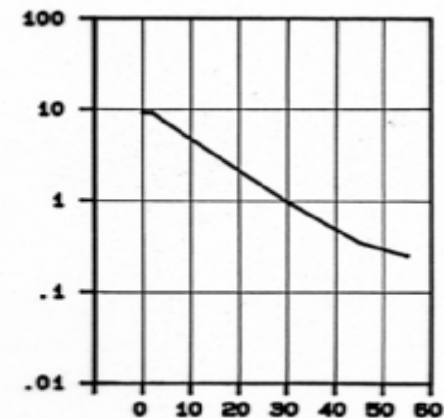
60 min: ~ 0.2 ml/min



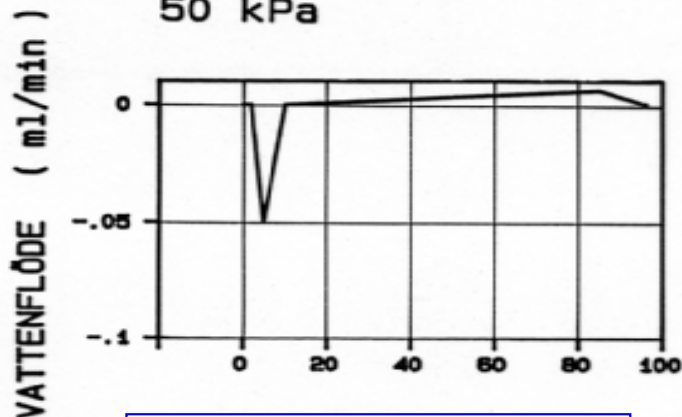
50 kPa



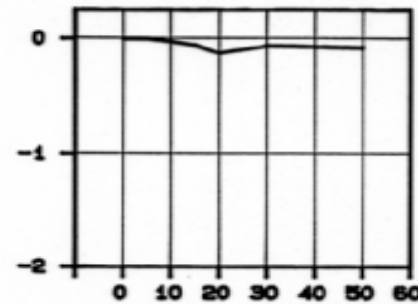
90 kPa



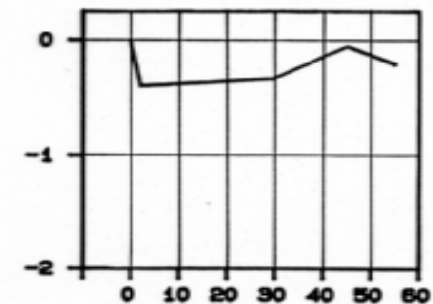
130 kPa



100 min: <0.1 ml/min



60 min: <0.1 ml/min



60 min: <0.1 ml/min

# Test 10 (Back pressure 120 kPa)

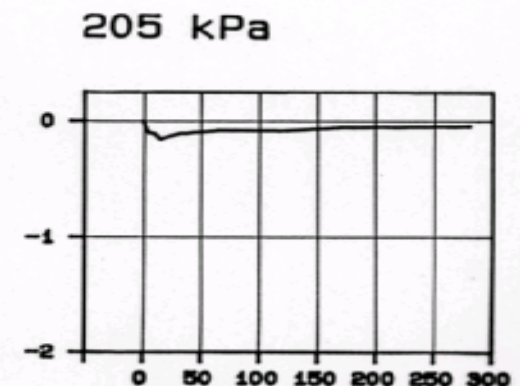
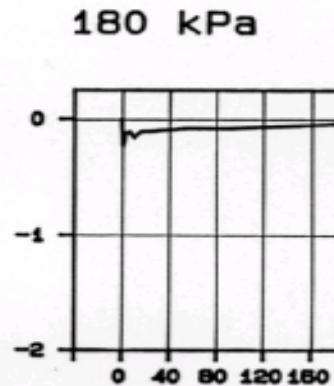
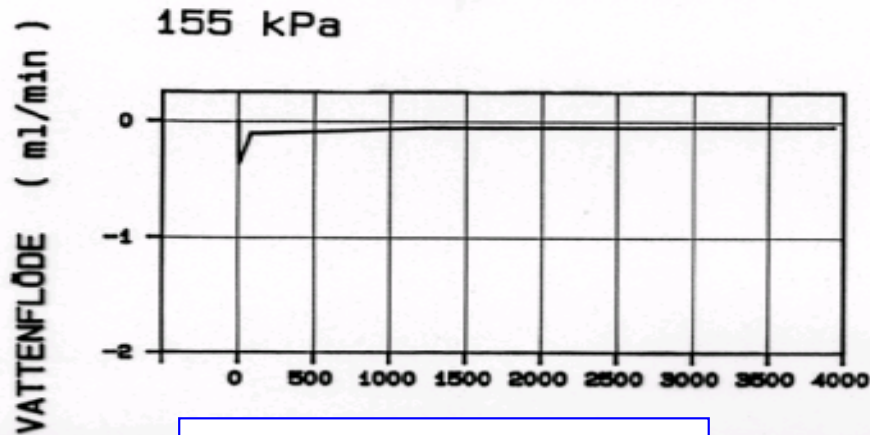
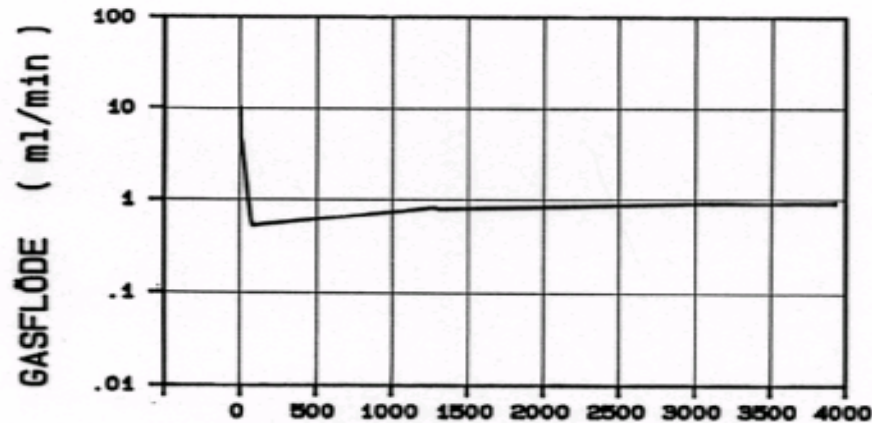
Pressure step 4: 155 kPa

Pressure step 5: 180 kPa

Pressure step 6: 205 kPa

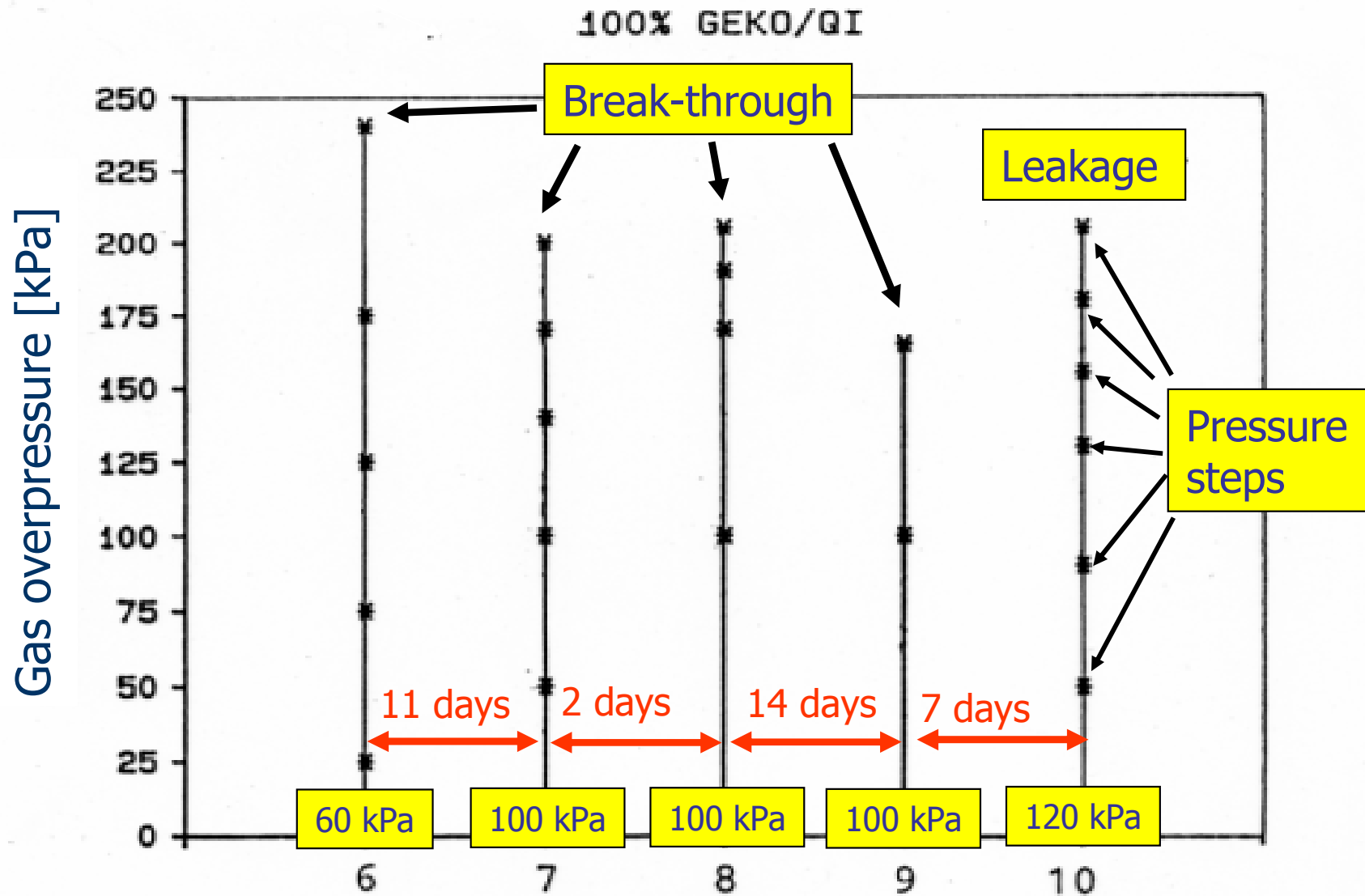
Upper: gas flow into sample;  
Lower: water flow out of sample

4000 min: 1 ml/min



4000 min: <0.1 ml/min

# Result summary





# Conclusions/Observations

- Gas phase break-through occurred at gas over-pressures in the range 165 kPa – 240 kPa
- The amount of water successively displaced during pressure build-up was, at most, a few per mille of the water contained in the sample.
- Only a small fraction of the pore space, i.e. the largest continuous pores, were involved in the gas transport
- Capillary analogy estimates suggest that the smallest diameter of the largest continuous pores was 1-2 $\mu$ m
- The first test (nr 6) gave a larger amount of water displaced before breakthrough than the following tests (at least twice as much).
- Because of leakage, the back pressure could not be varied within a sufficiently wide range to verify or falsify the critical pressure hypothesis.

ISSN 1404-0344

CM Digitaltryck AB, Bromma, 2005